



Utilisation of Rearrangement Chemistry in the Synthesis of Novel Fluorinated Ring Systems: A Computational and Experimental Study

David George Alexander Orr

Submitted in part fulfilment of the requirements of the degree of Doctor of
Philosophy

April 2016

Academic Supervisor: **Prof. Jonathan M. Percy** (Pure and Applied Chemistry)

Industrial Supervisor: **Dr. Zoë A. Harrison** (GlaxoSmithKline)

Internal Examiner: **Prof. Nick C. O. Tomkinson** (Pure and Applied Chemistry)

External Examiner: Prof. **Martin D. Smith** (University of Oxford)

Declaration

'This thesis is the result of the author's original research. It has been composed by the author and has not been previously submitted for examination which has led to the award of a degree.'

'The copyright of this thesis belongs to the author under the terms of the United Kingdom Copyright Acts as qualified by University of Strathclyde Regulation 3.50. Due acknowledgement must always be made of the use of any material contained in, or derived from, this thesis.'

Signed:

Print:

Date:

“When its all gone,
Something carries on,
And it’s not morbid at all,
Just that nature’s had enough of you,
When my blood stops,
Someone else’s will thaw,
When my head rolls off,
Someone else’s will turn,

And while I’m alive, I’ll make tiny changes to Earth.”

Frightened Rabbit

Heads Roll Off

Acknowledgements

First and foremost I would like to thank my supervisor Prof. Jonathan Percy for providing me with the opportunity to undertake this research project. His help and support throughout my PhD has been invaluable and has allowed me to develop a more critical approach to my chemistry and to become more confident in talking about my work.

Dr. Zoë Harrison (GlaxoSmithKline, Stevenage) is thanked for her advice throughout the project and for providing an industrial perspective of our work. Her organisation and planning of my Industrial CASE Placement was very much appreciated alongside her continued support and involvement during the 3 months.

I would also like to thank members of the Percy group, both past and present, for their support and helpful discussions throughout the years. I would like to specifically thank Dr. David Nelson and Dr. Peter Wilson for help synthesising Ni-catalyst or troubleshooting cross-coupling reactions, respectively.

The academic and technical staff and the University of Strathclyde have supported much of this work. Dr. Tell Tuttle is thanked for help with electronic structure calculations and Dr. Alan Kennedy for X-Ray crystallographic analysis. Craig Irving has been invaluable and is thanked for his assistances with NMR reaction monitoring. Pat Keating is thanked for her assistance with mass spectroscopy and Gavin Bain for ensuring the smooth running of our lab. All three are thanked for their trust is allowing me to help out and for their rants/chats which kept me sane! Alex Clunie is thanked for CHN analysis and the EPSRC NMSSC team in Swansea for accurate mass analysis.

Thanks goes to GlaxoSmithKline (specifically Dr. Vipulkumar Patel) and the University of Strathclyde for funding the studentship.

Last but certainly no means least, I would like to thank my friends and family for their support throughout. Special thanks are reserved for Krystyna who has always been there for me, through the good times and bad. Through her I have learned that life outside of the lab is much more fulfilling and knowing she was there for me at the end of everyday made the work so much easier.

Publication List

- **Poster Presentation:** “Developing a Coupling-based Route to Difluorinated Cyclopentenes” **Orr, D.**, Percy, J. M., Harrison, Z. A., WestCHEM Organic Postgraduate Symposium (University of Glasgow, July, **2013**).
- **Oral Presentation:** “Facile and Highly Stereospecific Rearrangement of a Difluorinated Vinylcyclopropane”, RSC Postgraduate Fluorine Group Meeting joint with Fluorine - Academia Meets Industry (University of St Andrews, July, **2014**) and 10th Annual WestCHEM Research Day (University of Strathclyde, August, **2014**).
- **Publication:** “Evaluating the Thermal Vinylcyclopropane Rearrangement (VCPR) as a Practical Method for the Synthesis of Difluorinated Cyclopentenes: Experimental and Computational Studies of Rearrangement Stereospecificity”, **Orr, D.**, Percy, J. M., Tuttle, T., Kennedy, A. R., Harrison, Z. A., *Chem. Eur. J.*, **2014**, *20*, 14305-14316.
- **Oral Presentation:** “Synergic Experimental and Theoretical Studies into the Stereoselective Synthesis of Difluorocyclopentenes using Vinylcyclopropane Rearrangements”, 26th SCI Postgraduate Symposium on Novel Organic Chemistry (University of Strathclyde, April, **2015**).
- **Oral Presentation:** “Stereoselective Synthesis of Difluorocyclopentenes using Vinylcyclopropane Rearrangements: Synergic Experimental and Theoretical Studies”, 21st International Symposium on Fluorine Chemistry & 6th International Symposium on Fluorous Technologies (Politecnico Di Milano, Como, Italy, August, **2015**).
- **Publication:** “A Computational Triage Approach to the Synthesis of Novel Difluorocyclopentenes and Fluorinated Heptadienes using Thermal Rearrangements”, *Chem. Sci.*, Accepted 15th June 2016, DOI:10.1039/C6SC01289B.

Abbreviation

| | |
|-------|--|
| acac | - Acetylacetone |
| BAIB | - (Diacetoxyiodo)benzene |
| B3LYP | - Becke, 3-parameter, Lee-Yang-Parr |
| BPin | - Pinacol Borane |
| Bn | - Benzyl ether |
| CI | - Chemical Ionisation |
| CM | - Cross Metathesis |
| COD | - 1,5-Cyclooctadiene |
| Cy | - Cyclohexyl |
| DAST | - Diethylaminosulfur trifluoride |
| dba | - Dibenzylideneacetone |
| DCM | - Dichloromethane |
| DEC | - Diethyl carbamate |
| DIBAL | - <i>Diisobutyl</i> aluminum hydride |
| DMC | - Dimethyl carbamate |
| DME | - Dimethoxyethane |
| dmpe | - 1,2- <i>Bis</i> (dimethylphosphino)ethane |
| DMPU | - N,N'-Dimethyl-N,N'-trimethyleneurea |
| dppf | - 1,1'-Bis(diphenylphosphino)ferrocene |
| ESC | - Electronic Structure Calculations |
| EWG | - Electron withdrawing group |
| FT-IR | - Fourier Transform Infrared |
| GC | - Gas Chromatography |
| IPr | - 1,3-Bis(2,6-diisopropylphenyl)imidazol-2-ylidene |
| IR | - Infrared |
| LDA | - Lithium <i>diisopropyl</i> amide |
| KHDMS | - Potassium hexamethyldisilazane |
| MDFA | - Methyl 2,2-difluoro-2-(fluorosulfonyl)acetate |
| MEM | - Methoxyethyl ether |

| | | |
|----------|---|---|
| Ms | - | Methanesulfonyl |
| MOM | - | Methoxymethyl ether |
| NFSI | - | <i>N</i> -fluorobenzenesulfonimide |
| NHC | - | <i>N</i> -heterocyclic carbene |
| NMR | - | Nuclear Magnetic Resonance |
| ONIOM | - | Our own <i>N</i> -layered Integrated molecular Orbital and |
| ORTEP | - | Oak Ridge Thermal-Ellipsoid Plot Program |
| RCM | - | Ring closing metathesis |
| RuPhos | - | 2-Dicyclohexylphosphino-2',6'-diisopropoxybiphenyl |
| SIPr | - | 1,3-Bis(2,6-di- <i>i</i> -propylphenyl)imidazolidin-2-ylidene |
| SPE | - | Solid Phase Extraction |
| TBAT | - | Tertrabutylammonium triphenyldifluorosilicate |
| TBS | - | <i>t</i> -Butyldimethylsilane |
| TEFDA | - | Triethylsilyl fluorosulfonyldifluoroacetate |
| TEMPO | - | 2,2,6,6-Tetramethyl-1-piperidinyloxy, free radical |
| TFDA | - | Trimethylsilyl 2,2-difluoro-2-(fluorosulfonyl)acetate |
| THF | - | Tetrahydrofuran |
| THP | - | Tetrahydropyran |
| TIPS | - | triisopropylsilane |
| TMS | - | Trimethylsilane |
| TMSCl | - | Chlorotrimethylsilane |
| TMSI | - | Iodotrimethylsilane |
| Ts | - | <i>p</i> -Toluenesulfonyl |
| UB3LYP | - | Unrestricted Becke, 3-parameter, Lee-Yang-Parr |
| VCP | - | Vinylcyclopropane |
| VCPR | - | Vinylcyclopropane rearrangement |
| Xantphos | - | 4,5-Bis(diphenylphosphino)-9,9-dimethylxanthene |
| Xphos | - | 2-Dicyclohexylphosphino-2',4',6'-triisopropylbiphenyl |
| XRD | - | X-Ray Diffraction |

Abstract

The rearrangement of vinylcyclopropanes to cyclopentenes (the vinylcyclopropane rearrangement, VCPR) has developed rapidly from its initial discovery and has become an important transformation in the synthesis of a variety of natural products. The beneficial effect of fluorine atom substitution on vinylcyclopropanes has been well documented but the rearrangement has yet to be deployed as an effective method for the synthesis of difluorocyclopentenes.

Work towards developing an efficient, building-block approach to difluorocyclopentenes by using the VCPR is presented. Two distinct precursors were selected as synthetic targets; focusing on accessing compounds with either *gem*-difluoroalkene or *gem*-difluorocyclopropane motifs. These routes relied on the successful development of novel cross-coupling chemistry and the utilisation of the most effective difluorocyclopropanation techniques.

Accessible precursors were subjected to thermal, photochemical and Ni-mediated VCPR conditions showing that difluorocyclopropane substitution underwent more efficient rearrangements than difluorovinyl precursors. Overall, a novel difluorocyclopentene could be accessed in 70% yield over 4 steps using commercial reagents and further functionalised to more complex molecules.

The ease of rearrangement was intriguing, and was investigated using a variety of physical organic chemistry tools such as spectroscopy, kinetic studies, density functional theory and reaction simulations. Reaction monitoring of the rearrangements uncovered both competing cyclopropane stereoisomerisation and an alternative [3,3]-sigmatropic rearrangement pathway which ultimately afforded a novel fluorinated benzocycloheptadiene. Furthermore, a dramatic reactivity difference was observed when different alkene isomers were subject to VCPR conditions. Experimental activation energies for the rearrangements could be obtained and used to conduct methodology screening for electronic structure calculations, leading to the development of a computational model which could triage synthetic targets.

This work contributes to better understanding of the VCPR and the synthetic limitations of accessing fluorinated precursors. The development of a computational model which can be effectively utilised by non-specialists is an excellent tool for aiding synthetic projects which utilise the VCPR.

Contents

| | |
|---|-------------|
| Declaration | i |
| Publication List | iv |
| Abbreviation..... | v |
| Abstract..... | vii |
| Contents..... | viii |
| Introduction | 1 |
| 1.1. Methods of Fluorination..... | 2 |
| 1.2. Building Block Approach..... | 3 |
| 1.2.1. 2,2,2-Trifluoroethanol..... | 3 |
| 1.2.2. Difluorocarbene | 10 |
| 1.3. Vinylcyclopropane Rearrangements | 21 |
| 1.3.1. Mechanism..... | 24 |
| 1.3.1.1. Thermolysis | 24 |
| 1.3.1.2. Transition Metal Catalysis | 29 |
| 1.3.1.3. Effects of Fluorine | 35 |
| 1.3.2. Applications of VCPR..... | 38 |
| 1.4. Difluorinated 5-Membered Ring Systems | 39 |
| 1.4.1. Difluorinated Cyclopentanes | 39 |
| 1.4.2. Difluorinated Cyclopentenones | 40 |
| 1.4.3. Difluorinated Cyclopentenenes | 41 |
| Aims | 43 |
| Chapter 1: Synthesis of 2,2-(Difluorovinyl)cyclopropanes | 45 |
| 2.1. 1 st Generation Optimisation | 46 |
| 2.2. Isolation of Oxidative Addition Intermediate 111 | 54 |

| | | |
|--|--|-----------|
| 2.2.1. | Suppressing the Formation of Diene 101 | 56 |
| 2.3. | 2 nd Generation Optimisation | 63 |
| 2.3.1. | Effect of Base | 65 |
| 2.4. | Best Coupling Conditions | 69 |
| 2.5. | Rearrangement of Cyclopropyl 99 | 70 |
| 2.5.1. | Nickel Catalysed Rearrangement..... | 70 |
| 2.5.2. | Thermolysis..... | 71 |
| 2.6. | Conclusion | 73 |
| Chapter 2: Synthesis of 1,1-Difluoro-2-vinylcyclopropanes | | 75 |
| 3.1. | Route I | 76 |
| 3.1.1. | Hydroboration | 76 |
| 3.1.2. | Difluorocyclopropanation of Vinyl Boronic Esters..... | 80 |
| 3.1.2.1. | Reactions with Sodium Chlorodifluoroacetate | 80 |
| 3.1.2.2. | Reactions with Sodium Bromodifluoroacetate..... | 82 |
| 3.1.2.3. | Reactions with Methyl 2,2-difluoro-(fluorosulfonyl)-acetate (MDFA) | 83 |
| 3.1.3. | Overview of Difluorocarbene Trapping with Alkene 123 | 86 |
| 3.2. | Route II | 88 |
| 3.2.1. | Optimising the Difluorocyclopropanation of Cinnamyl Acetate | 90 |
| 3.2.1.1. | Literature Conditions | 90 |
| 3.2.1.2. | Optimisation with MDFA..... | 91 |
| 3.2.2. | Complete Synthesis of VCPR Precursor 147 | 94 |
| 3.2.3. | Synthesis of <i>cis</i> -Difluorocyclopropane Precursors | 96 |
| 3.2.4. | Thermal Rearrangement of <i>E</i> -Difluorocyclopropane Precursors | 97 |
| 3.2.5. | Difluorocyclopentene Functionalisation..... | 99 |

| | | |
|---|--|------------|
| 3.2.6. | VCPR Reaction Monitoring | 102 |
| 3.2.7. | Thermal Rearrangement of Z-Difluorocyclopropane Precursors | 105 |
| 3.2.8. | Investigations using Electronic Structure Calculations..... | 107 |
| 3.2.8.1. | VCPR Methodology Screening | 107 |
| 3.2.8.2. | Cyclopropane Stereoisomerisation..... | 112 |
| 3.2.8.3. | [3,3]-Rearrangement..... | 115 |
| 3.2.9. | Assessment of Computational Methodology | 118 |
| 3.3. | Conclusion | 119 |
| Chapter 3: Computational Triage | | 122 |
| 4.1. | Computational Assessment..... | 123 |
| 4.1.1. | Effect of Difluorocyclopropane Substitution | 123 |
| 4.1.2. | Effect of Alkene Substitution | 131 |
| 4.2. | Synthetic Investigations | 133 |
| 4.2.1. | Synthesis of Cyclopropane Substituted Difluoro-VCP | 134 |
| 4.2.1.1. | 1 st Generation Synthetic Route..... | 134 |
| 4.2.1.2. | 2 nd Generation Synthetic Route | 136 |
| 4.2.1.3. | 3 rd Generation Synthetic Route | 142 |
| 4.2.2. | Functionalisation of Alkene Fragment..... | 145 |
| 4.3. | Thermal Rearrangement of Isolated Difluoro-VCP | 150 |
| 4.4. | Further Exploration of Electronic Structure Calculation Methods..... | 156 |
| 4.5. | Predictive Electronic Structure Calculations | 163 |
| 4.6. | Conclusion | 168 |
| Chapter 4: Alternative Rearrangement Conditions..... | | 170 |
| 5.1 | Photochemical Initiation | 170 |
| 5.2 | Transition Metal Mediated Rearrangements..... | 173 |

| | | |
|--------------------------------------|---|------------|
| 5.2.1 | Phosphine Ligand Screening | 175 |
| 5.2.2 | NHC-Ligand Screening..... | 176 |
| 5.2.3 | Investigating Alternative Ni(0) Sources | 178 |
| 5.3 | Computational Assessment of Ni-mediated VCPR..... | 181 |
| 5.3.1 | Method Comparison | 181 |
| 5.3.2 | Effect of Substitution | 183 |
| 5.3.3 | Investigating Full-NHC Ligand Systems..... | 188 |
| 5.4 | Conclusion | 193 |
| Conclusion | | 196 |
| Future Work | | 201 |
| 6.1.1. | Difluorovinyl Precursors | 201 |
| 6.1.2. | Functionalisation of Rearrangement Products..... | 202 |
| 6.1.3. | Improved Syntheses of Difluorocyclopropyl Alcohols..... | 203 |
| 6.1.4. | Further Utilisation of Computational Triage | 204 |
| 6.1.5. | Building Block Route to Fluorinated Furans | 204 |
| 6.1.6. | Ni-mediated Rearrangements | 207 |
| Chapter 7: Experimental | | 209 |
| 7.1. | General Experimental..... | 209 |
| 7.2. | Computational Methodology | 212 |
| 7.3. | Compounds from Chapter 1 | 214 |
| 7.4. | Compounds from Chapter 2 | 218 |
| 7.5. | Compounds from Chapter 3 | 240 |
| 7.6. | Compounds from Chapter 4..... | 278 |
| Appendix | | 281 |
| References..... | | 316 |

Introduction

Fluorinated compounds continue to enhance our day-to-day lives, with the fluorine atom found in a wealth of everyday materials¹ and in at least 20% of pharmaceuticals and 30% of agrochemicals.²

The high electronegativity of the fluorine atom modifies many chemical and physical properties; these include altering the dipole moment of a molecule and dramatically affecting the acidity and basicity of nearby groups. The steric difference between fluorine and hydrogen is minimal and switching atoms has shown to have little impact when fluorinated ligands bind to enzyme receptor sites.³ Fluorine atoms are also present in bioisosteres for a range of functional groups, which can be beneficial in drug molecule design by altering metabolic stability, modulating lipophilicity and increasing bioavailability (**Figure 1**).⁴

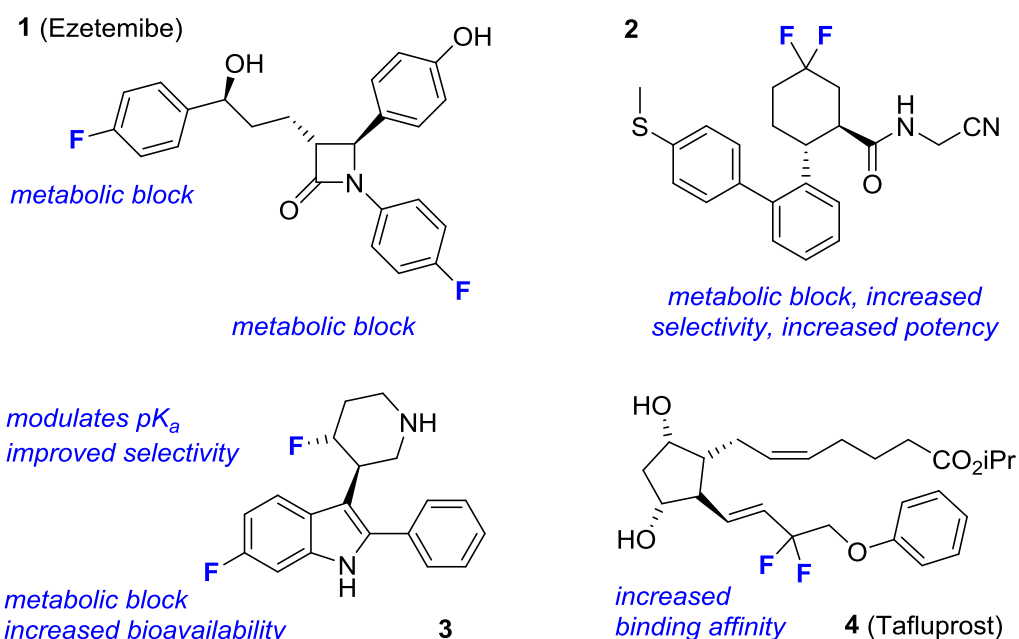


Figure 1: Drugs which have more desirable properties due to the introduction of fluorine atoms.

Cholesterol inhibitor Ezetemibe **1** uses fluorine atoms on the pendent phenyl rings to minimise oxidation by cytochrome P450 enzymes, improving metabolic stability and allowing the drug to be administered in a lower dose.⁵ Difluorocyclohexyl **2**, a potent inhibitor of cathepsin K for the treatment of diseases involving bone loss, utilises fluorine atoms in a similar manner but also benefits from increased

selectivity and potency.⁶ Antipsychotic 3-piperidinylindole **3** provides a good example of pK_a modification; the basicity of the amine was decreased by γ -fluorination, improving selectivity and reducing undesirable side effects.⁷ Talfluprost **4** is an approved drug molecule for lowering intraocular pressure and has higher potency than other species due to the favourable binding interactions between the fluorine substituents with motifs found in the receptor.⁸

The naturally abundant isotope of fluorine (¹⁹F) is also NMR active, with a spin of ½ and a large chemical shift range from +200 to -200 ppm, allowing fluorinated molecules to act as probes which can be followed in chemical and biological systems,⁹ as well as aiding in fragment based drug screens.¹⁰

Despite this focus on biologically-active molecules, there are many examples of the beneficial role fluorine atoms have across the chemical sciences¹¹ and methods for synthesising novel organofluorine compounds have become essential tools in the chemical industry.

1.1. Methods of Fluorination

The unique electronic properties of the fluorine atom makes fluorination less than trivial and accounts for the low incidence of fluorine atoms present in natural products.¹² In the laboratory, a wide range of fluorinating reagents have been developed, and many are now commercially available (**Figure 2**).¹³ Diethylaminosulfur trifluoride (DAST) was the classic nucleophilic fluorinating reagent, typically used for the fluorodeoxygenation of alcohols with inversion of stereocentres but the reagent is unstable at temperatures above 90 °C.^{13b} Deoxo-Fluor™ solved this issue by introducing ether oxygen atoms which can coordinate to the sulphur and stabilise the reagent.¹⁴ Fluolead™ has been developed as a crystalline solid with high thermal stability (decomposition at 150 °C) and has been utilised in the deoxyfluorination of alcohols, difluorination of ketones and the trifluorination of acids (**Figure 2a**).¹⁵ More recently, Doyle and co-workers reported the low-cost synthesis of thermally stable PyFluor which effectively carried out the deoxyfluorination of a broad range of alcohols in the presence of base;

proof of concept was also secured for the ^{18}F radiolabelling of a benzyl protected sugar.¹⁶

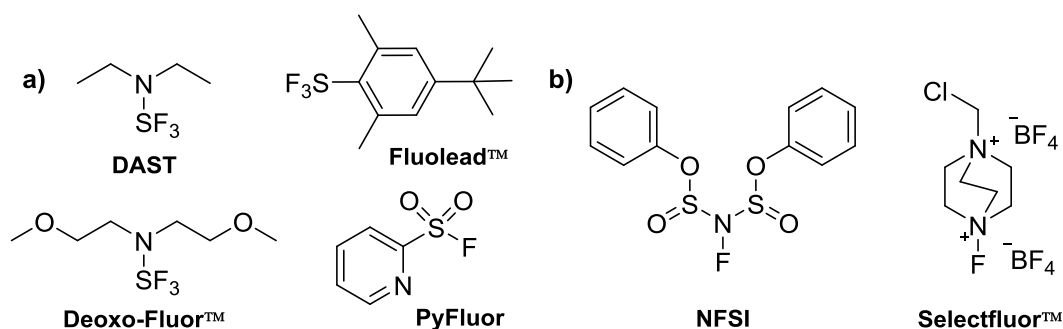


Figure 2: Common commercially available a) nucleophilic and b) electrophilic fluorinating reagents.

Alternatively, carbon-centred nucleophiles can be fluorinated using electrophilic reagents (**Figure 2b**). Despite the requirement for specialised equipment to handle elemental fluorine, the gas provides the most atom efficient electrophilic source of fluorine atoms and has been utilised successfully in the replacement of hydrogen in aliphatic, carbonyl and (hetero)aromatic compounds.¹⁷ *N*-fluorobenzenesulfonimide (NFSI) and Selectfluor are examples of more practical, commercially-available reagents which can carry out the same electrophilic fluorination reactions, as well as facilitating transition metal mediated aryl fluorinations.¹⁸

1.2. Building Block Approach

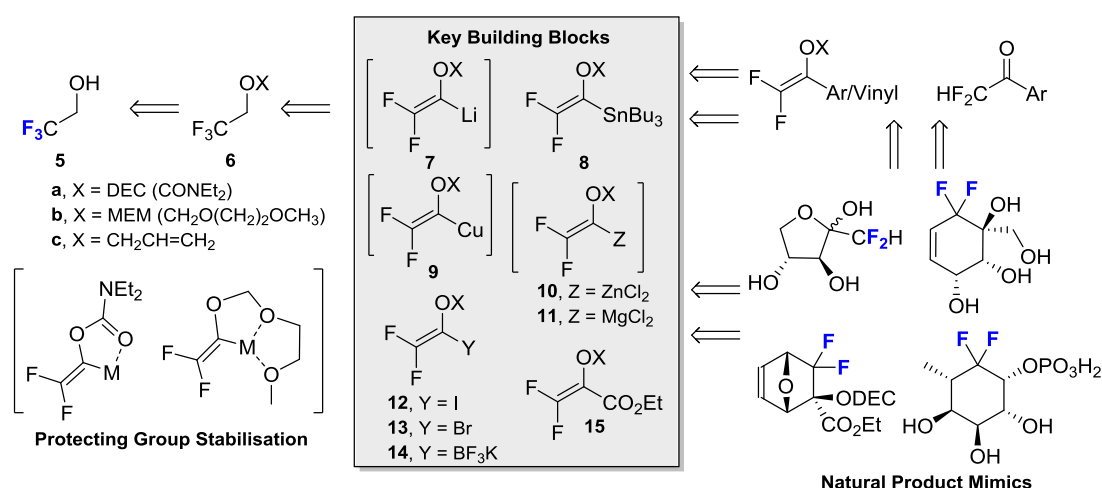
An alternative method is the building block approach which introduces fluorine into the synthesis at an early stage, typically from commercially available fluorinated compounds.¹⁹ Deploying fluorinated building blocks avoids the use of hazardous fluorinating reagents whilst also utilising the atom's electronic properties to aid in the synthesis of more complex molecules.

1.2.1. 2,2,2-Trifluoroethanol

Trifluoroethanol (**5**) is better known as a solvent used to speed up homogenous catalytic reactions, typically oxidations, without the need for other reagents or metal catalysts.²⁰ It is also an extremely attractive building block for the synthesis of complex difluorinated compounds due to it being commercially available in

industrial quantities and inexpensive (Fluorochem, 2.5 kg = £89, < £4 mol⁻¹). Two synthetic steps, protection then dehydrofluorination/metalation, provides valuable reactive intermediates which can be utilised in the synthesis of difluoromethyl ketones²¹ and substituted *gem*-fluoroalkenes (**Scheme 1**). Fluorinated mimics of carbohydrate analogues,²² difluorinated cyclohexene polyols,²³ and carbasugar phosphates²⁴ can be synthesised, creating bioisosteres for probing the biological role of the corresponding naturally occurring compounds.

Protection of alcohol **5** with base-stable (methoxy)ethoxymethyl ether (MEM) or diethyl carbamate (DEC) groups is key to providing stability for the reactive vinyl lithium species; chelation of the lithium by oxygen atoms helps to slow down the elimination of fluoride ion. Lithium species **7** can be trapped out effectively with electrophiles including halides in order to access difluorovinyl iodide **12** or bromide **13**.²⁵ Iodide **12**, successfully undergoes Suzuki-Miyaura cross coupling reactions to give access to valuable difluorovinyl aryl compounds.²⁶

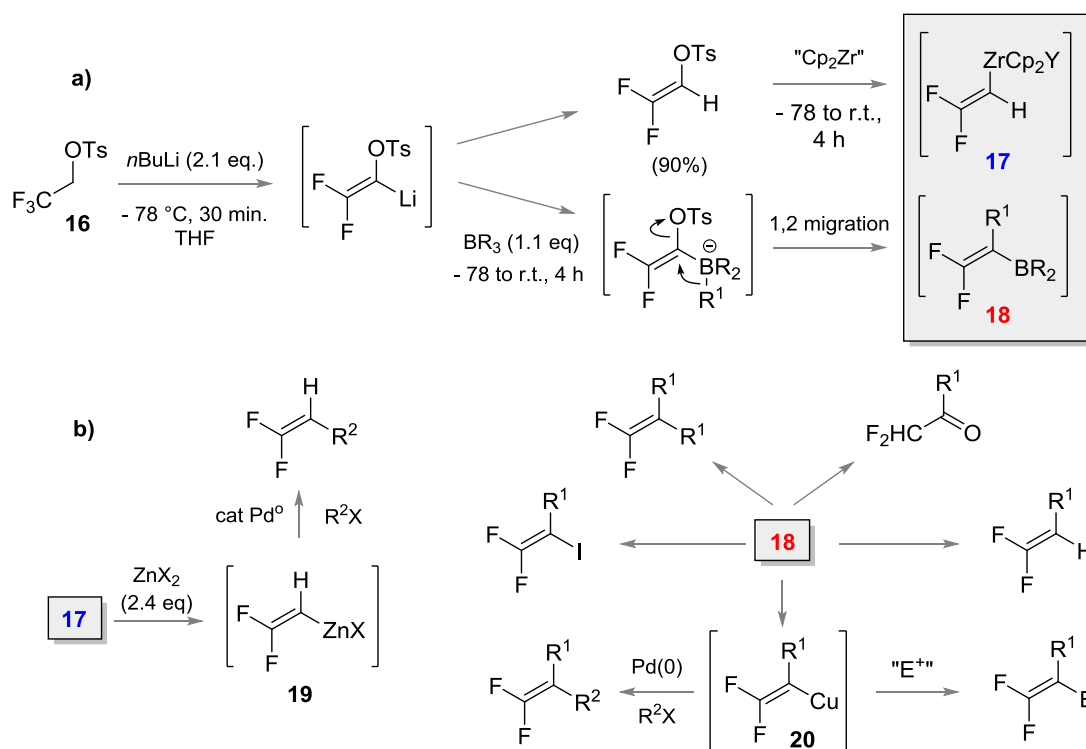


Scheme 1: Synthesis of complex sugar like compounds from reactive intermediates derived from 2,2,2-trifluoroethanol.

Transmetalation of **7** to the corresponding stannane **8** resulted in a storable species which readily underwent Stille cross coupling chemistry.^{21,27} Specifically, palladium-catalysed cross-coupling of **8** with ethyl chloroformate afforded alkenoate **15**, a reactive dienophile for the cycloaddition with furan.²⁸ Converting stannane **8** to the corresponding vinylcopper species **9**, increased the scope of the chemistry allowing reactions with haloalkanes and acid chlorides.²⁹ The undesirable cryogenic

temperatures required for handling difluorovinyl lithium **7** could be avoided by transmetallation to the corresponding zinc **10** and magnesium **11** reagents, allowing Negishi-based cross couplings and reactions with electrophiles to be conducted at near ambient temperatures, respectively.³⁰

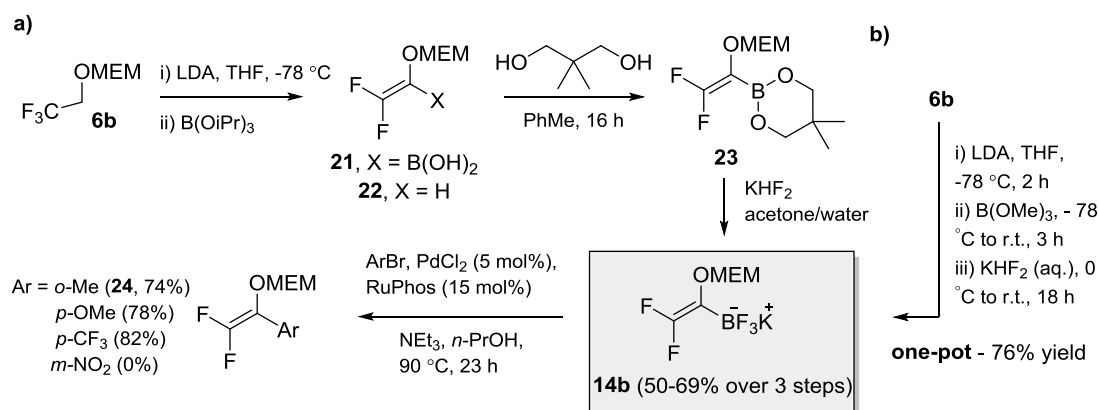
Ichikawa has used trifluoroethyl tosylate **16** in sequences which involve nucleophilic then electrophilic substitution on the vinyl carbon adjacent to the difluorinated carbon (**Scheme 2a**).³¹ Dehydrofluorination/metallation occurs with lithium bases, then trialkylboranes were used in the transmetallation step. Alkylation results via migration of an alkyl group from boron to carbon in the borate complex, with concerted loss of tosylate. The resulting borane **18** was thermally stable and underwent protonolysis to monosubstituted alkenes, oxidation to ketones, iodination and *bis*-alkylation. Cross coupling chemistry is also possible from the vinylcopper species **20**, and Negishi coupling with zinc reagent **19** (**Scheme 2b**).



Scheme 2: a) Synthesis of difluorovinyl building blocks **17** and **18** from tosyl protected trifluoroethanol **16**. b) Synthetic elaboration of **19** and **20** (Ts = *p*-toluenesulfonyl).

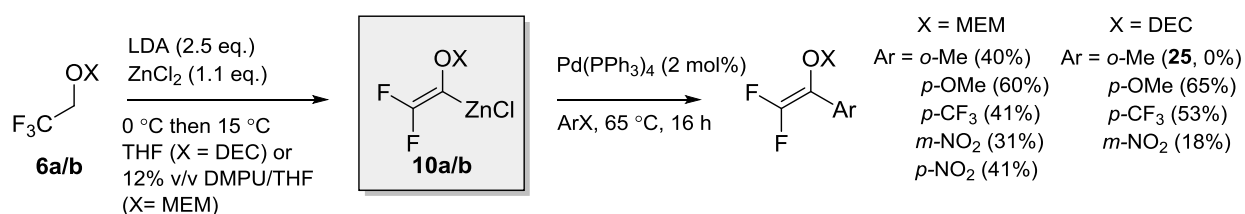
Katz *et al.*³² first reported the synthesis of stable potassium trifluoroborate salt **14b** using a modified Percy synthesis (**Scheme 3a**). Initial dehalogenation chemistry

remained the same, but the organolithium was trapped using tri-*isopropyl* borate to afford boronic acid **21** and enol ether **22**. Esterification to boronic ester **23** was necessary due to the poor stability of the boronic acid; **23** also showed signs of decomposing under coupling conditions. Conventional conversion to potassium trifluoroborate salt **14b** using KHF_2 provided a more stable coupling partner and Suzuki-Miyaura cross coupling chemistry was successful with aryl bromides. However, poor functional group tolerance was observed when ketones were present, and when the aryl bromide was based on a thiophene or was nitro-substituted. A more efficient, one-pot synthesis of **14b** from MEM-protected trifluoroethanol **6b** which avoids isolation of unstable boronic acid derivatives whilst improving isolated yields has now been developed within the group (**Scheme 3b**).³³



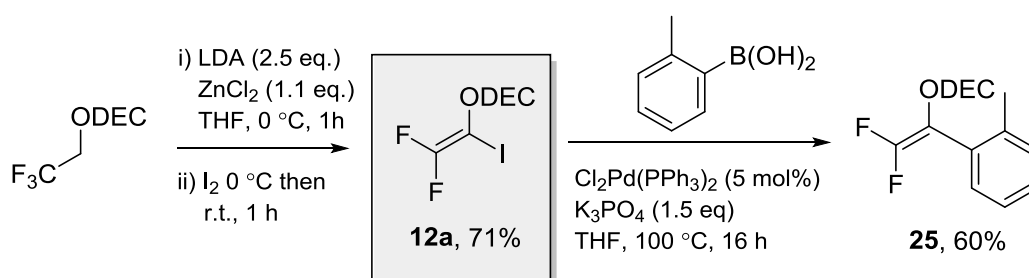
Scheme 3: a) Literature synthesis and coupling of potassium trifluoroborate salt (14b**). b) One pot synthesis of **14b** from **6b**.**

Vinylzinc chloride **10**, another nucleophilic cross coupling reagent, can be generated using ice bath temperatures from protected trifluoroethanol **6**, and reacted directly in one-pot under Negishi-conditions (**Scheme 4**).^{30a} Generally higher isolated yields were observed from **6b** compared to Katz's conditions (*c.a.* *m*-NO₂ compound) but Stille coupling with stannane **8b** gave better yields for more electron deficient aryl bromides (*c.a.* *p*-NO₂, 61%, $\text{X} = \text{MEM}$). The Negishi chemistry reached its limits when *ortho*-substituted aryl bromides (see product **25**, Ar = *o*-Me) were used, with steric factors being held responsible for slowing down transmetalation and reducing the yield.³⁴



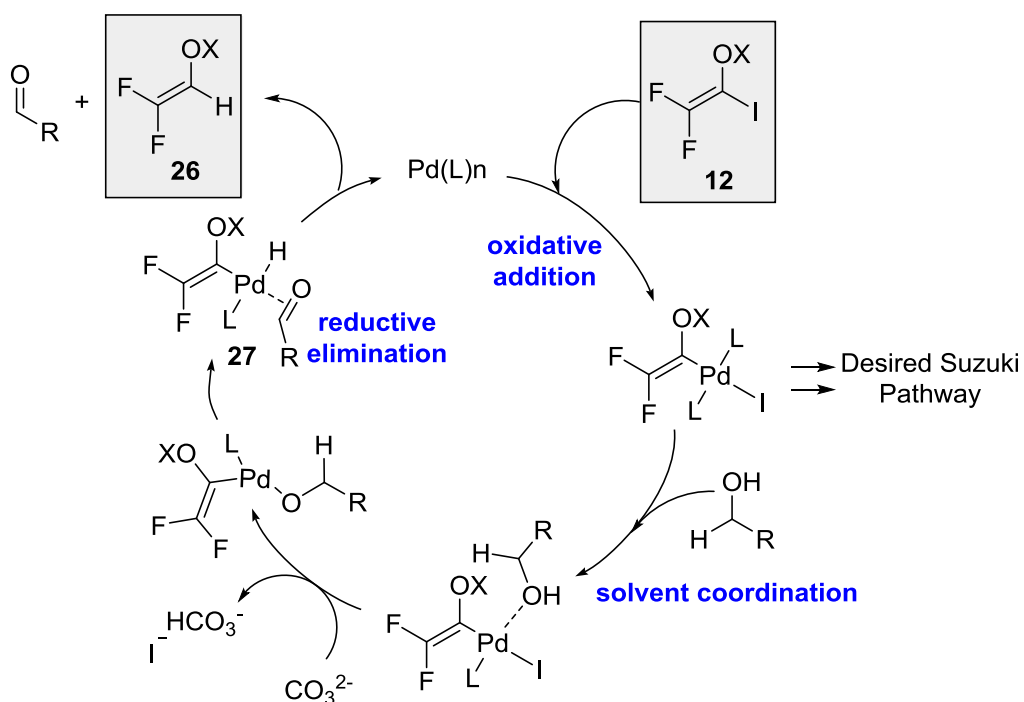
Scheme 4: Ice bath synthesis of zinc chloride 10 followed by Pd(0) catalysed Negishi coupling with aryl halides (DMPU = N,N'-Dimethyl-N,N'-trimethyleneurea).^{30a}

Zinc species **10a** can be quenched with elemental iodine to afford iodide **12a** at near ambient temperature (**Scheme 5**). This allowed the nucleophilic and electrophilic coupling species to be switched, affording a greatly improved yield of 60% for *ortho*-tolyl species **25**.



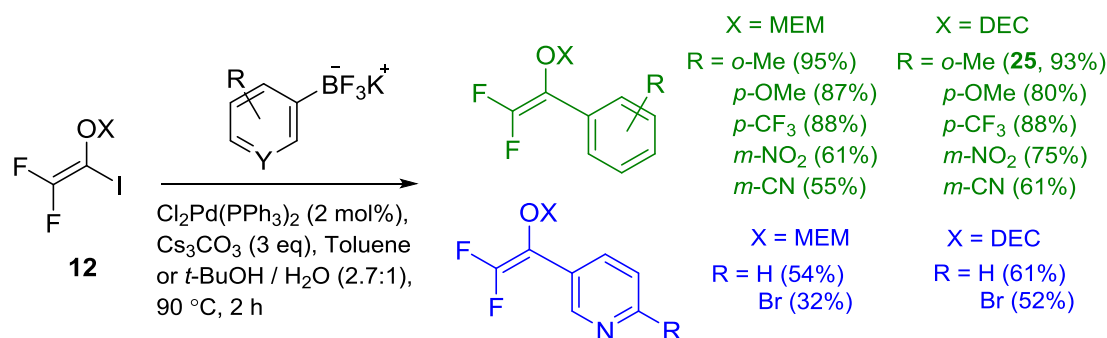
Scheme 5: Improved synthesis of 25 via difluorovinyl iodide 12a.²⁶

The major side product observed during either type of coupling from either building block was enol carbamate/ether **26**. Solvent change was key to decreasing the formation of **26**; non-coordinating toluene or the more polar *t*-BuOH (used for insoluble reagents) both stopped the unwanted side reaction. It was proposed that alcohol solvents can complex to palladium; β -hydride elimination affords palladium intermediate **27** which undergoes reductive elimination to side product **26** (**Scheme 6**). Despite still being able to coordinate to palladium, *t*-BuOH lacks the protons required for the β -hydride elimination step and suppresses formation of **26**.



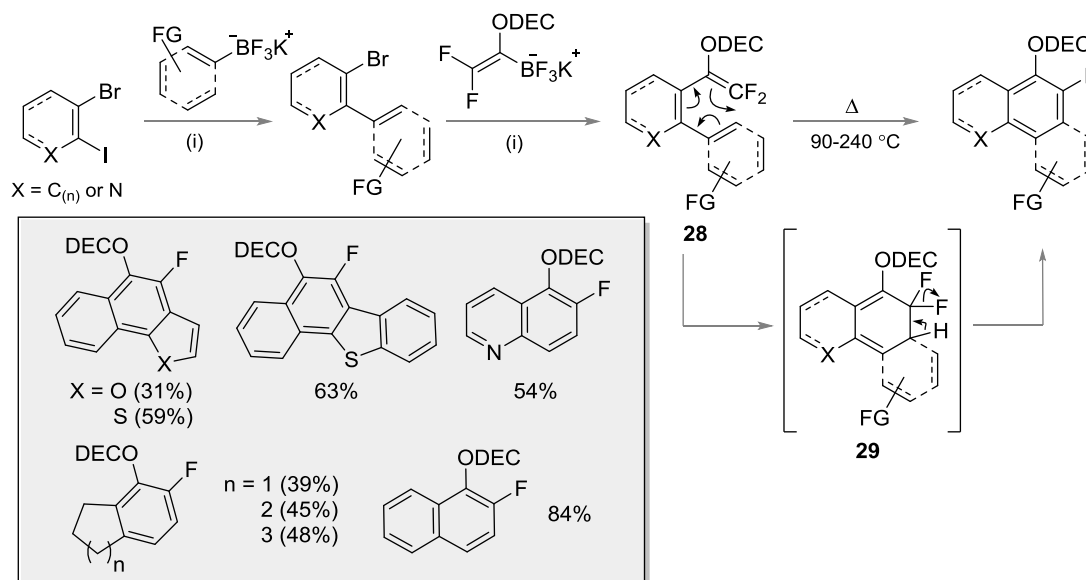
Scheme 6: Proposed catalytic cycle for formation of enol carbamate/ether **26** (X = DEC or MEM).

Yields were greatly improved from previous Negishi or Suzuki procedures when more stable aryl potassium trifluoroborate salts were coupled with iodide **12a/b**. Notably, an excellent yield for *ortho*-tolyl species **25** was obtained (93%), along with an increased tolerance for heteroaromatic systems (**Scheme 7**). Unfortunately, due to isolation issues from side products and unreacted starting materials, the limitation of this chemistry was reached with vinyl borates. To date, couplings of alkynyl borates have been poor and alkyl borates have failed completely under these conditions.



Scheme 7: Improved coupling yields using iodide 12a/b and aromatic potassium trifluoroborate salts.²⁶

These studies developed our knowledge of the scope and limitations of a range of difluorovinyl-based cross-coupling reagents, which was essential for the development of array-based synthesis of difluorinated electrocyclisation precursors (**Scheme 8**).



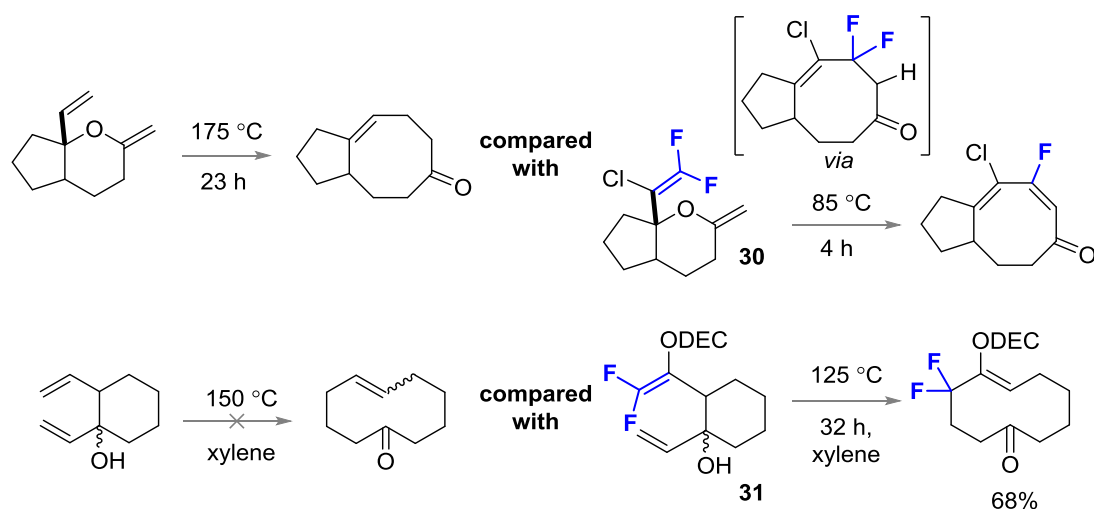
Scheme 8: Three step route to mono-fluorinated substituted aromatic compounds.

Conditions: (i) $\text{Cl}_2\text{Pd}(\text{PPh}_3)_2$ (2 mol%), Cs_2CO_3 (3 eq.), *t*-BuOH/ H_2O (2.7:1), 90 °C, overnight).

Suzuki-Miyaura mediated (hetero)aromatic-aromatic and vinyl-aromatic bond formations allowed direct access to difluorovinyl species **28**. A varied temperature range was required to initiate electrocyclisation (90-240 °C) in order to disrupt either none, one or two aromatic systems. However, the transformation from a sp^2 to a more stable sp^3 difluorinated carbon in intermediate **29**, lowers the activation energy for the cyclisation compared to the non-fluorinated systems. The

electrocyclisation is further driven by rearomatisation and HF elimination to afford a range of *mono*-fluorinated aromatic compounds in moderate to high yields (31-84%).

Further rate enhancements were observed when difluorovinyl species **30** and **31** underwent Claisen³⁵ and oxy-Cope³⁶ rearrangements, respectively (**Scheme 9**). The dramatic temperature difference observed from the corresponding non-fluorinated compounds was again attributed to the destabilisation effect of the CF₂ centre on *sp*²-hybridised alkenes.³⁷



Scheme 9: Beneficial effect of difluorovinyl unit on rearrangement reactions.

The group has developed a wide range of building blocks derived from 2,2,2-trifluoroethanol allowing the formation of complex natural product mimics as well as fluorinated aromatic systems. The introduction of fluorine atoms at the early stage of the synthesis is beneficial, playing a key role in facilitating rearrangement chemistry used in the development of the majority of these products.

1.2.2. Difluorocarbene

The difluorocarbene building block is used frequently in organofluorine chemistry. Carbenes are transient or reactive intermediates within organic chemistry but the isolation of stable metal complexes³⁸ and *N*-heterocyclic carbenes³⁹ has greatly expanded their reaction scope.⁴⁰ Four years before the first isolation of what are now known as Fischer carbenes, Birchall *et al.* reported the trapping of difluorocarbene with cyclohexene, laying the foundations for the

difluorocyclopropanation of alkenes.⁴¹ However, the chemistry has generally been restricted to electron-rich alkenes because difluorocarbene is electrophilic. This can be understood by comparing the energy level diagrams⁴² of carbenes containing electron-deficient or electron-rich substituents and rationalised by the high electron density around the two fluorine atoms directly attached to the carbene centre, donating into the empty $2p$ -orbital of the carbon.⁴³ This donation lowers the singlet energy level in which the carbene electrons lie, stabilising the carbene (**Figure 3**).

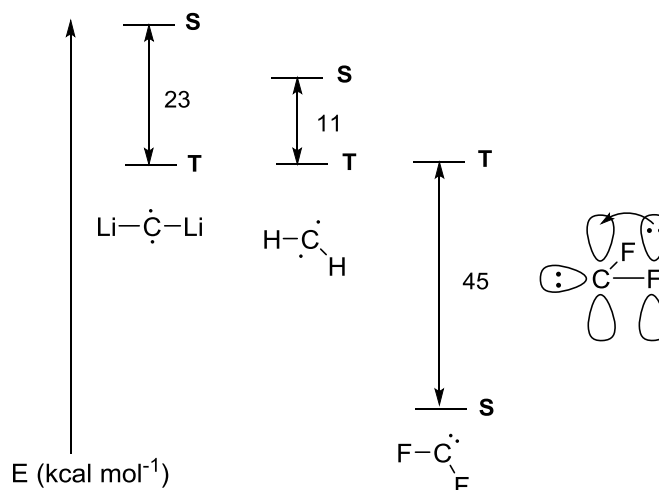
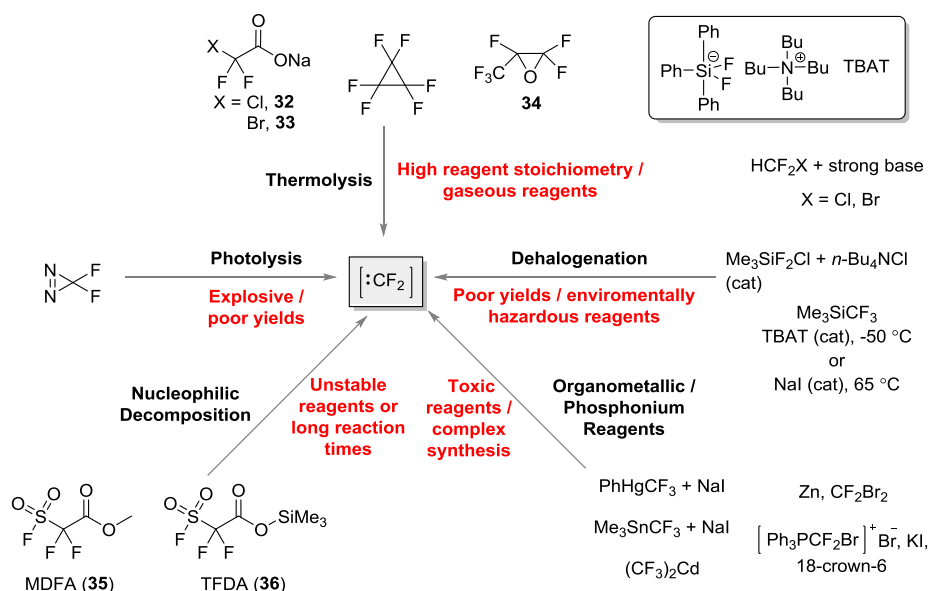


Figure 3: Singlet energy level stabilisation observed for difluorocarbene (S = singlet and T = triplet).

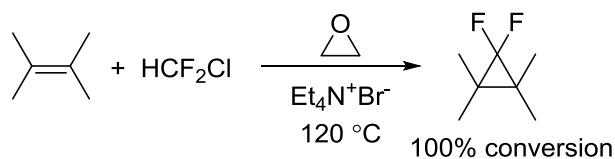
After Birchall's initial discovery, a wide variety of reagents were developed for the generation of difluorocarbene, and these have been reviewed extensively.⁴³⁻⁴⁴ A selection of reagents is discussed within, focusing on benefits and problems associated with each (**Scheme 10**). A comparison of reactivities between dimethylbutene and the slightly less nucleophilic cyclohexene is used to determine the limits of these difluorocarbene reagents (**Table 1**).



Scheme 10: Selected difluorocarbene generating reagents (TBAT = tetrabutylammonium triphenyldifluorosilicate).

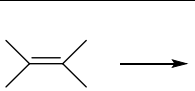
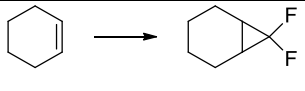
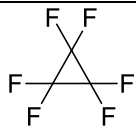

The pyrolysis of perfluorocyclopropane releases difluorocarbene at temperatures greater than 165 °C⁴⁵ and has been shown to difluorocyclopropanate cyclohexene in 67% yield (**Table 1**, Entry 1).⁴⁶ Hexafluoropropylene oxide **34** is another useful source of difluorocarbene⁴⁷ since it is commercially available, and forms volatile by-products which are easily removed from the reaction. However, neither reagent has ever been considered as a very practical source of difluorocarbene because of the need to use autoclave techniques.

Dehydrohalogenation⁴⁸ of chloro- or bromodifluoromethane under basic conditions generates difluorocarbene, but trapping with alkenes is impaired by competitive addition of the base to the carbene (**Table 1**, Entry 2).⁴⁹ Using conditions which limit the concentration of base (**Scheme 11**)⁵⁰ allows nucleophilic alkenes to be trapped in excellent yields; electron-deficient alkenes react in much lower yields (**Table 1**, Entry 3). Despite the good yields, the use of environmentally hazardous haloforms as reagents, or to synthesise reagents, is a major disadvantage.



Scheme 11: Base controlled dehydrohalogenation of chlorodifluoromethane.⁵⁰

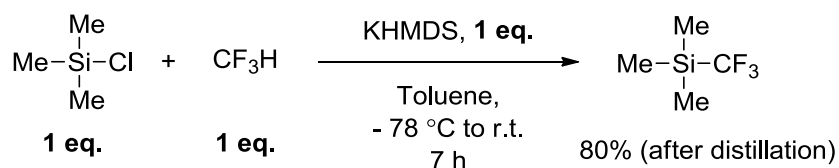
Table 1: Reactivity Comparison of Difluorocarbene Generating Reagents with Electrophilic and Nucleophilic Alkenes

| Entry | Difluorocarbene Reagent |  |  |
|-------|---|---|---|
| 1 |  | - | 67% |
| 2 | CHClF ₂ , NaOH | 6% | - |
| 3 | CHClF ₂ , Et ₃ N ⁺ Br ⁻ ,  | 100% | 29% |
| 4 | Me ₃ SiCF ₂ Cl + Cl ⁻ (cat) | 86% conversion | - |
| 5 | Me ₃ SiCF ₃ + NaI | 82% conversion | 83% conversion |
| 6 | CF ₂ Br ₂ , Zn | 96% | 7% |
| 7 | 2 eq. [Ph ₃ P ⁺ CF ₂ Br]Br ⁻ , KF | 74% | 21% |
| 8 | 2 eq. [Ph ₃ P ⁺ CF ₂ Br]Br ⁻ , KF 18-crown-6 | - | 70% |
| 9 | (CF ₃) ₂ Cd | - | 95% conversion |
| 10 | PhHgCF ₃ + NaI | - | 88% |
| 11 | Me ₃ SnCF ₃ + NaI | 77% | 89% |

All yields are isolated unless otherwise stated. References can be found within the text where each of the reagents is discussed.

In 2011, Wang and co-workers reported the difluorocyclopropanation of alkenes and alkynes using a chloride-catalysed decomposition of (chlorodifluoromethyl)trimethylsilane.⁵¹ Again, only reactions with electron-rich alkenes were high yielding (**Table 1**, Entry 4) and, despite the reagent itself being non-toxic, the synthesis from haloforms is environmentally unfriendly.⁵² Hu and Prakash⁵³ have recently reported that non-metallic fluoride sources can initiate the decomposition of commercially-available TMSCF₃ (Ruppert-Prakash reagent) at low temperatures (-50 °C) but NaI and higher temperatures (65 °C) are required for the difluorocyclopropanation of more electron-deficient alkenes (**Table 1**, Entry 5). Due to its use as a trifluoromethylating reagent,⁵⁴ the Ruppert-Prakash reagent was previously synthesised from CF₃Br gas which is strictly controlled under environmental protocols. However, Prakash and co-workers reported a more environmentally friendly synthesis from trimethylsilyl chloride (TMSCl) and fluoroform (**Scheme 12**).⁵⁵ Fluoroform is also an ozone-depleting gas, but it is formed in high concentrations in the production of Teflon, polyvinylidene fluoride,

fire-extinguishing agents, refrigerants and foams.⁵⁵ Its transformation to useful products is well established.

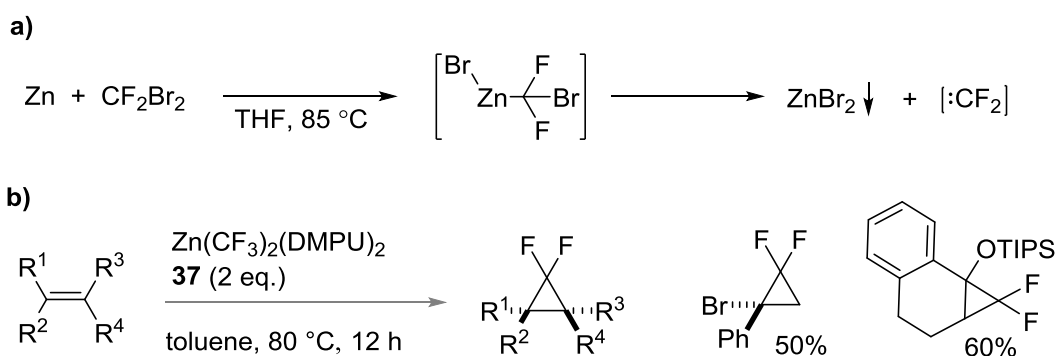


Scheme 12: More environmentally friendly synthesis of Ruppert-Prakash reagent (KHMDS = potassium hexamethyldisilazane).

Newly-developed reagents (TMSCF₃ and Me₃SiCF₂Cl) for difluorocarbene generation have shown that high temperatures are not always required for electron-rich alkenes but are generally needed to overcome the high activation barrier when trapping less nucleophilic alkenes.

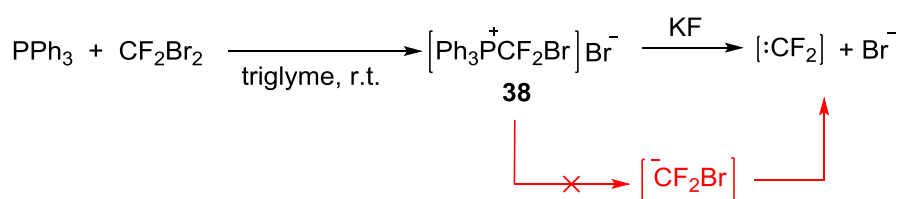
A notable rate difference of difluorocarbene addition to *cis*-but-2-ene was also observed when different temperatures were used for the decomposition of difluorodiazirine. Photolytic decomposition at room temperature gave modest yields (26%) but these were greatly improved when thermal decomposition was used instead (180 °C, 83%).⁵⁶ However, these yields are still poor compared to other less explosive reagents.

Other mild sources of difluorocarbene are derived from the trapping of haloform CF₂Br₂ with either Zn⁵⁷ or triphenylphosphine.⁵⁸ Dolbier's work with zinc suggested metal-halogen insertion occurred, resulting in free difluorocarbene (**Scheme 13a**), but yields are only high for nucleophilic alkenes (**Table 1**, Entry 6). More recently, Mikami and co-workers reported that isolable Zn(CF₃)₂(DMPU)₂ **37** successfully underwent thermal decomposition to generate difluorocarbene; successful trapping with a simple set of alkenes resulted in good to moderate NMR yields of the corresponding difluorocyclopropane (**Scheme 13b**).⁵⁹



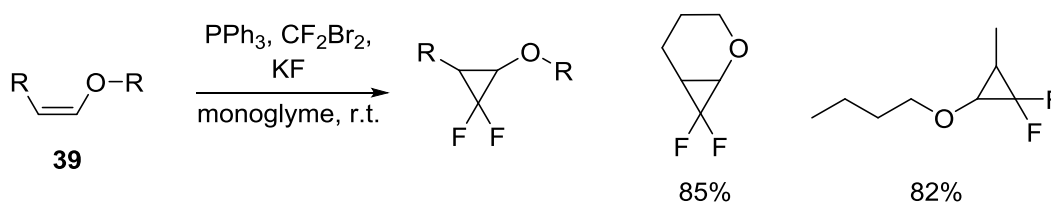
Scheme 13: a) Difluorocarbene formation from Zn insertion into haloform b) Difluorocarbene generation from **37** and successful trapping reaction with alkenes (NMR yields, TIPS = trisopropylsilane).⁵⁹

Burton and Nae^{58b} made the first report of difluorocarbene generation from phosphonium salt **38**, but trapping of the carbene with electrophilic alkenes was inefficient (**Table 1**, Entry 7). These salts can be formed *in situ* from phosphine and haloforms in the presence of a fluoride source. The formation of a strong P-F bond (117 kcal/mol)^{58b} facilitates decomposition and hydrolysis studies of the salts suggest that difluorocarbene forms without the need for a difluorobromomethyl anionic intermediate (**Scheme 14**).⁶⁰



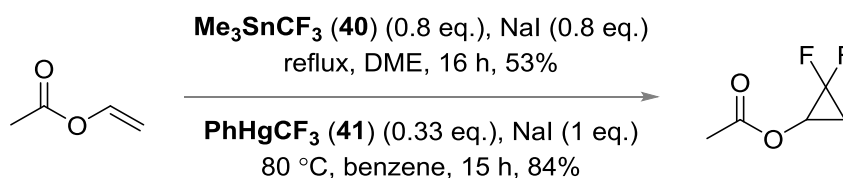
Scheme 14: Proposed decomposition of phosphonium salt **38** to difluorocyclopropane.

Bessard *et al.* improved the trapping yields for electrophilic alkenes (**Table 1**, Entry 8) by using 18-crown-6 ether to solvate the potassium, increasing fluoride concentration in solution and aiding the decomposition of the phosphonium salt.^{58a} Interestingly, electron-rich enol ethers **39** were difluorocyclopropanated in high yields, making the phosphonium reagent a very useful room temperature difluorocarbene source for more sensitive electrophiles (**Scheme 15**). Unfortunately, the use of toxic crown ethers and haloforms makes the reagent a poor choice in the current industrial climate.



Scheme 15: High yielding difluorocyclopropanation of enol ethers.^{58a}

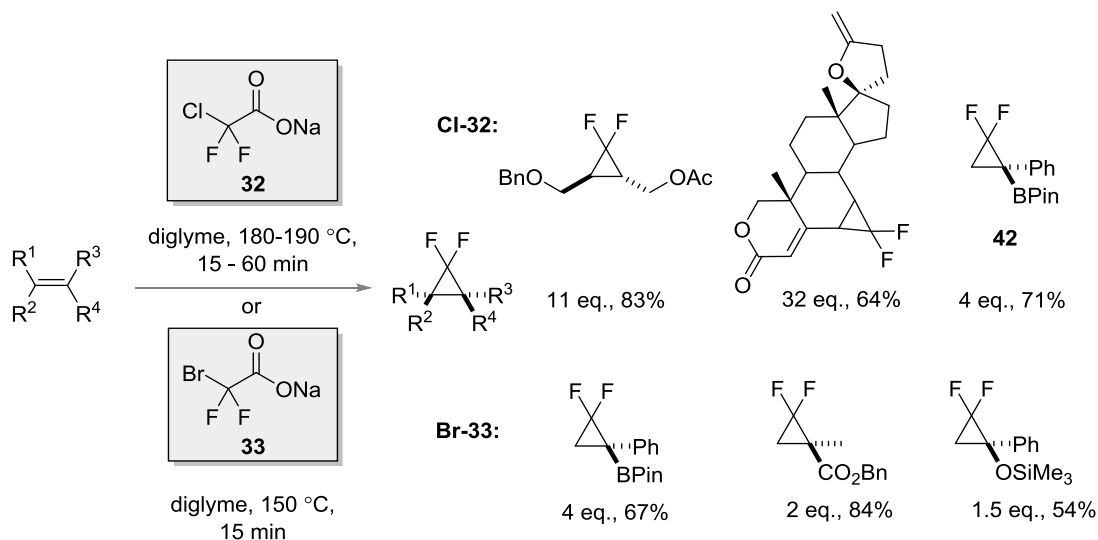
Difluorocarbene is also available from organometallic reagents; the most well-known precursor is Eujen and Hoge's bis(trifluoromethyl) cadmium reagent⁶¹ and Seyferth's trifluoromethyl(phenyl) mercury⁶² and trifluoromethyl(trimethyl) tin reagents.⁶³ While all showed promising reactivity, their major disadvantage is the high toxicity of the organometals and metals themselves. The cadmium reagent shows unprecedented reactivity at -5 °C (**Table 1**, Entry 9) but is known to be explosive when warmed to room temperature. Synthesis of the organotin reagent **40** is not trivial from commercially available compounds and it is unstable to atmospheric moisture. Despite these drawbacks it still shows high reactivity (**Table 1**, Entry 10), most notably with vinyl acetate (**Scheme 16**). Seyferth reported that organomercury reagent **41** is a more robust reagent compared to **40**, showing increased reactivity (**Scheme 16** and **Table 1**, Entry 11) but the toxic effects of this heavy metal means it is rarely used today.



Scheme 16: Difluorocyclopropanation of vinyl acetate using Seyferth reagents.^{62b,63}

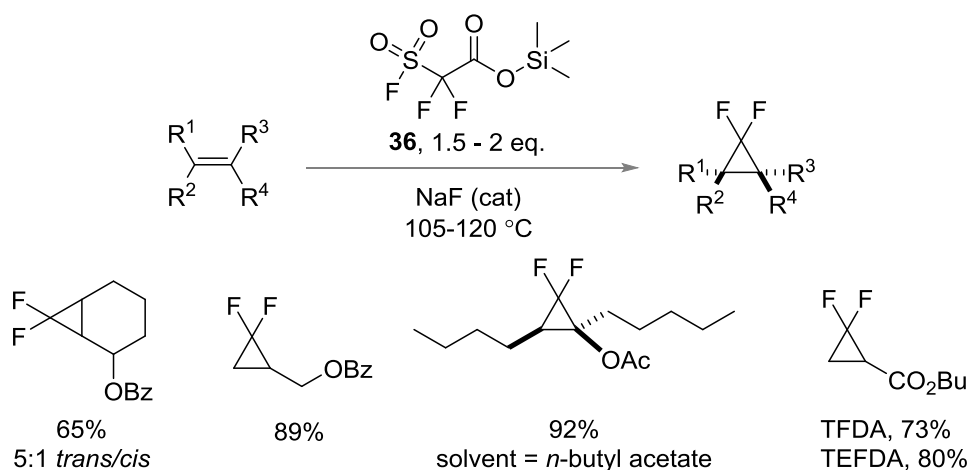
Despite the variety of competing difluorocarbene reagents, the thermolysis of sodium chlorodifluoroacetate **32** is still one of the favoured methods to date because of the ease of handling and non-toxic nature of the reagent.⁶⁴ High reactivity can be achieved with electron-rich alkenes but at the expense of excess reagent (generally 4-15 equivalents, **Scheme 17**). Recent work has shown that bromoacetate **33** can maintain reactivity at a lower loading of reagent⁶⁵ (**Scheme 17**). Difluorocyclopropyl pinacol borane **42** could be accessed in a comparable 70% yield using 3 equivalents of sodium chloro-acetate **32** after only 5 minutes

microwave irradiation.⁶⁶ These more energy efficient conditions developed by Sweeney and co-workers emphasise the preference for using sodium acetate based salts in industry but reactions must be run in open-vessels to avoid pressure build up from the release of CO₂.



Scheme 17: Difluorocyclopropanation of electron-deficient alkenes using sodium chloro-^{44b,67} or bromodifluoroacetate.⁶⁵

The first major progress with the trapping of highly electrophilic alkenes was only truly achieved in 2000 by Dolbier and co-workers,⁶⁸ they successfully difluorocyclopropanated *n*-butyl acrylate using trimethylsilyl fluorosulfonyldifluoroacetate (TFDA, **36**). Further work by the Gainesville group⁶⁹ has established TFDA as the most reactive difluorocarbene reagent to date (**Scheme 18**).



Scheme 18: Unprecedented reactivity of electrophilic alkenes with TFDA.⁶⁹

The highly reactive nature of the reagent is also its downfall, with poor shelf life due to its susceptibility to hydrolysis. Literature experimental procedures advise that only freshly prepared or distilled reagent be used in order to obtain high yields. Dolbier's group attempted to tackle the hydrolysis issue by adding bulkier groups onto the silicon; however hydrolysis then occurs faster at the carbonyl instead of at silicon, meaning bulkier alkylsilanes do not hydrolyse more slowly. Only the corresponding triethyl derivative (**Figure 4**) showed an improved yield for *n*-butyl acrylate but this was due to the increased purity of the isolated reagent (**Scheme 18**).

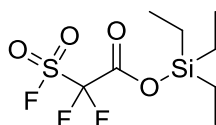
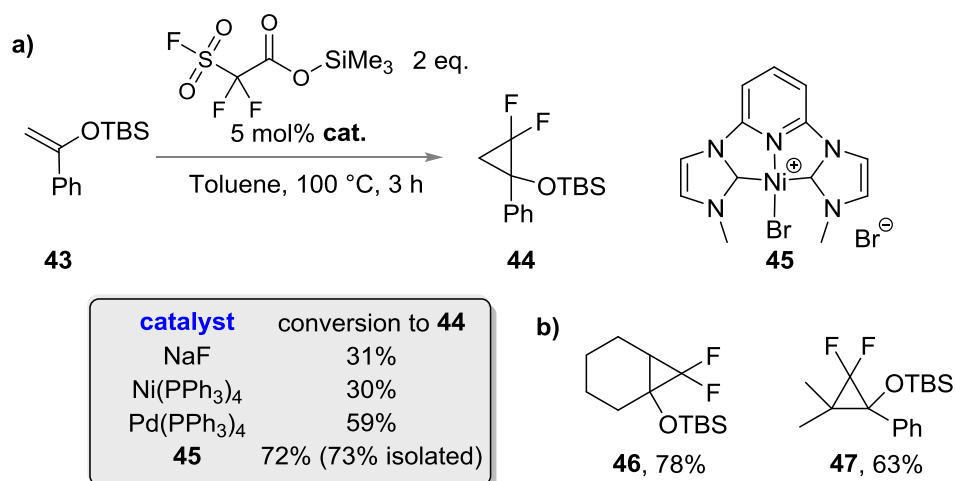


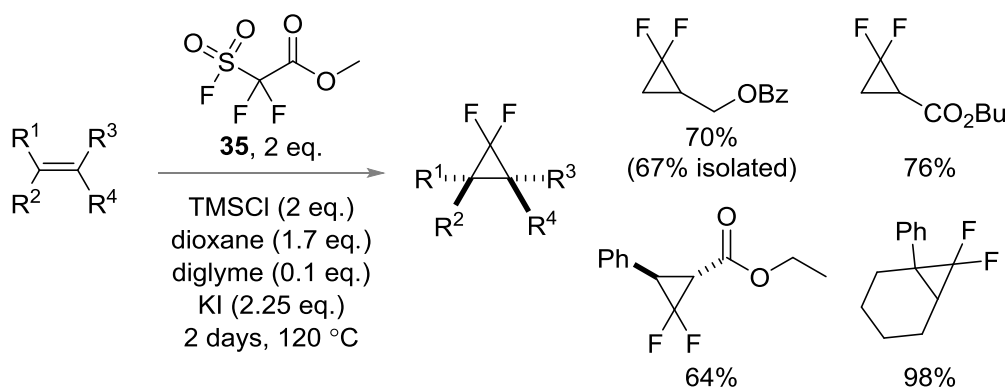
Figure 4: Triethylsilyl fluorosulfonyldifluoroacetate (TEFDA).

More recent work by Ichikawa and co-workers furthered the scope of TFDA mediated difluorocyclopropanations of silyl enol ethers.⁷⁰ Despite the full consumption of **43**, the literature conditions using catalytic quantities of NaF gave poor conversion of difluorocyclopropyl **44** (31%), presumably due to the instability of the silyl protecting group to fluoride reaction conditions (**Scheme 19a**). Use of Ni(0) and Pd(0) catalysts also facilitated the reaction, with the latter giving a higher 59% conversion. After screening other metal sources, Ni(II) pincer complex **45** gave the best conversion (72%), but the role of the transition metal in the generation of the difluorocarbene is still unclear. These modifications were also successful with silyl enol ethers **46** and **47** (**Scheme 19b**) and worked effectively in domino difluorocyclopropanations/ring-expansion sequences (*vide infra*).



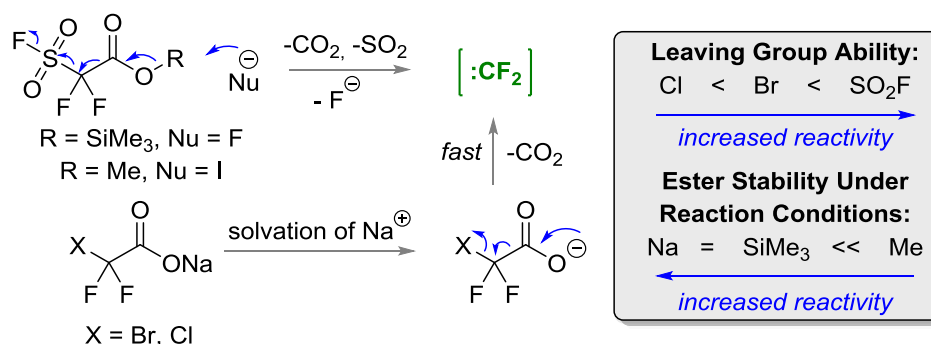
Scheme 19: a) Transition metal mediated difluorocyclopropanation of silyl enol ether 43. b) Accessible difluorocyclopropanes 46 and 47.

Reagent stability was greatly improved by replacing the silyl ester with the methyl analogue, allowing a safer alternative to TFDA to be developed. Dolbier *et al.* reported that methyl 2,2-difluoro-2-(fluorosulfonyl)acetate (MDFA, **35**) was almost as reactive as TFDA but required a longer reaction time of 2 days (**Scheme 20**).⁷¹ The prolonged course of the reaction allowed all the reagents to be mixed in one pot, instead of the slow addition rates typically required for sodium chlorodifluoroacetate and TFDA. Due to its high reactivity, cost and ease of use, MDFA has the potential to become the reagent of choice for difluorocarbene addition to a broad range of alkenes; more reactive styrene-based alkenes or oct-1-ene gave high yields and good yields were observed for the more electron deficient alkenoates.



Scheme 20: Reaction of MDFA (35) with selected alkenes (NMR yields unless otherwise stated).⁷¹

Formation of difluorocarbene from the decomposition of TFDA and MDFA relies on chemistry similar to that of the sodium halodifluoroacetate salts and is initiated by either nucleophilic attack, or by solvent coordination of the sodium cation, respectively (**Scheme 21**). Decomposition for both types of reagent is driven by elimination of carbon dioxide but Dolbier's reagents have a further entropic drive in the elimination of sulphur dioxide and fluoride; fluoride is either sequestered by an electrophile for MDFA, or initiates further decomposition with TFDA. The more controlled generation of difluorocarbene from MDFA is a result of the ester stability under reaction conditions, but at the cost of longer reaction times (*cf.* TFDA).



Scheme 21: Similarities between the generation of difluorocarbene from TFDA, MDFA and sodium halodifluoroacetates.

Despite the many advances in reagents which carry out the difluorocyclopropanation of alkenes, only a very select few are reactive with electron-deficient olefins. The recent advances by Dolbier and co-workers have allowed access to commercially available difluorocarbene generating reagents which maintain the high reactivity with electron-deficient olefins. Toxic organometallic reagents (PhHgCF_3 , $(\text{CF}_3)_2\text{Cd}$ or Me_3SnCF_3) were previously the only reagents available to react with vinyl acetates. Reagents which are likely to be used in an industrial environment (non-toxic, commercial and scalable reagents) are more desirable for method development. These reagents include sodium halodifluoroacetates, MDFA, TFDA and TMSCF_3 (**Figure 5**).

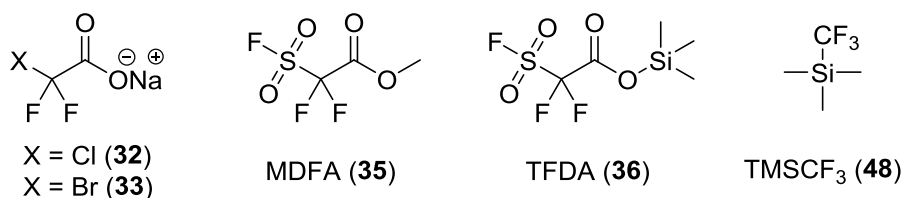
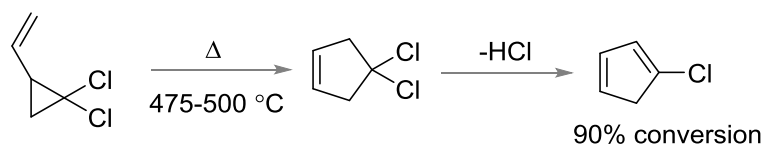


Figure 5: Difluorocarbene reagents selected for high reactivity and safety.

Just like the difluorovinyl motifs discussed previously, difluorocyclopropanes can also be used in the synthesis of more complex products by facilitating key rearrangements; the vinylcyclopropane rearrangement to cyclopentenes is a good example of one such rearrangement.

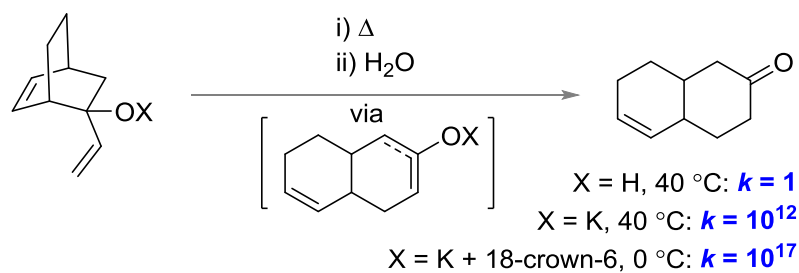
1.1. Vinylcyclopropane Rearrangements

The vinyl cyclopropane rearrangement (VCPR) is an often overlooked reaction in organic chemistry, even though it has been used in the synthesis of drug molecules and complex natural products.⁷² The reaction was first discovered in 1959 by Neureiter (**Scheme 22**), who showed that dichlorovinylcyclopropane underwent rearrangement at extremely high temperatures (475-500 °C) to dichlorocyclopentene. Loss of HCl gave a 90% conversion to chlorocyclopentadiene.⁷³ A year later, cyclopentene was synthesised from the pyrolysis of vinyl cyclopropane (**Table 2**, Entry 1)⁷⁴ and the effectiveness of the rearrangement started to become noticed.



Scheme 22: First reported VCPR reaction.

Developments over the following decades showed that heteroatoms could decrease the extremely high reaction temperatures (**Table 2**, Entries 2-3)⁷⁵, with room temperature reactions being accessible using lithium alkoxides (**Table 2**, Entry 4).⁷⁶ This increase in rate is comparable to that seen with oxy-Cope and anionic oxy-Cope rearrangements (**Scheme 23**).⁷⁷

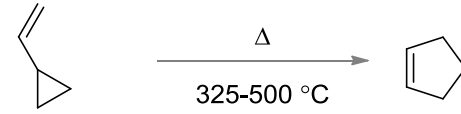
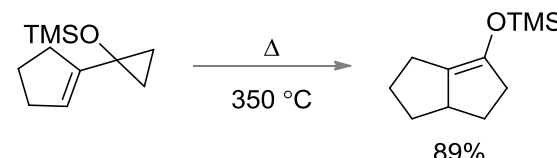
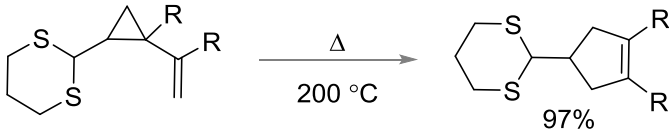
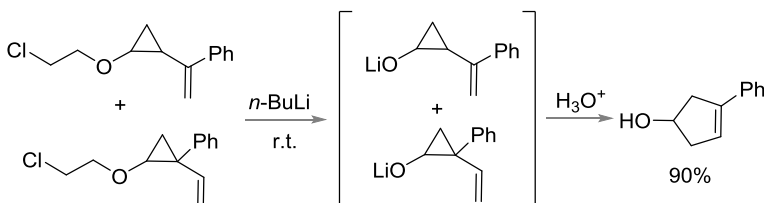
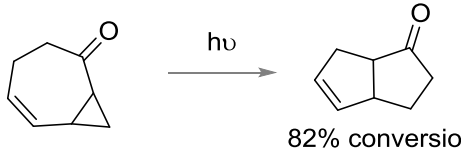
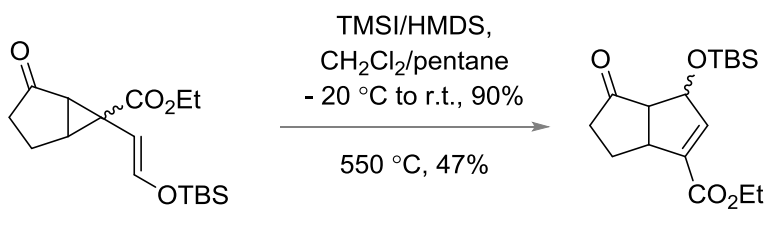
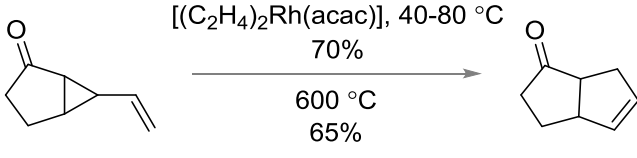


Scheme 23: Rate increase seen with anionic oxy-Cope over oxy-Cope.⁷⁷

Photolytic conditions have also been applied in the synthesis of bicyclo[3,3,0]octenone cores but polymerisation issues mean that the photochemical reactions are less efficient than pyrolysis methods (**Table 2**, Entry 5).⁷⁸ Low temperature, Lewis acid mediated conditions are sufficient to overcome the previously high barriers for rearrangement, giving increased yields compared with pyrolysis (**Table 2**, Entry 6).⁷⁹

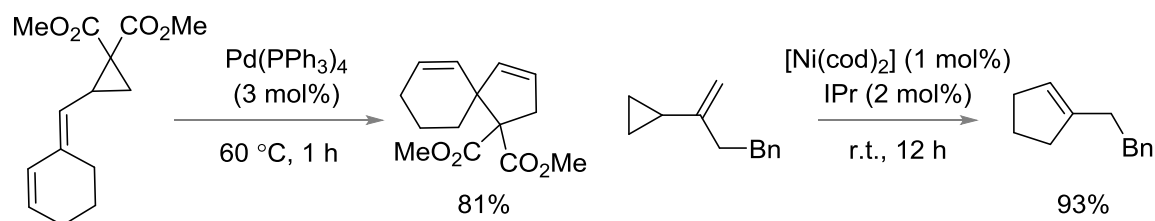
However, the biggest development came when stoichiometric amounts of a rhodium complex were found to lower the temperature of VCPR, whilst increasing yields compared with pyrolysis (**Table 2**, Entry 7).⁸⁰

Table 2: Key literature VCPR transformations.

| Entry | Reaction | Description |
|------------------|--|--|
| 1 ^[a] |  | Prototypical VCPR ⁷⁴ |
| 2 |  | Heteroatom Effects ^{75a} |
| 3 |  | Heteroatom Effects ^{75b} |
| 4 |  | Alkoxide Effects ⁷⁶ |
| 5 |  | Photolytic VCPR ⁷⁸ |
| 6 |  | Lewis Acid Effects ⁷⁹ |
| 7 |  | First Transition Metal ⁸⁰ |

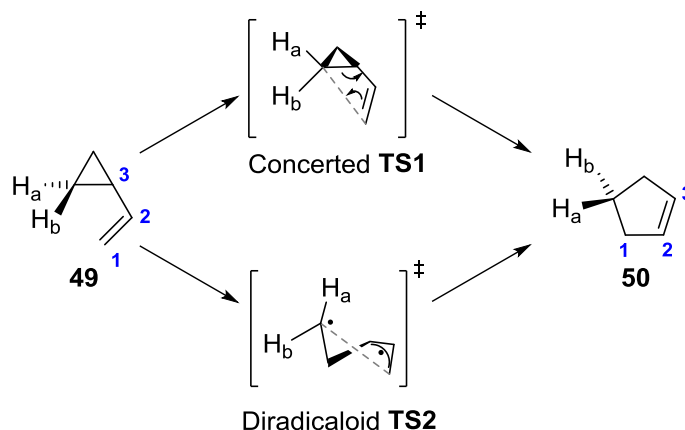
[a] No yield reported in the literature. acac = acetylacetonate, TMS = Trimethylsilane, TMSI = iodotrimethylsilane, TBS = *t*-butyldimethylsilane, HMDS = hexamethyldisiloxane.

Catalytic conditions have subsequently been developed using either Pd(0)⁸¹ or Ni(0)⁸² based catalysts (**Scheme 24**).



Scheme 24: Transition metal-catalysed VCPR.

The mechanism of the thermal VCPR has been a hotly debated subject; experimental and theoretical evidence has suggested that both concerted and diradicaloid mechanisms are feasible, depending on the nature of the precursor and initiator (**Scheme 25**).

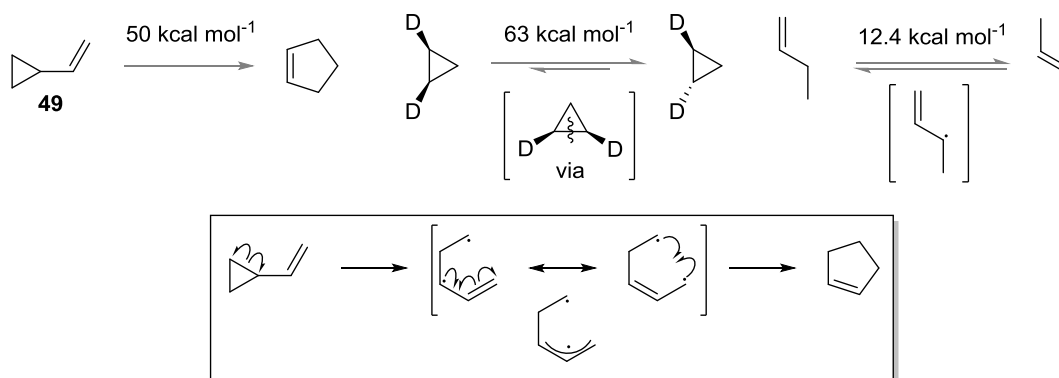


Scheme 25: Concerted (TS1) and diradicaloid (TS2) pathways connecting vinylcyclopropane 49 and cyclopentene 50.

1.3.1. Mechanism

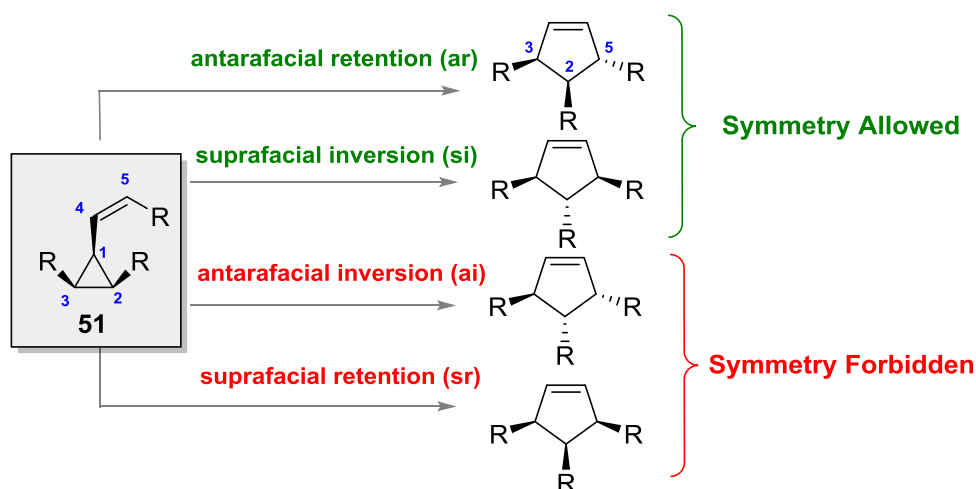
1.3.1.1. Thermolysis

Support for a diradicaloid mechanism (**Scheme 26**) came initially from kinetic evidence; the activation energy for the VCPR of **49** was reported at $50.0 \text{ kcal mol}^{-1}$ ($50.0 \pm 0.3 \text{ kcal mol}^{-1}$ by Wellington⁸³ and $51.7 \pm 0.5 \text{ kcal mol}^{-1}$ by Baldwin⁸⁴), $13.0 \text{ kcal mol}^{-1}$ less than the activation energy required to break a carbon-carbon bond in cyclopropane itself.⁸⁵ This difference is remarkably similar to the resonance stabilisation energy seen with allyl radicals (determined as $12.4 \pm 0.6 \text{ kcal mol}^{-1}$ by but-1-ene isomerisation in the presence of iodine⁸⁶).



Scheme 26: Kinetic results favouring a stepwise diradical mechanism.

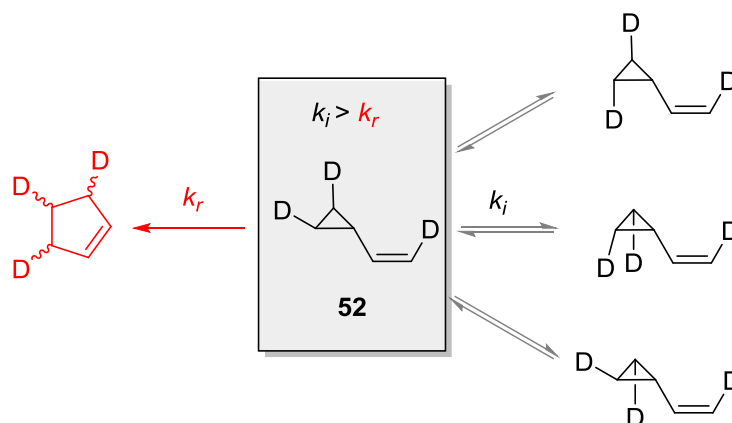
This stepwise mechanism was questioned when Woodward and Hoffman considered VCPR as a typical [1,3]-sigmatropic reaction.⁸⁷ They proposed that the symmetry-allowed concerted process would be evident in the stereochemical outcome of the vinylcyclopropane rearrangement of **51** (Scheme 27). If the percentage of product of the symmetry-allowed process outweighed the percentage of the symmetry forbidden product, then the mechanism is likely to be concerted. Definitive confirmation of the stereochemical outcome of reactions would confirm the mechanistic pathway for the rearrangement.



Scheme 27: Theoretically determined symmetry allowed products in the concerted VCPR of **51**.

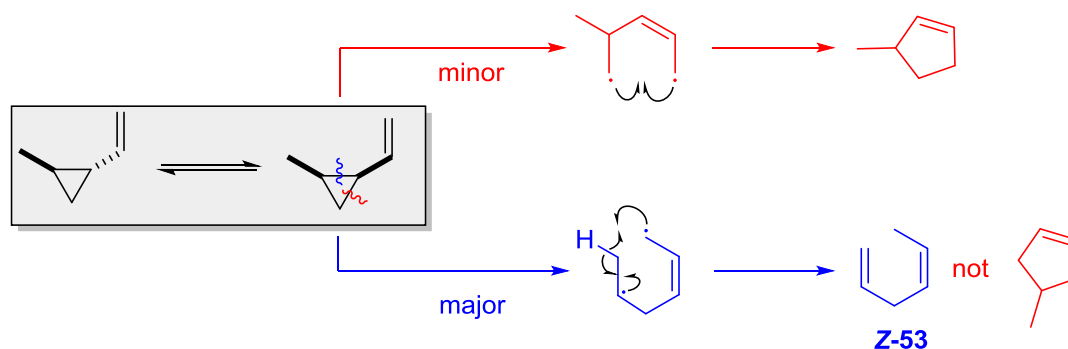
However, due to high temperatures required for the rearrangement, mechanistic proof of a concerted mechanism was hard to obtain. Stereomutation reported by Willcott and Cargle⁸⁸ showed that pyrolysis of deuterium-labelled vinyl cyclopropane **52** resulted in a lower rate of conversion to its stereoisomers than for

VCPR (**Scheme 28**). The pair believed that the stereoisomerisation can only occur via a rotatable diradical system, casting doubt over the concerted route.



Scheme 28: Preferential cyclopropane stereoisomerisation of [D3]cyclopropyl **52** over VCPR.

Another side reaction which has been reported at high temperatures involves rapid homodienyl [1,5]-hydrogen shifts.⁸⁹ The rate of isomerisation of *trans*-1-methyl-2-vinylcyclopropane to *Z*-diene **53** is reported to be equal to the *cis-trans*-isomerisation (**Scheme 29**).⁸⁹ During the pyrolysis, 3-methylcyclopentene was observed as a minor product, showing that different carbon-carbon bonds on the cyclopropane ring can be broken. The authors concluded that diradical intermediates were present and the formation of *Z*-diene **53** was favoured over rearrangement, accounting for the lack of experimental evidence for 4-methylcyclopentene.



Scheme 29: [1,5]-hydrogen shift reaction favoured at high temperatures.

Despite these rapid background reactions, Baldwin's group was still able to obtain valid stereochemical data for the desired [1,3]-rearrangement of vinylcyclopropanes (VCPs), showing that the mechanism is highly system-dependent.⁹⁰ Both concerted

and stepwise biradical methods were evident between 1,2-*trans*- and *cis*-vinylcyclopropanes; *trans*-species generally favour a concerted route whereas the *cis*-equivalent favours a stepwise mechanism (**Table 3**). However, if the *cis*-VCPs underwent cyclopropane stereoisomerisation first before undergoing VCPR, these product ratios would support a concerted process.

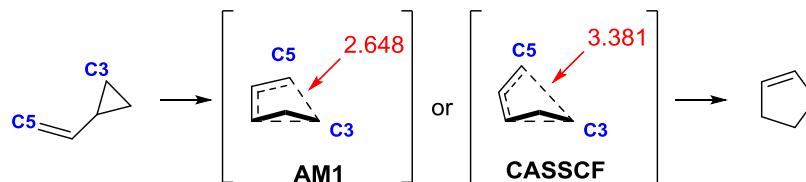
Table 3: Experimental Evidence for Both Concerted and Biradical VCPR Mechanisms

| Entry | R | R' | “Concerted” (<i>si+ar</i>)% | “Biradical” (<i>sr+ai</i>)% | “Concerted” (<i>si+ar</i>)% | “Biradical” (<i>sr+ai</i>)% |
|-----------------|-------------------|----|----------------------------------|----------------------------------|----------------------------------|----------------------------------|
| 1 ⁹⁰ | CN | Me | 67 | 33 | 36 | 64 |
| 2 ⁹¹ | Ph | Me | 64 | 36 | 10 | 90 |
| 3 ⁹² | Ph | Ph | 79 | 21 | 9 | 91 |
| 4 ⁹³ | Ph-d ₅ | D | 66 | 34 | 48 | 52 |
| 5 ⁹⁴ | D | D | 53 | 47 | - | - |

However, evidence that radical stabilising groups (**Table 3**, Entry 3) can both decrease the activation energy for rearrangement, and limit stereomutation, suggests strongly that radical intermediates are necessary for the rearrangement. Baldwin even suggests that, despite confirming Woodward and Hoffmann’s initial prediction, the data favouring a concerted mechanism relies on the assumption that the “allowed” stereochemical transformations are only controlled by molecular orbital theory and other important factors, such as steric effects, ring strain and bond elongations are all disregarded.⁹⁰

Further experimental results failed to distinguish between mechanisms^{90,95} and preliminary low level electronic structure calculations failed to help. The original semi-empirical method (RHF-AM1) predicted that **49** and **50** could be linked via an

allowed *si*-concerted transition state.⁹⁶ Unfortunately this method does not describe open-shelled diradical species accurately, so it is unsurprising that it favoured a concerted mechanism. Conflicting mechanisms were derived from the interatomic distances between the combining carbons in calculated transition states (**Scheme 30**); low level AM1 favoured a concerted pathway (2.648 Å),⁹⁶ whereas higher level CASSCF/3-12G favoured a stepwise, diradical mechanism (3.381 Å).⁹⁷



Scheme 30: Calculated bond distances in the transition state for VCPR (bond distances in Å).

It was only when further investigations using higher level calculations by Davidson and Gajewski (CASSCF(4o/4e)6-31G*)⁹⁸ and Houk and co-workers (UB3LYP/6-31G*)⁹⁹ that a good agreement between calculated and experimental activation energies emerged.¹⁰⁰ Both groups mapped the potential energy surface for the VCPR, showing that diradicaloid transition states lie only 1.6 kcal mol⁻¹ between a broad plateau on the energy surface, with the lowest energy structure favouring the formation of *si*-product (**Figure 6**). Despite being a symmetry allowed transformation, these results suggest that a concerted mechanism is highly unlikely.

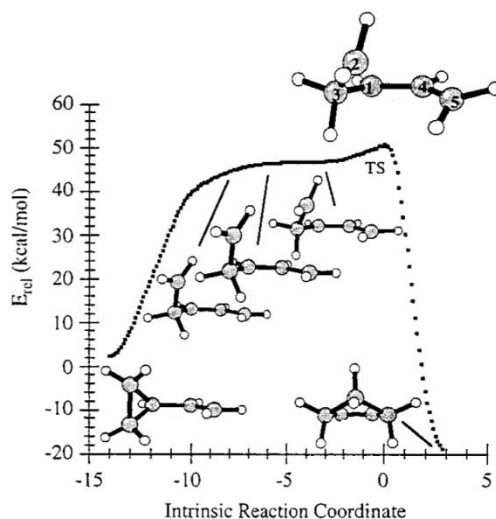


Figure 6: IRC of the transition structures involved in VCPR (UB3LYP/6-31G*, distance between bonding carbons in transition state = 2.681 Å).¹⁰⁰

Further theoretical investigations involving a detailed dynamic study¹⁰¹ and higher levels of theory (UM05-2X/6-311+G**) ¹⁰² also supported a diradicaloid pathway, which is now the accepted mechanism for VCPRs.

Houk and co-workers correlated their theoretical calculated activation energies with experimental results, showing that substituents with increasing potential for stabilising radicals, facilitate a bigger decrease in the activation energy for VCPR (Figure 7).

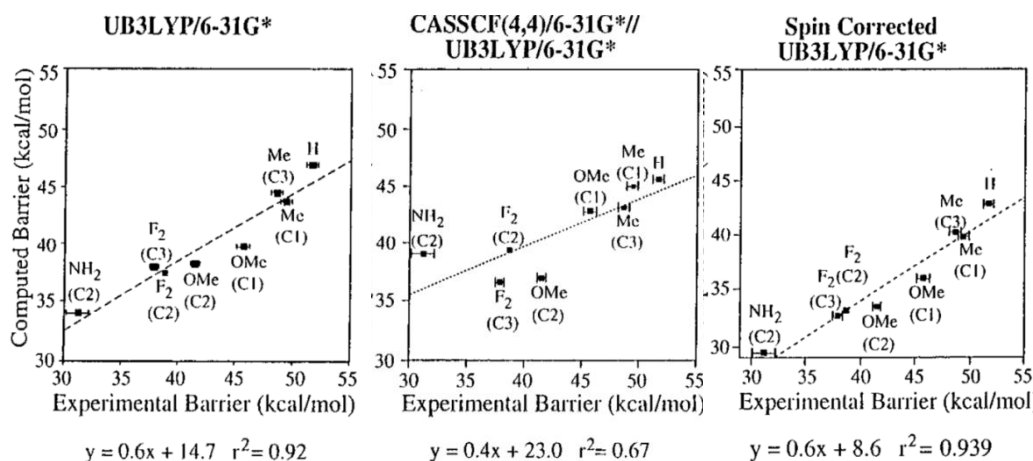


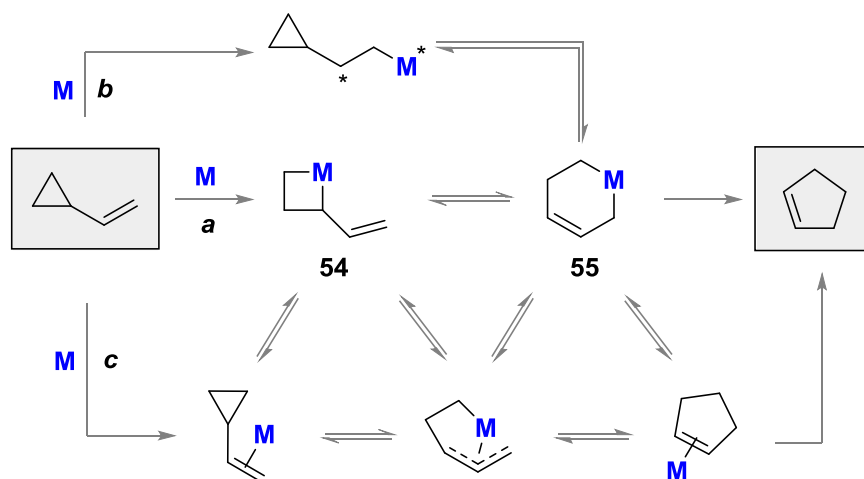
Figure 7: Experimental versus calculated activation energies for the VCPR of substituted-VCP.¹⁰⁰

This stabilisation allows the rearrangement temperatures to be decreased, suppressing the formation of unwanted side products. Transition metal catalysts have also been employed for this same purpose.

1.3.1.2. Transition Metal Catalysis

The use of metal catalysts in organic chemistry has become ubiquitous over the last century and transition metals such as ruthenium, palladium and nickel have allowed for the development of vinylcyclopropane rearrangements at ambient temperatures. A review in 2006 by Wang and Tantillo,¹⁰³ discussed the use of these metals and outlined the most likely steps for the rearrangement (Scheme 31). The majority of these conclude with metallocyclohexene **55** which reductively eliminates to form the desired cyclopentene. Pathway **a** is initiated by cyclopropane bond breaking via oxidative addition of the metal to form metallocyclobutane **54**. Direct conversion to **55** can be achieved with [1,3]-sigmatropic rearrangement or

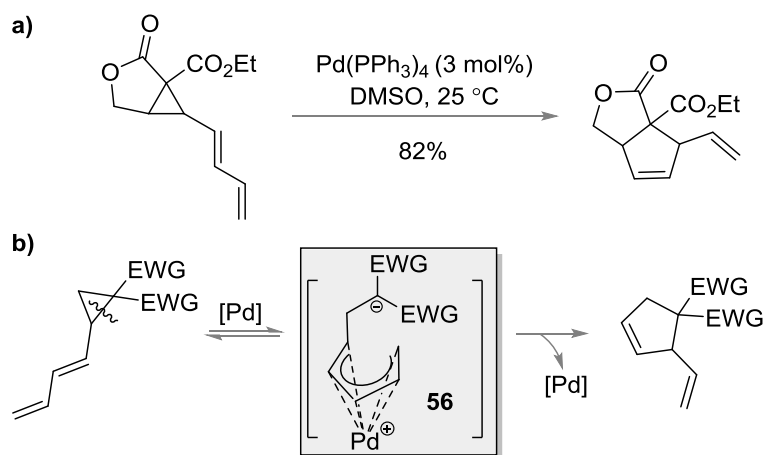
through the η^1 -alkyl/ η^3 -allyl intermediate. The formation of an η^1 -alkyl radical, anionic or cationic intermediate can also theoretically afford **55** after C-C bond breaking (pathway **b**). Transition metals can form π -complexes (pathway **c**) which can be involved in equilibrium reactions which culminate in the formation of metallacyclohexene **55**. Which pathway is undertaken, depends on the type of metal used.



Scheme 31: Transition states involved in metal catalyzed VCPR (* = radical, anion or cation).¹⁰³

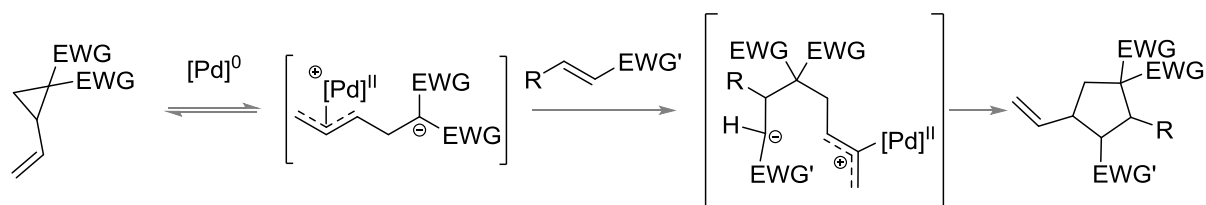
The first reported transition metal mediated VCPR used ruthenium based complexes (*vide supra*) but are limited due to the requirement for stoichiometric amounts of metal.

The effectiveness of palladium catalysis relies on the presence of electron-withdrawing groups on the cyclopropane, as well as on the presence of a conjugated diene rather than a single alkenyl group (**Scheme 32a**).⁸¹ This arrangement suggests that palladium(0) nucleophilically attacks the alkene to form zwitterionic intermediate **56**; stabilisation of the resulting anion and pentadienyl cation is achieved by electron-withdrawing groups and palladium complexation, respectively (**Scheme 32b**).



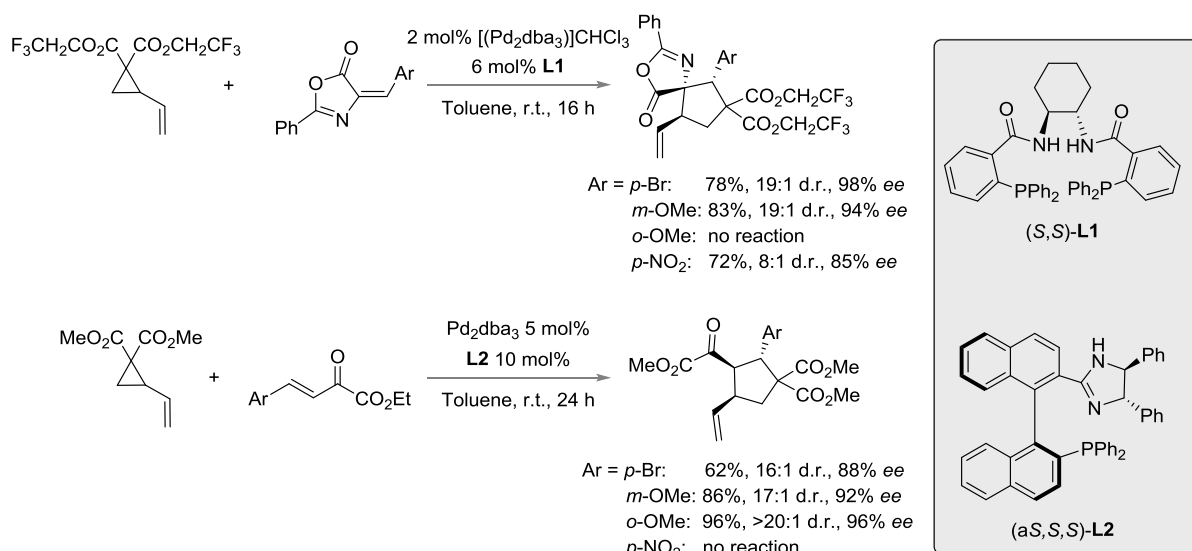
Scheme 32: a) VCP ring opening catalysed by Pd(0). b) Proposed Pd(0) mechanism involving zwitterionic intermediates.

The resulting zwitterionic intermediate is capable of undergoing intermolecular nucleophilic attack on electron-deficient olefins, followed by ring closure to afford cyclopentanes (**Scheme 33**).



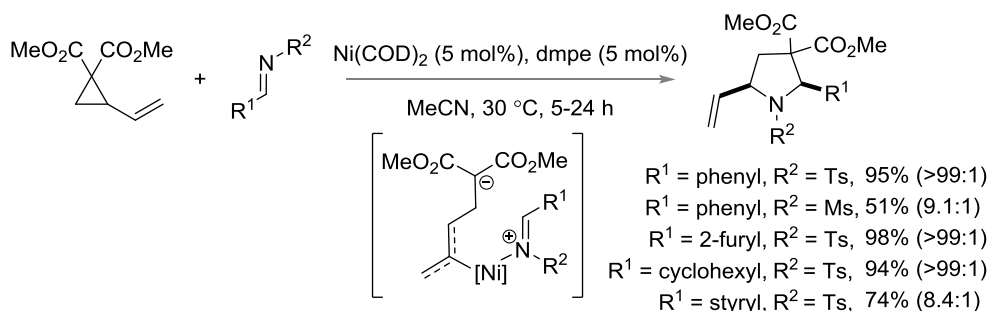
Scheme 33: Palladium mediated VCP ring opening followed by zwitterionic intermediate capture and cyclisation.

This sequence has been applied successfully in the development of routes to highly-substituted cyclopentanes, with high enantio- and diastereoselectivity derived from chiral ligands (**Scheme 34**).¹⁰⁴



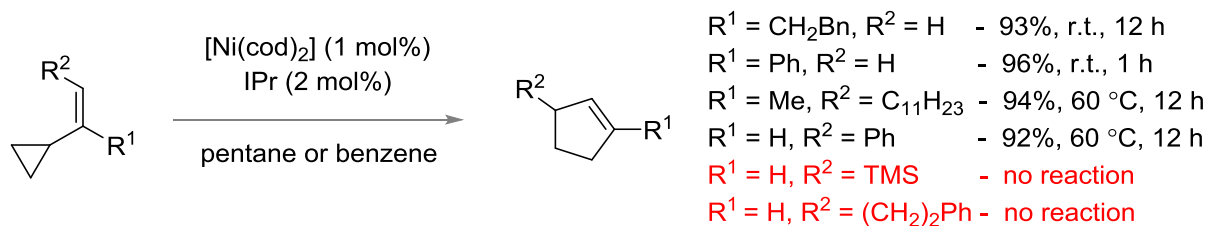
Scheme 34: Synthesis of highly functionalised cyclopentenes from Pd(0) mediated VCPR with chiral ligands.

More recent work has shown that nickel catalysts can promote a ring opening reaction of vinyl cyclopropanes in the presence of imines to synthesise substituted pyrrolidines.¹⁰⁵ The reaction is believed to proceed via a similar zwitterionic intermediate found in the palladium systems (**Scheme 35**).



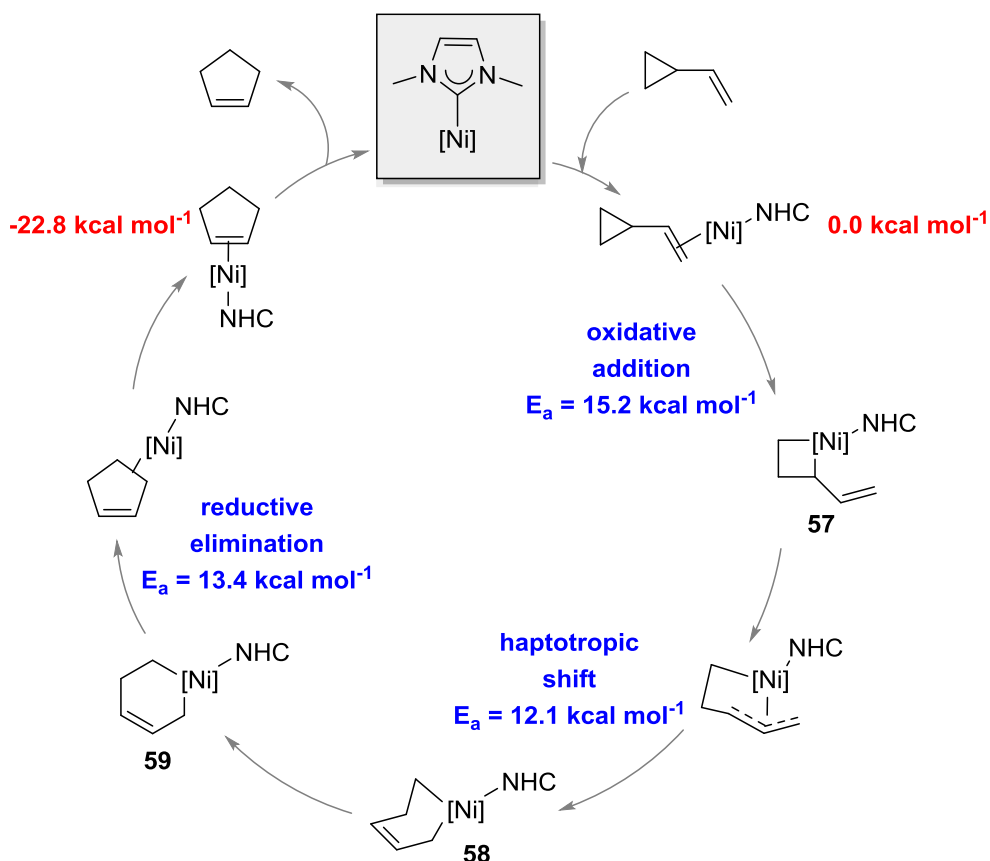
Scheme 35: Ni(0) mediated ring opening of VCP in the synthesis of pyrrolidines (diastereomeric ratio in parentheses).¹⁰⁵

In 2004, nickel complexes were reported to catalytically promote VCPR of unactivated vinyl cyclopropanes to cyclopentenes at room temperature.^{82b} 1,1-Disubstituted alkenes proceeded smoothly but 1,2-disubstituted olefins either reacted sluggishly or did not react at all (**Scheme 36**).



Scheme 36: Reaction scope for unactivated VCPs using a Ni(0) catalyst system.

High level computational and experimental investigation by the Louie and Tantillo groups, showed that radical species and zwitterions are not involved as intermediates.¹⁰⁶ Instead, an oxidative addition step occurs to form metallacyclobutane intermediate **57** which then undergoes haptotropic shifts to metallacyclohexene **58**. A conformation change to metallacyclohexane **59** was required to bring the two methylene centres attached to the nickel closer together. Subsequent reductive elimination regenerates the catalyst and forms the desired cyclopentene (**Scheme 37**).



Scheme 37: Intermediates in Ni(0)-promoted VCPR (relative energies, B3LYP/LANL2DZ, gas phase, 298 K).

The relief of the high cyclopropane ring strain is the major driving force for the reaction but steric factors and substitution around the alkene can affect the activation energy for rearrangement. Computational and experimental results were in agreement, predicting that 1,1-disubstituted alkenes have a lower activation energy than their 1,2-disubstituted counterparts (**Table 4**, Entry 2 compared with Entries 3 and 4, respectively). The activation energy for *gem*-dimethyl compounds is higher (**Table 4**, Entry 5) due to extra steric repulsion between the substituents and the carbene ligand (this can be avoided in the 1,2-disubstituted species because the substituent can twist away from the ligand¹⁰⁶). Finally a fully-substituted olefin is predicted to be the least reactive species, but the formation of a trisubstituted alkene in the product provides an extra driving force for rearrangement, providing a lower energy barrier than the 2,2-disubstituted compound (**Table 4**, Entry 6).

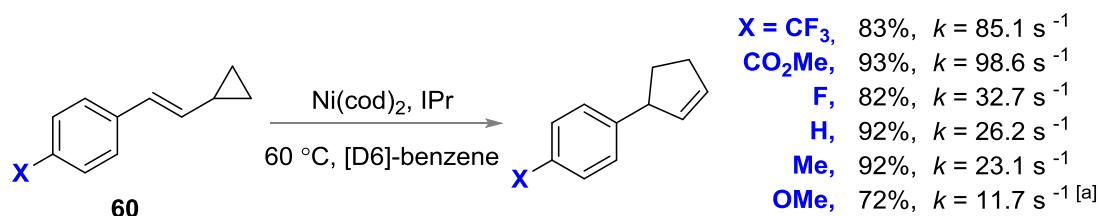
Table 4: Activation Energy Effects with Increased Alkene Substitution

| Entry | Alkene | Activation Energy (kcal mol ⁻¹) ^[a] | Highest Energy Process |
|-------|--------|--|------------------------|
| 1 | | 16.8 | Oxidative Addition |
| 2 | | 15.5 | Oxidative Addition |
| 3 | | 17.9 | Haptotropic Shift |
| 4 | | 19.6 | Haptotropic Shift |
| 5 | | 28.0 | Reductive Elimination |
| 6 | | 23.9 | Reductive Elimination |

[a] Relative energies calculated using B3LYP/DZVP2+//B3LYP/LANL2DZ +ZPE(B3LYP/LANL2DZ).

Electronic effects on the rearrangement were also studied using VCP-**60** and varying the substitution on the *para*-position (**Scheme 38**). Substrates with electron-withdrawing substituents (*p*-CO₂Me, *p*-CF₃, *p*-F) were found to rearrange more

quickly than the unsubstituted species, whereas electron-donating groups resulted in a slower reaction (*p*-OMe and *p*-Me). A Hammett treatment of these results gave a ρ value of 0.11; values greater than 0.2 suggest that the substitution plays a significant role in the reaction.¹⁰⁶ Therefore, it was concluded that the mechanism did not involve zwitterions or radicals because there is only a very small change in rate, despite quite large changes in the electronic properties of the aromatic ring.



Scheme 38: Electronic effects on Ni(0) catalysed VCPR. [a] GC yield.

Both the pyrolysis and metal-catalysed mechanistic investigations of the VCPR suggest that the rearrangement can proceed faster and at lower temperatures when electron-withdrawing substituents are introduced into the system. Fluorine is both a σ -acceptor and a π -donor so the effects on rearrangement rate are difficult to predict.

1.3.1.3. Effects of Fluorine

Despite the obvious potential benefits which would arise from fluorine atom substituents lowering the rate of rearrangement, very few published VCPR rearrangements actually investigate fluorine atom effects. This may originate at least partly in practical issues involved in handling fluorinating reagents used to synthesise the desired precursors.

The high energetic barrier for the prototypical VCPR ($51.7 \text{ kcal mol}^{-1}$) can be lowered by approximately 10 kcal mol^{-1} by *geminal* fluorination of the cyclopropane ring (**Table 5**, Entries 1 and 2, respectively). Perfluorinated vinylcyclopropanes show a further decrease (**Table 5**, Entry 3), with the pentafluorinated species giving the lowest activation energy of $28.4 \text{ kcal mol}^{-1}$ (**Table 5**, Entry 4). These experimental results allowed some mechanistic insight to be developed into why the fluorine atoms alter the reactivity so dramatically.

Table 5: Effects of Fluorine Substitution on VCPR

| Entry | VCPR Scheme | Activation Energy (E_a) ^[a] |
|-------|-------------|--|
| 1 | | 51.7 ⁸⁴ |
| 2 | | 41.5 ¹⁰⁷ |
| 3 | | 34.6 ¹⁰⁸ |
| 4 | | 28.4 ¹⁰⁹ |

[a] Energies reported in kcal mol⁻¹.

Difluorinated cyclopropane rings have been shown to have higher strain energy and a weaker distal carbon-carbon bond.^{44a} Computational work by Zeiger and Leibman¹¹⁰ showed the dramatic effect that increasing fluorine substitution has on the cyclopropane ring strain energy (**Figure 8**).

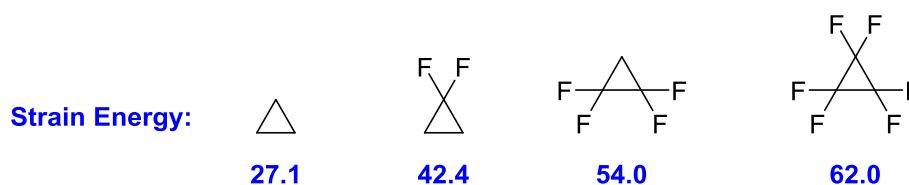
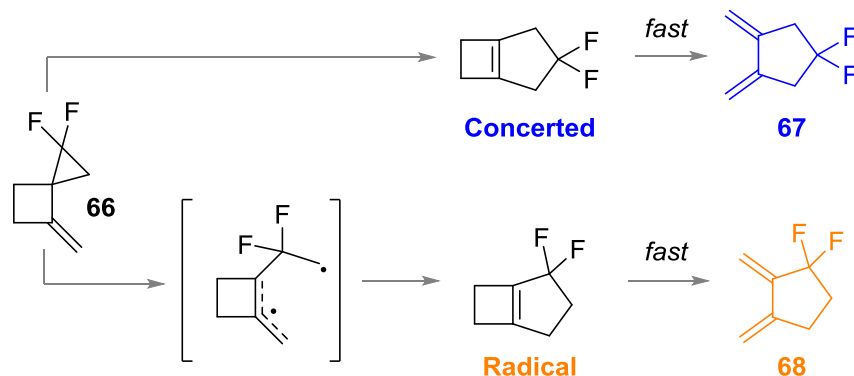


Figure 8: Increased cyclopropane strain energy with increasing fluorine substitution (calculated using Hartree-Fock with 6-311G** basis set, energies in kcal mol⁻¹).¹¹⁰

It was expected that compound **61** would rearrange via the scission of the weakest bond (C1-C3, **Table 5**, Entry 2), but Dolbier's initial report suggested that cleavage of the stronger C1-C2 bond occurred exclusively to give 3,3-difluorocyclopentene **62**.¹¹¹ However, the group quickly corrected their observation, stating that 4,4-

difluorocyclopentene **63** polymerised before analysis, falsely showing that **62** was the major isomer.^{107a} This false result led to the group studying the pyrolysis of **66** (Scheme 39), which resulted in a mixture of **67** and **68**, suggesting competition between a radical and concerted mechanism (ratio of products was not reported).



Scheme 39: Evidence of competing concerted and radical pathways in fluorinated VCPR.¹¹¹

Due to the increased strain energy associated with fully fluorinated (perfluorinated) cyclopropane ($62.0 \text{ kcal mol}^{-1}$), it is no surprise that perfluoro- and pentafluorinated vinyl cyclopropanes have the lowest activation energies (Table 5, Entries 3 and 4 respectively). However, understanding why there is a $6.2 \text{ kcal mol}^{-1}$ difference between the two species is more difficult. Smart *et al.*¹⁰⁹ suggested that the transition states have polar biradical character due to the high electron-withdrawing effects of the fluorine atoms; however, entropic values suggest that the formation of pentafluoro-transition state **TS3** ($\Delta S^\ddagger = -5.5 \text{ eu}$) is more ordering than the corresponding perfluoro-intermediate **TS4** ($\Delta S^\ddagger = 2.5 \text{ eu}$) (Figure 9). Both differences in energy and entropy are small, therefore making predictions into why **65** rearranges more readily than **64** difficult. There is no obvious reason why these transition states should involve different levels of entropy loss/gain.

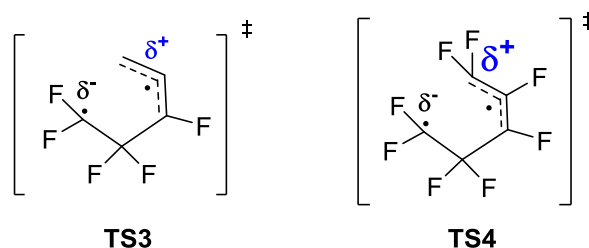
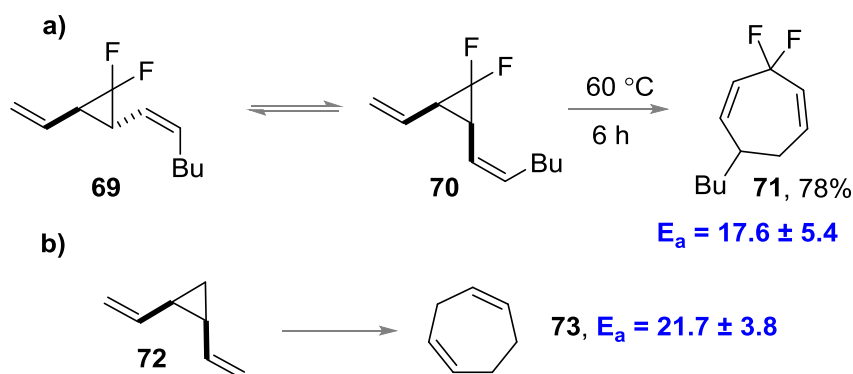


Figure 9: Proposed polar biradical transition states for pentafluoro- and perfluorinated VCP.¹⁰⁹

A related [3,3]-rearrangement pathway was reported by Erbes and Boland when divinylcyclopropane **69** rearranged to difluoroheptadiene **71**, presumably after cyclopropane stereoisomerisation to *cis*-**70** (**Scheme 40a**).¹¹² The facile reaction conditions (60 °C, 6 hours) were supported by a low experimental activation energy of 17.2 ± 5.4 kcal mol⁻¹ and attributed to the increased strain energy of the difluorocyclopropane. Surprisingly, the lowering of the activation energy compared with non-fluorinated **72** was not as dramatic as those observed in VCPR ($\Delta\Delta E_a = 4.4$ kcal mol⁻¹);¹¹³ large experimental errors and potential unfavourable steric interaction with the butyl group in **69** could account for these differences between pathways (**Scheme 40b**).



Scheme 40: a) Preferred divinylcyclopropane rearrangement over VCPR. b) Non-fluorinated comparison (all experimental values were recalculated to 298 K from reported kinetic data using methods described by Maskil¹¹⁴ to allow comparison, values are in kcal mol⁻¹).

These results highlight that even when VCP precursors undergo low temperature rearrangements, competing side reactions like [3,3]-rearrangements and cyclopropane stereoisomerisation can still occur. It is important to take account of these processes when designing new precursors.

1.3.2. Applications of VCPR

With the extensive mechanistic studies carried out into the VCPR the rearrangement has been used in a variety of total synthesis projects. The stereospecific nature of the rearrangement is appealing and only the initial cyclopropanation step is required to control configuration. VCPRs were utilised as key steps in securing the 5-membered cyclic cores for a range of complex

structures,⁷² including α -vetispirene **74**,¹¹⁵ specionin acetate **75**¹¹⁶ from the sesquiterpene family of compounds and prostaglandin E₂ methyl ester **76** (Figure 10).¹¹⁷

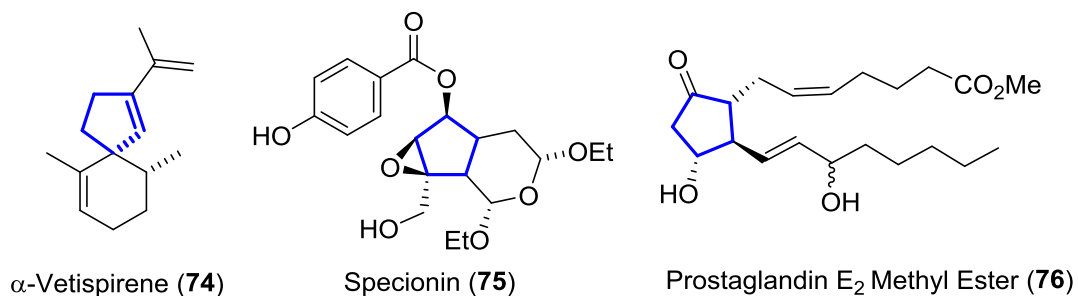


Figure 10: Selected natural products synthesised using VCPR (key ring structures formed during the rearrangements are highlighted in blue).

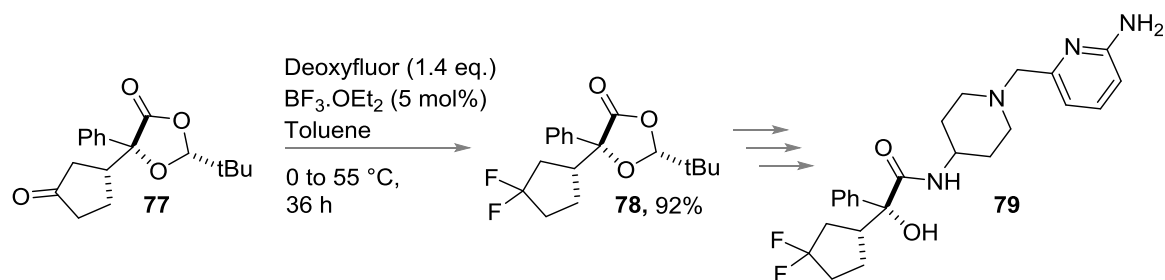
The key rearrangements in the synthesis of **74** and **75** required high and very high temperatures of 190 °C and 560 °C, respectively but the synthetic route to **76** benefited from anion-accelerated rearrangement and could be carried out at much a lower temperature range of -78 to -40 °C.

Despite the beneficial effect of fluorine atom substitution on VCPR precursors, there are very few synthetic applications of the rearrangement for difluorocyclopentenes; the ring structures themselves are relatively unusual motifs in the synthetic literature.¹¹⁸

1.4. Difluorinated 5-Membered Ring Systems

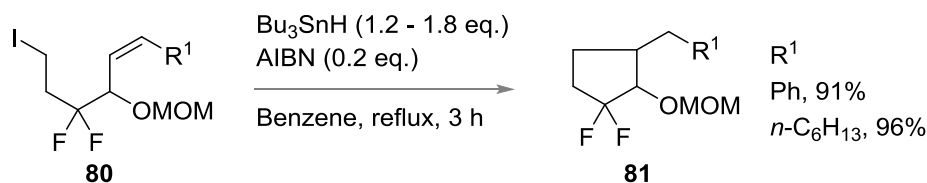
1.4.1. Difluorinated Cyclopentanes

The most widely used route to difluorocyclopentanes is the nucleophilic difluorination of ketones but these methods typically result in undesirable side products resulting from HF elimination. Mase and co-workers were faced with these issues during the large scale synthesis of muscarinic receptor antagonist **79** (Scheme 41).¹¹⁹ They developed a highly efficient synthesis of difluorocyclopentane **78** from the Deoxofluor mediated difluorination of ketone **77**, but the presence of catalytic amounts of Lewis acid was essential to suppress unwanted side product formation. Optimised conditions improved yields of **78** by 10-12% and aided in the group being able to access multi-kilogram quantities of **79**.



Scheme 41: Controlled difluorination of ketone 77 en route to 79.

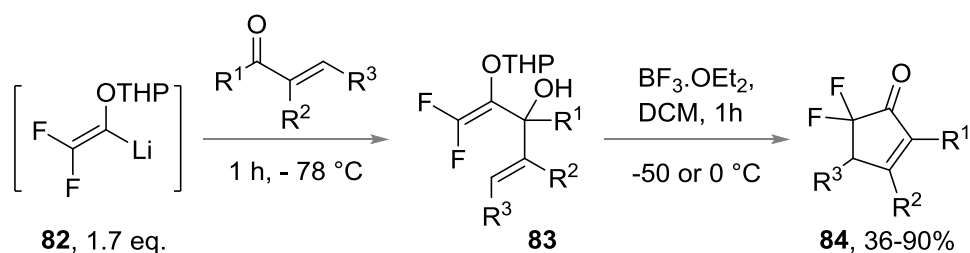
Building block routes to difluorocyclopentanes rely on intramolecular radical mediated cyclisations based around tin hydride chemistry.¹²⁰ Morikawa and co-workers demonstrated that β,β -difluoroalkyl iodide **80** underwent radical cyclisation to cyclopentene **81** in high yields of both aryl and alkyl substituents (**Scheme 22**).^{120a} This route can be further extended to the synthesis of difluorinated cyclohexane and tetrahydropyran derivatives, but lengthy synthetic steps are required to access precursors, and little stereocontrol was observed in the formation of the resulting products.



Scheme 42: Radical cyclisation of 80 to difluorocyclopentane 81.

1.4.2. Difluorinated Cyclopentenones

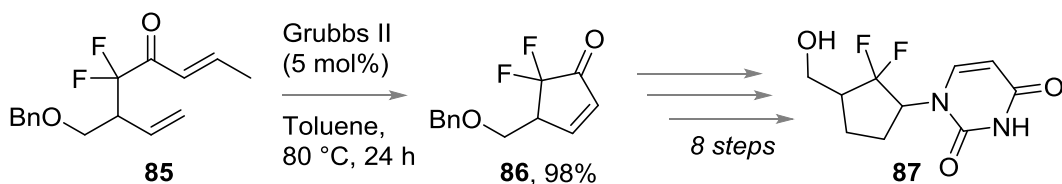
The Nazarov cyclisation is a classic method for accessing cyclopentenones and Tius and co-workers utilised the reaction to access difluorinated cyclopentenones (**Scheme 43**). A wide range of difluoroallylic alcohols **83** could be assembled rapidly from α,α,α -trifluoroethanol; vinyl lithium **82** reacted with a range of ketones and aldehydes. In order to obtain controlled addition, this step must be carried out at cryogenic temperatures, which limits the chemistry to smaller scales. The resulting alcohols proved difficult to purify so direct cyclisation of crude reaction mixtures were favoured and driven by addition of Lewis acid $\text{BF}_3 \cdot \text{OEt}_2$.



Scheme 43: Difluorinated cyclopentenones accessible from Nazarov cyclisations.

A range of cyclopentenones **84** incorporating a wide variety of functional groups (alkyl, (hetero)aryl and halogens) were prepared in moderate to excellent yields; hydroxyl groups could also be included.

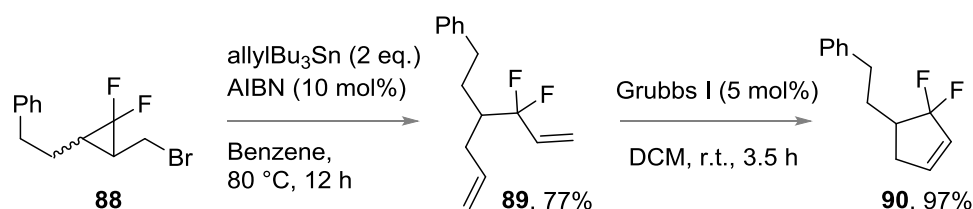
A route more applicable to large scale was developed by Qing and co-workers who synthesised difluorocyclopentenone **86** via the ring closing metathesis (RCM) of difluorinated precursor **85** (Scheme 44).¹²¹ Further functional group transformations afforded difluorocyclopentane **87** which they sought to use as a fluorinated mimic of the anti-HIV drug dideoxyinosine.



Scheme 44: High yield synthesis of difluorocyclopentenone 86 via the RCM of 85.

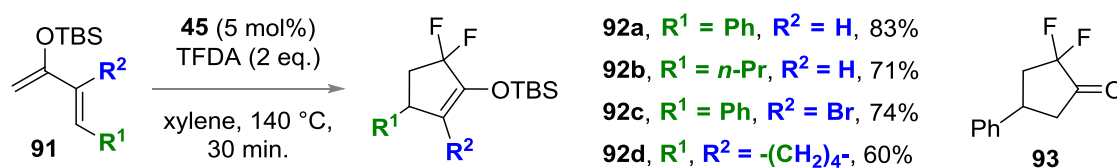
1.4.3. Difluorinated Cyclopentenes

Itoh and co-workers also utilised RCM chemistry in the synthesis of difluorocyclopentene **90** (Scheme 45).¹²² Nine difluorinated 1,6-dienes were accessed from free radical ring opening reactions of *gem*-difluorocyclopropanes, controlled by regioselective ring opening distal to the CF₂ group. Difluoromethylene building block **89** was accessed in 77% yield from **88** and successfully underwent RCM when treated with first generation Grubbs catalyst to afford **90**. This was the only compound to be functionalised further so functional group limitations are unknown.



Scheme 45: Synthesis of difluorocyclopentene 90 via RCM of 89.

To our knowledge, Ichikawa and co-workers reported the only synthetically-oriented investigations into the use of VCPR for accessing difluorocyclopentenes.³¹ Their Ni-mediated difluorocyclopropanation of silyl enol ether **91a** at 100 °C for 40 minutes (*vide supra*) gave poor yields of the corresponding vinyl difluorocyclopropane (12%, ¹⁹F NMR) and instead favoured rearrangement through to difluorocyclopentene **92a** (61%, ¹⁹F NMR). Increased reaction temperatures (140 °C) gave exclusive formation of **92a** in an isolated yield of 83% while maintaining a short reaction time of 30 minutes (**Scheme 46**). Alkyl (**92b**), bromide (**92c**) and cyclic (**92d**) systems could all be synthesised in good yields.



Scheme 46: Domino nickel-catalysed difluorocyclopropanation/ring-expansion of diene 91 to difluorinated cyclopentenes 92.

The group also showed that hydrolysis of **92a** under acidic conditions allowed access to difluorocyclopentanone **93** (80%, ¹⁹F NMR) which was unstable to purification and required further functionalisation to the corresponding hydrazine, oxime or cyclopentanol. The direct access to difluorocyclopentenes from the study is appealing but the effect of the nickel catalyst **45** on the VCPR was not obvious from experimental results.

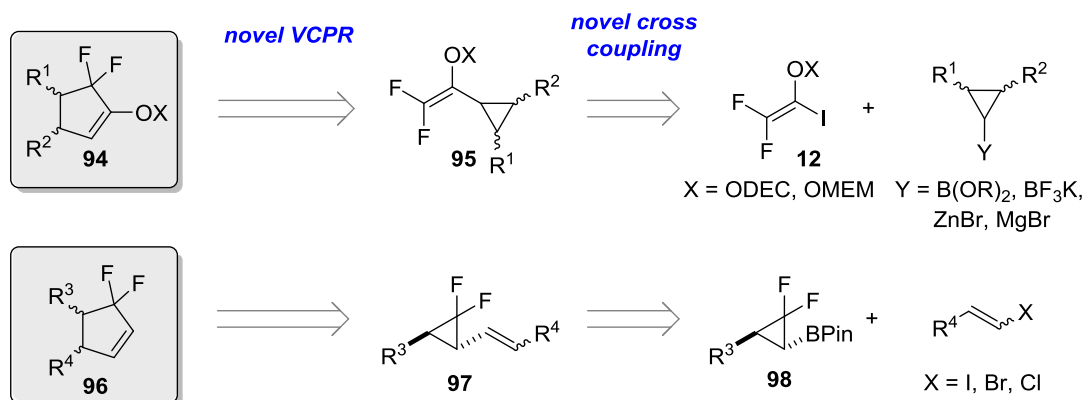
The promising application of the VCPR by Ichikawa and co-workers in 2015 for the synthesis of difluorocyclopentenes complements our investigations into the viability of a building block approach to these fluorinated ring systems. This work started in 2012 and is discussed within.

Aims

The beneficial effect of fluorine atom substitution on compounds which undergo VCPR has been well documented, but the harnessing of this attribute synthetically to access difluorocyclopentenes has not been achieved. These desirable ring systems represent relatively unexplored areas of fluorinated chemical space and one prerequisite would be the ability to further functionalise the resulting compounds to enable access to more complex systems.

The work reported in this thesis has three main aims focusing on the synthesis of precursors, the assessment of fluorine atom assisted VCPR as a viable synthetic method for synthesising difluorocyclopentenes and understanding the limitations of the developed chemistry.

The development of an efficient building block synthesis of difluorinated vinylcyclopropane precursors is essential to allow thorough investigations into the rearrangement. Developments in the cross coupling chemistry of difluorovinyl **12** and the reported literature synthesis of difluorocyclopropyl pinacol borane **98** provide strong starting points for accessing precursors **95** and **97**, respectively (**Scheme 47**). Our proposed route to **97** relies on only one potentially difficult difluorocarbene transfer reaction and relies on the more versatile cross-coupling chemistry to introduce diversity. Extensive optimisation of both cross coupling steps will be required but the development of novel sp^2 - sp^3 carbon-carbon bond forming reactions will be beneficial, not just in this study but also for other synthetic targets.



Scheme 47: Retrosynthesis of difluorocyclopentenes **94** and **96** from reported literature compounds.

Once synthesised, the VCPR of both precursors will be assessed using thermal conditions, metal catalysed or photochemical activation; the former will be preferred because it requires no additional reagents or specialised equipment. ^{19}F NMR spectroscopy will be used extensively for reaction monitoring alongside kinetic investigations into the rearrangement; these will allow effective comparisons between other literature rearrangements to be made. Electronic structure calculations are likely to complement this work strongly, and will be carried out throughout the study to confirm and guide experimental investigations.

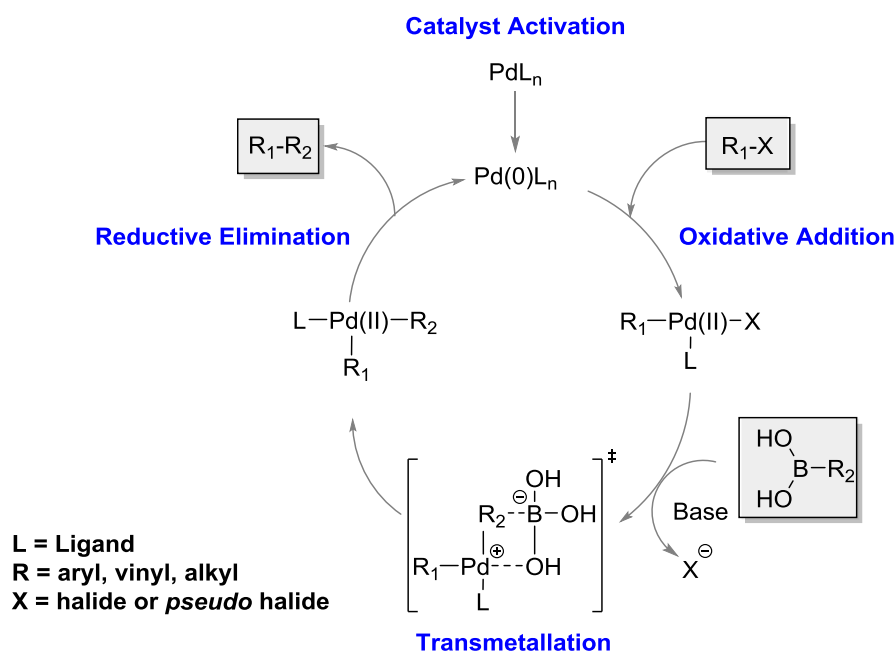
During the course of these investigations, issues in the synthesis of precursors arose, and side products from rearrangements required identification. It is important that the synthetic issues are discussed, to highlight the limitations of current literature methodology. It is from the understanding of these limitations that the precursor route design could be enhanced. Furthermore, extensive electronic structure calculations allowed the reasons for the formation of side products to be resolved. At the start of these investigations we lacked the power to foresee issues with the VCPR and alternative rearrangement pathways. Throughout our work we found that an *a priori* assessment of thermal rearrangements was imperative to minimise synthetic commitments. Developments of this triage approach are discussed within.

Together these aims represent our drive to develop and assess the synthetic viability of accessing novel difluorocyclopentenes using the VCPR. Both experimental and computational considerations were key for the effective assessment and understanding of the reactions.

Disclaimer: X-ray diffraction of intermediate **111** was obtained, processed and refined by Dr. Alan Kennedy (University of Strathclyde).

Chapter 1: Synthesis of 2,2-(Difluorovinyl)cyclopropanes

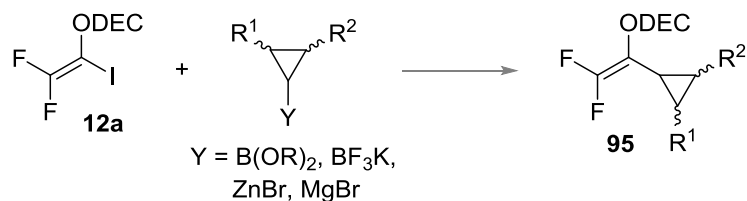
Carbon-carbon bond forming reactions are of critical importance in organic chemistry, and the cross-coupling of organometallic reagents is deployed in both routes proposed for the synthesis of difluorinated VCPR precursors. The Suzuki-Miyaura reaction,¹²³ one of the most utilised forms of cross-coupling in industry, is a palladium-catalysed reaction between an organo-boron species and an organo-(or *pseudo*) halide. The importance of the reaction has led to a huge level of interest in reaction, alongside extensive research into its mechanism. The catalytic cycle only proceeds in the presence of base and Pd(0) species, formed *in situ* from ligand dissociation, or the reduction of Pd(II) precatalysts. Once available, the catalyst undergoes three distinct transformations; oxidative addition, transmetalation and reductive elimination (**Scheme 48**).¹²⁴



Scheme 48: General mechanism for Suzuki-Miyaura reaction between a boronic acid and organohalide.

Matos and Soderquist were the first authors to suggest that transmetalation could proceed via two separate pathways; base mediated formation of a reactive palladium hydroxide intermediate or a reactive boron-ate complex.¹²⁵ Experimental

studies by Carrow and Hartwig¹²⁶ support the former and further work by Amatore and co-workers highlights the important role the base plays in controlling the cross coupling.¹²⁷ The transmetallation step in our proposed synthesis of difluorovinyl cyclopropane precursors **95** (**Scheme 49**) is likely to be difficult and optimisation will focus on conditions which increase the rate of transmetallation; oxidative addition with difluorovinyl iodide **12a** has been shown to be facile²⁶ and the β -hydride elimination common with alkyl coupling partners is slowed for cyclopropyl units.¹²⁸

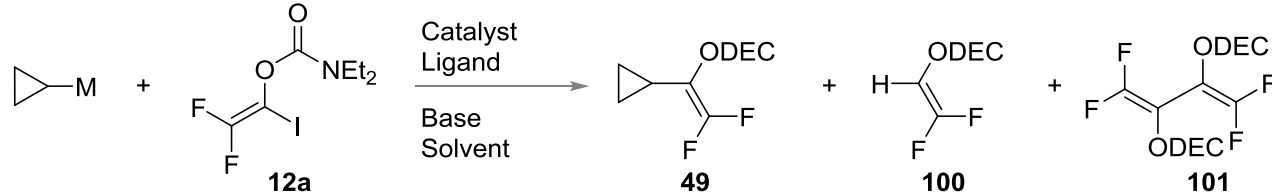


Scheme 49: Proposed novel cross-coupling route to difluoro-VCP 95.

In order to assess the problems that could arise from the cross coupling of vinyl iodide **12a** and nucleophilic cyclopropyl coupling partners fully, initial screening focused on conditions reported in the literature.¹²⁹

2.1. 1st Generation Optimisation

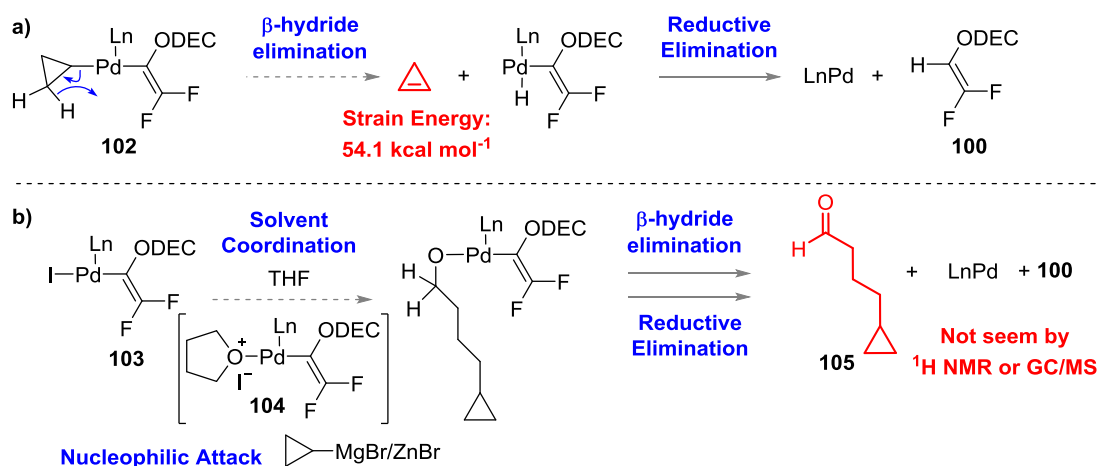
Kumada, Negishi and Suzuki-Miyaura coupling between iodide **12a** and cyclopropyl coupling species were investigated, focusing on literature conditions based on previous cyclopropane couplings but using a higher loading of catalyst for the initial screening (**Table 6**, Entries 1-3). It was proposed that reagents based on the more electropositive metals (Mg and Zn)¹³⁰ would react faster than potassium trifluoroborates, but all of the reactions attempted with these reagents favoured formation of enol carbamate **100**.

Table 6: Coupling Screen Varying the Cyclopropyl Nucleophile


| Entry | M (eq.) | Catalyst (mol%) | Base (eq.) | Solvent | Temp. (°C) | Time (h) | SM (12a) ^[a] | Product (99) ^[a] | Enol (100) ^[a,b] | Diene (101) ^[a,b] |
|------------------|---------------------------|---|-------------------------------------|--|------------|----------|-------------------------|-----------------------------|-----------------------------|------------------------------|
| 1 | MgBr ^[c] (1.1) | Pd(PPh ₃) ₄ (20) | - | THF | 70 | 4 | X | Trace | Major | Trace |
| 2 | ZnBr ^[c] (1.2) | Pd(PPh ₃) ₄ (20) | - | THF | r.t. | 130 | X | X | ✓ | X |
| 3 | ZnBr ^[c] (2) | Pd(PPh ₃) ₄ (20) | - | THF | 90 | 2 | X | X | ✓ | X |
| 4 ²⁶ | BF ₃ K (1.2) | (Ph ₃ P) ₂ PdCl ₂ (20) | Cs ₂ CO ₃ (3) | <i>t</i> BuOH / H ₂ O (2.7:1) | 110 | 17 | X | X | Minor | Major |
| 5 ¹³¹ | BF ₃ K (1.2) | PdCl ₂ (dppf) (20) | Cs ₂ CO ₃ (3) | THF / H ₂ O (3:1) | 110 | 17 | X | X | X | ✓ |
| 6 ¹³¹ | BF ₃ K (1.2) | PdCl ₂ (dppf) (20) | K ₃ PO ₄ (3) | THF / H ₂ O (3:1) | 110 | 17 | X | X | X | ✓ |
| 7 ¹³¹ | BF ₃ K (1.2) | Pd(PPh ₃) ₄ (20) | K ₃ PO ₄ (3) | Toluene / H ₂ O (3:1) | 110 | 17 | Major | Minor | X | Minor |
| 8 ¹³¹ | BF ₃ K (1.2) | Pd(OAc) ₂ (20) ^[d] | K ₃ PO ₄ (3) | Toluene / H ₂ O (4:1) | 110 | 17 | X | X | X | ✓ |
| 9 ¹³² | B(OH) ₂ | Pd(PPh ₃) ₄ (20) | K ₃ PO ₄ (3) | Toluene (wet) | 80 | 66 | X | Minor | X | Major (2.6:1) |

[a] Determined by ¹⁹F NMR. [b] ¹⁹F NMR consistent with reported literature compounds.²⁶⁻²⁷ [c] Titrated using procedure reported by Knochel and co-workers.¹³³ [d] (2-Biphenyl)dicyclohexylphosphine (CyJohnPhos, 40 mol%).

The conventional mechanism for formation of enol carbamate is through β -hydride elimination of intermediate **102** (Scheme 50a). However, the high strain energy of the cyclopropene side product makes this route unlikely.¹³⁴ Wilson and co-workers previously reported that alcohol solvents could undergo ligand exchange, then β -hydride elimination follows to afford enol carbamate **100**.²⁶ Theoretically, THF could coordinate to palladium intermediate **103** to form activated electrophile **104**. Nucleophilic attack with cyclopropylmagnesium or cyclopropylzinc species has the potential to form aldehyde **105**, but the lack of NMR or GC/MS evidence for this by-product also makes this mechanism unlikely (Scheme 50b).



Scheme 50: Proposed formation of enol carbamate **100** under Kumada or Negishi coupling conditions via a) β -hydride elimination or b) solvent coordination followed by nucleophilic attack.

Palladium compounds with coordinated THF have been isolated previously and reported in the literature¹³⁵ but all depicted THF bound as a neutral donor and not with a labilised C-O depicted in compound **104** (**Figure 11**).

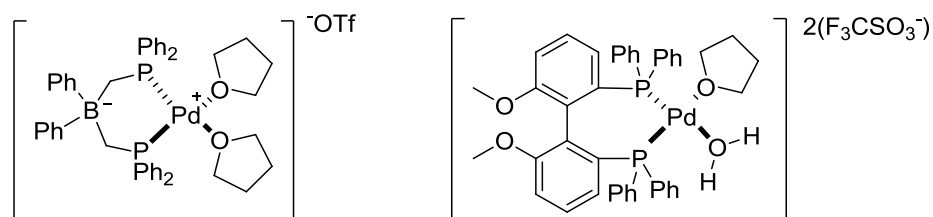
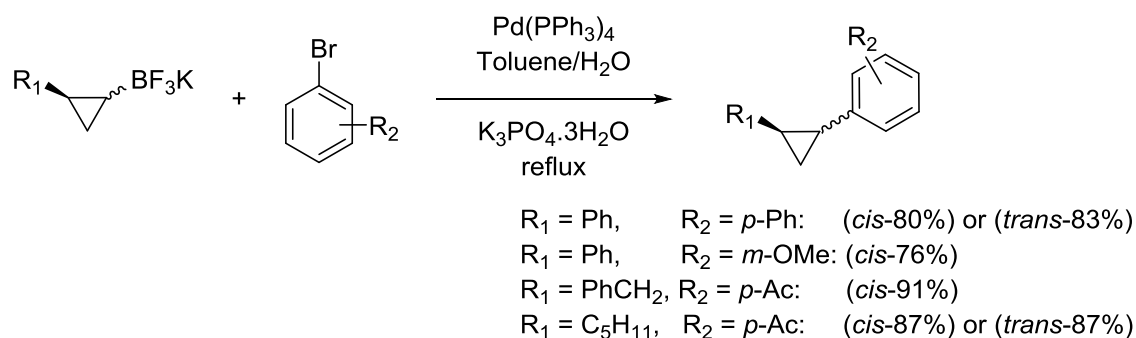


Figure 11: Known palladium complexes (confirmed by XRD) showing THF coordination.

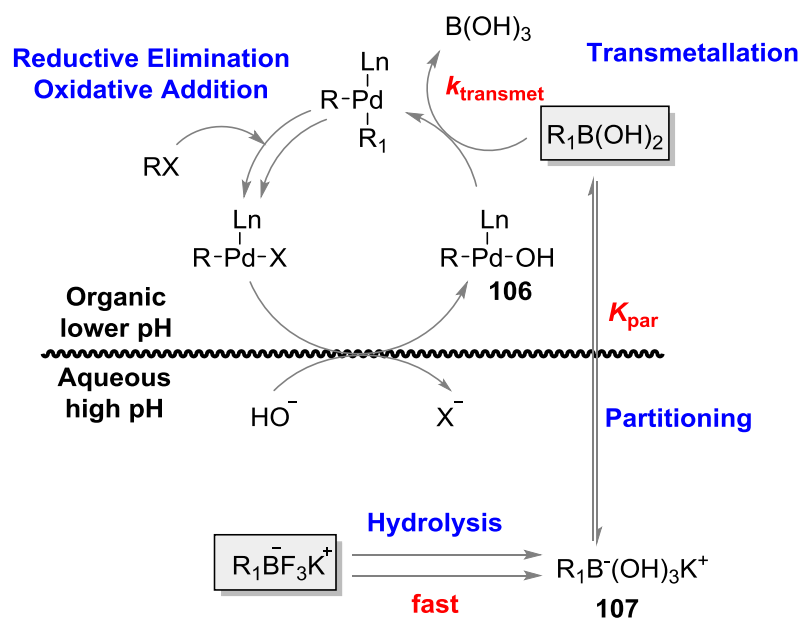
Since the more reactive Kumada and Negishi conditions failed to give the desired product, Suzuki-Miyaura conditions were investigated instead. Both Wilson's²⁶ (**Table 6**, Entry 4) and Deng's¹³¹ (Entries 5-8) coupling conditions failed to afford the desired product, favouring formation of homocoupled diene **101** instead. The latter conditions have previously been shown to couple substituted potassium cyclopropyl trifluoroborates with aryl bromides successfully (**Scheme 51**), so our failure to observe coupling with the unsubstituted species was disappointing.



Scheme 51: Suzuki-Miyaura cross coupling of substituted potassium trifluoroborates with aryl bromides.¹³¹

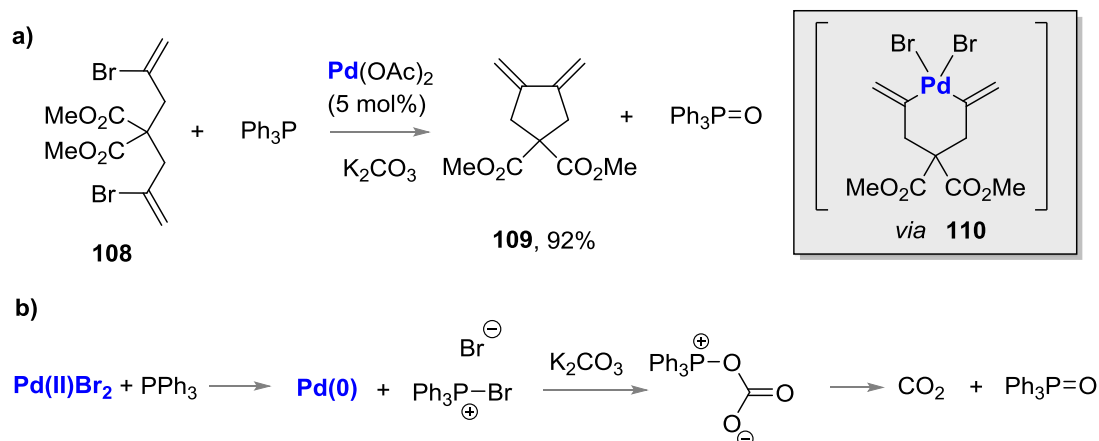
Since iodide **12a** was consumed fully in the majority of screened conditions, it can be concluded that oxidative addition is occurring, but that competitive side reactions are faster than the desired transmetallation step.

Lloyd-Jones and Lennox calculated that the hydrolysis of potassium cyclopropyl trifluoroborate is extremely rapid under basic conditions (hydrolytic half-life ($t_{1/2}$) = 7 minutes using Cs_2CO_3 in THF), with full conversion to the boronic acid in 2% of the time taken for a Suzuki-Miyaura coupling.¹³⁶ It was therefore surprising to see that coupling conditions which had previously failed with trifluoroborates (**Table 6**, Entry 7) gave full conversion with boronic acid, albeit with a longer reaction time and poor selectivity versus formation of diene **101** (**Table 6**, Entry 9). If we assume that transmetallation proceeds via palladium hydroxide intermediate **106**, then the rate of transmetallation (k_{transmet}) will be dependent of the concentration of boronic acid present in the organic phase (**Scheme 52**). A simple solubility experiment showed that cyclopropyl boronic acid was fully soluble in hot toluene whereas the corresponding trifluoroborate was only partially soluble. If a small equilibrium constant (K_{par}) exists for the partitioning of **107** between the two phases then the concentration of active boronic acid will be lowered, accounting for the poor conversion.



Scheme 52: Biphasic partitioning between boron species under cross coupling conditions (k_{transmet} = rate of transmetalation, k_{par} = rate of partitioning of active boronic acid between phases).

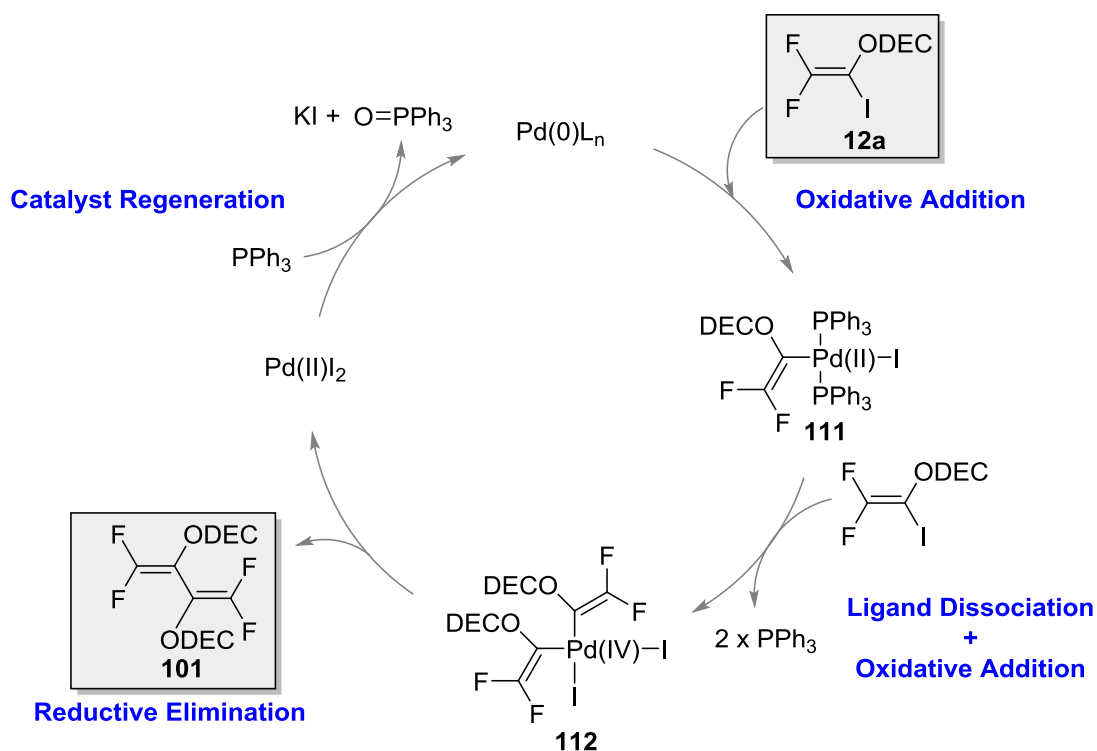
Further optimisation with cyclopropyl potassium trifluoroborate could focus on the effect of changing the base and solvent on increasing the concentration of active boronic acid in the organic phase; focus instead turned to investigating conditions which introduced the boronic acid directly. Despite the full consumption of iodide **12a**, the cross coupling of cyclopropyl boronic acid favoured the formation of diene **101** over desired VCP **49** (2.6:1, respectively, by ^{19}F NMR). The palladium-catalysed homocoupling of alkyl halides is not unknown¹³⁷ and the intramolecular coupling of alkenyl bromide **108** to 1,3-diene **109** provides some understanding of how diene **101** is forming (Scheme 53a).¹³⁸



Scheme 53: Intramolecular homocoupling of alkenyl bromide 108 via triphenylphosphine mediated regeneration of Pd(0).

Grigg and co-workers proposed that the reaction proceeds via two oxidative additions to form Pd(IV) intermediate **110**, which reductively eliminates to form the desired product and PdBr₂. Regeneration of the active Pd(0) catalyst is also known to be facilitated by triphenylphosphine and potassium carbonate (**Scheme 53b**).

In the formation of diene **101**, oxidative addition results in the formation of Pd(II) intermediate **111**, followed by a second oxidative addition to afford Pd(IV) intermediate **112** (**Scheme 54**). Despite it being an unusually high oxidation state, Pd(IV) species are known and reports from Muñiz show that they may be isolable and capable of catalytic reactions.¹³⁹ Reductive elimination of **112** results in PdI₂ which can be regenerated from the free triphenylphosphine present via ligand dissociation.



Scheme 54: Proposed catalytic cycle for the synthesis of diene 101.

During the first generation optimisation, ^{19}F NMR spectroscopy was used to understand how the reactions were proceeding, with distinctive peaks present for starting iodide **12a** and all of the products (**Figure 12**). In some reactions, two unknown peaks were observed (-89.6 and -115.8 ppm) containing an unexpected doublet of triplets coupling pattern ($^2J_{\text{F-F}} = 90.0$ Hz and $^4J_{\text{P-F}} = 7.0$ Hz, respectively). The smaller coupling correlated with a triplet in the $\{^1\text{H}\}$ ^{31}P NMR spectrum (18.36 ppm, t, $^4J_{\text{P-F}} = 7.7$ Hz) which allowed the compound to be tentatively identified as oxidative addition product **111**.

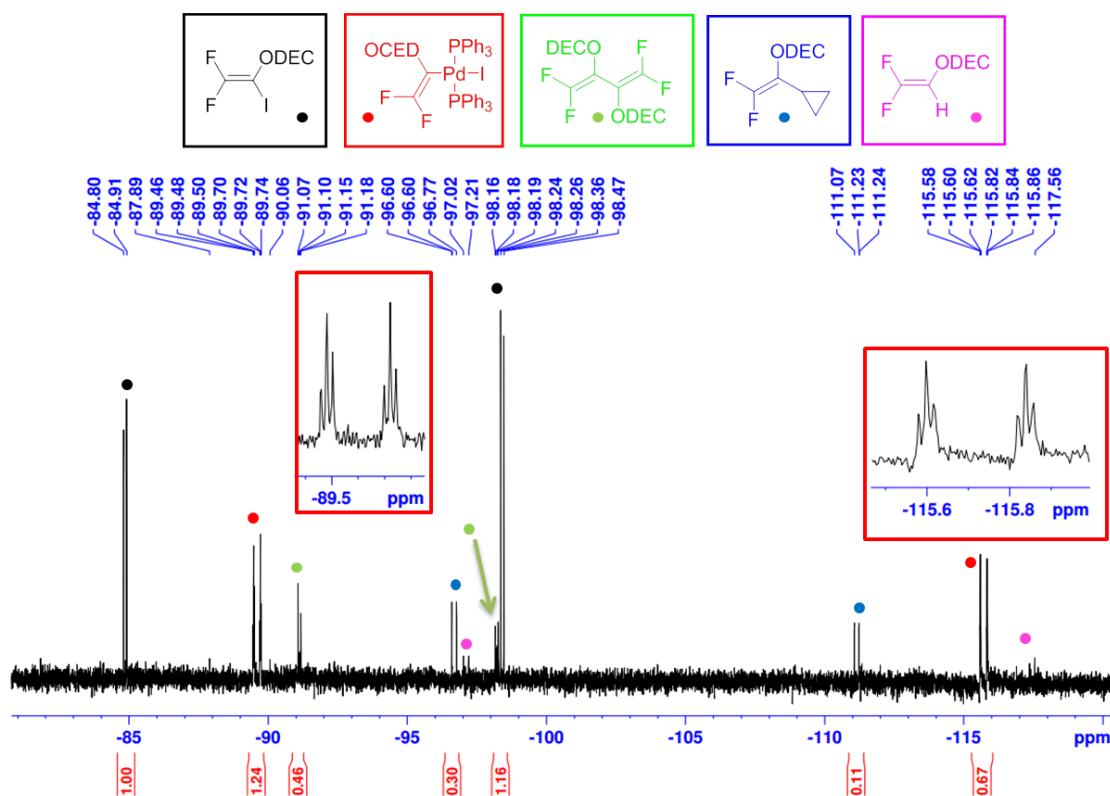
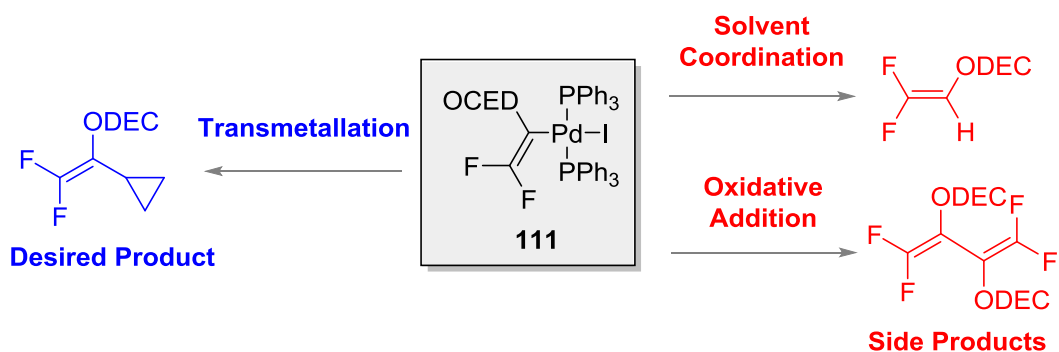


Figure 12: Crude ^{19}F NMR spectrum of coupling reaction mixture after 17 hours (Table 6, Entry 7) showing that starting material **12a**, oxidative addition intermediate **111** and all products are visible and distinguishable.

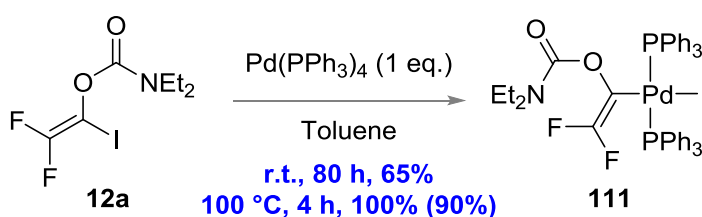
The presence of intermediate **111** after 17 hours under coupling conditions (Table 6, Entry 8) suggests that transmetallation is slow and that **111** is accumulating. The intermediate is also quite stable since it is still observed after aqueous work up. This intermediate is present in the proposed mechanism for all of the observed products, so isolation could help in understanding how to suppress the undesired side products (Scheme 55).



Scheme 55: Common intermediate **111** in the formation of desired product **99** and side products **100** and **101**.

2.2. Isolation of Oxidative Addition Intermediate **111**

Intermediate **111** was formed exclusively from iodide **12a** and stoichiometric amounts of *tetrakis*(triphenylphosphino)palladium(0) at room temperature by removing the transmetallation reagent from the reaction (**Scheme 56**), albeit with slow turnover and incomplete conversion after 80 hours. Increasing the reaction temperature to 100 °C afforded 100% conversion to **111** after 4 hours. The work up of the reaction mixture was simple, consisting of removing the toluene from the reaction mixture then precipitating intermediate **111** using DCM/MeOH. Filtration afforded a yellow solid in an excellent 90% yield; no signs of decomposition were observed after storage for over one year at -5 °C.



Scheme 56: Synthesis of oxidative intermediate **111** (relative conversion determined by ^{19}F NMR, isolated yield in parenthesis).

Oxidative addition occurs initially to form the *cis*-isomer, which quickly isomerises to the more stable *trans*-isomer.¹⁴⁰ The formation of **111** was followed by ^{19}F NMR but showed no evidence of two species, even at room temperature. This observation suggests strongly that the *cis*-isomer is short lived. The presence of only one distinct triplet in the $\{^1\text{H}\} \text{ }^{31}\text{P}$ NMR spectrum provided strong evidence that the *trans*-isomer had been isolated. X-ray quality crystals were grown by vapour diffusion from pentane and chloroform; the elucidation of the molecular structure in the crystal confirmed this analysis conclusively (**Figure 13**). The alkene carbons on intermediate **111** couple with fluorine and phosphorus atoms; 6144 scans with a relaxation time of 2 seconds in a 500 MHz spectrometer were required to observe them.

It has been proposed that the *N,N*-diethylcarbamoyloxy group is capable of chelating metal centres; from the structure, it looks like the oxygen is positioned over the metal centre. However, despite the carbonyl oxygen being close enough to

the palladium centre to represent an interaction (the Pd-O distance is 2.95 Å, the sum of the Van Der Waals radii is 3.15 Å), the group is more likely to be positioned this way to avoid a steric clash between the ethyl groups and phenyl rings. Looking at the bond lengths of the palladium ligands we can predict that the iodine is the most labile species (Pd-I distance 2.66 Å) and the alkene the most tightly bound (Pd-C distance 2.01 Å). Both the triphenylphosphine and iodide therefore have the potential to dissociate and facilitate transmetalation, consistent with the $[M-(Ph_3P+I)]$ mass ion of 546.1 a.u. observed during electrospray analysis.

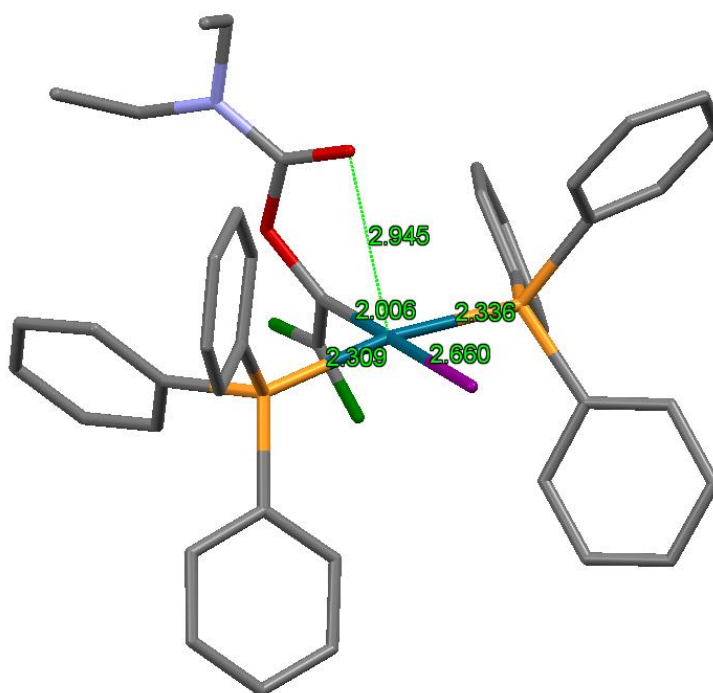
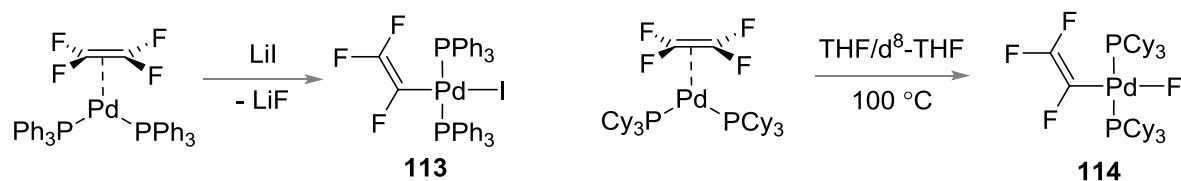


Figure 13: Crystal structure of intermediate **111** (hydrogen atoms omitted for simplicity, image from Mercury software).

Ogoshi and co-workers¹⁴¹ have reported two similar intermediates, **113** and **114**, but only the latter was synthesised via palladium oxidative addition (**Scheme 57**).



Scheme 57: Known literature examples of isolated Pd(II) intermediates (both confirmed by XRD).

A comparison between iodide **113** and intermediate **111** shows similar bond lengths (for **113**: Pd-I = 2.65 Å, Pd-C = 2.00 Å, Pd-P = 2.34 Å and 2.32 Å) but different

P-Pd-P angles (177.6° and 170.5° , respectively), suggesting that **111** is slightly skewed due to a steric clash between the diethyl carbamoyloxy and triphenylphosphino groups (**Figure 14**).

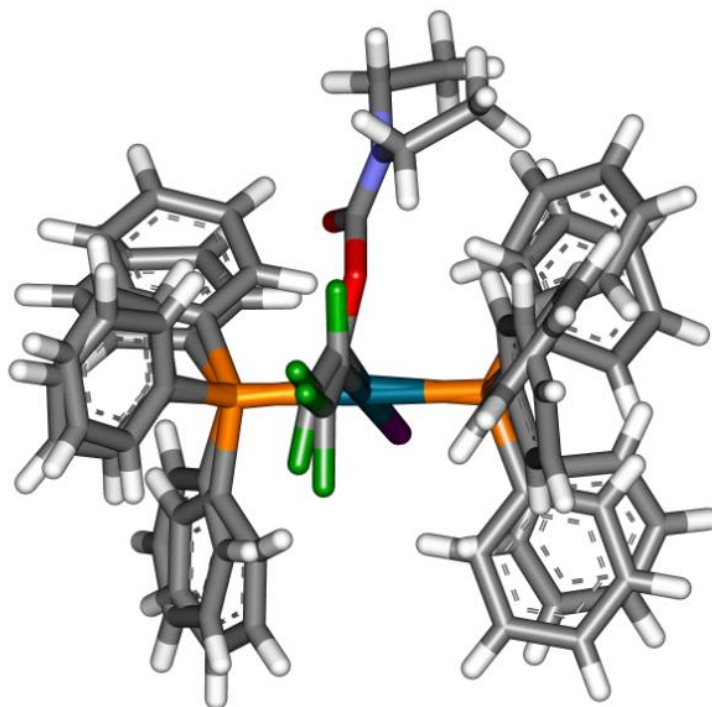


Figure 14: Crystal structure overlay of intermediate **111** and literature complex **113**^{141a} (overlay carried out using Accerlys software).

With the efficient synthesis and isolation of intermediate **111** secured, we sought to use the compound to investigate ways of suppressing formation of diene **101** and enol carbamate **100**.

2.2.1. Suppressing the Formation of Diene **101**

The proposed mechanism for formation of diene **101** can only operate catalytically if triphenylphosphine is present in the reaction mixture to reduce PdI_2 back to the active $\text{Pd}(0)$ catalyst. Therefore, the reaction between intermediate **111** and iodide **12a** was carried out in the presence of different quantities of added triphenylphosphine (**Table 7**). It was thought that the triphenylphosphine would speed up diene formation, but instead, it was completely suppressed, with both low and high loadings of triphenylphosphine (**Table 7**, Entries 1-3). The control reaction from which triphenylphosphine was absent confirmed that an extra ligand was needed to control diene formation (**Table 7**, Entry 4). Interestingly, the ^{19}F NMR for

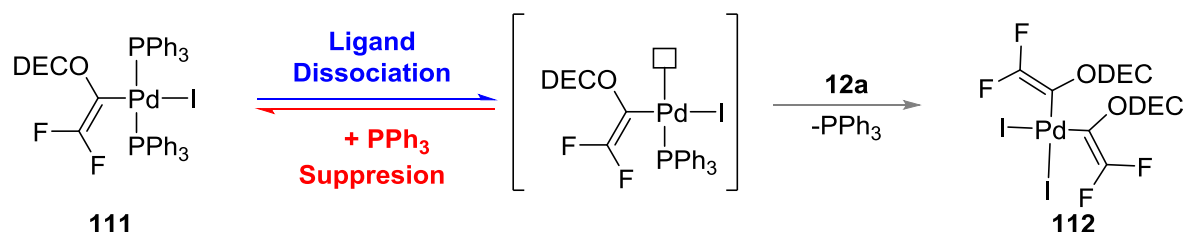
the control reaction showed the presence of iodide **12a** (60%) and diene **101** (40%) but no intermediate **111**. This suggests that an alternative mechanism, in which two molecules of **111** can react together to form diene **101** without the need for iodide **12a** is possible.

Table 7: Doping with Triphenylphosphine Suppresses Diene Formation

| Entry | PPh ₃ (eq.) | Diene (%) ^[a] |
|-------|------------------------|--------------------------|
| 1 | 0.3 | 0 |
| 2 | 0.5 | 0 |
| 3 | 1 | 0 |
| 4 | 0 | 40 |

[a] Determined by ¹⁹F NMR.

The proposed alternative mechanism for the formation of **111** goes via ligand dissociation, supporting the fact that an increased amount of triphenylphosphine will hinder the process, slowing the second oxidative addition to intermediate **112** by favouring ligand association.



Scheme 58: Triphenylphosphine addition suppressing the formation of diene **101** by slowing down formation of Pd(IV) intermediate **112**.

The crystal structure suggests strongly that the Pd-I bond was the weakest, allowing iodide to theoretically undergo ligand dissociation and promote a second oxidative addition or transmetalation.^{138a} Silver salts are often used to promote iodide dissociation from metals, and Deng's conditions¹⁴² were investigated with our system (**Table 8**). Attempts to couple **12a** with cyclopropyl boronic acid failed; diene **101** was the major product and trace amounts of enol carbamate **100** were formed (**Table 8**, Entry 1). Removal of boronic acid gave similar results (**Table 8**, Entry 2) suggesting that the second oxidative addition is favoured over transmetalation

when iodide is sequestered from palladium complex **111**. Confirmation of this was obtained by omitting both silver oxide and boronic acid from the reaction mixture, resulting in the slow formation of intermediate **111** only (**Table 8**, Entry 3).

Table 8: Effects of Iodide Dissociation in Side Product Formation

| Entry | 115 (eq.) | Base (eq.) | Solvent | SM ^[a] (12a) | Product ^[a] (99) | Enol ^[a] (100) | Diene ^[a] (101) | Ox. Int. ^[a] (111) |
|------------------|-----------|--------------------------------------|----------------------------------|-------------------------|-----------------------------|---------------------------|----------------------------|-------------------------------|
| 1 ^[b] | 1.1 | Ag ₂ O (1.3) | Dioxane | X | X | 3% | 97% | X |
| 2 | - | Ag ₂ O (1.3) | Dioxane | X | X | X | 100% | X |
| 3 | - | - | Dioxane | 83% | X | X | X | 17% |
| 4 | 1.1 | Ag ₂ O (1.3) / NaOH (3.3) | Dioxane / H ₂ O (1:1) | X | X | 69% | 31% | X |

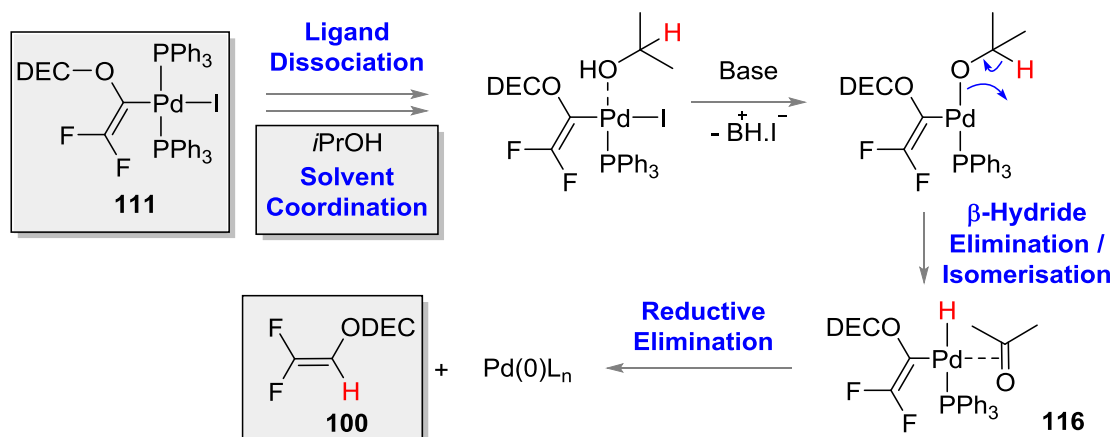
[a] Relative percentage determined by ¹⁹F NMR. [b] Conditions derived from Deng and co-workers.¹⁴²

Interestingly, conversion to enol carbamate **100** was favoured when NaOH and water were added to the reaction system (**Table 8**, Entry 4). This suggests that the second oxidative addition step is competing with an unknown mechanism which ultimately forms enol carbamate **100**. Solvent investigations were carried out on intermediate **111** in attempts to understand this alternative mechanism.

2.2.2. Suppression of Formation of Enol Carbamate **100**

Previous work within the group showed that alcohol solvents containing β-hydride protons facilitated the formation of enol carbamate **100** under cross coupling conditions.²⁶ The key step in the proposed mechanism is coordination of the alcohol to intermediate **111** (**Scheme 59**). Base-mediated HI elimination followed by β-

hydride elimination affords palladium complex **116**, which reductively eliminates enol carbamate **100** and regenerates the active catalyst.



Scheme 59: Previously proposed mechanism for enol carbamate **100 formation.**

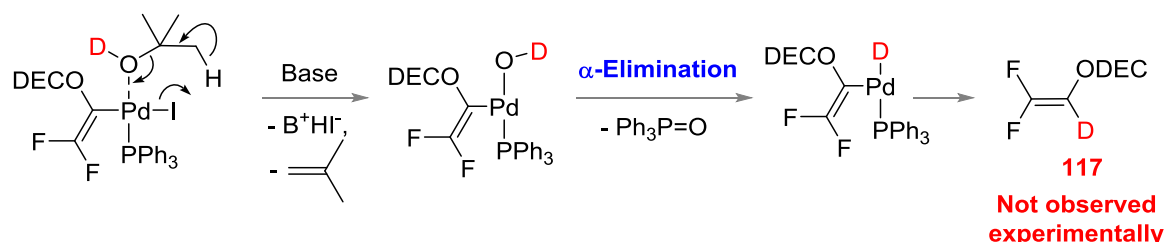
Refluxing intermediate **111** in *i*PrOH gave 100% conversion to enol carbamate **100** supporting the idea that the mechanism involves solvent coordination to the intermediate but does not require the presence of base (**Table 9**, Entry 1). Previously, formation of enol carbamate **100** could be suppressed (in part) by using tertiary alcohols. However when optimised coupling conditions using *t*-BuOH were screened, **100** still formed as a minor product. Heating **111** in *t*BuOH alone gave 10% conversion to enol carbamate **100** after 19 hours (**Table 9**, Entry 2) confirming an alternative mechanism must exist.

Table 9: Effects of Solvent on the Formation of Enol Carbamate **100**

| Entry | Solvent (v/v) | Temp. (°C) | Time (h) | Solubility | Enol ^[a] (100) | Diene ^[a] (101) | Ox. Int. ^[a] (111) |
|------------------|--|------------|----------|--------------------------|---------------------------|----------------------------|-------------------------------|
| 1 | <i>i</i> PrOH | 85 | 16.5 | Sparingly | 100 | 0 | 0 |
| 2 | <i>t</i> BuOH | 100 | 19 | Sparingly ^[b] | 10 | 0 | 90 |
| 3 | <i>t</i> BuOD | 100 | 19 | Sparingly ^[b] | 6 | 0 | 94 |
| 4 | THF/ <i>t</i> BuOH (1:1) | 100 | 19 | Partial | 13 | 0 | 87 |
| 5 | THF/ <i>t</i> BuOD (1:1) | 100 | 19 | Partial | 25 | 0 | 75 |
| 6 | <i>t</i> BuOH/H ₂ O (2.7:1) | 100 | 19 | Sparingly | 6 | 0 | 94 |
| 7 ^[c] | <i>t</i> BuOH/H ₂ O (2.7:1) | 100 | 19 | Sparingly | 62^[d] | 0 | 0 |

[a] Relative percentage conversion determined by ¹⁹F NMR. [b] Reaction mixture was frozen before heating. [c] K₃PO₄ (3 eq.) [d] No other side products formed but unknown impurities were present.

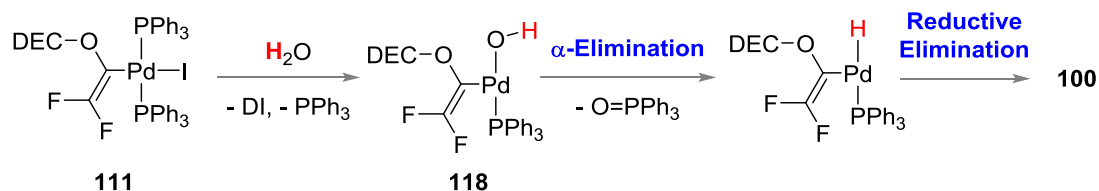
It was proposed that when *t*BuOH complexed with the palladium, α-hydride elimination could occur from the alcohol proton (**Scheme 60**) but refluxing in *t*BuOD only gave **100** and not the deuterated species **117** (**Table 9**, Entry 3).

**Scheme 60:** Proposed α-elimination mechanism for the formation of enol carbamate **117**.

The solubility of intermediate **111** was higher in mixtures of THF/*t*BuOH or THF/*t*BuOD and formation of **100** increased slightly but not significantly (**Table 9**, Entries 4 and 5, respectively). The less solubilising combination of *t*BuOH/H₂O gave poor conversion (**Table 9**, Entry 6; 6% conversion to enol carbamate) but the introduction of base dramatically increased the rate of conversion, with enol carbamate forming in 62% conversion over the same period of time (**Table 9**, Entry 7). These results highlight that an as yet unknown mechanism is operational in the

formation of enol carbamate **100** but stress that the presence of base and alcohol solvents do favour the side reaction.

Under Negishi and Kumada coupling conditions with iodide **12a**, the major product was always enol carbamate **100**. No alcohol was present under these conditions and refluxing **111** in THF alone showed no reaction (**Table 10**, Entry 1). Even though these couplings were run under anhydrous conditions, the presence of trace amounts of water could facilitate the formation of hydroxypalladium intermediate **118**. This can undergo α -elimination, then reductive elimination to form enol carbamate **100** (**Scheme 61**). Experiments using deuterated water and THF were carried out to investigate this proposed mechanism.



Scheme 61: Proposed mechanism for the formation of enol carbamate **100** via hydroxypalladium intermediate **118**.

Table 10: Effect of Water on the Formation of Enol Carbamate **100**

$$\text{111} \xrightarrow[\text{Solvent}]{\text{Base}} \begin{array}{c} \text{H} \quad \text{ODEC} \\ \diagdown \quad / \\ \text{C} \\ / \quad \diagdown \\ \text{F} \quad \text{F} \\ \text{100} \end{array} + \begin{array}{c} \text{ODECF} \\ \diagdown \quad / \\ \text{C} \\ / \quad \diagdown \\ \text{F} \quad \text{ODEC} \\ \text{101} \end{array}$$

| Entry | Solvent | Base (eq.) | Temp. (°C) | Time (h) | Solubility | Enol ^[a] (100) | Diene ^[a] (101) | Ox. Int. ^[a] (111) |
|------------------|--|------------------------------------|------------|----------|------------|---------------------------|----------------------------|-------------------------------|
| 1 | THF | - | 85 | 16.5 | Fully | 0 | 0 | 100 |
| 2 | THF/D ₂ O (4.6:1) | - | 80 | 14.5 | Fully | 0 | 0 | 100 |
| 3 | d ⁸ -THF/H ₂ O (4.6:1) | - | 100 | 90 | Fully | 0 | 25 | 75 |
| 4 | d ⁸ -THF/H ₂ O (4.6:1) | K ₃ PO ₄ (3) | 100 | 90 | Fully | 14 | 0 | 86 |
| 5 | THF/D ₂ O (4.6:1) | K ₃ PO ₄ (3) | 100 | 90 | Fully | 0 | Trace | > 95 |
| 6 ^[b] | THF/H ₂ O (4.6/1) | K ₃ PO ₄ (3) | 100 | 24 | Fully | 19 | 18 | 53 |

[a] relative percentage conversion determined by ¹⁹F NMR. [b] Cyclopropyl boronic acid (1 eq.) added to the reaction mixture (10% conversion to cyclopropyl **99**).

Unfortunately, intermediate **111** remained unchanged when heated in an equimolar solution of THF and D₂O (**Table 10**, Entry 2); the control reaction with *d*⁸-THF and H₂O gave no enol carbamate **100** (**Table 10**, Entry 3). Running the latter reaction in the presence of base gave 14% conversion to **100** after refluxing for 90 hours (**Table 10**, Entry 4). This rate enhancement could be due to the base facilitating the conversion of intermediate **111** to hydroxypalladium complex **118**. Interestingly, when the same conditions were used with THF/D₂O, no enol carbamate was observed either as the deuterated or protonated species (**Table 10**, Entry 5). Deuterium has a stronger bond than hydrogen to the oxygen atom¹⁴³ suggesting that the rate determining step for the formation of enol carbamate involves the breaking of a hydrogen-oxygen bond, providing strong support that water is the source of the proton. However, such a dramatic difference between the two solvents is rare when considering primary isotope effects. Finally, when cyclopropylboronic acid and K₃PO₄ were refluxed with intermediate **111** in THF and water, faster conversion to enol carbamate **100** and diene **101** was observed (**Table 10**, Entry 6). This suggests that the boronic acid may also have a role in aiding the formation of the hydroxyl-palladium **118**.

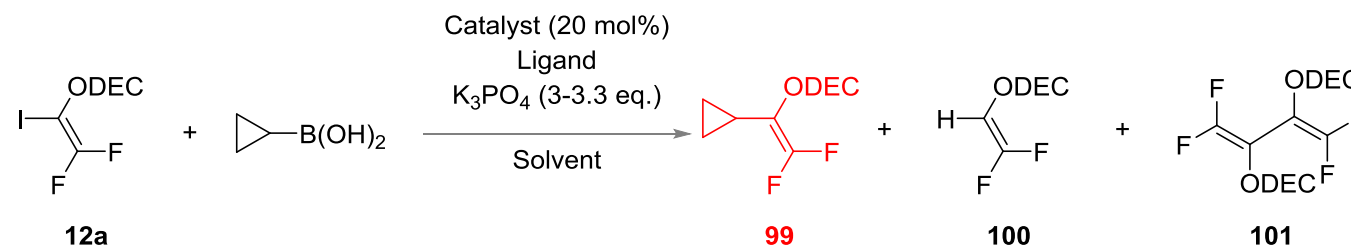
Some mechanistic understanding of the formation of diene **101** and enol carbamate **100** under coupling conditions has been obtained from investigating ligand and solvent effects on intermediate **111**, respectively. The results suggest that carrying out the coupling reactions with triphenylphosphine additive should slow down diene formation and allow transmetalation to proceed. It is beneficial that only a low concentration of ligand is required to stop diene formation (0.3 equivalents with respect to intermediate **111**) because the presence of ligand can also hinder catalyst activation. Suppression of enol carbamate formation was less clear but lowering the amount of water and base present within the reaction should help. Though experiments also showed that cyclopropyl boronic acid facilitated the formation of **100** and **101**, it was hoped that the other modifications would be enough to counteract this rate enhancement.

2.3. 2nd Generation Optimisation

The initial 1st generation optimisation focused on literature procedures for a range of cyclopropyl nucleophile coupling partners. Only cyclopropyl boronic acid gave full conversion of iodide **12a** but favoured formation of diene **101** and the reaction time of 66 hours was undesirable (**Table 11**, Entry 1). Using anhydrous, degassed toluene allowed the volume of water to be controlled and, with exactly 1 and 3 equivalents of water (with respect to base), conversion to product increased to 50% and 68% respectively (**Table 11**, Entries 2 and 3, respectively). At this stage a small assay was carried out based on literature conditions^{26,123a,132,144} to investigate the effects of varying catalyst, ligand or base. A combination of Pd(OAc)₂ and XPhos (**Table 11**, Entry 4) showed comparable results over a shorter time (65% conversion to **99** after 20 h) but the rest resulted in poorer conversion (**Table 11**, Entries 5-7). Since ligand dissociation is disfavoured with chelating ligands, it was thought that Cl₂Pd(dppf) could slow the formation of diene **101**; however, it formed as the major product (90% conversion to **101**, **Table 11**, Entry 7). Insights obtained from working with intermediate **111** were therefore implemented in the hope that formation of the unwanted side products would be suppressed.

It was shown that the rate of formation of enol carbamate **100** was directly related to the volume of water within the reaction mixture. A balance had to be obtained between having enough water to dissolve the base for transmetallation but not enough to trigger formation of **100**. A toluene/water ratio of 29:1 (v/v via syringe addition to microwave vial) was selected since it allowed full conversion of starting material and intermediate **111**, with formation of enol carbamate **100** only as a minor product (8% conversion to **100**, **Table 11**, Entry 3). Doping reactions with triphenylphosphine allowed for suppression of formation of diene **101**; however the presence of 40 mol% ligand slowed oxidative addition, leading to a low (46%) conversion to desired product after 48 hours (**Table 11**, Entry 8). Lowering the amount of ligand to 10 mol% allowed full turnover of iodide **12a** after 26 hours at a higher temperature (**Table 11**, Entry 9). Despite a high conversion to the desired product (65% conversion), a significant amount of intermediate **111** remained (24%

conversion), suggesting that transmetallation was sluggish. The heat source was changed to microwave irradiation which has previously been used to decrease reaction times of Suzuki-Miyaura cross-couplings.¹⁴⁵ Using the same conditions in the microwave at 150 °C, reaction times were decreased to 10 minutes while a good product conversion was maintained (62% conversion to **99**, **Table 11**, Entry 10). Further investigations into the faster Pd(OAc)₂/XPhos combination were not carried out because it was expected that more equivalents of the more expensive ligand would be required to suppress formation of diene **101**. The much shorter reaction times allowed rapid screening of specific variables within the reaction, starting with the effect different bases have on product formation.

Table 11: Cyclopropyl Boronic Acid Coupling Optimisation


| Entry | Catalyst | Ligand (mol%) | Solvent ^[a] | Temp. (°C) | Time (h) | SM ^[b] (12a) | Ox. Int. ^[b] (111) | Product ^[b] (99) | Enol ^[b] (100) | Diene ^[b] (101) |
|----------------------|--|-----------------------|----------------------------------|--------------------|----------|-------------------------|-------------------------------|-----------------------------|---------------------------|----------------------------|
| 1 ¹³² | Pd(PPh ₃) ₄ | - | Toluene (wet) | 80 | 66 | 0 | 0 | 28 | 0 | 72 |
| 2 | Pd(PPh ₃) ₄ | - | Toluene/H ₂ O (63:1) | 100 | 40 | 0 | 37 | 50 | 0 | 7 |
| 3 | Pd(PPh ₃) ₄ | - | Toluene/H ₂ O(20:1) | 100 | 40 | 0 | 0 | 68 | 8 | 24 |
| 4 ^[c] | Pd(OAc) ₂ | XPhos (45) | Toluene | 100 | 22 | 0 | 0 | 65 | 4 | 31 |
| 5 ¹²⁹ | Pd(OAc) ₂ | PCy ₃ (40) | Toluene/H ₂ O (20:1) | 100 | 20 | 33 | 0 | 10 | 14 | 43 |
| 6 ²⁶ | (Cl) ₂ Pd(PPh ₃) ₂ | - | Toluene | 100 | 22 | 0 | 0 | 6 | 0 | 94 |
| 7 ^{131/[c]} | (Cl) ₂ Pd(dppf) | - | Toluene/H ₂ O (3:1) | 100 | 45 | 0 | 0 | 10 | 0 | 90 |
| 8 | Pd(PPh ₃) ₄ | PPh ₃ (40) | Toluene/H ₂ O(28.6:1) | 100 | 48 | 27 | 27 | 46 | Trace | 0 |
| 9 | Pd(PPh ₃) ₄ | PPh ₃ (10) | Toluene/H ₂ O(28.6:1) | 120 | 26 | 0 | 24 | 65 | 7 | 7 |
| 10 | Pd(PPh ₃) ₄ | PPh ₃ (10) | Toluene/H ₂ O(28.6:1) | 150 ^[d] | 10 (min) | 0 | 0 | 62 | 11 | 27 |

[a] All organic solvents were anhydrous and degassed unless otherwise stated. [b] Relative percentage conversion determined by ¹⁹F NMR (predicted >5% error in integrations). [c] Cs₂CO₃ used as base. [d] Microwave irradiation.

2.3.1. Effect of Base

The base used during Suzuki-Miyaura cross couplings is crucial to controlling transmetalation and has even been shown to speed up the reductive elimination of *trans*-ligands in palladium complexes.^{127c} Lowering the stoichiometry in base within the reaction would be beneficial since less water would be required; this would help to suppress enol carbamate formation. A small linear screen was carried out in the

microwave, investigating the effect one, two and three equivalents of K_3PO_4 had on product conversion. No significant difference was observed between higher equivalents of base but lower numbers of equivalents gave approximately 10% decrease in product formation (^{19}F NMR conversion).

The type of base used during the cross coupling was also examined, focusing on the effect of varying base strength and counter ions (**Figure 15**). From this assay it was apparent that only KOH and K_3PO_4 gave full conversion of iodide **12a** after 20 minutes at 150 °C in the microwave, with the former giving a higher NMR yield of 50% (c.a. K_3PO_4 with 36% yield).

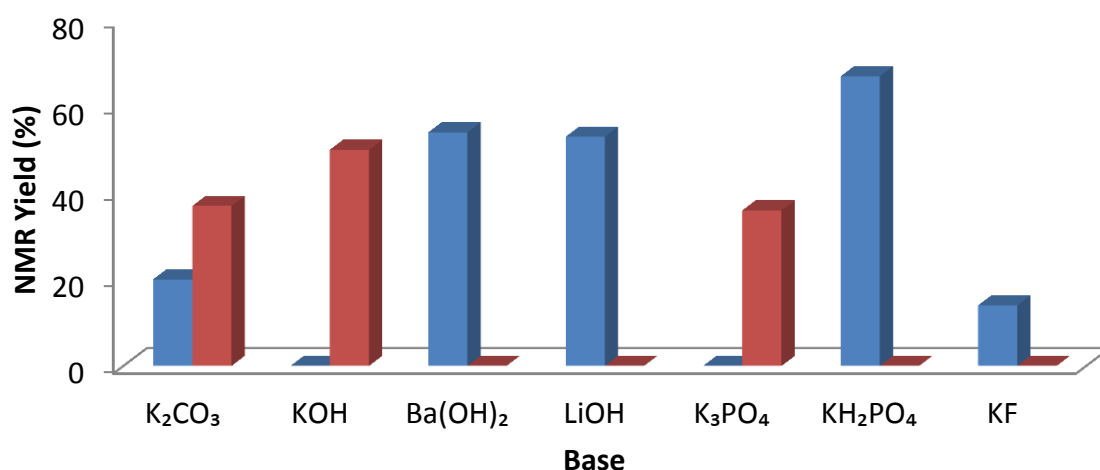


Figure 15: Effect of type of base on second generation coupling conditions (blue = iodide 12a, red = cyclopropyl 99). Conditions: Iodide 12a (0.18 mmol), cyclopropyl boronic acid (0.27 mmol), trihenylphosphine (0.02 mmol), *tetrakis*(triphenylphosphino)palladium(0) (0.04 mmol), trifluorotoluene (0.04 mmol), toluene (1 mL), water (0.035 mL) and base (0.36 mmol), 150 °C, μw , 20 minutes, yield determined by ^{19}F NMR and internal standard.

The range of results can be best explained by comparing product yield with the strength of the base. The aqueous pK_a of the conjugate acid gives a good guide to base strength since strong acids dissociate to weak bases. The assay above shows that a trend exists between product yield and base strength, with stronger bases giving increased yields (**Figure 16**).

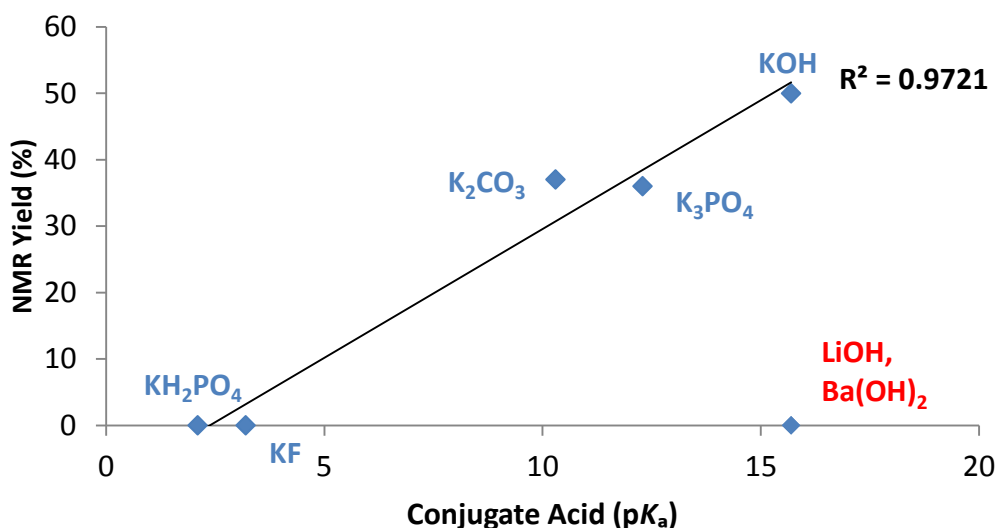


Figure 16: Linear correlation between base strength (conjugate acid pK_a) and product yield.

The graph also outlines the importance of the counter ion; both the lithium and barium hydroxide reactions stalled at oxidative intermediate **111** (only iodide **12a** and intermediate **111** were observed by ^{19}F NMR). Jutand and co-workers^{127c} have used electrochemical techniques to investigate the mechanistic roles of base within Suzuki-Miyaura couplings. One finding suggests that counter ions can have a rate retarding effect on the reaction of palladium complex **119** and phenyl boronic acid (Figure 17). A graph of reaction rate against equivalents of hydroxide base showed a distinct bell-shaped curve when phenyl boronic acid (1 equivalent) and base (approx. 0.4-1.0 equivalents) were used in the reaction with oxidative intermediate **119** (5 mol%). Lower numbers of equivalents of base were more detrimental during the coupling of iodide **12a**, so comparisons could not be made with our system; no further base investigations were carried out from intermediate **111**. However, similar to our screening into the type of base, Jutand and co-workers observed an obvious difference in rates between bases with different counter ions; quaternary ammonium cation $n\text{Bu}_4\text{N}^+$ showed higher reactivity than inorganic (K^+ , Cs^+ and Na^+) counter ions.

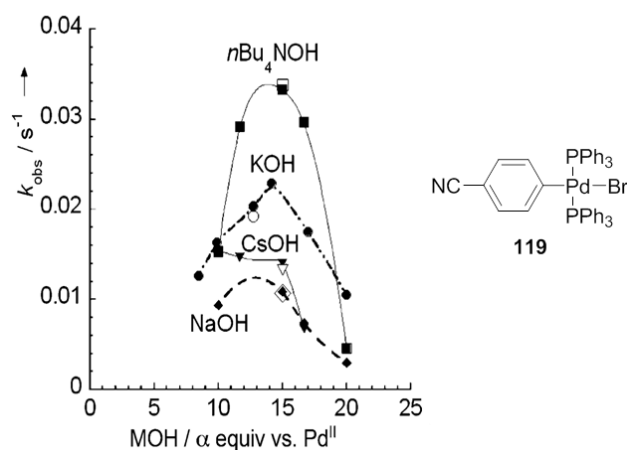
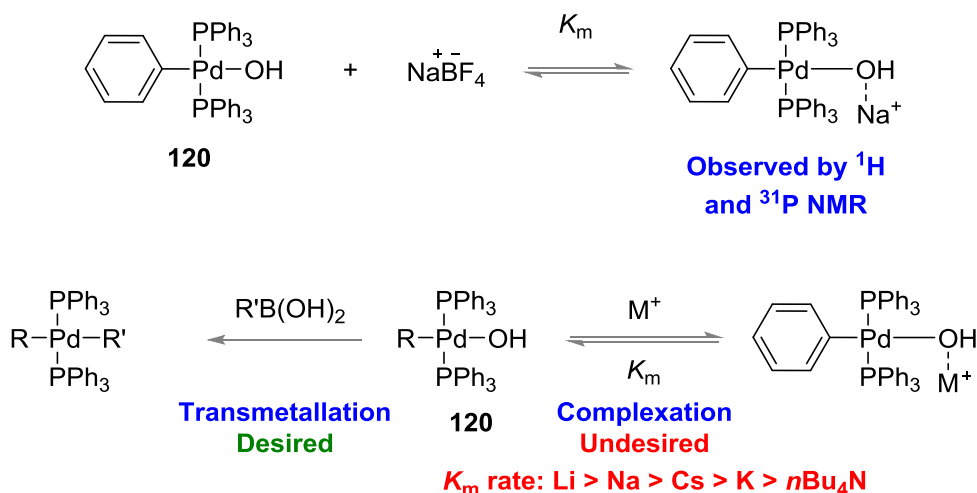


Figure 17: Base effect on the reaction rates of PhB(OH)_2 (20 eq.) and palladium intermediate **119** (1 eq.). Reaction mixtures also contained Ph_3P (2 eq.) and base (α eq.).^{127c}

They proposed that the base acts as a ligand throughout the catalytic cycle and the rate determining transmetalation step is dependent on the formation of hydroxypalladium intermediate **120**. Cations bind strongly to alcohols and NMR evidence has shown that Na^+ can effectively bind to **120** by reversible complexation to hydroxide ligand, removing the key intermediate from the cycle (**Scheme 62**).^{127b}



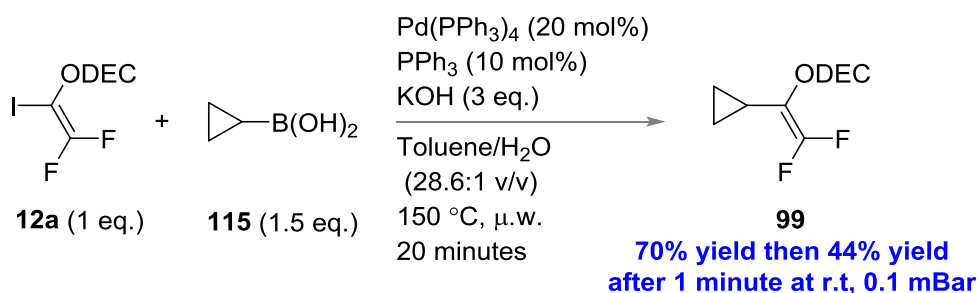
Scheme 62: Proposed counter cation binding to hydroxypalladium complex **120** has the potential to slow transmetalation.

There is a trend linking rate differences with cation-alcohol affinity, with decreased rates observed for stronger binding cations.¹⁴⁶ This is consistent with the rate difference observed between KOH and LiOH in couplings of iodide **12a**, since lithium

has a stronger affinity than potassium to bind to alcohol (determined by DFT, but for gas phase calculations).

2.4. Best Coupling Conditions

The isolation of cyclopropyl **99** was attempted at various points throughout the optimisation of cross coupling conditions but yields were always low and inconsistent with observed ^{19}F NMR conversions. These issues were attributed to the volatility of the product and confirmed from a low retention time after GC/MS analysis ($t_{\text{R}} = 9.78$ minutes, 40-320 °C temperature program, ramp rate = 20 °C min^{-1} with methane carrier gas flow at 1 $\text{cm}^3 \text{min}^{-1}$). Using the quicker microwave conditions designed to suppress side product formation resulted in a 60% conversion to desired product **99** (Scheme 63).



Scheme 63: Scaled up cross-coupling reaction (0.9 mmol) using optimised conditions.

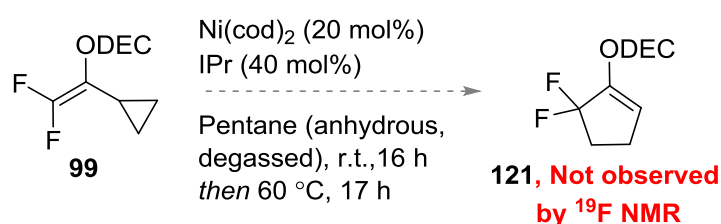
The remaining reaction mixture consisted of diene **101** (40%) and column chromatography was required to enable separation. Pentane was used in attempts to avoid unnecessary loss of product during evaporation of column fraction. Controlled evaporation resulted in a 70% crude yield but the compound still contained chromatography solvent; further evaporation under reduced pressure (r.t., 0.1 mbar) for one minute removed both solvent and product, decreasing the isolated yield to 44%. Despite these disappointing results sufficient amounts of precursor could be isolated to test VCPR and these were carried out first before committing to further optimisation of the cross coupling.

2.5. Rearrangement of Cyclopropyl **99**

The purest batch of cyclopropane **99** was used to test both nickel catalysed and thermal rearrangement conditions.

2.5.1. Nickel Catalysed Rearrangement

Louie and co-workers reported nickel catalysed rearrangement of various unactivated vinyl cyclopropanes.^{82b} These reaction conditions were appealing because they allowed the rearrangements to proceed at room temperature and attempts were made to implement the same conditions with cyclopropane **99** (Scheme 64).



Scheme 64: Failed attempt at nickel catalysed VCPR of cyclopropyl **99**.

Louie reported that glove box conditions were not necessary to prepare and handle the key catalyst, so the reaction was attempted within a fumehood using stringently anhydrous conditions. Unfortunately, neither the published room temperature nor more forcing 60 °C conditions showed any rearranged product, even with higher catalyst and ligand loading than reported in the literature (Louie reports Ni(cod)₂ at 1 mol% and IPr at 2 mol%).^{82b} As previously discussed, Louie and co-workers used electronic structure calculations to predict that, due to steric repulsion between reagents, tri- and tetrasubstituted olefins have a high activation barriers and are unlikely to rearrange.¹⁰⁶ Despite being tetrasubstituted, it was expected that cyclopropyl **99** could still rearrange because the fluorine atoms are smaller than the methyl substituents present in the substrates examined by Louie.

A greenish-black reaction solution was expected during the reaction but instead it remained beige throughout. This suggest that the required Ni/IPr catalyst complex never formed within the reaction, most likely due to catalyst poisoning from contact with air or impurities within the cyclopropane starting material. The obvious

requirement for more stringent anhydrous conditions and the highly toxic nature of the nickel catalyst makes these reactions undesirable, favouring investigations into thermal conditions.

2.5.2. Thermolysis

The same batch of cyclopropyl **99** used above was reacted in a sealed vial with incremental increases in temperature from 120 to 250 °C; low temperatures of 60 °C in the presence of nickel complexes showed no evidence of background thermal rearrangement. ^{19}F NMR was used to follow the reaction throughout but there were no signs of the formation of a difluorinated sp^3 -carbon centre (**Figure 18**). Instead, the starting cyclopropane remained and showed no signs of decomposition; even from the higher temperature reactions (no changes in product ^{19}F NMR signals were observed).

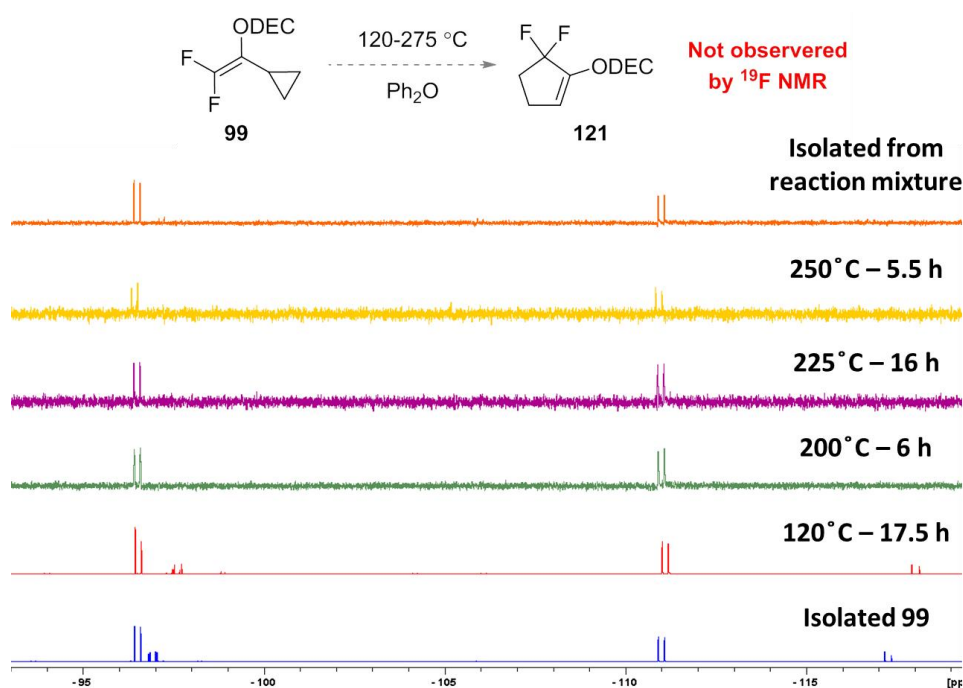
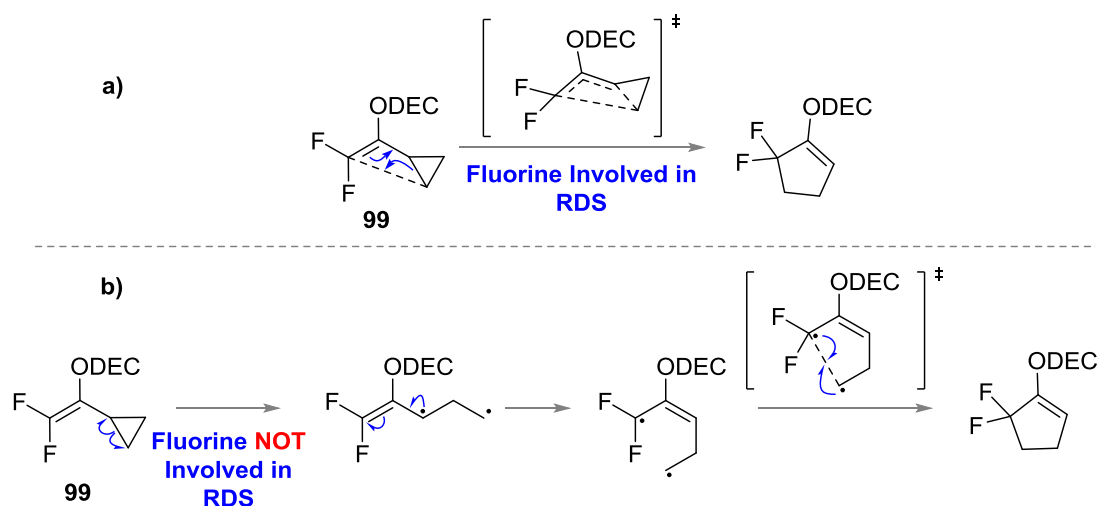


Figure 18: ^{19}F NMR analysis of the pyrolysis attempts of cyclopropyl **99**.

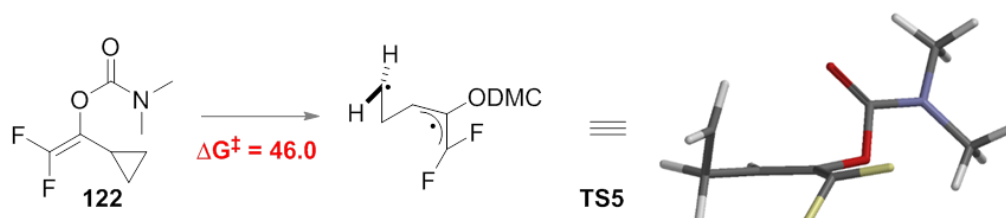
These results suggest that the mechanism is likely to involve a diradical species instead of being a concerted process. The latter would benefit from the favourable energy transformation of the difluorinated carbon, lowering the activation energy for the rearrangement (**Scheme 65a**). A diradical mechanism is initiated by the

homolytic cleavage of a cyclopropane bond. For compound **99**, the fluorine atoms are not involved in this process, so no lowering in activation energy is expected (**Scheme 65a**). Literature examples for unactivated, non-fluorinated vinyl cyclopropanes required higher temperatures (325-500 °C) to initiate rearrangement.⁷⁴ These high temperatures are unattainable with general laboratory equipment, making the thermal process unattractive.



Scheme 65: a) Concerted and b) diradical based VCPR mechanism for cyclopropyl **99**.

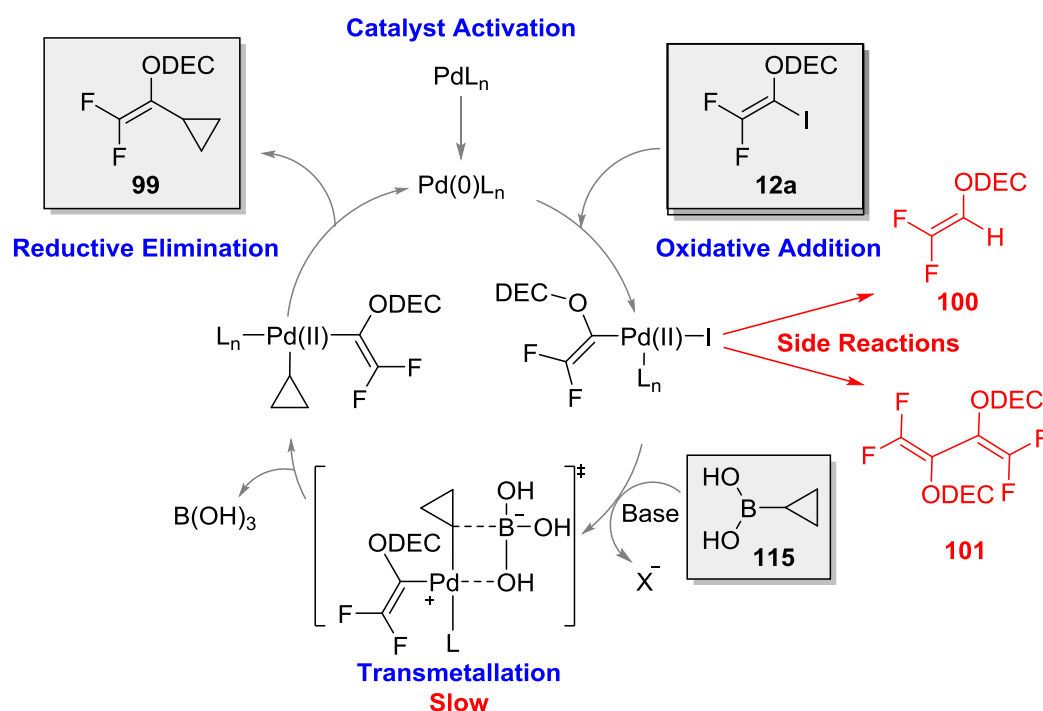
Further studies carried out into the VCPR allowed the development of computational methodology for assessing thermal rearrangements (*vide infra*). These were used in a retrospective manner to predict the ease of thermal rearrangement of precursor **99**. A very high calculated activation energy of 46.0 kcal mol⁻¹ from conformationally simpler methyl carbamate **122** to diradicaloid **TS5** suggested that extremely high temperatures would be required to induce rearrangement (**Scheme 66**).



Scheme 66: Electronic structure calculation for the thermal VCPR of **122** (DMC = dimethyl carbamate, Spartan'10, B3LYP/6-31G*, gas phase, 298 K, energy in kcal mol⁻¹).

2.6. Conclusion

The development of a one-step synthetic route for the synthesis of a novel difluorinated vinylcyclopropane has been examined using palladium-catalysed coupling reactions between iodide **12a** and cyclopropane coupling partners. Initial optimisation with different cyclopropyl nucleophiles suggested that the transmetallation step was rate determining, with only cyclopropyl boronic acid leading to product formation. This slow step allowed competing side reactions to dominate, resulting in the formation of enol carbamate **100** or diene **101** (Scheme 67).



Scheme 67: Catalytic cycle for Suzuki-Miyaura coupling of iodide **12a** and boronic acid **115**.

A simple reaction between iodide **12a** and stoichiometric amounts of tetrakis triphenylphosphine palladium(0) afforded key oxidative addition intermediate **111** in excellent yields. Experiments which varied solvent and ligand were performed, showing that type of solvent, number of equivalents of base and free ligand played an important role in the formation of enol carbamate **100** and diene **101**, respectively. Microwave conditions dramatically decreased reaction times (from 26 hours to 10 minutes) and successful implementation of suppression techniques allowed isolation of cyclopropane **99** in a moderate 44% yield (Scheme 63) from the

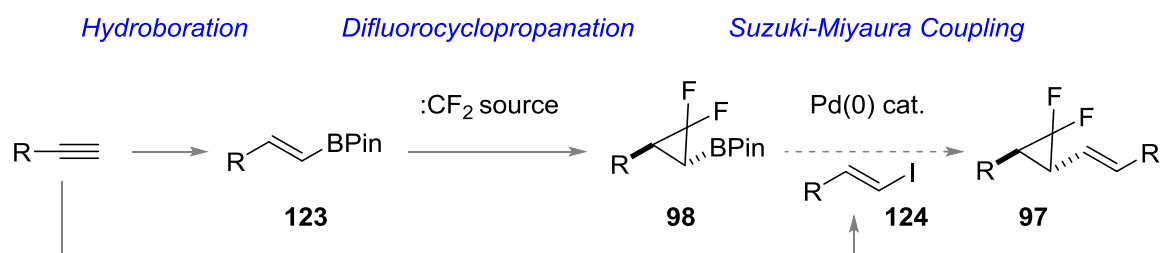
first successful alkyl-vinyl cross coupling with difluorovinyl iodide **12a**. Unfortunately, isolation of pure **99** proved problematic due to volatility and only spectroscopic characterisation could be obtained. Tests on the rearrangement could still be performed and screening of both metal and thermal mediated rearrangements were carried out. Disappointingly, no evidence of difluorocyclopentene **121** was observed, even when the VCP was heated to 220 °C. A very high calculated activation barrier of 46.0 kcal mol⁻¹ made it apparent that synthetically useful thermal rearrangements were unlikely to be achieved for this precursor.

The results from the rearrangement confirm that fluorine atom substitution on the alkene fragment of VCP precursors do not aid the thermal rearrangement to the same extent as *gem*-difluorinated cyclopropanes, consistent with a diradicaloid mechanism. Focus turned into developing the synthesis of these precursors over continued research into modification of cyclopropane **95**.

*Disclaimer: X-ray diffraction of epoxide **156** and acetal **158** were obtained, processed and refined by Dr. Alan Kennedy (University of Strathclyde). The identification of initial intermediates and transition states using electronic structure calculation was carried out by Jonathan Percy (University of Strathclyde, Spartan'08) and further screening on Gaussian'09 aided by Tell Tuttle (University of Strathclyde, structures processed and built by JMP).*

Chapter 2: Synthesis of 1,1-Difluoro-2-vinylcyclopropanes

The most efficient way of synthesising difluorocyclopropane units is the trapping of difluorocarbene with an alkene; the most recent and synthetically useful methods have been discussed previously. Promising results reported by Amii and co-workers into the synthesis of difluorocyclopropyl boronic esters **98**,⁶⁷ led to a proposed three step synthesis of precursors which could be used to test rearrangement conditions (**Scheme 68**).



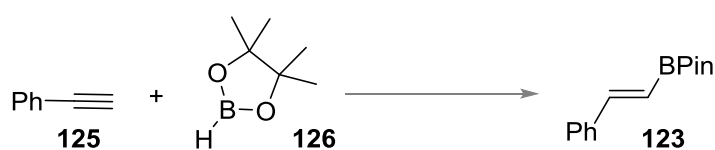
Scheme 68: Proposed route to substituted 1,1-difluoro-2-vinylcyclopropanes (R = aryl, alkyl).

Literature conditions exist for the proposed hydroboration of commercial alkynes;¹⁴⁷ vinyl iodide **124** is also accessible from the same starting material using zirconium based chemistry.¹⁴⁸ The least well-precedented step would be final vinyl-alkyl Suzuki-Miyaura cross coupling between **98** and iodide **124**. Our investigations started with phenyl acetylene, since all of the literature precedents had been secured for the corresponding compounds.

3.1. Route I

3.1.1. Hydroboration

The main aim for the chemistry at this stage was to use simple, quick, stereospecific reactions which allowed efficient access to vinyl boronic esters. Alkene **123** can be synthesised using Miyaura-borylation chemistry but this route was never investigated since it used the relatively expensive *bis*(pinacolato)diboran reagent.¹⁴⁹ Pinacol esters were preferred for these transformations because they are stable to aqueous workup and chromatography; direct hydroboration of phenyl acetylene with pinacol borane has been reported (**Scheme 69**).



Scheme 69: Hydroboration of phenyl acetylene (Pin = -OC(CH₃)₂C(CH₃)₂O-).

Knochel and co-workers previously reported the successful reaction between phenyl acetylene and two equivalents of **126**, affording vinyl boronic ester **123** in 64% yield after 2 hours (96:4 ratio of *E*:*Z* isomers).^{147a} Unfortunately, attempts to repeat this result failed, with only a 13% yield of **123** (**Table 12**, Entry 1). The reactions were easy to monitor by ¹H NMR due to the distinct changes in proton chemical shifts as alkyne **125** transformed to alkene **123**; no alkene peaks were visible by ¹H NMR when the reaction concentration (**Table 12**, Entry 2) or temperature (**Table 12**, Entry 3) was increased.

Table 12: Hydroboration Reaction without Transition Metal Catalyst

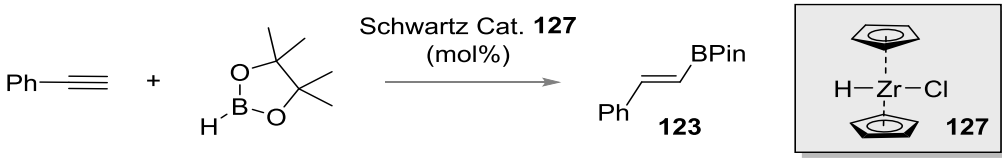
| Entry | Solvent | Temperature (°C) | Time (h) | Isolated Yield (%) |
|-------|---------|-------------------|----------|--------------------|
| 1 | DCM | r.t. | > 60 | 13 |
| 2 | - | r.t. | 22 | no reaction |
| 3 | - | 40 | 22 | no reaction |

Reactions performed using phenylacetylene (1 eq.) and pinacol borane (2 eq.).

After these initial results it was decided that a catalyst would be needed to increase reaction rate but, more importantly, allow the use of near stoichiometric quantities

of pinacol borane. Srebnick^{147b} first proposed the use of the zirconium catalyst known as Schwartz reagent; the reagent has been used for the functionalisation of alkenes, 1,3-dienes and alkynes¹⁵⁰ and is also useful for the halogenation and transmetallation of organic compounds.¹⁵¹ Srebnick's conditions with 5 mol% catalyst loading were not reproducible (**Table 13**, Entry 1; literature yield of 75% after 16 hours^{147b}), even after an increased reaction time. Decreasing the catalyst loading to 1 mol% while increasing the concentration improved product isolation (**Table 13**, Entry 2) but a higher loading of catalyst (10 mol%) was required for faster conversion and higher yields (**Table 13**, Entry 3).

Table 13: Optimisation of Phenyl Acetylene Hydroboration



| Entry | HBPIn (eq.) | 127 (mol%) | Solvent | Temp. (°C) | Time (h) | Yield (%) ^[a] | Isolated Yield (%) ^[b] |
|-------|-------------|------------|---------|------------|--------------------|--------------------------|-----------------------------------|
| 1 | 1.05 | 5 | DCM | r.t. | 72 | 15 | - |
| 2 | 1.05 | 1 | - | r.t. | 70 | 40 | - |
| 3 | 1.05 | 10 | - | r.t. | 23 | >90 | - |
| 4 | 1.05 | 10 | - | 60 | 2 ^[c] | 85 | 48 |
| 5 | 1.05 | 5 | - | 60 | 1.5 ^[d] | 82 | 48 |
| 6 | 1.1 | 10 | - | 60 | 1 ^[c] | - | 60 |

[a] Based on mass isolated (assuming 100% purity) [b] isolated yield after Kugelrohr distillation. [c] 90% conversion by ¹H NMR. [d] 50% conversion by ¹H NMR.

Reaction times could be decreased from 24 to 2 hours by increasing the temperature to 60 °C (**Table 13**, Entry 4). Halving the catalyst loading gave comparable yields (**Table 13**, Entry 5). A slight increase in pinacol borane stoichiometry provided the highest yield (60%, **Table 13**, Entry 6).

Isolated products after aqueous workup contained traces of white solid, expected to be either pinacol or catalyst-derived residue. Both of these should dissolve in the aqueous layer during work up, but Kugelrohr distillation was required to obtain analytically pure product (single peak in GC/MS to 231.1 [M+H]⁺). In order to avoid the reduction in yield seen with these two work ups, subsequent neat reactions were distilled directly after complete conversion had been detected by ¹H NMR.

Isolated alkene **123** was enriched in the *E*-isomer; however, on examining crude ^1H NMR spectra, it appeared that isomers may be forming during the reaction (**Figure 19**).

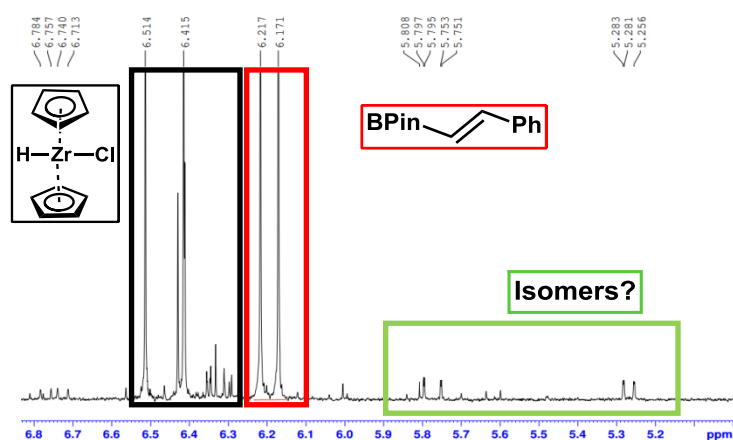


Figure 19: ^1H NMR spectra of crude reaction mixture showing distinct peaks for Schwartz reagent, alkene **123** and proposed isomers.

The key to decreasing reaction times was increasing the temperature; however this also brought about an observable colour change from pale yellow to a reddish brown. This colour change coincided with the appearance of the unassigned doublets, confirmed by heating catalyst **127** and phenyl acetylene together at 60 °C in the absence of the boron reagent (**Figure 20**).

This simple NMR experiment confirmed that an alkenylzirconium reagent was forming instead of the suspected stereoisomer. This is consistent with the proposed mechanism for the hydroboration,^{147b,152} which starts with alkyne insertion, followed by σ -bond metathesis to form activated alkene **128** (**Scheme 70**). Alkenyl/halide exchange with pinacol borane forms the desired alkene and regenerates the catalyst. The cyclopentadienyl ligands on the zirconium add bulk which establishes the regio- and stereochemistry of alkene **123** and is transcribed through the transmetallation step.

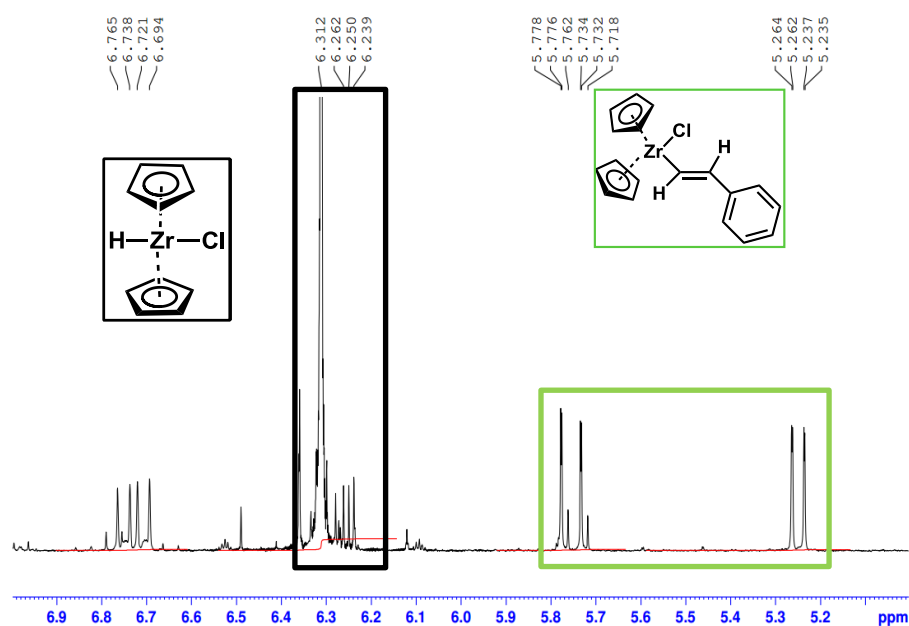
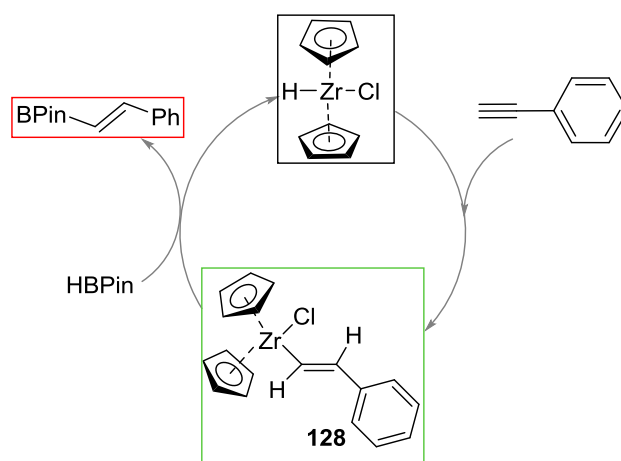


Figure 20: ^1H NMR spectra of catalyst **127** and phenyl acetylene at 60 °C.



Scheme 70: Proposed catalytic cycle for hydroboration of phenyl acetylene.

With the formation of alkenylzirconium species **128** detected, the reaction procedure was modified to pre-form this species. Previously, dropwise addition of pinacol borane followed cooling of alkyne and catalyst solution to 0 °C. The addition at low temperature was thought to aid stereocontrol but addition at room temperature followed by heating to 60 °C showed no other isomers by ^1H NMR (Table 13, Entries 4-6). A new procedure was proposed in an attempt to decrease reaction times further. Phenyl acetylene and catalyst **127** were pre-heated at 60 °C until a distinct colour change (yellow to red-brown) indicated that alkenylzirconium

128 had formed. Dropwise addition of pinacol borane afforded desired alkene **123** in a comparable yield of 59% (**Table 14**, Entry 1).

Table 14: Effects of Catalyst Loading on Optimised Hydroboration

| Entry ^[a] | Activation Time (h) | Reaction Time (h) | 127 (mol%) | P/SM ratio ^[b] | Yield (%) ^[c] |
|----------------------|---------------------|-------------------|-------------------|---------------------------|--------------------------|
| 1 | 0.5 | 1 | 10 | 1:0 | 59 |
| 2 | 0.5 | 7 | 5 | 1:0 | 82 |
| 3 | 0.5 | 36 | 2.5 | 1:0.23 | 42 |
| 4 | 5 | 88 | 1 | 1:0.13 | 63 ^[d] |

[a] all reactions used 1.1 equivalence of pinacol borane. [b] Determined by ¹H NMR. [c] Isolated yields from direct distillation. [d] <90% purity.

As expected, reactions took longer when the catalyst loading was decreased to 5 mol% but with an unexpected increase in isolated yield (82%, **Table 14**, Entry 2). Unfortunately attempts to decrease the loading further to 2.5 and 1 mol% gave unrealistic reaction times, incomplete conversion and a drop in yield (**Table 14**, Entries 3 and 4, respectively).

A direct hydroboration protocol with a quick work up procedure was successfully developed for our synthetic route using catalytic quantities of zirconium catalyst in an otherwise neat reaction mixture. The high yield is comparable with those quoted in the literature^{147b,152} and the optimised reaction gave only the desired *E*-isomer which was used in subsequent difluorocyclopropanation reactions.

3.1.2. Difluorocyclopropanation of Vinyl Boronic Esters

Only a selection of the reagents which generate difluorocarbene and successfully trap with alkenes are easy to handle and commercially available. Difluorocyclopropanation conditions examined for vinyl pinacol borane **123** focused on these reagents and started with sodium chlorodifluoroacetate **32** based on the reports of Amii and co-workers.⁶⁷

3.1.2.1. Reactions with Sodium Chlorodifluoroacetate

Two methods are used in the literature;⁶⁷ these involve either rapid reagent addition of **32** over 10 minutes (method A) or slow addition over 5-8 hours (method B). Method B was shown to be required for the reaction of alkene **123** (**Table 15**,

Entry 1). However, attempts to reproduce literature results failed, even after rigorous distillation of the alkene and diglyme (**Table 15**, Entries 2 and 3, respectively). Unfortunately, it also became apparent early on that the alkene and cyclopropyl compounds were inseparable, either by chromatography or distillation, so full conversion was imperative for isolation of cyclopropane **129**.

Table 15: Optimisation of Sodium Chlorodifluoroacetate Reaction with Alkene **123**

| Entry | 32 (eq.) | Addition Time (h) ^[a] | Reaction Time (h) | SM/Product Ratio ^[b] | Yield (%) ^[c] |
|------------------|--------------------|-------------------------------------|----------------------|---------------------------------|--------------------------|
| 1 ^[d] | 4 | 0.08 | 13 | 3.5 : 1 | - |
| 2 ^[d] | 4 | 8.5 | 4 | 4.8 : 1 | - |
| 3 ^[e] | 4 | 7 | 10 min. | 2 : 1 | - |
| 4 | 8 | 8.4 | 10 min. | Full conv. ^[f] | - |
| 5 | 8 | 7 | 15 | Full conv. | 15 |
| 6 | 8 | 9 | 14 | n.d. | 16 ^[g] |
| 7 | 8 | 4.5 | 17 | Full conv. | 27 ^[h] |

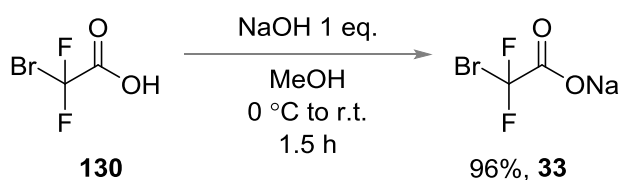
[a] Slow addition carried out using a syringe pump and septum/needle technique. [b] Determined by GC/MS. [c] Isolated yields unless otherwise stated. [d] Undistilled diglyme and alkene. [e] Exact repeat of literature conditions. [f] Majority unknown impurity. [g] 50% purity by GC/MS. [h] 80% purity by GC/MS.

Amii required only four equivalents of chloro-reagent **32** when method B was used to transform **123** but in our hands, doubling the number of equivalents was required for full conversion. A switch in inert atmosphere from nitrogen to argon was key to this conversion and it is believed that the more inert gas is better at excluding moisture from the reaction, avoiding unwanted difluorocarbene hydrolysis. A short reaction time after slow addition formed an unknown by-product, making purification more difficult (**Table 15**, Entry 4). Longer reaction times avoided this impurity but chromatography by wet loading (**Table 15**, Entry 5) or dry loading (**Table 15**, Entry 6) only afforded cyclopropane **129** in low yields and purity. An increase in yield was observed when Celite was used to dry load crude material onto a column of silica, but product purity was still low (**Table 15**, Entry 7).

The learnings in the conditions required for successful generation and trapping of difluorocarbene were transferred into investigations into other reagents.

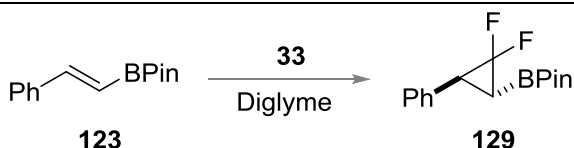
3.1.2.2. Reactions with Sodium Bromodifluoroacetate

Switching the halogen atoms in the difluoroacetate reagent to bromine makes decomposition to the difluorocarbene easier, allowing the reaction temperature and the stoichiometry of the reagent to be decreased and negating the need for slow addition.⁶⁵ Bromo species **33** is considerably more expensive than the corresponding chloro-species (the costs of 25 g from Sigma Aldrich are £199 and £40 for the bromo- and chloro-species, respectively); however acid **130** is available at a much lower price than the corresponding sodium salt (25 g from FluoroChem = £39). Reaction of bromodifluoroacetic acid **130** with sodium hydroxide afforded the desired sodium salt in quantitative yield after drying in a Kugelrohr oven (60 °C/0.1 mbar) (**Scheme 71**).⁶⁵



Scheme 71: Synthesis of sodium salt **33** from cheaper acid **130**.

It was still impossible to get full conversion of alkene **123** using salt **33** under a nitrogen atmosphere, with slow addition affording more product than rapid addition (**Table 16**, Entries 1 and 2 respectively). Switching to argon and increasing the temperature by 30 °C gave better conversion with rapid addition of carbene reagent (**Table 16**, Entry 3) but conversion only started to favour product when the excess of this reagent was increased to 6 equivalents (**Table 16**, Entry 4).

Table 16: Optimisation of Sodium Bromodifluoroacetate Reaction with Alkene **123**

| Entry ^[a] | 33 (eq.) | Temp (°C) | Addition Time | Reaction Time (h) | SM/P Ratio ^[b] | Yield (%) ^[c] |
|----------------------|--------------------|--------------|------------------|----------------------|------------------------------|-----------------------------|
| 1 ^[d] | 4 | 150 | 10 min. | 1 | 5 : 1 | - |
| 2 ^[d] | 4 | 150 | 7 h | 1 | 1.3 : 1 | - |
| 3 | 4 | 180 | 10 min. | 6 | 2.5 : 1 | - |
| 4 | 6 | 180 | 8 min. | 1 | 0.5 : 1 ^[e] | 28 ^[f] |
| 5 | 6 | 180 | 10 min. | 4.5 | 0.5 : 1 ^[e] | 48 ^[f] |
| 6 | 6 | 180 | 10 min. | 18 | 0.01 : 1 | 5 |
| 7 | 6.5 | 180 | 10 min. | 16 | 0.04 : 1 | 19 ^[g] |
| 8 | 7.0 | 180 | 6 min. | 16 | Full Conv. | 20 |

[a] **123** (0.5-1.0 mmol). [b] Determined by GC/MS. [c] Isolated unless otherwise stated. [d] Under nitrogen. [e] Determined by ¹H NMR after chromatography. [f] Mixture of product and starting material after chromatography. [g] 80% purity.

Leaving the reaction mixture for an extra 4.5 hours resulted in no change (**Table 16**, Entry 5) but a prolonged reaction time of 18 hours gave nearly full conversion (**Table 16**, Entry 6). The excess of carbene precursor **33** was increased to 6.5 and 7.0 equivalents (**Table 16**, Entries 7-8), with full conversion being observed with the latter; purification on silica gel afforded the desired product in a 20% yield (>95% purity). The low efficiency of isolation from the reactions with both salts **32** and **33** was disappointing due to previous success reported in the literature. The results suggest that decomposition of pinacol borane **129** may occur either under the reaction conditions or during silica chromatography. However, the sodium salts are only one of the reagents used recently to afford difluorinated cyclopropanes; another is MDFA.

3.1.2.3. Reactions with Methyl 2,2-difluoro-(fluorosulfonyl)-acetate (MDFA)

A study published in 1995 used MDFA with catalytic amounts of copper to trifluoromethylate organic halides, but it was also noticed that the carbene generated during the reaction could be trapped with 2,3-dimethylbut-2-ene.¹⁵³ However it was only recently that this observation was examined further by Dolbier

and co-workers, resulting in the development of highly effective conditions for the difluorocyclopropanation of alkenes through the controlled and efficient generation of difluorocarbene.⁷¹ They reported that a minimal amount of solvent and high temperatures were required due to the surprisingly low reactivity of the carbene. The key to their optimisation was finding a solvent system which could withstand the high temperatures required; consistent results were obtained with a combination of diglyme and 1,4-dioxane though these conditions were not necessarily optimal for all alkenes examined.

Unfortunately, the literature MDFA conditions failed to give full conversion of electron deficient alkene **123** to cyclopropane **129** (**Table 17**, Entry 1); using 50% less alkene in the reaction was more detrimental to conversion and confirmed that reaction concentration was important for product conversion (**Table 17**, Entry 2). Since an extensive optimisation (changes in temperature, solvent, nucleophilic source, electrophilic trap and reagent stoichiometry) had previously been carried out in the literature,⁷¹ optimisation of the reaction for alkene **123** focused on solvent effects.

Table 17: Optimisation of MDFA Cyclopropanation of Alkene **123**

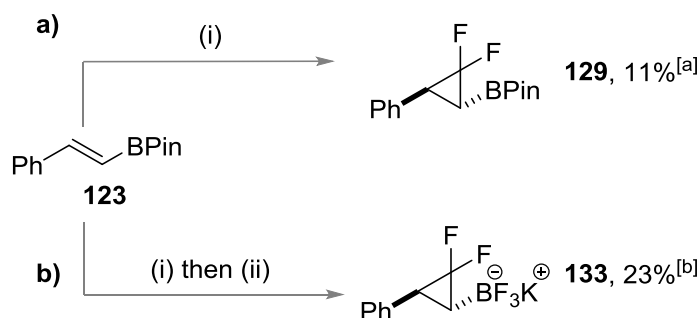
| Entry | 131 (eq.) | 132 (eq.) | SM:P Ratio ^[a] | Yield (%) ^[b] |
|------------------|-----------|-----------|---------------------------|--------------------------|
| 1 | 1.7 | 0.1 | 1 : 2 | - |
| 2 ^[c] | 3.4 | 0.2 | 3 : 1 | - |
| 3 | 1.7 | 0.55 | Full Conv. | - |
| 4 | 1.7 | 0.96 | 1.1 : 1 ^[d] | - |
| 5 | 1.7 | 1.3 | Full Conv. | 18 |
| 6 | 1.7 | 1.3 | 0.16 : 1 ^[d] | - |

[a] Determined by GC/MS or ¹H NMR. [b] Isolated yield. [c] 50% less alkene in reaction mixture (i.e. MDFA (5 eq.), TMSCl (5 eq.) and KI (4.5 eq.)). [d] Incomplete conversion potentially due to tarring.

Increasing the total number of equivalents of solvent to match those of potassium iodide was attempted; the hypothesis was that more iodide would then be free to

react with MDFA and carbene generation would be faster. This proved to be the case and full conversion was achieved (**Table 17**, Entry 3). The use of a minimal volume of solvent in the reaction proved to be troublesome since the conversion of MDFA to gaseous side products reduces the total volume of liquid causing the formation of black tar after two days. Increasing the total volume of the reaction by increasing the number of equivalents of the higher boiling point solvent solved this tarring issue while maintaining full conversion. However, it was necessary to carry out the reactions on a larger scale to avoid tarring. Attempts to assess the solvent effects using small scale reactions failed due to tarring (**Table 17**, Entry 4) and even attempted repeats of successful reactions (**Table 17**, Entry 5) still had the potential to form tar, decreasing conversion and yields (**Table 17**, Entry 6). The unreliability and low yields from both MDFA and sodium halodifluoroacetate reactions led to the investigation into a more efficient route to the desired precursors.

One of these alternative routes led to new MDFA conditions which decreased reaction times while maintaining full conversion of alkene (*vide infra*). Interest in the synthesis of precursors from vinyl boronic ester still remained, so these new conditions were tested retrospectively (**Scheme 72a**). Near full conversion was observed after difluorocyclopropanation over 24 hours, half the reaction time observed with previous optimisations. More importantly no tarring was observed which gave good possibilities of further optimisation. However, low yields and purity of difluorocyclopropyl **129** (11%, 80% purity) resulted from decomposition during purification.

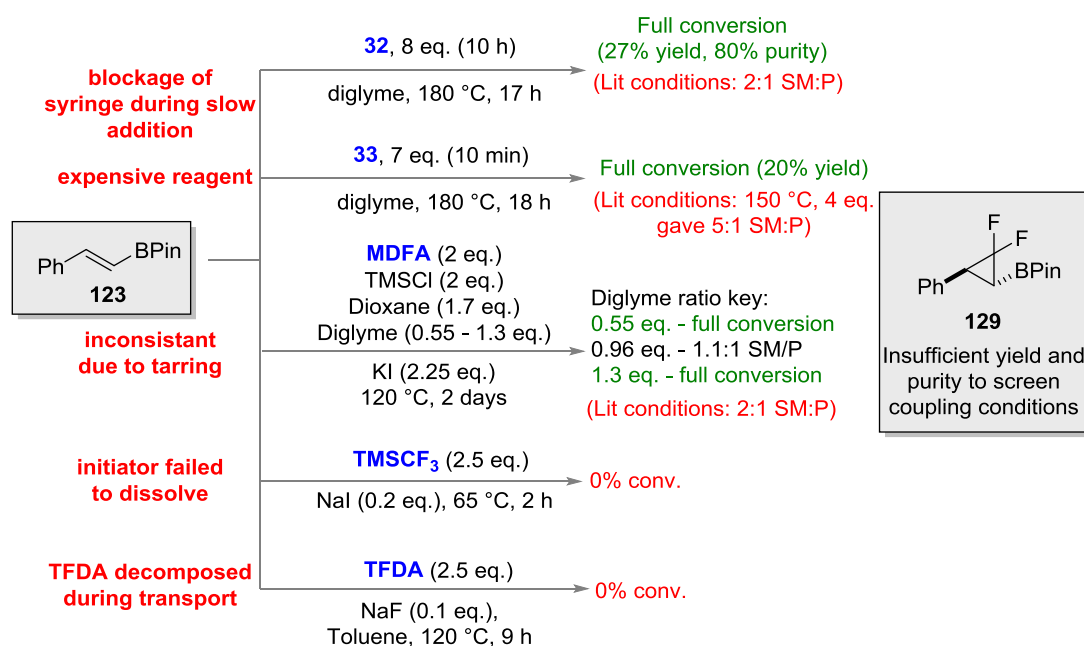


Scheme 72: Optimised MDFA conditions used in the attempted synthesis of a) boronic ester 129 and b) potassium trifluoroborate 133. Conditions: (i) MDFA (2.3 eq.), TMSCl (2.3 eq.), KI (2.8 eq.), diglyme, 120 °C, 24 h (ii) KHF₂ (2.5 eq.) in H₂O (4.5 M), MeOH, 1 h. [a] 80% purity by ¹H NMR. [b] >95% purity by ¹H NMR.

Attempts to convert crude **129** to the corresponding potassium trifluoroborate **133** resulted in isolation of purer, solid product in a slightly higher yield (23%, **Scheme 72b**). A final year MChem project was set up to seek improvements in the isolation of **133** and to assess the viability of using the compound in cross-coupling reactions.¹⁵⁴ Despite reports that cyclopropyl trifluoroborates undergo extremely fast hydrolysis to the corresponding boronic acid,¹³⁶ it was found that hydrolysis rates for difluorocyclopropyl **133** were extremely slow, and all attempt cross coupling with aryl halides failed. These results demanded that alternative synthetic routes to rearrangement precursors be found.

3.1.3. Overview of Difluorocarbene Trapping with Alkene **123**

The synthesis of cyclopropyl pinacol borane **129** from alkene **123** was investigated using the most desirable difluorocarbene reagents from the literature but gave undesirably low yields of product. The Ruppert-Prakash reagent⁵³ and TFDA⁶⁹ were also screened but both reactions were unsuccessful, either due to failed initiation or instability of the reagents, respectively (**Scheme 73**).

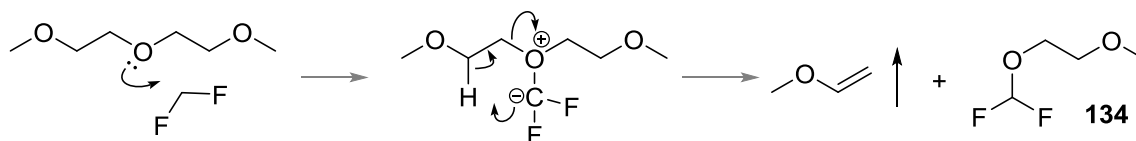


Scheme 73: Problems associated with difluorocarbene addition to alkene **123.**

Despite the disappointing results with alkene **123**, insight into the different reactivities of the screened reagents could be obtained. Despite the quick addition times for bromo-**33**, the price of the reagent made it inefficient when compared

with chloro-**32**. Reaction conditions were developed for both acetate **32** and MDFA which allowed full conversion of alkene **123** and these conditions could be taken forward and screened with more reactive alkenes.

Analysis of crude reaction mixtures from reactions carried out with both acetate **32** and MDFA showed the presence of a common impurity by ^{19}F NMR (- 84.6 ppm, d, $J_{\text{F-H}} = 74.6$ Hz). The nature of the impurity was unknown; however both reaction conditions contain diglyme and difluorocarbene. From analysis of ^{19}F NMR spectra, it was proposed that difluorocarbene had added to one of the oxygen atoms in diglyme because the chemical shift (- 84.6 ppm) was consistent with fluorine atom attached to an ether carbon.¹⁵⁵ The coupling constant of 74.6 Hz correlated with a triplet in the ^1H NMR, confirming that two fluorine atoms remain on the molecule. A mechanism was proposed from this analysis, with nucleophilic attack of oxygen from diglyme onto difluorocarbene followed by deprotonation and elimination to form ether **134** (Scheme 74). Unfortunately, confirmation of this side product could not be confirmed by GC/MS analysis and isolation was impossible from diglyme.



Scheme 74: Proposed reaction between diglyme and difluorocarbene resulting in the formation of side product **134 seen during unsuccessful difluorocyclopropanation reactions.**

A simple thermal experiment showed that acetate **32** fully decomposed after approximately one hour refluxing in diglyme (Figure 21). The small change in ^{19}F chemical shift from -63.0 ppm to -64.1 ppm suggests that the salt has been replaced by a similar species, likely to be the corresponding acid **135**. The formation of the unknown impurity at -84.6 ppm gives strong evidence for the difluoro-diglyme adduct **134** since there is nothing else to trap the difluorocarbene after decomposition.

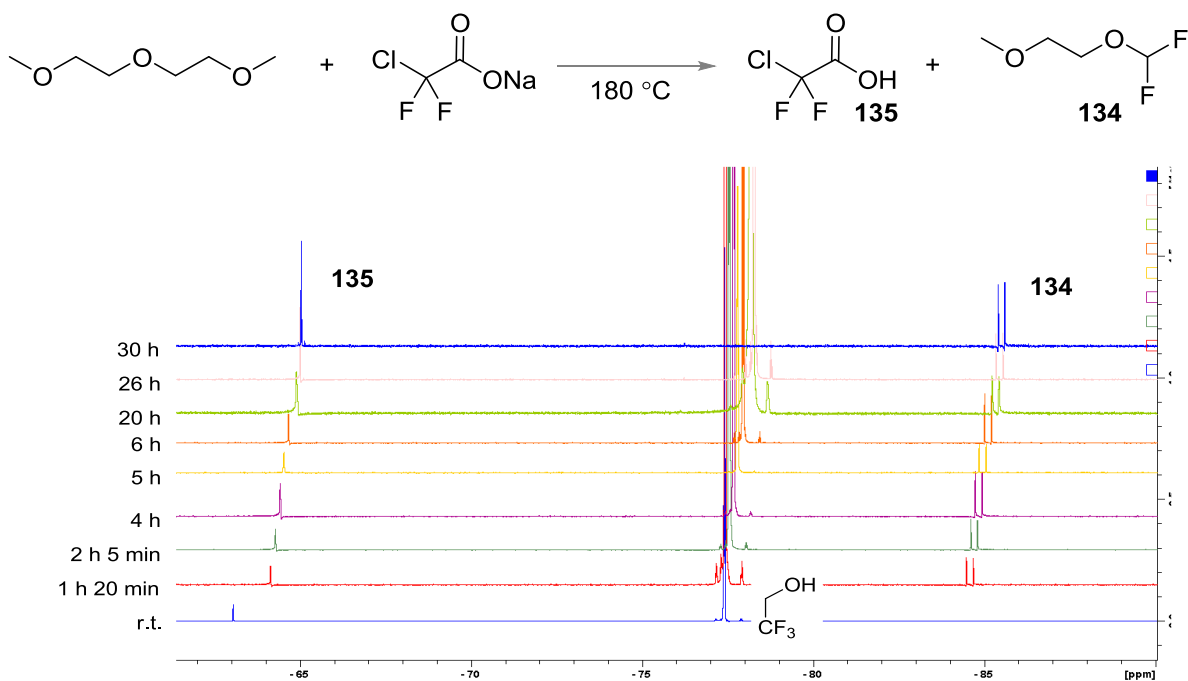


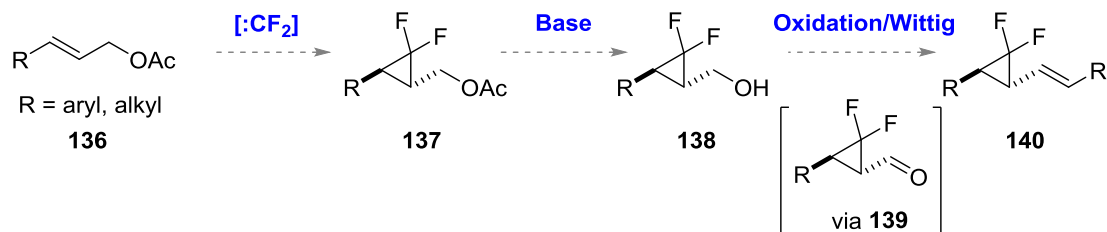
Figure 21: ^{19}F NMR (CDCl₃, 400 MHz) spectrum of reaction time-points showing difluorocarbene generated from sodium chlorodifluoroacetate reacting with diglyme (horizontal offset = 0.15 ppm, trifluoroethanol used as external reference).

The observed ^{19}F NMR experimental data for the proposed side product **134** (-84.6 ppm, d, $^2J_{\text{F-H}} = 74.6$ Hz) is extremely similar to 1-(difluoromethoxy)-2-(2-methoxyethoxy)ethane reported by Rozen and co-workers (-84.6 ppm, d, $^2J_{\text{F-H}} = 75.0$ Hz).¹⁵⁶ Houk *et. al.* previously performed low level calculations (MP2/3-21G) showing that the attack by water on difluorocarbene was exergonic with a stabilisation energy of 9.7 kcal mol^{-1} compared with the separate species, concluding that the ether stabilisation was greater than that seen with alkenes.¹⁵⁷ The presence of **134** in attempted difluorocyclopropanation reaction gives a good indication of poor reactivity with alkenes, and could account for the need for excess difluorocarbene reagent to ensure complete conversion of less reactive alkenes.

3.2. Route II

An alternative three step synthetic route was proposed for the synthesis of vinyl difluorocyclopropane **140**, focusing on using simple and efficient chemical transformations (**Scheme 75**). If (acetoxymethyl)cyclopropane **137** could be successfully synthesised then deprotection would afford alcohol **138**. Oxidation to

aldehyde **139** has the potential to be low yielding because the inherent reactivity of aldehydes could cause problems during isolation. However, tandem oxidation/olefination chemistry avoids the isolation of **139** and initial development focused on this chemistry.



Scheme 75: Proposed three step route to VCPR precursors.

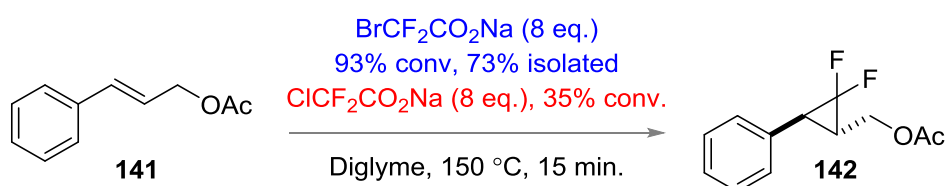
It was predicted that the most problematic step would once again be the addition of difluorocarbene to alkene **136**. Electronic structure calculations were used in attempts to quantify the activation barrier involved in difluorocarbene addition to vinyl boronic ester **123** and cinnamyl acetate **136**. Houk, Rondan and Mareda previously calculated the relative activation energy for difluorocarbene addition to ethylene to be $28.9 \text{ kcal mol}^{-1}$ (RHF/3-21G*) from a stabilised complex formed between the olefin and difluorocarbene.¹⁵⁷ This work was repeated by finding the difluorocyclopropanation transition state between difluorocarbene and ethene (confirmed by the existence of one imaginary frequency) and relaxing the optimised molecule backwards and forwards along the forming bond to obtain similar geometries of complexed difluorocarbene-alkene and difluorocyclopropane product, respectively. Our energy profile agreed well with the literature (relative activation energy = $28.9 \text{ kcal mol}^{-1}$) but we were unable to obtain good correlation with experimental activation energies calculated by Moss and co-workers for cyclohexene ($\Delta G^\ddagger = (7.6 \pm 0.5) \text{ kcal mol}^{-1}$) or tetramethylethylene ($\Delta G^\ddagger = (5.5 \pm 0.3) \text{ kcal mol}^{-1}$).^{56b} Higher level calculations with B3LYP functional with a range of basis sets (6-31G*, 6-311G*, 6-31+G* and 6-31G**) also failed to correlate with experimental activation energies. Sader and Houk reported a calculated activation energy for the difluorocarbene addition to cyclohexene of $7.4 \text{ kcal mol}^{-1}$ using M06-2X/6-31+G** level of theory¹⁵⁸ but due to the lack of confidence in our preliminary computational

models of the difluorocyclopropanation, experimental comparisons in reactivity were preferred in order to screen alternative alkene substrates.

3.2.1. Optimising the Difluorocyclopropanation of Cinnamyl Acetate

3.2.1.1. Literature Conditions

Difluorocarbene addition to **141** has been reported in the literature using both halodifluoroacetates **32** and **33**; the best conversion was obtained when 8 equivalents of **33** was reacted at 150 °C for 15 minutes (**Scheme 76**).⁶⁵



Scheme 76: Literature examples of successful difluorocarbene addition to alkene **141**.

Reported conditions which relied on the quick addition of sodium bromodifluoroacetate **33** (10 minutes) were reproducible, but product and starting material were inseparable using flash chromatography on silica gel (**Table 18**, Entry 1). The corresponding chloro-salt **32** also gave similar results to the literature; a quick addition time of 20 minutes gave a 50% conversion to **142** (**Table 18**, Entry 2). The required full conversion could be obtained with an increased reaction time of 45 hours but with an undesirably low yield (17% yield, **Table 18**, Entry 3). The total reaction time could be decreased to 20 hours whilst maintaining full conversion when slow addition techniques described by Barnett and co-workers were employed (70% yield, **Table 18**, Entry 4).¹⁵⁹ Full conversion could not be maintained at higher scale due to the practical issues involved in slowly adding large volumes of diglyme solution of **32** via a syringe pump. Low volumes of diglyme favour high alkene conversion, but acetate **32** requires sonication and heating in order to solubilise the salt fully. Precipitation of salt occurred in the syringe during prolonged addition times, causing blocked needles and decreasing the concentration of difluorocarbene within the reaction mixture (45% yield, **Table 18**, Entry 5). Attempts

with lower temperature initiating reagent TMSCF_3 failed to result in the desired full conversion when literature conditions were implemented (**Table 18**, Entry 6).⁵³

Table 18: First Generation Difluorocyclopropanation Optimisation with **141**.

| Conditions: | | | | | |
|--|------------|--|-------------------|---|----------------------|
| A | | B | | C | |
| $\text{ClF}_2\text{CCO}_2\text{Na}$ Diglyme, 180 °C | | $\text{BrF}_2\text{CCO}_2\text{Na}$ Diglyme, 150 °C | | Me_3SiCF_3 , NaI (0.2 eq.) THF (an), 65 °C | |
| Entry | Conditions | Addition Time | Reaction Time (h) | Conversion (141:142) ^[a] | Yield ^[b] |
| 1 | B | 10 min. | 21 | 1:16 | 45 |
| 2 | A | 20 min. | 0.5 | 1:1 | n.d. |
| 3 | A | 20 min. | 45 | 0:1 | 17 |
| 4 | A | 7 h | 14 | 0:1 | 70 |
| 5 ^[c] | A | 14 h | 10 | 1:19 | 45 |
| 6 | C | - | 2 | 1:0 | - |

[a] Ratio determined by ^1H NMR; [b] Isolated yield. [c] 4 mmol scale.

Higher addition rates of **32** could be implemented if the reagent was added in portions; however, it is predicted that more than 8 equivalents of reagent would be required. The optimised conditions with MDFA (obtained during difluorocyclopropanation attempts with vinyl pinacol borane **123**), required only 2 equivalents of the reagent. These conditions are more applicable on scale because the chance of unwanted tarring is lower; subsequent investigation into the synthesis of cyclopropyl **142** focused on this reagent.

3.2.1.2. Optimisation with Methyl 2,2-difluoro-2-(fluorosulfonyl)-acetate (MDFA)

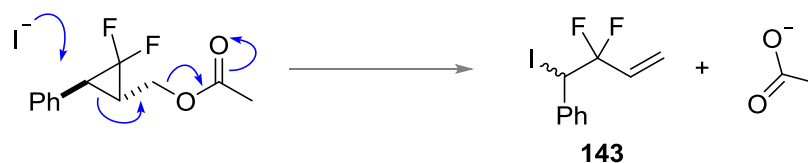
Previous optimisation work with MDFA showed that the ratio of 1,4-dioxane to diglyme was important in obtaining full conversion of pinacol borane **123**. Interestingly, when literature conditions were attempted for **141**, a previously unseen side product was observed by ^{19}F NMR, and chromatographic separation afforded a modest 32% yield of desired product **142** (**Table 19**, Entry 1).

Table 19: Difluorocyclopropanation Optimisation of Acetate **141** with MDFA

| Entry | MDFA (eq.) | TMSCl (eq.) | Dioxane (eq.) | Diglyme (eq.) | KI (eq.) | Time (h) | Conv. (%) ^[a] (141:142) | Yield (%) ^[b] |
|------------------|------------|-------------|---------------|---------------|---------------------|----------|------------------------------------|--------------------------|
| 1 | 2 | 2 | 1.7 | 0.1 | 2.25 | 48 | 4:80 ^[c] | 32 |
| 2 | 2 | 2 | 1.7 | 1.3 | 2.25 | 48 | 18:82 | n.d. |
| 3 | 2.46 | 2.46 | 1.87 | 0.11 | 2.77 | 17 | 1:19 | 43 ^[d] |
| 4 ^[e] | 2.46 | 2.46 | 0 | 2.77 | 2.77 | 24 | 9:91 | n.d. |
| 5 ^[f] | 2.46 | 2.46 | 0 | 1.2 | 2.77 ^[g] | 24 | 0:100 | 94 |
| 6 | 2.46 | 2.46 | 0 | 1.2 | 2.77 | 4 | 0:100 | 85 |

[a] Relative percentage determined by ¹H NMR. [b] Isolated yield unless otherwise stated. [c] Crude reaction mixture contained 16% of **143** (¹H NMR). [d] 97% purity determined by ¹H NMR. [e] 2.5 M concentration. [f] 6.0 M concentration. [g] Reaction mixture went to dryness after 5 hours and an extra 1.2 eq. of diglyme was added.

This side product was never seen when chloro-acetate **32** was used for difluorocyclopropanation so it was proposed that the reagents used to initiate the decomposition of MDFA, specifically potassium iodide, facilitated the formation of the side product. Nucleophilic attack of iodide on product **142** has the potential to open the strained difluorocyclopropane ring resulting in the elimination of an acetate anion (**Scheme 77**). The side product was highly unstable and decomposed quickly so full characterisation could not be achieved. However, the pink colouration of the sample during NMR analysis and deconvolution of ¹H NMR spectra supported the formation of iodide **143**. It was found that when slightly wet reagents or solvents were used the formation of iodide **143** was favoured. Surprisingly, when optimised MDFA conditions designed to increase the dissociation of potassium iodide were utilised, no side product formation was seen and instead 82% conversion to product was obtained (**Table 19**, Entry 2).

**Scheme 77:** Proposed mechanism for side product formation in MDFA mediated difluorocyclopropanation of acetate **141**.

A 0.25-fold increase in reagent excess over alkene **141** gave near full conversion to cyclopropane **142** in half the reaction time required for literature conditions (95% conversion after 17 hours, **Table 19**, Entry 3). Decreasing the reaction time was beneficial because it lowered the potential for tarring; it was observed that the reaction mixture thickened considerably after 2-3 hours and solid started to precipitate out.

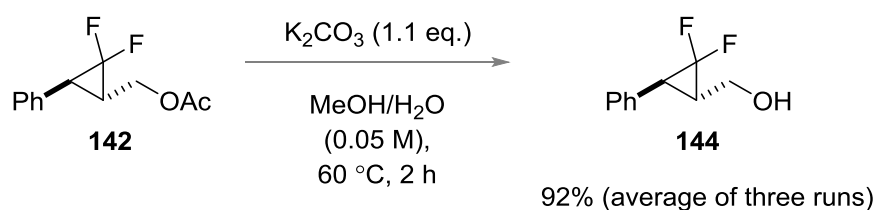
It was decided that the number of equivalents of diglyme (the higher boiling point solvent) would be altered to match the potassium iodide to ensure as much of the reaction mixture remained in solution for as long as possible. The dioxane was removed to maintain the required low reaction concentration; a smaller reaction flask and low boiling point condenser were also essential to provide the best set-up for enabling the reaction mixture to remain fully soluble over 24 hours. Full conversion was not achieved with these changes (91% conversion, **Table 19**, Entry 4) but increasing the reaction concentration to 6.0 M afforded **142** in high yields if an additional portion of diglyme was added when the reaction mixture started to solidify (94% yield, **Table 19**, Entry 5). When the reaction was stopped after only 4 hours, full conversion was achieved and the high yield of **142** was maintained (85% yield, **Table 19**, Entry 6).

Two successful methods for the difluorocyclopropanation of **141** have been developed using either acetate **32** or MDFA. The procedure based on chlorodifluoroacetate **32** gave a good 70% yield but could only be used on small scale (1.5 mmol). MDFA conditions were more applicable to larger scales (8 mmol) and gave an increase 94% yield. Pleasingly, full conversion could be maintained when the latter conditions were run on a 16 mmol scale allowing access to gram quantities of material (77% isolated yield representing 2.8 g of **142**).

The MDFA methodology developed was selected as the preferred method to probe the limitations of the difluorocyclopropanation conditions since it enabled faster carbene formation whilst facilitating full conversion of alkene **141** at relatively low temperatures.

3.2.2. Complete Synthesis of VCPR Precursor 147

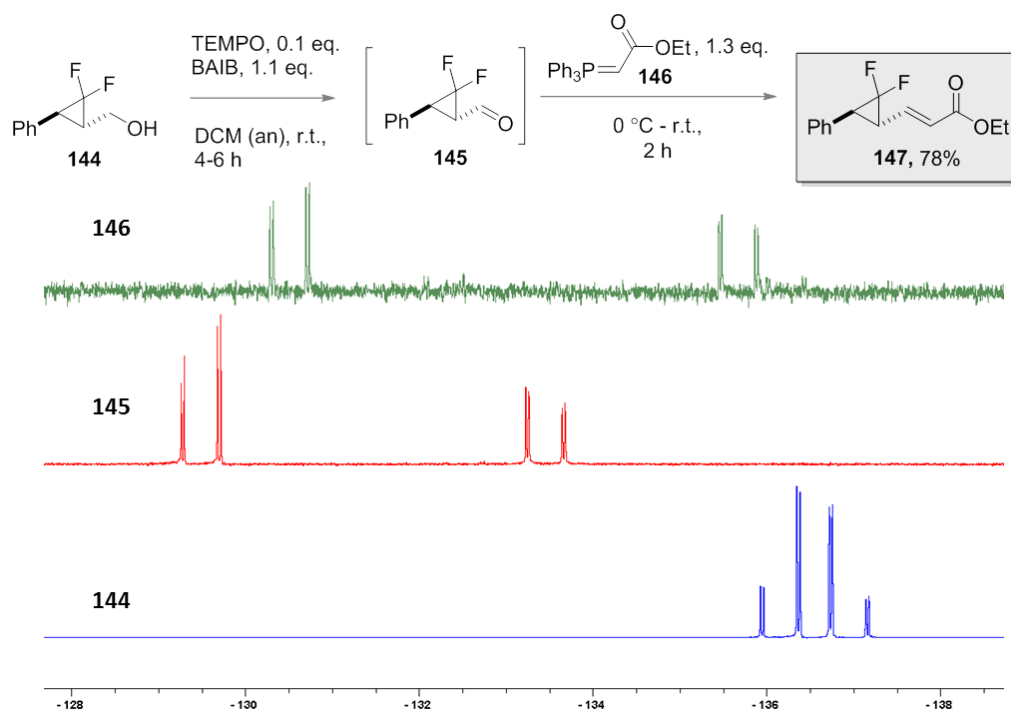
With a successful synthesis of cyclopropane **142** in hand, the proposed deprotection and tandem oxidation/olefination procedures were investigated. Base-catalysed hydrolysis of acetate **142** was implemented successfully using potassium carbonate in aqueous methanol (**Scheme 78**). Excellent yields of alcohol **144** could be obtained (highest isolated yield 99%, 92% average of three reactions) using a simple work up procedure in which the reaction mixture was concentrated and the solid base was removed using a small Celite pad.



Scheme 78: Deprotection of acetate 142.

A variety of tandem oxidation/olefination conditions are reported in the literature but many use either expensive metal catalysts¹⁶⁰ or require cryogenic temperatures.¹⁶¹ Vatéle's one-pot oxidation/Wittig conditions were favoured for the next step because they used commercially-available starting materials and mild reaction conditions; the latter was important to ensure rearrangement of precursor was not induced during synthesis.¹⁶² The oxidation step was initiated by a TEMPO-BAIB combination to give full conversion to aldehyde **145** after 4-6 hours at room temperature (**Scheme 79**). The addition of stabilised phosphorane **146** successfully converted aldehyde **145** *in situ* to *E*-cyclopropyl alkene **147** in a high (78%) isolated yield. ¹⁹F NMR reaction monitoring was crucial to confirming that full conversion was achieved at each of the stages.

Under these olefination conditions the *E*-isomer is favoured (>95:5 by ¹H NMR) but trace amounts of the *Z*-isomer could also be isolated (5% yield) allowing the effects of alkene stereochemistry, if any, on VCPR to be investigated.



Scheme 79: Oxidation/olefination of alcohol **144** with ^{19}F NMR monitoring at each stage.

Our synthesis relied on the stereochemistry of the starting acetate **142** being transcribed through the difluorocyclopropanation chemistry and subsequent transformations. Before subjecting **147** to thermal rearrangement conditions, it was important to determine if this was indeed the case. Through space correlations between cyclopropane proton and aromatic or alkene protons confirmed that the expected *trans*-difluorocyclopropane **147** had been synthesised (**Figure 22**).

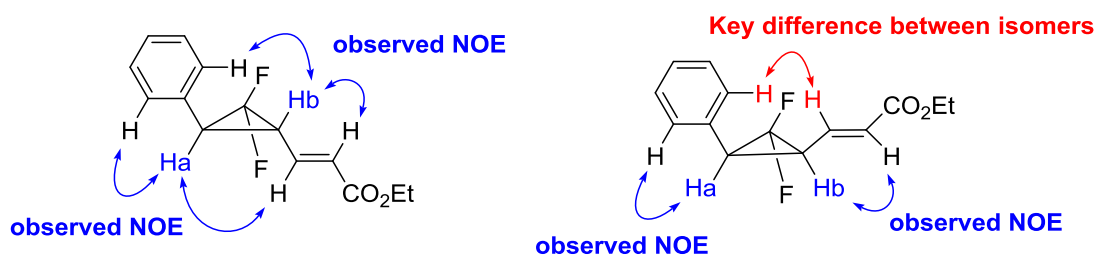
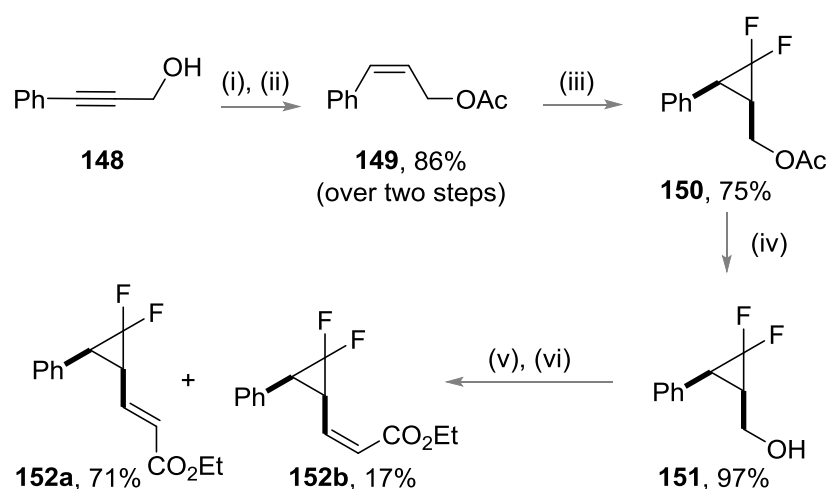


Figure 22: Through space correlations used to confirmation of cyclopropane stereochemistry by NOESY NMR.

Since both alkene stereoisomers could be accessed for *trans*-cyclopropane **147**, it was important that the corresponding *cis*-isomers were also isolated.

3.2.3. Synthesis of *cis*-Difluorocyclopropane Precursors

Vinyl acetate **149** was prepared from the Lindlar reduction of propargyl alcohol **148** followed by acetylation in a high (86%) yield over two steps (**Scheme 80**).



Scheme 80: Synthesis of *cis*-VCP compounds.

Conditions: (i) H₂ (1 eq., atm.), Lindlar cat. (5 mol% Pd), EtOH, r.t., 10 h; (ii) Ac₂O (1.05 eq.), DMAP (10 mol%), DCM/pyridine, r.t., 22 h; (iii) MDFA (2.46 eq.), TMSCl (2.46 eq.), KI (2.77 eq.), diglyme (1.2 eq.), 120 °C, 24 h; (iv) K₂CO₃ (1 eq.), MeOH/H₂O, 60 °C, 2 h; (v) TEMPO (0.1 eq.), BAIB (1.15 eq.), DCM, r.t., 6 h; (vi) Ph₃P=CHCO₂Et (1.3 eq.), 14 h.

Optimised MDFA conditions translated readily, giving full conversion to difluorocyclopropane **150**; hydrolysis afforded the corresponding alcohol **151** (73% over two steps). Elaboration of **151** using Vatele's oxidation/olefination conditions allowed access to both *cis*-alkene isomers; *E*-**152a** (71%) was favoured over *Z*-**152b** (17%). Cyclopropane and alkene configuration were confirmed by NOESY and ¹H NMR, respectively.

The synthetic route developed allows access to all four isomers of the desired precursor from commercially-available material using Dolbier's robust and effective difluorocarbene transfer reagent MDFA (**Figure 23**). Thermal rearrangement conditions were investigated for all precursors but initial optimisations focused on *trans*-*E* **147a** since it was synthetically easiest to access; the overall yield of **147a** from cinnamyl acetate was 70% over four steps.

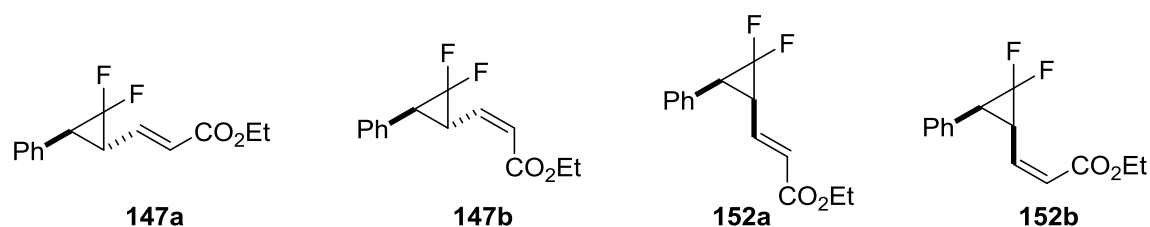
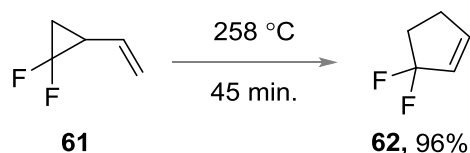


Figure 23: Four synthetically accessible diastereoisomers used to test VCPR conditions.

3.2.4. Thermal Rearrangement of *E*-Difluorocyclopropane Precursors

Dolbier and Sellers previously showed that simple difluorovinyl cyclopropane **61** rearranged successfully to difluorocyclopentene **62** in the gas phase at 260 °C after 45 minutes (**Scheme 81**).¹⁶³ The VCPR proceeds through a diradicaloid mechanism so it was expected that the rearrangement temperature for our precursors could be reduced further due the formation of a benzylic radical.



Scheme 81: Literature thermolysis of unsubstituted vinyl difluorocyclopropane **61**.

The rearrangement of *trans-E* precursor **147a** was examined first in high boiling point solvent diphenyl ether, with the expectation of screening high temperatures. Pleasingly, VCPR of **147a** was observed after 19 hours at 100 °C; a high (87%) yield of difluorocyclopentene **153** was obtained after chromatography (**Table 20**, Entry 1).

Table 20: Selected optimisation results for thermal VCPR of **147a** and **152a**

| Entry | VCP | Solvent | Temp (°C) | Time (h) | Conversion (%) ^[a] | | | | Yield (%) ^[b] |
|------------------|------|-------------------|-----------|----------|-------------------------------|------|------|------|--------------------------|
| | | | | | 147a | 152a | 153 | 154a | |
| 1 | 147a | Ph ₂ O | 100 | 19 | 1 | 0 | 19 | 0 | 87 |
| 2 | 147a | [D8]Tol. | 90 | 6 | 1 | 0.19 | 0.63 | 0 | - |
| | | | | 26 | 1 | 0 | 4.6 | 0 | - |
| 3 ^[c] | 147a | Tol. | 90 | 6 | 1 | 0.14 | 0.11 | 0 | - |
| 4 ^[d] | 147a | - | 100 | 16 | 0 | 0 | 1 | 0 | n.d. |
| 5 ^[e] | 147a | - | 100 | 22 | 1 | 0 | 33 | 16.5 | - ^[f] |
| 6 | 147a | Ph ₂ O | 180 | 19 | 0 | 0 | 1 | 0 | n.d. |
| 7 | 147a | Tol. | 100 | 17 | 0 | 0 | 1 | 0 | 99 |
| 8 | 152a | Tol. | 100 | 24 | 0 | 0 | 1 | 0 | 93 |

[a] Relevant conversion determined by ¹⁹F NMR integration. [b] Isolated yields. [c] Microwave irradiation. [d] 0.36 mmol scale. [e] 1.3 mmol scale. [f] **154a** isolated in 19% yield.

Swapping to [D8]-toluene allowed the rearrangement to be monitored by ¹⁹F NMR; **147a** rearranged smoothly to difluorocyclopentene **153** even at 90 °C but still showed evidence of VCP precursor after 26 hours (**Table 20**, Entry 2); full conversion was more desirable due to difficult chromatographic separation between **147a** and **153**. During this rearrangement the *cis*-diastereoisomer **152a** formed from pure *trans*-**147a** (6 h NMR time point), but the thermolysis of the **147a/152a** mixture resulted in the formation of unique difluorocyclopentene product **153**. Microwave irradiation resulted in slower rearrangement (**Table 20**, Entry 3), but neat **147a** was consumed more rapidly under conventional heating (**Table 20**, Entry 4). Attempts to scale this reaction from 0.4 mmol to 1.3 mmol maintained the high consumption of starting VCP **147a** but side product **154a** was also formed (**Table 20**, Entry 5). Benzocycloheptadiene **154a** could be isolated from the crude reaction mixture and the connectivity established by 2D NMR method. [3,3]-Rearrangement of the *cis*-cyclopropane **152a**, followed by

dehydrofluorination/rearomatisation of the initial educt (*vide infra*) results in the formation of the observed side product **154a**. Reintroduction of solvent (Ph₂O) and the use of excessive rearrangement temperature of 180 °C showed exclusive formation of difluorocyclopentene **153** (Table 20, Entry 6); re-subjecting isolated product to the same conditions showed only decomposition and no formation of benzocycloheptadiene **154a**. These control reactions confirm that the side product originates from the VCP precursors; why its formation was observed in the larger scale neat reaction is unknown, but it is thought to originate from poor heat transfer through the reaction and the possible formation of hot spots.

The side reaction could be avoided when the reaction was run in toluene at 100 °C (Table 20, Entry 7). After full conversion under these conditions, the reaction solvent was removed to afford a very high yield of **153** from **147a** (99%); *cis*-cyclopropane also rearranged exclusively to **153** in excellent (93%) yield under the same conditions (Table 20, Entry 8). This VCPR represents a direct and effective way of making difluorinated cyclopentenes. Compared with methods discussed previously, our approach combines ease of precursor preparation (four high-yielding steps from commercially available reagents) and purification-free rearrangement at useful temperatures.¹⁶⁴ Difluorocyclopentene **153** bears an attractive range of functional groups on for further functionalisation, and the utility of these groups was investigated synthetically.

3.2.5. Difluorocyclopentene Functionalisation

Functional group transformations on ester motifs and alkene groups have been well documented and studies into using these transformation for difluorocyclopentene **153** were carried out. It also became apparent in subsequent computational screening that the presence of the aromatic ring was necessary to maintain low VCPR temperatures (*vide infra*) so being able to base further transformations on this group would be highly beneficial (Figure 24).

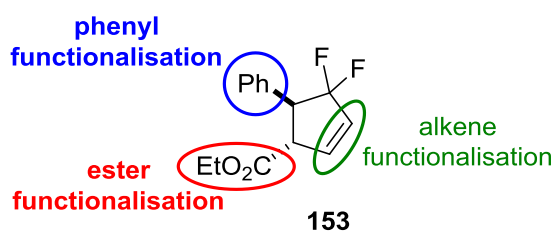
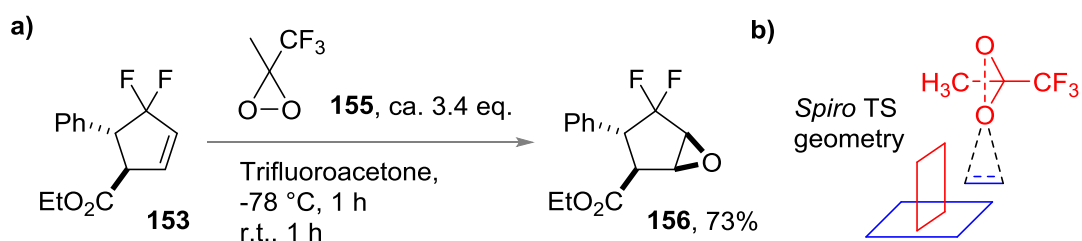


Figure 24: Potential sites for functionalisation of difluorocyclopentene **153**.

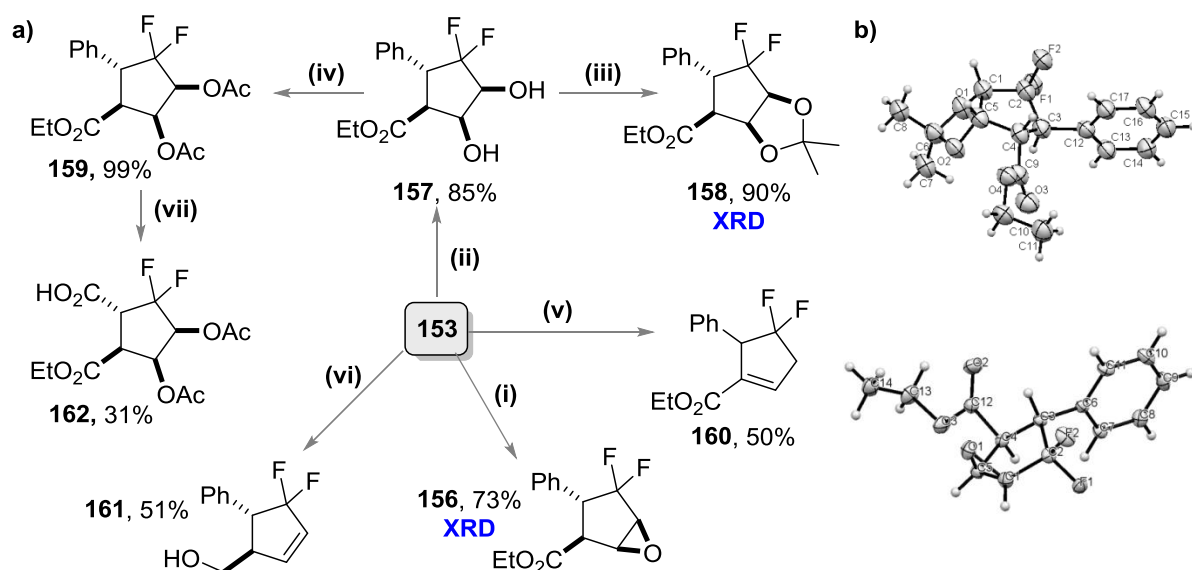
Initial investigations focused on using the olefin as a vector for functionalisation. Conventional epoxidation methods using *m*-CPBA, as well as conditions which facilitated the *in situ* generation of the more reactive methyl trifluoromethyldioxirane **155** (the latter was used previously within the group for the epoxidation of difluorinated cyclooctenes),¹⁶⁵ failed to react with difluorocyclopentene **153**. Instead, preparation of **155** using a modification of a published procedure¹⁶⁶ described by the Baran group¹⁶⁷ was required, and treatment with **153** resulted in a good yield of epoxide **156** (Scheme 82a). The original *trans*-relationship between the aromatic and ester groups on **153** and the unexpected facial selectivity was confirmed from the X-ray diffraction of **156**. It is well documented that the dioxirane epoxidation proceeds via a *spiro*-transition state (Scheme 84b)¹⁶⁸ and comparisons between relative free energies for the epoxidation transition states which arise from **156** support the observed facial selectivity. This is likely to originate from undesirable steric interactions with the *ortho*-aromatic protons from the alternative face.



Scheme 82: a) Successful epoxidation of **153**. b) Representation of transition state geometry from dioxirane mediated epoxidations.

Upjohn dihydroxylation on alkene **153** allowed access to diol **157** in 85% yield; protection of **157** through to *bis*-acetate **159** and acetonide **158** proceeded in high yields (Scheme 83a). X-ray diffraction analysis of the latter confirmed that the

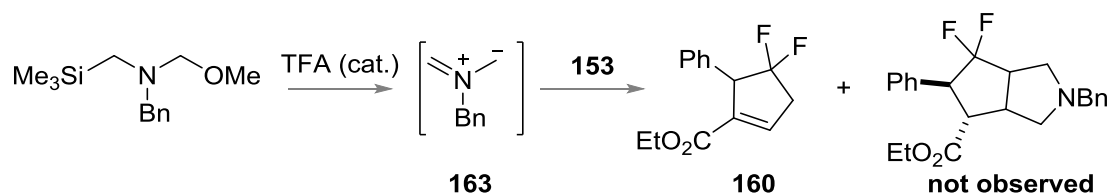
dihydroxylation occurred with the same facial selectivity observed with epoxidation (Scheme 83b).



Scheme 83: a) Functionalisation of 153 (XRD = X-ray diffraction obtained for these compounds). b) ORTEP diagram of crystal structures used to confirm stereochemistry.

Conditions: Methyl(trifluoromethyl)dioxirane (ca. 3.4 eq.) in trifluoroacetone, -78 °C, 1 h then r.t., 1 h. (ii) $\text{K}_2\text{Os}_4 \cdot 2\text{H}_2\text{O}$ (2 mol%), NMO (10 mol%), $\text{H}_2\text{O}/\text{THF}/\text{acetone}$, r.t., 45 h (iii) 2,2-dimethoxypropane (2 eq.), Amberlyst 15 (cat.), DCM, r.t., 19 h (iv) Ac_2O (3 eq.), pyridine, r.t., 16 h (v) DBU (10 mol%), acetone, r.t., 1 h (vi) LiAlH_4 (1.4 eq.), Et_2O , 0 °C to r.t., 5.5 h (vii) $\text{RuCl}_3 \cdot x\text{H}_2\text{O}$ (20 mol%), H_5IO_6 (14.2 eq.) MeCN/acetone, r.t., 19 h.

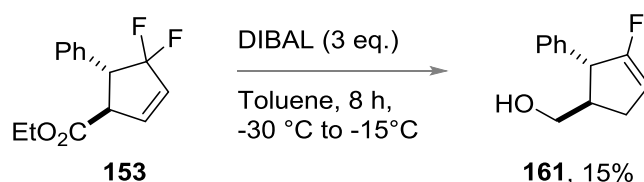
Attempts to trap alkene **153** with azomethine ylide **163** failed,¹⁶⁹ with crude NMR spectra suggesting that the alkene had isomerised to the more conjugated unsaturated ester **160** (Scheme 84).



Scheme 84: Failed attempts at [1,3]-cycloaddition between azomethine ylide 163 and difluorocyclopentene 153.

This result sparked investigations of the alkene isomerisation, revealing that the process was base-mediated; solvent screening in NMR reactions confirmed that acetone was the optimum solvent, allowing full conversion to be achieved after 2.5 hours at room temperature in the presence of catalytic quantities of 1,8-diazabicycloundec-7-ene (DBU, Scheme 83a).

Ester reduction with LiAlH_4 at cryogenic temperatures gave access to alcohol **161** in a moderate yield (51%) but with recovery of starting ester **153** (25%). Attempts to increase the reactivity by conducting the reaction at higher temperatures with DIBAL (3 equivalents) were successful, but also facilitated fluoride elimination via alkene isomerisation to afford fluorinated alkene **161** as the major product (**Scheme 85**). NMR characterisation confirmed product connectivity and distinctive vibrations in the IR confirmed ester reduction to alcohol.



Scheme 85: Fluorinated alkene 161 observed in higher temperature reductions.

Finally, proof of concept for oxidising the phenyl ring in *bis*-acetate **159** to the corresponding carboxylic acid **162** has been secured (**Scheme 83a**). Following literature conditions¹⁷⁰ but crucially, without the use of toxic carbon tetrachloride as a solvent, we observed 92% conversion to **162** using $\text{RuCl}_3 \cdot n\text{H}_2\text{O}$ (20 mol%) and excess periodic acid. Chromatographic purification gave a moderate 31% yield of acid **162** alongside an unknown side product. Tentative attempts at lowering catalyst loading (10 mol%) gave full conversion but more of the side product was formed; further investigations are required to improve the procedure but evidence that the aromatic ring could be oxidatively cleaved was extremely promising.

The above set of simple functional group transformations was not only key for assigning the stereochemistry of difluorocyclopentene **153** but also started to illustrate the flexibility of **153** as a robust building block for the synthesis of more complex fluorinated molecules.

3.2.6. VCPR Reaction Monitoring

Evidence of cyclopropane stereoisomerisation uncovered during the investigations of the thermal rearrangement of **147a** was intriguing and reaction monitoring was used to investigate this process more fully.

The thermolysis of both *trans*-**147a** and *cis*-**152a** was conducted in [D₈]-toluene in the NMR probe at 100 °C; ¹⁹F NMR spectra were recorded at appropriate time intervals and integration of resulting peaks provided relative percentages of compounds forming in the reaction. As shown previously, *trans*-**147a** transformed smoothly to **153**, but *cis*-**152a** also formed, reaching a maximum at about 13% of the reaction mixture after 10 minutes, and then decaying slowly, confirming that cyclopropane stereoisomerisation competes effectively with VCPR (**Figure 25a**). This could be observed more clearly when the reaction was started from *cis*-**152a**; within 15 minutes, most of the *cis*-cyclopropane had isomerised to the *trans*-diastereoisomer **147a**, which then reacted through to the cyclopentene **153** (**Figure 25b**).

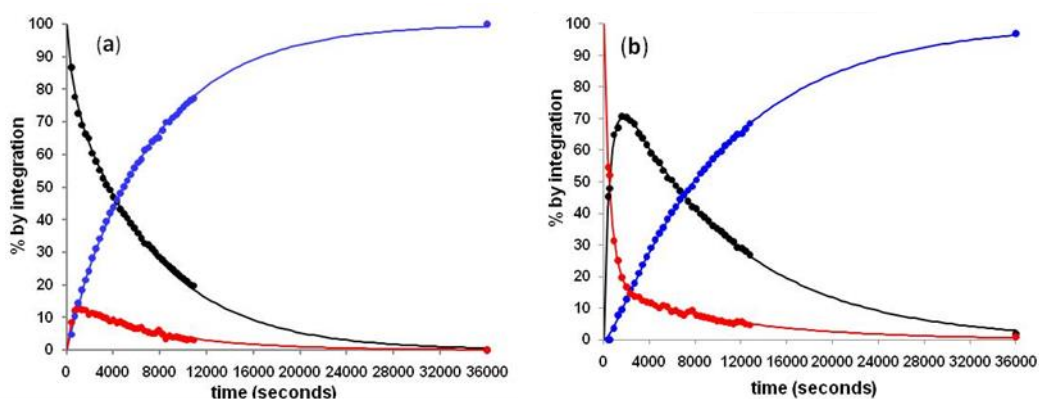
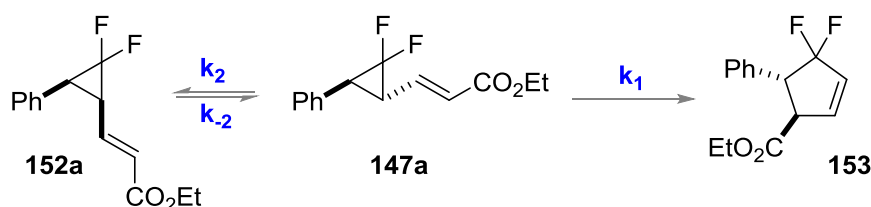


Figure 25: Experimental (points) and simulated (lines) concentration/time profile for thermolysis (373 K) of a) *trans*-**147a** and b) *cis*-**152a** (*trans*-**147a** = black, *cis*-**152a** = red, difluorocyclopentene **153** = blue).

The resulting concentration/time profiles could be simulated successfully as far as experimental endpoints at 10 hours using numerical integration software¹⁷¹ based on the simple kinetic model described in **Scheme 86**.



Scheme 86: Kinetic model used in the simulation of parallel VCPR and stereoisomerisation pathways.

Deconvolution of the calculated rate constants (**Table 21**) highlighted the modest equilibrium constant between *trans* and *cis* cyclopropanes (k_2/k_1) and supports facile cyclopropane stereoisomerisation (5.4 starting from *trans*-**147a** and 5.6 starting from *cis*-**152a**, favouring the *trans*-cyclopentene). The rate constant is an order of magnitude higher than that observed for the VCPR and is consistent with stereoisomerisation running in parallel with the rearrangement.

Table 21: Rate constants extracted from reaction simulation

| Substrate | $10^4 k_1$ (s ⁻¹) | $10^4 k_2$ (s ⁻¹) | $10^4 k_2$ (s ⁻¹) | k_2/k_1 |
|----------------------------|-------------------------------|-------------------------------|-------------------------------|-----------|
| <i>trans</i> - 147a | 1.6 | 3.5 | 19.1 | 5.4 |
| <i>cis</i> - 152a | 1.1 | 2.6 | 14.7 | 5.6 |

An approximate Arrhenius determination of the activation parameter for VCPR was carried out by taking the best first-order fit of the data from the rearrangement of **147a** using VT ¹⁹F NMR experiments conducted between 90 °C and 120 °C (**Figure 26**).

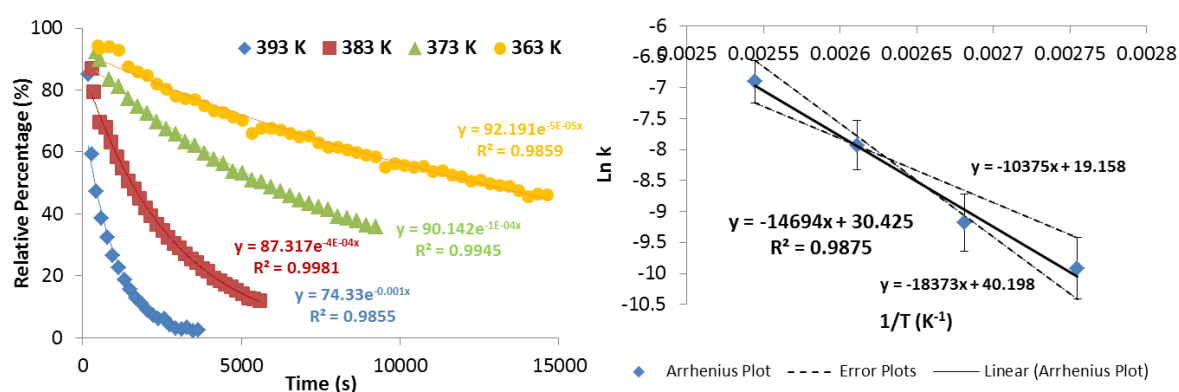


Figure 26: First order decay plot of the thermolysis of **147a** at different temperatures and the resulting Arrhenius plot from extracted rate data.

The experimental activation energy (E_a) for the VCPR of **147a** was calculated at 28.6 ± 0.6 kcal mol⁻¹ (373 K), not unlike the value obtained by Smart and co-workers for the thermolysis of pentafluorinated precursor **65** ($E_a = 28.4$ kcal mol⁻¹ at 373 K).¹⁰⁹ Furthermore, this value is approximately 10 kcal mol⁻¹ lower than Dolbier's unsubstituted difluorocyclopropane **81** and confirms the stabilising effect of the ester group and aromatic ring on the VCPR transition state; the phenyl is likely to have the greatest effect because it is better at stabilising radicals.

This experimental evidence provided a clear explanation into why lower temperature rearrangements are accessible from *trans*-precursor **147a** and definitively showed that competing stereoisomerisation pathways are active during VCPR. Investigations of the minor *Z*-alkenoates were also conducted to understand the effect alkene geometry has, if any, on the rearrangement.

3.2.7. Thermal Rearrangement of *Z*-Difluorocyclopropane Precursors

Similar temperature screening was conducted to investigate the rearrangement of minor *Z*-alkenoates, but no VCPR was observed from either *cis*-**152b** or *trans*-**147b**; only cyclopropane stereoisomerisation in favour of *trans*-**147b** was detected when the precursors were heated in [D₈]-toluene at 100 °C (**Figure 27**). Equilibrium constants of 3.7 (from *trans*-**147b**) and 3.6 (from *cis*-**152b**) were extracted from the simulation data and confirmed by integration of the ¹⁹F NMR spectra.

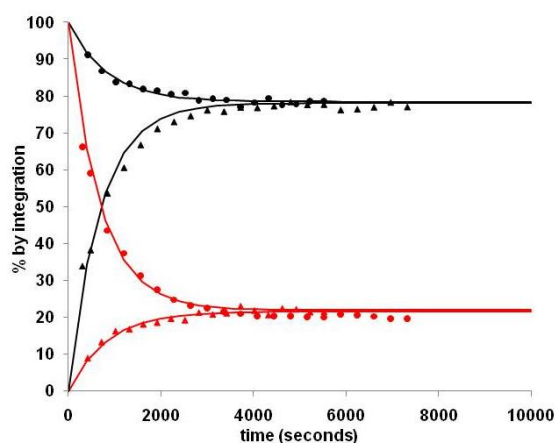
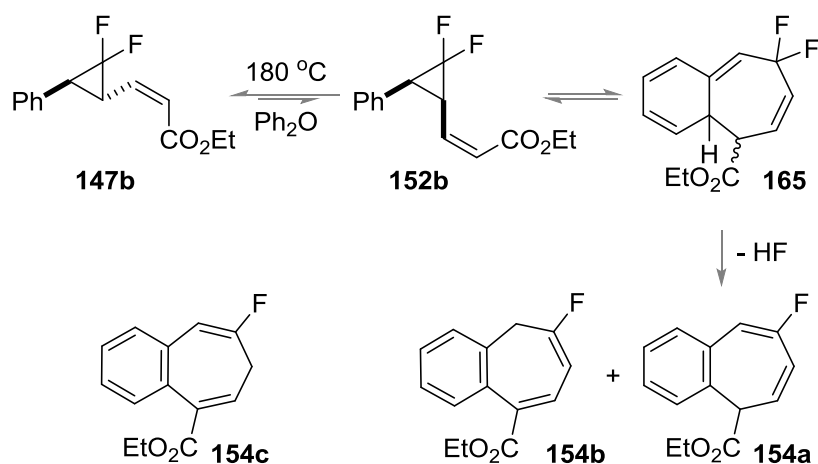


Figure 27: Experimental (points) and simulated (lines) concentration/time profile for thermolysis starting from: • *trans*-**147b** from *trans*-**147b**, ▲ *cis*-**152b** from *trans*-**147b**, • *cis*-**152b** from *cis*-**152b** and ▲ *trans*-**147b** from *cis*-**152b**; solid simulate lines are for *trans*-**147b** (black) and *cis*-**152b** (red).

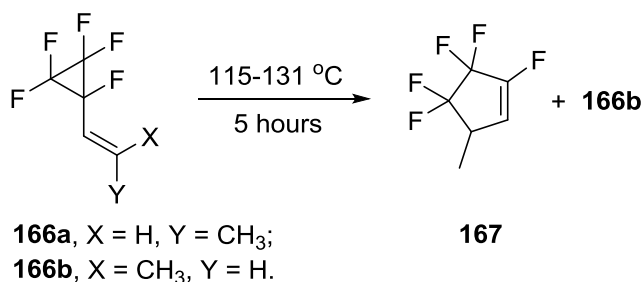
Higher temperatures were screened to try to facilitate VCPR, but *trans*-**152b** favoured a [3,3]-pathway to **154a** and **154b** at 180 °C (**154a**:**154b** ratio of 10:1 by ¹⁹F NMR integration). Stronger heating of *cis*-**152b** also returned a very similar mixture of **154a** and **154b** (9:1 by ¹⁹F NMR integration); similar to previous results, the de-aromatised intermediate **165** was never observed (**Scheme 87**).

Heating an isolated sample of **154a** at 180 °C (Ph₂O, 17.5 hours) returned the more fully conjugated **154b**, presumably via a [1,5]-hydride shift mechanism; the product of a [1,3]-hydride shift from **154a** (**154c**) was never detected.



Scheme 87: [3,3]-Rearrangement of Z-alkenoate precursors **147b** and **152b**.

The inertness of the Z-alkenoate precursors towards VCPR surprised us, but we failed to find literature examples of Z-alkenyl groups participating, apart from the deuterated alkene species of Baldwin and co-workers.⁹³⁻⁹⁴ Sustmann⁶² and co-workers prepared precursors with Z-alkenyl groups but did not report their behaviour under rearrangement conditions. Smart *et al.*²¹ heated a 5:1 mixture of **166a** and **166b**, to form a 19:1 mixture of pentafluorocyclopentene **167** and unreacted Z-isomer **166b** (**Scheme 88**). To our knowledge, Smart's result provides the only example of a Z-alkenyl component in VCPR; ΔG^\ddagger (373 K) for the VCPR of **166b** was measured at 31.1 kcal mol⁻¹, only ca. 3 kcal mol⁻¹ higher than that for **166a** (28.5 kcal mol⁻¹).



Scheme 88: Convergence of diastereoisomeric alkene precursors through VCPR.

The *E/Z*-alkene reactivity difference is more dramatic in our system and we looked to electronic structure calculations to help us understand this and other aspects of the stereospecific nature of the VCPR.

3.2.8. Investigations using Electronic Structure Calculations

3.2.8.1. VCPR Methodology Screening

The detailed computational studies of the VCPR of **49** through transition state **TS2** conducted by Houk and co-workers¹⁰⁰ provided the ideal starting point for our computational investigations. The Cartesian coordinates for **TS2** were used to provide a core model for building more substituted transition states (**TS6**, **TS7** and **TS8**) which represented the VCPR of **61**, **65** and **168a** (a conformationally simpler analogue of *trans*-**147a**) (**Figure 28**).

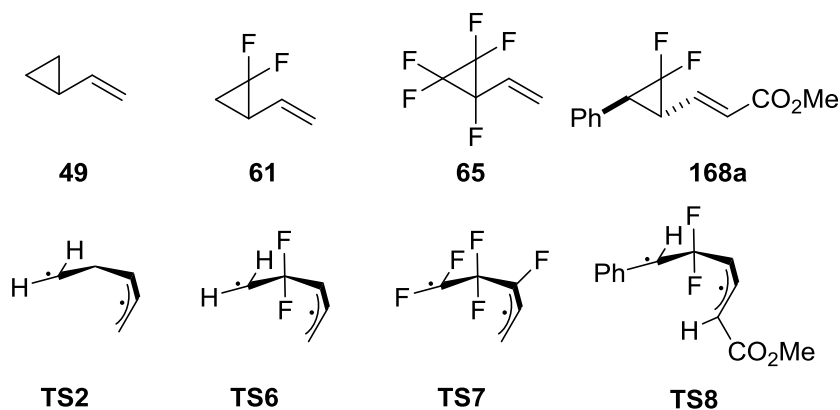


Figure 28: Precursors and their corresponding transition states used to investigate the VCPR.

We chose to explore the effectiveness of a small matrix of methods for predicting VCPR barriers. Both literature and our precursors were examined, using B3LYP,¹⁷² M05-2X,¹⁷³ M06-2X¹⁷⁴ and B97-D¹⁷⁵ functionals (all in unrestricted mode) with 6-31G*, 6-31+G* and 6-311+G** basis sets to calculate barrier energies (ΔG^\ddagger). Initial optimisations were carried out on Spartan'08¹⁷⁶ or Spartan'10¹⁷⁷ software due to the ease of handling lists, then the reported activation energies were calculated on Gaussian'09.¹⁷⁸ Optimised geometries were characterised as minima or transition structures by analysis of calculated frequency calculations; the diradical character of the transition states could be confirmed by examining the spin operator (S^2) values. The focus of our work is primarily synthetic, so larger methods or higher level basis

sets were not considered; instead we wished to establish the most accurate lowest cost method. The dipoles of all the precursors and transition states were small and similar (2.25-3.00 Debyes), and the toluene solvent used for the experimental work has a low dielectric constant ($\epsilon = 2.38$); therefore no solvation methods were applied. The values for barrier heights calculated using electronic structure calculations (ΔG^\ddagger) were compared with experimental Arrhenius parameters (E_a , recalculated to 298K) from the literature and from this work to assess how well the methods deal with the VCPR (**Table 22** and **Figure 29**).

Table 22: Barriers (ΔG^\ddagger , gas phase, 298 K, kcal mol⁻¹) for VCPR from electronic structure calculations and recalculated¹¹⁴ from Arrhenius data.^{84,107b,111}

| Method | 49 → TS2 | 61 → TS6 | 65 → TS7 | 168a → TS8 |
|-------------------|---------------------|---------------------|---------------------|-----------------------|
| UB3LYP 6-31G* | 46.9 | 38.3 | 24.8 | 26.6 |
| UB3LYP 6-31+G* | 46.2 | 36.0 | 22.9 | 25.1 |
| UB3LYP 6-311+G** | 45.9 | 36.0 | 23.0 | 24.8 |
| UM05-2X 6-31G* | 50.8 | 41.6 | 28.5 | 31.1 |
| UM05-2X 6-31+G* | 50.0 | 39.4 | 26.4 | 29.8 |
| UM05-2X 6-311+G** | 49.5 | 39.5 | 26.8 | 29.8 |
| UM06-2X 6-31G* | 55.1 | 46.4 | 31.8 | 36.0 |
| UM06-2X 6-31+G* | 54.0 | 44.0 | 29.9 | 34.7 |
| UM06-2X 6-311+G** | 53.2 | 43.6 | 29.8 | 34.6 |
| UB97-D 6-31G* | 45.3 | 36.2 | 29.7 | 22.5 |
| UB97-D 6-31+G* | 44.6 | 33.9 | 28.0 | 21.3 |
| UB97-D 6-311+G** | 44.4 | 36.8 | 27.9 | 21.1 |
| Experiment | 49.2 | 39.0 | 28.5 | 28.6 |

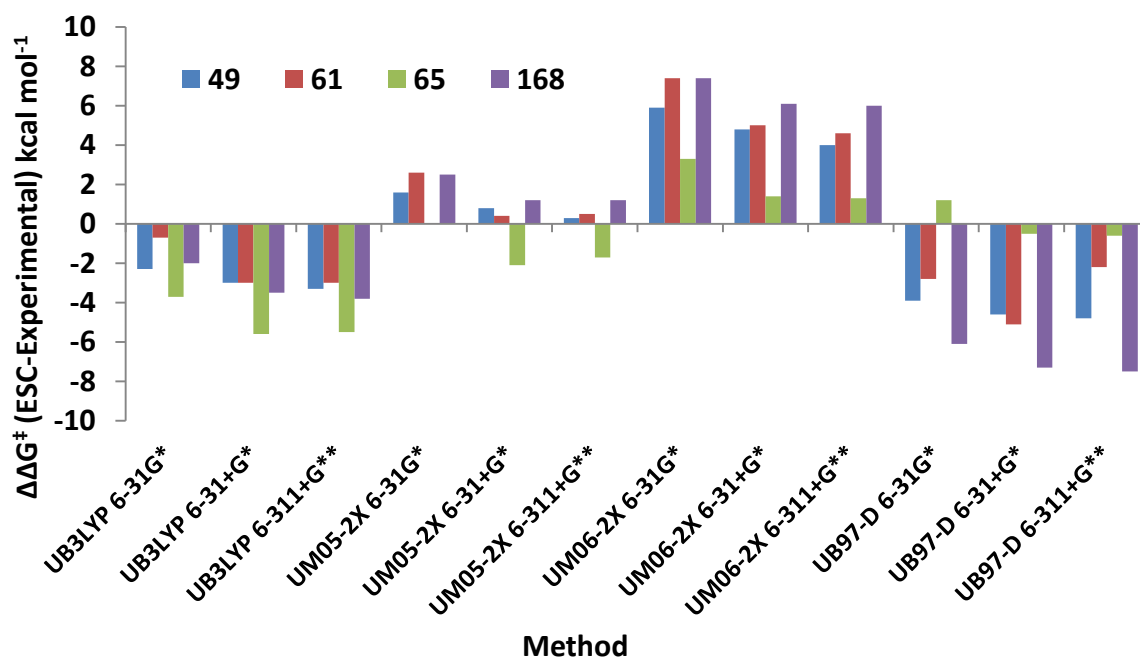


Figure 29: Differences between experimental E_a (298 K, re-calculated from activation parameters) and ΔG^\ddagger from electronic structure calculations (298 K), plotted as $\Delta\Delta G^\ddagger$ ($\Delta G^\ddagger - E_a$, kcal mol⁻¹). Expected error associated with the data is ± 0.5 kcal mol⁻¹.

Significant differences were noted between the levels of performance of the various functionals. UB3LYP underestimated the experimental barriers for all systems, with the discrepancy increasing with basis set size. UB97-D performed best with Smart's pentafluorinated system but greatly under-estimated barriers for the other systems. This method dealt with the diradical nature of **TS7** and **TS8** less well, with S^2 values of 0 and 0.31, respectively. Consistently higher values, closer to 0.75, were obtained with the other methods across all systems.

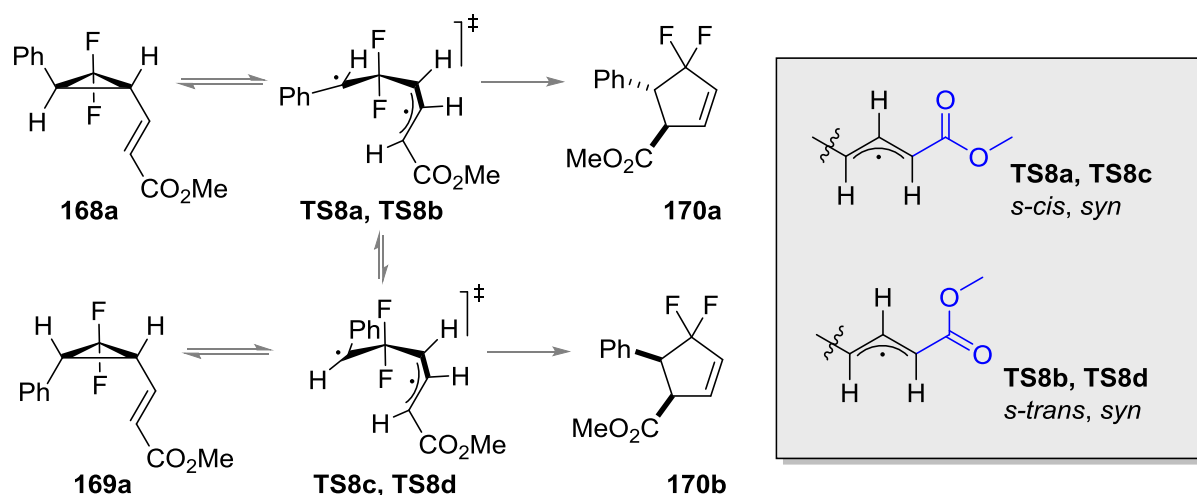
The closest agreement with experimental values was obtained with UM05-2X/6-31+G* and UM05-2X/6-311+G** methods with $\Delta\Delta G^\ddagger$ values within 1 kcal mol⁻¹ (overestimate) for **49**, **61** and **168a**, and within 2 kcal mol⁻¹ (underestimate) for **65**, respectively. These observations were consistent with the results of studies carried out by Sustmann and co-workers of the computational assessment of non-fluorinated precursors, but also show that the lower 6-31+G* basis set performs just as well as larger, more time-consuming alternatives.

The UM06-2X functional over-estimated the rearrangement barrier for **49**, **61** and **168a** by a larger 4.0 kcal mol⁻¹ or more, but performed better for the more highly-fluorinated **65**. Comparison between transition states showed that **TS7** had a different radical terminus from the other three systems due to the presence of fluorine atoms. In **TS7**, the radical centre was pyramidal, whereas it has a trigonal geometry in others. There is no reason why the different levels of theory should deal with the VCPR of **65** less well but there is an obvious step change in transition state structures.

While the UM05-2X/6-31G* method gave the closest agreement between prediction and experimental values in this small test set, the consistency of performance of the lower cost UB3LYP/6-31G* method was impressive. Both methods were applied in subsequent investigations and the difference in free energies obtained are identified by a suffix in G_{UM05-2X} and G_{UB3LYP}.

The transition states examined focus on the lowest energy *si*-pathway but previous studies have shown that the *si*-pathway competes with others (*ar*, *ai* and *sr*) to varying degrees, depending on the level and type of precursor substitution. Larger groups seem to favour the major *si*-pathway more decisively; this was the expectation with our system due to the formation of a single *trans*-cyclopentene product. It was important to confirm this hypothesis using electronic structure calculations.

From experimental results, the logical progression of *trans*-**168a** would be through **TS8a** or **TS8b**; these transition states differ only in the ester conformation (**Scheme 89**). Inversion at the migrating benzylic centre means that by the time the transition state is reached, the phenyl group has swung into the correct orientation for the formation of *trans*-cyclopentene **170a**.



Scheme 89: Diastereoisomeric VCPR transition state from **168a** and **169a**.

TS8a ($\Delta G^{\ddagger}_{\text{UM05-2X}} = 29.8 \text{ kcal mol}^{-1}$) has the alkenoate in the *s-cis, syn* conformation, which is the favoured orientation for simpler systems like methyl acrylate;¹⁷⁹ **TS8b** has the ester *s-trans, syn* at a cost of an additional $1.0 \text{ kcal mol}^{-1}$ at the barrier ($\Delta G^{\ddagger}_{\text{UM05-2X}} = 30.8 \text{ kcal mol}^{-1}$).¹⁸⁰ Unexpectedly, transition states **TS8c** and **TS8d** which represent VCPR from *cis*-**169a** have very similar barrier heights (both within 1 kcal mol^{-1} from **TS8a**, **Table 23**). On the basis of these calculations, the formation of *cis*-cyclopentene **170b** would be anticipated strongly, contrary to what was observed experimentally. In contrast, the UB3LYP method predicted a kinetically *trans*-selective VCPR, with bigger free energy differences between the diastereoisomeric transition states. The values of $\Delta\Delta G^{\ddagger}_{\text{UB3LYP}}$ of $2.3 \text{ kcal mol}^{-1}$ corresponds to a kinetic ratio of **170a:170b** of >20:1, in this instance the *cis*-product **170b** would not be detectable in product mixtures by ^{19}F NMR.

Table 23: Barriers for VCPR from diastereoisomeric transition states.

| TS | $\Delta G^{\ddagger}_{\text{UM05-2X}}$ | $\Delta G^{\ddagger}_{\text{UB3LYP}}$ |
|-------------|--|---------------------------------------|
| TS8a | 29.8 | 25.9 |
| TS8b | 30.8 | 26.6 |
| TS8c | 30.1 | 28.2 |
| TS8d | 30.8 | 28.9 |
| TS9d | 34.7 | 32.8 |

The same set of structures with alternative alkene geometries were used to assess the VCPR from *Z*-alkenoate **168b**; only one (**TS9d**) out of the four transition states

optimised to a geometry recognisable as a VCPR transition state, 34.7 kcal mol⁻¹ above **168b** ($\Delta G_{\text{UM05-2X}}^\ddagger$) (**Table 23**).

Therefore, only one pair of transition states could be used to determine the effect of opposite alkene configurations. The transition state **TS9d** from the *Z*-alkenoate was 3.9 kcal mol⁻¹ higher in energy than **TS8d** for the corresponding *E*-alkenoate; the additional cost of access to this structure could arise from the close approach (2.65 Å) between the benzylic proton and the alkenoate carbonyl carbon (**Figure 30**).

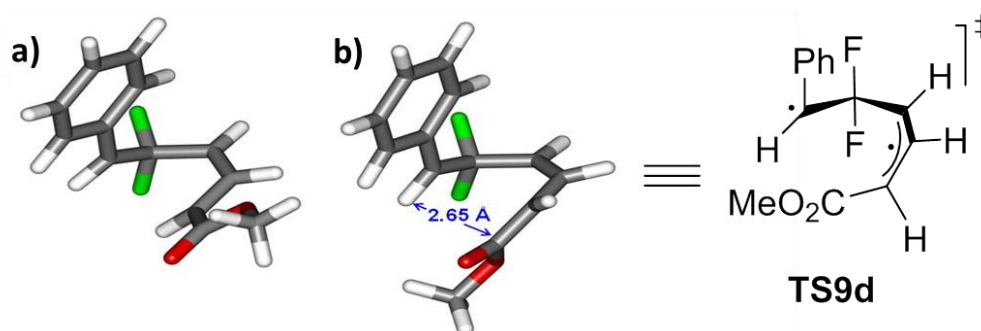
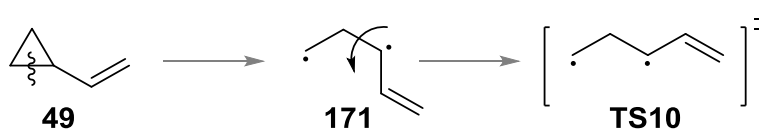


Figure 30: Diastereoisomeric transition structures, both with *s-trans, syn* alkenoate conformation for a) **TS8d** for *E*-alkenoate series and b) **TS9d** for *Z*-alkenoate series where an H...C close contact is highlighted.

Both computational methods support the fact that the *Z*-alkenoate requires higher energy to promote VCPR; insight into the cyclopropane stereoisomerisation and alternative [3,3]-rearrangement pathway would also help us to understand our system more fully.

3.2.8.2. Cyclopropane Stereoisomerisation

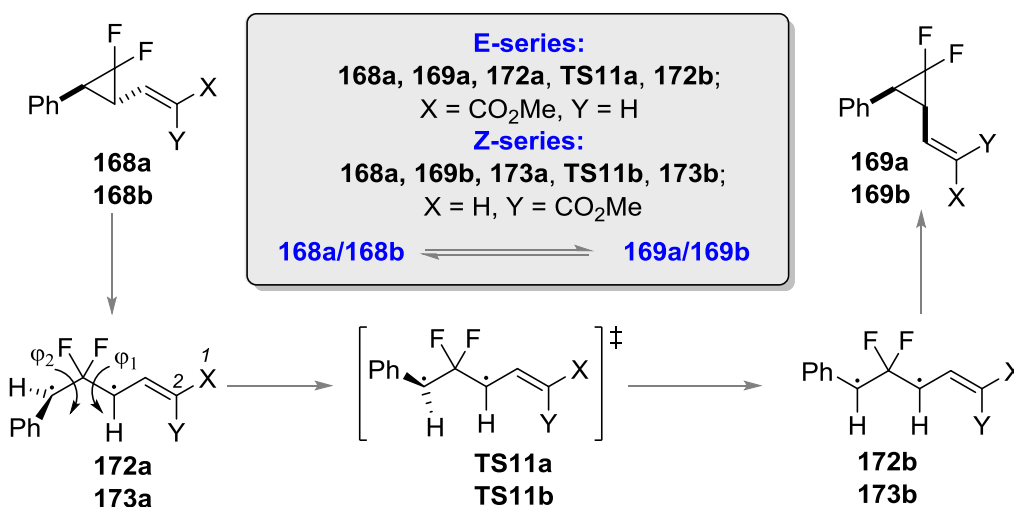
We looked to secure a minimal pathway which interconnected the *cis*- and *trans*-cyclopropane precursors; Houk and co-workers previously mapped the quite complex potential energy surface accessible from simple VCP **49**.¹⁰⁰ They identified that intermediate **171** and transition state **TS10**, were connected by rotation around a C-C σ -bond which cost approximately 15 kcal mol⁻¹ from precursor **49** (from single point calculations, **Scheme 90**).



Scheme 90: Diradical species implicated in cyclopropane stereoisomerisation of **49**.

We could access similar intermediates of this type from *trans*-**168** or *cis*-**169** by stretching the ring bond distal to the CF₂ centre (using AM1 and energy profile algorithm in Spartan'10). A minimal set of triplet diradicals corresponding to the full VCPR system were built and used to access transition states which would interconnect the two systems (**Scheme 91**).

Transoid triplet diradical **172a** could be converted to *cisoid* triplet **172b** either by rotation around C-4/C-5 (dihedral φ_1) or C-5/C-6 (dihedral φ_2) bonds; carbons C-1 through to C-4 stay mutually coplanar in order to preserve allyl radical stabilisation (**Scheme 91**). This explains why alkenoate *E/Z*-stereoisomerisation was never observed experimentally. Transition state **TS11a** relating both intermediates **172a** and **172b** was found through rotation of dihedral φ_2 at a cost of 24.5 kcal mol⁻¹ ($\Delta G_{\text{UM05-2x}}^{\ddagger}$) or 22.0 kcal mol⁻¹ ($\Delta G_{\text{UB3LYP}}^{\ddagger}$) from precursor **168a** (**Figure 31a**).



Scheme 91: *Trans*-/*cis*-cyclopropane stereoisomerisation via triplet intermediates and transition states.

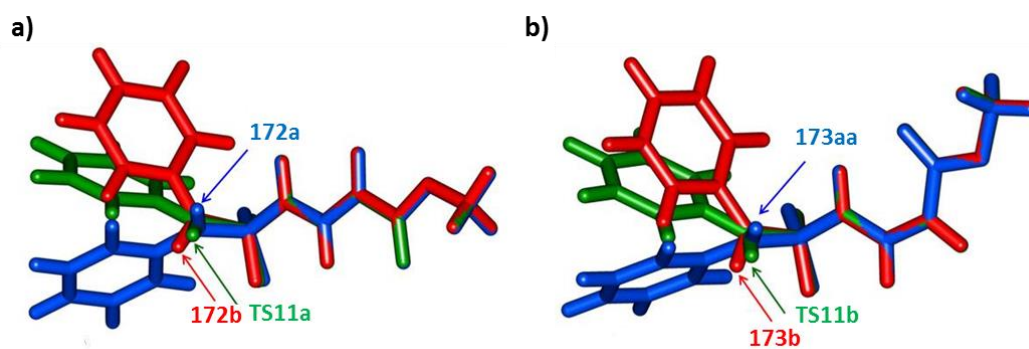


Figure 31: Triplet diradical structures which interconnect *cis*- and *trans*-cyclopropane structures for a) *E*-alkenoate and b) *Z*-alkenoate series.

The *Z*-cyclopropane **168b** and **169b** could be interconnected by rotation around dihedral φ_2 via triplet **173a** and **173b**, through transition state **TS11b** at a similar cost (**Figure 31b**). Both methods predicted the interconversion to be more facile than VCPR, consistent with experimental findings (**Table 24**).

Table 24: Relative free energies (*G*, gas phase, 298 K, kcal mol⁻¹, Spartan'08) for cyclopropanes (**168**, **169**), ring opened triplets (**172**, **173**) and triplet interconversion transition states (**TS11a**, **TS11b**).

| Species | $G_{(\text{UM05-2X})\text{rel}}$ | $G_{(\text{UB3LYP})\text{rel}}$ | Species | $G_{(\text{UM05-2X})\text{rel}}$ | $G_{(\text{UB3LYP})\text{rel}}$ |
|--------------|----------------------------------|---------------------------------|--------------|----------------------------------|---------------------------------|
| 168a | 0.0 | 0.0 | 168b | 0.0 | 0.0 |
| 172a | 23.4 | 19.4 | 173a | 24.1 | 19.8 |
| TS11a | 24.5 | 22.0 | TS11b | 27.7 | 23.0 |
| 172b | 24.1 | 20.5 | 173b | 26.6 | 20.1 |
| 169a | 0.5 | 0.6 | 169b | 0.0 | 0.8 |

A more detailed investigation into rotation around dihedral φ_2 was carried out, obtaining structures after every 10° rotation through 180° from triplet intermediate **172a**. The resulting 18 structures were optimised as triplet intermediates and transition states, revealing an intermediate/transition state system interconnecting the two cyclopropane isomers with two transition states between three intermediates (**Figure 32a**). These species remain on a flat energy plateau between both *E*- and *Z*-alkenoates and both remain the lowest energy pathway compared with VCPR (**Figure 32b**).

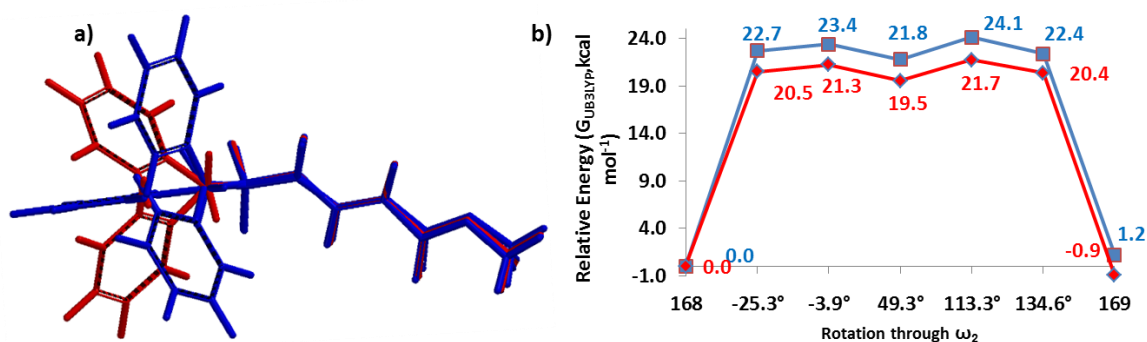


Figure 32: a) Full triplet intermediate (blue) and transition state (red) system interconnecting *trans*- and *cis*-cyclopropanes. b) Flat energy plateau of relative energies for *E*- (blue) and *Z*-alkenoate (red) systems observed for cyclopropane stereoisomerisation (Spartan'10, relative energies in kcal mol⁻¹, gas phase, 298 K).

Computational investigations of the [3,3]-rearrangement were also carried out in order to assess this higher energy process compared with VCPR.

3.2.8.3. [3,3]-Rearrangement

The concerted [3,3]-rearrangement observed in our system represent an aromatic-vinylcyclopropane Cope rearrangement and these are less common than the divinylcyclopropane rearrangement discussed previously.¹⁸¹ Though the rearrangement had been utilised in the successful synthesis of marine sponge-derived natural product Frodosin B **174** and the highly potent SIRT-inhibitor **175**, the synthetic use of the aromatic-vinylcyclopropane rearrangement is much less common than the divinyl counterpart (Figure 33).

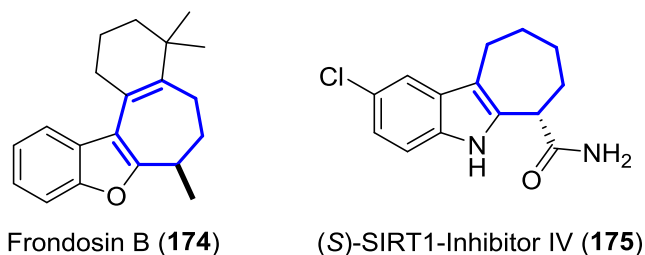


Figure 33: A natural product and an active pharmaceutical compound synthesised using the aromatic-vinylcyclopropane rearrangement (the key ring structure formed during the rearrangement is highlighted in blue).

The disruption of aromaticity leads to a high energy penalty for the rearrangement, but in our system, this is likely to be recovered during the dehydrofluorination/re-aromatisation step. Computational assessment of the later step is likely to be

difficult but the initial [3,3]-rearrangement would be more manageable. Özkan and Zora carried out a DFT study on the rearrangement of *cis*-1,2-divinylcyclopropane and found that the optimised transition structures remained closed-shell even when they ran spin-unrestricted calculations.

We therefore focused our investigations on the concerted [3,3]-rearrangement pathway for the formation of benzocycloheptadienes from the *cis*-cyclopropanes. From M05-2X/6-31+G* calculations, the *cis*-*E* **TS12a** lies 27.7 kcal mol⁻¹ above precursor **169a**; *cis*-*Z* **TS12b** had a significantly higher barrier at 34.7 kcal mol⁻¹ (**Figure 34**). The corresponding values using our B3LYP method were 27.8 and 32.9 kcal mol⁻¹, respectively.

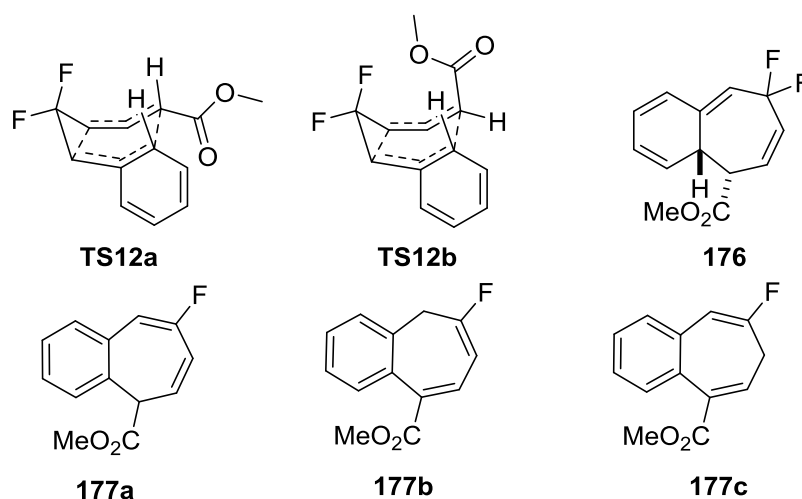


Figure 34: Initial (**176**) and final (**177a-c**) [3,3]-rearrangement products and transition state (**TS12a**, **TS12b**) from *cis*-cyclopropanes.

Once again, the alkene geometry had a decisive effect on reactivity, consistent with the experimental observations in which *Z*-species only reacted at significantly higher temperatures. The increased barrier for **TS12b** is likely to originate from an eclipsing interaction between a C-H and C-C bond at the reacting centres which become bonded during rearrangement.

The immediate product **176** has lost aromaticity and therefore lies above precursor **169a** ($(G_{\text{M05-2X}})_{\text{rel}} = 9.3 \text{ kcal mol}^{-1}$ or $(G_{\text{B3LYP}})_{\text{rel}} = 14.5 \text{ kcal mol}^{-1}$); loss of HF leads to benzoheptadienes **177a-c**. Both sets of calculations identified thermodynamic

product **177b** correctly (for **177a** $(G_{M05-2X})_{rel} = -19.0 \text{ kcal mol}^{-1}$, $(G_{B3LYP})_{rel} = -9.4 \text{ kcal mol}^{-1}$; for **177b** $(G_{M05-2X})_{rel} = -22.8 \text{ kcal mol}^{-1}$, $(G_{B3LYP})_{rel} = -14.5 \text{ kcal mol}^{-1}$; for **177c** $(G_{M05-2X})_{rel} = -19.6 \text{ kcal mol}^{-1}$, $(G_{B3LYP})_{rel} = -11.1 \text{ kcal mol}^{-1}$); the favourable energetic drive from **177a** to **177b** was consistent with observed experimental rearrangement and the proposed [1,5]-hydride shift was also investigated.

Hess and Baldwin carried out DFT studies on the [1,5]-hydride shift for a range of cyclic dienes, predicting an activation energy of $33.7 \text{ kcal mol}^{-1}$ in the cycloheptadiene system;¹⁸² we could obtain an identical barrier height locally using B3LYP/6-31G* methodology. From this basic model, we looked at larger systems to assess the effects of alkene, benzene, ester and fluorine substituents; the outcome was a calculated barrier for the [1,5]-hydride shift from **177a** to **177b** (Figure 35a).

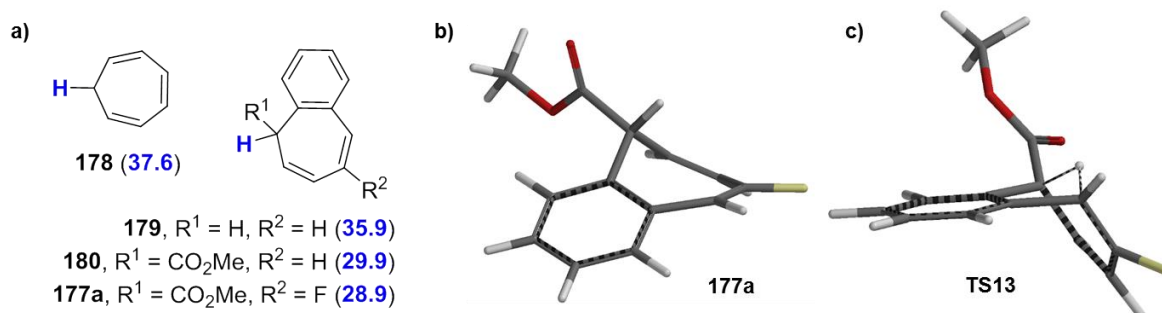


Figure 35: a) Barrier height for the [1,5]-hydride shift for cycloheptadiene compounds (Spartan'10, B3LYP/6-31G*, gas phase, 298 K, kcal mol⁻¹). b) Computational image of **177a** highlighting the position of the shifting hydrogen atom. c) Transition state (TS13) representing the [1,5]-hydride shift observed between **177a** and **177b**.

An increase activation energy of $3.9 \text{ kcal mol}^{-1}$ for the [1,5]-hydride shift was observed with cycloheptatriene **178** ($\Delta G_{B3LYP}^\ddagger = 37.6 \text{ kcal mol}^{-1}$) compared with cycloheptadiene ($\Delta G_{B3LYP}^\ddagger = 33.7 \text{ kcal mol}^{-1}$); less of an effect was observed with benzocycloheptadiene **179** ($\Delta G_{B3LYP}^\ddagger = 35.9 \text{ kcal mol}^{-1}$). Interestingly, barrier heights decreased to $29.9 \text{ kcal mol}^{-1}$ when methyl ester **180** was investigated and fluorination gave a further $1.0 \text{ kcal mol}^{-1}$ decrease ($\Delta G_{B3LYP}^\ddagger = 28.9 \text{ kcal mol}^{-1}$); the latter model represents the rearrangement observed between **177a** and **177b**. In the benzoheptadiene systems the shifting hydride in optimised intermediates is in a geometry which looks capable of facilitating rearrangement; ordering this species for [1,5]-shift should have a very low entropic cost (Figure 35b). The energy

lowering effect observed between benzoheptadiene **179** and methyl ester **180** is likely to be electronically driven, supporting the modest benefit conferred by fluorine atom substitution.

Transition state **TS13** (**Figure 35c**) sits 28.9 kcal mol⁻¹ above intermediate **177a**, the product of [3,3]-rearrangement of Z-alkenoate **169b** through **TS12b** and adduct **176** ($\Delta G_{\text{B3LYP}}^{\ddagger} = 32.9$ kcal mol⁻¹). Intermediate **177a** has a lower relative free energy than the cyclopropane and the similarities in barrier height account for the competitiveness of the [1,5]-hydride shift at the [3,3]-rearrangement temperature.

3.2.9. Assessment of Computational Methodology

Two computational methods, UM05-2X/6-31+G* and UB3LYP/6-31G*, were found to be the most accurate at predicting VCPR barrier heights across a set of compounds and were used to assess competing rearrangement pathways. Our initial interest in carrying out these calculations arose from a desire to order the reactivities of the competing pathways successfully; *cis/trans*-cyclopropane stereoisomerisation, stereoselective *trans*-cyclopentene formation by VCPR, [3,3]-rearrangement versus VCPR and the low reactivity of the Z-alkenonates versus the *E*-diastereoisomer all required explanations.

Of the two methods used, (U)B3LYP/6-31G* ordered the pathways correctly by reactivity, predicted the stereoselectivity of the VCPR in agreement with experiment and rationalised the effect of alkene configuration on VCPR and [3,3]-rearrangement rates (**Table 25**). While the UM05-2X/6-31+G* method provided the highest accuracy at lowest cost for the VCPR test set, the agreement between predicted and experimental reactivity order suggests strongly that the older UB3LYP/6-31G* method may prove most effective for assessing the overall rearrangement pathways (**Figure 36**).

Table 25: Barriers (ΔG^\ddagger) and differences ($\Delta\Delta G^\ddagger$) between barriers (gas phase, 298 K, kcal mol⁻¹) relating to selectivities between isomerisation, VCPR and [3,3]-rearrangement pathways.

| Pathway/process | (U)M05-2X 6-31+G* | (U)B3LYP 6-31G* |
|--|----------------------|--------------------|
| Cyclopropane isomerisation 168a/169a , ΔG^\ddagger | 24.5 | 22.0 |
| Cyclopropane isomerisation 168b/169b , ΔG^\ddagger | 27.7 | 23.0 |
| Lowest cost VCPR, ΔG^\ddagger | 29.8 | 25.9 |
| Lowest cost [3,3]-rearrangement from 169b , ΔG^\ddagger | 27.7 | 27.8 |
| Selectivity for formation of kinetic <i>trans</i> -product, 170a versus 170b , $\Delta\Delta G^\ddagger$ | 0.3 | 2.3 |
| <i>E</i> versus <i>Z</i> selectivity for VCPR, $\Delta\Delta G^\ddagger$ | 5.5 | 3.9 |
| <i>E</i> versus <i>Z</i> selectivity for [3,3]-rearrangement, 169a versus 169b , $\Delta\Delta G^\ddagger$ | 7.0 | 5.1 |

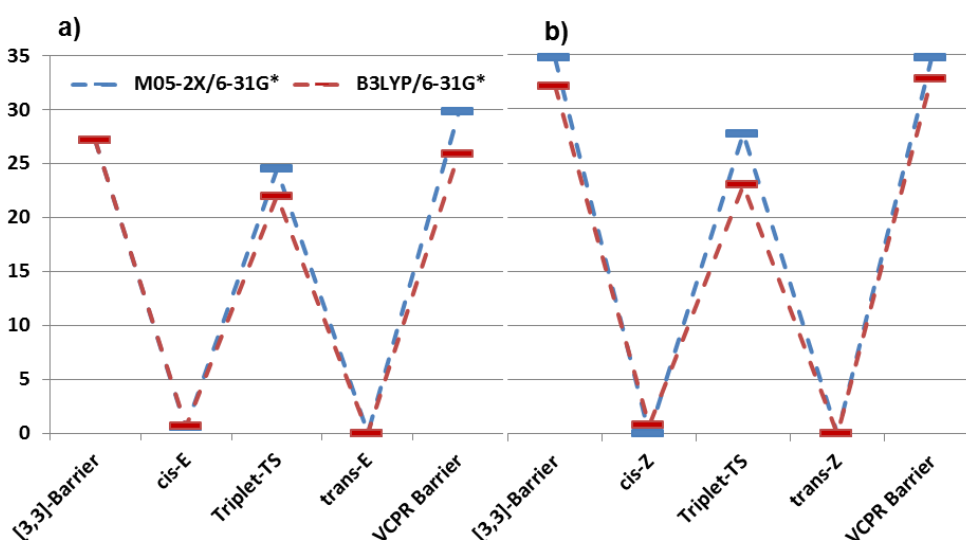


Figure 36: Comparison between (U)M05-2X/6-31G* and (U)B3LYP/6-31G* methodology at assessing rearrangement pathways for a) *E*-alkenoates and b) *Z*-alkenoates.

3.3. Conclusion

Two separate synthetic routes to *gem*-difluorocyclopropane precursors for VCPR were investigated. The first looked to focus on developing novel cyclopropyl-vinyl cross coupling chemistry of difluorocyclopropyl boronic ester reported in the literature. However, issues in controlling the difluorocyclopropanation chemistry, and the stability of the boronic ester, proved too problematic for a synthetically useful route to be developed.

The learnings from the screening of difluorocarbene transfer reagents carried out for vinyl boronic ester **123** were important for the development of new routes. Solvent trapping of the difluorocarbene (which was readily detectable by ^{19}F NMR) was a strong sign of a failed reaction. The second route focused on the difluorocyclopropanation of cinnamyl acetate, showing that Dolbier's robust and effective difluorocarbene transfer reagent MDFA was the most efficient on scale (using 2.81 g (16 mmol) of cinnamyl acetate afforded 2.79 g (77%) of difluorocyclopropane **142**). Optimisation of literature conditions, focusing on solvent type and reaction concentration, increased the decomposition rate of the reagent and allowed reactions to be complete after 4 hours compared with the 2 days reported in the literature. Ester hydrolysis followed by tandem oxidation/olefination afforded the desired precursors; all four isomers of 3-(1'(2'2'-difluoro-3'-phenyl)cyclopropyl) propenoate could be accessed using this route.

Investigations of the thermal VCPR of these precursors showed that the major *trans-E* isomer **147a** rearranged to difluorocyclopentene **153** in close to quantitative yields at a relatively low temperature (100 °C); the overall yield of **153** over the four steps from cinnamyl acetate was 70%. Following rearrangements by ^{19}F NMR showed that cyclopropane stereoisomerisation was facile and occurred at lower temperatures than the VCPR. The minor *Z*-alkenoates required much higher temperatures to induce rearrangement (180 °C) and underwent aromatic-vinylcyclopropane rearrangement instead of VCPR. The control of rearrangement pathway by VCP precursor alkene geometry was unprecedented and required further understanding using electronic structure calculations.

Computational methodology screening revealed that the UM05-2X/6-31G* method provided the highest accuracy at lowest cost for the VCPR test set. Only one transition state which represented VCPR could be accessed for the Z-alkenoate; comparison with the corresponding Z-alkenoate not only predicted a higher activation barrier but proposed that this was due to steric clashes at the reactive centres. Further analysis of the cyclopropane stereoisomerisation through triplets, and the [3,3]-rearrangement through closed shell species allowed all the rearrangement pathways to be assessed effectively. Only the UB3LYP/6-31G* method provided a useful agreement with experimental results. The clear comparisons in this study between computational and experimental results strongly suggest that electronic structure calculations could be used with some confidence to triage synthetic work.

Chapter 3: Computational Triage

The continual rise in the processing power of modern computer systems has allowed the computational chemist to perform ever larger and more accurate calculations over shorter and shorter periods of time. Calculations are routinely performed for synthetically interesting reactions in order to characterise pathways in detail and rationalise experimental observations.¹⁸³ Typically, these calculations are performed *after* considerable synthetic optimisation, which can be time consuming and expensive. Computational evaluation of reactions prior to the commitment of experimental resource is now becoming less rare having been shown to streamline investigations into a range of organic transformations.¹⁸⁴

We now look to understand more fully what effect changing the functional groups around our difluorinated precursors has on the interplay between these two rearrangement pathways; we wish to be able to design precursors which rearrange at relatively low temperatures. By securing accurate transition structures for all three possible rearrangement pathways (**Figure 37**, See **Chapter 2**), we have ensured an opportunity to assess the scope and limitations of our system using electronic structure calculations, before committing to any synthetic chemistry.

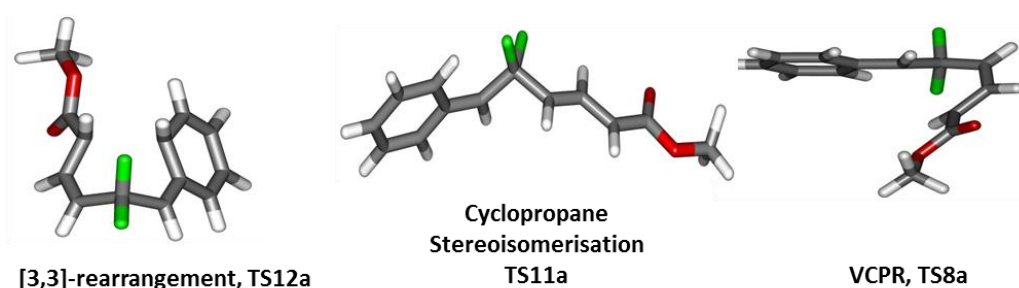


Figure 37: Geometries found representing the diradicaloid-VCPR, closed-shell [3,3]-sigmatropic rearrangement and triplet cyclopropane stereoisomerisation transition states.

4.1. Computational Assessment

Our computational screening would start by separately assessing the effect of different substituents, attached either to the difluorocyclopropane or the alkene portions of the precursor, have on the barrier for VCPR. A selection of interesting compounds based on the predicted ease of rearrangement would then be synthesised to assess the accuracy of the theoretical predictions. The overall goal is to obtain computational models that are easily accessible to synthetic chemists, so off-the-peg methods which are quicker would be preferred over more complex calculations.

4.1.1. Effect of Difluorocyclopropane Substitution

We previously found that the most cost effective method for calculating VCPR activation energies was an unrestricted B3LYP¹⁷² ((U)B3LYP) method with the 6-31G* basis set.¹⁶⁴ This method was used to assess the impact of modification of the left hand side of difluoro-VCP **181**, with calculated activation barriers ranked alongside phenyl-substituted precursor **168a** (Figure 38 and Table 20).

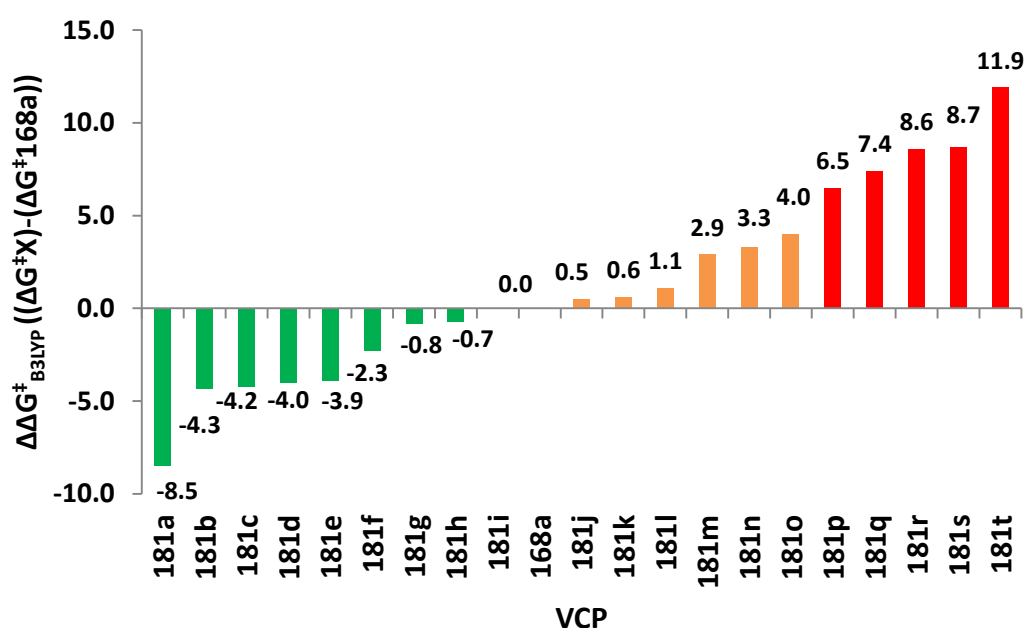


Figure 38: Difference in free energies of activation ($\Delta\Delta G^{\ddagger}_{\text{B3LYP}}$) between cyclopropane-substituted difluoro-VCP and reference 186a. Green = lower ΔG^{\ddagger} (< 25.3 kcal mol⁻¹), orange = 0-5 kcal mol⁻¹ higher ΔG^{\ddagger} and red = > 5 kcal mol⁻¹ increase in ΔG^{\ddagger} .

Table 26: Predicted effects on Substitution on Difluorocyclopropane Precursors **181** ((U)B3LYP/6-31G*, gas phase, 298 K, Spartan'10).

| VCP | R ¹ | R ² | $\Delta G_{\text{B3LYP}}^{\ddagger}$ | $\Delta\Delta G_{\text{B3LYP}}^{\ddagger}$ ^[a] |
|-------------|--|----------------|--------------------------------------|---|
| 181a | 2-pyrrolyl | H | 16.8 | -8.5 |
| 181b | 2-furyl | H | 21.0 | -4.3 |
| 181c | 4-pyridyl-N-oxide | H | 21.1 | -4.2 |
| 181d | 2-thiophenyl | H | 21.3 | -3.8 |
| 181e | 2-N-Boc-pyrrolyl | H | 21.4 | -3.9 |
| 181f | 5-benzo[d][1,3]dioxolyl | H | 23.0 | -2.3 |
| 181f | H ₂ C=CH ₂ (vinyl) | H | 24.5 | -0.8 |
| 181h | 3-thiophenyl | H | 24.6 | -0.7 |
| 181i | 2-thiazolyl | H | 25.3 | 0.0 |
| 168a | <i>Ph</i> | <i>H</i> | <i>25.3</i> | <i>0.0</i> |
| 181j | Ph | Ph | 25.8 | +0.5 |
| 181k | HC≡C (alkynyl) | H | 25.9 | +0.6 |
| 181l | 4-pyridyl | H | 26.4 | +1.1 |
| 181m | 2-pyridyl | H | 28.2 | +2.9 |
| 181n | 2,6-dimethylphenyl | H | 28.6 | +3.3 |
| 181o | CN | H | 29.3 | +4.0 |
| 181p | Me | Me | 31.8 | +6.5 |
| 181q | -CH ₂ (CH ₂) ₃ CH ₂ - | | 32.7 | +7.4 |
| 181r | Me | H | 33.9 | +8.6 |
| 181s | C ₆ H ₁₁ | H | 34.0 | +8.7 |
| 181t | H | H | 37.2 | +11.9 |

$$^{[a]} \Delta\Delta G_{\text{B3LYP}}^{\ddagger} = (\Delta G_{\text{B3LYP}}^{\ddagger} \mathbf{181}) - (\Delta G_{\text{B3LYP}}^{\ddagger} \mathbf{168a})$$

We observed a dramatic rise in calculated activation energy when there was no additional substitution on the difluoro-VCP (**181t**, +11.9 kcal mol⁻¹). Compounds with no aromatic functionality but one (**181r** and **181s**) or two alkyl (**181p** and **181q**) substituents were also found to have higher barriers for rearrangement (ranging from +6.5 to +8.6 kcal mol⁻¹). Previously we observed that temperatures of 180 °C facilitated a [3,3]-rearrangement pathway with a calculated activation energy of 32.9 kcal mol⁻¹ ($\Delta G_{\text{B3LYP}}^{\ddagger}$, (U)B3LYP/6-31G*, gas phase, 298 K, Gaussian'09),¹⁶⁴ suggesting that low rearrangement temperature with alkyl substituents would be unlikely. Higher reaction temperatures also have the potential to activate a

competitive [1,5]-hydride shift pathway⁸⁹ so these substitution patterns were ruled out of our synthetic study.

We observed a higher activation energy for 2,6-dimethylphenyl **181o** (+3.3 kcal mol⁻¹) due to steric interactions between the methyl protons and the proton (2.26 Å) and fluorine atoms (2.23 and 2.25 Å) attached to the cyclopropane ring in the transition state (**Figure 39**). These small steric interactions are tolerated in the transition state to ensure the benzylic radical remains coplanar with the aromatic ring.

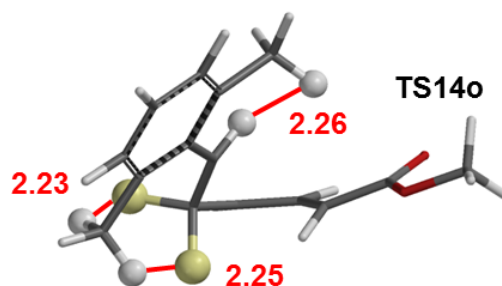


Figure 39: Steric interactions arising from *ortho*-dimethyl substitution on the phenyl ring in VCPR transition state TS14o (ball and spoke model used to highlight atoms which are within Van der Waals radii, distances in Å).

Unlike the *bis*-alkyl substituents, no barrier-lowering was observed for *bis*-phenyl **168j** (+0.5 kcal mol⁻¹). Steric repulsion between the *ortho*-protons in **TS14j** induces a slight rotation of each ring, forcing stabilising aryl groups out of the plane of the benzylic radical (**Figure 40**). Sustmann and co-workers investigated this twist angle effect in more detail,¹⁰² but no further investigations into *bis*-arylated difluoro-VCP systems were undertaken because the $\Delta G_{\text{B3LYP}}^\ddagger$ values were so similar to those for **168a**.

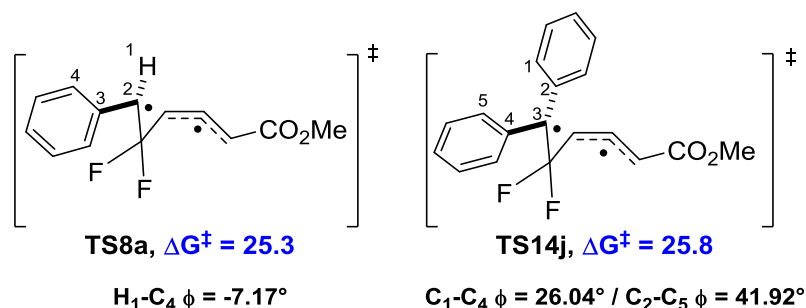


Figure 40: Aromatic ring planarity effects on benzylic radical stabilisation in TS8a and TS14j (dihedral angles represented by ϕ , ΔG^\ddagger values (blue) calculated using (U)B3LYP/6-31G*, gas phase, 298 K, Spartan'10, all energy values are in kcal mol⁻¹).

The lower activation energy calculated for the more electron rich phenyl-substituted **181f** (-2.3 kcal mol⁻¹) prompted further investigations into the electronic effects of phenyl ring substitution. The VCPR activation energies for a range of precursors with electron-donating and electron-withdrawing groups were assessed (**Table 27**), focusing solely on *para*-substituents, since these show the greatest effects for resonance stabilisation of benzylic radicals. Substrates containing electron-donating groups were predicted to undergo faster rearrangement (**Table 27**, Entries 1-6) than unsubstituted **168a** (**Table 27**, Entry 7), whereas substrates bearing electron-withdrawing groups only showed a modest increase in activation energy (**Table 27**, Entries 8-12).

Table 27: Calculated VCPR free energies of activation for difluoro-VCP **182a-k** ($\Delta G^\ddagger_{\text{B3LYP}}$, (U)B3LYP/6-31G*, gas phase, 298 K, Spartan'10) and σ and σ^\bullet constants used to generate Hammett Plot in **Figure 41a** and **Figure 41b**, respectively.

| Entry | VCP | XX | ΔG^\ddagger | $\Delta\Delta G^\ddagger$ ^[a] | σ^{185} | $\sigma^{\bullet 186}$ |
|-------|-------------|--------------------|---------------------|--|----------------|------------------------|
| 1 | a | N(Me) ₂ | 21.2 | -4.1 | -0.83 | 0.9 |
| 2 | b | NH ₂ | 21.9 | -3.4 | -0.66 | 0.7 |
| 3 | c | OH | 23.5 | -1.8 | -0.37 | 0.26 |
| 4 | d | OMe | 23.3 | -2.0 | -0.27 | 0.27 |
| 5 | e | Me | 24.5 | -0.8 | -0.17 | 0.34 |
| 6 | f | NHC(O)Me | 23.7 | -1.6 | 0 | 0.16 |
| 7 | 168a | H | 25.3 | 0 | 0 | 0 |
| 8 | g | Cl | 25.3 | 0 | 0.23 | 0.11 |
| 9 | h | Br | 25.4 | 0.1 | 0.23 | 0.11 |
| 10 | i | CF ₃ | 25.4 | 0.1 | 0.54 | 0.05 |
| 11 | j | CN | 25.6 | 0.3 | 0.66 | 0.47 |
| 12 | k | NO ₂ | 25.9 | 0.6 | 0.78 | 0.57 |

^[a] $\Delta\Delta G^\ddagger_{\text{B3LYP}} = (\Delta G^\ddagger_{\text{B3LYP}} \mathbf{182}) - (\Delta G^\ddagger_{\text{B3LYP}} \mathbf{168a})$

The Hammett plot¹⁸⁵ (**Figure 41a**) constructed from this data gave an extremely low ρ value of 0.05 and supported a radical (rather than a polar) mechanism. A variety of free radical substituent constants (σ^\bullet) have been reported in the literature^{38a,187}

but only those reported by Creary and co-workers (σ_c^\bullet) are applicable to the more commonly used substituents.¹⁸⁶ Our calculated activation energies correlated poorly when σ_c^\bullet constants were used ($R^2 = 0.4259$) but still gave a ρ value close to zero (**Figure 41b**). The relatively small increases in activation barriers, suggest that even substrates bearing electron-deficient phenyl rings should undergo VCPR at or close to 100 °C.

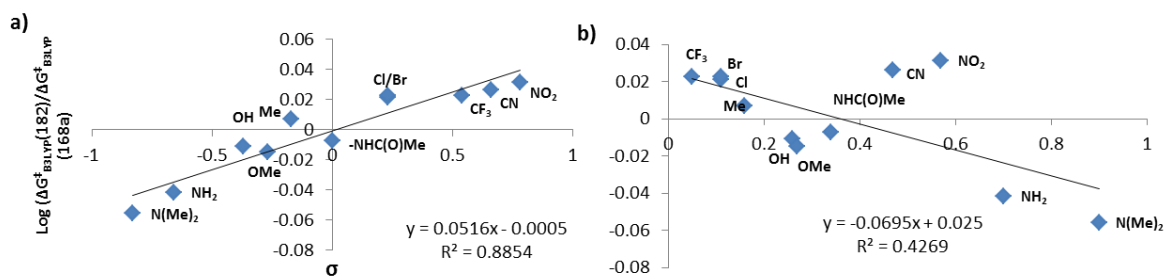
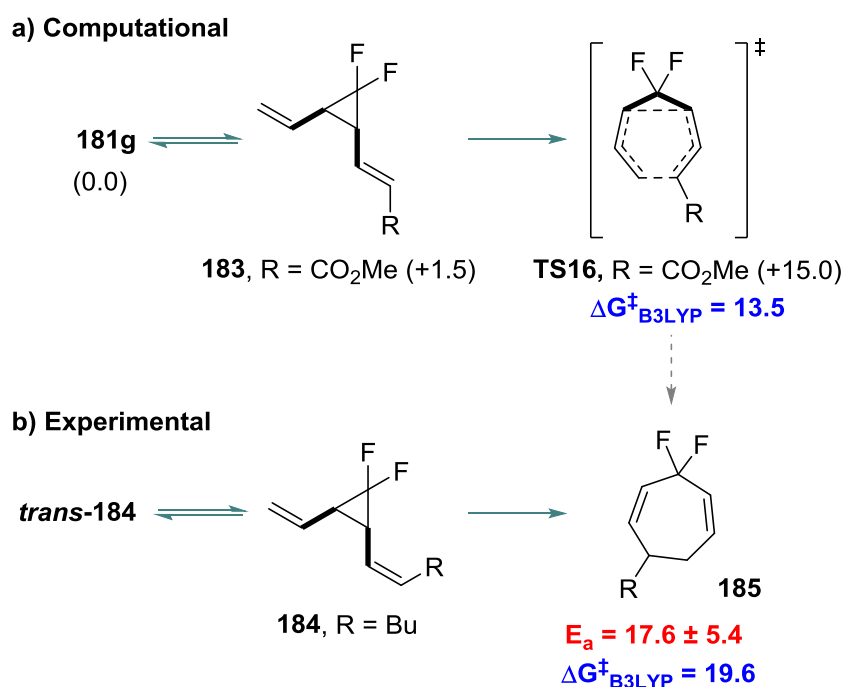


Figure 41: Hammet Plot generated from a) σ and b) σ^\bullet data in Table 27.

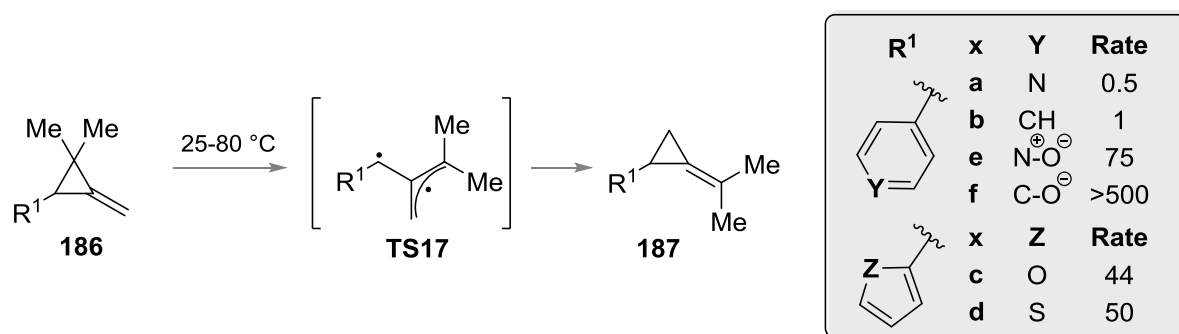
As our prime goal was to lower VCPR reaction temperatures, our screening was directed towards vinyl, (hetero)aryl and alkynyl substituents because the most effective mechanism for radical stabilisation is delocalisation through adjacent π -systems.¹⁸⁸ The lower activation energy observed for **181g** (ethenyl, 24.5 kcal mol⁻¹) compared with **168a** (phenyl, 25.3 kcal mol⁻¹) and **181k** (ethynyl, 25.9 kcal mol⁻¹) showed good correlation with the increased radical stabilisation energy reported for these substituents (calculated as 17.6, 14.6 and 14.5 kcal mol⁻¹, respectively).^{188b} The higher activation energy observed for **181o** (cyano, 29.3 kcal mol⁻¹) can be rationalised by a decreased radical stabilisation energy (7.9 kcal mol⁻¹),^{188b} which arises from the higher electronegativity of the nitrogen atom. These calculations suggested that *bis*-vinyl VCP-**181g** has the potential to rearrange at temperatures lower than 100 °C, but electronic structure calculations predicted that *cis*-isomer **183** would favour divinylcyclopropane rearrangement via **TS16** ($\Delta G_{\text{B3LYP}}^\ddagger = 13.5$ kcal mol⁻¹, VCPR vs [3,3] difference of 11.5 kcal mol⁻¹, **Scheme 92a**). Erbes and Boland showed experimentally that a similar dialkenyl-substituted *gem*-difluorocyclopropane (**184**) favoured the [3,3]-pathway through to cycloheptadiene **185** (**Scheme 92b**) exclusively.¹¹² Previous computational methodology screening for the VCPR of **168a** showed that the (U)B3LYP/6-31G* method under-estimated

the activation energy ($\Delta\Delta G^\ddagger_{\text{UB3LYP}} = -2.3 \text{ kcal mol}^{-1}$) consistently;¹⁶⁴ analysis of the [3,3]-rearrangement of **184** actually showed an over-prediction of barrier height ($\Delta\Delta G^\ddagger_{\text{B3LYP}} = +4.2 \text{ kcal mol}^{-1}$). Dialkenyl-**181g** was omitted from any subsequent synthetic investigations due to the unlikelihood of selective VCPR; however further electronic structure investigations into the [3,3]-rearrangement were undertaken in this study (*vide infra*).



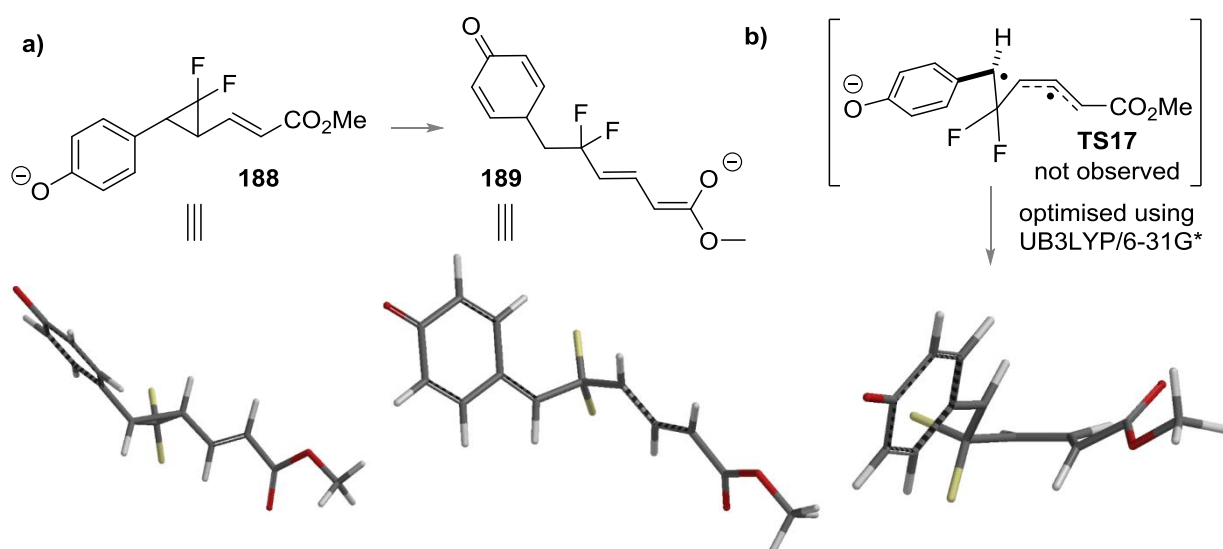
Scheme 92: a) Predicted lower energy [3,3]-pathway for *bis*-vinyldifluorocyclopropane **183** (free energies are relative to **181g**). b) Experimental example of preferential divinylcyclopropane rearrangement from *bis*-vinyl-difluorocyclopropane **184** to difluoroheptadiene **185**¹¹² (experimental activation energy (E_a) is derived from an Arrhenius determination of reported kinetic data,¹¹² all free energies (blue) calculated using B3LYP/6-31G*, 298 K, gas phase and quoted in kcal mol⁻¹).

Of the heteroaromatic substituents examined, only the 2- and 4-pyridyl species gave higher VCPR barriers than **168a** (**181m**, +2.9 kcal/mol⁻¹ and **181l**, +1.1 kcal mol⁻¹); the nitrogen atom cannot help stabilise radicals in these cases. Creary and co-workers reported similar results during investigations into the radical rearrangement of methylenecyclopropane **186** to isopropylidenecyclopropane **187** (Scheme 93).^{186,189}



Scheme 93: Substituent group radical stability determined from the rate of rearrangement of 186 to 187.¹⁸⁶

They reported higher rearrangement rates when heterocycles **186c-e** and phenolate **186f** were present. These substituents were dubbed “super radical stabilisers” by Creary. Unfortunately all computational attempts at incorporating the most strongly-activating 4-phenoxide substituent into our VCPR system failed. During the optimisation of precursor **188**, ring opening occurred via a donor-acceptor mechanism¹⁹⁰ to **189** (**Scheme 94a**). All attempts at obtaining a diradicaloid transition state which represented the VCPR failed; **TS17** optimised as a transition state ($\nu_i = i107 \text{ cm}^{-1}$) but lacked any diradical character ($S^2 = 0.0001$). Our focus was on using electronic structure calculations to assess the VCPR so no further investigations were carried out on cyclopropane precursor **188**; if the compound could be accessed synthetically, a very low energy barrier between **189** and **TS17** (11.0 kcal mol⁻¹) suggests that rearrangement would be very facile. The calculated activation energy was 12.5 kcal mol⁻¹ lower than the corresponding phenol precursors **182c** (see **Table 27**) and is consistent with the higher reactivity observed by Creary and co-workers.¹⁸⁶



Scheme 94: Failed attempts at obtaining optimised electronic structures for a) intermediate **189** and b) transition state **TS17**; the resulting species react via a donor-acceptor mechanism.

When the heteroarenes were embedded in our VCPR system, the calculated activation energies (for **181b-181d**) were consistently lower (ranging from a 4.2 to 5.3 kcal mol⁻¹ under-estimate) than for phenyl **168a**. Two regioisomeric transition-states exist for the unsymmetrical species; the 2-pyrrolyl and 2-thiophenyl species favoured **TS14a** whilst the 2-furyl favoured **TS14b** (Figure 42a).

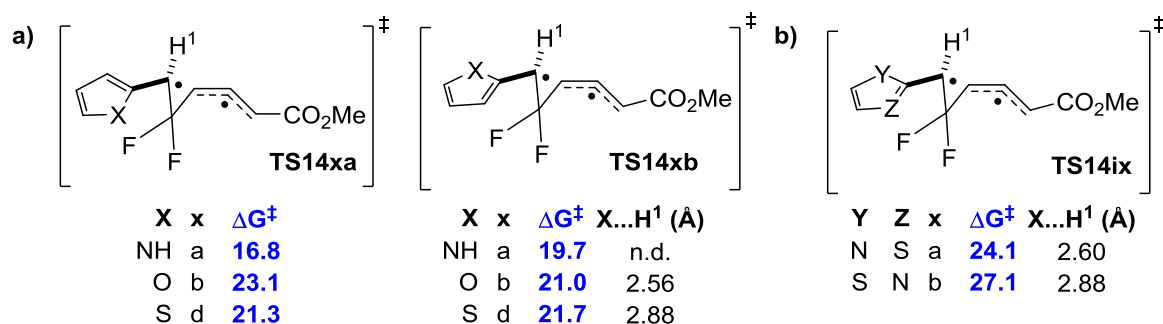


Figure 42: Two alternative VCPR transition states available for difluoro-VCP substituted with heteroarenes (ΔG^\ddagger energies calculated on Spartan'10, (U)B3LYP/6-31G*, 298 K, gas phase, energies quoted in kcal mol⁻¹).

We propose that the lower energies observed for **TS14bb** compared with **TS14ba** arose from a complementary polar interaction between the δ^+ proton (H¹) and the oxygen atom in the furan ring (calculated distances are within the sum of the Van der Waals radii used in Spartan'10). The absence of additional stabilisation observed in **TS14db** over **TS14da** can be attributed to lower strength S...H interactions. This was consistent with calculated activation energies for thiazolyl **TS14i**, favouring the

stronger N...H interaction over S...H (**Figure 42b**).¹⁹¹ Furthermore, 2-pyrrolyl **181a** favoured **TS14aa** due to an unfavourable N-H...H interaction in **TS14ab**. The extra stabilisation experience by furyl **181b** over thiophenyl **181d** offered some explanation as to why our calculated rearrangement rates were ordered differently from those reported by Creary and co-workers. Our lowest calculated activation energy was observed with 2-pyrrolyl **181a** ($\Delta\Delta G^\ddagger = -8.5 \text{ kcal mol}^{-1}$), a substituent which to our knowledge has not previously been reported as a strong radical stabiliser.

The low activation energies calculated for heteroaromatic compounds **181b**, **181d-f** and **181i** promised that lower temperature VCPRs would be possible with fluorinated precursors. We selected this set of compounds for synthesis, alongside 4-pyridyl **181m** as a control, to test our predictions.

4.1.2. Effect of Alkene Substitution

We used **190** as a template to investigate modifications to the alkene fragment of the precursors, focusing on the effects of alkene configuration (R^2 versus R^3), radical stabilising substituents and vinyl ether functionalisation ($R^1 = \text{OEt}$) (**Figure 43** and **Table 28**).

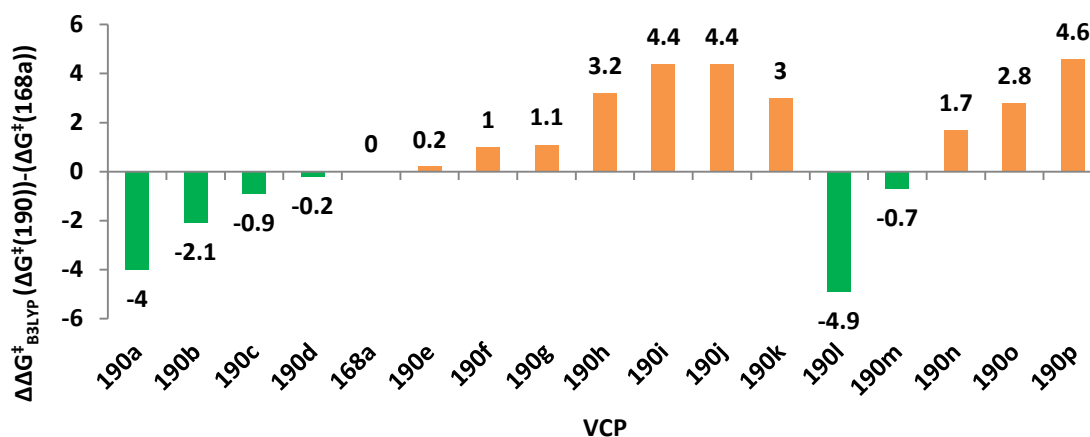
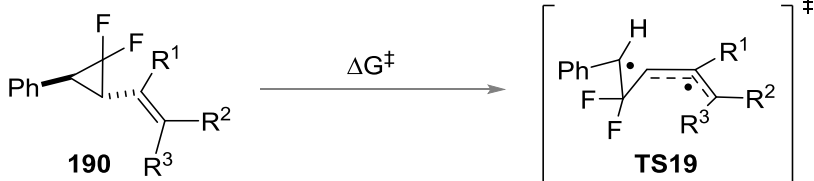


Figure 43: Difference in free energy ($\Delta\Delta G^\ddagger_{\text{B3LYP}}$) between alkene substituted difluorovinylcyclopropanes and reference 168a. **Green** = lower ΔG^\ddagger ($< 25.3 \text{ kcal mol}^{-1}$) and **orange** = $0-5 \text{ kcal mol}^{-1}$ greater ΔG^\ddagger .

Table 28: Effect of Alkene Substitution on VCP **190** ((U)B3LYP/6-31G*, gas phase, 298 K, Spartan'10).



| Entry | VCP | R ¹ | R ² | R ³ | $\Delta G^\ddagger_{\text{B3LYP}}$ | $\Delta\Delta G^\ddagger_{\text{B3LYP}}^{[a]}$ |
|-------|-------------|----------------|--------------------|--------------------|------------------------------------|--|
| 1 | 190a | H | Ph | H | 21.3 | -4.0 |
| 2 | 190b | H | CN | H | 23.2 | -2.1 |
| 3 | 190c | H | CON(Me)OMe | H | 24.4 | -0.9 |
| 4 | 190d | H | CH ₂ OH | H | 25.1 | -0.2 |
| 5 | 168a | H | CO ₂ Me | H | 25.3 | 0.0 |
| 6 | 190e | H | Me | H | 25.5 | 0.2 |
| 7 | 190f | H | H | H | 26.3 | 1.0 |
| 8 | 190g | H | H | Ph | 26.4 | 1.1 |
| 9 | 190h | H | H | CH ₂ OH | 28.5 | 3.2 |
| 10 | 190i | H | H | Me | 29.7 | 4.4 |
| 11 | 190j | H | H | CN | 29.7 | 4.4 |
| 12 | 190k | H | CO ₂ Me | Me | 28.3 | 3.0 |
| 13 | 190l | OEt | Ph | H | 20.4 | -4.9 |
| 14 | 190m | OEt | Me | H | 24.6 | -0.7 |
| 15 | 190n | OEt | H | Ph | 27.0 | 1.7 |
| 16 | 190o | OEt | H | H | 28.1 | 2.8 |
| 17 | 190p | OEt | H | Me | 29.9 | 4.6 |

^[a] $\Delta\Delta G^\ddagger_{\text{B3LYP}} = (\Delta G^\ddagger_{\text{B3LYP}} \mathbf{190}) - (\Delta G^\ddagger_{\text{B3LYP}} \mathbf{168a})$

The dramatic reactivity difference between the *E*- and *Z*-alkene isomers of **168a** previously reported¹⁶⁴ was maintained when a range of alkene substituents was examined. Calculated activation energies for *E*-substituted precursors (**Table 28**, Entries 1-6) were lower than for the unsubstituted precursor **190f** (**Table 28**, Entry 7), whilst the barriers for the corresponding *Z*-diastereoisomers were higher (**Table 28**, Entries 8-10). The narrow range of free energies of activation observed for the *E*-diastereoisomers (21.3 to 25.6 kcal mol⁻¹) suggest that all of these precursors should rearrange at temperatures close to or below 100 °C. The narrow spread of barrier heights ($\Delta\Delta G^\ddagger_{\text{B3LYP}} = 4.3$ kcal mol⁻¹) as the alkene substituents vary between aryl and alkyl is half that observed when the same functionality change is made on the cyclopropane (see **Table 26**). This suggests that a wider range of substituents

could be tolerated on the alkene fragment since the radical is already stabilised through allyl resonance.

The transition states for the diastereotopic *Z*-isomer of Weinreb amide **190c** and methyl ester **168b** failed to optimise, but the phenyl (**190g**, +1.1 kcal mol⁻¹), allyl (**190h**, +3.2 kcal mol⁻¹), methyl (**190i**, +4.4 kcal mol⁻¹) and cyano (**190j**, +4.5 kcal mol⁻¹) species all optimised with higher activation energies than the corresponding *E*-series. Disubstituted alkene **190k** (Table 28, Entry 12) had a higher free energy of activation than ester **168a** (+3.0 kcal mol⁻¹) but the introduction of the ester functionality lowered the activation energy for the rearrangement of *Z*-methyl **190i** (difference of 1.0 kcal mol⁻¹ between **190i** and **190k**). Successful synthetic investigations (*vide infra*) were made to follow up these predictions.

A set of aryl and alkyl substituted vinyl ethers were also examined (Table 28, Entries 13-17); an increase in activation energy of 1.8 kcal mol⁻¹ was observed from unsubstituted alkene **190f** (26.3 kcal mol⁻¹) to unsubstituted vinyl ether **190o** (28.1 kcal mol⁻¹). It was predicted that lower temperature rearrangements (< 100 °C) could be facilitated by either aryl (**190l**, 20.4 kcal mol⁻¹) or alkyl (**190m**, 24.6 kcal mol⁻¹) substitution in the less sterically hindered R² position. Surprisingly, despite previously leading to increased barrier heights, phenyl substitution at R³ (**190n**, 27.0 kcal mol⁻¹) resulted in an activation energy lower than that of the corresponding unsubstituted vinyl ether **190o** ($\Delta\Delta G_{\text{B3LYP}}^\ddagger$ between **190n** and **190o** = -1.1 kcal mol⁻¹). The less effective methyl radical stabilising group in the same position had the highest reported activation energy out of all the alkene-substituted compounds examined (**190p**, 29.9 kcal mol⁻¹).

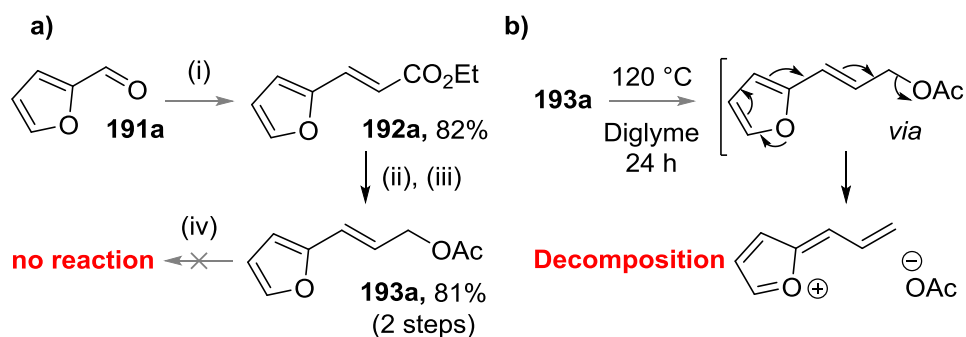
4.2. Synthetic Investigations

After the systematic examination of the functional group tolerance of the VCPR using electronic structure calculations, the synthesis of a selection of compounds was undertaken in order to test our computational predictions.

4.2.1. Synthesis of Cyclopropane Substituted Difluoro-VCP

4.2.1.1. 1st Generation Synthetic Route

The efficient synthesis of phenyl-VCP **147a** (73% over three steps) previously reported, relied on the successful difluorocyclopropanation of commercially available cinnamyl acetate with methyl 2,2-difluoro-2-(fluorosulfonyl)acetate (MDFA, **35**). It was believed that more electron-rich heteroaromatic substituents would help the cyclopropanation reaction by raising the nucleophilicity of the alkene. 2-Furyl propene **193a** was used to test this theory. Olefination of furfural **191a** with (carbethoxymethylene)triphenylphosphorane **146**, allowed access to gram quantities of furyl alkenoate **192a** (Scheme 95).



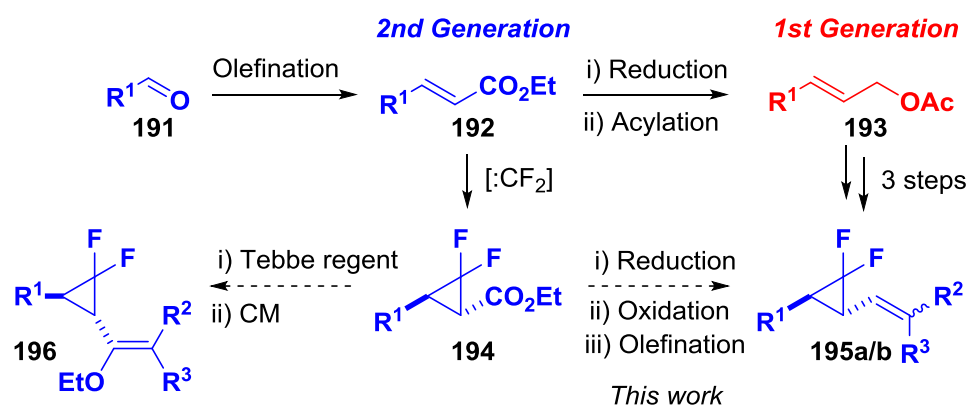
Scheme 95: a) Synthesis and failed difluorocyclopropanation of 2-furyl allyl acetate **193a** due to b) faster thermal decomposition.

Conditions: (i) (carbethoxymethylene)triphenylphosphorane (1.1 eq.), DCM, r.t., 17 h (ii) DIBAL (3 eq.), toluene, -78 °C to r.t., 8 h (iii) Ac₂O (1.2 eq.), pyridine (1.2 eq.), DCM, 45 °C, 5 h (iv) MDFA (2.5 eq.), TMSCl (2.5 eq.), KI (2.8 eq.), diglyme (1.17 eq.), 120 °C, 24 h.

Subsequent reduction of **192a** using diisobutylaluminium hydride (DIBAL) followed by acetylation of the crude reaction mixture, afforded **193a** in good yield over all three steps (66%). Disappointingly, only decomposition was observed when **193a** was subjected to the previously optimised difluorocyclopropanation conditions. It was proposed that the high reaction temperatures facilitated the elimination of acetic acid via donation of electrons from the furan ring system (Scheme 95b). A control reaction which heated a solution of acetate **193a** alone in diglyme for 24 h at 120 °C resulted in the formation of a black tarry mixture; cinnamyl acetate was shown to be stable under the same conditions. The strong odour of AcOH from the

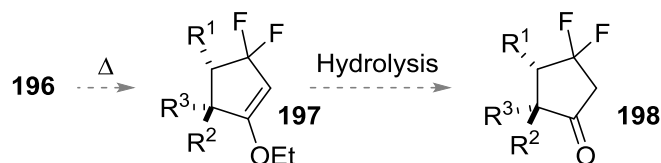
resulting crude reaction mixture supported the proposed decomposition mechanism but no other by-product could be detected.

A more divergent 2nd generation synthesis from alkenoate **192** was proposed which allowed potential access to both vinyl ether **196** and alkene **195** precursors (**Scheme 96**); alkenoates **192** are easily accessible on a gram scale from the corresponding commercial or easily-accessible aldehydes and are more stable olefins for the high temperature reactions involving electron-rich aromatic substituents than allyl acetate **193**.



Scheme 96: 1st generation and the more divergent 2nd generation synthetic routes for accessing difluoro-VCPs **195** and **196**, from aldehydes **191**.

Olefination of ester **194** using Tebbe's reagent¹⁹² followed by functionalisation via cross methathesis¹⁹³ chemistry could afford Z-vinyl ether precursors **196**. Subsequent VCPR on these substrates, which we have predicted to rearrange close to or below 100 °C (*vide supra*), would afford difluorocyclopentene **197**. This could be readily transformed into difluorovinylcyclopentanone **198** via enol ether hydrolysis¹⁹⁴ (**Scheme 97**).



Scheme 97: Proposed synthesis of difluorocyclopentanone **198** via VCPR of **196** then ester hydrolysis of enol ether **197**.

This work focused on accessing difluoro-VCP precursor **195** from the reduction of ester **194**, followed by the oxidation and olefination of the corresponding alcohol; these species are more comparable to phenyl **147a** examined previously.¹⁶²

4.2.1.2. 2nd Generation Synthetic Route

The olefination reaction between (carbethoxymethylene)triphenylphosphorane and commercial (hetero)aromatic aldehydes **191a-e** afforded the desired alkenoates **192a-e** in good to excellent yields (60-98%, **Table 29**, Entries 1-8). Formylation of thiazole (via the thiazolyl lithium reagent)¹⁹⁵ afforded 2-thiazoyl carboxaldehyde **191g** which was used crude in the olefination reaction to afford alkenoate **192g** in 74% yield over 2-steps (**Table 29**, Entry 9). After experimental investigations into the rearrangement of 2-furyl-difluoro-VCP precursor, we became interested in the effect methyl substitution in the 3'-position had on the outcome of the rearrangement (*vide infra*). To allow a complete discussion of the effect a range of heteroaromatic alkenoates on the difluorocyclopropanation chemistry, the synthesis of **191h** is described within this section. DIBAL-mediated reduction of methyl 3'-methyl-2-furoate afforded the corresponding primary alcohol (81% crude yield) which was used without purification in Vatele's room temperature oxidation/olefination¹⁶² to afford novel alkenoate **192h** in 45% yield over two steps (**Table 29**, Entry 10).

Table 29: Synthesis of Difluorocyclopropyl Allyl Alcohols **199a-h** from Aldehydes **191a-h**.

| Entry | R ¹ | x | 192 Yield (%) ^[a] | 194 Conv. (%) ^[b] | 199 Yield (%) ^[a] |
|-------|------------------------|------------------|------------------------------------|------------------------------------|------------------------------------|
| 1 | 2-furyl | a | 82 | 66 | 40 |
| 2 | Ph | b | - | 28 ^[c] | - |
| 3 | | | 73 | n.d. ^[e] | - |
| 4 | 2-thiophenyl | c | - | 37 | n.d. ^[e] |
| 5 | | | 98 | 77 | 71 |
| 6 | 5-benzo[d][1,3]dioxole | d | 94 | 50 | 43 |
| 7 | 2-pyridyl | e | 87 | 0 | - |
| 8 | 2-N-Boc-pyrrolyl | f | 60 | 92 | 54 |
| 9 | 2-thiazolyl | g ^[f] | 74 ^[g] | 0 | - |
| 10 | 3-Me-2-furyl | h ^[h] | 45 ^[i] | 80 | 45 |

Conditions: (i) (carbethoxymethylene)triphenylphosphorane (1.1-1.3 eq.), DCM, r.t., 6-20 h (ii) MDFA (2.5 eq.), TMSCl (2.5 eq.), KI (2.8 eq.), diglyme (1.17 eq.), 120 °C, 4 h (iii) DIBAL (3 eq.), toluene or DCM, -78 °C to r.t., 8 h. ^[a] Isolated yields. ^[b] Determined by ¹H NMR. ^[c] Reaction time of 24 h. ^[d] Starting from commercial ethyl cinnamate **192b**. ^[e] **192b** and **194b** were inseparable via column chromatography or distillation. ^[f] Aldehyde **191g** synthesised from thiazole and used crude in the olefination reaction. ^[g] Calculated over two steps from thiazole, 4:1 mixture of *E:Z*-isomers ^[h] Aldehyde synthesised *in situ* from the oxidation of 2-hydroxymethyl-3-methyl furan. ^[i] Calculated over two steps from methyl 3-methyl-2-furoate.

Furyl alkenoate **192a** proved to be more stable under MDFA-mediated difluorocyclopropanation conditions than acetate **193a** but only when a shorter reaction time of 4 hours was used (**Table 29**, Entry 1); prolonged reaction times of 24 h resulted in a decreased conversion to ester **194a** (66% compared with 50%, respectively). The conversion to **194a** could be increased to 87% by using sodium chlorodifluoroacetate (Na-CDFA, 10 eq.) conditions,^{64c,64d,67} but a drop in isolated yield was observed (22%) and attributed to product decomposition at the higher reaction temperature of 180 °C over a longer reaction time of 25 hours. Depending on the ease of chromatographic separation, a variety of heteroaromatic functionalised difluorocyclopropyl esters could be isolated in moderate to good yields (40-71%) using our shorter difluorocyclopropanation conditions from the corresponding alkenoates (**Table 29**). 2-Pyridyl **192e** and 2-thiazoyl **192g** failed to

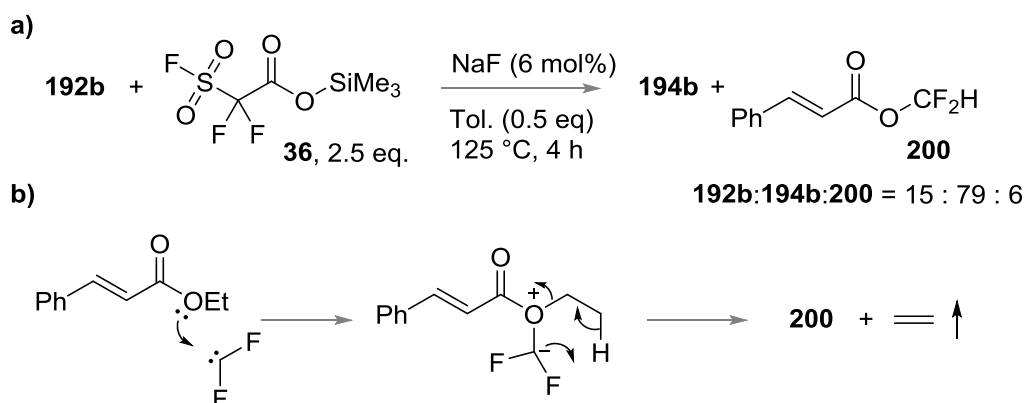
show any signs of reaction. Successful difluorocyclopropanation of a more reactive vinyl pyridine was reported in the patent literature using higher temperature decomposition of sodium chlorodifluoroacetate (Na-CDFA);¹⁹⁶ these conditions also failed to cause alkenoate **192e** to react.

DIBAL mediated reduction of the isolated difluorocyclopropyl esters to the corresponding alcohols gave mixed results with moderate to excellent yields (50-94%) observed for furyl **199a**, thiophenyl **199c**, piperonyl **199d** and 3-methyl-furyl **199e** analogues (**Table 29**). Unfortunately, N-Boc pyrrolyl **194f** was unstable under reduction conditions and gave a poor 6% yield of **199f**.

We were disappointed in the overall success of the difluorocyclopropanation conditions, so further investigations were carried out to determine how we could improve them. Both synthesised and commercial ethyl cinnamate **192b** gave similarly low conversion after difluorocyclopropanation (28% and 29%, respectively) so we were confident that there were no side products from the previous olefination step which were responsible for the poor conversion (**Table 29**, Entries 2-3). Again, slightly higher conversions could be obtained by decreasing the reaction time to 4 hours (**Table 29**, Entry 4, 37% conversion) but **194b** could not be separated from **192b** using either chromatography or distillation. Under the same conditions, cinnamyl acetate **141** had given 100% conversion to the desired difluorocyclopropane.¹⁶⁴ The dramatic reactivity difference between **141** and **192b** can be attributed to increased electron-deficiency of the alkene in **192b**. Selectivity experiments carried out by Dolbier and co-workers showed that difluorocarbene addition to a 1:1 mixture of butyl acrylate and 1-octene favoured the latter at 120 °C (product ratio of 1:3.3), consistent with the lower reactivity observed for **192b**.⁶⁹ Other literature methods^{53,65} using commercial reagents were previously unsuccessful when used for the difluorocyclopropanation of cinnamyl acetate **141**¹⁶⁴ and were therefore not investigated for these less reactive alkenoates.

Dolbier and co-workers reported more success in the synthesis of **194b** using alternative MDFA conditions (64%, ¹⁹F NMR conversion);⁷¹ we were able to replicate

their results (69% ^1H NMR conversion) but felt that the longer reaction time of 48 hours would be detrimental to the product recovery of the more reactive alkenoates. Higher conversion of 81% was achieved for this substrate by the same group using trimethylsilyl 2,2-difluoro-2-(fluorosulfonyl)acetate (TFDA, **36**) as the difluorocarbene precursor but it is unclear if this is an isolated or NMR yield.⁶⁹ This reagent is less practical than others since it is prone to hydrolysis; purification is necessary before every reaction. We observed similar conversion with **36** (79%, determined by ^1H NMR) but the isolation of synthetically useful quantities of **194b** proved difficult due to the presence of starting alkenoate **192b** and the previously unreported difluoromethyl ester side product **200** (Scheme 98a). We currently do not have a reason for the formation of **200** but it is proposed to proceed via a mechanism similar to that of the difluoromethylation of acids reported by Wu and Chen¹⁹⁷ and driven by the elimination of ethene (Scheme 98b); we observed similar difluorocarbene side reactions with diglyme (*vide supra*).



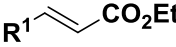
Scheme 98: a) Difluorocyclopropanation of **192b** using TFDA (ratio determined by ^1H NMR). b) Proposed mechanism for the formation of side product **200**.

Reported difluorocyclopropanation methodologies are generally screened against a set of simple alkene substrates but reactivity issues are rarely discussed. We used alkenoates **192a** and **192b** to assess the most reactive procedures in the literature and highlighted the synthetic limitations for electron deficient olefins. For this study, the main purpose of the synthetic investigations was to obtain a range of substituted cyclopropane precursors in order to test computational predictions. No further screening of conditions was carried out, but recent synthetic advances with metal-mediated difluorocyclopropanation reported by Ichikawa and co-worker, look

to be a more promising method for the synthesis of difluorocyclopropyl esters **194**.⁷⁰

The capricious nature of the difluorocyclopropanation made it difficult to predict which functional groups would be tolerated. The HOMO energy for a reactive species is generally considered to give a good representation of the compounds' nucleophilicity, but only a weak trend was observed between the reactivity of the alkenoates (determined by percentage conversion) and the HOMO energies of **192a-c**, **192f** and **192h** (Table 30 and Figure 44).

Table 30: Difluorocyclopropanation conversion and calculated HOMO energies for (hetero)arene alkenoates.

|  R ¹ = | Percentage Conversion (%) | HOMO Energy (eV) |
|---|---------------------------|------------------|
| 2-Pyridyl | 0 | -6.70 |
| 2-Thiazolyl | 0 | -6.47 |
| Piperonyl | 50 | -5.68 |
| Phenyl | 37 | -6.36 |
| 2-Furyl | 66 | -5.96 |
| 2-Thiophenyl | 77 | -6.10 |
| 3'-Methyl-2-furyl | 80 | -5.84 |
| 2-NBoc-Pyrrolyl | 92 | -5.68 |

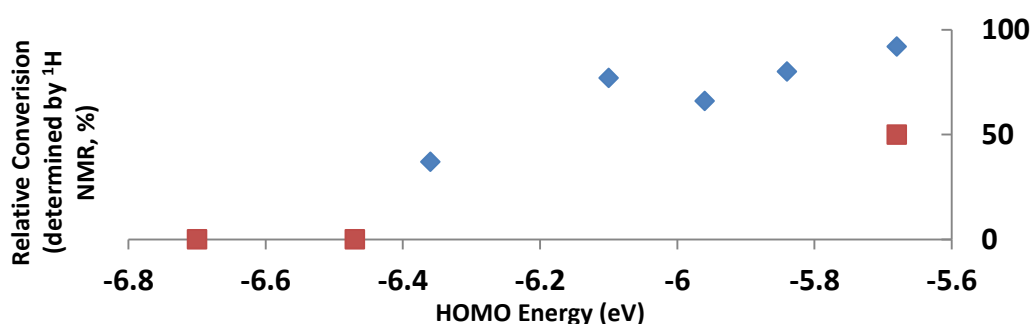


Figure 44: Plot of percentage conversion in difluorocyclopropanation reactions against calculated HOMO energies (eV, Spartan'10, B3LYP/6-31G*, gas phase, 298 K). Blue substrates show slight trend but red substrates do not.

This model only assessed the reactivity of the olefin and did not take into consideration the alternative trapping reactions difluorocarbene can undergo; difluoromethylation of carboxylic acids, ketones, alcohols, thiols, heterocyclic

amines and hydrophosphine oxides have all been reported.¹⁹⁸ We found that a better indication of functional group tolerance was to measure the effects of heterocycles as additives in the previously successful difluorocyclopropanation of cinnamyl acetate **141** (Table 31, Entry 1).¹⁶⁴

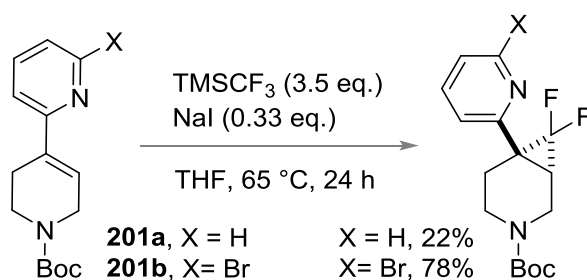
Table 31: Effect of Heterocyclic Additives on the Difluorocyclopropanation of Cinnamyl Acetate **141**.

Reaction scheme: Cinnamyl acetate (**141**) reacts with MDFA (2.5 eq.), TMSCl (2.5 eq.), KI (2.8 eq.), Diglyme (1.17 eq.), and an additive (X eq.) at 120 °C for 24 h to form 1,1-difluoro-2-phenylpropanoate (**142**).

| Entry ^[a] | Additive | Equivalents | Conversion to 142 (%) ^[b] |
|----------------------|---------------------------|-------------|---|
| 1 ^[c] | none | n.a. | 100 |
| 2 | Pyridine | 1.0 | 0 |
| 3 | Pyridine | 0.5 | 4 |
| 4 ^[c] | Pyridine | 0.1 | 85 |
| 5 | Thiazole | 0.5 | 34 |
| 6 | Pyridine-N-oxide | 0.5 | 14 |
| 7 | N-Boc-pyrrole | 0.5 | 88 |
| 8 | Methyl-3-methyl-2-furoate | 0.5 | 100 |
| 9 | 1,3-Benzodioxole | 0.5 | 50 |

^[a] All reactions run on an 8 mmol scale with respect to **141** unless otherwise stated. ^[b] Determined by ¹H NMR. ^[c] 16 mmol scale.

We observed that 1.0 equivalence of pyridine completely hindered the trapping of difluorocarbene with **141** (Table 31, Entries 2) and as little as 50 mol% completely inhibited product formation (Table 31, Entry 3); even small quantities of the heterocycle (10 mol%) lowered the conversion to **142** by 15% (Table 31, Entry 4). Addition of thiazole to the reaction had a smaller effect, but a low 34% conversion confirmed that both of these heterocycles do suppress the difluorocarbene-alkene reaction (Table 31, Entry 5). DeNinno and co-workers reported similar issues when the difluorocyclopropanation of **201a** gave a poor 22% yield, but shielding the pyridine nitrogen using *ortho*-bromo substitution gave a highly improved 78% yield from **201b** (Scheme 99).¹⁹⁹ This result suggests strongly that pyridine nucleophilicity is responsible for the impairment of the carbene transfer reaction.

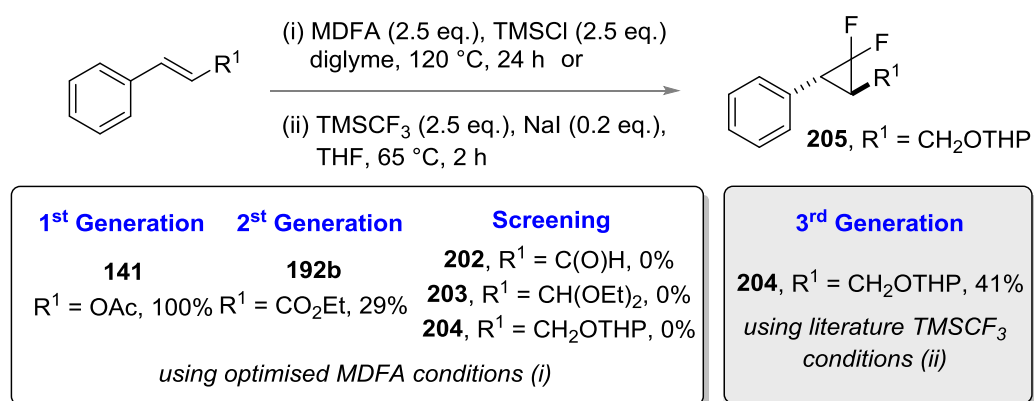


Scheme 99: Increased difluorocyclopropanation yields by blocking aromatic nitrogen atom.¹⁹⁹

We hoped that blocking the nitrogen atom directly via the N-oxide would help the difluorocyclopropanation reaction in a similar way and potentially give access to a more reactive VCPR precursor. However, since a poor 14% conversion to **142** was observed when pyridine-N-oxide was used as an additive, no further synthetic investigations were carried out (**Table 31**, Entry 6). Heterocycles which were tolerated during the difluorocyclopropanation of alkenoate **141**, gave lower (12-0%) reductions in conversions to **142** when used as additives (**Table 31**, Entries 7-8). This experimental approach of assessing functional group tolerance was a more effective way to prioritising the synthesis of heteroaromatic olefins and can be used to predict which substrates will be tolerated during difluorocyclopropanation without competing side reactions.

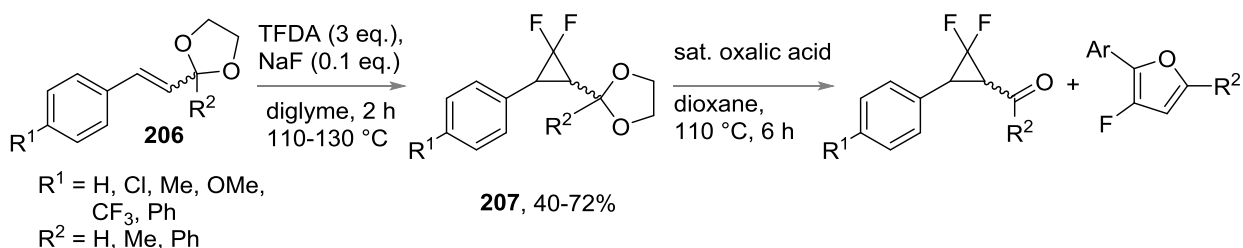
4.2.1.3. 3rd Generation Synthetic Route

Despite successfully accessing difluorocyclopropyl alcohol compounds with the second generation route, we were disappointed in the poor difluorocyclopropanation of (hetero)aryl alkenoates. We initially looked to improve our synthesis by screening alternative functional groups to the ester group whilst still maintaining the ability to access the required oxidation state for the olefination chemistry. Unfortunately, cinnamaldehyde **202**, its acetal **203** and THP-protected cinnamyl alcohol **204** all failed to react under optimised MDFA conditions (**Scheme 100**).



Scheme 100: Effect of changing alkene functional group substitution on difluorocyclopropanation conversions (percentage conversion determined by ¹H NMR).

Conditions using sodium halodifluoroacetate salts were likely to afford similar results due high reaction temperatures; lower temperature conditions with TMSCF₃ seemed more promising after 41% conversion to difluorocyclopropyl **205** was observed using literature conditions.⁵³ Xu and Chen reported that TFDA-mediated difluorocyclopropanation of acetals/ketals **206** was successful in moderate to good yields but hydrolysis to the corresponding aldehydes or ketones proved difficult, resulting in the unexpected formation of monofluorinated furan compounds (**Scheme 101**).²⁰⁰



Scheme 101: Literature TFDA mediated synthesis of difluorocyclopropyl acetal/ketal **207 and unexpectedly difficult acid mediated hydrolysis.**

In order to avoid similar issues in our synthesis, optimisation of the TMSCF₃ conditions focused on THP-protected **204** which could be accessed in lower-than-expected yield (60%) from the acid-catalysed protection of cinnamyl alcohol with 3,4-dihydro-2H-pyran. Literature conditions for the difluorocyclopropanation of **204** to **205** could be improved by *ca.* 20% conversion by doubling the number of equivalents of difluorocarbene-generating reagents present in the reaction (**Table 32**, Entry 1 and 2, respectively); prolonging the reaction time to 18 h gave a slight increase in formation of **205** (65%, **Table 32**, Entry 3). Further attempts at increasing

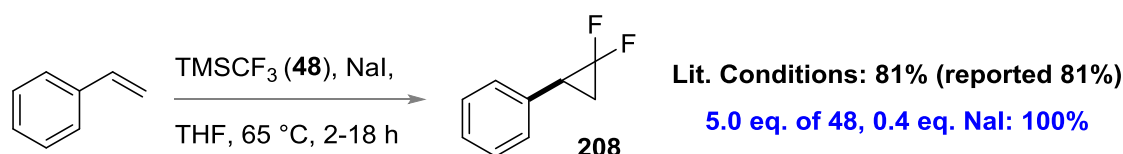
reagent stoichiometry (7.5 eq and 10 eq.) with longer reaction times gave modest or no increase in conversion to **205** (Table 32, Entry 4-5).

Table 32: TMSCF₃ Optimisation for the Difluorocyclopropanation of THP-**204**

| Entry | 48 (eq.) | NaI (eq.) | Time (h) | Concentration (M) | Conversion (%) ^[a] |
|-------|----------|-----------|----------|-------------------|-------------------------------|
| 1 | 2.5 | 0.2 | 2 | 0.17 | 41 |
| 2 | 5.0 | 0.4 | 2 | 0.17 | 60 |
| 3 | 5.0 | 0.4 | 18 | 0.17 | 65 |
| 4 | 7.5 | 0.6 | 18 | 0.17 | 75 |
| 5 | 10.0 | 0.8 | 18 | 0.17 | 61 |
| 6 | 5.0 | 0.4 | 18 | 0.34 | 65 |
| 7 | 5.0 | 0.4 | 18 | 0.68 | 78 |
| 8 | 5.0 | 0.4 | 18 | 1.36 | 89 ^[b] |
| 9 | 5.0 | 0.4 | 18 | 2.72 | 20 |
| 10 | 5.0 | 0.4 | 18 | no solvent | 0 |
| 11 | 5.0 | 0.4 | 18 | 0.09 | 43 |

[a] Relative conversion determined by ¹H NMR. [b] Average of two reactions.

The difluorocyclopropanation of styrene was used to compare the conditions reported by Prakash and co-workers with the semi-optimised conditions from **204** (Scheme 102). We observed exactly the same percentage conversion to difluorocyclopropane **208** when literature conditions were used (81%, ¹H NMR) but 100% conversion was achievable when the number of equivalents of **48** was increased, and a longer reaction time was utilised (the same conditions after 2 hours gave 93% conversion of **208**).

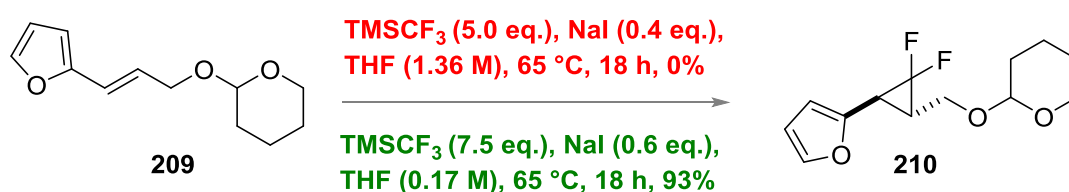


Scheme 102: TMSCF₃ mediated difluorocyclopropanation of styrene.⁵³

The use of an even larger excess of the most expensive reagent was not practical so investigations into the effects of concentration and longer reaction times, were carried out instead (Table 32, Entry 6-11). An optimal concentration of 1.36 M (8 times higher than literature conditions) gave the highest 89% conversion to **205**

(Table 32, Entry 8); attempts to increase (Table 32, Entry 9-10) or decrease (Table 32, Entry 11) reaction concentrations gave poorer outcomes.

Issues were again encountered when difluorocyclopropanation conditions were attempted with more reactive heteroaromatic olefins. Furyl **209** showed no evidence of trapping with difluorocarbene with the higher concentration conditions (1.36 M) but 93% conversion was observed when a larger excess of TMSCF_3 (7.5 eq) was used (Scheme 103). The high cost of TMSCF_3 makes these conditions undesirable and low reproducibility on scale (0%, 0.88 mmol ca. 93%, 0.1 mmol) meant this route offered no advantage over the 2nd generation conditions.



Scheme 103: Inconsistent TMSCF_3 mediated difluorocyclopropanation results for furyl **209** (relative percentage conversion by ^1H NMR).

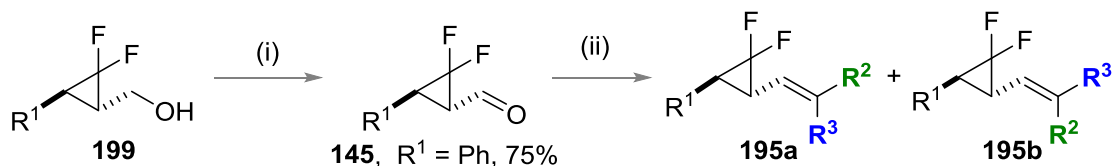
Despite the disappointing reactivity observed with furyl **209**, the proof of concept for the lower temperature difluorocyclopropanation of cinnamyl-derived olefins was promising and further work into this 3rd generation synthetic route may prove beneficial.

Despite the synthetic challenges posed by the incorporation of heteroaromatic substituents onto the difluorocyclopropane ring, it was promising that five novel primary alcohols could be accessed and used to complete the synthesis of precursors in order to test our computational predictions.

4.2.2. Functionalisation of Alkene Fragment

Vatele's room temperature tandem oxidation/olefination conditions were again utilised as the final step in the precursor synthesis, minimising rearrangements during alkenoate formation.¹⁶² Though this one-pot method previously had proved successful for making ethyl esters, it performed variably with other commercially available phosphoranones (Scheme 104, Method A). However, aldehyde **145** could be

isolated in good yield using the same room temperature oxidation chemistry, allowing direct Wittig reactions to proceed more smoothly (**Scheme 104, Method B**).



Method A: One Pot / Method B: 145 Isolated First

Scheme 104: Oxidation and olefination chemistry used to access a range of alkene functionality.

Conditions: (i) BAIB (1.1 eq.), TEMPO (0.1 eq.), DCM, r.t., 5-6 h, (ii) $\text{Ph}_3\text{P}=\text{C}(\text{R}^1)\text{R}^2$, DCM, r.t., 15-16 h.

Three more alkenes were accessed in good yields from phenyl **199b**; these were Weinreb amide **211a**, α -methyl ester **212a** and cyanide **213** (**Table 33**, Entry 1-3, respectively). Furthermore, heteroaromatic based building blocks all underwent functionalisation successfully but only piperonal-based precursor **214a** could be isolated (50%, **Table 33**, Entry 4); the 2-furyl, 2-thiophenyl and 3-methyl-2-furyl congeners all rearranged before isolation (**Table 33**, Entry 5-10).

Table 33: Complete Synthesis of Difluoro-VCP Precursors **211-219**.

| Entry (Method) ^[a] | R ¹ | R ² | R ³ | VCP | Yield (%) ^[b] | |
|----------------------------------|----------------|--------------------|----------------|------------|--------------------------------|---------------------|
| | | | | | E-alkene (a) | Z-alkene (b) |
| 1 (A) | Ph | CON(OMe)Me | H | 211 | 74 | 9 |
| 2 (A) | Ph | CO ₂ Et | Me | 212 | 74 | 0 |
| 3 (B) | Ph | H/CN | H/CN | 213 | 84 ^[c] | |
| 4 (A) | 2-piperonyl | CO ₂ Et | H | 214 | 50 | n.d. ^[d] |
| 5 (A) | 2-furyl | CO ₂ Et | H | 215 | Full conversion ^[e] | |
| 6 (A) | 2-thiophenyl | CO ₂ Et | H | 216 | Full conversion ^[e] | |
| 7 (A) | 2-furyl | CO ₂ Et | Me | 217 | Full conversion ^[e] | |
| 8 (A) | 2-thiophenyl | CO ₂ Et | Me | 218 | Full conversion ^[e] | |
| 9 (A) | 3-Me-2-furyl | CO ₂ Et | H | 219 | Full conversion ^[e] | |

Compounds represented by numbers and suffix **a** and **b** correspond to *E*- and *Z*-isomers, respectively. [a] Synthetic methodology based on **Scheme 104**. [b] Isolated yields unless otherwise stated. [c] **213a** and **213b** could not be separated by column chromatography and instead were isolated as a 3:2 mixture, respectively (mixture determined by ¹H NMR). [d] **214b** formed during the reaction but could not be separated out from a mixture with **214a** (21% isolated yield of **214a/214b** mixture). [e] All precursors were successfully formed but reactions resulted in complex mixtures due to competing low temperature rearrangements.

Although 2-furyl **181b** and 2-thiophenyl **181d** had some of the lowest predicted VCPR activation energies (21.0 and 21.3 kcal mol⁻¹ respectively), the observed low temperature rearrangements were still surprising; all reactions were conducted at room temperature and only warmed briefly during the evaporation of solvent (maximum temperature of 40 °C). In a repeated synthesis of VCP-**215** (furan), the reaction solvent was evaporated under a stream of nitrogen at ambient temperature and even then, resulted a similar mixture of products was detected. These results suggest that the rearrangements occurred at room temperature (<18 °C) and not during work up. To our knowledge, these are the first examples of VCP precursors undergoing low temperature thermolysis without additional additives or special patterns of functional groups; previously only transition metal mediated^{82b,201} or charge-accelerated rearrangements^{76,79,202} facilitated reactions at similar or lower temperatures.

Deconvolution of crude oxidation/Wittig reaction mixtures for furyl and thiophenyl substrates was difficult due to the presence of triphenylphosphine oxide side product. All of these reaction mixtures were purified twice, first to remove impurities arising from the reaction, then a final separation to isolate products free from phosphine oxide (**Table 34**).

Table 34: Reaction Outcomes from Furyl and Thiophenyl Precursors **215-218**.

a, R¹ = H, b, R¹ = Me **220, X = O, 221, X = S** **222, X = O, 223, X = S**

| Entry | VCP | X | R ¹ | Crude Observations (% conversion) ^[a] | Product (% ^[b]) | |
|-------|------------|---|----------------|---|-----------------------------|--------------------------------|
| | | | | | 220/221 | 222/223 |
| 1 | 215 | O | H | 220a (>95), 222a (trace) | n.a. ^[c] | |
| 2 | 216 | S | H | 221a major, 223a minor, evidence of 216 | 221a (12) | 223a (3) ^[d] |
| 3 | 217 | O | Me | 220b (100) | 220b (48) | 222b (0) |
| 4 | 218 | S | Me | 221b (100) | 221b (55) | 223b (0) |

[a] Percentage conversion determined by ¹H NMR after 1st purification. [b] Isolated yield. [c] Compound decomposed during purification attempts. [d] 50% purity (determined by ¹H NMR) containing **221a**.

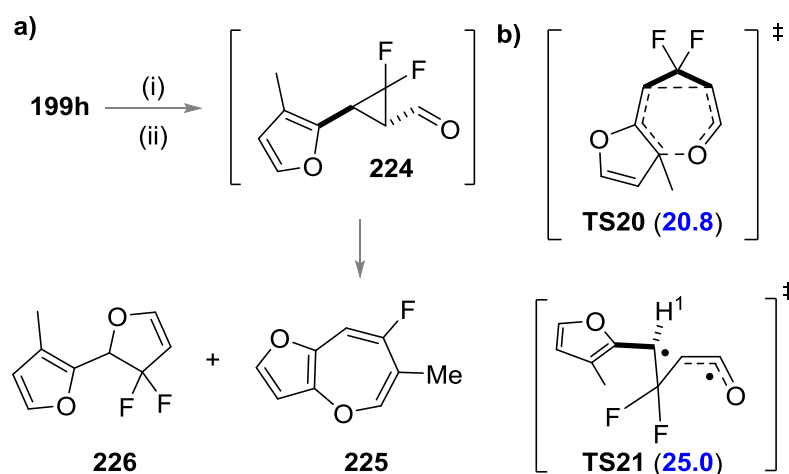
No VCP precursors derived from furyl **215** were evident after the reaction; instead mixed fractions from the first purification confirmed that mono-fluorinated cycloheptadiene **220a** has formed (more rapidly than difluorocyclopentene **222a** (**Table 34**, Entry 1)). Attempts at isolating rearrangement product **220a** failed due to product decomposition which was attributed to the lability of furyl-containing species, but distinctive ¹⁹F NMR signals which were consistent with data obtained for isolated thiophene product were used for assigning rearrangement outcomes.

In the synthesis of thiophenyl **216**, more complex mixtures resulted from the first purification, with NMR evidence for VCP **216a** and **216b**, as well as rearrangement products **221a** and **223a** (**Table 32**, Entry 2). Further thermolysis reactions of mixtures containing VCP precursors showed that *E*-isomer **216a** rearranged at 40 °C whereas the corresponding *Z*-isomer **216b** required the higher temperature of 50 °C (See Appendix for crude spectra). The major mono-fluorinated cycloheptadiene **221a** could be isolated in 12% yield and minor difluorocyclopentene **223a** in a lower 3% yield (50% purity containing cycloheptadiene **221a**).

Previous computational investigations predicted that an α -methyl substitution on the alkene for VCP precursor **190k** would increase the activation barrier for VCPR

rearrangement (*vide supra*). It was proposed that similar substitution would enable better temperature control of the rearrangement of highly reactive heterocyclic precursors. However, despite an increase in calculated activation energies for furyl **217a** ($\Delta G_{\text{B3LYP}}^{\ddagger} = 23.5 \text{ kcal mol}^{-1}$, +2.5 *cf.* **181b**) and thiophenyl **218a** ($\Delta G_{\text{B3LYP}}^{\ddagger} = 23.7 \text{ kcal mol}^{-1}$, + 2.4 *cf.* **181d**), experimental results still gave room temperature rearrangements (**Table 34**, Entries 3-4). Interestingly, both these precursors exclusively favoured the [3,3]-pathway, leading to moderate yields of both **220b** (48%) and **221b** (55%).

We also attempted the synthesis of 3'-methyl furyl precursor **219** intending that the methyl group would cause unfavourable steric interactions in the [3,3]-transition state and instead favour VCPR (Scheme **105a**). However, like all other heteroarene substituted precursors, rearrangement was observed before isolation; however, ^{19}F NMR reaction monitoring of the tandem oxidation/olefination of alcohol **199h** suggested that rearrangement had occurred directly from aldehyde **224**.

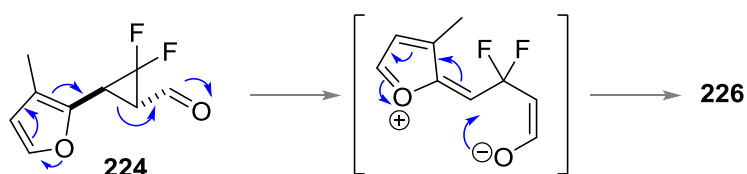


Scheme 105: a) Oxidation/olefination of alcohol **199h** resulting in unexpected rearrangement of aldehyde **224**. b) Electronic structure calculations for proposed rearrangement ((U)B3LYP/6-31G*, Spartan'10, gas phase, kcal mol⁻¹).

Conditions: (i) BAIB (1.1 eq.), TEMPO (10 mol%), DCM (3 mL) (ii) Ph₃P=CHCO₂Et (1.3 eq.).

The two major products were tentatively assigned as dihydrofuran **226** and 1-furanooxepine **225** (formed after a [1,5]-hydride shift and dehydrofluorination) due to the strong similarities between ^{19}F NMR chemical shifts reported by Hammond²⁰³ and ourselves,¹⁶⁴ respectively. Electronic structure calculations for the [3,3]-rearrangement via **TS20** supported room temperature rearrangement with a low

$\Delta G^{\ddagger}_{\text{UB3LYP}}$ value of 20.8 kcal mol⁻¹ (**Scheme 105b**). Analysis of the VCPR of aldehyde **224** through **TS21** gave a higher calculated barrier for rearrangement ($\Delta G^{\ddagger}_{\text{UB3LYP}} = 25.0$ kcal mol⁻¹) but a low spin operator value ($S^2 = 0.291$) suggested that the rearrangement is more likely to be concerted with diradicaloid character or through an alternative donor-acceptor ring-opening/ring-closing mechanism (**Scheme 106**).¹⁹⁰ Purification of the resulting crude reaction mixture failed, due to either decomposition or volatility of the proposed products. Further synthetic and computational investigations into these appealing fluorinated products would be worthwhile, but they do not contribute to the development of the computational model in this study.



Scheme 106: Potential donor-acceptor ring-opening/ring-closing mechanism for the formation of **226**.

The observed experimental results with heterocyclic precursors link well to the calculated low activation energies for VCPR. However the lack of control, and in some cases dominance of the [3,3]-pathway, was surprising because temporary dearomatisation is required. The thermolysis of precursor **147a** with varying numbers of equivalents (0.1, 0.5 and 1 eq.) of TEMPO showed no effect on VCPR pathway, confirming that the presence of this reagent during the oxidation reaction does not suppress the rearrangement. These experimental results suggest that the activation energy for the [3,3]-rearrangement must be lower than those calculated for VCPR. Experimental activation energies were required from more controlled rearrangements in order to screen for the best computational methods for assessing this competing pathway.

4.3. Thermal Rearrangement of Isolated Difluoro-VCP

The rearrangement temperatures for precursors which could be isolated were optimised to give full consumption of VCP after 17 hours (± 5 °C). Normalising the reaction temperature against a fixed reaction time allows for a greater

understanding into the role different substituents have on rearrangement rates (**Table 35**), and puts the data into a very practical context.

Table 35: Thermal Rearrangement of Isolated VCP **211-214** and **227**

| Entry | VCP Precursor | | | | | Temp. (°C) | VCPR Product | | |
|------------------|------------------------------|---|----------------|--------------------|----------------|------------|--------------|--------------------------|--------------------------|
| | # | X | R ¹ | R ² | R ³ | | # | Conv. (%) ^[a] | Yield (%) ^[b] |
| 1 | 211a | F | Ph | CON(Me)OMe | H | 95 | 228 | 100 | 97 |
| 2 | 211b | F | Ph | H | CON(Me)OMe | 160 | 228 | 0 ^[c] | - ^[d] |
| 3 | 212a | F | Ph | CO ₂ Et | Me | 155 | 229 | 0 ^[c] | - ^[e] |
| 4 | 213a/b ^[f] | F | Ph | H/CN | H/CN | 90 | 230 | 71 ^[g] | - |
| 5 ^[h] | 213b | F | Ph | CN | H | 160 | 230 | 100 | 48 ^[i] |
| 6 | 227a | H | Ph | CO ₂ Et | H | 220 | 231 | 100 | 40 ^[j] |
| 7 | 214a | F | Pip. | CO ₂ Et | H | 70 | 232 | 42 ^[k] | 18 ^[l] |

[a] Conversion to product (determined by ¹H or ¹⁹F NMR). [b] Isolated yields unless otherwise stated.

[c] Full conversion of VCP precursor was observed. [d] Decomposition was observed. [e] Clean

product could not be isolated from crude reaction mixture. [f] 3:2 mixture of **213a** and **213b**, respectively. [g] Crude mixture also contains 26% **213b** and 3% *cis*-**235b** (determined by ¹⁹F NMR).

[h] Using crude reaction mixture from Entry 4. [i] 6:1 ratio of difluorocyclopentene **230** and alkene

isomer **236** (by ¹H NMR) [j] 22% of *cis*-cyclopentene **213b** was also isolated. [k] Crude reaction

mixture also contains 58% of [3,3]-product (**237**, by ¹⁹F NMR). [l] 11% of **237** was also isolated. Pip. = piperonyl.

Weinreb amide **211a** rearranged at 95 °C, 5 °C lower than the corresponding ethyl ester **147a**, to afford a near quantitative yield of difluorocyclopentene **228** (**Table 35** Entry 1), consistent with the slightly lower calculated activation energy ($\Delta\Delta G^\ddagger = -0.9$ kcal mol⁻¹). Minor stereoisomer **211b** required higher temperatures to induce rearrangement, favouring what seemed to be a [3,3]-pathway over VCPR consistent with previously investigated *Z*-alkenoates. Diene **233** was proposed as one of the major products (**Figure 45**) but these harsher conditions resulted in decomposition and poor recovery of products observed in the reaction mixtures by ¹⁹F NMR (**Table 35**, Entry 2). Despite the slightly lower temperature of 155 °C required for

methylated alkenoate **212a** (Table 35, Entry 3), decomposition was again observed and only ^{19}F NMR assignment of diene **234** could be obtained. The higher temperature required for rearrangement of **212a** compared with ester **147a** was consistent with an increased calculated barrier height (+3.0 kcal mol $^{-1}$, *vide supra*).

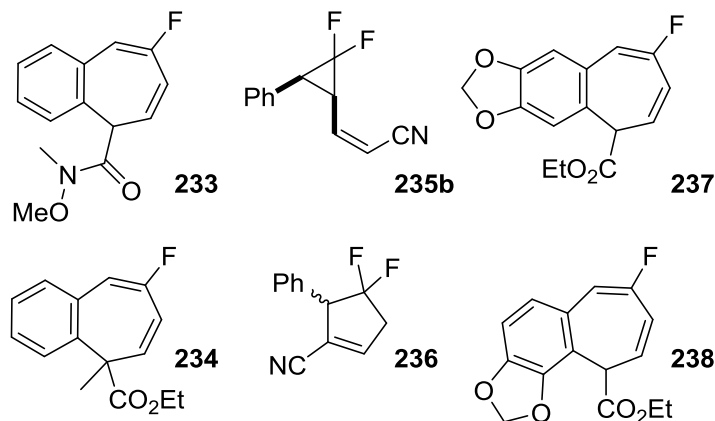
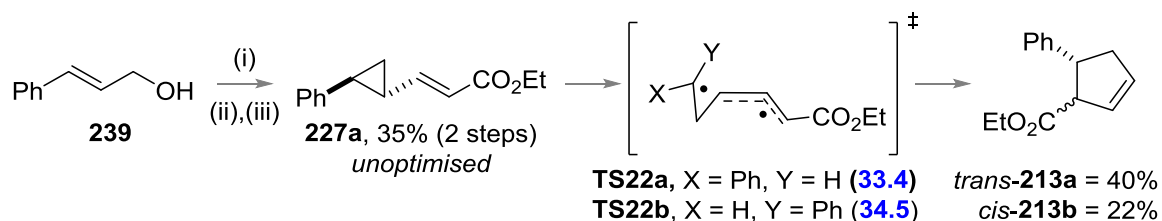


Figure 45: Potential side products from the rearrangement of difluorinated VCP discussed in Table 35.

It was predicted that the *E*-isomer (**213a**) would rearrange more rapidly in the isolated mixture of nitriles-**213a** and **213b** since the calculated activation energy for **213a** was 6.5 kcal mol $^{-1}$ lower than that of the *Z*-isomer (**213b**). Thermolysis of the mixture at 90 °C over 17 hours gave full conversion of **213a** to difluorocyclopentene **230**; **213b** only showed cyclopropane stereoisomerisation to *cis*-**235b** at this temperature (Table 35, Entry 4). Only when the resulting mixture was re-heated to 160 °C was full conversion of the *Z*-isomers observed (Table 35, Entry 5), affording difluorocyclopentene **230** in a 48% yield in a 6:1 ratio with alkene isomer **236**.

The computational triage was not limited to fluorinated precursors; VCP **227a** had a calculated activation barrier of 33.4 kcal mol $^{-1}$ for rearrangement through **TS22a** (Scheme 107). Simmons-Smith cyclopropanation²⁰⁴ of commercially available cinnamyl alcohol **239**, followed by tandem oxidation/olefination, afforded the desired precursor **227a** in an unoptimised 35% yield over two steps. A much higher temperature of 220 °C was required for full conversion of **227a** to cyclopentene **213** over 17 hours (Table 35, Entry 6), 120 °C higher than required for the corresponding difluorinated precursor **147a**. A mixture of *trans*-**213a** and *cis*-**213b**

diastereoisomers was observed and chromatographic separation gave a 40% and 22% yield of each product, respectively. Electronic structure calculations showed that transition states representing the VCPR from both *trans*-**227a** (**TS22a**, $\Delta G^{\ddagger}_{\text{B3LYP}} = 33.4 \text{ kcal mol}^{-1}$) and the corresponding *cis*-isomer (**TS22b**, $\Delta G^{\ddagger}_{\text{B3LYP}} = 34.5 \text{ kcal mol}^{-1}$) had similar barrier heights and could both be active at high temperatures.

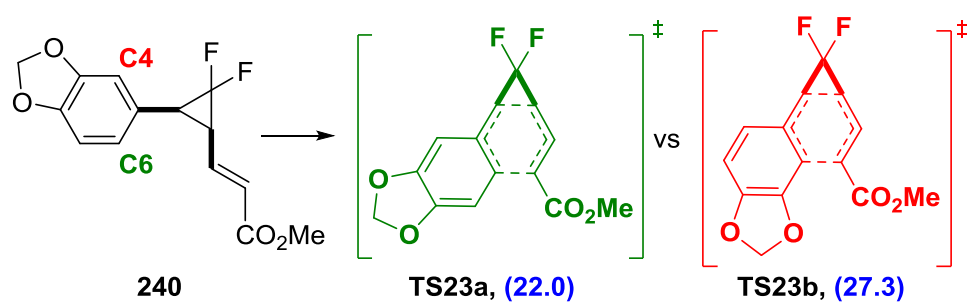


Scheme 107: Two step synthesis of non-fluorinated VCP-227 and calculated activation energy to TS22 (ΔG^{\ddagger} values (in blue) were calculated using (U)B3LYP/6-31G* from intermediate 227a, gas phase, 298 K, Spartan'10, using conformationally simpler Me ester, units are kcal mol⁻¹).

Conditions: (i) ZnEt₂ (1M in hexane, 5 eq.), CH₂I₂ (10 eq.), 0 °C to r.t., 2.5 h; (ii) TEMPO (0.1 eq.), BAIB (1.1 eq.), DCM, r.t., 3.5 h; (iii) Ph₃P=C(H)CO₂Et (1.3 eq.), 20 h.

This result conclusively showed the accelerative effect of *gem*-difluorination, and justifies the decision not to invest time in the synthesis of precursors predicted to have activation energies greater than 30 kcal mol⁻¹. In fact, experimental results from compounds **212a** and **213b** suggest that the maximum temperature for synthetically useful VCPR with fluorinated precursors could be much lower than expected due to the onset of product decomposition.

Piperonyl species **214a** had a much lower predicted activation energy ($\Delta G^{\ddagger}_{\text{B3LYP}} = 23.0 \text{ kcal mol}^{-1}$) and subsequently rearranged at a much lower optimised temperature of 70 °C (**Table 35**, Entry 7). However, like other highly activated heteroaromatic substituents, both difluorocyclopentene **232** and cycloheptadiene **237** were observed and could be isolated after preparative-HPLC in low yields of 18% and 11%, respectively. Diene **237** was the exclusive product of the [3,3]-rearrangement, despite the possibility of the formation of regioisomer **238** via reaction at aromatic carbon centre C4 (**Scheme 108**). Electronic structure calculations were consistent with experimental results, showing that the observed pathway through **TS23a** had a lower activation energy than that through **TS23b** ($\Delta\Delta G^{\ddagger} = 5.3 \text{ kcal mol}^{-1}$).



Scheme 108: Electronic structure calculations used to predict the favoured [3,3]-rearrangement pathway from **240** (ΔG^\ddagger values are relative to **240** (blue) and calculated using ((U)B3LYP/6-31G*, gas phase, 298 K, Spartan'10, units are in kcal mol⁻¹).

The greater thermal control observed from the rearrangement of **214a**, allowed the competition between VCPR and [3,3]-pathways to be examined more fully using ¹⁹F NMR spectroscopy at 373 K in [D₈]toluene. Unlike the VCPR of phenyl **147a** monitored previously, no evidence of the *cis*-VCP **241a** was observed during thermolysis because the [3,3]-pathway (which removes the *cis*-diastereoisomer from the equilibrium) was now competitive with VCPR (Figure 46). At this higher rearrangement temperature (100 °C), full consumption of **214a** was observed after 30 minutes, contrasting with the 10 hours required for full conversion of **147a** and providing further experimental evidence that the activation energy for the latter was higher, as predicted.

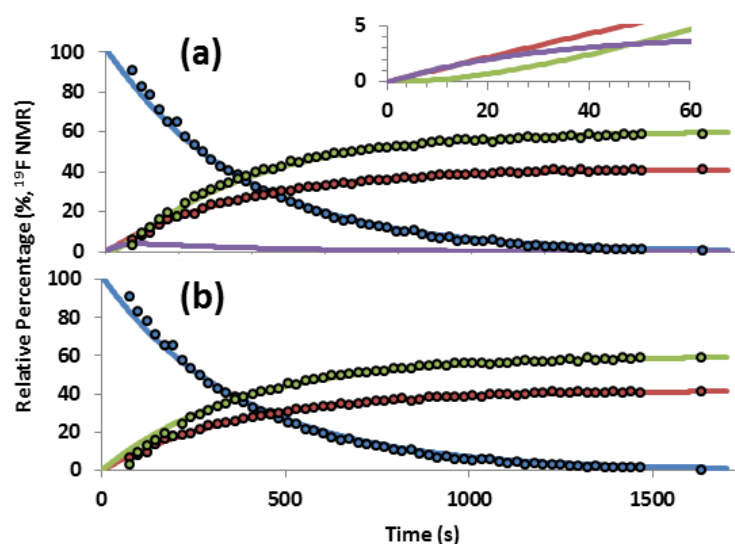
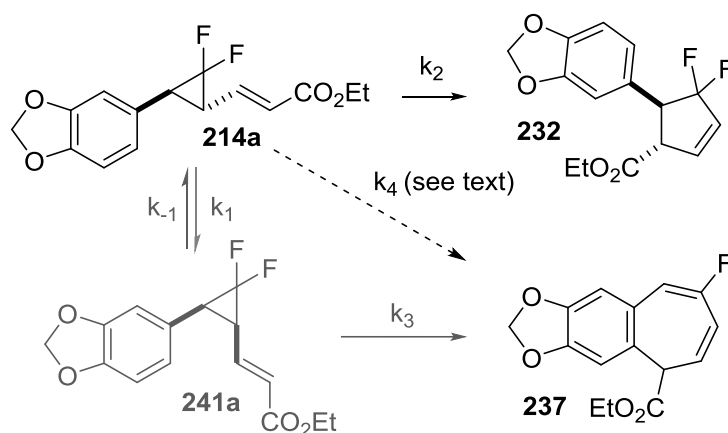


Figure 46: Experimental (points) and simulated (lines) concentration/time profile for thermolysis (373 K) of **214a**; a) simulation Model A takes into account *cis*-**241a**; insert shows the first simulated 30 seconds of the rearrangement b) Model B utilising a steady state approximation for *cis*-**241a** (blue = *trans*-**214a**, green = **237**, red = **232**, purple = *cis*-**241a**).

The experimental concentration/time profile could be simulated successfully as far as experimental end points using numerical integration software¹⁷¹ based on two kinetic models expressed in **Scheme 109**.



Scheme 109: Kinetic models used in the simulation of parallel VCPR and [3,3]-pathways.

Model A used successfully with phenyl **147a**, takes into account the equilibrium set up between *cis*-**241a** and *trans*-**214a** due to cyclopropane stereoisomerisation and the subsequent first order rearrangement through to diene **237** and cyclopentene **232**, respectively. Simulated data using this model showed formation of *cis*-**241a**, rising to a maximum at about 3% in the reaction mixture after 30 seconds before slowly decaying (**Figure 46a**). These values are below the lower limit of experimental detection and explain why **241a** was not observed. Deconvolution of rate constants predicted that rearrangement of **214a** should be selective for the [3,3]-pathway, with a rate approximately 40 times faster than VCPR (**Table 36**). This does not match experimental findings and may be due to an overestimation in rates involving *cis*-**241a** due to the lack of experimental data points to fit profiles to.

Table 36: Rate constants extracted from reaction simulations.

| Rate | k_2 | k_1 | k_{-1} | k_3 | k_4 | k_3/k_2 | k_4/k_2 |
|----------------|-------|-------|----------|-------|-------|-----------|-----------|
| Model A | 11.2 | 21.8 | 153.2 | 439.4 | - | 39.2 | - |
| Model B | 11.1 | - | - | - | 15.8 | - | 1.4 |

This issue was resolved by treating both rearrangement pathways as first order with respect to *trans*-**214a** (Model B); k_4 now represents an overall rate for the

conversion of **214a** to **241a** and incorporates the cyclopropane stereoisomerisation and [3,3]-rearrangement rates associated with **241a**. Again, simulated data showed good correlation with experimental values (**Figure 46b**) and this time the rate constants favoured the [3,3] pathway only slightly (1.5 times faster than VCPR), consistent with experimental conversions of 59% and 41% to diene **237** and cyclopentene **232**, respectively. Furthermore, the much higher rate for VCPR from **214a** ($11.5 \times 10^{-4} \text{ s}^{-1}$) than from phenyl **147a** ($1.6 \times 10^{-4} \text{ s}^{-1}$), matched the predicted differences in calculated activation energies.

An Arrhenius determination of activation parameters within a limited temperature range (30 K) was carried out from the calculated rate data from kinetic Model B (344-374 K, $[D_8]$ toluene (**Figure 47**)); the value for VCPR E_a from piperonyl **214a** of (23.4 ± 0.2) kcal mol⁻¹ was very close to the calculated $\Delta G^\ddagger_{\text{B3LYP}}$ (23.0 kcal mol⁻¹). A slightly higher E_a value of (24.9 ± 0.3) kcal mol⁻¹ was calculated for the [3,3]-pathway and was used to screen for the best computational method for treating this manifold of reactions.

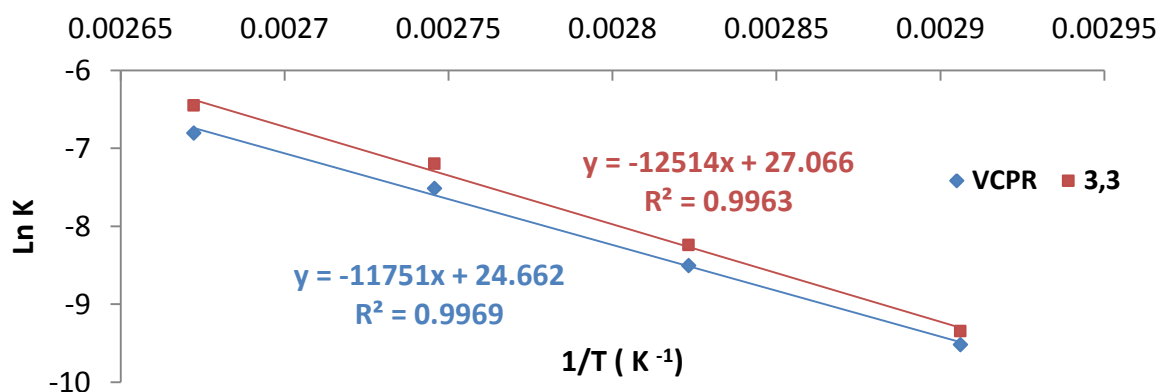


Figure 47: Combined Arrhenius plots for VCPR and [3,3]-rearrangement of **214a**.

4.4. Further Exploration of Electronic Structure Calculation Methods

In order to assess the accuracy of the electronic structure calculations efficiently, all experimental activation energies were recalculated to 298 K using the Arrhenius data and methods described by Maskill.¹¹⁴ We previously reported that for VCPRs, changes to the basis set either had detrimental effects (with UB3LYP, UM06-2X and UB97-D functionals) or gave slightly more accurate values of ΔG^\ddagger when the diffuse

function was introduced (6-31+G*) with the UM05-2X functional. Increasing polarisation and diffuse functions (6-31+G**) gave no improvement in the agreement between experimental and calculated values for a benchmarking set of VCPRs; these trends were followed for piperonyl **181f**. Initial methodology screening was carried out using Spartan'10 software due to the ease of local implementation. All activation energies were then recalculated on Gaussian'09 since the software generally dealt with the diradicaloid character of the VCPR better (S^2 values closer to 0.75) and energies would be more comparable with the literature.

Investigating the barrier height for the rearrangement of VCP **181f** to **TS14f**, gave results comparable to those observed with phenyl **168a**. The M05-2X functional¹⁷³ with the 6-31+G* basis set still proved to be the most accurate methodology, with a $\Delta\Delta G^\ddagger = 0.2 \text{ kcal mol}^{-1}$ (**Figure 48**). Truhlar and co-workers reported that the M06-2X functional, with a similar HF-exchange (56% for M05-2X and 58% M06-2X), was slightly more accurate overall in assessing kinetic parameters than M05-2X.¹⁷⁴ However in our system this was not the case, with a $4.5 \text{ kcal mol}^{-1}$ increased overestimation by the M06-2X functional with the same basis set.

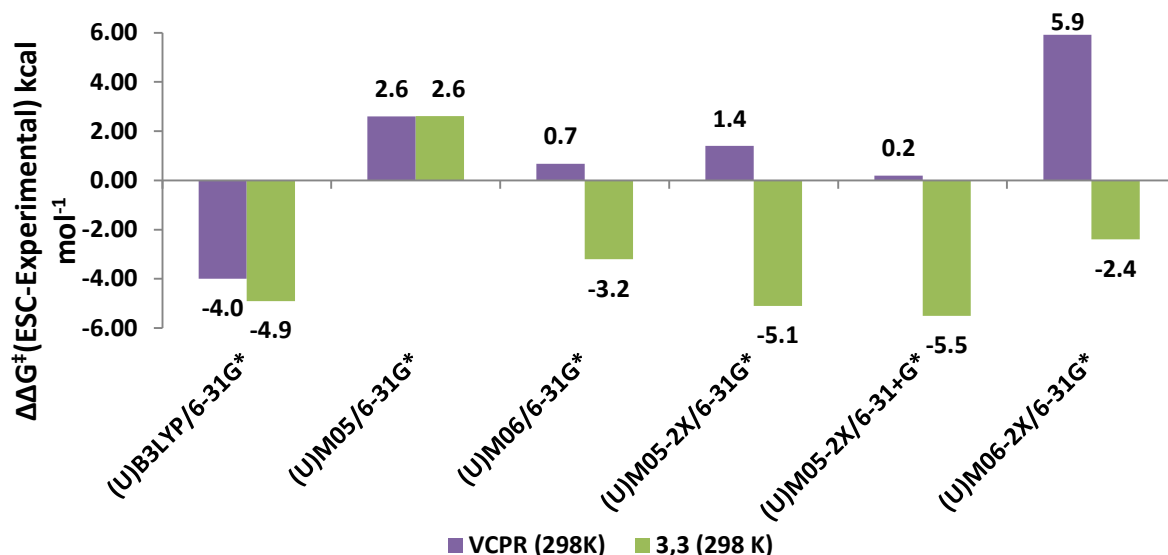
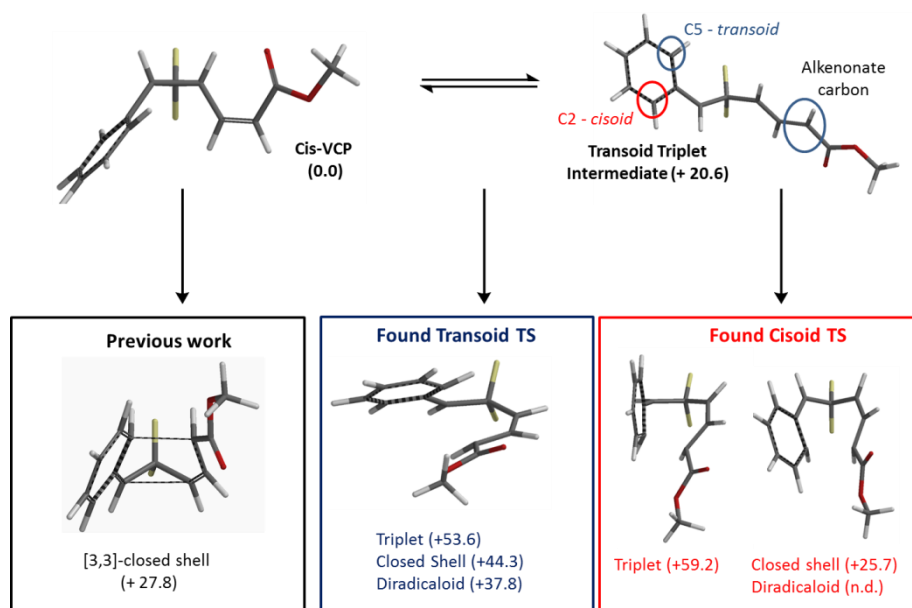


Figure 48: Differences between experimental ΔG^\ddagger (298 K, re-calculated from activation parameters) and ΔG^\ddagger from electronic structure calculations (298 K, gas phase, Spartan'10) plotted as $\Delta\Delta G^\ddagger$ ($\Delta G^\ddagger(\text{ESC}) - \Delta G^\ddagger(\text{experimental})$, kcal mol⁻¹) for the VCPR and [3,3]-rearrangement of VCP **181f** and **240a**, respectively. Expected error associated with calculated data is $\pm 0.5 \text{ kcal mol}^{-1}$.

During the peer-review process for our computational investigations into the rearrangements from phenyl **168a**, it was suggested that the different amount of HF-exchange used in each method could have some role in determining the accuracy of the calculated free energies of activation for the VCPR. The M06 functional, with a lower HF-exchange of 27%, gave the closest agreement with experimental values when the 6-31G* basis set was used ($\Delta\Delta G^\ddagger = 0.7 \text{ kcal mol}^{-1}$). Electronic structure calculations using M05/6-31G* methodology were less accurate ($\Delta\Delta G^\ddagger = 2.6 \text{ kcal mol}^{-1}$) despite having a similar HF-exchange value (28%) to the M06 functional. However, we observed little difference between the M05-2X and M06 functionals when the same VCPR barrier heights were calculated on Gaussian'09 for piperonyl **181f**, simple precursor **49** and phenyl **168a**. Furthermore, for the VCPR of non-fluoro **49**, M06/6-31+G* calculations were only within $1.6 \text{ kcal mol}^{-1}$ (underestimate) whereas M05-2X/6-31+G* methods gave $\Delta\Delta G^\ddagger$ values within $0.8 \text{ kcal mol}^{-1}$ (overestimate). DFT methods either underestimated experimental barrier heights when 20% HF-exchange was used (B3LYP), or overestimated ($+1.8 \text{ kcal mol}^{-1}$) when a hybrid exchange-correlation was used with 19% HF-exchange at short range and 65% at long range (CAM-B3LYP²⁰⁵). These results suggest that HF-exchange alone does not determine the accuracy of calculated VCPR activation energies.

Previously, only a concerted closed-shell transition state was investigated for the [3,3]-rearrangement of *cis*-**240a**. This was consistent with Özkan and Zora's DFT study of the divinylcyclopropane rearrangement; despite running spin-unrestricted calculations, no low energy diradical or triplet intermediates or transition states were found.²⁰⁶ We used our previously optimised triplet intermediate of ring opened phenyl VCP **172a** as a starting point to search for alternative triplet or diradicaloid pathways for the [3,3]-rearrangement ((U)B3LYP/6-31G*, gas phase, 298 K, Spartan'10). Two transition states with triplet character which connected the alkenoate radical with the alternative ortho-carbon centred radicals on the aromatic ring were found; both had uncompetitive calculated activation energies of $53.6 \text{ kcal mol}^{-1}$ and $59.2 \text{ kcal mol}^{-1}$. Only one of these optimised with diradical

character, but still had a much higher barrier for rearrangement ($37.8 \text{ kcal mol}^{-1}$) than the closed shell pathway ($27.8 \text{ kcal mol}^{-1}$, **Scheme 110**).



Scheme 110: Closed-shell, diradical and triplet transition states for [3,3]-rearrangement (kcal mol^{-1}).

For subsequent computational methodology screening, the [3,3]-rearrangement was treated using closed shell methodology.

One difference which was observed between phenyl and piperonyl substituents was the change in dipole moment calculated from precursor to transition state; **168a** showed a slight decrease in calculated polarity during VCPR and [3,3]-rearrangement (change in dipole = -0.39 and -0.22 Debyes, respectively) whereas **181f** showed a slight increase (change in dipole = $+1.2$ and $+0.95$ Debyes, respectively, UB3LYP/6-31G*, Gaussian'09, gas phase, 298 K). The calculated activation energies for the two rearrangement pathway from **181f** were assessed using M05-2X/6-31+G* method with different solvation parameters which had varying dielectric constants (range of $\epsilon = 2.37$ - 35.7), but only a slight decrease in barrier height for the [3,3]-rearrangement in acetonitrile compared with gas phase was predicted ($\Delta G_{\text{Gas}}^{\ddagger} - \Delta G_{\text{MeCN}}^{\ddagger} = -0.9 \text{ kcal mol}^{-1}$). Maas reported that the experimental rate for the [3,3]-rearrangement of non-fluorinated 1-aryl-2-vinylcyclopropanes was more than 8 times faster in acetonitrile than in benzene,

but VCPR rates were not affected by reaction solvent.²⁰⁷ VCP **214a** showed no significant change in rearrangement outcome when heated in either [D3]acetonitrile (52% (**237**([3,3]) and 48% (**232**(VCPR)) conversion, determined by ¹⁹F NMR) or [D8]toluene (58% (**237**([3,3]) and 42% (**232**(VCPR)) conversion, determined by ¹⁹F NMR). Therefore, no solvation methods were applied and all electronic structure calculations were carried out in the gas phase (see Appendix for data).

Irrespective of the basis set used, the M05-2X functional was found to be the least accurate of those examined for calculating the free energy of activation of **181f** to **TS14f** (6-31G*, $\Delta\Delta G^\ddagger = -5.1$ kcal mol⁻¹ and 6-31+G*, $\Delta\Delta G^\ddagger = -5.5$ kcal mol⁻¹). Instead, the M06-2X/6-31G* combination was found to be the best at predicting barrier height with a $\Delta\Delta G^\ddagger = -2.4$ kcal mol⁻¹ (**Figure 48**). This is opposite to what was observed for the VCPR and gives a strong indication of the functional's differing abilities in dealing with diradicaloid character or the loss of aromaticity at transition states. The (U)B3LYP/6-31G* method gave a similar underestimation in barrier height for both pathways ($\Delta\Delta G^\ddagger$ values were within error of ± 0.5 kcal mol⁻¹) but (U)M05/6-31G* gave exactly the same overestimate of 2.6 kcal mol⁻¹. If required, these two combinations of functions and basis sets provide a universal method for assessing both rearrangement pathways in Spartan'10.

Electronic structure calculations for VCP **181f** which were carried out in Gaussian'09 dealt with the diradicaloid character of the VCPR better (S^2 value closer to 0.75) than Spartan'10, resulting in barrier heights which we were more confident in; M05/6-31G* was the key exception, with higher $\Delta\Delta G^\ddagger$ values for both VCPR and [3,3]-pathways (+3.7 kcal mol⁻¹ and +5.2 kcal mol⁻¹, respectively). Pleasingly, DFT methodology using B3LYP/6-31G* still gave consistent underestimation in barrier height for both pathways, $\Delta\Delta G^\ddagger$ values were within 0.3 kcal mol⁻¹ of each other (**Figure 49**). Out of the Minnesota functionals, the M06-2X/6-31G* method remained the most accurate for the [3,3]-rearrangement ($\Delta\Delta G^\ddagger = -0.5$ kcal mol⁻¹) and M05-2X/6-31+G* for the VCPR ($\Delta\Delta G^\ddagger = +1.1$ kcal mol⁻¹).

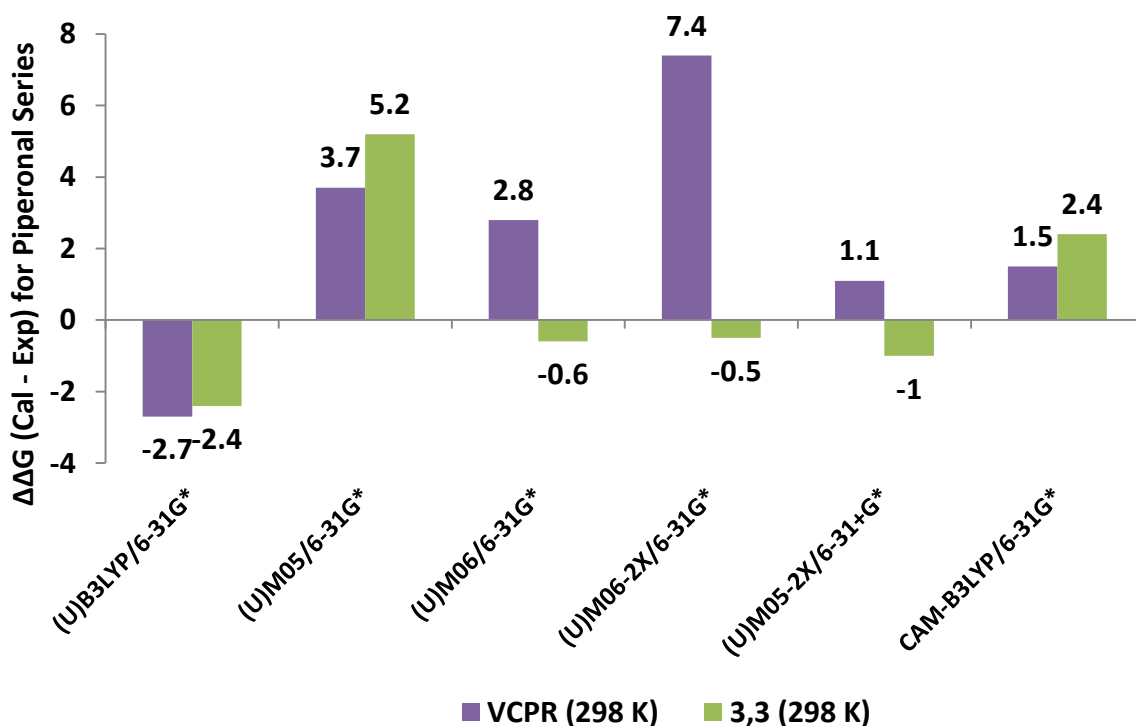
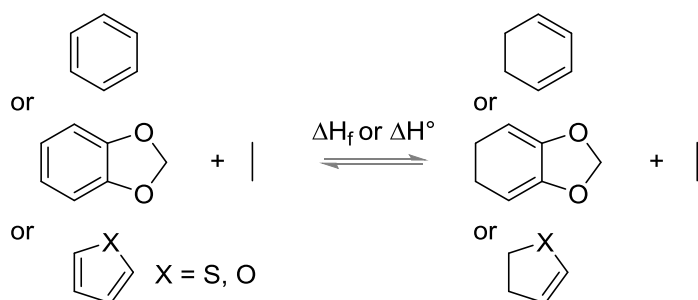


Figure 49: Differences between experimental ΔG^\ddagger (298 K, re-calculated from activation parameters) and ΔG^\ddagger from electronic structure calculations (298 K, gas phase, Gaussian'09) plotted as $\Delta\Delta G^\ddagger$ ($\Delta G^\ddagger(\text{ESC}) - \Delta G^\ddagger(\text{experimental})$, kcal mol⁻¹) for the VCPR and [3,3]-rearrangement of VCP 181f and 240a, respectively. Expected error associated with calculated data is ± 0.5 kcal mol⁻¹.

We looked to explore the effectiveness of the B3LYP/6-31G* and M06-2X/6-31G* calculations of barrier heights for divinylcyclopropane¹¹²⁻¹¹³ and heteroaromatic-vinylcyclopropane rearrangements²⁰⁸ reported in the literature but the experimental errors were so big (in the reported data) that it was impossible to distinguish between accurate and inaccurate calculated barriers.

Instead, the isodesmic reaction represented in **Scheme 111** was used to assess how well both methods dealt with the disruption of aromaticity in the transition state for aromatic-vinylcyclopropane rearrangement.



Scheme 111: Isodesmic reactions used to model the cost of disruption of aromaticity.

There was little difference between the calculated heats of formation for either T1²⁰⁹ or G3(MP2)²¹⁰ thermochemical recipes (within computational error of ± 0.5 kcal mol⁻¹), but when compared with experimental values,²¹¹ T1 was more accurate for ethane and ethene whereas G3(MP2) was slightly more accurate for aromatic compounds (**Figure 50**); both recipes gave $\Delta\Delta H_f$ values within computational error of each other.

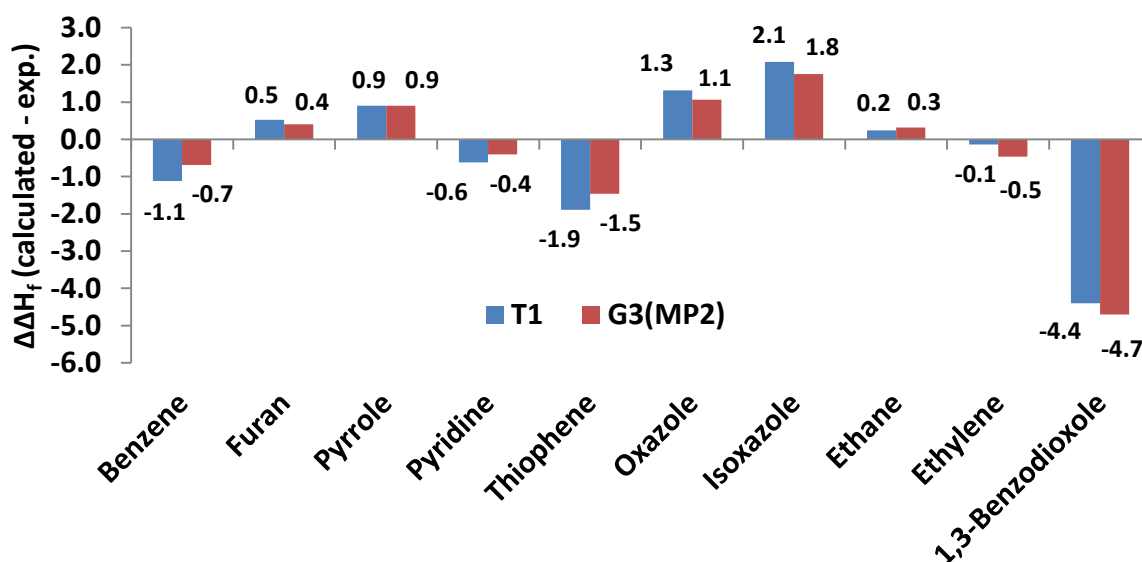


Figure 50: Differences in calculated and experimental heats of formation (Spartan'10 values in kcal mol⁻¹).

The average error associated with the calculated heats of formation for benzene, furan, pyrrole, pyridine, thiophene, oxazole and isoxazole were ± 1.21 kcal mol⁻¹ and ± 0.95 kcal mol⁻¹ for T1 and G3(MP2), respectively. Calculated data for 1,3-benzodioxole had an underestimation greater than 4 kcal mol⁻¹ for both methods when compared with experimental values.²¹²

The G3(MP2) values were used to assess the accuracy of the calculated enthalpy change for the dearomatisation of benzene, benzodioxole, furan and thiophene using either B3LYP/6-31G* or M06-2X/6-31G* methodology (**Figure 51**). The B3LYP method had an average overprediction in enthalpy of 5.3 kcal mol⁻¹ for benzene, furan, thiophene and 1,3-benzodioxole. In contrast, M06-2X consistently overestimated the enthalpic cost of dearomatisation, ranging from 3.6 kcal mol⁻¹ to 6.4 kcal mol⁻¹ (total average error of 4.8 kcal mol⁻¹). Similar differences were observed from the T1 values.

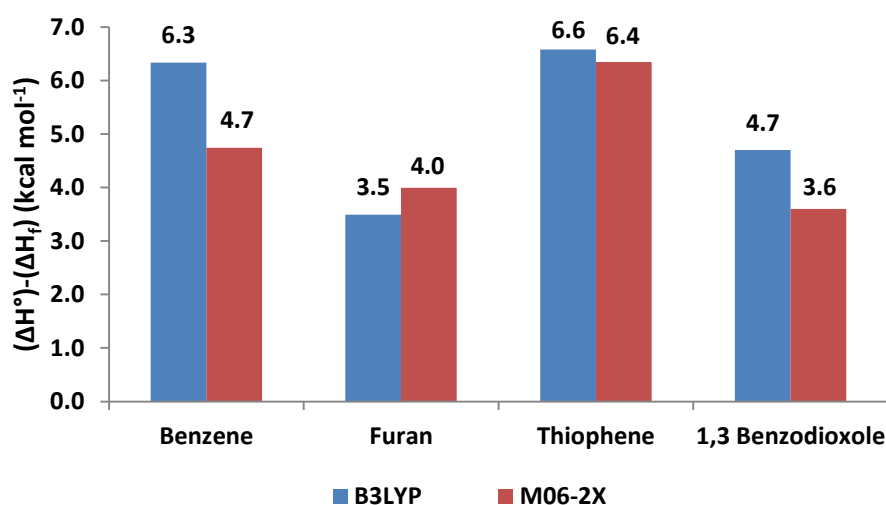


Figure 51: Difference in change in enthalpy (ΔH°) calculated using B3LYP or M06-2X (6-31G*) methods and G3(MP2) heats of formation (ΔH_f) for the isodesmic reactions represented in Scheme 111 (gas phase, 298 K, Spartan'10, units are in kcal mol⁻¹).

This thermochemical analysis suggests that the two desirable methods for assessing the aromatic-vinylcyclopropane rearrangement do not deal with the loss of aromaticity at the transition state well. This is important since M06-2X/6-31G* calculations were perceived to be the most accurate, but are likely to over-predict the calculated free energy (ΔG^\ddagger) for rearrangements involving benzene, furan, thiophene and 1,3-benzodioxole.

4.5. Predictive Electronic Structure Calculations

After our assessment of the accuracy of the electronic structure calculations, we were interested to see how well these methods could be used to predict which rearrangement pathway would be favoured. The UM05-2X/6-31+G* method gave

the closest agreement between experimental values for the VCPR of **168a** and **181a**, while the M06-2X/6-31G* method was the best for the [3,3]-rearrangement of **240a**; these Minnesota functionals were selected as the most accurate methods for assessing the two pathways. Because of its consistency of performance, the B3LYP/6-31G* was also retained as a low cost method able to handle both rearrangements at a useful level of accuracy. The calculated ΔG^\ddagger values for VCPR using each of these methods were corrected by the average error ($\Delta\Delta G^\ddagger$) from **168a** and **181a**; these values are +2.7 kcal mol⁻¹ for UB3LYP and -1.2 kcal mol⁻¹ for UM05-2X. Since the experimental activation energy for the [3,3]-rearrangement could only be determined for **240a**, the correcting values are based solely on this compound's $\Delta\Delta G^\ddagger$ values, which are +2.4 kcal mol⁻¹ for B3LYP and +0.5 kcal mol⁻¹ for M06-2X.

The differences in corrected $\Delta G^\ddagger_{\text{VCPR}}$ and corrected $\Delta G^\ddagger_{[3,3]}$ values ($(\Delta G^\ddagger_{\text{VCPR}}) - (\Delta G^\ddagger_{[3,3]})$) were used to predict which rearrangement pathway would be favoured by either DFT or Minnesota methods; values greater than +1.0 kcal mol⁻¹ would favour VCPR and values less than -1.0 kcal mol⁻¹ would favour sigmatropic rearrangement. Small differences between these values could result from computational error (± 0.5 kcal mol⁻¹) and would represent the limit of our ability to predict the composition of rearrangement product mixtures or the identity of the dominant pathway (**Table 37**).

Table 37: Predicting thermal rearrangement pathways (VCPR or [3,3]) from VCPs using corrected free energies of activation (ΔG^\ddagger).

| Entry | VCP | ΔG^\ddagger (U)B3LYP | | $\Delta\Delta G^\ddagger$ [c] | ΔG^\ddagger UM052X | | $\Delta\Delta G^\ddagger$ [f] | Experimental Observation |
|-------|-------------|------------------------------|----------------------|-------------------------------|----------------------------|----------------------|-------------------------------|--------------------------|
| | | VCPR ^[a] | [3,3] ^[b] | | VCPR ^[d] | [3,3] ^[e] | | |
| 1 | 147a | 29.4 | 30.2 | +0.9 | 28.6 | 30.0 | +1.4 | VCPR |
| 2 | 214 | 27.0 | 26.3 | -0.7 | 26.9 | 27.3 | +0.9 | Mixture |
| 3 | 215 | 24.8 | 19.0 | -4.9 | 24.5 | 21.2 | -3.3 | [3,3] |
| 4 | 216 | 25.2 | 20.9 | -4.3 | 24.8 | 21.7 | -3.1 | [3,3] |
| 5 | 212 | 33.3 | 36.3 | +3.0 | 31.5 | 35.5 | +4.0 | [3,3] |
| 6 | 217 | 28.0 | 26.6 | -1.4 | 26.7 | 26.6 | -0.1 | [3,3] |
| 7 | 218 | 28.4 | 27.4 | -1.0 | 28.0 | 28.0 | 0.0 | [3,3] |
| 8 | 211 | 28.9 | 35.7 | +6.8 | 28.0 | 36.1 | +9.3 | VCPR |
| 9 | 213a | 27.4 | 30.3 | +2.9 | 27.6 | 31.3 | +3.7 | VCPR |
| 10 | 213b | 32.4 | 35.1 | +2.7 | 32.8 | 37.2 | +4.4 | VCPR |
| 11 | 227 | 37.8 | 37.9 | +0.1 | 36.9 | 37.0 | +0.1 | VCPR |

[a] Calculated $\Delta G^\ddagger + 2.7 \text{ kcal mol}^{-1}$ (UB3LYP/6-31G*) [b] Calculated $\Delta G^\ddagger + 2.4 \text{ kcal mol}^{-1}$ (B3LYP/6-31G*) [c] $\Delta\Delta G^\ddagger = (\text{corrected VCPR } \Delta G^\ddagger_{\text{UB3LYP}}) - (\text{corrected [3,3] } \Delta G^\ddagger_{\text{B3LYP}})$ [d] Calculated $\Delta G^\ddagger - 1.2 \text{ kcal mol}^{-1}$ (UM05-2X/6-31+G*) [e] Calculated $\Delta G^\ddagger + 0.5 \text{ kcal mol}^{-1}$ (M06-2X/6-31G*) [f] $\Delta\Delta G^\ddagger = (\text{corrected VCPR } \Delta G^\ddagger_{\text{UM052X}}) - (\text{corrected [3,3] } \Delta G^\ddagger_{\text{M062X}})$. All calculations were performed in gas phase at 298 K using Gaussian'09, units are in kcal mol^{-1} . **Blue** values predict VCPR pathway, **orange** values predict a mixture of pathways and **green** values predict [3,3]-rearrangement.

Since the correcting factors were derived from their experimental values, it was no surprise that phenyl **147a** was correctly predicted to undergo VCPR and that piperonyl **214** was predicted to give a mixture of products (**Table 37**, Entry 1 and 2, respectively). More pleasingly, the major rearrangement pathways for the nine out of the ten novel difluoro-VCP examined were all predicted correctly using B3LYP/6-31G* calculations; phenyl **147a** correctly predicts VCPR pathway but is within computational error ($\Delta\Delta G^\ddagger = +0.9 \text{ kcal mol}^{-1}$, **Figure 52**). Both methods failed to deal with the non-fluorinated system, predicting a mixture of rearrangement products instead of only VCPR observed experimentally. Trulhar's functionals also failed to deal with more sterically hindered heteroaromatic VCPs **217** and **218** but it is unknown whether the error is associated with the VCPR or [3,3]-rearrangement calculations, or a combination of both. These results strongly suggest that the low cost DFT method is comparable and in some cases more effective in this context than the more expensive Minnesota methods, consistent with studies carried out by Simón and Goodman.²¹³

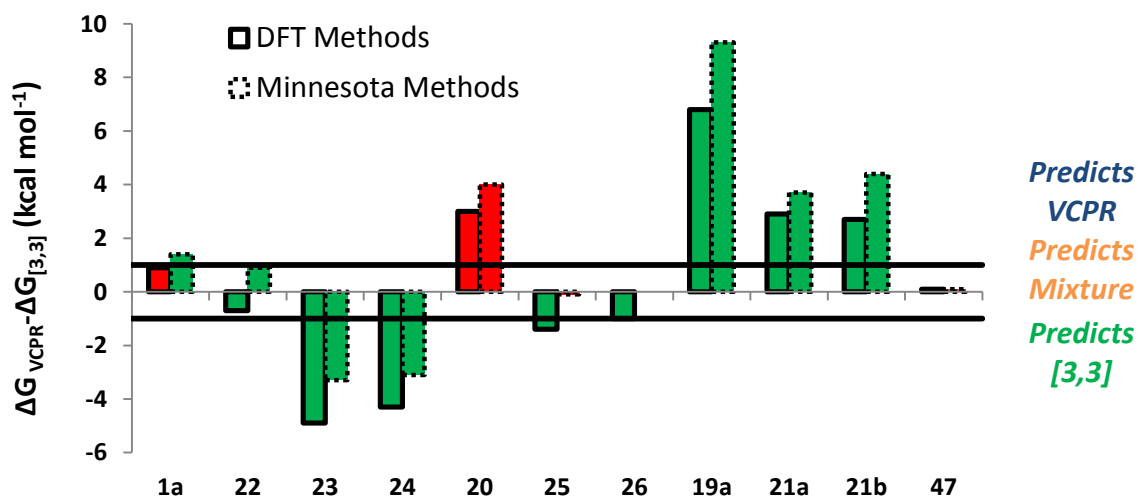


Figure 52: Prediction plot of the difference between corrected $\Delta G^{\ddagger}_{VCP}$ ((U)B3LYP/6-31G* or (U)M05-2X/6-31+G*) and corrected $\Delta G^{\ddagger}_{[3,3]}$ (B3LYP/6-31G* or M06-2X/6-31G*, respectively) for synthesised VCP. Colour used to represent the correct (green) or incorrect (red) predictions compared with experimental observations.

Since all experimental rearrangements were optimised to give full conversion of VCP after 17 hours, a strong trend was apparent between the corrected ΔG^{\ddagger} values for VCPR with reaction temperatures using either M05-2X/6-31+G* (Figure 53) or B3LYP/6-31G* methods (See Appendix).

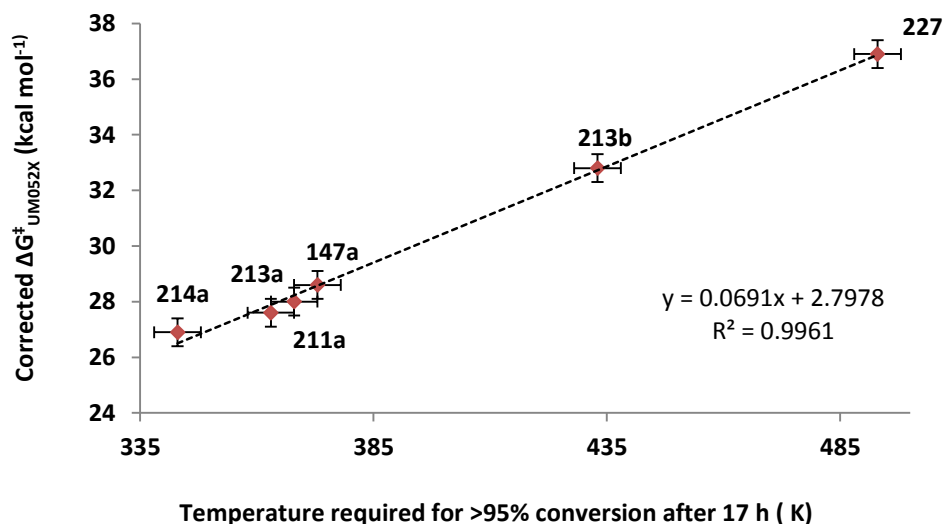


Figure 53: Correlation between corrected $\Delta G^{\ddagger}_{UM052X}$ values (kcal mol^{-1}) for VCPR and the optimised reaction temperatures (K) which gave 100% conversion of VCP. Error in $\Delta G^{\ddagger}_{UM052X}$ values = $\pm 0.5 \text{ kcal mol}^{-1}$. Error in temperature = $\pm 5 \text{ K}$.

As more compounds are synthesised, the error associated with these models may be reduced. However, from the small set of varied difluorinated vinylcyclopropanes that were examined, the most effective computational models look reliable enough to be used with confidence in the design and assessment of new precursors before any synthetic commitments are required.

A set of VCP from the literature were selected to test the predictive capability of the computational models developed, and the major rearrangement pathway observed for all four compounds was predicted successfully using the lower cost (U)B3LYP/6-31G* method (**Figure 54**).

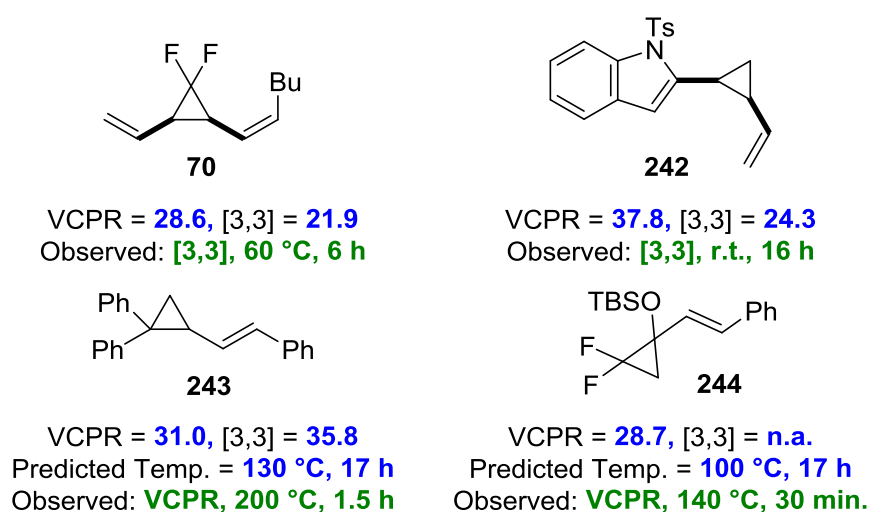


Figure 54: Testing the predictive capability of electronic structure models against compounds which undergo selective VCPR or [3,3]-rearrangement (simplified computational models were used for **242** (Ts replaced with Ms) and **244** (TBS replaced with TMS). Free energies of activation (ΔG^\ddagger) calculated on Gaussian'09 using (U)B3LYP/6-31G* (gas phase, 298 K) and quoted in kcal mol⁻¹. Predicted temperature derived from the straight line equation $y = 0.0721x + 2.0341$ from a plot of corrected $\Delta G^\ddagger_{\text{B3LYP}}$ against VCPR rearrangement temperatures.

The indole-vinylcyclopropane rearrangement of **242**^{181b} and divinylcyclopropane rearrangement of **70**¹¹² were both favoured over VCPR, whereas Sustmann and co-workers *bis*-aryl VCP **243** was correctly predicted to undergo VCPR.²¹⁴ The calculated $\Delta G^\ddagger_{\text{VCPR}}$ value of 31.0 ± 0.5 kcal mol⁻¹ for **243** is within error of the reported experimental activation energy of 32.8 ± 1.6 kcal mol⁻¹ (corrected to 298 K). Our temperature prediction suggests that the rearrangement could give full conversion after 17 hours at 130 °C, 70 °C lower than the reported conditions (reaction time of 1.5 hours). Difluoro-VCP **244** could only undergo VCPR and a calculated $\Delta G^\ddagger_{\text{B3LYP}}$ value of 28.7 kcal mol⁻¹ was very similar to phenyl **147a** and was

predicted to rearrange at the same temperature of 100 °C. These results strongly suggest that the Ni-catalyst present during the reaction at 140 °C does not facilitate the rearrangement, a factor that was not obvious from experimental observation.⁷⁰

4.6. Conclusion

A low cost computational assessment ((U)B3LYP/6-31G*) of substituent effects on the VCPR of difluorinated vinyl cyclopropanes was used to guide the synthesis of novel difluorocyclopropanes. Radical stabilising groups, specifically heteroaromatics, were found to lower calculated free energies of activation more when bound directly to the cyclopropane instead of the alkene, consistent with the accepted diradicaloid mechanism. Our synthetic investigations pushed the most recent difluorocarbene transfer methodology to the limits, highlighting the issues with functional group tolerance. Key difluorocyclopropyl alcohols (**199a**, **199c-d** and **199h**) could be accessed over two steps in moderate yields (32-38%) despite the capricious nature of the difluorocyclopropanation chemistry. Oxidation/olefination chemistry completed the syntheses of precursors, but the more reactive heteroaromatic compounds underwent rearrangements at unexpectedly low temperatures, through VCPR and aromatic-vinylcyclopropane rearrangements to give access to both novel difluorocyclopentenes and fluorinated benzoheptadienes, respectively. Optimised rearrangement temperatures for isolated precursors showed a good trend with calculated activation energies, allowing estimates of rearrangement temperatures to be made before synthesis. Assessment of electronic structure calculations with experimental activation energies for piperonyl **181f** and literature examples showed that the (U)M05-2X/6-31+G* method remained the most accurate for assessing VCPR but M06-2X/6-31G* calculations were better for the aromatic-vinylcyclopropane rearrangement. No single method proved to be the best overall but the consistency in error observed with (U)B3LYP/6-31G* calculations for both pathways, meant that it was considered closest to a universal method for dealing with the system. The selectively for rearrangement pathways could be predicted accurately using electronic structure calculations, either with the Minnesota functionals or lower cost DFT methods

((U)B3LYP/6-31G*). The computational design model developed was tested against literature compounds and correctly predicted observed experimental results.

The ability to determine whether a VCP molecule will rearrange thermally at a synthetically useful temperature, whilst also predicting which pathway it will undergo, is extremely powerful. These computational models could be used extensively to streamline further investigations into the application of these rearrangements.

Disclaimer: David Nelson (University of Strathclyde) synthesised the in house Ni-catalysts used during transition metal screening and Jonathan Percy (University of Strathclyde) ran the electronic structure calculations for intermediates and transition states representing Ni-mediated VCPR on Spartan'08.

Chapter 4: Alternative Rearrangement Conditions

From the computational triage we found that the incorporation of certain functional groups into our precursors led to barriers for VCPR of greater than 30 kcal mol⁻¹; the reaction temperatures required to induce rearrangement of these compounds were too high to make the process synthetically viable because of the accompanying decomposition reactions.

Both photochemical-initiated and transition metal-catalysed rearrangements of VCP precursors have been reported in the literature. Investigations into these procedures were important to assess if less reactive difluorinated-VCP species could still undergo rearrangement. Difluoro-**147a** was accessible in the largest quantities and used in our preliminary investigations into alternative rearrangement conditions; all cyclopropane-diastereoisomers and products have previously been isolated and fully characterised (**Figure 55**).

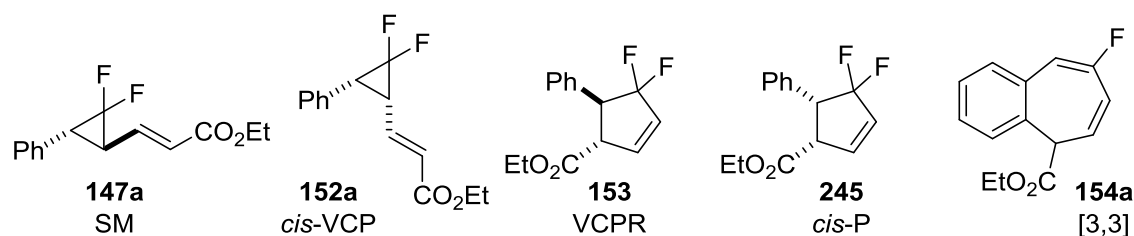
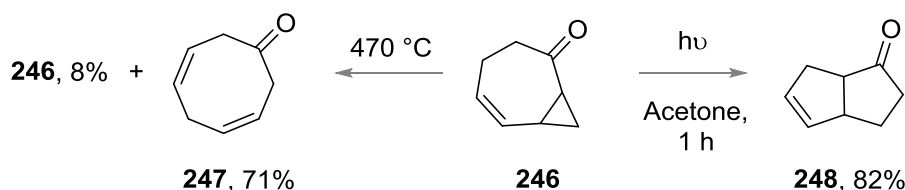


Figure 55: Compounds observed during the rearrangement of **147a** (naming system refers to key in **Figure 57**).

5.1 Photochemical Initiation

Paquette and co-workers studied both the thermal and photochemical rearrangement of ketone **246** (**Scheme 112**).⁷⁸ The extremely high pyrolysis temperatures of 470 °C favoured formation of cyclooctadienone **247** (71% conversion) but irradiation with a 450-W mercury bulb (a pyrex filter used to absorb

light of wavelength below 280 nm) favoured VCPR through to ketone **248** (82% conversion).



Scheme 112: Thermal and photochemical rearrangement of cyclooctadienone **246** (conversion determined by vapour phase chromatography analysis).

Inspired by these results, we looked to assess the effect of photochemical irradiation on *trans-E* **147a** and non-fluorinated precursor **227a**. Prior to running any experiments the UV/vis spectra were recorded and showed that the introduction of fluorine atoms on the cyclopropane ring caused a 20 nm shift in λ_{max} ; difluorocyclopropyl **147a** had a $\lambda_{\text{max}} = 222\text{ nm}$ ($\epsilon_0 = 26900\text{ M}^{-1}\text{ cm}^{-1}$, MeCN) and non-fluorinated **227a** had a $\lambda_{\text{max}} = 244\text{ nm}$ ($\epsilon_0 = 24900\text{ M}^{-1}\text{ cm}^{-1}$, MeCN) (**Figure 56**).

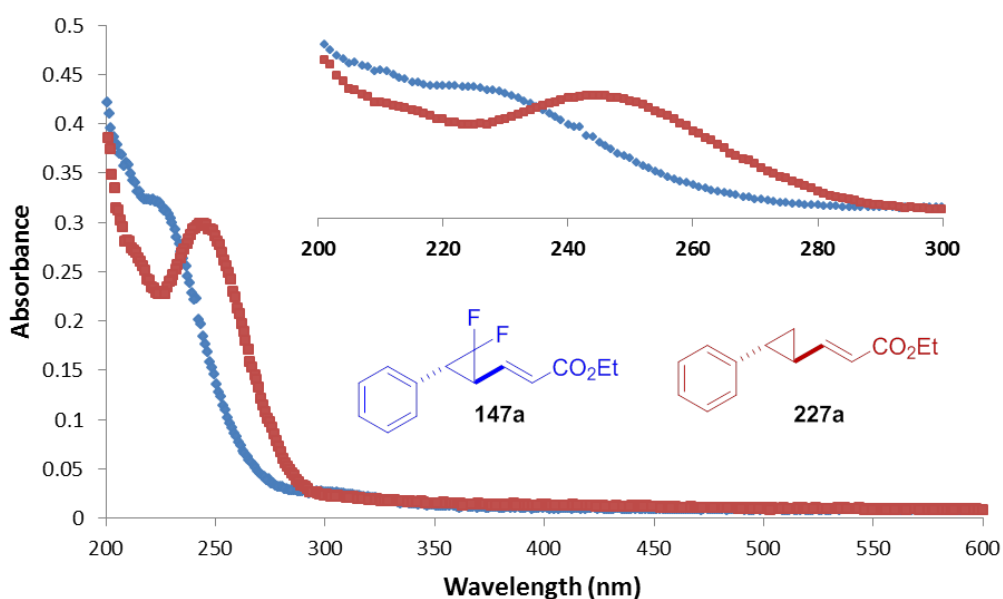
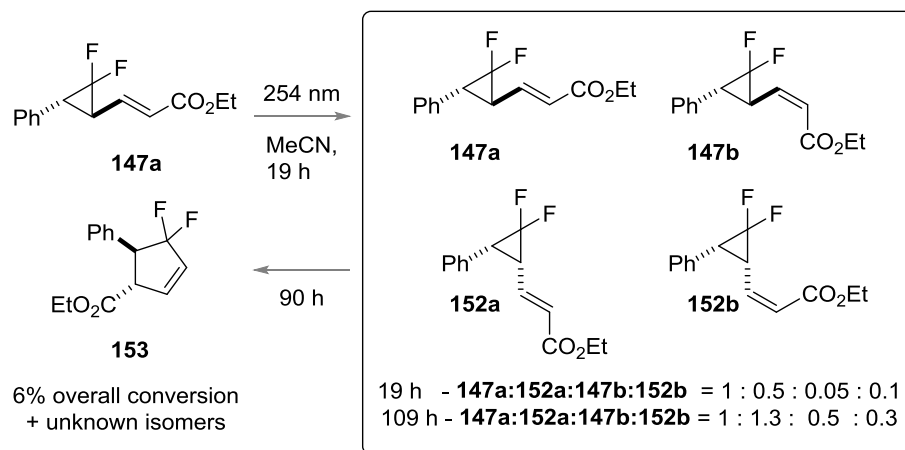


Figure 56: UV/vis spectrum for difluoro-**147a** and non-fluoro **227a** (insert is expanded view of λ_{max} region).

The similarities with the reported λ_{max} for methyl acrylate ($\lambda_{\text{max}} = 258\text{ nm}$, hexane) and methyl crotonate ($\lambda_{\text{max}} = 250\text{ nm}$, ethanol)²¹⁵ strongly suggest that the observed absorption with **147a** and **227a** is from the alkenoate group. We selected a 19-W low-pressure mercury lamp as a source of short wave (100-280 nm) ultraviolet

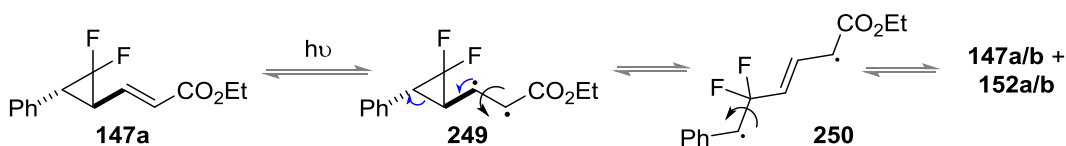
radiation for carrying out photochemical reactions because this would irradiate our precursors close to their λ_{max} .

However, only cyclopropane and alkene isomerisation of clean difluoro-**147a** was observed after irradiation for 19 hours (**Scheme 113**). Prolonged exposure for a further 90 hours (total reaction time of 109 hours) resulting in only 6% conversion to desired difluorocyclopentene **153** (determined by ^{19}F NMR) and instead favoured further isomerisation.



Scheme 113: Low pressure photochemical irradiation of precursor **147a** (relative ratios determined by ^{19}F NMR).

The observed isomerisation confirmed that photons were being absorbed by the precursor to form diradical intermediates **249** and **250** which, after bond rotation and reformation of the cyclopropane ring, allow access to the observed diastereoisomers (**Scheme 114**). However, the energy provided during this process was not large enough to overcome the energy barrier for VCPR.



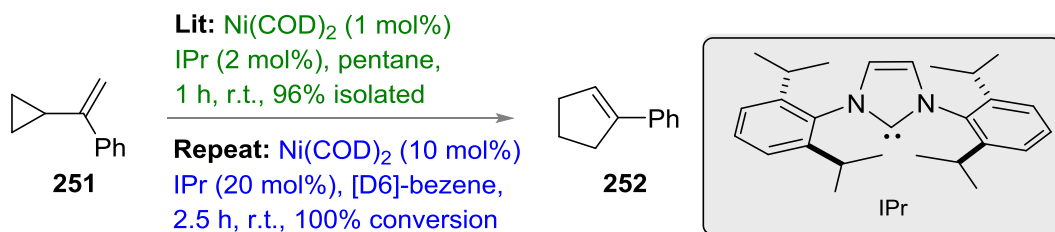
Scheme 114: Formation of diradical intermediates which result in stereochemical scrambling during photochemical irradiation.

These results were disappointing and showed that photochemical rearrangement of our VCP-precursors was unlikely. Further optimisation into light source, solvent type, reaction concentration and temperature could be beneficial but evidence for stereochemical scrambling and the potential lack of stereo-control in the

rearrangement meant that no further investigation were carried out. Instead focus turned into transition-metal catalysed VCPR conditions.

5.2 Transition Metal Mediated Rearrangements

A range of transition metals have been utilised to facilitate rearrangement of VCP but only nickel-NHC complexes were successful in catalysing the VCPR of unactivated vinyl cyclopropane precursors.^{82b} The effect of solvent, ligand type and loading were all assessed, revealing that the bulky IPr NHC ligand performed best and enabled pre-catalyst loading to be as low as 1 mol% for Ni(COD)₂. Louie and co-worker reported that the VCPR of 1-(cyclopropylvinyl)benzene **251** to cyclopentene **252** was complete after 1 hour at room temperature; we were able to repeat this observation, obtaining full conversion of **252** using the same reagents (**Scheme 115**), though under different conditions.



Scheme 115: Successful repeat of Ni-mediated VCPR of **251** to **252**.

The literature procedure reported that a solution of Ni(COD)₂/IPr was equilibrated for 12 hours (r.t., pentane) prior to carrying out the reaction. In our experiment, the catalyst and ligand were only mixed immediately before the reaction, which could explain the need for a longer reaction time and increased catalyst/ligand loading; solvent change has also been shown to affect reaction times.¹⁰⁶ This difference was not a concern since we initially only wanted to understand how difluoro-precursor **147a** would react under these conditions; our procedure still facilitated turnover and resulted in full conversion of **251** to **252**.

Trans-E precursor **147a** was exposed to the Ni(0)/IPr reaction system; no reaction was observed after 20 hours at room temperature or 40 °C. Thermally, this precursor undergoes full conversion to difluorocyclopentene **153** after 17 hours at 100 °C, so 80 °C was selected as the maximum screening temperature for the Ni-

catalysed reactions to avoid unwanted background thermal reactions. At this temperature, only a modest increase in rearrangement was observed after 3 days (12% increased conversion of rearrangement products compared with background thermal reaction) (**Figure 57**).

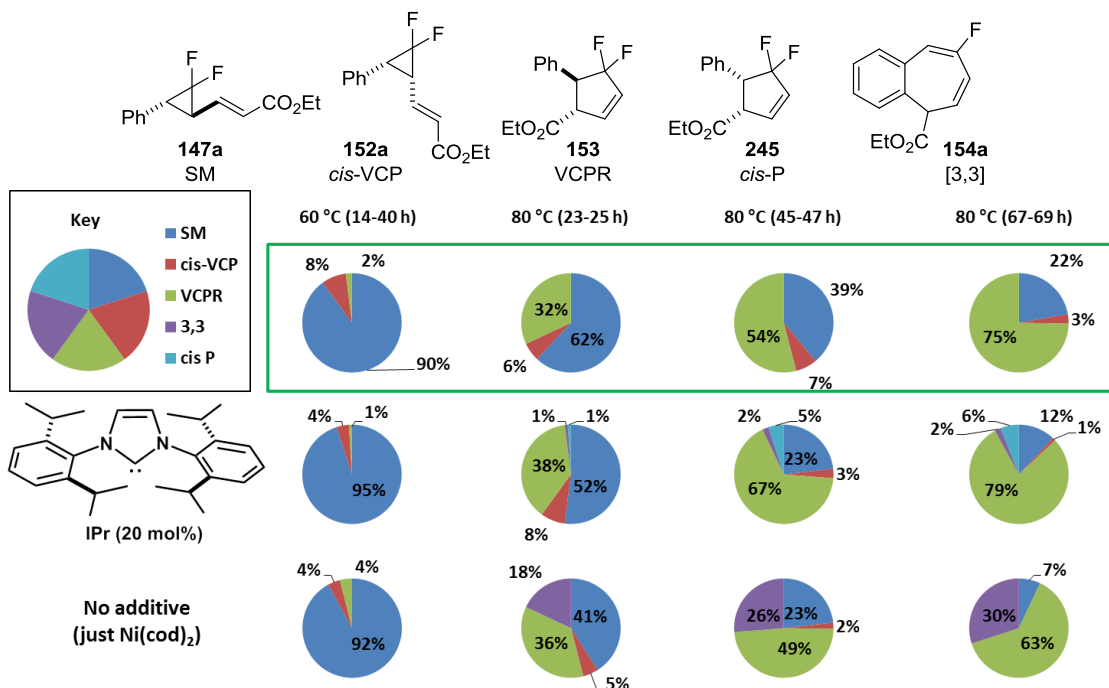
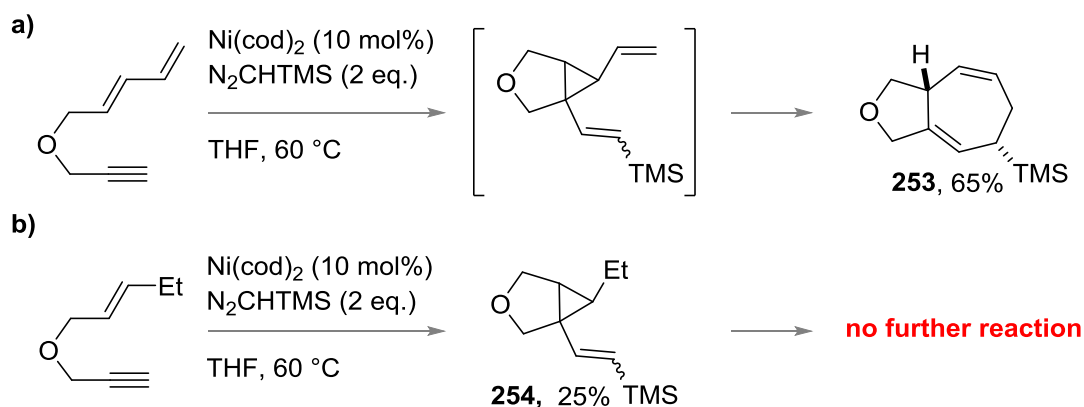


Figure 57: Pie charts representing fluorinated compounds present during the rearrangement of **147a** (relative percentage conversion by ¹⁹F NMR). The background thermal rearrangement is represented by the control reaction in the green box with no catalyst or ligand present. Conditions: Ni(COD)₂ (10 mol%), ligand (20 mol%), [D₆]-benzene.

However, a similar 79% conversion to *trans*-difluorocyclopentene **153** was observed for the Ni-reaction (*cf.* 75% from the background thermal reaction) but the formation of both *cis*-cyclopentene **245** (6%, tentatively assigned based on ¹⁹F NMR signals) and benzocycloheptadiene **154a** (2%) indicated that alternative rearrangement pathways were active in the presence of nickel complexes. Control experiments in the literature where either no Ni(COD)₂ or no IPr ligand were present in the reactions, failed to facilitate VCPR. This indicated that the formation of a Ni-IPr complex was required to induce rearrangement. However, when difluoro-**147a** was heated over 3 days at 80 °C in the presence of only Ni(COD)₂ (10 mol%), the [3,3]-rearrangement pathway became more active resulting in a 30% conversion to benzocycloheptadiene **154a** (*cf.* 0% in control thermal and 2% with

Ni(COD)₂/IPr conditions). These results are consistent with Yike and Montgomery's investigations into the Ni(COD)₂ mediated divinylcyclopropane rearrangement to **253**.²¹⁶ The rearrangement was part of a cascade [4+2+1] cycloaddition reaction (Scheme 116a) but substrates which could only undergo VCPR (**254**) showed no reactivity (Scheme 116b).



Scheme 116: Ni-mediated cascade reaction in the synthesis of a) **253** through a divinylcyclopropane rearrangement and b) **254** which shows no Ni-mediated VCPR.

Despite the undesirably long reaction time of 3 days, the activation of different rearrangement pathways for **147a** in the presence of nickel-complexes was intriguing and warranted further screening of ligand and catalyst type.

5.2.1 Phosphine Ligand Screening

Catalysts based on Ni(0) and phosphines (PBU₃, PPh₃) have been reported to successfully facilitate VCPR but at the cost of high temperatures and long reaction times.^{82a,217} However, when Louie and co-workers screened PCy₃ as an additive for unactivated precursors, no rearrangement was observed (100 °C, 24 h).^{82b} Further studies using a small set of NHC ligands with similar electronic properties showed a significant range of VCPR rates, suggesting that steric factors play a significant role in the rearrangement; increasing bulk close to the metal centre appears to be desirable.¹⁰⁶

These findings led us to investigate the effect of more bulky phosphine ligands (RuPhos, Xphos, dppf, Xantphos) on the Ni-mediated rearrangement of difluoro-**147a** (Figure 58). Unfortunately, no rate enhancement was observed over the

background thermal reaction (80 °C); the only new observation was the formation of benzocycloheptadiene **154a** when RuPhos (11%) or XPhos (20%) were used as additives.

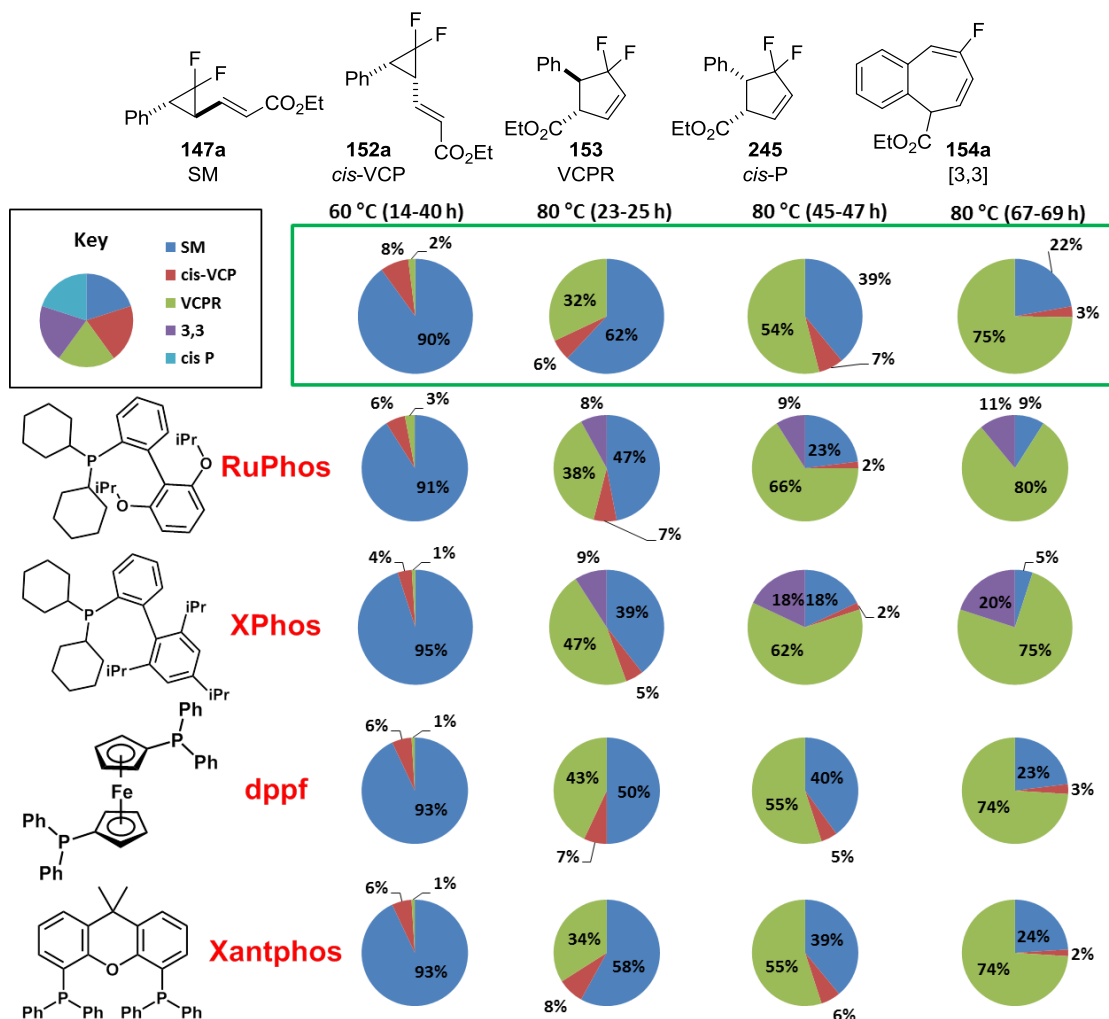


Figure 58: Effect of phosphine additives on Ni(0) mediated VCPR of difluoro-147a (relative percentage conversion by ^{19}F NMR). The background thermal rearrangement is represented by the control reaction in the green box with no catalyst or ligand present.

Conditions: Ni(COD) $_2$ (10 mol%), phosphine (20 mol%), [D $_6$]-benzene.

5.2.2 NHC-Ligand Screening

Previous screening of NHC-ligands effect on Ni-catalysed VCPR was carried by Louie and co-workers; they reported that a 3.2-fold rate enhancement was observed when SIPr was used, over the reaction with IPr in [D $_6$]-benzene.¹⁰⁶ We looked to use this combination in an attempt to reduce the reaction times for our system, but no

benefit was observed and instead [3,3]-rearrangement was active alongside [1,5]-hydride shift forming conjugated benzocycloheptadiene **154b** (Figure 59).

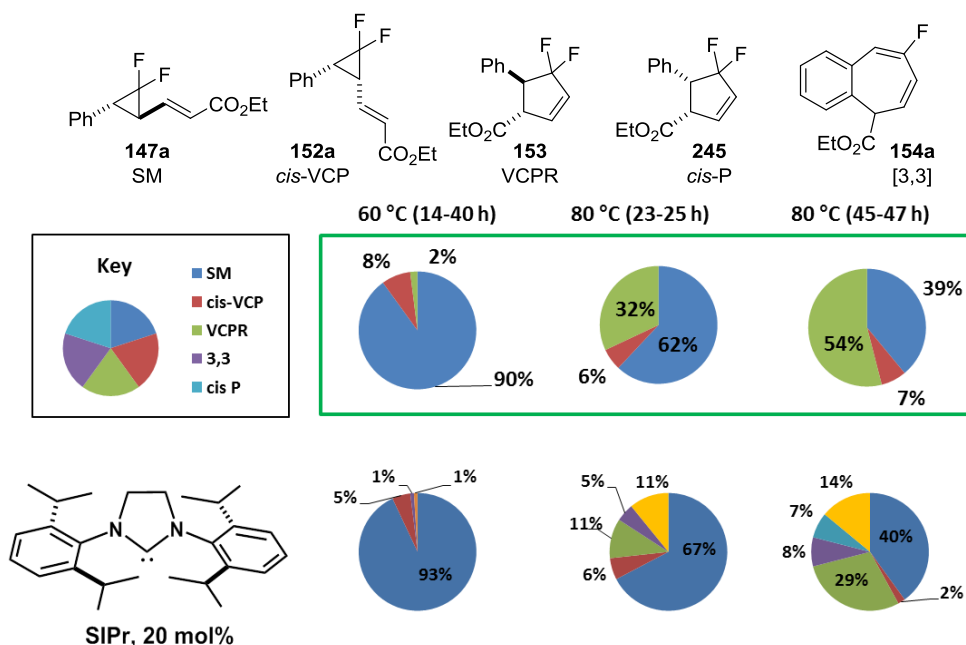


Figure 59: Effect of SIPr ligand on Ni(0) mediated VCPR of difluoro-147a (relative percentage conversion by ^{19}F NMR). The background thermal rearrangement is represented by the control reaction in the green box with no catalyst or ligand present. The yellow wedge represent conjugated benzocycloheptadiene **154b.**

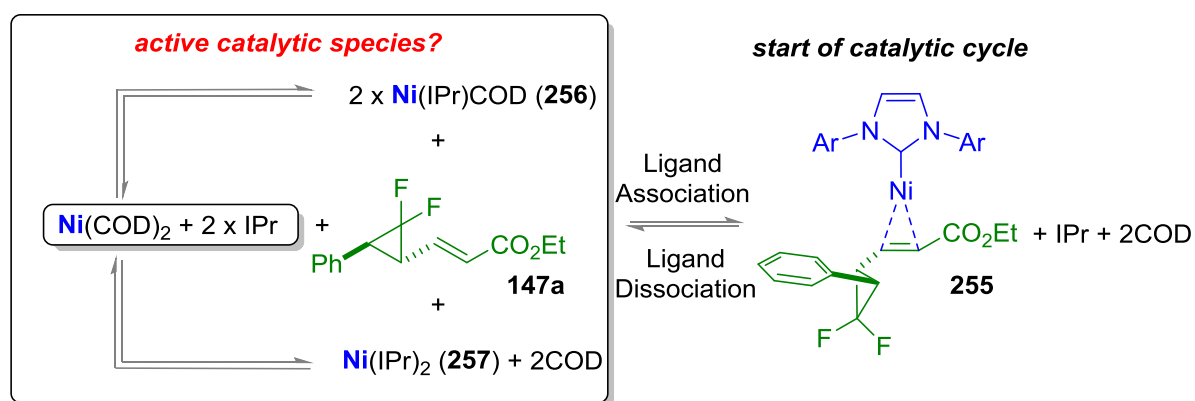
Conditions: Ni(COD)₂ (10 mol%), SIPr (20 mol%), [D₆]-benzene.

The activation of all rearrangement pathways, specifically those which would normally require temperatures of 180 °C, was interesting, but the lack of control was unpromising for the development of an efficient synthetic process. A slight change in the steric demands made by the NHC ligand enabled alternative pathways to become active, so extensive ligand screening would be required to obtain a better understanding of optimum conditions for our system.

A large commitment of resource would be required to conduct this investigation and in the context of this study, we were concerned that our initial conditions still involved long reaction times and gave no real benefit compared to the background thermal reaction. Instead of carrying out an intensive screening process, we looked to try and obtain a better understanding of the reason behind the poor reactivity by studying alternative Ni(0) sources, and gain a better mechanistic understanding using electronic structure calculations.

5.2.3 Investigating Alternative Ni(0) Sources

Mechanistic investigations of the catalytic cycle^{103,106} by Tantillo and co-workers predicted that catalysis would start from intermediate **255** in our systems. However, they did not take into account the active catalytic species which is required to form the complex (**Scheme 117**). Louie and co-workers conducted their experimental work with Ni(COD)₂/IPr solutions which had pre-equilibrated for 12 hours beforehand;^{82b} internal studies carried out by the same group showed that a mixture of Ni(COD)₂ and IPr exists in equilibrium with Ni(IPr)₂ and COD ($K_{eq} = 1$). However, the mono-NHC complex, Ni(iPr)COD (**256**) could also form under same conditions so understanding what is the active catalyst species remains difficult (**Scheme 117**).



Scheme 117: Catalyst/equilibrium system in play before accessing the start of the VCPR catalytic cycle (COD = 1,5-cyclooctadiene, Ar = 2,6-diisopropylphenyl).

The synthesis of the *bis*-IPr-nickel complex **257** has been reported²¹⁸ but Louie and co-workers found that the preparation was not as straightforward as reported and that the *in situ* generation from Ni(COD)₂ and IPr was more practical.²¹⁹ Interestingly, when Louie and co-workers subjected *bis*-IPr-nickel **257** to VCPR conditions, they observed that rearrangement still occurred, but with a much lower yield and rate, suggesting that the COD ligand plays an important role in the formation or stabilisation of the active catalyst.¹⁰⁶

These findings suggest that Ni(IPr)COD **256** is likely to be the most active catalytic species; in order to access intermediate **255**, ligand dissociation of the COD is

required followed by association of the alkenyl group of the difluoro-VCP **147a** to form an η^2 -complex. We were interested in the trying to understand this process more, but isolation of **256** has not been reported and is likely to be less than trival. Instead, Ni-complexes which mimic **256** were synthesised; these included hexadiene **258**, *bis*-styrene **259** and $(\eta^3\text{-allyl})\text{Ni}(\text{IPr})\text{Cl}$ **260** (Figure 60) complexes.

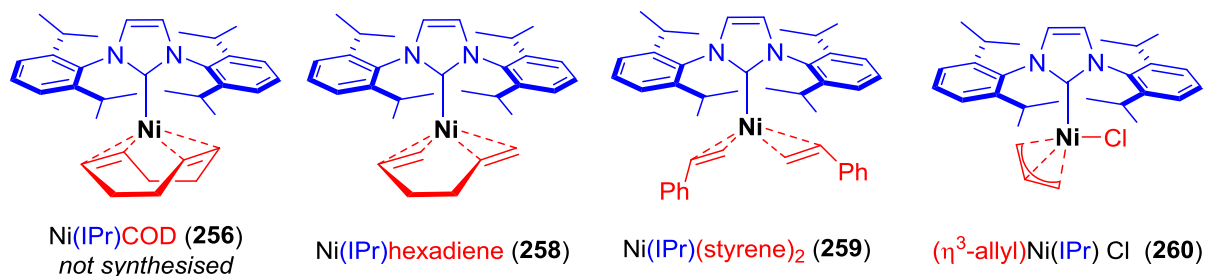


Figure 60: $\text{Ni}(\text{IPr})\text{COD}$ **256** mimics used to investigation ligand dissociation/association in the VCPR; $\text{Ni}(\text{IPr})\text{hexadiene}$ (**258**),²²⁰ $\text{Ni}(\text{IPr})(\text{styrene})_2$ (**259**)²²¹ and $(\eta^3\text{-allyl})\text{Ni}(\text{IPr})\text{Cl}$ (**260**)²²² were synthesised using literature methods.

Hexadiene-based catalyst **258** showed similar reactivity to the $\text{Ni}(\text{COD})_2/\text{IPr}$ mixture (82% conversion to **153** *cf.* 79%) and the background thermal reaction (75%) (Figure 61); other side rearrangements were also active. The similarities between the two catalytic reactions give some support into the active catalyst being an NHC-Ni-alkene complex.

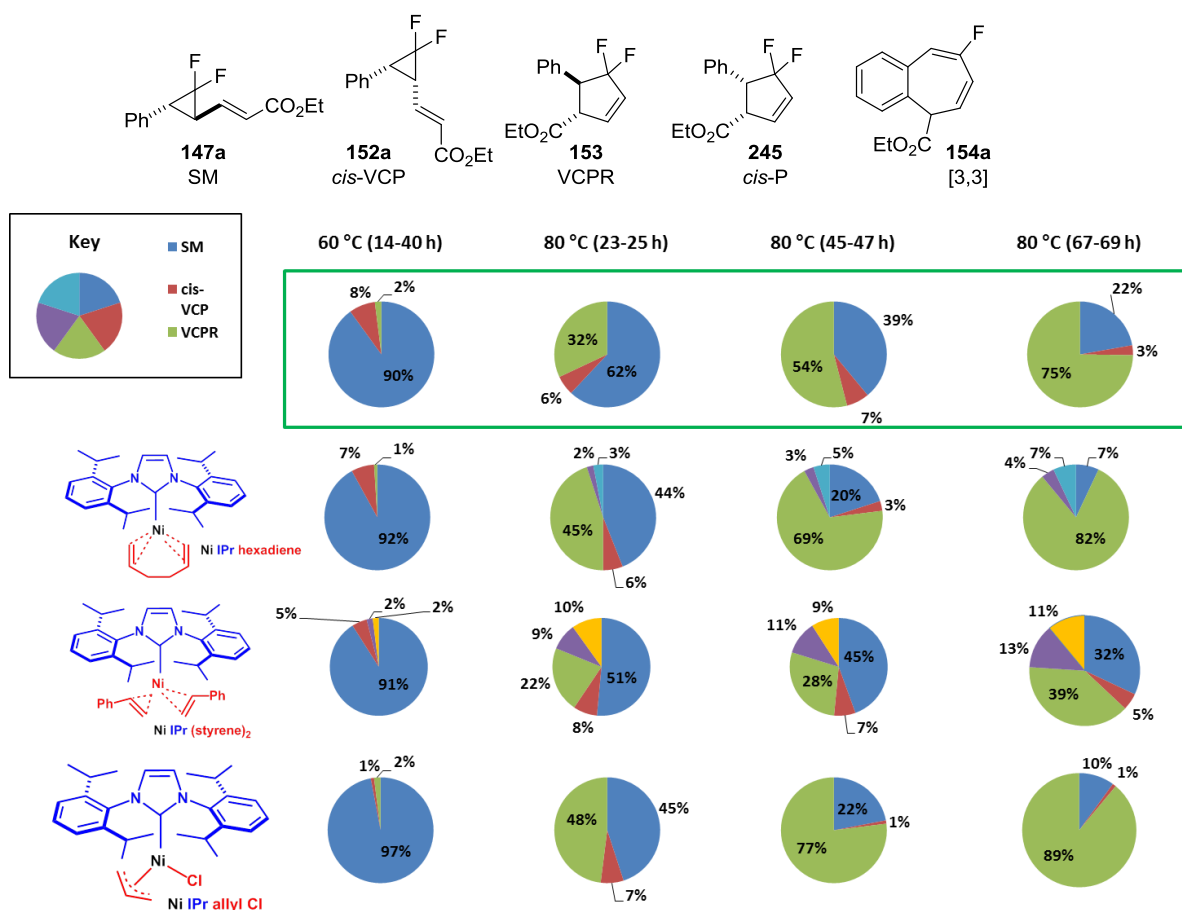


Figure 61: Reaction compositions for the VCPR of 147a using different Ni-precatalysts (yellow wedge represent the conjugated benzocycloheptadiene (154b) product). Conditions: Ni-catalyst (10 mol%), [D6]-benzene.

It was proposed that ligand dissociation from either COD **256** or hexadiene **258** complexes through to intermediate **255** would be disfavoured due to the favourable chelation found in the initial catalysts. It was therefore proposed that *bis*-styrene **259** would be a better complex to favour ligand exchange; however, suppression of the rearrangement was observed with 32% difluoro-VCP **147a** remaining after 3 days at 80 °C (*cf.* background thermal reaction had 22% of **147a** remaining). Furthermore, all rearrangement pathways were still active, including [1,5]-hydride shifts to conjugated benzocycloheptadiene **154b**.

Pleasingly, when IPr-Ni(II) catalyst **260** was utilised, an 89% conversion to difluorocyclopentene **153** was observed (*cf.* 75% for background thermal reaction) with no other rearrangement pathways active. Typically base is required to initiate catalysis by forming the active Ni(0) complex²²³ but no rate increase was observed

when the VCPR reaction with **147a** was carried out in the presence of KOtBu (20 mol%, 80% conversion to **153** after 3 days at 80 °C). How the active Ni(0) complex forms in our reaction is unknown, but the reported cross coupling of heteroaromatic chlorides with aryl ethers with **260** was also successful in the absence of base.²²⁴ Unfortunately, no VCPR was observed when 1,1-disubstituted olefin **251** was exposed to the same catalyst system.

The Ni-catalysed VCPR of our difluorinated precursors is of low synthetic value, with long reaction times and very modest rate increases over the background thermal reactions; the activation of undesirable rearrangement pathways is also problematic. Difluorocyclopropane precursors were expected to benefit from Ni-mediated VCPR as the non-fluorinated species had, and we looked towards electronic structure calculations to confirm our hypothesis. We also hoped that access to computational models for the rearrangement would reveal why precursor **147a** did not respond to the presence of a catalyst system. This knowledge would aid the design of more suitable compounds to carry out further synthetic screening.

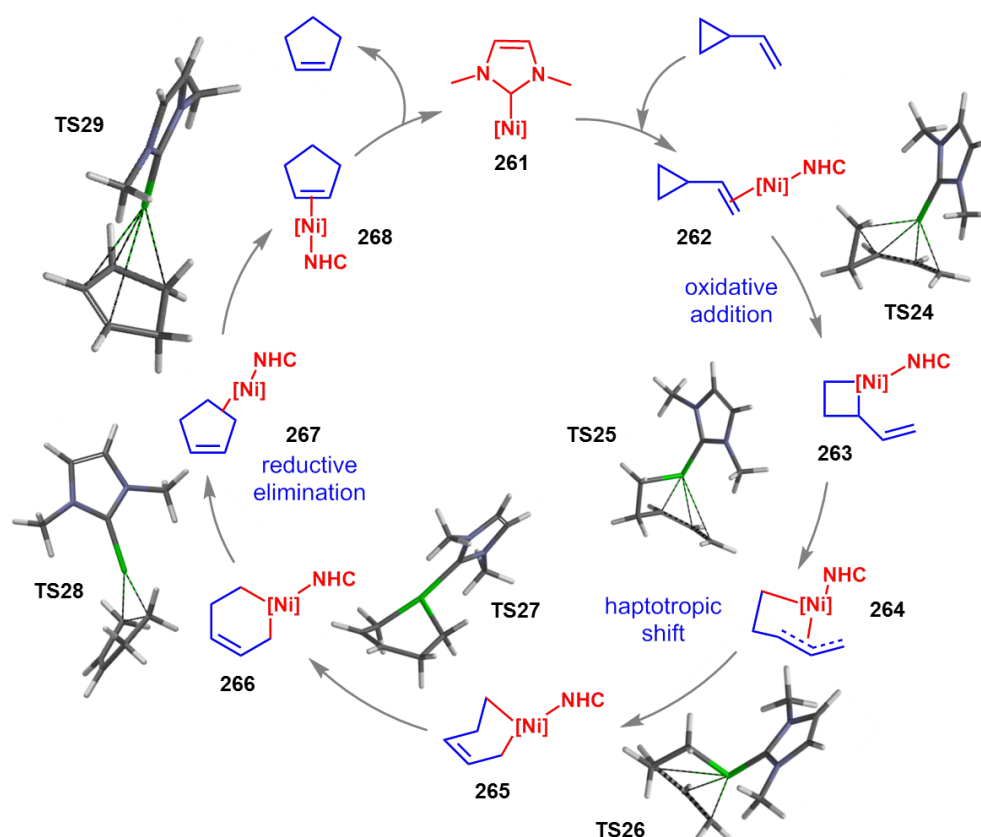
5.3 Computational Assessment of Ni-mediated VCPR

Tantillo and co-workers carried out extensive studies on the effect of alkene substitution on the activation energies for Ni-mediated VCPR but no work was conducted the effect of substituents on the cyclopropane ring.¹⁰⁶ From their extensive investigations, a detailed mechanistic pathway was analysed using electronic structure calculations (*vide supra*) and we looked to utilise their structure as the basis to help understand the effect substituents on our system have on the rearrangement.

5.3.1 Method Comparison

The intermediates and transition states reported in the literature were optimised using Gaussian'03 at the B3LYP/LANL2DZ level of theory; method testing relied on the optimisation and comparison of several Ni-allyl and Ni-NHC complexes for which X-ray structures had been obtained; according to Tantillo and co-workers no significant deviations in geometry were observed between experimental and

calculated geometries.¹⁰⁶ We were interested to see how Spartan software dealt with these systems due to the ease of local access and the efficient use of list functions within the software. Using literature Cartesian coordinates, we could obtain optimised structures for all intermediates and transition states reported for the Ni-mediated VCPR of vinyl cyclopropane with simplified Ni-NHC model (Me replacing the (2,6-diisopropylphenyl) ligands, **Scheme 118**).¹⁰⁶



Scheme 118: Intermediates and transition states used to assess the Ni-mediated VCPR and based on literature compounds.¹⁰⁶

We found that a very similar reaction profile could be obtained when the intermediates and transition states were optimised on Spartan'08 software using B3LYP/LACVP* methodology (**Figure 62a**). An expected change in our calculated relative energies from **262** compared to those reported in the literature was observed (overestimate of 0.7 to 4.5 kcal mol⁻¹) but this was not an issue since the simplified NHC model does not fully represent the reaction system. More

importantly, the geometries and motion of transition states obtained were very similar (**Figure 62b**) between the two methods.

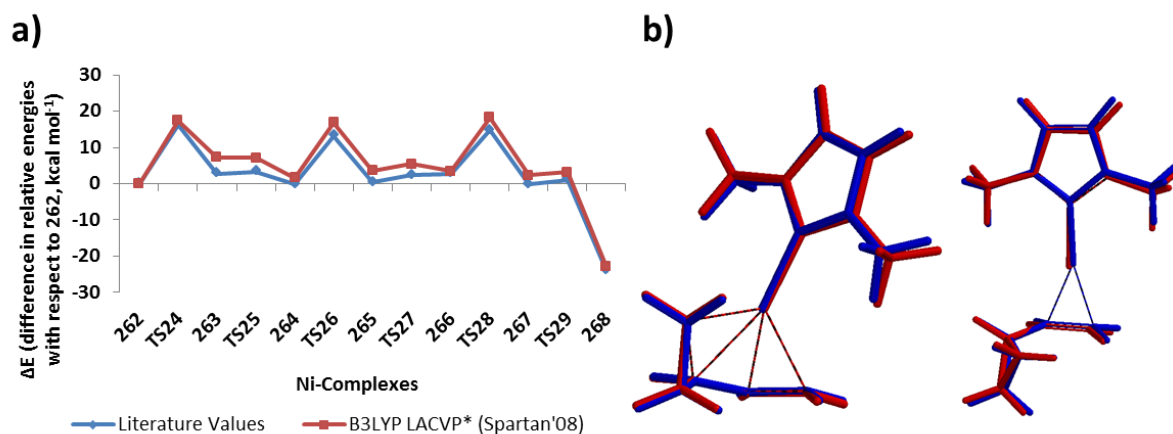


Figure 62: a) Relative energies for the Ni-mediated VCPR of vinyl cyclopropane, comparing literature methodology (B3LYP/LANL2DZ) and B3LYP/LACVP* methodology (Spartan'08, gas phase, 298 K) b) overlay of literature (red) and optimised (blue) electronic structures for TS25 and 261).

With confidence secured in obtaining similar Ni-intermediates and transition states to those reported in the literature, we used these base structures to assess the effect substitution had on the barrier for rearrangement.

5.3.2 Effect of Substitution

From the calculated reaction profile, it was observed that only the three transition states which represented oxidative addition, hapotropic shift and reductive elimination (**TS24**, **TS25** and **TS26**, respectively) had barriers high enough to influence the rate of rearrangement. In order to minimise the number of calculations required and still effectively assess the effects of substitution, we focused on these key steps in the rearrangement as well as the intermediates which surround them. It is also worth noting that the most subtle structural changes (e.g. transformation of intermediate **265** to **266**) could not be represented adequately using the Spartan method, and instead optimised to the same species.

All of the energies were calculated relative to intermediate **262** so it was important to assess the effect individual substituents had on the approach of the metal; *gem*-difluoro cyclopropyl **262b**, *trans*-phenyl **262c** and vinyl methyl ester **262d** were used

and geometries compared with simpler intermediate **262a**. Difluorination of the cyclopropyl ring had no effect on the geometry but phenyl-cyclopropyl **262c** and vinyl methyl ester **262d** both showed the nickel approaching from an angle, instead of directly above the alkene (**Figure 63**).

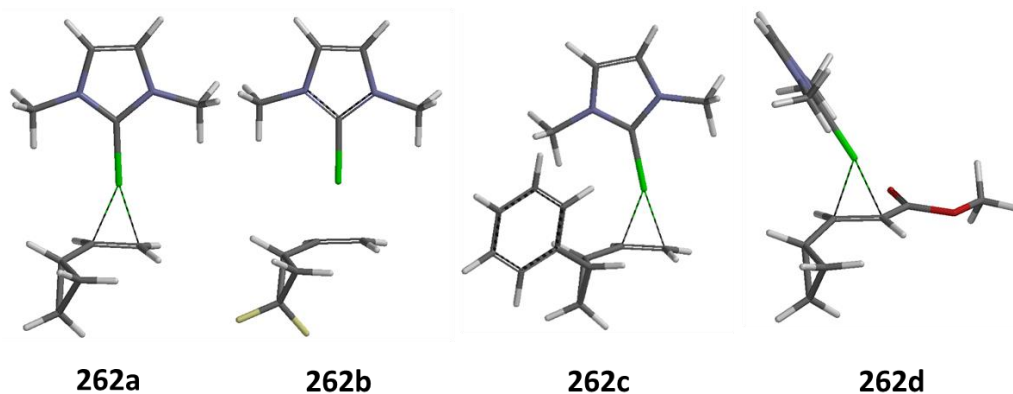


Figure 63: Effect of substitution on the approach of Ni-alkene coordination of intermediate **262**.

An accurate comparison of relative energies which derive from intermediate **262** would be difficult due to these differences in metal/ligand approach geometry. We therefore used the sum of the relative energies for the VCP and the mono-Ni-NHC complex **261** to normalise the energies for the intermediates and transition states examined (**Table 38** and **Figure 64a**).

Table 38: Relative energy (ΔE , relative to sum of separate Ni-NHC and VCP system) differences with substitution on the cyclopropane ring and alkene (kcal mol^{-1}).

| Compound | Prototypical | Difluoro | <i>Trans</i> -Ph | <i>cis</i> -Ph | Methyl Ester |
|-------------|--------------|----------|------------------|----------------|--------------|
| 262 | -34.1 | -35.5 | -34.2 | -32.4 | -38.1 |
| TS24 | -16.7 | -22.5 | -19.7 | -16.0 | -21.3 |
| 264 | -32.6 | -50.6 | -35.2 | -37.6 | -38.0 |
| TS26 | -17.2 | -30.3 | -18.3 | -20.7 | -25.6 |
| 265 | -30.6 | -47.9 | -31.3 | -33.4 | -43.7 |
| TS28 | -15.9 | -28.0 | - | -15.7 | - |
| 267 | -31.7 | -41.7 | -44.6 | -30.6 | -46.4 |

Adding two fluorine atoms to the cyclopropane ring, distal to the scissile bond, resulted in all intermediates and transition states having a lower normalised energy than with the non-fluorinated system. The highest energy process remained

oxidative addition but the barrier was 5.8 kcal mol⁻¹ lower than that of the prototypical rearrangement (**Figure 64b**).

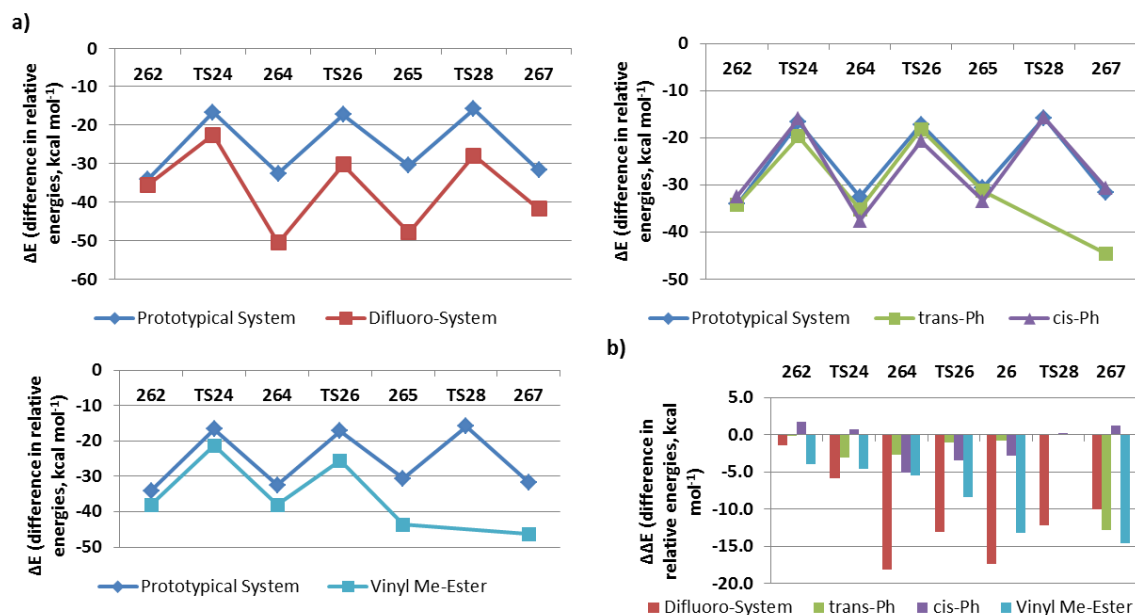


Figure 64: a) Relative energy (ΔE , relative to sum of separate Ni-NHC and VCP system) differences with substitution on the cyclopropane ring and alkene (kcal mol⁻¹). b) Difference in relative energy for substituted system and unsubstituted system ($\Delta\Delta E$, B3LYP/LACVP*, gas phase, 298 K, kcal mol⁻¹).

Both *trans*- and *cis*-phenyl VCPs were examined since the two isomers were present at experimental reaction temperatures. By working through the complexes involved in Ni-mediated VCPR, it was found that *trans*-substituted VCP resulted in the formation of the corresponding *cis*-cyclopentene; the observed difluoro *trans*-cyclopentene **147a** in our experiments would form from *cis*-VCP **245** under Ni-catalysis. Only the *cis*-phenyl VCP gave a higher normalised energy (+1.7 kcal mol⁻¹) when intermediate **262** was compared with the prototypical system; only a slight change in approach of the Ni-NHC was observed (**Figure 65a**). The *trans*-phenyl VCP system had a similar approach but did not show any significant differences from the prototypical system ($\Delta\Delta E$ value = -0.1 kcal mol⁻¹). For the *cis*-phenyl system, the remaining key intermediates and transition states were either within experimental error or had a lower barrier ($\Delta\Delta E$ values ranged from +0.7 kcal mol⁻¹ to -5.1 kcal mol⁻¹). For the oxidative addition step and haptotropic shift, the *trans*-phenyl system was lower in energy ($\Delta\Delta E$ values ranged from -1.0 kcal mol⁻¹ to -3.1 kcal mol⁻¹) but a transition state for reductive elimination could not be obtained. Attempts to obtain

a minimised structure which represented *trans*-phenyl intermediate **267c** resulted in the η^2 -complexation between the edge of the phenyl ring and nickel centre (**Figure 65b**). A similar pathway was uncovered when Tantillo and co-workers examined the Ni-mediated VCPR of (*E*)-(2-cyclopropylvinyl)benzene.¹⁰⁶ They could obtain a transition state which resulted in a similar intermediate but a 1.2 kcal mol⁻¹ increase in energy was observed over the normal reductive elimination pathway. However, the resulting Ni-benzene complex which resulted from this pathway was 15.0 kcal mol⁻¹ more stabilised than intermediate **267a** for the same system; *trans*-phenyl cyclopropane intermediate **267c** had a $\Delta\Delta E$ value of -12.8 kcal mol⁻¹ compared with the prototypical system.

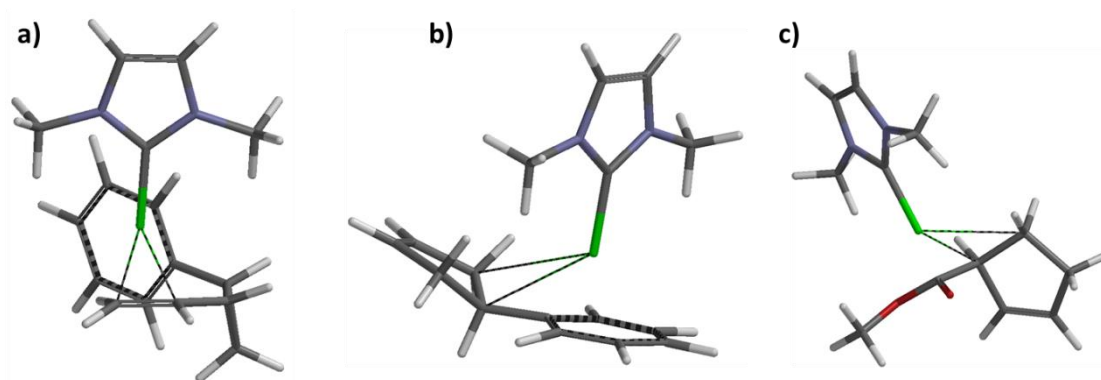
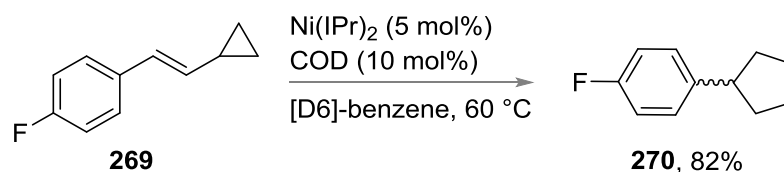


Figure 65: a) Intermediate **262** for *cis*-phenyl system. b) Intermediates **267c** for *trans*-phenyl system. c) Intermediate **267d** for vinyl Me-ester system.

A similar alternative pathway was observed when the Me-vinyl ester system was examined; no reductive elimination transition state could be found but intermediate **267d** for this system showed η^2 -coordination of the carbonyl group to Ni, rather than Ni/ σ -alkyl formation (**Figure 65c**). All species were lower in energy than those of the prototypical reaction system ($\Delta\Delta E$ values ranging from -3.9 kcal mol⁻¹ to -14.6 kcal mol⁻¹).

These preliminary computational results suggest that, when assessed separately, the substituents on difluoro-VCP **147a** do not have a dramatic effect on the barrier for rearrangement compared with the energies required for the Ni-mediated VCPR of **49**. In fact, the beneficial effect of both *gem*-difluorination and vinyl ester functionality suggest that the rearrangement should be faster; this was not

consistent with experimental findings. The only detrimental effects observed were potential steric clashes when a phenyl ring was incorporated onto the cyclopropane. Our comparisons with literature results use a simplified NHC model (Me instead of 2,6-diisopropylbenzene attached to the nitrogen atoms) and this dramatically underestimates steric influences on the VCPR. Tantillo and co-workers touched on this issues when they reported that the highest calculated energy barrier in the nickel-mediated rearrangement of VCP **269** was 19.3 kcal mol⁻¹ (**Scheme 119**); the experimental activation energy was determined to be 27.0 kcal mol⁻¹ (computational underestimation of 7.7 kcal mol⁻¹).¹⁰⁶



Scheme 119: Ni-mediated VCPR of VCP 269.

The same group carried out an ONIOM-based assessment of the VCPR of the prototypical system with the full-sized carbene, but no significant changes in relative energies were observed; interestingly, the reductive elimination transition state which is most influenced by steric effects could not be located.¹⁰⁶ The steric influences on our system are more significant but we struggled to obtain optimised systems using Spartan'08 methodology. An overlay of literature coordinates for the prototypical transition state **TS24** containing the full NHC ligand with our full VCP system using the basic NHC model highlighted potential steric clashes between both the phenyl and ester substituents with the bulkier ligand (**Figure 66**).

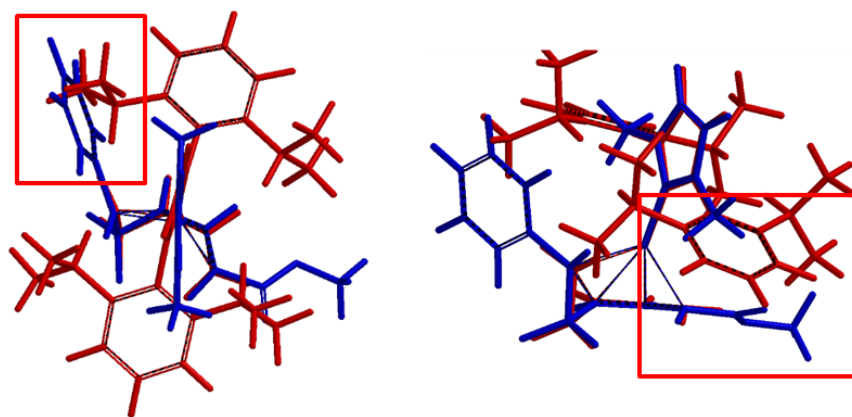


Figure 66: Overlay of TS24 for basic VCP system with full NHC (red structures) and full VCP system with basic NHC model (blue structures) – red squares highlight likely areas for steric repulsion.

Obtaining optimised intermediates and transition states for our full difluoro-VCP system with a full NHC system was important in order to determine where our system is likely to fail on the Ni-mediated pathway, and how we can design more effective substrates.

5.3.3 Investigating Full-NHC Ligand Systems

In order to handle these much larger structures effectively, we moved to Gaussian'09 software due to the amount of computing resource and time available in house. This setup allowed our full difluoro-VCP system to be computed with the Ni metal bound to an IPr ligand; B3LYP methodology was employed with LANL2DZ basis set for the Ni atom and 6-31G* for all others. We also looked to use free energy values derived from thermodynamic calculations to give a more accurate representation of energy levels and changes.

We started our investigations with the prototypical VCP system using the full NHC ligand; these optimised structures could then be used as templates for building our full VCP system. We found that the key steps had similar barrier heights ($\Delta\Delta G^\ddagger$ spread of $3.3 \text{ kcal mol}^{-1}$) with the haptotropic shift being the rate-determining step ($\Delta G^\ddagger = 21.4 \text{ kcal mol}^{-1}$ with respect to intermediate **262**) (Figure 67). This differs from the ΔE° values reported in the literature, which suggested that the initial oxidative addition step had the highest energy barrier by a modest margin.

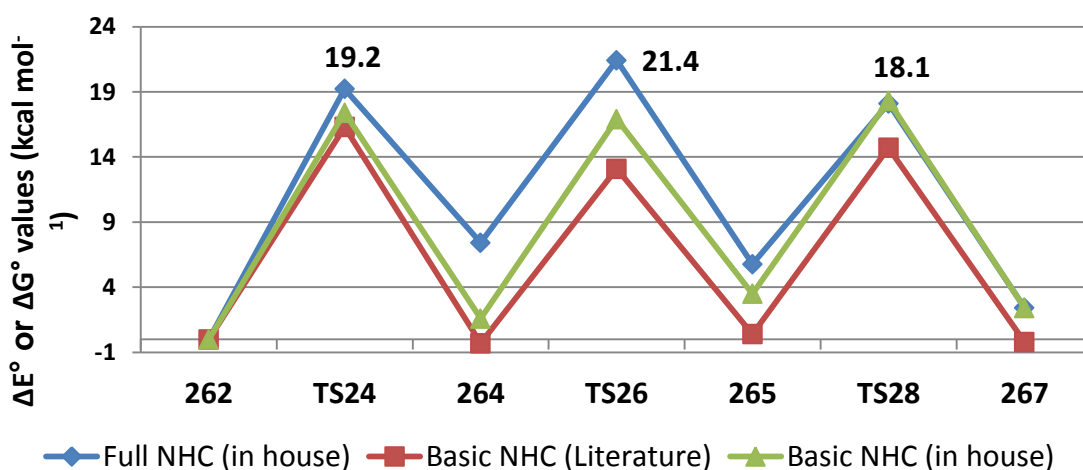


Figure 67: Comparison of full NHC system (ΔG° values, B3LYP/LANL2DZ/6-31G*, gas phase, 298 K, Gaussian'09) with basic NHC system reported in the literature (ΔE° values, B3LYP/LANL2DZ, gas phase, 298 K, Gaussian'03) and in house (ΔE° values, B3LYP/LACVP*, gas phase, 298 K, Spartan'08). All energies are relative to intermediate 262 and reported in kcal mol⁻¹.

All intermediates and transition states had a higher relative energy than those reported in the literature, suggesting that the steric influence of the IPr ligand needs to be modelled in order to assess energy barriers effectively. Interestingly, we could obtain a transition state which represented the reductive elimination step (**TS28**) when the full ligand was used and the ΔG° value was very similar to the ΔE° for our simpler system (difference of 0.2 kcal mol⁻¹). The steric influence of the IPr ligand was expected to be more dramatic when our full difluoro-VCP system was incorporated.

Comparison of the stabilisation energy resulting from complexation between the simple VCP system alkene and a basic NHC model or full IPr ligand showed little difference when relative energies ($\Delta E^\circ = (E \text{ for intermediate } \mathbf{262}) - (E \text{ for Ni-NHC} + E \text{ for free VCP } \mathbf{261})$) were compared, at -34.1 kcal mol⁻¹ and -32.8 kcal mol⁻¹, respectively. The change in free energy for the latter was also calculated ($\Delta G^\circ = -19.1$ kcal mol⁻¹) and similar stabilisation energies were calculated for the full *trans*- and *cis*-systems ($\Delta G^\circ = -16.3$ kcal mol⁻¹ and -18.5 kcal mol⁻¹, respectively). Due to the conformation of the phenyl ring in the *cis*-system (**Figure 68a**), it was expected that the energy of the complexed species (**262**) would be higher than that of the corresponding *trans*-system where the phenyl ring points away from the metal

centre. However, the structure for *cis*-**262** did not minimise to the intermediate which enables oxidative addition through **TS24**; instead, optimisation resulted in rotation of the cyclopropane ring to relieve steric clashes between the aromatic rings (**Figure 68b**).

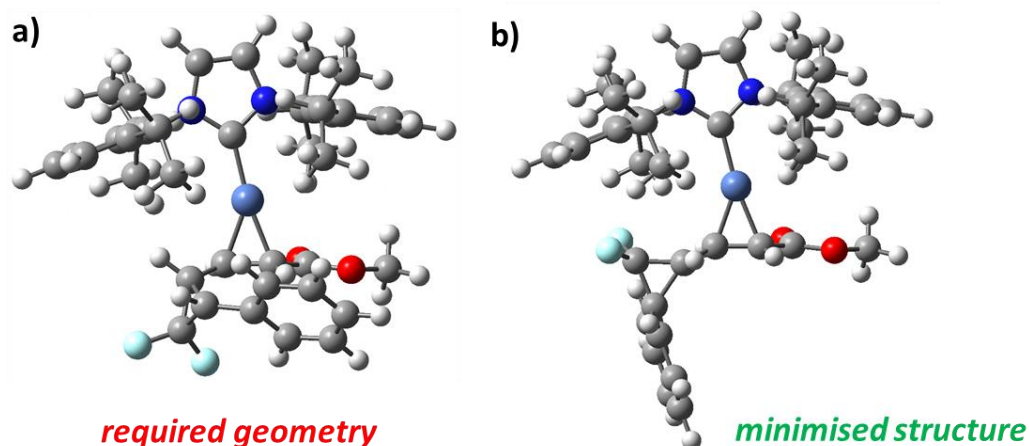


Figure 68: Intermediate 262 for full *cis*-system showing a) the desired conformation to facilitate oxidative addition and b) the resulting structure after equilibrium geometry optimisation (Gaussian'09, B3LYP/LAND2DZ/6-31G*, gas phase, 298 K).

No adverse changes in the barrier for oxidative addition between simple VCP and full *trans*-system were observed when the full NHC model was used; an oxidative addition transition state could not be obtained for the *cis*-system (**Table 39** and **Figure 69**).

Table 39: Energy Barriers for different VCP systems using Full-NHC Model

| Process | Species | ΔG° (relative to intermediate 262, kcal mol ⁻¹) | | |
|-----------------------|---------|--|---------------------------|-------------------------|
| | | Basic VCP | <i>Trans</i> -Full System | <i>Cis</i> -Full System |
| Oxidative Addition | 262 | 0.0 | 0.0 | 0.0 |
| | TS24 | 19.2 | 19.5 | n.d. ^[a] |
| Haptotropic Shift | 264 | 7.4 | 9.4 | 1.6 |
| | TS26 | 21.4 | 28.6 | 21.0 |
| Reductive Elimination | 265 | 5.8 | -2.6 | 7.8 |
| | TS28 | 18.1 | 11.6 ^[b] | 4.3 ^[b] |
| | 267 | 2.4 | 7.9 ^[c] | 3.2 ^[c] |

[a] Representative transition state could not be found. [b] Transition state does not represent reductive elimination. [c] Intermediates not representative of Ni- η_2 -alkyl coordination.

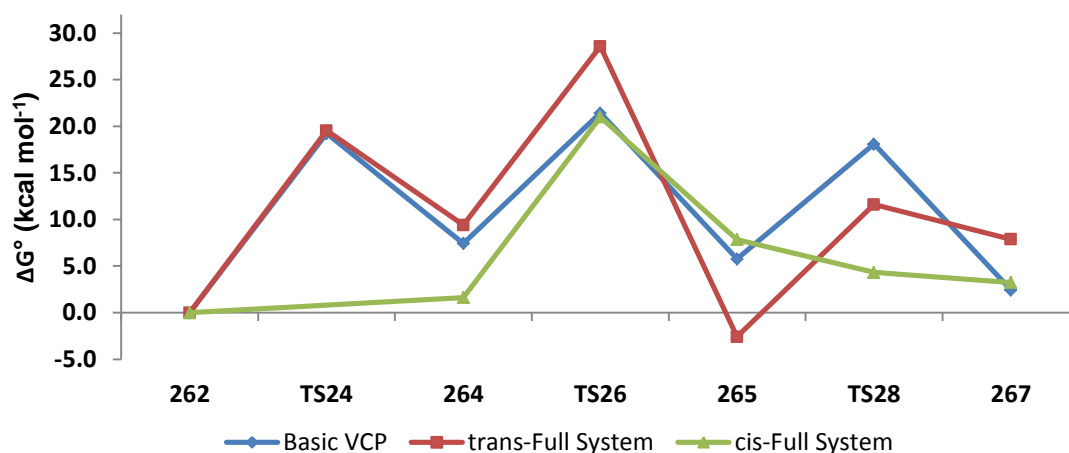


Figure 69: Graphical representation of relative free energies in Table 39.

The structure representing the transition state for oxidative addition with the full *cis*-system before optimisation suggested adverse steric interactions between the *iso*-propyl groups and the phenyl ring (**Figure 70a**). The transition state with this structure could not be optimised fully; the resulting complex maintained the Ni- η^2 -alkene coordination, but a new Ni- η^2 -phenyl interaction emerged (**Figure 70b**). The relative energy difference of this species compared with the Ni- η^2 -alkene intermediate (**262**) was +21.7 kcal mol⁻¹ and is likely to be more favourable than the sterically hindered **TS24**.

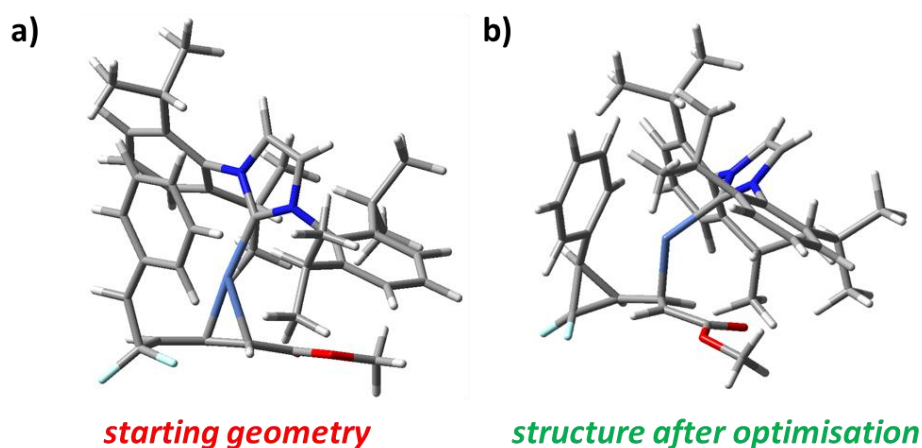


Figure 70: Attempts to optimise **TS24** for *cis*-full system; starting geometry (**a**) resulted in a new Ni-complex (**b**).

This complex has the Ni-metal connecting the alkenoate with the phenyl ring and supports an alternative Ni-mediated pathway which could be related to the [3,3]-

sigmatropic rearrangement through to benzocycloheptadiene **154a**. Further investigations are required to secure electronic structures for this pathway, but a Ni-mediated rearrangement pathway would be consistent with what was observed experimentally.

The activation energies for both the *trans*- and *cis*-**TS26** (ΔG^\ddagger , (free energy for **TS26**)-(free energy for **264**)) for the haptropic shift were similar ($\Delta G^\ddagger = 19.2 \text{ kcal mol}^{-1}$ and $19.4 \text{ kcal mol}^{-1}$, respectively) but more than 5 kcal mol^{-1} greater than the simplified VCP system ($\Delta G^\ddagger = 14.0 \text{ kcal mol}^{-1}$). However, the *trans*-system has a much greater ΔG° ($28.6 \text{ kcal mol}^{-1}$, relative to **262**) than the other two systems. This is very similar to the calculated thermal rearrangement barrier and supports experimental observation that metal-mediated rearrangement of these systems did not differ significantly from the background thermal rearrangement.

Relative free energies for the final step were lower than simple VCP system but the transition states obtained for the larger systems did not represent the expected reductive elimination pathway; optimised structures had one imaginary frequency with a motion that suggested the metal moves towards either the ester motif in the *cis*-system or a very low value representing Me-group spinning in the *trans*-systems. These were consistent with observed alternative pathways when the basic NHC model was used to investigate individual substituents (*vide supra*). Intermediates resulting directly from these transition states (**267**) optimised to different structures; the *cis*-system developed η^2 -coordination of the ester carbonyl to the metal (**Figure 71a**) while in the *trans*-system (**Figure 71b**), the metal was η^2 -coordinated to the ester carbonyl, and to the phenyl group.

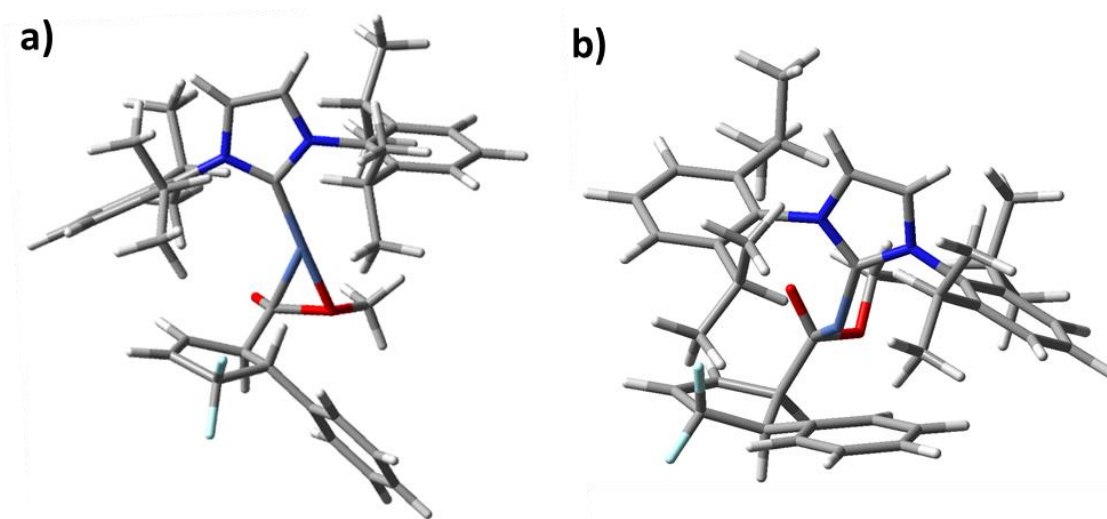


Figure 71: Optimised intermediate 267 for a) *cis*-full system and b) *trans*-full system showing nickel coordinating to both the carbonyl unit of the ester and phenyl ring.

The high energy barriers and difficulties in obtaining optimised transition states for the Ni-mediated VCPR of difluoro-VCP **147a** precursors were consistent with the lengthy reaction times and high temperature required to induce rearrangement experimentally. Steric conflicts between the NHC and the cyclopropane substituents were the main issue in these systems, but now that models are available, they could be used to design better precursor/ligand combinations.

5.4 Conclusion

The photochemical and transition metal-mediated VCPRs were investigated for difluoro-VCP **147a** in order to provide some understanding into whether reported room temperature conditions could be successful with our precursors.

Unfortunately, irradiation of **147a** with UV-C light failed to facilitate any VCPR; only cyclopropane and alkene stereoisomerisation was observed. This is consistent with the formation of triplet intermediates but these species are not on the diradicaloid pathway which facilitates VCPR. We failed to find a triplet transition state which represented the VCPR but these result suggests that the energy barrier is likely to be higher than stereochemical scrambling observed experimentally.

The effects of catalytic quantities of nickel and NHC ligands on the rearrangement of **147a** were investigated. Our procedure and reagents could facilitate the room

temperature VCPR of 1,1-disubstituted olefin **251** successfully, but no rearrangement of **147a** was observed; prolonged heated (80 °C, 3 days) gave only a modest increase in VCPR compared to the background reaction. This was disappointing and attempts to identify effective ligands failed to lower the reaction temperature. Instead side reactions which appeared to be [3,3]-rearrangements were facilitated. Understanding the identity of the active nickel catalyst formed under these conditions (catalyst formed from the mixing of Ni(COD)₂ and free IPr) was difficult so alternative Ni-IPr sources were investigated. We saw more controlled VCPR of **147a** when (η^3 -allyl)Ni(IPr) Cl **260** was used as the pre-catalyst (89% conversion, 3 days, 80 °C) and we believed the slight increase in conversion compared to other conditions was due to easier formation of the η^2 -Ni-alkene complex **255**, the first key intermediate in the catalytic cycle.

Synthetically, these rearrangements were still of very limited use, with the majority of difluorocyclopentene product formed from the background thermal rearrangement. It was believed that the substituents present on our precursor hindered catalysis and we turned to electronic structure calculations to understand this more fully. We could obtain geometries similar to those reported in the literature for intermediates and transition states based on a simplified NHC model.¹⁰⁶ However, when difluorocyclopropane, phenyl cyclopropane and methyl vinyl alkenoyl substrates were all assessed individually, the barriers for rearrangement were either similar or lower than those for the literature system which had undergone catalytic reaction.

This literature model fails to express any steric effects on the cycle; we had to use full IPr model systems to assess the rearrangement of both *trans*-**147a** and *cis*-**152a**. Oxidative addition proved difficult to model in the *cis*-system due to the unfavourable steric interactions between the phenyl ring and the *iso*-propyl groups on the ligand; intermediate **262** did not optimise in the orientation required for progression, and **TS24** failed to optimise, with the nickel moving into coordination with the phenyl ring. This step was comparable for the *trans*- and unsubstituted

systems, but the hapotropic shift had a much higher relative free energy (+28.6 kcal mol⁻¹) than any other system investigated; calculated energy barriers at this level predicted temperatures close to 100 °C to facilitate rearrangements at synthetically useful rates. Interestingly, transition states for the final reductive elimination step could not be obtained for either system but a lower energy pathway which brought phenyl or ester carbonyl groups into coordination seemed to be active.

These preliminary experimental and computational studies into the Ni-mediated VCPR of difluoro-VCP **147a** illustrate the incompatibility of the precursor towards the most convenient catalytic system reported to date in the literature. However, we showed that a more practical, easier-to-handle pre-catalyst, (η^3 -allyl)Ni-Cl **255**, could begin to facilitate rearrangement more effectively than the literature conditions. Furthermore, the larger computational models revealed the reason for ineffective catalysis; the resulting geometries can be used to design new, less bulky systems and/or precursors which could undergo more successful Ni-mediated rearrangements.

Conclusion

The results documented in this thesis effectively evaluate the use of the VCPR in the building block synthesis of difluorocyclopentenes at a number of levels, from developing an efficient synthetic procedure to access precursors, to utilising both computational and experimental methods for assessing all of the active rearrangement pathways.

Initially, synthetic routes which had strong literature precedents were studied, focusing on obtaining precursors which contained either difluorovinyl or difluorocyclopropyl functionality using building block fluorination methodology. We hoped that previous cross-coupling chemistry with difluorovinyl iodide **12a** could be optimised to react with nucleophilic cyclopropyl coupling partners; it quickly became apparent that competing side reactions dominated the process. However, the isolation of novel palladium(II) oxidative addition intermediate **111** was crucial in understanding the different pathways involved in side-product formation. Rapid, microwave-mediated conditions were developed which successfully suppressed these pathways but inherent volatility issues with precursor **99** made isolation difficult.

Our initial route to difluorocyclopropyl precursors also relied on the development of novel cross-coupling conditions, since difluorocyclopropyl boronic ester **129** had previously been accessed in the literature. Unfortunately, difluorocyclopropanation conditions used to access **129** proved to be very capricious, and decomposition during purification made isolation difficult. The knowledge gained in the handling of commercial reagents which generate difluorocarbene were essential assisted the development of an efficient alternative route to similar precursors. Optimisation of MDFA-mediated difluorocyclopropanation conditions, which relied on the faster generation of difluorocarbene, were developed; these allowed for the high yielding, reproducible synthesis of difluorocyclopropane **142** from commercial cinnamyl acetate (94% isolated yield). Deprotection, followed by oxidation/olefination afforded the major *trans-E* precursor **147a** in an overall 71% yield from cinnamyl

acetate. The procedure developed readily transferred to the synthesis of the corresponding *cis*-isomer (**152a**); minor *Z*-alkene isomers **147b** and **152b** were also isolable as minor products. Access to all four diastereomer enabled the effective assessment of the VCPR on this system.

All attempts to initiate the VCPR of difluorovinyl **99** failed, even after thermolysis at the extremely high temperature of 220 °C. This was a disappointing outcome but focused our efforts into investigating difluorocyclopropyl precursors. Difluorocyclopentene **153** could be accessed in near quantitative yields from the thermolysis of *trans-E* **147a** at 100 °C for 17 hours, a much more practical reaction temperature compared to those required for the prototypical system (325-500 °C). The obvious contrast between the thermolyses of precursors **147a** and **147b** was consistent with literature mechanistic work where the concerted diradicaloid transition state for VCPR keeps the divinyl unit locked in *sp*²-geometry to allow sufficient orbital overlap of the allyl radical. Therefore, the usual destabilisation resulting from fluorination on the alkene group is negated and does not lower the energy of the rate determining step but *gem*-difluorocyclopropane rings are reactive and undergo regiospecific ring opening. The naturally abundant ¹⁹F isotope also allowed reactions to be monitored *in situ* using NMR techniques.

Kinetic data from the VCPR of *trans-E* **147a** was obtained using variable temperature ¹⁹F NMR experiments, unravelling a competing cyclopropane stereoisomerisation pathway (favouring *trans*-**147a**) and allowing the activation energy of 28.6 kcal mol⁻¹ (298 K) for the VCPR to be measured. Attempts at running similar experiments with the minor *Z*-alkenoates failed due to the lack of any rearrangement under the same conditions; elevated temperature of 180 °C were required to facilitate [3,3]-sigmatropic rearrangement through to benzocycloheptadiene **154a**. This was the first time such a dramatic reactivity difference was observed by changing only the alkene geometry and we sought to understand this more fully using electronic structure calculations.

Our system has three different reaction pathways available; diradicaloid, triplet and closed-shell pathways all active from different isomers of **147/152**. Obtaining a universal method for dealing with all three pathways simultaneously provided a unique challenge for computational methodology. We started our methodology screening for the VCPR by assessing the accuracy of predictions of experimental activation energies of literature systems, and our rearrangement of **147a**. We found the combination of the UM05-2X function and 6-31+G* basis set was the most accurate method ($\Delta\Delta G^\ddagger$ for **168a** = +1.2 kcal mol⁻¹); the older UB3LYP/6-31G* methodology consistently under-estimated barrier heights ($\Delta\Delta G^\ddagger$ for **168a** = -2.0 kcal mol⁻¹). Both methods correctly identified that rearrangements of Z-alkenoates had higher energy barriers because they were more sterically compressed. Cyclopropane stereoisomerisation were modelled through a series of triplet intermediates and transition states for the [3,3]-rearrangement were found using closed-shell calculations. The more accurate (U)M05-2X/6-31G* performed less well when all three systems were reviewed, predicting that barrier heights for the [3,3]-rearrangement were lower than VCPR in our system. Pleasingly, barrier heights calculated using (U)B3LYP/6-31G* methodology were consistent with experimental results; calculated ΔG^\ddagger values were ordered as follows: cyclopropane stereoisomerisation < VCPR < [3,3]-sigmatropic rearrangement.

By obtaining accurate electronic models for assessing all of the active rearrangement pathways we carried out a computational triage of our system before synthetic commitments. This approach to screening substrate scope is becoming more favourable in today's research climate due to the time saved in synthetic commitments. We strategically investigated the effect different substituents had when introduced into either the cyclopropane ring or the alkene portion of the precursor. Groups which had better radical stabilising capabilities worked better when incorporated into the cyclopropane ring, lower VCPR activation barriers compared to our reference phenyl system (**168a**). This affect was less dramatic on the alkene portion since the radical is already stabilised through allyl resonance; *E*-isomers were consistently predicted to have lower barriers than the

corresponding Z-isomers. A small set of key compounds were selected for synthetic studies to test our predictions and focused on incorporating heteroaromatic groups onto the cyclopropane ring. Our previous synthetic route from allyl acetates failed for these more sensitive precursors and decomposition competed strongly with difluorocyclopropanation. A range of difluorocarbene transfer reagents were assessed in both 2nd and 3rd generation routes; trapping reactions with both heteroaryl alkenoates and THP protected allyl alcohols were investigated. Unfortunately, difluorocyclopropanation conditions remained low-yielding; side-reactions which removed difluorocarbene competitively and overtook the cyclopropanations of less reactive alkene substrates were revealed. Despite these disappointing results, four novel difluorocyclopropyl allyl alcohols could be isolated over two steps from alkenoates (32-38% isolated yields over 2 steps) and the oxidation/olefination conditions developed previously were used to complete the syntheses of a range of precursors successfully.

Substrates which were predicted to be most reactive showed room temperature rearrangement with the [3,3]-sigmatropic rearrangement now effectively competing, and in some cases becoming more selective over VCPR. We were able to monitor the competition between these pathways using NMR studies into the rearrangement of isolable piperonal precursors **214a**. Experimental activation energies for both VCPR and [3,3]-pathways were obtained and used to reassess our computational methodology. (U)B3LYP/6-31G* systems consistently underestimated barriers for both pathways but no single Minnesota functional could be used effectively with both the diradicaloid and closed-shell rearrangements; M05-2X/6-31+G* remained the most accurate for VCPR but M06-2X/6-31G* was best for the [3,3]-rearrangement.

Taking our optimised methodology forward, we were able to predict which rearrangement pathway would be favoured using electronic structure calculations. Furthermore, a strong trend between calculated ΔG^\ddagger values and optimised reaction temperatures emerged, allowing a good estimate of VCPR rearrangement

temperature to be obtained from calculated activation energies. Both these models were tested against literature substrates which undergo either [3,3]-rearrangement or VCPR; the observed experimental results were predicted successfully. Some mechanistic insight into the role of metal complexes in VCPR rearrangement was also developed; the role of the metal was not obvious from the limited experimental data in the literature report.

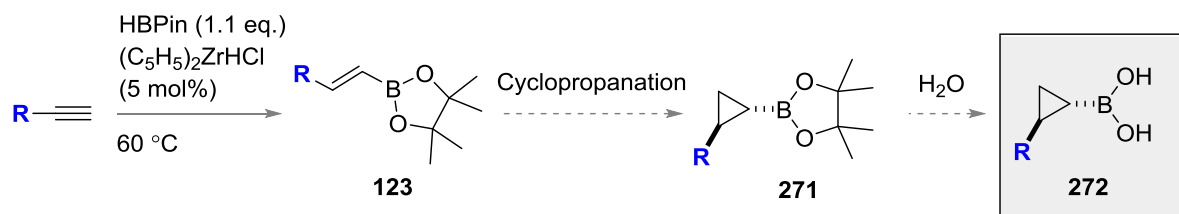
Some precursors which were evaluated during the computational triage had calculated barrier heights which were too high for synthetically useful thermolysis ($\Delta G^\ddagger > 30 \text{ kcal mol}^{-1}$, Spartan'10)., Alternative conditions were therefore investigated for *trans-E* **147a** (all isomers and rearrangement products from this system had previously been characterised) but neither photochemical initiation nor Ni-catalysed conditions facilitated ambient temperature rearrangements. Further experimental and computational investigations into the Ni-catalysed conditions uncovered an alternative pre-catalyst (**260**) which gave comparable results to literature conditions but more importantly, showed that the increased steric bulk present in our precursor impaired catalysis. The electronic structures of key intermediates and transition states on the catalytic cycle secured, could now be used to design and assess less bulky systems for experimental screening.

Overall, our philosophy of trying to understanding the three parallel and competitive rearrangement pathways by using accurate electronic structure calculations has been moderately successful leading to the development of models with effective predictive capability; preliminary studies into the Ni-mediated VCPR also led to a model which could be used to assess how well precursors performed in the reaction. The ability to determine how a precursor will rearrange, at what temperature and under what conditions, is potentially extremely powerful, and could be used to streamline further synthetic investigations extensively.

Future Work

6.1.1. Difluorovinyl Precursors

The volatility issues encountered with cyclopropane **99** must be resolved before the utility of the cross-coupling chemistry and subsequent rearrangement of difluorovinyl precursors can be assessed fully. Since iodide **12a** has been reported to undergo successful cross-coupling reactions in the literature, changes to the nucleophilic coupling partner would be preferred. Deng and co-workers successfully synthesised a range of potassium cyclopropyl trifluoroborates from vinyl boronic esters **123** via the palladium mediated decomposition of diazomethane.¹³¹ This route could be modified for the synthesis of cyclopropyl boronic acids but the use of explosive reagents is not appealing. Simmons-Smith reaction conditions²²⁵ have also been implemented successfully but require the use of extremely pyrophoric diethylzinc. A proposed three step synthetic route to cyclopropyl boronic acids **270** utilises the above cyclopropanation techniques and start from commercially available alkynes (**Scheme 120**).



Scheme 120: Proposed route to more substituted cyclopropyl boronic acids.

We anticipate that the more substituted cyclopropyl boronic acids would still undergo cross-coupling and being less volatile, make isolation of the resulting precursors more straightforward. This would be a key development before further screening into metal-mediated VCPR could be investigated.

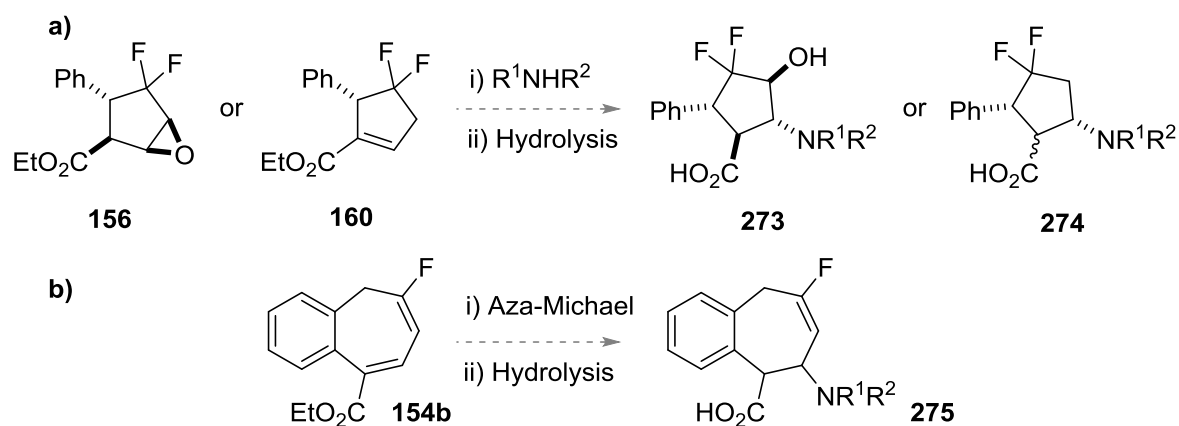
The use of nickel catalysts with NHC ligands is currently the most synthetically viable way of promoting the VCPR of unactivated cyclopropanes and further investigations could be launched from these preliminary results. 1,1-Disubstituted alkenes have been tolerated in the investigations carried out previously by Louie and co-workers^{82b} but the sterically demanding *N,N*-diethylcarbamoyloxy group

present in our precursor may be an issue. Assessment of this effect using electronic structure calculations derived from our investigations in **Chapter 4** would be extremely useful before synthetic commitments were made.

6.1.2. Functionalisation of Rearrangement Products

Functionalisation of different vectors on difluorocyclopentene **153** has been achieved; further work would expand the scope. Proof-of-concept into the synthesis of acid **162** has been obtained, but purification proved difficult and initial work should focus on securing this compound. Recent advances solid phase extraction techniques may work well with these compounds; ISOLUTE® NH₂ cartridges (Biotage) contain a weak anion exchange sorbent which can be used to catch acidic compounds from a mixture and separate any basic or neutral impurities.

Amines and amides are commonly found in pharmaceutical compounds but, apart from Weinreb amide **228**, we have yet to incorporate these motifs into our final product. However, epoxide ring opening²²⁶ reactions of **156** and aza-Michael²²⁷ reaction of alkene isomer **160** could be developed to synthesise β -aminoacids **273** and **274**, respectively (**Scheme 121a**). Similar aza-Michael conditions could be utilised with conjugated benzocycloheptadiene **154b**, potentially allowing access to novel fluorinated β -aminoacid **275** (**Scheme 121b**).



Scheme 121: Proposed synthesis of β -aminoacid compounds from a) difluorocyclopentene building blocks **273 and **274** or b) benzocycloheptadiene **275**.**

Securing these compounds will only enhance the use of difluorocyclopentene **153** as a building block for more complex structures.

6.1.3. Improved Syntheses of Difluorocyclopropyl Alcohols

A range of synthetic routes were explored to try to access the required difluorocyclopropyl alcohols during the synthesis of VCP precursors. Unfortunately, no method proved universal when the heteroarene substituent was varied, and side-reactions started to compete. The additive experiment we developed allowed some prediction of which functional groups would be tolerated in difluorocyclopropanation reactions, but the reactivity of the alkenoates remained generally low. Two different approaches are available to try to improve the synthesis; these could involve the investigation of alternative alkene substrates, or the development of a new reagent for generating difluorocarbene. We tried extensive optimisation of the first approach, and it was evident that reactivity of the alkene was lower when alkenoates were used. Alternative methods of hydroxyl group protection were not investigated, but poorer leaving groups may result in more stable substrates for difluorocyclopropanation (**Figure 72a**). More stable protecting groups were avoided in our initial methodology screening due to the harsher conditions anticipated for their removal; the stability of the difluorocyclopropane products may then be limiting.

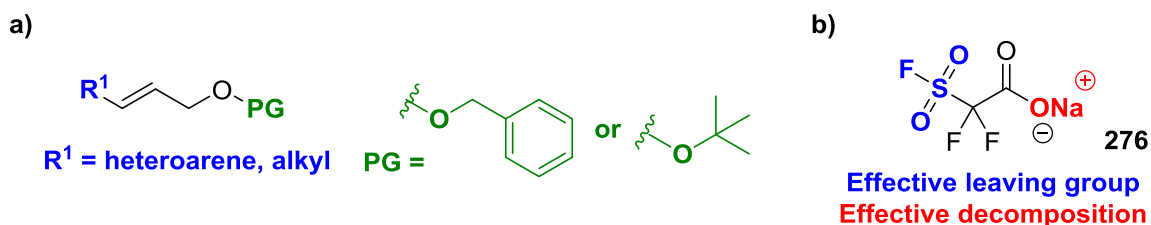


Figure 72: Improving synthetic route via a) more robust protecting groups on allyl alcohols or b) more reactive difluorocarbene generating reagent.

The literature which describes difluorocarbene generating reagents is extensive, but many of the more reactive difluorocyclopropanation reactions are derived from modifications to previous conditions. Ichikawa and co-workers' recent developments with metal-mediated difluorocarbene transfer look to be extremely useful and should be used initially to try and improve the outcomes with alkenoates.⁷⁰ Ichikawa modified the literature conditions used for TFDA; an alternative approach would be to redesign the reagent completely, maintaining the

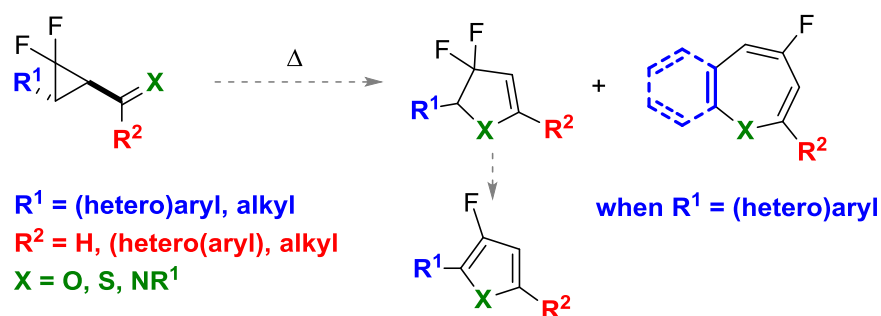
effective fluorosulfonyl leaving group but improving the profile for reagent decomposition by forming the sodium acetate salt (**Figure 72b**). Sodium salt **276** has previously been synthesised in the patent literature²²⁸ from the commercially available acid, but the stability of the reagent could be a major safety issue and scrupulous care would be required if such studies were to be carried out.

6.1.4. Further Utilisation of Computational Triage

During development of the computational models used to estimate activation barriers and determine rearrangement pathways, we predicted that enol ethers **190m-p** should undergo VCPR to difluorocyclopentene **197** (see **Scheme 97, Chapter 3**) effectively. Literature precedents exist for the synthesis of these precursors from previously accessible difluorocyclopropyl esters and the resulting difluorocyclopentenones **197** could be used to access the corresponding difluorocyclopentanones **198**. Investigations into these species would not only make our 2nd generation synthetic route more divergent but would also provide further experimental data against which our computational predictions could be tested.

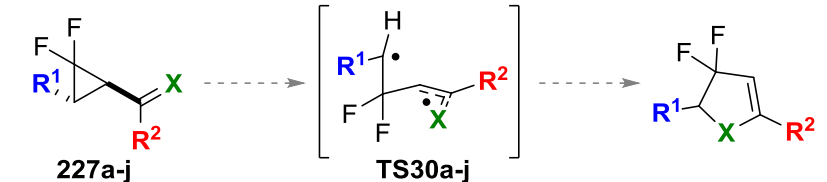
6.1.5. Building Block Route to Fluorinated Furans

During the synthesis of 3'-methyl-furyl precursor, it was surprising to see that aldehyde **224** was highly reactive and underwent room temperature rearrangement to dihydrofuran **226** and furanooxepine **225** (see **Scheme 105, Chapter 3**). There are no similar fluorinated furanooxepines reported in the literature; routes to difluoro-dihydrofurans or the corresponding 3-fluorofurans required either the use of metal salts²⁰³ or use excess amount of base to facilitate rearrangements.²²⁹ A room temperature rearrangement without any additives seems possible from our precursors which are highly amenable to functional group interconversions to access a range of novel heterocycles (**Scheme 122**).



Scheme 122: Proposed synthesis of novel heterocycles through potential low temperature rearrangements.

Similar kinetic investigations carried out previously with phenyl **147a** and piperonyl **214a** would be required to allow effective computational methodology screening to be carried out, but preliminary investigations into these heteroatom-derived VCPR have been conducted and electronic structure calculations suggest that a range of precursors could undergo low temperature rearrangements (**Table 40**). Aldehyde **145** which had been isolated previously, and had proved stable at room temperature, had a high calculated barrier for VCPR through **TS30a** of 32.2 kcal mol⁻¹ (**Table 40**, Entry 1). Little effect was observed when the corresponding methyl ketone **277b** was investigated (32.0 kcal mol⁻¹) but phenyl ketone **277c** had a lower barrier height of 28.2 kcal mol⁻¹ (**Table 40**, Entries 2-3).

Table 40: Calculated ΔG^\ddagger for VCPR reactions involving heteroatoms

| Entry | x | R ¹ | R ² | X | ΔG^\ddagger (kcal mol ⁻¹) |
|-------|---|----------------|----------------|------|---|
| 1 | a | phenyl | H | O | 32.2 |
| 2 | b | phenyl | Me | O | 32.0 |
| 3 | c | phenyl | Ph | O | 28.2 |
| 4 | d | 2-furyl | H | O | 25.2 |
| 5 | e | phenyl | H | S | 22.7 |
| 6 | f | phenyl | Me | S | 22.5 |
| 7 | g | phenyl | Ph | S | 20.8 |
| 8 | h | phenyl | H | N-Ph | 25.2 |
| 9 | i | phenyl | Me | N-Ph | 25.7 |
| 10 | j | phenyl | Ph | N-Ph | 15.6 |

Electronic structure calculations performed on Spartan'10, B3LYP/6-31G*, gas phase, 298 K (all transition states had S^2 values ranging from 0.47-0.81).

Introducing better radical-stabilising groups on the cyclopropane ring (R^1 = furyl, **227d**) lowered the VCPR barrier height to 25.2 kcal mol⁻¹ (**Table 40**, Entry 4); furyl **227d** was synthesised previously but was never isolated. The close similarity to the calculated activation energy for phenyl **147a** (25.3 kcal mol⁻¹) suggested that aldehyde **277d** may undergo rearrangement at temperatures close to 100 °C. Less demanding rearrangements were predicted for thioaldehyde **227e** or thioketones **227f-g** (**Table 40**, Entries 5-7); these precursors could be accessible from the corresponding aldehyde and ketones using alumina-supported Lawesson's reagent.²³⁰ Imine precursors **277h** and **277i** would be predicted to undergo rearrangement at 100 °C (**Table 40**, Entry 8-9) but phenyl substituted imine **277j** had an extremely low predicted barrier height of 15.6 kcal mol⁻¹ (**Table 40**, Entry 10). Non-fluorinated heteroatom-based VCPR have been reported in the literature⁷² but our system once again provides a base for understanding these process more fully using both experimental techniques (¹⁹F NMR) and electronic structure calculations.

6.1.6. Ni-mediated Rearrangements

Before further synthetic commitments to the Ni-mediated rearrangement of fluorinated-VCP are made, it is important to obtain more confidence in the computational models. Louie and co-workers calculated the experimental activation energy for VCP **269** (see **Scheme 119, Chapter 4**);¹⁰⁶ this should provide the basis for computational methodology screening, focusing on the identification of the most accurate low cost method to assess the VCPR.

We used our full-NHC model to assess the key intermediate and transition states for the Ni/IPr mediated VCPR of *para*-fluorophenyl VCP **269**; all species optimised with correct geometries expect for the reductive elimination (**TS28**). The haptotropic shift was calculated as the highest energy process, ($\Delta G^\circ = 21.5 \text{ kcal mol}^{-1}$, relative to **262**) which is still an under-estimate of $5.5 \text{ kcal mol}^{-1}$ (**Table 41**).

Table 41: Free Energy Differences for the Ni-Mediated VCPR of **269** using IPr Ligand Models

| Species | ΔG° (kcal mol ⁻¹) |
|--|--|
| 262 | 0.0 |
| TS24 (oxidative addition) | 21.4 |
| 264 | 9.2 |
| TS26 (haptotropic shift) | 25.5 |
| 265 | 5.6 |
| TS28 (reductive elimination) | - |
| <i>Experimental $\Delta G^{\ddagger 106}$</i> | 27.0 |

It is obvious that higher level methodology is required but once confidence is secured, the computational model could be used to assess the energy barrier for the rearrangement of less reactive difluorovinyl precursor **147a**.

From our preliminary experimental and computational investigations (**Chapter 4**), we showed that the steric influences of the phenyl ring in difluorocyclopropane **147a** were detrimental to the Ni-mediated rearrangement. With a computational model in hand, we could assess the effect of less bulky cyclopropane ring substituents on the barrier heights (**Figure 73a**). Realistically, these compounds would be species which are unlikely to undergo low temperature thermal

rearrangements; our triage suggests that compounds bearing alkyl (rather than aryl) groups would benefit most from metal-mediated methodology. Strong confidence in a successful rearrangement would be required before committing to what could be quite difficult synthesis.

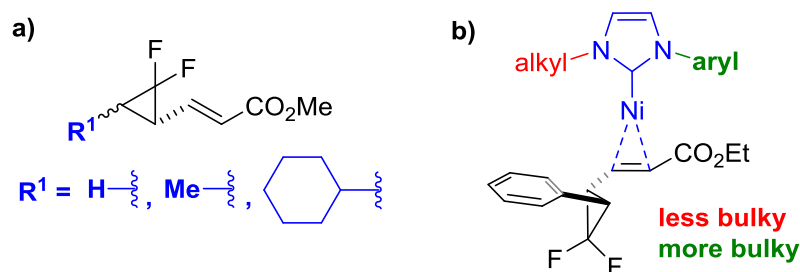


Figure 73: a) Alternative difluoro-VCP and b) potential beneficial effect of unsymmetrical-NHC ligands for Ni-mediated VCPR.

Only commercial NHC-ligands were investigated in the literature and the less sterically demanding phosphine ligands required much higher reaction temperatures. The synthesis of unsymmetrical-NHC ligands has been reported²³¹ but no studies have been carried out to determine their effect on VCPR reactions. Decreasing the steric demand close to the cyclopropane ring may lower the energy of key steps for the rearrangement (**Figure 73b**) and these effects can be investigated with the intermediates and transition states already obtained for difluoro-VCP **147a**.

Chapter 7: Experimental

All characterisation spectra for all synthesised compounds and Cartesian coordinates are compiled as Supplementary Information and available on request.

7.1. General Experimental

NMR spectra were recorded on Bruker DPX-400, AV-500 Avance-II+ 600 spectrometers. ^1H , ^{19}F and ^{13}C NMR spectra were recorded using the deuterated solvent as the lock and the residual solvent as the internal reference. The multiplicities of the spectroscopic data are presented in the following manner: s = singlet, d = doublet, dd = double doublet, ddd = doublet of double doublets, etc up to ddddd, dt = doublet of triplets, ddt = doublet of double triplet, dddt = doublet of double double triplet, dq = doublet of quartet; t = triplet, td = triple doublet; tt = triple triplet, q = quartet, ABq = AB system quartet, m = multiplet and br. = broad. Unless stated otherwise, all couplings refer to 3J homocouplings. All ^1H spectra are fully assigned as much as possible. Relevant 2D-NMR spectra are supplied to confirm assignment. **IR spectra** were recorded on a Shimadzu IRAffinity-1 FT-IR Spectrophotometer using a MIRacle™ Single Reflection Horizontal ATR Accessory. **UV/Vis spectra** were recorded on a Varian Cary® 50 UV-Vis Spectrophotometer using Quartz UV cuvettes (1.2 cm diameter) in MeCN. Data was processed using the Varian UV scan application. **Melting points** were recorded on a Griffin melting point apparatus and are uncorrected. **GC/MS spectra** were obtained on an Agilent 7890A GC System fitted with a DB5-type column (30 m × 0.25 μm) running a 40–320 °C temperature program, ramp rate 20 °C min^{-1} with helium carrier gas flow at 1 $\text{cm}^3 \text{min}^{-1}$. Chemical ionisation (CI) (methane) mass spectra were recorded on an Agilent Technologies 5975C mass spectrometer. **Direct Infusion** mass spectra were recorded on a Thermo Finnigan LCQ DUO using Electrospray Ionisation (ESI ion trap). **HRMS measurements** were obtained from a Waters GCT Premier MS (CI-MS), Finnigan MAT 95 XP (EI-MS and/or APCI-MS), Waters XEVO G2-S (ESI, APCI, ASAP) or Thermo Scientific LTQ Orbitrap XL via Advion TriVersa NanoMate infusion (NSI-ES) spectrometers (carried out by EPSRC National Mass Spectrometry Service Centre, Swansea). **Thin layer chromatography** was performed on pre-coated aluminium-

backed silica gel plates (E.Merck, A.G.Darmstadt, Germany. Silica gel 60 F254, thickness 0.2 mm). Visualisation was achieved using potassium permanganate or UV detection at 254 nm. **Column chromatography** was performed on silica gel (Zeochem, Zeoprep 60 HYD, 40-63 μm) using a Büchi Sepacore system. Hexane was distilled before chromatography. **Carbon, Hydrogen and Nitrogen analysis** was carried out on a Perkin Elmer 2400 Series II CHNS Analyser (data acquired by Alexander J. Clunie). **Preparative HPLC** was performed using Grace Reveleris PREP purification system with a Kromasil 100-10-C18 column (L = 250 mm, ID = 200 mm). Compound was loaded in a minimum volume of 1:1 DMSO:MeOH in a 5 mL sample loop. Flow rates varied depending on separation (5-30 ml/min) and peaks determined using ELSD and UV detection. **Microwave reactions** were carried out in sealed vials in a Biotage Initiator 2.5 instrument. Data for **X-ray crystal structure determination** were obtained with an Oxford Diffraction Gemini S Diffractometer with Mo K α radiation ($\lambda = 0.71073 \text{ \AA}$) at 123 K or 150 K **Crystallography**. Single crystal diffraction measurements were made at 150(2) K with an Oxford Diffraction Xcalibur E instrument and $\lambda = 0.71073 \text{ \AA}$ radiation. Refinement to convergence was with F^2 and against all unique reflections using the program SHELXL-97²³² (performed by Dr Alan Kennedy). Anhydrous hexane, toluene, DCM, THF and Et₂O were dried using a **PureSolv system** from Innovative Technology, Inc.. Needles and glass syringes used for anhydrous reactions were oven dried (150 °C) overnight before use.

Specific Experimental Information

Chapter 1:

Phase separation of cross-coupling reactions was accomplished with Isolute SPE Accessories phase separators. Iodide **12a** was synthesised according to literature procedures.²⁶ *Tetrakis*(triphenylphosphino)palladium(0) was synthesised according to literature procedures.²³³

Chapter 2:

Phenyl acetylene was percolated through alumina before use. Pinacol borane was transferred immediately into an Aldrich SureStor flask and stored under nitrogen in the fridge. (Z)-3-phenylprop-2-en-1-ol was synthesised via selective hydrogenation of 3-phenyl-2-propyn-1-ol (Sigma Aldrich) following the procedure reported by Greene and co-workers.^{S156} 1,4-Dioxane was distilled from CaH₂ (48 °C/140 mbar) and stored under nitrogen over CaH₂. Diglyme was distilled from CaH₂ (60 °C/23 mbar) and stored under nitrogen over CaH₂. Trimethylsilyl chloride was distilled from CaH₂ (60 °C/430 mbar) and stored under nitrogen over CaH₂ in the refrigerator. Methyl 2,2-Difluoro-2-(fluorosulfonyl)acetate (MDFA) was purchased from Fluorochem and stored under a headspace of nitrogen. Potassium iodide (Sigma Aldrich) was dried in the oven (150 °C) before use. All glassware used in the synthesis of methyl(trifluoromethyl)dioxirane was washed with an aqueous solution of ethylenediaminetetraacetic acid (0.1 M) to removed trace metals and then oven dried (150 °C) before use.

Chapter 3:

Commercial furfural (black) was percolated through a pad of alumina to afford an orange solution which was used immediately in reactions. Commercial butyl lithium was titrated using 4-phenylbenzylidene benzylamine by the procedure described by Duhamel and Plaquevent.^{S234} 2-Formyl-pyrrole-1-carboxylic acid tert-butyl ester **191f** was synthesised from NaH and Boc anhydride using conditions described by Carreira and co-workers.^{S235} 2-thiazolyl-carboxaldehyde **191g** was synthesised from thiazole, BuLi and DMF using conditions described by Glorius and co-workers.¹⁹⁵ Due to the volatility of the aldehyde, crude product was used directly in subsequent Wittig olefinations. Triethylorthoformate was refluxed with molecular sieves (3 Å, pre-dried at 220 °C, < 0.1 mbar) for 2 hours then distilled onto fresh molecular sieves (52 °C, 65 mbar) before use.

Chapter 4:

Low pressure UV experiments were carried out in FEP tubing (capacity 53 mL) coiled around a double-walled quartz immersion well (L = 390 mm) with a 16 W low

pressure mercury lamp (L = 380 mm, discharge = 230 mm, diameter = 15 mm, 3×10^{18} photons s^{-1}). Reaction could be run in batch mode or flow using an HPLC pump to control flow rate. Reaction temperatures could be monitored with an external temperature probe placed on the FEP tubing. [D6]-Benzene was distilled from 3 Å molecular sieves (pre-dried at 220 °C, < 0.1 mbar) into a Schleck flask, transferred into a glovebox, dispensed into vials and stored in the freezer. Alternative nickel catalysts were synthesised by Dr. David J. Nelson according to literature procedures: (η^3 -allyl)Ni Cl **260** was synthesised according to Dible and co-workers;²²² Ni *bis*-styrene **259** was synthesised according to Nicoso and co-workers²²¹ and Ni hexadiene **258** was synthesised according to Hazari and co-workers.²²⁰ Catalyst purity was confirmed by CHN analysis before being used in reactions.

All other chemicals were purchased from Sigma Aldrich, Apollo Scientific, Alfa Aesar, or Fluorochem and used as received.

7.2. Computational Methodology

Structures were built in Spartan'10 using previously published compounds as models and geometry optimisation calculations were carried out for all closed shell compounds. For known diradical compounds unrestricted methodology was invoked using the keywords MIX and SCF=UNRESTRICTED, with CONVERGE deprecated. In cases where SCF convergence was difficult, the keyword NODIIS was used. All calculations were performed *in vacuo*. Spartan'10 software was run on a Dell Precision T7500 (2 x Intel E5530 processors, four cores each, 2.40 GHz) with 24 GB RAM Debian GNU/Linux 5.

The calculation methods used in Spartan have been documented in: Y. Shao, L.F. Molnar, Y. Jung, J. Kussmann, C. Ochsenfeld, S.T. Brown, A.T.B. Gilbert, L.V. Slipchenko, S.V. Levchenko, D.P. O'Neill, R.A. DiStasio Jr., R.C. Lochan, T. Wang, G.J.O. Beran, N.A. Besley, J.M. Herbert, C.Y. Lin, T. Van Voorhis, S.H. Chien, A. Sodt, R.P. Steele, V.A. Rassolov, P.E. Maslen, P.P. Korambath, R.D. Adamson, B. Austin, J. Baker, E.F.C. Byrd, H. Dachsel, R.J. Doerksen, A. Dreuw, B.D. Dunietz, A.D. Dutoi, T.R. Furlani, S.R. Gwaltney, A. Heyden, S. Hirata, C-P. Hsu, G. Kedziora, R.Z. Khalliulin, P.

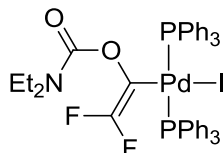
Klunzinger, A.M. Lee, M.S. Lee, W.Z. Liang, I. Lotan, N. Nair, B. Peters, E.I. Proynov, P.A. Pieniazek, Y.M. Rhee, J. Ritchie, E. Rosta, C.D. Sherrill, A.C. Simmonett, J.E. Subotnik, H.L. Woodcock III, W. Zhang, A.T. Bell, A.K. Chakraborty, D.M. Chipman, F.J. Keil, A. Warshel, W.J. Hehre, H.F. Schaefer, J. Kong, A.I. Krylov, P.M.W. Gill and M. Head-Gordon, *Phys. Chem. Chem. Phys.*, **2006**, *8*, 3172.

Full reference for the Gaussian09 programme: Gaussian 09, Revision A.1, Frisch, M. J.; Trucks, G. W.; Schlegel, H. B.; Scuseria, G. E.; Robb, M. A.; Cheeseman, J. R.; Scalmani, G.; Barone, V.; Mennucci, B.; Petersson, G. A.; Nakatsuji, H.; Caricato, M.; Li, X.; Hratchian, H. P.; Izmaylov, A. F.; Bloino, J.; Zheng, G.; Sonnenberg, J. L.; Hada, M.; Ehara, M.; Toyota, K.; Fukuda, R.; Hasegawa, J.; Ishida, M.; Nakajima, T.; Honda, Y.; Kitao, O.; Nakai, H.; Vreven, T.; Montgomery, Jr., J. A.; Peralta, J. E.; Ogliaro, F.; Bearpark, M.; Heyd, J. J.; Brothers, E.; Kudin, K. N.; Staroverov, V. N.; Kobayashi, R.; Normand, J.; Raghavachari, K.; Rendell, A.; Burant, J. C.; Iyengar, S. S.; Tomasi, J.; Cossi, M.; Rega, N.; Millam, N. J.; Klene, M.; Knox, J. E.; Cross, J. B.; Bakken, V.; Adamo, C.; Jaramillo, J.; Gomperts, R.; Stratmann, R. E.; Yazyev, O.; Austin, A. J.; Cammi, R.; Pomelli, C.; Ochterski, J. W.; Martin, R. L.; Morokuma, K.; Zakrzewski, V. G.; Voth, G. A.; Salvador, P.; Dannenberg, J. J.; Dapprich, S.; Daniels, A. D.; Farkas, Ö.; Foresman, J. B.; Ortiz, J. V.; Cioslowski, J.; Fox, D. J. Gaussian, Inc., Wallingford CT, **2009**.

7.3. Compounds from Chapter 1

6.3.1. Experimental Procedure

1-((Diethylcarbamoyl)oxy)-2,2-difluorovinyl)bis(triphenylphosphino) palladium(II) iodide (**111**)



1-(N,N-Diethylcarbamoyloxy)-2,2-difluoro-1-iodoethene (**12a**) (258 mg, 0.82 mmol), palladium *tetrakis*(triphenylphosphino)palladium(0) (946 mg, 0.82 mmol) and anhydrous toluene (7 mL, degassed with argon) in that order were added to a flamed-dried Radleys Carousel tube, which was flushed with nitrogen. The reaction mixture was sonicated to afford a red solution which was heated to 100 °C for 4 hours. Full conversion was confirmed by the ^{19}F NMR spectrum of an aliquot. After cooling, the reaction mixture was diluted with water (10 mL) and the crude product was extracted with DCM (2 x 10 mL). The organic extracts were combined and dried through a hydrophobic frit, then concentrated under reduced pressure to afford a brown oil. The crude product was redissolved in DCM (10 mL) and crystallisation was encouraged by addition of MeOH (5 mL). The yellow solid was collected by filtration and the solid was washed with DCM (10 mL) to afford palladium intermediate **111** (693 mg, 90%). m.p. = 189-192 °C (dec., (chloroform/pentane)); crystals turned black at temperatures >120 °C); decomposition; $\bar{\nu}$ /(film) = 3047, 2950, 2901, 1679, 1480, 1433, 1275, 1223, 1095, 745, 693 cm^{-1} ; ^1H NMR (400 MHz, CDCl_3): δ = 7.81-7.77 (m, ArH, 12H), 7.43-7.36 (m, ArH, 18H), 3.19-3.14 (br. q, 6.6 Hz, N(CH_2CH_3), 2H), 2.45-2.40 (br. q, J = 6.6 Hz, N(CH_2CH_3), 2H), 1.10-1.06 (br. t, J = 6.7 Hz, N(CH_2CH_3), 3H), 0.65-0.61 ppm (br. t, J = 6.7 Hz, N(CH_2CH_3), 3H); ^{13}C NMR (125 MHz, CDCl_3): δ = 153.1, 149.7 (ddt, $^1J_{\text{C-F}}$ = 303.4, 245.3 Hz, $J_{\text{C-P}}$ = 7.9 Hz), 135.1 (t, $^2J_{\text{C-P}}$ = 6.0 Hz), 132.6 (t, $^1J_{\text{C-P}}$ = 23.8 Hz), 130.0, 127.7 (t, $J_{\text{C-P}}$ = 4.7 Hz), 114.3 (ddt, $^2J_{\text{C-F}}$ = 94.8, 87.6 Hz, $^2J_{\text{C-P}}$ = 6.3 Hz), 41.6, 41.4, 13.7 ppm (represents two carbons; see HSQC); ^{19}F NMR (400 MHz, CDCl_3): δ = - 89.6 (dt, $^1J_{\text{F-F}}$ = 90.1 Hz $^4J_{\text{F-P}}$ = 8.2 Hz, 1F), - 115.7 ppm (dt, $^1J_{\text{F-F}}$ = 90.1 Hz $^4J_{\text{F-P}}$ = 8.2 Hz, 1F); ^{155}P NMR (162 MHz, CDCl_3): δ =

18.4 ppm (t, $^4J_{\text{P-F}} = 8.2$ Hz); elemental analysis calcd (%) for $\text{C}_{43}\text{H}_{40}\text{F}_2\text{INO}_2\text{P}_2\text{Pd}$: C 55.17, H = 4.31, N = 1.50; found: C 54.38, H 4.35, N 1.21; m/z (EI): 546 (^{106}Pd , 100) [(M-I+PPh₃)], 440 (10), 401 (20), 369 (22), 263 (42) [PPh₃+H] (see spectra for Pd isotope splitting).

| | | | | | |
|-------------------|---|---|---|---|--------------|
| empirical | - | $\text{C}_{86}\text{H}_{80}\text{F}_4\text{I}_2\text{N}_2\text{O}_4\text{P}_4\text{Pd}_2$ | Z | - | 4 |
| M_r | - | 1872.00 | ρ_{calcd} [g cm ⁻³] | - | 1.557 |
| crystal system | - | Monoclinic | reflins measured | - | 32741 |
| space group | - | P 2 ₁ /c | unique reflns | - | 15792 |
| a [Å] | - | 19.209(4) | R _{int} | - | 0.0471 |
| b [Å] | - | 18.2643(17) | Goof | - | 1.054 |
| c [Å] | - | 22.761(7) | R [on F, obs rflns only] | - | 0.0808 |
| β [°] | - | 90.52(2) | wR [on F ² , all data] | - | 0.1190 |
| [Å ³] | - | 1552.3(3) | Largest diff. peak/hole | - | 1.937/-1.096 |

Coupling Screening and Assays

Intermediate 111 - Diene Suppression

A mixture of intermediate **111** (93.3 mg, 0.1 mmol), iodide **12a** (31 mg, 0.1 mmol) and triphenylphosphine (0, 0.03, 0.5 or 0.1 mmol) was taken up in toluene (1 mL) in a Radleys' carousel tube. The mixture was heated at 100 °C for 21 hours under nitrogen, then allowed to cool to room temperature. Aliquots of the crude reaction mixture were analysed by ^{19}F NMR and the relative percentage of diene **101** reported.

Intermediate 111 - Solvent Effect

Intermediate **111** was taken up in reaction solvent in a Radley's Carousel tube and refluxed for 16.5-90 hours under nitrogen, then allowed to cool to room temperature. The reaction mixture was partitioned between DCM (5 mL) and water (5 mL). The organic phase was separated and dried through a hydrophobic frit, then concentrated to afford crude material. Integration of the ^{19}F NMR spectra provided the percentage relative conversion.

Coupling Screens

A mixture of base (0.9 - 3.0 mmol), triphenylphosphine (0-0.36 mmol.), palladium(0) catalyst (0.2 mmol), cyclopropyl boronic acid (177.5 mg, 1.35 mmol) and iodide **12a** (271 mg, 0.9 mmol) was taken up in reaction solvent in a Radleys' Carousel tube; the mixture was heated at a set temperature and for a set time under nitrogen. Reaction aliquots were analysed by ^{19}F NMR to determine when full conversion was achieved. After cooling to room temperature, the reaction mixture was partitioned between DCM (3 x 5 mL) and water (5 mL). The organic phase was separated and dried through a hydrophobic frit and concentrated to afford crude material. Integration of ^{19}F NMR spectra provided relative percentage conversion.

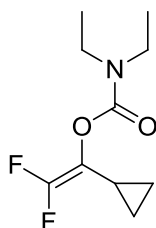
Base Assay

A mixture of base (0.36 mmol), triphenylphosphine (5 mg, 0.02 mmol), *tetrakis*(triphenylphosphino)palladium (0) (43 mg, 0.04 mmol), cyclopropylboronic acid (23 mg, 0.27 mmol), iodide **12a** (54 mg, 0.18 mmol) and α,α,α -trifluorotoluene (4.4 μL , 0.036 mmol) was taken up in toluene (1 mL) and water (0.035 mL) in a microwave vial. The reactions were heated to 150 °C for 20 minutes in a microwave reactor then allowed to cool to room temperature. After venting and opening the vial, the reaction mixture was partitioned between DCM (5 mL) and water (5 mL). The organic phase was separated and dried through a hydrophobic frit and the remaining aqueous phase was washed with DCM (5 mL). The organic extracts were combined and concentrated under reduced pressure to afford crude product. Integration of the ^{19}F NMR spectra was used to determine the NMR yield of product, and quantify the amount of iodide remaining.

Base Coupling Screen

| Base | pK_a | Iodide 12a Yield (%) | Cyclopropane 99 Yield (%) |
|---------------------------------|--------|-----------------------------|----------------------------------|
| K ₂ CO ₃ | 10.3 | 20 | 37 |
| KOH | 15.7 | 0 | 50 |
| Ba(OH) ₂ | 15.7 | 54 | 0 |
| LiOH | 15.7 | 53 | 0 |
| K ₃ PO ₄ | 12.3 | 0 | 36 |
| KH ₂ PO ₄ | 2.1 | 67 | 0 |
| KF | 3.2 | 14 | 0 |

Preparation 1-(N,N-Diethylcarbamoyloxy)-2,2-difluoro-1-cyclopropane (**99**)



A mixture of potassium hydroxide (103.5 mg, 1.8 mmol), triphenylphosphine (22.8 mg, 0.09 mmol), *tetrakis*(triphenylphosphino)palladium(0) (192.7 mg, 0.18 mmol), cyclopropyl boronic acid (177.5 mg, 1.35 mmol) and iodide **12a** (271 mg, 0.9 mmol) were taken up in degassed toluene (5 mL) and water (0.175 mL) in a microwave vial. The orange solution was heated to 150 °C for 20 minutes in a microwave reactor and then allowed to cool to room temperature. After venting and opening the vial, the brown reaction mixture was partitioned between DCM (5 mL) and water (5 mL). The organic phase was separated and dried by passing through a hydrophobic frit and the remaining aqueous phase was washed with DCM (2 x 10 mL). The organic extracts were combined and concentrated under reduced pressure to afford crude product as a brown oil. Column chromatography on silica gel (1:9 to 1:4 diethyl ether in pentane) afforded cyclopropane **99** as an orange oil (58.7 mg, 44%). R_f = 0.38 (1:4 diethyl ether/pentane); ^1H NMR (400 MHz, CDCl₃): δ = 3.35-3.27 (br. m, N(CH₂CH₃)₂, 4H), 1.66-1.59 (m, CH - cyclopropane, 1H), 1.16 (t, J = 7.1 Hz, N(CH₂CH₃)₂, 6H), 0.77-0.72 (m, CH₂, 2H), 0.65-0.61 ppm (m, CH₂, 2H); ^{13}C NMR (100 MHz, CDCl₃): δ = 154.7 (dd, $^1J_{\text{C-F}}$ = 288.0, 281.3 Hz), 151.8, 111.9 (dd, $^2J_{\text{C-F}}$ = 42.1, 16.9 Hz), 41.9, 41.3, 13.4, 12.7, 7.3 (d, $^4J_{\text{C-F}}$ = 3.1 Hz), 3.5 ppm (d, $^4J_{\text{C-F}}$ = 2.6 Hz). The signal at 3.5 ppm represents two carbons (confirmed by HSQC); ^{19}F NMR (400 MHz,

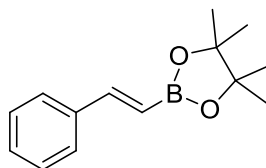
CDCl₃): δ = -96.7 (dd, 2J = 64.0, $^4J_{F-H}$ = 2.7 Hz), -111.2 (dd, 2J = 64.0 Hz, $^4J_{F-H}$ = 3.6 Hz); MS (CI): m/z (%): 248 (12) [M+C₂H₅]⁺, 220 (100) [M+H]⁺, 100 [M-ODEC]; t_R (GC) = 9.78 minutes.

7.4. Compounds from Chapter 2

6.4.1. Experimental Procedure

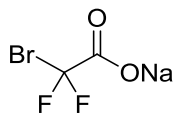
Alkyne Hydroboration:

Preparation of (*E*)-4,4,5,5-Tetramethyl-2-styryl-1,3,2-dioxaborolane (**123**)



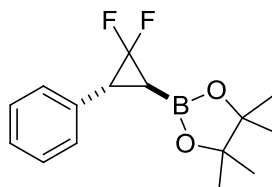
Bis(cyclopentadienyl)zirconium(IV) chloride hydride (51.6 mg, 0.20 mmol) was added to a flame-dried round-bottomed flask under nitrogen. The solid was lightly flamed dried under vacuum to remove any moisture, then the flask was flushed with nitrogen and sealed with a SubaSeal. Phenyl acetylene (0.44 mL, 4 mmol) was added by syringe and the colourless reaction mixture was heated to 60 °C for 30 minutes to afford a red/brown solution. Pinacol borane (0.64 mL, 4.4 mmol) was added dropwise to the reaction mixture, which was stirred for 7 hours until the ¹H NMR spectrum of an aliquot showed complete conversion. The crude reaction mixture was purified by distillation (Kugelrohr, 110 °C/0.11 mbar) to afford (*E*)-4,4,5,5-tetramethyl-2-styryl-1,3,2-dioxaborolane **123** as a colourless oil (756 mg, 82%). R_f = 0.33 (1:9 diethyl ether/hexane); ¹H NMR (400 MHz, CDCl₃): δ = 7.51-7.49 (m, ArH, 2H), 7.42 (d, J = 18.6 Hz, ArCH=CHB, 1H), 7.36-7.27 (m, ArH, 3H), 6.12 (d, J = 18.6 Hz, ArCH=CHB, 1H), 1.32 ppm (s, CH₃, 12H); ¹³C NMR (100 MHz, CDCl₃): δ = 149.0, 137.0, 128.4, 128.1, 126.6, 82.9, 24.3 ppm. The alkene carbon attached to boron was not visible; this was confirmed by the HSQC spectrum; $\bar{\nu}$ /(film) = 2978, 2359, 2341.6, 1624, 1352, 1209, 1144 cm⁻¹; MS (CI): m/z (%): 259 (25) [M+C₂H₅]⁺, 231 (100) M+H]⁺, 187 (30), 101 (32); t_R (GC) = 13.08 minutes. The data was in agreement with that reported by Knochel and co-workers.^{147a}

Sodium bromodifluoroacetate (**33**)⁶⁵



Sodium hydroxide (845 mg, 21 mmol) was added to a flame-dried round-bottomed flask, purged with nitrogen and cooled to 0 °C. A solution of bromodifluoroacetic acid (4.0 g, 21 mmol) in methanol (6 mL) was added dropwise over 10 minutes then the colourless reaction mixture was allowed to warm to 25 °C and stirred for 1.5 hours until the ¹⁹F NMR spectrum of an aliquot showed complete conversion. Methanol was removed under reduced pressure and the resulting colourless oil was dried using a Kugelrohr oven (60 °C/0.1 mbar) to afford sodium bromodifluoroacetate **33** as a colourless solid (3.9 g, 95%): ¹³C NMR (100 MHz, *d*-acetone): δ = 162.0 (t, ²*J*_{C-F} = 25.8 Hz), 133.8 ppm (t, ¹*J*_{C-F} = 319.5 Hz); ¹⁹F NMR (376 MHz, *d*-acetone): δ = 121.77 ppm (s), $\bar{\nu}$ /(film) = 1661, 1398, 1105, 939, 820, 710 cm⁻¹. No characterisation data were presented in the literature.

rac-2-[(1*R**,3*S**)-2,2-Difluoro-3-phenylcyclopropyl]-4,4,5,5-tetramethyl-1,3,2-dioxaborolane (**129**)



(*E*)-4,4,5,5-Tetramethyl-2-styryl-1,3,2-dioxaborolane **123** (171 mg, 0.71 mmol) and diglyme (1 mL) were added in that order to an oven dried three-necked 50 mL flask with a condenser and the mixture was heated to 180 °C under argon. A solution of sodium bromodifluoroacetate (1.03 g, 5.18 mmol) in diglyme (5 mL) was added dropwise to the reaction mixture over 6 minutes; the mixture was heated at 180 °C for 16 h. The resulting dark brown solution was filtered under vacuum and the white precipitate washed with diethyl ether (20 mL). The filtrate was collected and concentrated under reduced pressure to remove volatiles, then the diglyme was removed by distillation (Kugelrohr 60 °C/0.15 mbar). The ¹H NMR spectrum of the resulting black viscous oil confirmed full conversion. Column chromatography on

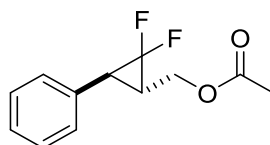
silica gel (1:19 to 1:9 gradient of ethyl acetate in hexane) afforded boronic ester **129** as an orange oil (43.2 mg, 21%). $R_f = 0.33$ (1:20 ethyl acetate/hexane); $^1\text{H NMR}$ (400 MHz, C_6D_6): $\delta = 7.00\text{--}6.95$ (m, ArH, 5H), 3.16 (dd, $J_{\text{H-F}} = 11.1$ Hz, $J = 9.3$ Hz, CH, 1H), 1.45 (ddd, $J_{\text{H-F}} = 16.2$, 4.7 Hz, $J = 9.3$ Hz, CH, 1H), 1.01 (s, CH_3 , 6H), 1.00 ppm (s, CH_3 , 6H); $^{13}\text{C NMR}$ (100 MHz, CDCl_3): $\delta = 132.9$, 127.4, 126.8, 126.1, 113.4 (dd, $^1J_{\text{C-F}} = 288.5$, 283.8 Hz), 83.2, 30.4 (t, $^2J_{\text{C-F}} = 10.8$ Hz), 23.8, 23.5 ppm; $^{19}\text{F NMR}$ (376 MHz, C_6D_6): $\delta = -124.33$ (ddd, $^2J = 145.8$ Hz, $J_{\text{F-H}} = 11.1$, 4.7 Hz, CF_aF_b , 1F), -135.1 ppm (dd, $^2J = 145.8$ Hz, $J_{\text{F-H}} = 16.2$ Hz, CF_aF_b , 1F); $\bar{\nu}$ /(film) = 2980, 2363, 2344, 1439, 1371, 1339, 1227, 1138 cm^{-1} ; MS (CI): m/z (%): 309 (5) $[\text{M}+\text{C}_2\text{H}_5]^+$, 281 (45) $[\text{M}+\text{H}]^+$, 261 (15) $[\text{M}-\text{F}]$, 203 (17) $[\text{M}-\text{Ph}]$, 181 (8), 147 (20), 101 (100), 85 (92); t_R (GC) = 12.84 minutes. The data was in agreement with that reported by Amii and Fujioka.⁶⁷

Evidence of Difluorocarbene-Diglyme Reaction

An oven dried two-necked round bottom flask containing sodium chlorodifluoroacetate (275 mg, 1.8 mmol) was sealed with a SubaSeal, and the salt lightly flame dried under vacuum. The atmosphere was replaced with nitrogen and the flask allowed to cool to room temperature. A low boiling point water condenser with a gas outlet connected to an argon/vacuum manifold was attached to the reaction flask and the atmosphere was purged three times. Diglyme (1 mL) was added and a reaction aliquot (< 0.1 mL) was taken and analysed by $^{19}\text{F NMR}$. The saturated mixture was heated to 180 °C and reaction aliquot taken at different time points and analysed by $^{19}\text{F NMR}$ (see **Chapter 2, Figure 21**).

General Procedure A: Difluorocyclopropanation with MDFA

Preparation of ((1S*,3S*)-1-Acetoxy(methyl)-2,2-difluoro-3-phenylcyclopropane (142)



An oven dried two-necked round bottom flask containing potassium iodide (3.68 g, 22.2 mmol) was sealed with a SubaSeal, and the salt was stirred and lightly flame

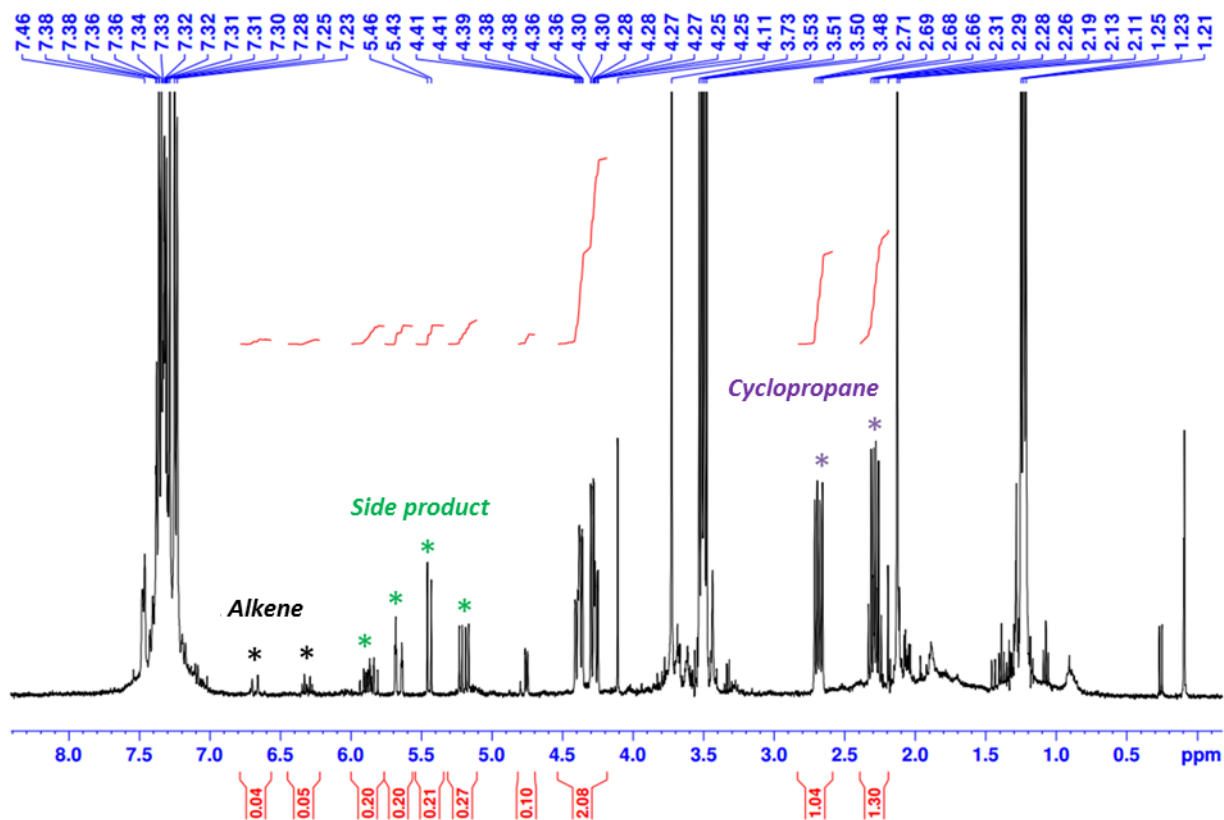
dried under an atmosphere of argon. A low boiling point water condenser with a gas outlet connected to an argon/vacuum manifold was attached and the reaction flask and the atmosphere were purged three times. Cinnamyl acetate **141** (1.34 mL, 8.0 mmol) followed by diglyme (1.3 mL) were added and the yellow suspension was heated to 120 °C. Once the reaction temperature had been reached, TMSCl (2.6 mL, 19.7 mmol) and MDFA (2.6 mL, 19.7 mmol) were added dropwise in that order. After 5 hours, the reaction mixture had evaporated to dryness and a further portion of diglyme (1.3 mL) was added. The mixture was stirred for a further 19 hours (total reaction time of 24 hours). The resulting brown solution was cooled to room temperature and the reaction mixture was quenched with aqueous NaCl (10 mL) and diethyl ether (10 mL) added. The organic layer was separated and the aqueous layer was extracted with diethyl ether (2 x 10 mL). The original organic layer and the extracts were combined, dried (MgSO₄) and concentrated under reduced pressure to remove volatiles. The ¹H NMR spectrum of the resulting brown oil confirmed full conversion. Column chromatography on silica gel (2:23 diethyl ether in hexane) afforded acetate **142** as a pale yellow oil (1.7 g, 94%). R_f = 0.26 (1:9 diethyl ether/hexane); ¹H NMR (400 MHz, CDCl₃): δ = 7.36-7.29 (m, ArH, 3H), 7.23-7.21 (br. d, J = 7.9 Hz, ArH, 2H), 4.38 (br. ddd, J = 11.9, ⁴J = 2.5 and 1.0 Hz, CH_oH_bOAc, 1H), 4.25 (br. dd, J = 7.8, ⁴J = 1.6 Hz, CH_aH_bOAc, 1H), 2.68 (dd, J_{H-F} = 14.5 Hz, J = 7.8 Hz, PhCH, 1H), 2.33-2.24 (m, C(H)CH₂OAc, 1H), 2.10 ppm (s, OC(O)CH₃, 3H); ¹³C NMR (100 MHz, CDCl₃): δ = 170.9, 132.7, 128.6, 128.2, 127.5, 113.1 (t, ¹J_{C-F} = 289.4 Hz), 60.9 (d, J_{C-F} = 5.6 Hz), 32.0 (t, ²J_{C-F} = 11.2 Hz), 28.0 (t, ²J_{C-F} = 10.3 Hz), 20.8 ppm; ¹⁹F NMR (376 MHz, CDCl₃): δ = -135.4 (dd, ²J = 157.8 Hz, J_{F-H} = 14.5 Hz, CF_aF_b, 1F), -137.3 ppm (dd, ²J = 158.6 Hz, J_{F-H} = 14.0 Hz, CF_aF_b, 1F); $\bar{\nu}$ /(film) = 2386, 2354, 1737, 1225, 1017, 999, 972, 696 cm⁻¹; MS (CI): m/z (%): 167 (55) [M-OAc]⁺, 147 (100); HRMS (EI): calcd for C₁₂H₁₂F₂O₂, 226.0800 [M], found 226.0861; t_R (GC) = 11.37 minutes. The data was in agreement with that reported by Kobayashi and co-workers but no ¹³C NMR data was previously reported.²³⁶

The reaction was repeated on a larger scale using cinnamyl acetate (2.7 mL, 16 mmol), MDFA (5.2 mL, 39.5 mmol), TMSCl (5.2 mL, 39.5 mmol), KI (7.36 g, 44.4

mmol) and diglyme (2.6 mL) according to the procedure above to afford acetate **142** (2.8 g, 77%).

Evidence for the Identity of Iodide Side Product **143**

The following crude ^1H NMR spectrum was acquired after using literature MDFA conditions⁵¹¹ for the difluorocyclopropanation of cinnamyl acetate (**141**).

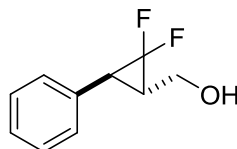


^1H NMR of crude reaction mixture (400 MHz, CDCl_3).

Flash chromatography on silica gel for the above crude product (1:9 diethyl ether in hexane) afforded side product **143** as a yellow/brown oil. Analytical data below was acquired immediately after purification but after storage (4 °C), decomposition to a pink oil occurred. **143** was found to decompose on the GC/MS and decomposition occurred before an acceptable ^{13}C NMR spectrum could be obtained. Data for iodide **143**: R_f = 0.52 diethyl ether/hexane, ^1H NMR (400 MHz, CDCl_3): δ = 7.48-7.46 (m, ArH, 2H), 7.35-7.31 (m, ArH, 3H), 5.94-5.81 (dddd, J = 17.2, 10.9 Hz, $J_{\text{H-F}}$ = 11.3, 10.1 Hz, $\text{HC}=\text{CH}_a\text{H}_b$, 1H), 5.68 (dt, J = 17.3, $^4J_{\text{F-F}}$ = 2.4 Hz, $\text{HC}=\text{CH}_a\text{H}_b$, 1H), 5.45 (d, J = 10.9 Hz, $\text{HC}=\text{CH}_a\text{H}_b$, 1H), 5.20 ppm (dd, J = 18.6, 8.3 Hz, CF_2CIH , 1H); ^{19}F NMR (376

MHz, CDCl₃): δ = - 92.2 (ddd, $^2J_{F-F}$ = 237.1 Hz, J_{F-H} = 11.3, 8.3 Hz, 1F), - 96.7 ppm (ddd, $^2J_{F-F}$ = 237.1 Hz, J_{F-H} = 18.8, 10.1 Hz, 1F); $\bar{\nu}$ /(film) = 1495, 1454, 1443, 1152, 1044, 990 cm⁻¹; HRMS (APCI): calcd for C₁₀H₉F₂, 293.9712 [M+H]⁺ found 293.9716.

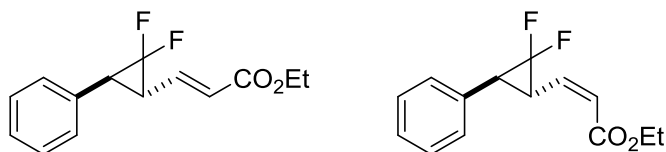
**General Procedure B: Ester Hydrolysis of Difluorocyclopropyl Acetate
((1S*,3S*)-2,2-Difluoro-1-hydroxy(methyl)-3-phenylcyclopropane (144))**



A solution of potassium carbonate (443 mg, 3.2 mmol) in H₂O (2 mL) was added to a solution of acetate **142** (718.7 mg, 3.2 mmol) in MeOH (60 mL, 0.05 M) and the mixture was heated to 60 °C for 1 hour. Full conversion was confirmed by TLC. The reaction mixture was concentrated under reduced pressure and the resulting suspension taken up in MeOH (5 mL) and evaporated onto Celite (6.4 g). The solid was transferred onto a sinter funnel and the product was eluted with diethyl ether (60 mL). The filtrate was concentrated under reduced pressure to afford alcohol **144** as a colourless oil (583.5 mg, 99%). Compound was of a high analytical standard that no purification was required. R_f = 0.16 (1:4 diethyl ether/hexane); ¹H NMR (400 MHz, CDCl₃): δ = 7.38-7.30 (m, ArH, 3H), 7.27-7.25 (m, ArH, 2H), 4.01-3.86 (br. m, CH₂OH, 2H), 2.65 (ddd, J_{H-F} = 13.5, J = 7.6, 4J = 1.4 Hz, PhCH, 1H), 2.23 (m, CHCH₂OH, 1H), 1.72 ppm (t, J = 5.9 Hz, CH₂OH, 1H); ¹³C NMR (100 MHz, CDCl₃): δ = 132.5, 128.1, 127.6, 126.8, 113.9 (t, $^1J_{C-F}$ = 289.1 Hz), 59.3 (d, J_{C-F} = 5.5 Hz), 31.0 (t, $^2J_{C-F}$ = 10.7 Hz), 30.7 ppm (t, $^2J_{C-F}$ = 9.6 Hz); ¹⁹F NMR (376 MHz, CDCl₃): δ = -136.2 (dd, 2J = 158.1 Hz, J_{F-H} = 14.0 Hz, 1F), -136.9 ppm (dd, 2J = 157.6 Hz, J_{F-H} = 13.5 Hz, 1F); $\bar{\nu}$ /(film) = 3321 (br.), 1500, 1474, 1447, 1269, 1013, 698 cm⁻¹; MS (CI): m/z (%): 185 (4) [M+H]⁺, 167 (21) [M-OH], 147 (100) [(M+H)-F₂]⁺, HRMS (APCI): calcd for C₁₀H₁₀F₂O, 184.0694 [M-H]⁺, found 184.0688; t_R (GC) = 10.56 minutes. Alcohol **144** has been reported in the literature but no characterisation data was reported.²³⁶ The compound was also reported recently by Itoh and co-workers¹²² though the material isolated was of lower quality than that used in our study.

General Procedure C: Oxidation/Wittig of Difluorocyclopropyl Alcohols

Preparation of ethyl 3-((1'R*,3'S*)-2',2'-difluoro-3'-phenylcyclopropyl) prop-2E-enoate (**147a**) and ethyl 3-((1'R*,3'S*)-2',2'-difluoro-3'-phenylcyclopropyl) prop-2Z-enoate (**147b**)

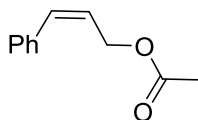


Bis(acetoxy)iodobenzene (1.35g, 4.23 mmol) was added to a solution of alcohol **144** (678 mg, 3.68 mmol) and TEMPO (54 mg, 0.368 mmol) in anhydrous DCM (15 mL) and the reaction mixture was stirred at room temperature under nitrogen for 6 hours. The ^1H NMR spectrum showed complete conversion to the corresponding aldehyde. (Ethoxycarbonylmethylene)triphenylphosphorane (1.64 g, 4.7 mmol) was then added to the reaction mixture and stirred for 2 hours until the ^1H or ^{19}F NMR spectrum showed complete conversion. The resulting orange solution was concentrated under reduced pressure and column chromatography on silica gel (1:19 diethyl ether in hexane) afforded **147a** (728 mg, 78%) and **147b** (43 mg, 5%).

Data for 147a: R_f = 0.30 (1:9 diethyl ether/hexane); ^1H NMR (500 MHz, CDCl_3): δ = 7.40-7.31 (m, ArH, 3H), 7.27-7.25 (m, ArH, 2H), 6.79 (ddt, J = 15.6, 9.5 Hz, $^4J_{\text{H-F}}$ = 1.5 Hz, HC=CHCO₂Et, 1H), 6.09 (d, J = 15.6 Hz, HC=CHCO₂Et, 1H), 4.25 (q, J = 7.2 Hz, CO₂CH₂CH₃, 2H), 2.91 (dd, $J_{\text{H-F}}$ = 14.7 Hz, J = 7.3 Hz, PhCH, 1H), 2.66-2.60 (ddd, $J_{\text{H-F}}$ = 13.4 Hz, J = 9.5, 7.3 Hz, CHCH=CH, 1H), 1.33 ppm (t, J = 7.2 Hz, CO₂CH₂CH₃, 3H); ^{13}C NMR (100 MHz, CDCl_3): δ = 165.0, 139.8, 131.8, 128.2, 127.4, 127.2, 123.2, 112.9 (t, $^1J_{\text{C-F}}$ = 292.6 Hz), 59.9, 35.4 (t, $^2J_{\text{C-F}}$ = 9.8 Hz) 33.1 (t, $^2J_{\text{C-F}}$ = 12.7 Hz), 13.7 ppm; ^{19}F NMR (376 MHz, CDCl_3): δ = 130.6 (dd, 2J = 157.4 Hz, $J_{\text{F-H}}$ = 14.7 Hz, 1F), -135.6 ppm (dd, 2J = 156.6 Hz, $J_{\text{F-H}}$ = 13.4 Hz, 1F); $\bar{\nu}$ /(film) = 2359, 2342, 1715, 1281 cm^{-1} ; MS (CI): m/z (%): 233 (100) [M-F], 187 (44), 159 (26); HRMS (APCI): calcd for C₁₄H₁₅F₂O₂, 253.1035 [M+H]⁺, found 253.1034; t_r (GC) = 12.13 minutes. **Data for 147b:** R_f = 0.43 (1:9 ethyl acetate/hexane); ^1H NMR (400 MHz CDCl_3): δ = 7.40-7.29 (m, ArH, 5H), 6.06-5.99 (m, HC=CHCO₂Et, 2H), 4.234 (q, J = 7.2 Hz, OCH_aH_bCH₃, 1H), 4.225 (q, J = 7.2 Hz, OCH_aH_bCH₃, 1H), 4.18-4.10 (m, HCCH=CHCO₂Et, 1H), 2.84 (dd, $J_{\text{H-F}}$ = 14.8 Hz, J

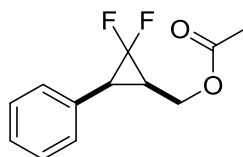
= 7.1 Hz, *CHPh*, 1H), 1.32 ppm (t, $J = 7.2$ Hz, CH_3 , 3H); ^{13}C NMR (100 MHz, $CDCl_3$): $\delta = 165.7, 140.1$ (d, $J_{C-F} = 6.3$ Hz), 131.7, 128.1, 127.7, 127.1, 121.3, 113.5 (t, $^1J_{C-F} = 291.1$ Hz), 59.8, 36.2 (dd, $^2J_{C-F} = 11.8, 9.1$ Hz), 30.1 (dd, $^2J_{C-F} = 13.6, 9.9$ Hz), 13.7 ppm; ^{19}F NMR (376 MHz, $CDCl_3$): $\delta = -132.3$ (dd, $^2J = 154.3$ Hz $J_{F-H} = 14.8$ Hz, 1F), -136.2 ppm (dd, $^2J = 154.6$ Hz $J_{F-H} = 13.7$ Hz, 1F); $\bar{\nu}$ /(film) = 2359, 2342, 1715, 1194, 1018, 806 cm^{-1} ; MS (CI): m/z (%): 281 (4) $[M+C_2H_5]^+$, 253 (70) $[M+H]^+$, 233 (35) $[M-F]$, 225 (36), 205 (60) $[(M+H)-(F+Et)]^+$, 187 (100), 179 (30) $[M-CO_2Et]$, 169 (18) $[M-F_2+OEt]$, 159 (45), 141 (28) $[M-F_2+CO_2Et]$; HRMS (APCI): calcd for $C_{14}H_{15}F_2O_2$, 253.1035 $[M+H]^+$, found 253.1035; t_R (GC) = 12.36 minutes.

Preparation of 1-Acetoxy-3-phenylprop-2Z-ene (149)



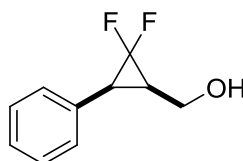
4-Dimethylaminopyridine (85.5 mg, 0.7 mmol) was added to a solution of (*Z*)-3-phenylprop-2-en-1-ol (952 mg, 7 mmol) and acetic anhydride (0.69 mL, 7.35 mmol) in DCM/pyridine (30 mL, 1:1 v/v) and stirred at room temperature for 22 hours until TLC showed full conversion. The reaction mixture was quenched with 1M HCl (50 mL) and the partitioned organic layer separated. The aqueous layer was extracted with DCM (4 x 50 mL) and the organic extracts were combined, and backwashed with sodium bicarbonate (2 x 40 mL). The organic phase was dried ($MgSO_4$) and concentrated under reduced pressure. Any remaining pyridine in the resulting oil was removed by co-evaporation with toluene (4 x 30 mL) to afford acetate **149** as a yellow oil (1.19 g, 97%). $R_f = 0.41$ (1:19 diethyl ether/hexane); 1H NMR (400 MHz, $CDCl_3$): $\delta = 7.41-7.25$ (m, *ArH*, 5H), 6.70 (br. dt, $J = 11.8$ Hz, $^4J = 1.6$ Hz, *PhCH*, 1H), 5.85 (dt, $J = 11.8, 6.7$ Hz, $=CHCH_2$, 1H), 4.88 (dd, $J = 6.7$ Hz, $^4J = 1.6$ Hz, CH_2OAc , 2H), 2.11 ppm (s, $OCOCH_3$, 3H); ^{13}C NMR (100 MHz, $CDCl_3$): $\delta = 170.3, 135.6, 132.5, 128.2, 127.9, 127.0, 125.3, 61.0, 20.4$ ppm; $\bar{\nu}$ /(film) = 1736, 1371, 1225, 1024 cm^{-1} ; MS (CI): m/z (%): 145 (11), 117 (100) $[M-OAc]^+$, 60 (11); t_R (GC) = 11.00 minutes. The data was in agreement with that reported by Jung and co-workers.²³⁷

Preparation of ((1R*,3S*)-1-Acetoxy(methyl)-2,2-difluoro-3-phenylcyclopropane (150)



Ester **150** was prepared from Z-cinnamyl acetate **149** (713 mg, 4.06 mmol), MDFA (1.3 mL, 10 mmol), TMSCl (1.3 mL, 10 mmol), potassium iodide (1.87 g, 11.25 mmol) and diglyme (0.7 mL) as a yellow oil (689 mg, 75%) according to General Procedure A. $R_f = 0.42$ (1:19 diethyl ether/hexane); $^1\text{H NMR}$ (400 MHz, CDCl_3): $\delta = 7.35\text{-}7.31$ (m, ArH, 5H), 4.17-4.11 (m, $\text{CH}_a\text{H}_b\text{OAc}$, 1H), 3.88 (br. ddd, $^2J = 12.2$ Hz, $J = 8.4$ Hz, $^4J = 0.8$ Hz, $\text{CH}_a\text{H}_b\text{OAc}$, 1H), 3.03 (br. t, $J = 13.2$ Hz, PhCH, 1H), 2.36-2.27 (m, CHCH_2OAc , 1H), 2.07 ppm (s, OCOCH_3 , 3H); $^{13}\text{C NMR}$ (100 MHz, CDCl_3): $\delta = 107.1, 129.2, 129.4, 128.1, 127.2, 112.8$ (t, $^1J_{\text{C-F}} = 287.3$ Hz), 58.2 (d, $J_{\text{C-F}} = 5.8$ Hz), 28.6 (t, $^2J_{\text{C-F}} = 11.1$ Hz), 25.0 (t, $^2J_{\text{C-F}} = 10.2$ Hz), 20.1 ppm; $^{19}\text{F NMR}$ (376 MHz, CDCl_3): $\delta = -121.7$ (dtd, $^2J = 160.9$ Hz, $J_{\text{F-H}} = 13.7$ Hz, $^4J_{\text{F-H}} = 2.8$ Hz, 1F), -147.6 ppm (d, $^2J = 161.0$ Hz, 1F); $\bar{\nu}$ /(film) = 1739, 1501, 1470, 1447, 1230 cm^{-1} ; MS (CI): m/z (%): 167 (40) $[\text{M-OAc}]^+$, 147 (100); HRMS (APCI): calcd for $\text{C}_{12}\text{H}_{18}\text{F}_2\text{O}_2\text{N}$, 244.1144 $[\text{M} + \text{NH}_4]^+$, found 244.1139; t_R (GC) = 10.88 minutes. Compound **150** has been reported in the literature but no characterisation data was reported.²³⁸

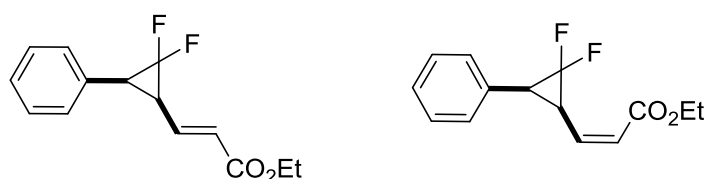
Preparation of ((1R*,3S*)-2,2-Difluoro-1-hydroxy(methyl)-3-phenylcyclopropane (151)



Alcohol **151** was prepared from acetate **150** (681 mg, 3 mmol), potassium carbonate (458 mg, 3.3 mmol) and MeOH (50 mL) as a yellow oil (536 mg, 97%) according to General Procedure B. $R_f = 0.29$ (1:1 diethyl ether/hexane); $^1\text{H NMR}$ (400 MHz, CDCl_3): $\delta = 7.36\text{-}7.31$ (m, ArH, 5H), 3.71-3.68 (br. m, $\text{CH}_a\text{H}_b\text{OAc}$, 1H), 3.63-3.57 (br. m, $\text{CH}_a\text{H}_b\text{OAc}$, 1H), 3.00 (dd, $J = 12.1$ Hz, $J_{\text{H-F}} = 13.6$ Hz, PhCH, 1H), 2.33-2.23 (m, CHCH_2OAc , 1H), 1.33 ppm (t, 5.9 Hz, OH, 1H); $^{13}\text{C NMR}$ (100 MHz, CDCl_3): $\delta = 130.5,$

129.3, 128.1, 127.0, 113.3 (dd, $^1J_{C-F} = 285.3, 288.9$ Hz), 56.5 (d, $J = 5.9$ Hz), 28.8 (dd, $^2J_{C-F} = 9.8, 12.2$ Hz), 28.5 (t, 9.9 Hz); ^{19}F NMR (376 MHz, $CDCl_3$): $\delta = -120.8$ (dtd, $^2J = 161.5$ Hz, $J_{F-H} = 13.6$ Hz, $^4J_{F-H} = 2.7$ Hz, 1F), -148.0 ppm (d, $J = 161.5$ Hz, 1F); $\bar{\nu}$ /(film) = 3352 (br.), 1501, 1470, 1445, 1109, 1015 cm^{-1} ; MS (CI): m/z (%): 167 (33) [M-OH], 147 (100) [(M+H)-F₂]⁺; HRMS (APCI): calcd for C₁₀H₁₄F₂ON, 202.1038 [M+NH₄]⁺ found 202.1036; t_R (GC) = 10.42 minutes.

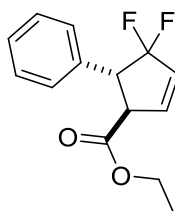
Preparation of ethyl 3-((1'S*,3'S*)-2',2'-difluoro-3'-phenylcyclopropyl) prop-2E-enoate (152a) and ethyl 3-((1'S*,3'S*)-2',2'-difluoro-3'-phenylcyclopropyl) prop-2Z-enoate (152b)



Esters **152a** and **152b** were prepared from alcohol **151** (125.2 mg, 0.68 mmol), TEMPO (11.2 mg, 0.068 mmol), BAIB (260 mg, 0.79 mmol), (ethoxycarbonylmethylene)triphenylphosphorane (306 mg, 0.88 mmol) and DCM (2.8 mL) as yellow oils **152a** (122 mg, 71%) and **152b** (29 mg, 17%) according to general procedure C. The 1H NMR spectrum showed complete conversion to the corresponding aldehyde after 5 hours. After addition of phosphorane, the reaction mixture was stirred for 14 hours until the ^{19}F NMR spectrum showed complete conversion. **Data for 152a:** $R_f = 0.26$ (1:19 diethyl ether/hexane); 1H NMR (400 MHz, $CDCl_3$): $\delta = 7.36-7.28$ (m, ArH, 5H), 6.42 (ddt, $J = 15.5, 10.2$ Hz, $^4J_{H-F} = 1.5$ Hz, CH=CHCO₂Et, 1H), 6.07 (dd, $J = 15.7$ Hz, $^4J = 0.9$ Hz, CH=CHCO₂Et, 1H), 4.16 (q, $J = 7.1$ Hz, OCH₂CH₃, 2H), 3.22 (dd, $J = 11.6$ Hz, $J_{H-F} = 12.8$ Hz, PhCH, 1H), 2.78 (ddd, $J = 11.6, 10.3$ Hz $J_{H-F} = 12.8$ Hz, CHCH=CH, 1H), 1.26 ppm (t, $J = 7.1$ Hz, CH₂CH₃, 3H); ^{13}C NMR (100 MHz, $CDCl_3$): $\delta = 164.9, 138.1$ (d, $J_{C-F} = 5.5$ Hz), 129.5, 129.4, 128.2, 127.4, 124.0, 113.0 (dd, $^1J_{C-F} = 287.3, 293.4$ Hz), 59.9, 32.5 (t, $^2J = 10.4$ Hz), 30.6 (dd, $^2J = 13.4, 9.9$ Hz), 13.7 ppm; ^{19}F NMR (376 MHz, $CDCl_3$): $\delta = -119.7$ (dt, $^2J = 157.1$ Hz, $J_{F-H} = 12.8$ Hz, 1F), -142.9 ppm (d, $^2J = 157.1$ Hz, 1F); $\bar{\nu}$ /(film) = 2359, 2342, 1715, 1651, 1501, 1445, 1258, 1148, 1017 cm^{-1} ; MS (CI): m/z (%): 273 (6), 233 (100) [M-F], 215 (10) [(M+H)-F₂]⁺, 205 (8), 187 (27), 159 (19); HRMS (APCI): calcd for C₁₄H₁₅F₂O₂,

253.1035 [M+H]⁺ found 253.1033; t_R (GC) = 11.87 minutes. **Data for 152b:** R_f = 0.41 (1:19 diethyl ether/hexane); ¹H NMR (300 MHz, CDCl₃): δ = 7.35-7.31 (m, ArH, 5H), 5.91 (br. d, J = 11.6 Hz, CHCO₂Et, 1H), 5.68-5.62 (m, CH=CHCO₂Et, 1H), 4.25 (q, J = 7.2 Hz, CH₂CH₃, 2H), 4.12 (ddd, J = 12.0, 10.8 Hz, J_{H-F} = 13.4 Hz CHCH=CH, 1H), 3.26 (dd, J = 12.0, Hz, J_{C-F} = 13.4 Hz, PhCH, 1H), 1.35 ppm (t, 7.2 Hz, CH₂CH₃, 3H); ¹³C NMR (100 MHz, CDCl₃): δ = 165.7, 138.4 (d, J_{C-F} = 6.6 Hz), 130.1, 129.5, 128.1, 127.1, 121.9, 113.8 (dd, ¹J_{C-F} = 286.2, 293.2 Hz), 59.8, 32.5 (t, ²J_{C-F} = 10.5 Hz), 28.0 (dd, ²J_{C-F} = 9.0, 14.2 Hz), 13.7 ppm; ¹⁹F NMR (376 MHz, CDCl₃): δ = -119.7 (dt, ²J = 155.8, J_{F-H} = 13.4 Hz, 1F), -144.0 ppm (d, ²J = 155.8 Hz, 1F); ν̄/(film) = 2361, 2342, 1715, 1418, 1188, 1159, 1092, 1017 cm⁻¹; MS (CI): m/z (%): 281 (5) [M+C₂H₅]⁺, 253 (88) [M+H]⁺, 233 (27) [M-F], 225 (38), 215 (19) [(M+H)-F₂]⁺, 205 (63) [(M+H)-(F+Et)]⁺, 187 (100), 179 (27) [M-CO₂Et], 161 (38), 159 (29), 141 (21) [M-F₂+CO₂Et]; HRMS (EI): calcd for C₁₄H₁₅O₂F₂, 253.1035 [M+H]⁺ found 253.1030; t_R (GC) = 12.29 minutes.

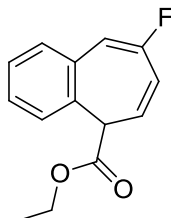
Preparation of Ethyl (1S*,5S*)- 4,4-difluoro-5-phenylcyclopent-2-ene-1-carboxylate (153)



A solution of **147a** (104 mg, 0.4 mmol) in toluene (0.5 mL) was heated to 100 °C in a sealed microwave vial for 17 hours in a DrySyn block. After cooling and venting the vial, fluorine NMR confirmed complete conversion. The reaction mixture was transferred to a round bottom flask using DCM (5 mL) and concentrated under reduced pressure to afford difluorocyclopentene **153** (102 mg, 99%) as a pale yellow oil. R_f = 0.34 (1:4 diethyl ether/hexane); ¹H NMR (400 MHz, CDCl₃): δ = 7.41-7.33 (m, ArH, 5H), 6.50 (dt, J = 6.0, ⁴J_{H-F} = 1.6 Hz, =CHCO₂Et, 1H), 6.09 (dd, J = 6.0, J_{H-F} = 2.5 Hz, =CHCF₂, 1H), 4.18 (q, J = 7.1 Hz, OCH₂CH₃, 2H), 4.04-3.92 (m, CHCO₂Et, CHPh, 2H), 1.26 ppm (t, J = 7.1 Hz, OCH₂CH₃, 3H); ¹³C NMR (400 MHz, CDCl₃): δ = 170.3 (d, ⁴J_{C-F} = 4.8 Hz), 138.6 (t, J_{C-F} = 10.4 Hz), 133.8, 129.3 (t, ¹J_{C-F} = 245.7 Hz), 128.7, 128.5 (dd, ²J_{C-F} = 25.0, 30.3 Hz), 128.0, 127.3, 61.0, 54.1 (d, J_{C-F} = 6.0 Hz), 53.2 (t, ²J_{C-F} = 24.6

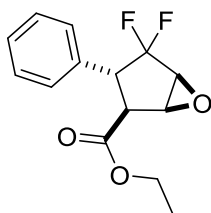
Hz), 13.6 ppm; ^{19}F NMR (376 MHz, CDCl_3): $\delta = -89.3$ (ddd, $^2J = 252.8$ Hz, $J_{\text{F-H}} = 16.6$, 8.9 Hz, 1F), -92.7 ppm (ddd, $^2J = 253.2$ Hz, $J_{\text{F-H}} = 14.2$, 5.8 Hz, 1F); $\bar{\nu}/(\text{film}) = 2359$, 2340, 1732, 1254, 1194, 1167, 698 cm^{-1} ; MS (CI): m/z (%): 253 (3) $[\text{M}+\text{H}]^+$, 233 (100) $[\text{M}-\text{F}]$, 215 (8), 187 (40), 159 (33); HRMS (APCI): calcd for $\text{C}_{14}\text{H}_{15}\text{FO}_2$, 253.1035 $[\text{M}+\text{H}]^+$ found 253.1033; t_{R} (GC) = 12.13 minutes.

Preparation of Ethyl 8-fluoro-5H-benzo[7]annulene-5-carboxylate (**154a**)



Neat **147a** (331 mg, 1.3 mmol) was heated to 90 °C in a sealed microwave vial for 22 hours in a DrySyn block. After cooling and venting the vial, the crude ^{19}F NMR spectrum showed 33% conversion to **154a**. Column chromatography on silica gel (1:9 diethyl ether in hexane) afforded **154a** as a colourless oil (63 mg, 19%). $R_{\text{f}} = 0.21$ (1:9 diethyl ether/hexane); ^1H NMR (400 MHz, CDCl_3): $\delta = 7.44$ -7.39 (m, ArH, 2H), 7.33-7.28 (m, ArH, 1H), 7.12 (d, $J = 7.8$ Hz, ArH, 1H), 6.93 (dd, $J_{\text{H-F}} = 18.2$ Hz, $^4J = 1.7$ Hz, ArHC=CF, 1H), 6.33-6.28 (m, =CHCHCO₂Et, 1H), 6.22-6.18 (br. m, FC-CH=CH, 1H), 4.33 (q, $J = 7.2$ Hz, OCH₂CH₃, 2H), 3.81 (d, $J = 9.4$ Hz, =CHCHCO₂Et, 1H), 1.32 ppm (t, $J = 7.2$ Hz, OCH₂CH₃, 3H); ^{13}C NMR (100 MHz, CDCl_3): $\delta = 171.0$, 158.9 (d, $^1J_{\text{C-F}} = 246.5$ Hz), 131.8 (d, $J_{\text{C-F}} = 11.9$ Hz), 131.2, 129.1 (d, $J_{\text{C-F}} = 12.7$ Hz), 128.9, 127.9 (d, $^4J_{\text{C-F}} = 3.6$ Hz), 126.1, 124.9, 119.6 (d, $^2J = 35.8$ Hz), 113.1 (d, $^2J = 27.0$ Hz), 60.8, 49.3, 13.7 ppm; ^{19}F NMR (376 MHz, CDCl_3): $\delta = -100.7$ ppm (dt, $J_{\text{F-H}} = 18.2$, 5.2 Hz, $^4J_{\text{F-H}} = 5.2$ Hz, 1F); $\bar{\nu}/(\text{film}) = 2982$, 2359, 2342, 1732, 1641, 1192, 1130, 1020, 750 cm^{-1} ; MS (CI): m/z (%): 261 (5) $[\text{M}+\text{C}_2\text{H}_5]^+$, 233 (100) $[\text{M}+\text{H}]^+$, 213 (53) $[\text{M}-\text{F}]$, 187 (88) $[\text{M}-\text{OEt}]$, 159 (50) $[\text{M}-\text{CO}_2\text{Et}]$; HRMS (APCI): calcd for $\text{C}_{14}\text{H}_{14}\text{FO}_2$, 233.0972 $[\text{M}+\text{H}]^+$ found 233.0972; t_{R} (GC) = 13.08 minutes.

Preparation of ethyl (1*S**,2*S**,3*R**,5*S**)-4,4-difluoro-3-phenyl-6-oxabicyclo[3.1.0]hexane-2-carboxylate (**156**)

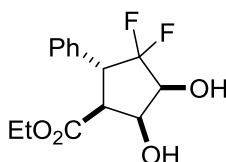


A slurry of sodium bicarbonate (13 g, 155 mmol) in water (13 mL) was added to the a 500 mL three necked round bottomed flask at 0 °C which was connected *via* rubber tubing to a cold-finger condenser (containing solid CO₂/acetone, -78 °C), attached to a cooled receiving flask (cooled in a solid CO₂/acetone bath, -78 °C) fitted with a gas outlet. Powdered oxone (24 g, 39.1 mmol) was added in 5 g portions to the vigorously stirred slurry resulting in the evolution of CO₂. After stirring for 5 minutes, a pre-cooled (-20 °C) dropping funnel was attached to the three necked flask and quickly charged with trifluoroacetone (12 mL, 134 mmol) and added in one portion to the reaction mixture. After a few seconds a yellow solution condensed into the receiving flask, stopping after 10 minutes, the yellow solution was (methyl(trifluoromethyl)dioxarane in trifluoroacetone (assumed 2% yield from trifluoroacetone, 2.7 mmol). The condenser was removed and difluorocyclopentene **153** (201 mg, 0.8 mmol) was added in one portion and stirred at -78 °C for 1 hour, then allowed to warm to room temperature over 1 hour. The ¹⁹F NMR spectrum of the mixture confirmed complete consumption of **153** to a single fluorinated product. The reaction mixture was concentrated under reduced pressure to afford crude product and column chromatography on silica gel (1:1 diethyl ether in hexane) afforded epoxide **156** as a colourless oil (158 mg, 73%). On standing the colourless oil solidified and vapour diffusion with chloroform/pentane afforded colourless crystals which were analytically consistent (R_f, δ_F) with bulk epoxide **156**: m.p. = 68-70 °C; R_f = 0.16 (1:4 diethyl ether/hexane); ¹H NMR (500 MHz, CDCl₃): δ = 7.38-7.31 (m, ArH, 3H), 7.27 (d, J = 7.1 Hz, ArH, 2H), 4.175 (q, J = 7.2 Hz, CH₃CH_aH_bCO, 1H), 4.165 (q, J = 7.2 Hz, CH₃CH_aH_bCO, 1H), 4.00-3.98 (m, C(O)HCHCO₂Et, 1H), 3.78 (br. d. J = 2.8 Hz, F₂CCH(O), 1H), 3.69 (ddd, J_{H-F} = 20.1, 12.3

Hz, $J = 10.5$ Hz, PhCH, 1H), 3.38 (dt, $J = 10.5$ Hz, $^4J_{\text{H-F}} = 1.4$ Hz, CHCO₂Et, 1H), 1.23 ppm (t, $J = 7.2$ Hz, OCH₂CH₃, 3H); ¹³C NMR (100 MHz, CDCl₃): $\delta = 168.8, 131.2, 129.1, 128.0, 127.6, 123.9$ (dd, $^1J_{\text{C-F}} = 257.8, 247.9$ Hz), 61.1, 53.9 (d, $J_{\text{C-F}} = 6.4$ Hz), 52.9 (dd, $^2J_{\text{C-F}} = 45.1, 31.0$ Hz), 47.1 (d, $^3J_{\text{C-F}} = 6.2$ Hz), 46.1 (dd, $^2J_{\text{C-F}} = 24.8, 20.2$ Hz), 13.5 ppm; ¹⁹F NMR (376 MHz, CDCl₃): $\delta = -110.9$ (dd, $^2J = 250.3$ Hz, $^3J_{\text{F-H}} = 20.1$ Hz, 1F), -112.3 ppm (dd, $^2J = 250.3$ Hz, $^3J_{\text{F-H}} = 12.3$ Hz, 1F); $\bar{\nu}$ /(film) = 2361, 2342, 1736, 1319, 1234, 1161, 905 cm⁻¹; MS (CI): m/z (%): 297 (3) [M+C₂H₅]⁺, 269 (89) [M+H]⁺, 249 (66) [M-F], 223 (97) [M-OEt], 203 (74), 179 (100), 175 (86); HRMS (APCI): calcd for C₁₄H₁₅F₂O₃, 269.0984 [M+H]⁺ found 269.0980; t_R (GC) = 12.43 minutes.

| | | | | | |
|-------------------|---|---|---|---|--------------|
| empirical | - | C ₁₄ H ₁₄ F ₂ O ₃ | Z | - | 4 |
| M_r | - | 268.25 | ρ_{calcd} [g cm ⁻³] | - | 1.441 |
| crystal system | - | Monoclinic | reflins measured | - | 5831 |
| space group | - | P 2 ₁ /c | unique reflins | - | 2924 |
| a [Å] | - | 12.1734(4) | R_{int} | - | 0.0173 |
| b [Å] | - | 10.1680(3) | Goof | - | 1.064 |
| c [Å] | - | 11.0157(4) | R [on F , obs rflns only] | - | 0.0366 |
| β [°] | - | 114.964(4) | wR [on F^2 , all data] | - | 0.0967 |
| [Å ³] | - | 1236.12(7) | Largest diff. peak/hole [eÅ ⁻³] | - | 0.339/-0.264 |

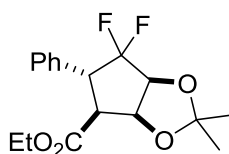
Preparation of ethyl (1S*,2R*,4S*,5S*)-3,3-difluoro-4,5-dihydroxy-2-phenylcyclopentane-1-carboxylate (**157**)



4-Methylmorpholine (101 mg, 0.078 mmol) and potassium osmate(VI)dihydrate (6.1 mg, 0.016 mmol) were added in that order to a solution of difluorocyclopentene **153** (196 mg, 0.78 mmol) in H₂O (2 mL), THF (2 mL) and acetone (2 mL) and the mixture was stirred at room temperature for 45 hours. TLC of the reaction mixture confirmed complete consumption of **153**. The reaction mixture was quenched with saturated Na₂S₂O₃ (5 mL) and volatile materials were removed under reduced pressure. EtOAc (10 mL) was added to the reaction mixture, the organic layer

separated and the aqueous layer extracted further with EtOAc (2 x 10 mL). The original organic layer and the extracts were combined, dried (MgSO₄) and concentrated under reduced pressure to afford diol **157** as a white solid (188 mg, 85%). m.p. = 112-114 °C (fine needles obtained *via* vapour diffusion from chloroform/pentane); R_f = 0.33 (7:3 EtOAc in hexane); ¹H NMR (400 MHz, CDCl₃): δ = 7.39-7.32 (m, ArH, 3H), 7.28 (d, *J* = 6.7 Hz, ArH, 2H), 4.64 (dd, *J* = 5.9, 5.6 Hz, CHOH, 1H), 4.22 (ddd, *J*_{H-F} = 13.9, 3.7 Hz, *J* = 5.9 Hz, F₂CCHOH, 1H), 4.16 (q, *J* = 7.2 Hz, OCH₂CH₃, 2H), 4.11 (ddd, *J*_{H-F} = 19.5, 15.4 Hz, *J* = 12.4 Hz, PhCH, 1H), 3.50 (br. s, OH, 1H), 3.36 (br. s, OH, 1H) 3.32 (dd, *J* = 12.4, 5.6 Hz, COCH, 1H), 1.19 ppm (t, *J* = 7.2 Hz, CH₂CH₃, 3H); ¹³C NMR (100 MHz, CDCl₃): δ = 170.9, 133.3, 129.1, 128.5, 128.0, 124.7 (dd, ¹*J*_{C-F} = 261.4, 252.1 Hz), 75.0 (dd, ²*J*_{C-F} = 33.2, 20.2 Hz), 69.3 (d, *J*_{C-F} = 6.5 Hz), 61.6, 50.3 (dd, ²*J*_{C-F} = 24.5, 23.6 Hz), 49.2 (d, *J*_{C-F} = 7.9 Hz), 14.0 ppm; ¹⁹F NMR (376 MHz, CDCl₃): δ = -103.8 (ddd, ²*J* = 240.0 Hz, *J*_{H-F} = 19.5, 14.0 Hz, 1F), -106.9 ppm (ddd, ²*J* = 239.4 Hz, *J*_{F-H} = 15.1 ⁴*J*_{F-H} = 3.9 Hz, 1F); $\bar{\nu}$ /(film) = 3462, 3445, 2986, 2361, 2342, 1730, 1287, 1215, 1175, 1123, 1067, 1034 cm⁻¹; MS (CI): *m/z* (%): 287 (25) [M+H]⁺, 269 (15) [M-OH]⁺, 249 (24), [(M+H)-F₂], 241 (100) [M-OEt]⁺; HRMS (APCI): calcd for C₁₄H₁₇F₂O₄, 287.1089 [M+H]⁺ found 287.1091; t_R (GC) = 13.63 minutes.

Preparation of ethyl (3aS*,4S*,5R*,6aS*)-6,6-difluoro-2,2-dimethyl-5-phenyltetrahydro-4H-cyclopenta[d][1,3]dioxole-4-carboxylate (158)

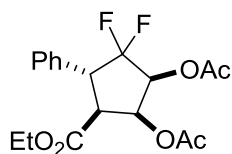


2,2-Dimethyloxypropane (0.07 ml, 0.52 mmol) was added to a solution of diol **157** (75 mg, 0.26 mmol) in DCM (1.5 mL) containing Amberlyst 15 (12 mg) and the reaction mixture stirred at room temperature for 19 hours. ¹⁹F NMR spectrum of the reaction mixture confirmed full conversion of diol **157**. The reaction mixture was filtered through a sinter funnel under reduced pressure and remaining Amberlyst-15 was washed with DCM (2 x 5 mL). The filtrate was collected and concentrated under reduced pressure. Any remaining 2,2-dimethyloxypropane in the resulting solid was removed by co-evaporation with toluene (2 x 10 mL) to

afford acetonide **158** as a white solid (77 mg, 90%). Vapour diffusion with chloroform/pentane afforded colourless crystals which were analytically consistent (^1H , ^{19}F) with bulk acetonide **158**. m.p. = 113-115 °C (fine needles obtained *via* vapour diffusion with chloroform/pentane); R_f = 0.68 (1:1 EtOAc in hexane); ^1H NMR (400 MHz, CDCl_3): δ = 7.40-7.31 (m, ArH, 5H), 5.07 (t, J = 5.8 Hz, OCH, 1H), 4.58 (dd, $J_{\text{H-F}}$ = 11.2, J = 5.8 Hz, CF_2CHO , 1H), 4.15 (q, J = 7.2 Hz, OCH_2CH_3 , 2H), 3.98 (ddd, $J_{\text{H-F}}$ = 19.3, 6.5 Hz, J = 13.0 Hz, PhCH, 1H), 3.37 (dd, J = 13.0, 5.8 Hz, EtO_2CCH , 1H), 1.60 (s, CH_3 , 3H), 1.40 (s, CH_3 , 3H), 1.22 ppm (t, J = 7.2 Hz, CH_3 , 3H); ^{13}C NMR (100 MHz, CDCl_3): δ = 167.7, 131.7, 128.7, 127.9, 127.5, 124.0 (dd, $^1J_{\text{C-F}}$ = 267.0, 243.2 Hz), 122.6, 79.2 (dd, $^2J_{\text{C-F}}$ = 40.9, 19.1) 76.7 (d, $J_{\text{C-F}}$ = 3.5 Hz), 60.6, 47.8 (d, $J_{\text{C-F}}$ = 8.1 Hz), 46.5 (t, $^2J_{\text{C-F}}$ = 21.5 Hz), 25.3, 23.9, 13.6 ppm; ^{19}F NMR (376 MHz, CDCl_3): δ = -113.1 (ddd, 2J = 245.8 Hz, $J_{\text{H-F}}$ = 28.3, 11.3 Hz, 1F), -117.4 ppm (dd, 2J = 246.1 Hz, $J_{\text{H-F}}$ = 6.7 Hz, 1F); $\bar{\nu}$ /(film) = 2968, 2934, 2361, 2342, 1742, 1456, 1377, 1281, 1221, 1159, 1082, 1067, 1057 cm^{-1} ; MS (CI): m/z (%): 355 (3) $[\text{M}+\text{C}_2\text{H}_5]^+$, 237 (34) $[\text{M}+\text{H}]^+$, 281 (100) $[(\text{M}-\text{O}_2\text{C}(\text{CH}_3)_2)+\text{C}_2\text{H}_5]^+$, 249 (43), 223 (9) $[\text{M}- (\text{O}_2\text{C}(\text{CH}_3)_2 + \text{Et})]^+$; HRMS (APCI): calcd for $\text{C}_{17}\text{H}_{20}\text{F}_2\text{O}_4$, 327.1402 $[\text{M}+\text{H}]^+$ found 327.1400; t_R (GC) = 13.89 minutes.

| | | | | | |
|-------------------|---|--|--|---|---------------|
| empirical | - | $\text{C}_{17}\text{H}_{20}\text{F}_2\text{O}_4$ | Z | - | 4 |
| M_r | - | 326.33 | ρ_{calcd} [g cm^{-3}] | - | 1.396 |
| crystal system | - | Monoclinic | reflins measured | - | 4487 |
| space group | - | P 2 ₁ /c | unique reflns | - | 2632 |
| a [Å] | - | 15.2633(18) | R_{int} | - | 0.0570 |
| b [Å] | - | 5.6553(5) | Goof | - | 0.981 |
| c [Å] | - | 18.237(2) | R [on F , obs rflns only] | - | 0.0939 |
| β [°] | - | 99.560(12) | wR [on F^2 , all data] | - | 0.2839 |
| [Å ³] | - | 1552.3(3) | Largest diff. peak/hole [eÅ^{-3}] | - | 0.342 /-0.368 |

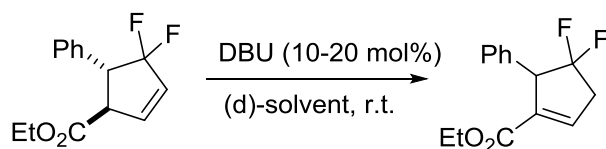
Preparation of ethyl (1S*,2S*,4R*,5S*)-5-(ethoxycarbonyl)-3,3-difluoro-4-phenylcyclopentane-1,2-diyl diacetate (159)



Acetic anhydride (54 μ L, 0.57 mmol) was added in one portion to a solution of diol **157** (55mg, 0.19 mmol) in pyridine (1.2 mL) and the mixture was stirred under nitrogen at room temperature for 16 hours. TLC analysis of the reaction mixture confirmed full consumption of diol. The reaction mixture was quenched with H₂O (10 mL) and DCM (10 mL). The organic layer was separated and washed with 1M HCl (2 x 20 mL). The organic layer was separated again, dried (MgSO₄) and concentrated under reduced pressure. Any remaining pyridine in the resulting solid was removed by co-evaporation with toluene (2 x 10 mL) to afford *bis*-acetate **159** as a colourless oil which solidified on standing to a white solid (72 mg, 99%). m.p. = 65-66 °C (fine needles obtained *via* vapour diffusion with chloroform/pentane); R_f = 0.2 (1:4 EtOAc in hexane); ¹H NMR (400 MHz, CDCl₃): δ = 7.39-7.31 (m, ArH, 3H), 7.28 (d, J = 7.2 Hz, ArH, 2H), 5.82 (dd, J = 5.3, 4.9 Hz, HCOAc, 1H), 5.42 (ddd, J_{H-F} = 13.9, 6.9 Hz, J = 4.9 Hz, CF₂CHOAc, 1H), 4.21 (ddd, J_{H-F} = 18.2, 15.9 Hz, J = 12.2 Hz, PhCH, 1H), 4.16-4.01 (m, OCH₂CH₃, 2H), 3.46 (dd, J = 12.2, 5.3 Hz, HCCO₂Et, 1H), 2.13 (s, COCH₃, 3H), 2.10 (s, COCH₃, 3H), 1.17 ppm (t, J = 7.1 Hz, CH₂CH₃, 3H); ¹³C NMR (100 MHz, CDCl₃): δ = 168.5, 168.1, 167.0, 132.1 (d, J_{C-F} = 2.0 Hz), 128.0, 127.6, 127.1, 122.6 (dd, $^1J_{C-F}$ = 262.9, 252.2 Hz), 72.5 (dd, $^2J_{C-F}$ = 34.0, 18.9 Hz), 68.7 (d, J_{C-F} = 7.8 Hz), 60.5, 49.8 (dd, $^2J_{C-F}$ = 26.3, 22.8 Hz), 46.9 (d, J_{C-F} = 7.3 Hz), 19.4, 19.2, 13.0 ppm; ¹⁹F NMR (376 MHz, CDCl₃): δ = -100.5 (ddd, 2J = 238.7 Hz, J_{H-F} = 15.7, 14.1 Hz, 1F), -102.8 ppm (ddd, 2J = 238.7 Hz, J_{H-F} = 18.3, 7.2 Hz, 1F); $\bar{\nu}$ /(film) = 2965, 2932, 2359, 2342, 1751, 1375, 1375, 1240, 1213, 1179, 1068 cm⁻¹; MS (CI): m/z (%): 399 (11) [M+C₂H₅]⁺, 339 (10) [(M-OAc)+C₂H₅], 311 (100) [M-OAc]⁺, 283 (16) [(M+H)-OAc-Et]⁺, 249 (15); HRMS (APCI): calcd for C₁₈H₂₀F₂O₆Na, 393.1120 [M+Na]⁺ found 393.1122; t_R (GC) = 14.25 minutes.

Alkene Isomerisation Solvent Screen

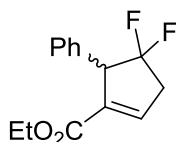
General Procedure H: Base Mediated Alkene Isomerisation



1,8-Diazabicyclo[5.4.0]undec-7-ene (DBU, 10-20 mol%) was added to a solution of difluorocyclopentene **153** (0.01-0.4 mmol) in deuterated solvent (0.3-0.5 mL, see below for specific solvents) in an NMR tube and shaken on a Heidolph Vibramax 100 at room temperature. Integration of ^{19}F NMR spectra at different reaction times (2.5-28 h) was used to determine the extent of conversion to alkene **160**.

| Solvent | DBU (mol%) | Time (h) | % conversion |
|----------------|------------|----------|--------------|
| d_8 -toluene | 20 | 28 | 71 |
| d_8 -THF | 10 | 24 | 88 |
| d_3 -MeCN | 10 | 24 | 22 |
| DMSO | 10 | 2.5 | 75 |
| d_6 -acetone | 10 | 2.5 | 100 |

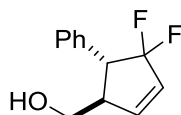
Preparation of ethyl (*S**)-4,4-difluoro-5-phenylcyclopent-1-ene-1-carboxylate (**160**)



1,8-Diazabicyclo[5.4.0]undec-7-ene (12 μL , 0.08 mmol) was added to a solution of difluorocyclopentene **153** (200 mg, 0.8 mmol) in acetone (0.5 ml) and stirred at room temperature for 1 hour. ^{19}F NMR spectrum of the reaction mixture confirmed full conversion to alkene **160**. The volatile organic solvents were removed under reduced pressure. Column chromatography on silica gel (1:4 Et_2O in hexane) afforded alkene **160** as an orange solid (100 mg, 50%). m.p. = 120-123 $^\circ\text{C}$ (fine colourless needles obtained *via* vapour diffusion with chloroform/pentane); R_f = 0.5 (1:4 Et_2O in hexane); ^1H NMR (400 MHz, CDCl_3): δ = 7.39-7.30 (m, ArH, 3H), 7.20-7.18 (m, ArH, 2H), 7.00-6.97 (m, C=CH, 1H), 4.40 (br. d, $J_{\text{H-F}}$ = 21.4 Hz, PhCH, 1H),

4.13 (q, $J = 7.2$ Hz, $\text{OCH}_a\text{H}_b\text{CH}_3$, 1H), 4.11 (q, $J = 7.2$ Hz, $\text{OCH}_a\text{H}_b\text{CH}_3$, 1H), 3.12-3.05 (m, $\text{CF}_2\text{CH}_a\text{H}_b$, 1H), 3.07 (ddd, $J_{\text{H-F}} = 19.1$ Hz, $J = 2.6, 1.0$ Hz, $\text{CF}_2\text{CH}_a\text{H}_b$, 1H), 1.16 ppm (t, $J = 7.1$ Hz, CH_2CH_3 , 3H); ^{13}C NMR (100 MHz, CDCl_3): $\delta = 162.6, 138.0$ (br. d, $J_{\text{C-F}} = 6.4$ Hz), 136.4 (t, $J_{\text{C-F}} = 3.2$ Hz), 133.8 ($J_{\text{C-F}} = 5.6, 3.4$ Hz), 128.4 (dd, $^1J_{\text{C-F}} = 259.0, 252.1$ Hz), 128.0, 127.8, 127.3, 60.1, 57.1 (dd, $^2J_{\text{C-F}} = 29.2, 24.2$ Hz), 41.7 (t, $^2J_{\text{C-F}} = 28.4$ Hz), 13.5 ppm; ^{19}F NMR (376 MHz, CDCl_3): $\delta = -86.6$ (dq, $^2J = 231.5$ Hz, $J_{\text{F-H}} = 19.0$ Hz, 1F), (-99.9) – (-100.2) (m including app. d, $^2J = 231.5$ Hz, 1F); $\bar{\nu}/(\text{film}) = 2954, 2361, 2342, 1717, 1329, 1236, 1167, 1084, 1051$ cm^{-1} ; MS (CI): m/z (%): 253 (21) $[\text{M}+\text{H}]^+$, 233 (49) $[\text{M}-\text{F}]^+$, 207 (100) $[\text{M}-\text{OEt}]^+$; HRMS (APCI): calcd for $\text{C}_{14}\text{H}_{15}\text{F}_2\text{O}_2$, 253.1035 $[\text{M}+\text{H}]^+$ found 253.1035; t_{R} (GC) = 12.35 minutes.

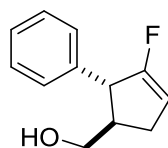
Preparation of ((1R*,5R*)-4,4-difluoro-5-phenylcyclopent-2-en-1-yl)methanol (161)



An oven dried round bottom flask containing lithium aluminium hydride (10 mg, 0.27 mmol) was sealed with a SubaSeal and connected to an argon/vacuum manifold, and the atmosphere was purged three times. Anhydrous diethyl ether (0.5 mL) was added and the grey suspension was cooled to 0 °C. Ester **153** (48 mg, 0.19 mmol) in anhydrous diethyl ether (0.5 ml) was added dropwise to the reaction mixture and stirred under argon at 0 °C from 1 hour. The reaction mixture was allowed to warm to room temperature and stirred for a further 4.5 hours. The reaction mixture was then cooled to 0 °C and quenched with H_2O (0.5 ml), 10% aqueous NaOH (0.5 ml) then H_2O (0.5 ml) dropwise in that order. The reaction mixture was allowed to warm to room temperature and stirred for 20 minutes until the excess LiAlH_4 was fully quenched (solid white precipitate formed). Ethyl acetate (20 mL) was added and the organic layer separated. The aqueous layer was extracted with ethyl acetate (2 x 20 mL). The original organic layer and extracts were combined, dried (MgSO_4) and concentrated under reduced pressure to remove volatile materials. ^{19}F NMR of the crude reaction mixture showed 78%

conversion to **161**. Column chromatography on silica gel (1:1 Et₂O in hexane) afforded alcohol **161** as a yellow oil (20 mg, 51%). *R_f* = 0.13 (1:1 Et₂O in hexane); ¹H NMR (400 MHz, CDCl₃): δ = 7.41-7.32 (m, ArH, 5H), 6.50 (br. dt, *J* = 6.1 Hz, 1.5 Hz, ⁴*J*_{H-F} = 1.5 Hz, CH=CH, 1H), 6.06 (dd, *J* = 6.0, 2.2 Hz, CF₂CH=CH, 1H), 3.84 (dd, ²*J* = 10.6 Hz, *J* = 4.9 Hz, HOCH_aH_b, 1H), 3.67 (dd, ²*J* = 10.6 Hz, *J* = 5.7 Hz, HOCH_aH_b, 1H), 3.45 (ddd, *J*_{H-F} = 17.2, 13.8 Hz, *J* = 6.6 Hz, PhCH, 1H), 3.30-3.21 (m, HOCH₂CH, 1H), 1.62 ppm (br. s, OH, 1H); ¹³C NMR (100 MHz, CDCl₃): δ = 141.8 (t, *J*_{C-F} = 10.4 Hz), 134.5 (d, *J*_{C-F} = 2.4 Hz), 130.0 (t, ¹*J*_{C-F} = 245.5 Hz), 128.9, 128.02 (dd, ²*J*_{C-F} = 29.4, 25.9 Hz), 127.99, 127.2, 62.8 (d, ⁴*J*_{C-F} = 4.8 Hz), 53.1 (t, ²*J*_{C-F} = 23.6), 51.9 ppm (d, *J*_{C-F} = 5.0 Hz); ¹⁹F NMR (376 MHz, CDCl₃): δ = -88.1 (dd, ²*J* = 250.8 Hz, *J*_{F-H} = 17.2, 9.5 Hz, 1F), -92.3 ppm (ddd, ²*J* = 251.4 Hz, *J*_{F-H} = 13.8, 4.7 Hz, 1F); $\bar{\nu}$ /(film) = 3370, 2930, 2867, 2359, 2342, 1497, 1450, 1367, 1352, 1200, 1172, 1019 cm⁻¹; MS (CI): *m/z* (%): 213 (4), 201 (10), 191 (32) [M-F]⁺, 173 (100) [(M+H)-F₂], 161 (15); HRMS (APCI): calcd for C₁₂H₁₆F₂ON, 228.1194 [M+NH₄]⁺ found 228.1190; *t_R* (GC) = 11.51 minutes.

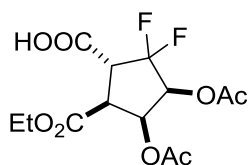
Preparation of ((1R*,2R*)-3-fluoro-2-phenylcyclopent-3-en-1-yl) methanol (**164**)



Diisobutylaluminium hydride (1.5 ml of a 1.1 M solution in cyclohexane, 1.65 mmol) was added dropwise to a solution of difluorocyclopentene **153** (100 mg, 0.4 mmol) in anhydrous toluene (5 mL) under nitrogen at -30 °C for 10 minutes. The reaction mixture was allowed to warm to -15 °C and stirred for a further 8 hours then quenched by dropwise addition of H₂O (1 mL), 0.1 M aqueous NaOH (1 mL) and H₂O (1 mL) in that order. MgSO₄ was added to quenched mixture until the solid was free flowing and the mixture was left overnight at room temperature (17 h). The resulting white emulsion was washed with EtOAc (4 x 20 mL) and the organic extracts were combined and concentrated under reduced pressure. ¹H NMR spectrum confirmed full consumption of ester. Column chromatography on silica gel (1:1 Et₂O in hexane) afforded mono-fluorinated product **164** (15 mg, 19%) as a pale yellow oil. *R_f* = 0.28 (1:1 Et₂O in hexane); ¹H NMR (400 MHz, CDCl₃): δ = 7.38-7.34

(m, ArH, 2H), 7.30-7.27 (m, ArH, 3H), 5.23 (tdd, $J = 2.7, 1.5$ Hz, $J_{H-F} = 1.0$ Hz, C(F)=CH, 1H), 3.79-3.76 (br. m, ArCH, 1H), 3.74 (m (containing d, $J = 6.4$ Hz), CH₂OH, 2H), 2.60-2.52 (m, CH-CH_aH_b-CH, 1H), 2.51-2.42 (m, CHCH₂OH, 1H), 2.18-2.11 (m, CH-CH_aH_b-CH, 1H), 1.49 ppm (br. s, OH, 1H); ¹³C NMR (100 MHz, CDCl₃): $\delta = 161.2$ (d, $^1J_{C-F} = 281.9$ Hz), 141.70 (d, $J_{C-F} = 3.4$ Hz), 128.7, 127.6, 126.9, 103.2 (d, $^2J_{C-F} = 11.5$ Hz), 65.7, 50.6 (d, $^2J_{C-F} = 20.7$ Hz), 48.5 (d, $J_{C-F} = 5.9$ Hz), 28.4 ppm (d, $J_{C-F} = 8.9$ Hz); ¹⁹F NMR (376 MHz, CDCl₃): $\delta = -124.2$ ppm (br. t, $J_{F-H} = 6.6$ Hz); $\bar{\nu}$ /(film) = 3324, 2930, 2859, 1680, 1602, 1495, 1294, 1175, 1156, 1032 cm⁻¹; MS (CI): m/z (%): 203 (6), 192 (4) [M+H]⁺, 175 (100) [M-OH]⁺, 155 (40), 143 (20), 129 (10), 115 (28), 97 (54); HRMS (ASAP): calcd for C₁₂H₁₂F, 175.0918 [M-OH]⁺, found 175.0913; t_R (GC) = 12.00 minutes.

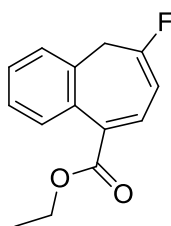
Preparation of (1R*,3S*,4S*,5S*)-3,4-diacetoxy-5-(ethoxycarbonyl)-2,2-difluorocyclopentane-1-carboxylic acid (162)



Periodic acid (456 mg, 2 mmol) was added to a solution of *bis*-acetate **159** (50 mg, 0.14 mmol) in a 2:3 mixture of MeCN (0.28 mL) and acetone (0.42 mL) and the mixture was stirred at room temperature until all of the solid dissolved to afford a clear solution (5 minutes). Ruthenium(III)chloride hydrate (6 mg, 0.02 mmol) was added and the mixture was stirred at room temperature for 19 hours. The black reaction mixture was cooled to 0 °C, diluted with diethyl ether (10 mL) and H₂O (10 mL) and stirred for 10 minutes. The organic layer was separated and the aqueous layer was extracted with diethyl ether (3 x 10 ml). The original organic layer and extracts were combined, dried (MgSO₄) and concentrated under reduced pressure to remove volatile organic solvents. The crude reaction mixture was transferred onto a pad of silica (3.2 g) in a sinter funnel which had been conditioned with 1:39:60 AcOH and EtOAc in hexane. Elution with the same solvent mixture afforded acid **162** (18 mg, 39%). $R_f = 0.35$ (1:39:60 AcOH in EtOAc in hexane); ¹H NMR (400 MHz, CDCl₃): $\delta = 5.77$ -5.65 (m, CF₂CHOAc, 1H), 5.31 (ddd, $^4J_{H-F} = 13.8$ Hz, $J = 9.2, 4.6$

Hz, CHCHOAc, 1H), 4.71 (br. s. HO₂C, 1H), 4.23 (q, *J* = 7.2 Hz, OCH_aH_bCH₃, 1H), 4.19 (q, *J* = 7.2 Hz, OCH_aH_bCH₃, 1H), 3.99 (ddd, *J*_{H-F} = 17.4, 13.2 Hz, *J* = 11.7 Hz, HO₂CCH, 1H), 3.62 (dd, *J* = 11.5, 4.8 Hz, EtO₂CCH, 1H), 2.12 (s, COCH₃, 3H), 2.07 (s, COCH₃, 3H), 1.25 ppm (t, *J* = 7.2 Hz, OCH₂CH₃, 3H); ¹⁹F NMR (376 MHz, CDCl₃): δ = -98.7 (ddd, ²*J* = 240.9 Hz, *J*_{F-H} = 17.4, ⁴*J*_{F-H} = 9.0 Hz, 1F), -99.9 ppm (ddd, ²*J* = 241.7 Hz, *J*_{F-H} = 13.8, 12.2 Hz, 1F); $\bar{\nu}$ /(film) = 2930, 2361, 2342, 1736, 1375, 1213 cm⁻¹.

Preparation of Ethyl 6-fluoro-5H-benzo[7]annulene-9-carboxylate (**154b**)



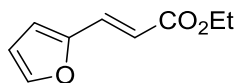
A solution of **154a** (28 mg, 0.07 mmol) in diphenyl ether (0.5 mL) was heated to 180 °C in a sealed microwave vial for 17.5 hours in a DrySyn block. After cooling and venting the vial, the crude reaction mixture was transferred onto a pad of silica (1.5 g) in a sinter funnel which had been conditioned with hexane. Diphenyl ether was eluted using hexane, then a mixture of **154a** and **154b** was eluted with diethyl ether (19 mg, 68% yield, 94% conversion to **154b** by ¹⁹F NMR). *R*_f = 0.21 (1:9 diethyl ether/hexane); ¹H NMR (400 MHz, CDCl₃): δ = 7.61 (dd, *J* = 7.9 Hz, ⁴*J* = 1.0 Hz, ArH, 1H), 7.55 (dd, ⁴*J*_{H-F} = 6.7 Hz, *J* = 6.5 Hz, HC=CCO₂Et, 1H), 7.45-7.23 (m, ArH, 3H), 5.81 (dd, *J*_{H-F} = 11.1 Hz, *J* = 6.5 Hz, HC=CF, 1H), 4.37 (q, *J* = 7.2 Hz, COCH₂CH₃, 2H), 3.34 (d, *J*_{H-F} = 16.7 Hz, CH₂CF, 2H), 1.39 ppm (t, *J* = 7.2 Hz, COCH₂CH₃, 3H); ¹³C NMR (100 MHz, CDCl₃): δ = 167.0, 160.0 (d, ¹*J*_{C-F} = 285.6 Hz), 135.8, 132.9 (*J*_{C-F} = 11.1 Hz), 132.5, 132.4, 128.9, 128.8, 126.9, 125.5, 101.8 (d, ²*J*_{C-F} = 23.1 Hz), 60.7, 36.4 (d, ²*J*_{C-F} = 26.3 Hz), 13.8 ppm; ¹⁹F NMR (376 MHz, CDCl₃): δ = -82.7 ppm (tdd, *J*_{F-H} = 16.7, 11.1 Hz, ⁴*J*_{F-H} = 6.7 Hz, 1F); $\bar{\nu}$ /(film) = 2359, 2342, 1713, 1659, 1225 cm⁻¹; MS (CI): *m/z* (%): 261 (10) [M+C₂H₅]⁺, 233 (100) [M+H]⁺, 213 (32) [M-F], 187 (64) [M-OEt], 159 (38) [M-CO₂Et]; HRMS (APCI): C₁₄H₁₄FO₂, 233.0972 [M+H]⁺ found 233.0968; *t*_R (GC) = 12.652 minutes.

7.5. Compounds from Chapter 3

6.5.1. Experimental Procedure

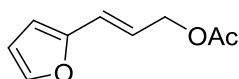
General Procedure D: Alkenoate Synthesis using Wittig Chemistry

Preparation of ethyl 3-(2'-furyl) prop-2*E*-enoate (**192a**)



(Carbethoxymethylene)triphenylphosphorane (3.7 g, 10.4 mmol) was added to a solution of furfural **191a** (0.79 mL, 9.5 mmol) in anhydrous DCM (50 mL) and the reaction mixture stirred at room temperature under nitrogen for 7 hours. An aliquot was taken and TLC confirmed full conversion of aldehyde. The reaction mixture was concentrated under reduced pressure and column chromatography on silica gel (1:9 Et₂O in hexane) afforded alkenoate **192a** (1.36 g, 82%) as a yellow oil. R_f = 0.31 (1:4 Et₂O in hexane); ¹H NMR (400 MHz, CDCl₃): δ = 7.49 (d, J = 1.8 Hz; ArH, 1H), 7.45 (d, J = 15.8 Hz, ArCH=CH, 1H), 6.62 (d, J = 3.4 Hz, ArH, 1H), 6.48 (dd, J = 3.4, 1.8 Hz, ArH, 1H), 6.33 (d, J = 15.8 Hz, ArCH=CH, 1H), 4.26 (q, J = 7.1 Hz, OCH₂CH₃, 2H), 1.34 ppm (t, J = 7.1 Hz, OCH₂CH₃, 3H); ¹³C NMR (100 MHz, CDCl₃): δ = 166.5, 150.5, 144.1, 130.4, 115.5, 114.0, 111.7, 59.9, 13.8 ppm; $\bar{\nu}$ /(film) = 2361, 2342, 1703, 1638, 1302, 1258, 1207, 1159, 1017 cm⁻¹; MS (CI): m/z (%): 195 (12) [M+C₂H₅]⁺, 167 (100) [M+H]⁺, 139 (61), 121 (80) [M-OEt]⁺; t_R (GC) = 9.62 minutes. The data was in agreement with that reported by Lebel and Davi.²³⁹

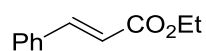
Preparation of (*E*)-3-(furan-2-yl)allyl acetate (**193a**)



Diisobutylaluminium hydride (14.0 mL of a 1.1 M solution in cyclohexane, 15.0 mmol) was added dropwise to a solution of ester **192a** (1.12 g, 5.0 mmol) in anhydrous toluene (40 mL) under nitrogen at 0 °C for 10 minutes. The reaction mixture was allowed to warm to room temperature and stirred for a further 8 hours, cooled to 0 °C and quenched by dropwise addition of H₂O (1 mL), 0.1 M aqueous NaOH (1 mL) and H₂O (1 mL) in that order. MgSO₄ was added to quenched mixture until the solid was free flowing and the mixture was left overnight at room

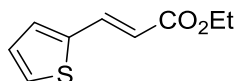
temperature (17 h). The resulting white emulsion was washed with EtOAc (3 x 50 mL) and the organic extracts were combined and concentrated under reduced pressure. ^1H NMR spectrum confirmed full conversion to the corresponding alcohol (603 mg, 97%) which was directly acetylated without further purification. Acetic anhydride (0.78 ml, 8.3 mmol) was added dropwise to a solution of crude alcohol (860 g, 6.9 mmol) and pyridine (0.67 ml, 8.3 mmol) in DCM (7 mL) under nitrogen and the reaction mixture was heated to 45 °C for 5 hours. The TLC of the reaction mixture showed complete consumption of alcohol. H_2O (20 mL) was added to the reaction mixture and the organic layer separated. The aqueous layer was extracted with DCM (2 x 10 mL) and the organic layer and extracts were combined and backwashed with HCl (2 x 20 mL of a 1 M aqueous solution), NaOH (3 x 20 mL of a 10 M aqueous solution) and aqueous NaCl (20 mL) in that order. The resulting organic layer was dried (MgSO_4) and concentrated under reduced pressure. Any remaining pyridine in the resulting oil was removed by co-evaporation with toluene (2 x 25 mL) to afford acetate **193a** as a colourless oil (950 g, 83%). $R_f = 0.43$ (1:4 Et_2O in hexane); ^1H NMR (400 MHz, CDCl_3): $\delta = 7.37$ (d, $J = 1.8$ Hz, ArH, 1H), 6.49 (dt, $J = 15.8$ Hz, $^4J = 1.3$ Hz, ArCH=CHCH₂, 1H), 6.40 (dd, $J = 3.5, 1.8$ Hz, ArH, 1H), 6.30 (d, $J = 3.4$ Hz, ArH, 1H), 6.23 (dt, $J = 15.8, 6.5$ Hz, CH=CHCH₂, 1H), 4.72 (dd, $J = 6.4$ Hz, $^4J = 1.3$ Hz, CH₂OAc, 2H), 2.12 ppm (s, COCH₃, 3H); ^{13}C NMR (100 MHz, CDCl_3): $\delta = 170.3, 151.3, 141.9, 121.6, 121.2, 110.9, 108.4, 64.1, 20.5$ ppm; $\bar{\nu}/(\text{film}) = 2359, 1734, 1377, 1360, 1223, 1013$ cm^{-1} ; MS (CI): m/z (%): 166 (5) [M], 123 (8) [M-COMe]⁺, 107 (100) [M-OAc]⁺, 61 (75); t_R (GC) = 10.26 minutes. The data were in agreement with those reported by Iwasaki and co-workers.²⁴⁰

Preparation of cinnamyl acetate (**192b**)



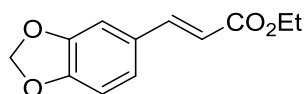
Ester **192b** was prepared from benzaldehyde **191b** (1.06 ml, 10 mmol), (carbethoxymethylene)triphenylphosphorane (3.83 g, 11.0 mmol) and DCM (20 ml) according to General Procedure D. Column chromatography on silica gel (1:4 Et_2O in hexane) afforded ester **192b** as a yellow oil (930 mg, 87%). ^1H NMR data was consistent with a commercial sample.

Preparation of ethyl 3-(2'-thiophenyl)-prop-2E-enoate (**192c**)



Ester **192c** was prepared from thiophene-2-carbaldehyde **191c** (0.92 ml, 10 mmol), (carbethoxymethylene)triphenylphosphorane (4.6 g, 11.2 mmol) and DCM (30 ml) over 20 hours according to General Procedure D. Column chromatography on silica gel (1:4 Et₂O in hexane) afforded ester **192c** as a yellow oil (1.79 g, 98%). $R_f = 0.31$ (1:1 Et₂O in hexane); ¹H NMR (400 MHz, CDCl₃): $\delta = 7.81$ (d, $J = 15.7$ Hz, ArCH=CH, 1H), 7.39 (d, $J = 5.1$ Hz, ArH, 1H), 7.27 (d, $J = 3.6$ Hz, ArH, 1H), 7.07 (dd, $J = 5.1, 3.6$ Hz, ArH, 1H), 6.26 (d, $J = 15.7$ Hz, ArCH=CH, 1H), 4.27 (q, $J = 7.0$ Hz, OCH₂CH₃, 2H), 1.35 ppm (t, $J = 7.0$ Hz, OCH₂CH₃, 3H); ¹³C NMR (100 MHz, CDCl₃): $\delta = 166.4, 139.1, 136.5, 130.3, 127.8, 127.6, 116.5, 60.0, 13.8$ ppm; $\bar{\nu}/(\text{film}) = 2358, 2342, 1703, 1624, 1369, 1304, 1202, 1159, 1042$ cm⁻¹; MS (CI): m/z (%): 211 (13) [M+C₂H₅]⁺, 183 (100) [M+H]⁺, 137 (80) [M-OEt]⁺; t_R (GC) = 11.85 minutes. The data was in agreement with that reported by Lebel and Davi.²³⁹

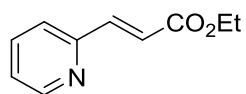
Preparation of ethyl 3-(5'-benzo[d][1,3]dioxolyl)-prop-2E-enoate (**192d**)



Ester **192d** was prepared from benzo[d][1,3]dioxole-5-carbaldehyde **191d** (1.39 g, 6.3 mmol), (carbethoxymethylene)triphenylphosphorane (3.47 g, 8.4 mmol) and DCM (30 ml) over 18 hours according to General Procedure D. Column chromatography on silica gel (1:4 Et₂O in hexane) afforded ester **192d** as a white solid (1.88 g, 98%). m.p. = 63-65 °C (obtained from powdered solid isolated after chromatography); $R_f = 0.38$ (1:4 Et₂O in hexane); ¹H NMR (400 MHz, CDCl₃): $\delta = 7.63$ (d, $J = 15.9$ Hz, ArCH=CH, 1H), 7.06 (d, $^4J = 1.6$ Hz, ArH, 1H), 7.03 (dd, $J = 8.1, ^4J = 1.6$ Hz, ArH, 1H), 6.83 (d, $J = 8.1$ Hz, ArH, 1H), 6.29 (d, $J = 15.9$ Hz, ArCH=CH, 1H), 6.03 (s, O₂CH₂, 2H), 4.28 (q, $J = 7.1$ Hz, OCH₂CH₃, 2H), 1.35 ppm (t, $J = 7.1$ Hz, OCH₂CH₃, 3H); ¹³C NMR (100 MHz, CDCl₃): $\delta = 166.7, 149.1, 147.8, 143.8, 128.4, 123.9, 115.7, 108.1, 106.0, 101.1, 59.9, 13.9$ ppm; $\bar{\nu}/(\text{film}) = 2359, 2342, 1701, 1632, 1489, 1445, 1236, 1163$ cm⁻¹; MS (CI): m/z (%): 249 (19) [M+C₂H₅]⁺, 221 (95) [M+H]⁺, 193 (12),

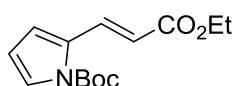
175 (100) [M-OEt]⁺, 147 (10) [M-CO₂Et]⁺; t_R (GC) = 13.91 minutes. The data was in agreement with that reported by Lebel and Davi.²³⁹

Preparation of ethyl 3-(2'-pyridyl)-prop-2E-enoate (**192e**)



Ester **192e** was prepared from picolinaldehyde **191e** (0.57 ml, 6 mmol), (carbethoxymethylene)triphenylphosphorane (2.7 g, 6.6 mmol) and DCM (25 ml) according to General Procedure D. Column chromatography on silica gel (1:1 Et₂O in hexane) afforded ester **192e** as a yellow oil (930 mg, 87%). R_f = 0.34 (1:1 Et₂O in hexane); ¹H NMR (400 MHz, CDCl₃): δ = 8.66 (br. d, *J* = 4.7 Hz, ArH, 1H), 7.72 (td, *J* = 7.8 Hz, ⁴*J* = 1.9 Hz, ArH, 1H), 7.70 (d, *J* = 15.7 Hz, ArCH=CH, 1H), 7.44 (dt, *J* = 7.8 Hz, ⁴*J* = 1.0 Hz, ArH, 1H), 7.27 (ddd, *J* = 7.8, 4.7 Hz, ⁴*J* = 1.0 Hz, ArH, 1H), 6.93 (d, *J* = 15.7 Hz, ArCH=CH, 1H), 4.29 (q, *J* = 7.14 Hz, OCH₂CH₃, 2H), 1.35 ppm (t, *J* = 7.14 Hz, OCH₂CH₃, 3H); ¹³C NMR (100 MHz, CDCl₃): δ = 166.3, 152.5, 149.6, 142.8, 136.2, 123.7, 123.6, 122.0, 60.2, 13.8 ppm; ν̄/(film) = 2981, 2359, 2342, 1717, 1201, 1167 cm⁻¹; MS (CI): *m/z* (%): 218 (5) [M+C₃H₅]⁺, 206 (10) [M+C₂H₅]⁺, 178 (100) [M+H]⁺, 150 (15), 132 (20) [M-OEt]⁺; t_R (GC) = 12.10 minutes. The data was in agreement with that reported by Lebel and Davi.²³⁹

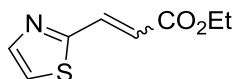
Preparation of ethyl 3-(2'-pyrrolyl-1-carboxylic acid *tert*-butyl ester)-prop-2E-enoate (**192f**)



Ester **192f** was prepared from aldehyde **191f** (3.9 g, 20 mmol), (carbethoxymethylene)triphenylphosphorane (9.25 g, 26 mmol) and DCM (125 ml) according to General Procedure A. Column chromatography (1:19 Et₂O in hexane to 1:4 Et₂O in hexane) afforded alkenoate **192f** as a yellow oil (3.4 g, 60%). R_f = 0.40 (1:4 Et₂O in hexane); ¹H NMR (400 MHz, CDCl₃): δ = 8.30 (d, *J* = 15.9 Hz, ArCH=CH, 1H), 7.42 (br. dd, *J* = 3.6 Hz, ⁴*J* = 1.6 Hz, ArH, 1H), 6.72-6.70 (m, ArH, 1H), 6.23 (t, *J* = 3.6 Hz, ArH, 1H), 6.22 (d, *J* = 15.9 Hz, CH=CHCO₂Et, 1H), 4.26 (q, *J* = 7.1 Hz, OCH₂CH₃, 2H), 1.65 (s, OC(CH₃)₃, 9H), 1.3 ppm (t, *J* = 7.1 Hz, OCH₂CH₃, 3H); ¹³C NMR (100 MHz,

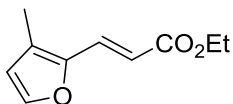
CDCl₃): δ = 166.6, 148.5, 134.4, 130.6, 124.3, 116.1, 114.3, 110.9, 84.4, 59.8, 27.5, 13.9 ppm; $\bar{\nu}$ /(film) = 2976, 1742, 1705, 1621, 1316, 1299, 1245, 1158, 1117 cm⁻¹; MS (CI): m/z (%): 194 (12) [M+ C₂H₅-Pyrrolyl-N-Boc]⁺, 166 (50) [M-Pyrrolyl-N-Boc]⁺, 120 (100); t_R (GC) = 12.58 minutes. The data was in agreement with that reported by Jeffrey and co-workers.²⁴¹

Preparation of ethyl 3-(2'-thiazolyl)-prop-2E-enoate (**192g**)



Aldehyde **191g** was synthesised from thiazole (1.75 mL, 25 mmol), DMF (3.9 mL, 20 mmol), BuLi (14.3 mL of a 2.1 M in THF, 30 mmol) in THF (100 mL) according to Glorius and co-workers¹⁹⁵ as a yellow oil. ¹H NMR confirmed full conversion to aldehyde. Ester **192g** was prepared from crude aldehyde **191g** (assumed 25 mmol), (carbethoxymethylene)triphenylphosphorane (9.75 g, 27 mmol) and DCM (150 ml) according to general procedure A. Column chromatography (7:20 Et₂O in hexane) afforded ester **192g** as a yellow oil (3.38 g, 74%) with a 4:1 mixture of alkene isomers (*E*-isomer major). **Data for Mixture:** R_f = 0.20 (1:4 Et₂O in hexane); $\bar{\nu}$ /(film) = 2978, 1708, 1630, 1468, 1480, 1299, 1266, 1175 1030 cm⁻¹; HRMS (FTMS): calcd. for C₈H₁₀O₂N₁S₁, 184.0423 [M+H]⁺ found 184.0427. **Data for E-192g:** ¹H NMR (400 MHz, CDCl₃): δ = 7.94 (d, *J* = 3.3 Hz, ArH, 1H), 7.82 (d, *J* = 15.9 Hz, ArCH=CH, 1H), 7.45 (d, *J* = 3.3 Hz, ArH, 1H), 6.77 (d, *J* = 15.9 Hz, CH=CHCO₂Et, 1H), 4.31 (q, *J* = 7.3 Hz, OCH₂CH₃, 2H), 1.36 ppm (t, *J* = 7.3 Hz, CH₂CH₃, 3H); ¹³C NMR (100 MHz, CDCl₃): δ = 165.3, 162.9, 144.2, 135.2, 122.5, 120.8, 60.3, 13.7 ppm; MS (CI): m/z (%): 224 (17), [M+C₃H₅]⁺, 212 (25) [M+C₂H₅]⁺, 184 (100) [M+H]⁺, 156 (42), 138 (59) [M-OEt]; t_R (GC) = 11.83 minutes. **Data for Z-192g:** ¹H NMR (400 MHz, CDCl₃): δ = 7.97 (d, *J* = 3.3 Hz, ArH, 1H), 7.57 (dd, *J* = 3.3 Hz, ⁵*J* = 1.0 Hz, ArH, 1H), 7.37 (dd, *J* = 12.7 Hz, ⁵*J* = 1.0 Hz, ArCH=CH, 1H), 6.15 (d, *J* = 12.7 Hz, CH=CHCO₂Et, 1H), 4.32 (q, *J* = 7.2 Hz, OCH₂H₃, 2H), 1.37 ppm (t, *J* = 7.2 Hz, CH₂H₃, 3H); ¹³C NMR (100 MHz, CDCl₃): δ = 165.3, 160.2, 142.6, 136.4, 123.7, 118.9, 60.2, 13.6 ppm; MS (CI): m/z (%): 224 (11), [M+C₃H₅]⁺, 212 (18) [M+C₂H₅]⁺, 184 (100) [M+H]⁺, 156 (20), 138 (97) [M-OEt]; 112 (14); t_R (GC) = 11.59 minutes.

Preparation of ethyl 3-(2'-furyl-3-methyl)-prop-2E-enoate (**192h**)

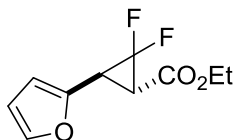


Diisobutylaluminium hydride (50 mL of a 0.9 M solution in cyclohexane, 45 mmol) was added dropwise to a solution of methyl 3-methyl-2-furoate (2.04 g, 14.6 mmol) in anhydrous toluene (120 mL) under nitrogen at -78 °C for 5 minutes. The reaction mixture was allowed to warm to room temperature and stirred for a further 8 hours, cooled to -78 °C and quenched with aqueous potassium sodium tartrate tetrahydrate (sat. Rochelle salt, 40 mL) and EtOAc (50 mL). The resulting organic layer was separated and collected. The aqueous layer was extracted further with EtOAc (50 mL x 6) and the separated extracts combined with the original organic layer, dried (MgSO₄) and concentrated under reduced pressure to afford (3-methylfuran-2-yl)methanol as a yellow oil (1.33 g 81%). ¹H NMR confirmed full conversion to desired alcohol which was used without further purification. Bis(acetoxy)iodobenzene (BAIB, 4.18 g, 13 mmol) was added to a solution of (3-methylfuran-2-yl)methanol (1.33 g, 11.8 mmol), TEMPO (184 mg, 1.18 mmol), in anhydrous DCM (90 mL) and the reaction mixture was stirred at room temperature under nitrogen for 4 hours. The ¹H NMR spectrum of a reaction aliquot showed complete conversion to corresponding aldehyde **191h**. (Carbethoxymethylene)triphenylphosphorane (5.2 g, 15 mmol) was then added and the reaction mixture stirred for 17 hours. ¹H NMR of a reaction aliquot showed complete consumption of aldehyde. The resulting orange solution was concentrated under reduced pressure and column chromatography on silica gel (2:25 Et₂O in hexane) afforded alkenoate **192h** as a yellow oil (1.26 g, 45%). R_f = 0.44 (1:10 Et₂O in hexane); $\bar{\nu}$ /(film) = 2976, 1703, 1632, 1299, 1253, 1164 cm⁻¹; ¹H NMR (400 MHz, CDCl₃): δ = 7.50 (d, *J* = 15.5 Hz, ArCH=CH, 1H), 7.40 (dq, *J* = 1.6 Hz, ⁴*J* = 0.5 Hz, ArH, 1H), 6.34 (d, *J* = 1.6 Hz, ArH, 1H), 6.26 (d, *J* = 15.5 Hz, CH=CHCO₂Et, 1H), 4.27 (q, *J* = 7.1 Hz, OCH₂H₃, 2H), 2.18 (s, ArCH₃, 3H), 1.35 ppm (t, *J* = 7.1 Hz, CH₂CH₃, 3H); ¹³C NMR (100 MHz, CDCl₃): δ = 166.9, 146.6, 143.4, 128.5, 125.1, 114.1, 113.5, 59.7, 13.8, 9.7 ppm; MS (CI): *m/z* (%): 209 (18), [M+C₂H₅]⁺, 181 (100), [M+H]⁺, 153 (12),

135 (72), [M-OEt]; HRMS (NSI): calcd. for C₁₀H₁₃O₃, 181.0859 [M+H]⁺ found 184.0857; t_R (GC) = 11.43 minutes.

General Procedure E: Difluorocyclopropanation of Alkenoates **192** with MDFA

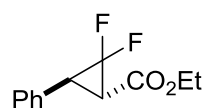
Preparation of ethyl (1S*,3S*)-2,2-difluoro-3-(fur-2-yl)cyclopropane-1-carboxylate (194a)



An oven dried two-necked round bottom flask containing potassium iodide (1.87 g, 11.2 mmol) was sealed with a SubaSeal, and the salt was stirred and lightly flame dried under an atmosphere of argon. A low boiling point water condenser with a gas outlet connected to an argon/vacuum manifold was fitted to the reaction flask and the atmosphere was purged three times. Alkenoate **192a** (1.48 g, 8.9 mmol) followed by diglyme (1.43 mL) were added and the yellow suspension purged with argon/vacuum once and then heated to 120 °C. Once the reaction temperature had been reached, TMSCl (2.9 mL, 22.3 mmol) and MDFA (2.9 mL, 22.3 mmol) were added dropwise in that order. After 4 hours, the black reaction mixture was allowed to cool to room temperature and the reaction mixture was quenched with aqueous NH₄Cl (10 mL) and diethyl ether (10 mL) was added. The organic layer was separated and the aqueous layer was extracted with diethyl ether (3 x 10 mL). The original organic layer and the extracts were combined, dried (MgSO₄) and concentrated under reduced pressure to remove volatile materials. The ¹H NMR spectrum of the resulting brown oil confirmed 66% conversion to difluorocyclopropyl **194a**. Column chromatography on silica gel (1:20 Et₂O in hexane) afforded difluorocyclopropyl **194a** as a yellow oil (760 mg, 40%) and recovered starting alkenoate **192a** (340 mg, 23%). R_f = 0.4 (1:19 Et₂O in hexane); ¹H NMR (400 MHz, CDCl₃): δ = 7.39 (dd, J = 2.0 Hz, ⁴J = 0.8 Hz, ArH, 1H), 6.38 (dd, J = 3.4, 2.0 Hz, ArH, 1H), 6.29 (dd, J = 3.4 Hz, ⁴J = 0.8 Hz, ArH, 1H), 4.28 (q, J = 7.1 Hz, OCH₂CH₃, 2H), 3.48 (ddd, J_{H-F} = 12.3 Hz, J = 7.7 Hz, ⁴J_{H-F} = 1.8 Hz, ArCHCF₂, 1H), 2.79 (dd, J_{H-F} = 13.4 Hz, J = 7.7 Hz, CF₂CHCO₂Et, 1H), 1.34 ppm (t, J = 7.2 Hz, OCH₂CH₃,

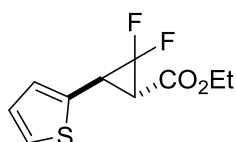
3H); ^{13}C NMR (100 MHz, CDCl_3): δ = 165.5, 145.1, 142.6, 110.6, 108.8 (dd, $^1J_{\text{C-F}}$ = 294.6, 289.7 Hz) 108.4, 61.9, 32.1 (t, $^2J_{\text{C-F}}$ = 10.9 Hz), 26.7 (dd, $^2J_{\text{C-F}}$ = 13.3, 8.9 Hz) 14.1 ppm; ^{19}F NMR (376 MHz, CDCl_3): δ = -133.1 (dd, 2J = 151.7 Hz, $J_{\text{F-H}}$ = 13.4 Hz, 1F), -135.1 ppm (dd, 2J = 152.8 Hz, $J_{\text{F-H}}$ = 12.2 Hz, 1F); $\bar{\nu}$ /(film) = 2986, 2932, 2359, 2342, 1736, 1447, 1331, 1290, 1153, 1009 cm^{-1} ; MS (CI): m/z (%): 257 (4) $[\text{M}+\text{C}_3\text{H}_5]^+$, 245 (9) $[\text{M}+\text{C}_2\text{H}_5]^+$, 217 (45) $[\text{M}+\text{H}]^+$, 197 (100) $[\text{M}-\text{F}]^+$, 189 (58), 171 (42) $[\text{M}-\text{OEt}]^+$, 169 (70) $[(\text{M}+\text{H})-\text{F}-\text{Et}]^+$, 143 (20), 125 (16); t_{R} (GC) = 9.49 minutes; HRMS (APCI): calcd for $\text{C}_{10}\text{H}_{11}\text{F}_2\text{O}_3$, 217.0668 $[\text{M}+\text{H}]^+$ found 217.0671.

Preparation of ethyl (1S*,3S*)-2,2-difluoro-3-phenylcyclopropane-1-carboxylate (194b)



The preparation of ester **194b** was attempted from alkenoate **192b** (0.67 mL, 4.03 mmol), MDFA (2.6 mL, 10 mmol), TMSCl (2.6 mL, 10 mmol), potassium iodide (1.87 g, 11.2 mmol) and diglyme (1.4 mL) according to General Procedure E with a total reaction time of 24 hours. The resulting ^1H NMR of the crude reaction mixture after work up confirmed incomplete conversion of **192b** (28% conv. to **194b**). The reaction was repeated using commercial ethyl cinnamate (**192b**) according to general procedure E on twice the scale. The resulting ^1H spectrum of the resulting brown oil confirmed incomplete conversion of **192b** (29% conv. to **194b**).

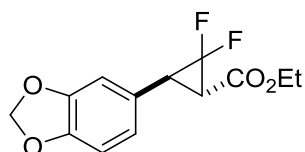
Preparation of ethyl (1S*,3R*)-2,2-difluoro-3-(thiophen-2-yl)cyclopropane-1-carboxylate (194c)



Ester **192c** was prepared from alkenoate **192c** (1.45 mg, 8 mmol), MDFA (2.6 mL, 20 mmol), TMSCl (2.6 mL, 20 mmol), potassium iodide (3.68 g, 22.6 mmol) and diglyme (1.3 mL) according to general procedure E with a reaction time of 4 hours. ^1H NMR of the resulting crude product showed 77% conversion to desired ester **194c**.

Column chromatography on silica gel (1:19 Et₂O in hexane) afforded ester **194c** as a yellow oil (1.32 g, 71%) and recovered alkenoate **192c** (310 mg, 21%). *R_f* = 0.42 (1:24 Et₂O in hexane); ¹H NMR (500 MHz, CDCl₃): δ = 7.26 (dd, *J* = 3.3, 3.1 Hz, ArH, 1H), 7.00 (d, *J* = 3.3 Hz, ArH, 1H), 7.00 (d, *J* = 3.1 Hz, ArH, 1H), 4.27 (q, *J* = 7.2 Hz, OCH₂CH₃, 2H), 3.63 (ddd, *J*_{H-F} = 13.1, 2.3 Hz, *J* = 7.7 Hz, ArCH, 1H), 2.67 (dd, *J*_{H-F} = 13.6, *J* = 7.7 Hz, CHCO₂Et, 1H), 1.33 ppm (t, *J* = 7.2 Hz, OCH₂CH₃, 3H); ¹³C NMR (100 MHz, CDCl₃): δ = 165.7, 133.3, 127.0, 126.7, 125.4, 110.4 (dd, ¹*J*_{C-F} = 296.8, 290.3 Hz), 61.9, 34.5 (²*J*_{C-F} = 10.9 Hz), 28.6 (dd, ²*J*_{C-F} = 13.0, 9.2 Hz), 14.1 ppm; ¹⁹F NMR (376 MHz, CDCl₃): δ = -132.8 (ddd, ²*J*_{F-F} = 151.7 Hz, *J*_{F-H} = 13.6, 2.4 Hz, 1F), -134.2 ppm (dd, ²*J*_{F-F} = 151.2 Hz, *J*_{F-H} = 13.3 Hz, 1F); $\bar{\nu}$ /(film) = 2965, 2359, 2342, 1732, 1466, 1431, 1325, 1285, 1215, 1152, 1009 cm⁻¹; MS (CI): *m/z* (%): 261 (7) [M+C₂H₅]⁺, 233 (33) [M+H]⁺, 213 (100) [M-F]⁺, 205 (43), 187 (36), 185 (66) [M-(F+Et)]⁺, 159 (16), 139 (18); HRMS (APCI): calcd for C₁₀H₁₄F₂O₂S₁N₁, 250.0708 [M+NH₄]⁺ found 250.0706; *t_R* (GC) = 11.15 minutes.

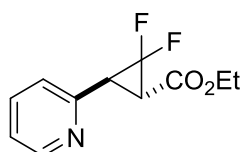
Preparation of ethyl (1S*,3S*)-3-(benzo[d][1,3]dioxol-5-yl)-2,2-difluorocyclopropane-1-carboxylate (194d)



Ester **194d** was prepared from alkenoate **192d** (1.66 g, 7.5 mmol), MDFA (2.4 mL, 18.5 mmol), TMSCl (2.4 mL, 18.5 mmol), potassium iodide (3.45 g, 20.7 mmol) and diglyme (1.2 mL) according to general procedure E. ¹H NMR of the resulting crude product showed 50% conversion to desired ester **194d**. Column chromatography on silica gel (1:9 Et₂O in hexane) afforded ester **194d** as a yellow oil (880 mg, 43%) and recovered alkenoate **192d** (700 mg, 42%). *R_f* = 0.59 (1:4 Et₂O in hexane); ¹H NMR (400 MHz, CDCl₃): δ = 6.82-6.73 (m, ArH, 3H), 6.00 (s, OCH₂O, 2H), 4.28 (q, *J* = 7.2 Hz, OCH₂CH₃, 2H), 3.44 (ddd, *J*_{H-F} = 13.2, 2.9 Hz, *J* = 7.9 Hz, ArCH, 1H), 2.65 (dd, *J*_{H-F} = 13.2 Hz, *J* = 7.9 Hz, CHCO₂Et, 1H), 1.34 (t, *J* = 7.2 Hz, OCH₂CH₃, 3H); ¹³C NMR (100 MHz, CDCl₃): δ = 165.8, 147.5, 146.9, 124.1, 121.3, 110.2 (t, ¹*J*_{C-F} = 294.2, 287.2 Hz), 107.9 (represents 2 carbons), 100.8, 61.3, 32.4 (dd, ²*J*_{C-F} = 11.2, 8.8 Hz), 32.0 (t, ²*J*_{C-F}

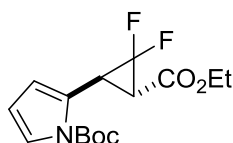
= 11.1 Hz) 13.6 ppm; ^{19}F NMR (376 MHz, CDCl_3): δ = -133.1 (dd, $^2J_{\text{F-F}} = 151.9$ Hz, $J_{\text{F-H}} = 13.6$ Hz, 1F), -134.1 (ddd, $^2J_{\text{F-F}} = 151.3$ Hz, $J_{\text{F-H}} = 13.5, 2.7$ Hz, 1F), $\bar{\nu}/(\text{film}) = 2359, 2342, 1732, 1506, 1466, 1449, 1290, 1242, 1213, 1152, 1038, 1013, 989$ cm^{-1} ; MS (CI): m/z (%): 299 (19) $[\text{M}+\text{C}_2\text{H}_5]^+$, 271 (44) $[\text{M}+\text{H}]^+$, 251 (94) $[\text{M}-\text{F}]^+$, 223 (75) $[(\text{M}+\text{H})-\text{F}-\text{OEt}]^+$, 206 (24), 197 (26) $[\text{M}-\text{CO}_2\text{Et}]^+$, 177 (100); HRMS (APCI): calcd for $\text{C}_{13}\text{H}_{13}\text{F}_2\text{O}_4$, 271.0776 $[\text{M}+\text{H}]^+$ found 271.0776; t_{R} (GC) = 13.50 minutes.

Preparation of ethyl (1*S,3*S**)-2,2-difluoro-3-(pyridin-2-yl)cyclopropane-1-carboxylate (194e)**



The preparation of ester **194e** was attempted from alkenoate **192e** (400 mg, 2.3 mmol), MDFA (0.74 mL, 5.7 mmol), TMSCl (0.74 mL, 5.7 mmol), potassium iodide (1.1 g, 6.6 mmol) and diglyme (0.45 mL) according to general procedure E with a total reaction time of 4 hours. The resulting ^1H NMR of the resulting crude black solid showed diglyme and diethyl ether with trace amounts of alkenoate **192e**. The desired product **194e** was not observed (0% conversion).

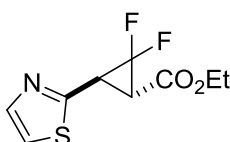
Preparation of ethyl (1*S,3*S**)-2,2-difluoro-3-(2'-pyrrolyl-1-carboxylic acid *tert*-butyl ester)cyclopropane-1-carboxylate (194f)**



Ester **194f** was prepared from alkenoate **192f** (2.12 g, 8 mmol), MDFA (2.6 mL, 20 mmol), TMSCl (2.6 mL, 20 mmol), potassium iodide (3.74 g, 22.4 mmol) and diglyme (1.6 mL) according to general procedure E. ^1H NMR of the resulting crude product showed 92% conversion to desired product. Column chromatography on silica gel (1:20 Et_2O in hexane) afforded ester **194f** as a yellow oil (1.37 g, 54%) and recovered alkenoate **192f** (140 mg, 7%). $R_f = 0.35$ (1:4 Et_2O in hexane); ^1H NMR (400 MHz, CDCl_3): δ = 7.29 (ddd, $J = 3.3$ Hz, $^4J = 1.7$ Hz, $^5J = 0.7$ Hz, ArH, 1H), 6.17-6.15 (br. m, ArH, 1H), 6.14 (t, $J = 3.4$ Hz, ArH, 1H), 4.28 (ABq, $J = 7.4$ Hz, $^2J = 3.1$ Hz, $\text{OCH}_a\text{H}_b\text{CH}_3$,

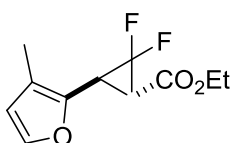
2H), 3.73 (br. dd, $J_{\text{H-F}} = 12.8$ Hz, $J = 7.8$ Hz, ArCH, 1H), 2.63 (dd, $J = 13.4$ Hz, $J = 7.8$ Hz, HCCO_2Et , 1H), 1.63 (s, $\text{C}(\text{CH}_3)_3$, 9H), 1.34 (t, $J = 7.2$ Hz, CH_2CH_3 , 3H); ^{13}C NMR (100 MHz, CDCl_3): $\delta = 165.7, 148.4, 124.0, 122.1, 112.9, 110.3$ (dd, $^1J_{\text{C-F}} = 297.3, 287.2$ Hz), 109.6, 84.1, 61.1, 31.7 (t, $^2J_{\text{C-F}} = 10.9$ Hz), 27.6 (t, $^2J_{\text{C-F}} = 12.9, 8.0$ Hz), 27.5, 13.7 ppm; ^{19}F NMR (376 MHz, CDCl_3): $\delta = -133.4$ (dd, $^2J = 149.8$ Hz, $J_{\text{F-H}} = 12.8$ Hz, CF_aF_b , 1F), -134.9 ppm (dd, $^2J = 149.8$ Hz, $J_{\text{F-H}} = 13.4$ Hz, CF_aF_b , 1F); $\bar{\nu}/(\text{film}) = 2980, 1742, 1459, 1325, 1158, 1128$ cm^{-1} ; MS (CI): m/z (%): 224 (17) $[\text{M}-(\text{F}+\text{CO}_2\text{Et})+\text{H}]^+$, 196 (100) $[\text{M}-(\text{F}+\text{Boc})+\text{H}]^+$, 168 (29), 150 (72) $[\text{M}-(\text{N-Boc-pyrrolyl})+\text{H}]^+$; HRMS (APCI): calcd for $\text{C}_{15}\text{H}_{23}\text{F}_2\text{N}_2\text{O}_4$, 333.1620 $[\text{M}+\text{NH}_4]^+$ found 333.1623; t_{R} (GC) = 12.07 minutes.

Preparation of ethyl (1S*,3S*)-2,2-difluoro-3-(2'-thiazolyl)cyclopropane-1-carboxylate (194g)



The preparation of ester **194g** was attempted from alkenoate **192g** (1.18 g, 6.4 mmol), MDFA (2.1 mL, 16.2 mmol), TMSCl (2.1 mL, 16.2 mmol), potassium iodide (3.0 g, 18 mmol) and diglyme (1.28 mL) according to general procedure E with a total reaction time of 4 hours. The resulting ^1H NMR of the resulting crude black solid showed diglyme and diethyl ether the desired product **194g** was not observed (0% conversion).

Preparation of ethyl (1S*,3S*)-2,2-difluoro-3-(2'-furyl-3-methyl) cyclopropane-1-carboxylate (194h)

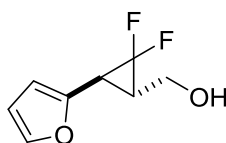


Ester **194h** was prepared from alkenoate **192h** (721 mg, 4.0 mmol), MDFA (1.3 mL, 10 mmol), TMSCl (1.3 mL, 10 mmol), potassium iodide (1.84 g, 12 mmol) and diglyme (0.7 mL) according to general procedure E. ^1H NMR of the resulting crude product showed 80% conversion to desired product. Column chromatography on silica gel (1:20 Et_2O in hexane) afforded ester **194h** as a yellow oil (417 mg, 45%)

and recovered alkenoate **192h** (136 mg, 19%). $R_f = 0.56$ (1:4 Et₂O in hexane); ¹H NMR (400 MHz, CDCl₃): $\delta = 7.26$ (d, $J = 1.8$ Hz, ArH, 1H), 6.23 (d, $J = 1.8$ Hz, ArH, 1H), 4.26 (q, $J = 7.1$ Hz, OCH₂CH₃, 2H), 3.67 (ddd, $J_{H-F} = 12.2, 2.3$ Hz, $J = 7.7$ Hz, ArCH, 1H), 2.92 (dd, $J_{H-F} = 13.5$ Hz, $J = 7.7$ Hz, HCCO₂Et, 1H), 2.05 (s, ArCH₃, 3H), 1.33 ppm (t, $J = 7.1$ Hz, CH₂CH₃, 3H); ¹³C NMR (100 MHz, CDCl₃): $\delta = 165.9, 141.4, 139.8, 119.0, 113.4, 110.1$ (t, $^1J_{C-F} = 294.1, 287.4$ Hz), 61.9, 30.8 (t, $J_{C-F} = 11.0$ Hz), 25.5 (dd, $J_{C-F} = 13.5, 9.5$ Hz), 14.1, 9.6 ppm; ¹⁹F NMR (376 MHz, CDCl₃): $\delta = -132.8$ (ddd, $^2J = 150.5$ Hz, $J_{F-H} = 13.5, 2.3$ Hz, CF_aF_b, 1F), -131.5 ppm (dd, $^2J = 150.5$ Hz, $J_{F-H} = 12.2$ Hz, CF_aF_b, 1F); $\bar{\nu}$ /(film) = 2985, 1738, 1454, 1329, 1290, 1208, 1154, 1091, 1013, 989 cm⁻¹; MS (CI): m/z (%): 259 (6) [M+C₂H₅]⁺, 231 (25) [M+H]⁺, 211 (100) [M-F]⁺, 203 (23), 185 (25) [M-OEt]⁺, 183 (28); HRMS (APCI): calcd for C₁₁H₁₁F₂O₃, 229.0671 [M-H]⁺ found 229.0676; t_R (GC) = 10.61 minutes.

General Procedure F: Reduction of Difluorocyclopropyl Ethyl Esters

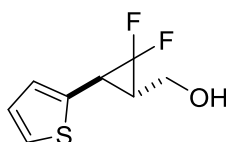
Preparation of ethyl ((1S*,3S*)-2,2-difluoro-3-(furan-2-yl)cyclopropyl)methanol (**199a**)



Diisobutylaluminium hydride (24 ml of a 1.1 M solution in cyclohexane, 23.7 mmol) was added dropwise to a solution of ester **194a** (1.71 g, 7.9 mmol) in anhydrous toluene (70 mL) under nitrogen at -78 °C over 10 minutes. The reaction mixture was allowed to warm to room temperature and stirred for a further 8 hours, then cooled to 0 °C and quenched by dropwise addition of H₂O (2 mL), 0.1 M aqueous NaOH (2 mL) and H₂O (2 mL) in that order. MgSO₄ was added to the quenched mixture until the solid was free flowing and the mixture was left overnight at room temperature (14-17 h). The resulting white emulsion was washed with EtOAc (4 x 50 mL) and the organic extracts were combined and concentrated under reduced pressure to afford alcohol **199a** as a pale yellow oil (1.3 g, 94%). $R_f = 0.19$ (1:2 Et₂O in hexane); ¹H NMR (400 MHz, CDCl₃): $\delta = 7.37$ (dd, $J = 1.9$ Hz, $^4J = 0.8$ Hz, ArH, 1H), 6.38 (dd, $J = 3.3, 1.9$ Hz, ArH, 1H), 6.21 (br. d, $J = 3.3$ Hz, ArH, 1H), 3.99-3.91 (br. m,

$\text{CH}_a\text{H}_b\text{OH}$, 1H), 3.90-3.83 (br. m, $\text{CH}_a\text{H}_b\text{OH}$, 1H), 2.64 (dd, $J_{\text{H-F}} = 13.1$ Hz, $J = 7.3$ Hz, ArCH, 1H), 2.32-2.23 (m, CHCH_2O , 1H), 1.62 ppm (br. s, CH_2OH , 1H); ^{13}C NMR (100 MHz, CDCl_3): $\delta = 146.6, 141.6, 112.1$ (t, $^1J_{\text{C-F}} = 289.0$ Hz), 110.1, 106.9, 58.6 (d, $J_{\text{C-F}} = 5.9$ Hz), 30.4 (t, $^2J_{\text{C-F}} = 9.5$ Hz), 24.2 ppm (dd, $^2J_{\text{C-F}} = 13.6, 10.6$ Hz); ^{19}F NMR (376 MHz, CDCl_3): $\delta = -135.5$ (ddd, $^2J = 158.7$ Hz, $J_{\text{F-H}} = 13.6, 2.0$ Hz, 1F), -138.3 ppm (dd, $^2J = 158.8$ Hz, $J_{\text{F-H}} = 13.1$ Hz, 1F); $\bar{\nu}$ /(film) = 2926, 2359, 2342, 1458, 1263, 1167, 1009, 736 cm^{-1} ; MS (CI): m/z (%): 175 (13) $[\text{M}+\text{H}]^+$, 157 (100) $[\text{M}-\text{OH}]^+$, 139 (13), 127 (12), 109 (18); HRMS (TOF): calcd for $\text{C}_8\text{H}_8\text{O}_2\text{F}_2$, 174.0492 [M] found 174.0496; t_{R} (GC) = 9.39 minutes.

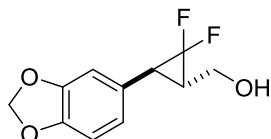
Preparation of ((1S*,3R*)-2,2-difluoro-3-(thiophen-2-yl)cyclopropyl)methanol (199b)



Alcohol **199b** was prepared from ester **194b** (272 mg, 0.85 mmol), DIBAL (2.3ml of a 1.1 M solution in cyclohexane, 2.55 mmol) and DCM (6 mL) according to general procedure F. ^1H NMR of the result crude reaction mixture confirmed 83% conversion. Column chromatography on silica gel (2:3 Et_2O in hexane) afforded alcohol **194b** as a yellow oil (81 mg, 50%). $R_f = 0.19$ (1:2 Et_2O in hexane); ^1H NMR (400 MHz, CDCl_3): $\delta = 7.23$ (dd, $J = 5.2, ^4J = 1.3$ Hz, ArH, 1H), 6.99 (dd, $J = 5.2, 3.6$ Hz, ArH, 1H), 6.95 (br. d, $J = 3.6$ Hz, ArH, 1H), 3.94 (dddd, $^2J = 12.1$ Hz, $J = 6.6, 1.1$ Hz, $^4J_{\text{H-F}} = 2.7$ Hz, $\text{CH}_a\text{H}_b\text{OH}$, 1H), 3.84 (ddd, $^2J = 12.1$ Hz, $J = 7.8, 1.6$ Hz, $\text{CH}_a\text{H}_b\text{OH}$, 1H), 2.77 (dd, $J_{\text{H-F}} = 13.6$ Hz, $J = 7.3$ Hz, ArCH, 1H), 2.33 (br. s, CH_2OH , 1H), 2.17 ppm (dddd, $J_{\text{H-F}} = 13.4$ Hz, $J = 7.8, 7.4, 6.6$ Hz, $^4J = 0.9$ Hz, CHCH_2OH , 1H); ^{13}C NMR (100 MHz, CDCl_3): $\delta = 135.1, 126.5, 125.4, 124.2, 112.7$ (t, $^1J_{\text{C-F}} = 290.1$ Hz), 58.7 (d, $J_{\text{C-F}} = 5.7$ Hz), 32.9 (t, $^2J_{\text{C-F}} = 9.6$ Hz), 26.1 ppm (dd, $^2J_{\text{C-F}} = 12.5, 11.1$ Hz); ^{19}F NMR (376 MHz, CDCl_3): $\delta = -135.4$ (ddd, $^2J = 158.0$ Hz, $J_{\text{F-H}} = 13.5$ Hz, $^4J_{\text{F-H}} = 2.7$ Hz, 1F), -137.5 ppm (dd, $^2J = 158.0$ Hz, $J_{\text{F-H}} = 13.5$ Hz, 1F); $\bar{\nu}$ /(film) = 3324, 2930, 2885, 1472, 1435, 1245, 1080, 1037, 1007 cm^{-1} ; MS (CI): m/z (%): 219 (6) $[\text{M}+\text{C}_2\text{H}_5]^+$, 191 (26) $[\text{M}+\text{H}]^+$, 173

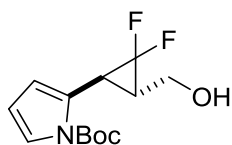
(100) $[M-OH]^+$, 153 (42) $[M-F_2]^+$, 123 (22); HRMS (ASAP): calcd for $C_8H_7F_2S_1$, 173.0231 $[M-H_2O+H]^+$ found 173.0229; t_R (GC) = 10.51 minutes.

Preparation of ((1S*,3R*)-2,2-difluoro-3-(benzo[d][1,3]dioxol-5-yl)cyclopropyl)methanol (194d)



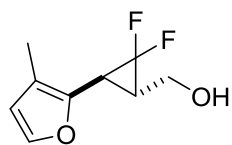
Alcohol **194d** was prepared from ester **192d** (550 mg, 2 mmol), DIBAL (1.0 M in cyclohexane, 6.0 mL, 6 mmol) and toluene (30 mL) according to general procedure F. Column chromatography on silica gel (1:1 Et₂O in hexane) afforded desired alcohol **194d** as a colourless oil (342 mg, 75%). R_f = 0.35 (1:1 Et₂O in hexane); ¹H NMR (400 MHz, CDCl₃): δ = 6.80-6.72 (m, ArH, 3H), 5.97 (s, OCH₂O, 2H), 3.95-3.83 (m, CHCH₂OH, 2H), 2.57 (ddd, J_{H-F} = 11.2 Hz, J = 7.6 Hz, 4J = 3.3 Hz, ArCH, 1H), 2.12 (dddd, J_{H-F} = 11.2 Hz, J = 7.6, 7.5, 7.1 Hz, 4J = 3.3 Hz, CHCH₂OH, 1H), 1.92 ppm (br. s, CH₂OH, 1H); ¹³C NMR (100 MHz, CDCl₃): δ = 147.3, 146.4, 126.1, 121.1, 113.1 (t, $^1J_{C-F}$ = 289.1 Hz), 108.0, 107.8, 100.6, 59.1 (d, J_{C-F} = 4.3 Hz), 30.8 (t, $^2J_{C-F}$ = 9.1 Hz), 30.7 ppm (t, $^2J_{C-F}$ = 11.1 Hz); ¹⁹F NMR (376 MHz, CDCl₃): δ = -136.5 (ddd, 2J = 158.2 Hz, J_{F-H} = 10.8 Hz, $^4J_{F-H}$ = 4.2 Hz, CHCF_aF_bCHCH₂, 1F), -136.6 ppm (ddt, 2J = 157.8 Hz, J_{F-H} = 10.8 Hz, $^4J_{F-H}$ = 3.7 Hz, CHCF_aF_bCHCH₂, 1F). Reported chemical shifts are representative of an AB system; $\bar{\nu}$ /(film) = 3292, 1495, 1476, 1437, 1236, 1167, 1036, 1011, 930 cm⁻¹; MS (CI): m/z (%): 269 (2) $[M+C_3H_5]^+$, 257 (10) $[M+C_2H_5]^+$, 229 (32) $[M+H]^+$, 211 (100) $[M-OH]^+$, 191 (90) $[(M+H)-F_2]^+$, 181 (48), 161 (74), 131 (26); HRMS (APCI): calcd for $C_{11}H_{11}F_2O_3$, 229.0671 $[M+H]^+$ found 229.0668; t_R (GC) = 12.96 minutes.

Preparation of ((1S*,3R*)-2,2-difluoro-3-(2'-pyrrolyl-1-carboxylic acid *tert*-butyl ester)methanol (194f)



Alcohol **194f** was prepared from ester **192f** (600 mg, 1.9 mmol), DIBAL (1.0 M in cyclohexane, 5.7 mL, 5.7 mmol) and toluene (40 mL) according to general procedure F. Column chromatography on silica gel (1:1 Et₂O in hexane) afforded desired alcohol **194f** as a pale yellow oil (30 mg, 6%). *R_f* = 0.32 (1:1 Et₂O in hexane); ¹H NMR (400 MHz, CDCl₃): δ = 7.23 (ddd, *J* = 3.4 Hz, ⁴*J* = 1.8 Hz, ⁵*J* = 0.8 Hz, Ar*H*, 1H), 6.25 (m, Ar*H*, 1H), 6.14 (t, *J* = 3.4 Hz, Ar*H*, 1H), 3.98 (ddd, ²*J* = 12.0 Hz, *J* = 5.7, 1.8 Hz, CHCH_aH_bOH, 1H), 3.74 (dt, ²*J* = 11.9 Hz, *J* = 1.8 Hz, CHCH_aH_bOH, 1H), 2.96 (br. s, OH, 1H), 2.86 (dd, ³*J*_{H-F} = 15.3 Hz, *J* = 7.3 Hz, ArCH, 1H), 1.99 (m, CHCH₂OH, 1H), 1.63 ppm (s, OC(CH₃)₃, 9H); ¹³C NMR (100 MHz, CDCl₃): δ = 149.3, 126.5, 121.2, 113.3 (dd, ¹*J*_{C-F} = 290.3, 287.3 Hz), 112.3 (d, ⁴*J*_{C-F} = 3,3 Hz), 110.0, 84.2, 59.0 (d, *J*_{C-F} = 4.4 Hz), 32.9 (t, ²*J*_{C-F} = 9.3 Hz), 23.5, 23.3 ppm (dd, ²*J*_{C-F} = 13.0, 9.6 Hz); ¹⁹F NMR (376 MHz, CDCl₃): δ = -132.6 (dd, ²*J* = 160.0 Hz, *J*_{F-H} = 13.6 Hz, CF_aF_b, 1F), -134.7 ppm (dd, ²*J* = 159.0 Hz, *J*_{F-H} = 15.1 Hz, CF_aF_b, 1F); $\bar{\nu}$ /(film) = 3443, 2982, 2835, 1740, 1478, 1405, 1372, 1323, 1260, 1164, 1128 cm⁻¹; MS (CI): *m/z* (%): 180 (23), 152 (100); *t_R* (GC) = 10.12 minutes. Due to lack of *m/z* consistent with product accurate mass analysis was not attempted.

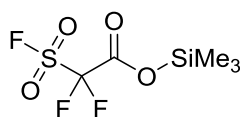
Preparation of ((1S*,3R*)-2,2-difluoro-3-(2'-furyl-3-methyl)cyclopropyl)methanol (199h)



Alcohol **199h** was prepared from ester **192h** (234 mg, 1.0 mmol), DIBAL (1.0 M in cyclohexane, 3.0 mL, 3.0 mmol) and toluene (6.2 mL) according to general procedure F to afford desired alcohol **199h** as a pale yellow oil (160 mg, 84%). *R_f* = 0.21 (1:1 Et₂O in hexane); ¹H NMR (400 MHz, CDCl₃): δ = 7.25 (d, *J* = 1.8 Hz, Ar*H*, 1H), 6.22 (d, *J* = 1.8 Hz, Ar*H*, 1H), 3.97-3.84 (br. m., CHCH₂OH, 2H), 2.52 (dd, *J*_{H-F} =

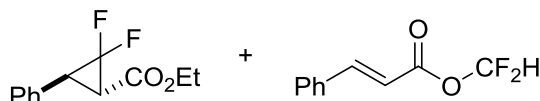
12.7, $J = 7.3$ Hz, ArCH, 1H), 2.40 (dddd, $J_{\text{H-F}} = 13.9, 2.0$ Hz, $J = 7.6, 7.3, 6.4$ Hz), 2.04 (s, ArCH₃, 3H), 1.62 ppm (br. s, OH, 1H); ¹³C NMR (100 MHz, CDCl₃): $\delta = 141.5, 141.0, 118.2, 113.3, 113.0$ (t, $^1J_{\text{C-F}} = 289.0$ Hz), 59.1 (d, $J_{\text{C-F}} = 5.6$ Hz), 29.5 (t, $^2J_{\text{C-F}} = 9.5$ Hz), 23.4 (dd, $^2J_{\text{C-F}} = 13.4, 10.8$ Hz), 9.6 ppm; ¹⁹F NMR (376 MHz, CDCl₃): $\delta = -134.8$ (ddd, $^2J = 157.3$ Hz, $J_{\text{F-H}} = 13.9, 2.2$ Hz, CF_aF_b, 1F), -138.4 ppm (dd, $^2J = 157.3$ Hz, $J_{\text{F-H}} = 12.7$ Hz, CF_aF_b, 1F); $\bar{\nu}$ /(film) = 3333, 2928, 2887, 1632, 1455, 1271, 1180, 1041, 1013 cm⁻¹; MS (CI): m/z (%): 189 (9) [M+H]⁺, 171 (100) [M-OH]⁺, 153 (16), 121 (14); HRMS (APCI): calcd for C₉H₉F₂O₁, 171.0616 [M-H₂O+H]⁺ found 171.0615; t_{R} (GC) = 9.99 minutes.

Preparation of trimethylsilyl 2,2-difluoro-2-(fluorosulfonyl)acetate (**36**)



A mixture of chlorotrimethylsilane (4.9 mL, 38.8 mmol) and commercial trimethylsilyl 2,2-difluoro-2-(fluorosulfonyl)acetate (TFDA, **36**, 1 mL, 9.7 mmol, 80% purity determined by ¹⁹F NMR) was refluxed (110 °C) for 1 hour under an atmosphere of argon. The reaction mixture was cooled to room temperature and the water condenser was replaced with an oven dried distillation apparatus and the glassware cooled under an atmosphere of argon. Excess TMSCl was removed (90 °C, 600 mbar) and the residual **36** was stored under argon at room temperature. The ¹⁹F NMR spectrum of the residue confirmed reagent purity at > 95% and **36** used immediately for a difluorocyclopropanation reaction. ¹⁹F NMR (376 MHz, CDCl₃): $\delta = -41.2$ (dd, $J = 4.6, 4.2$ Hz, FSO₂CF₂, 1F), -103.1 ppm (d, $J = 4.4$ Hz, FSO₂CF₂, 2F). The data was in agreement with that reported by Tian and co-workers.⁶⁸

Attempted difluorocyclopropanation of ethyl cinnamate with TFDA



An oven dried two-necked round bottom flask containing sodium fluoride (7 mg, 0.17 mmol) was sealed with a SubaSeal, and the salt was stirred and lightly flame dried under an atmosphere of argon. A low boiling point water condenser with a

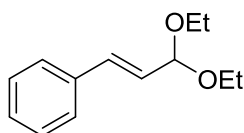
gas outlet connected to an argon/vacuum manifold was attached to the reaction flask and the atmosphere was purged three times. Ethyl cinnamate (0.48 mL, 2.84 mmol) followed by toluene (0.15 mL, 1.42 mmol) were added and the colourless suspension was heated to 125 °C. Once the reaction temperature had been reached, freshly distilled TFDA (1.4 mL, 7.1 mmol) was added dropwise over a period of 3 hours using a syringe pump. The mixture was stirred for a further 1 hour (total reaction time of 4 hours). The reaction mixture was cooled to room temperature and the reaction mixture was quenched with addition of water (10 mL) and diethyl ether (10 mL). The organic layer was separated and the aqueous layer was extracted with diethyl ether (4 x 10 mL). The original organic layer and the extracts were combined, dried (MgSO₄) and concentrated under reduced pressure to remove volatile materials. The ¹H NMR spectrum of the crude reaction mixture was used to determine the ratio of **192b**, **194b** and **200**. A similar crude reaction mixture was purified by column chromatography on silica gel (1:19 to 1:9 Et₂O in hexane) and a mixture of **200** and **192b** (4:1 ratio determined by NMR) was isolated. Extracted data for **200**: R_f = 0.26 (1:4 Et₂O in hexane); ¹H NMR (400 MHz, CDCl₃): δ = 7.88 (d, *J* = 16.0 Hz, ArCH=CH, 1H), 7.60-7.58 (m, ArH, 3H), 7.49-7.43 (m, ArH, 2H), 7.22 (t, ²*J*_{H-F} = 71.2 Hz, CF₂H, 1H), 6.56 ppm (d, *J* = 16.0 Hz, CH=CHCO, 1H); ¹³C NMR (100 MHz, CDCl₃): δ = 162.8 (t, *J*_{C-F} = 3.4 Hz), 149.2, 133.6, 131.6, 129.2, 128.8, 115.1, 112.8 ppm (t, ¹*J*_{C-F} = 257.1 Hz); ¹⁹F NMR (376 MHz, CDCl₃): δ = -91.4 ppm (d, ²*J*_{F-H} = 71.2 Hz); $\bar{\nu}$ /(film) = 1738, 1634, 1059, 980 cm⁻¹; MS (CI): *m/z* (%): 227 (4) [M+C₂H₅]⁺, 199 (47) [M+H]⁺, 157 (6), 131 (100) [M-OCF₂H]⁺; t_R (GC) = 10.45 minutes.

Testing Functional Group Capability in Difluorocyclopropanation Chemistry

An oven dried two-necked round bottom flask containing potassium iodide (3.68 g, 22.2 mmol) was sealed with a SubaSeal, and the salt was stirred and lightly flame dried under an atmosphere of argon. A low boiling point water condenser with a gas outlet connected to an argon/vacuum manifold was attached and the reaction flask and the atmosphere were purged three times. Cinnamyl acetate **141** (1.34 mL, 8.0 mmol) followed by a solution of additive (X eq., see report) in diglyme (1.3 mL)

were added and the resulting suspension was heated to 120 °C. Once the reaction temperature had been reached, TMSCl (2.6 mL, 19.7 mmol) and MDFA (2.6 mL, 19.7 mmol) were added dropwise in that order. After 5 hours, the reaction mixture had evaporated to dryness and a further portion of diglyme (1.3 mL) was added. The mixture was stirred for a further 19 hours (total reaction time of 24 hours). The resulting brown solution was cooled to room temperature and the reaction mixture was quenched with aqueous NaCl (10 mL) and diethyl ether (10 mL) was added. The organic layer was separated and the aqueous layer was extracted with diethyl ether (2 x 10 mL). The original organic layer and the extracts were combined, dried (MgSO₄) and concentrated under reduced pressure to remove volatiles. The ¹H NMR spectrum of the resulting brown oil was used to determine conversion of **141** to difluorocyclopropyl **142**.

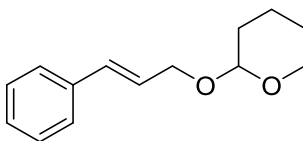
Preparation of (E)-(3,3-diethoxyprop-1-en-1-yl)benzene (**203**)



An oven dried round bottom flask containing Amberlyst-15 (435 mg) was attached to an argon/vacuum manifold and the atmosphere purged three times. Cinnamaldehyde (1.25 mL, 10 mmol) was added followed by the dropwise addition of distilled triethylorthoformate (17 mL, 25.5 mmol). The reaction mixture was stirred under argon for 17 h and ¹H NMR of a reaction aliquot showed full consumption of starting aldehyde. The reaction mixture was filtered through a celite pad and washed with hexane (50 mL) to removed residual acid. The collected filtrate was concentrated under reduced pressure to remove any remaining triethylorthoformate and EtOH side product. A repeat reaction on the same scale was carried out and the crude product from both reactions were combined and purified by distillation (75 °C, 1.1 x 10⁻¹ mbar) to afford desired acetal **203** (2.1 g, 10.3 mmol, 51%) as a colourless oil. ¹H NMR (400 MHz, CDCl₃): δ = 7.44-7.42 (m, ArH, 2H), 7.36-7.32 (m, ArH, 2H), 7.30-7.26 (m, ArH, 1H), 6.73 (d, *J* = 15.9 Hz, ArCH=CH, 1H), 6.23 (dd, *J* = 15.9, 5.1 Hz, CH=CHCH, 1H), 5.09 (dd, *J* = 5.1, 0.9 Hz,

CH(OEt)₂, 1H), 3.74 (qd, $J = 7.1$ Hz, $^2J = 2.4$ Hz, OCH_aH_bCH₃, 2H), 3.59 (qd, $J = 7.1$ Hz, $^2J = 2.4$ Hz, OCH_aH_bCH₃, 2H), 1.28 ppm (t, $J = 7.1$ Hz, CH₂CH₃, 3H); ¹³C NMR (100 MHz, CDCl₃): $\delta = 135.8, 132.4, 127.5, 126.31, 126.26, 101.0, 60.5, 14.8$ ppm; $\bar{\nu}$ /(film) = 2973, 2926, 2872, 1679, 1450, 1335, 1121, 1048, 998, 946 cm⁻¹; m/s (CI): m/z (%): 207 (4) [M+H]⁺, 161 (57) [M-OEt]⁺, 133(100) [M-(OEt+Et)+H], 117 (10), 105 (15); t_R (GC): 11.84 minutes. The data was in agreement with that reported by Page and co-workers.²⁴²

Preparation of 2-(cinnamyloxy)tetrahydro-2H-pyran (**204**)

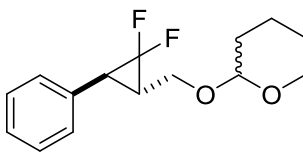


Tosic acid (10 mg, 0.05 mmol) was added to a solution of cinnamyl alcohol (134 mg, 1 mmol) and 3,4-dihydro-2H-pyran (0.11 mL, 1.2 mmol) in DCM (5 mL) and stirred for 2 hours. TLC analysis of a reaction aliquot confirmed full consumption of starting alcohol. The crude reaction mixture was quenched with addition of sodium bicarbonate (sat., 10 mL) and the resulting organic layer separated and collected. The aqueous layer was extracted further with DCM (2 x 5 mL) and the extracts combined with the original layer, dried (MgSO₄) and concentrated under reduced pressure. Crude product was purified on silica gel (1:19 Et₂O in hexane) to afford pyran **204** (130 mg, 60%) as a colourless oil. R_f = 0.38 (1:4 Et₂O in hexane); ¹H NMR (400 MHz, CDCl₃): $\delta = 7.43\text{-}7.40$ (m, ArH, 2H), 7.35-7.32 (m, ArH, 2H), 7.26 (tt, $J = 7.3$ Hz, $^4J = 1.6$ Hz, ArH, 1H), 6.66 (br. dt, $J = 15.9$ Hz, $^4J = 1.9$ Hz, ArCH=CH, 1H), 6.35 (ddd, $J = 15.9, 6.6, 5.6$ Hz, CH=CHCH₂, 1H), 4.74 (dd, $J = 4.0, 3.2$ Hz, OCHO, 1H), 4.43 (ddd, $^2J = 12.9$ Hz, $J = 5.6$ Hz, $^4J = 1.6$ Hz, CHCH_aH_bO, 1H), 4.20 (ddd, $^2J = 12.9$ Hz, $J = 6.6$ Hz, $^4J = 1.4$ Hz, CHCH_aH_bO, 1H), 3.97-3.92 (m, OCH_aH_bCH₂, 1H), 3.60-3.54 (m, OCH_aH_bCH₂, 1H), 1.95-1.86 (m, cyclohexyl, 1H), 1.82-1.75 (m, cyclohexyl, 1H), 1.71-1.55 ppm (m, cyclohexyl, 4H); ¹³C NMR (100 MHz, CDCl₃): $\delta = 134.3, 131.8, 128.0, 127.1, 126.0, 125.5, 97.4, 67.1, 61.7, 30.2, 25.0, 19.0$ ppm; $\bar{\nu}$ /(film) = 2937, 2865, 2846, 1441, 1450, 1364, 1351, 1130, 1117 cm⁻¹; m/s (CI): m/z (%): 161 (6) [M+C₂H₅]⁺, 133 (100) [M+H]⁺; t_R (GC): 10.547 minutes.

General Procedure G: Difluorocyclopropanation with TMSCF_3

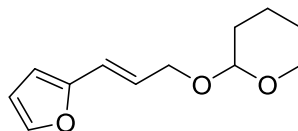
A known mass of sodium iodide was added to a 5 mL microwave vial, sealed with a suba seal and lightly flame dried under vacuum to remove any residual water. The atmosphere was replaced with nitrogen, cooled to room temperature and THF added. The solution was gently heated and sonicated to aid dissolution of the salt, then the suba seal was replaced with a microwave vial cap and sealed. Alkene then TMSCF_3 were added in that order and the reaction mixture heated at 60 °C for the desired reaction time on a DrySyn block under nitrogen. On completion, the reaction mixture was allowed to cool to room temperature, vented and concentrated under reduced pressure to afford crude product. ^1H NMR was used to determine product conversion using the relative integration between distinctive alkene (6.66 ppm, 1H) and cyclopropane (2.61 ppm, 1H) proton signals.

Preparation of 2-(((1S*,3S*)-2,2-difluoro-3-phenylcyclopropyl)methoxy)tetrahydro-2H-pyran (205)



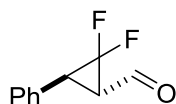
Difluorocyclopropyl pyran **205** was prepared from sodium iodide (30 mg, 0.20 mmol), alkene **204** (111 mg, 0.51 mmol), TMSCF_3 (0.38 mL, 2.55 mmol) and anhydrous THF (0.38 mL) according to General Procedure **G**. ^1H NMR of the resulting crude reaction mixture confirmed 89% relative conversion to desired product. ^{19}F NMR (376 MHz, CDCl_3): δ = -135.2 (dd, 2J = 156.2 Hz, $J_{\text{F-H}}$ = 14.4 Hz, 1F, diastereoisomer A), -135.9 (dd, 2J = 156.4 Hz, $J_{\text{F-H}}$ = 13.9 Hz, 1F, diastereoisomer B), -137.1 (ddd, 2J = 156.3 Hz, $J_{\text{F-H}}$ = 14.3, 2.3 Hz, 1F, diastereoisomer A), -137.4 ppm (ddd, 2J = 156.4 Hz, $J_{\text{F-H}}$ = 13.7, 2.7 Hz, 1F, diastereoisomer B). Purification was attempted by chromatography (1:19 Et_2O in hexane) but failed to separate starting alkene from product **205**.

Unoptimised Synthesis of (*E*)-2-((3-(furan-2-yl)allyl)oxy)tetrahydro-2H-pyran (**209**)



DIBAL (18.6 mL of a 1.1 M solution in cyclohexane, 20.5 mmol) was added dropwise to a solution of furyl alkenoate **192a** (1.03 g, 6.2 mmol) in anhydrous toluene (50 mL) at -78 °C under nitrogen. The reaction mixture was allowed to warm to room temperature and stirred for a further 7 hours, then cooled to 0 °C and quenched by dropwise addition of H₂O (2 mL), 0.1 M aqueous NaOH (2 mL) and H₂O (2 mL) in that order. MgSO₄ was added to the quenched mixture until the solid was free flowing and the mixture was left overnight at room temperature (14-17 h). The resulting white emulsion was washed with EtOAc (4 x 50 mL) and the organic extracts were combined and concentrated under reduced pressure to afford the corresponding alcohol as a yellow oil (630 mg, 5.1 mmol) which was used immediately in the next step. 3,4-Dihydro-2H-pyran (0.39 mL, 4.3 mmol) was to a suspension of Amberlyst-15 (200 mg) and crude alcohol in DCM (3.6 mL) and gently stirred for 7 hours at room temperature. The reaction mixture was filtered through a pad of celite (400 mg) and washed with DCM (20 mL) and the filtrate collected and concentrated under reduced pressure to afford crude product. Purification on silica gel (1:4 Et₂O in hexane) to afford pyran **209** (410 mg, 32% over two steps) as a yellow oil. *R*_f = 0.29 (1:4 Et₂O in hexane); ¹H NMR (400 MHz, CDCl₃): δ = 7.37 (d, *J* = 1.6 Hz, ArH, 1H), 6.48 (dt, *J* = 15.9 Hz, ⁴*J* = 1.4 Hz, ArCH=CH, 1H), 6.38 (dd, *J* = 3.0, 1.6 Hz, ArH, 1H), 6.27 (dt, *J* = 15.8, 6.0 Hz, CH=CHCH₂, 1H), 6.26 (d, *J* = 3.0 Hz, ArH, 1H), 4.73 (t, *J* = 3.5 Hz, O₂CH, 1H), 4.40 (ddd, ²*J* = 13.4 Hz, *J* = 5.5 Hz, ⁴*J* = 1.6 Hz, CHCH_oH_bO, 1H), 4.15 (ddd, ²*J* = 13.4 Hz, *J* = 6.4 Hz, ⁴*J* = 1.4 Hz, CHCH_aH_bO, 1H), 3.95-3.89 (m, OCH_oH_bCH₂, 1H), 3.58-3.53 (m, OCH_aH_bCH₂, 1H), 1.94-1.84 (m, cyclohexyl, 1H), 1.81-1.74 (m, cyclohexyl, 1H), 1.70-1.54 ppm (m, cyclohexyl, 4H); ¹³C NMR (100 MHz, CDCl₃): δ = 152.0, 141.4, 124.1, 119.8, 110.7, 107.4, 97.2, 66.5, 61.6, 30.1, 25.0, 18.9 ppm; $\bar{\nu}$ /(film) = 2945, 2874, 1459, 1467, 1262, 1210, 1134, 1123, 1037, 1024 cm⁻¹; m/s (CI): m/z (%): 123 (2) [M-C₅H₉O]⁺, 107 (100) [M-OTHP], 85 (93) [pyran]; t_R (GC): 12.743 minutes.

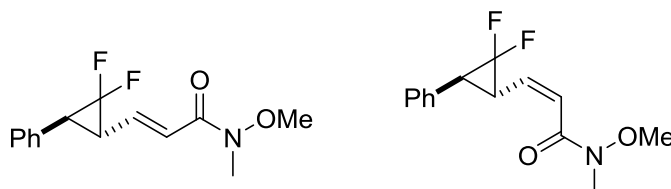
Preparation of (1S*,3S*)-2,2-difluoro-3-phenylcyclopropane-1-carbaldehyde (**145**)



BAIB (3.0 g, 9.3 mmol) was added to a solution of ((1S*,3S*)-2,2-difluoro-3-phenylcyclopropyl)methanol (**144**) (1.58 g, 8.6 mmol) and TEMPO (133 mg, 0.9 mmol) in anhydrous DCM (45 mL) and the reaction mixture was stirred at room temperature under nitrogen for 6 hours. The ^1H NMR spectrum showed complete conversion to aldehyde **145**. Kugelrohr distillation (50 °C, 20 mbar) removed iodobenzene side product then (60 °C, 0.1 mbar) afforded aldehyde **145** as a pale yellow oil (1.17 g, 75%). $R_f = 0.26$ (1:4 Et₂O in hexane); ^1H NMR (400 MHz, CDCl₃): $\delta = 9.51$ (dd, $J = 4.4$ Hz, $^4J = 2.0$ Hz, C(O)H, 1H), 7.42-7.34 (m, ArH, 3H), 7.29-7.27 (m, ArH, 2H), 3.63 (ddd, $J_{\text{H-F}} = 14.8$ Hz, $J = 7.6$ Hz, $^4J = 2.1$ Hz, ArCH, 1H), 2.97 (ddd, $J_{\text{H-F}} = 12.8$ Hz, $J = 7.5, 4.4$ Hz, CHC(O)H, 1H); ^{13}C NMR (100 MHz, CDCl₃): $\delta = 191.8$ (d, $J_{\text{C-F}} = 3.9$ Hz), 130.0, 128.4, 127.8, 127.6, 111.0 (t, $^2J_{\text{C-F}} = 291.3$ Hz), 40.3 (t, $J_{\text{C-F}} = 40.4$ Hz), 32.8 ppm (dd, $J_{\text{C-F}} 12.1, 8.8$ Hz); ^{19}F NMR (376 MHz, CDCl₃): $\delta = -129.4$ (dd, $^2J = 158.0$ Hz, $J_{\text{F-H}} = 15.0$ Hz, 1F), -133.4 ppm (dd, $^2J = 157.9$ Hz, $J_{\text{F-H}} = 12.9$ Hz, 1F); $\bar{\nu}$ /(film) = 1738, 1634, 1059, 980 cm⁻¹; MS (CI): m/z (%): 183 (11) [M+H]⁺, 163 (73) [M-F]⁺, 135 (100) [(M+H)-F-CO], 115 (24) [(M+H)-F₂-CO]; HRMS (APCI): calcd for C₁₀H₉F₂O, 183.0616 [M+H]⁺ found 183.0615; t_R (GC) = 10.03 minutes.

General Procedure H: Tandem Oxidation/Olefination of Difluorocyclopropyl Alcohols

Preparation of (E)-3-((1R*,3S*)-2,2-difluoro-3-phenylcyclopropyl)-N-methoxy-N-methylacrylamide (211a**) and (Z)-3-((1R*,3S*)-2,2-difluoro-3-phenylcyclopropyl)-N-methoxy-N-methylacrylamide (**211b**)**

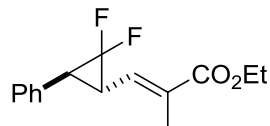


Bis(acetoxy)iodobenzene (BAIB, 304 mg, 0.92 mmol) was added to a solution of alcohol **144** (148 mg, 0.8 mmol) and TEMPO (12 mg, 0.08 mmol) in anhydrous DCM

(3.2 mL) and the reaction mixture was stirred at room temperature under nitrogen for 6 hours. The ^1H NMR spectrum showed complete conversion to the corresponding aldehyde. *N*-methoxy-*N*-methyl (triphenylphosphoranylidene) acetamide (378 mg, 1.04 mmol) was then added, and the reaction mixture stirred for 16 hours until the ^1H or ^{19}F NMR spectrum showed complete conversion. The resulting orange solution was concentrated under reduced pressure and column chromatography on silica gel (1:1 to 3:2 diethyl ether in hexane) afforded **211a** (157 mg, 74%) as a pale yellow solid and **211b** (25 mg, 9%) as a yellow oil. Data for **211a**: m.p. = 52-55 °C (chloroform/pentane); R_f = 0.14 (1:1 Et₂O in hexane); ^1H NMR (400 MHz, CDCl₃): δ = 7.39-7.31 (m, ArH, 3H), 7.30-7.25 (m, ArH, 2H), 6.82 (dd, J = 15.6, 9.6 Hz, CHCH=CH, 1H), 6.69 (d, J = 15.4 Hz, CH=CHCO, 1H), 3.74 (s, OCH₃, 3H), 3.28 (s, NCH₃, 3H), 2.91 (dd, $J_{\text{H-F}}$ = 14.6 Hz, J = 7.1 Hz, ArCHCF₂CH, 1H), 2.70 ppm (ddd, $J_{\text{H-F}}$ = 13.1 Hz, J = 9.6, 7.2 Hz, CHCH, 1H); ^{13}C NMR (100 MHz, CDCl₃): δ = 165.3, 138.5 (d, $^4J_{\text{C-F}}$ = 4.8 Hz), 132.1, 128.2, 127.4, 127.1, 120.6, 112.9 (t, $^1J_{\text{C-F}}$ = 292.7 Hz), 61.3, 35.6 (dd, $J_{\text{C-F}}$ = 11.2, 9.0 Hz), 33.8 (t, $J_{\text{C-F}}$ = 11.5), 31.9 ppm; ^{19}F NMR (376 MHz, CDCl₃): δ = -130.5 (dd, 2J = 156.1 Hz, $J_{\text{F-H}}$ = 14.1 Hz, 1F), -135.7 ppm (dd, 2J = 156.0 Hz, $J_{\text{F-H}}$ = 13.5 Hz, 1F); $\bar{\nu}$ /(film) = 1661, 1630, 1383, 1273, 1152, 986 cm⁻¹; MS (CI): m/z (%): 288 (8) [(M-F)+C₃H₅]⁺, 276 (9) [(M-F)+C₂H₅]⁺, 248 (100) [M-F]⁺; HRMS (APCI): calcd for C₁₄H₁₆F₂NO₂, 268.1144 [M+H]⁺ found 268.1145; t_R (GC) = 11.30 minutes. Data for **211b**: R_f = 0.33 (1:1 Et₂O in hexane); ^1H NMR (400 MHz, CDCl₃): δ = 7.36-7.34 (m, ArH, 4H), 7.32-7.27 (m, ArH, 1H), 6.53 (d, J = 11.4 Hz, CH=CHCO, 1H), 5.95 (dddd, J = 11.4, 10.1 Hz, $^4J_{\text{H-F}}$ = 1.4, 1.3 Hz, CHCH=CH, 1H), 4.29 (br. ddd, $J_{\text{H-F}}$ = 14.0 Hz, J = 10.1, 7.2 Hz, CHCH=CH, 1H), 3.74 (s, OCH₃, 3H), 3.27 (s, NCH₃, 3H), 2.81 (dd, $J_{\text{H-F}}$ = 14.9 Hz, J = 7.2 Hz, ArCHCF₂CH, 1H); ^{13}C NMR (100 MHz, CDCl₃): δ = 166.2 (d, $^5J_{\text{C-F}}$ = 3.7 Hz), 133.3 (d, $^4J_{\text{C-F}}$ = 6.0 Hz), 131.8, 128.1, 127.7, 126.9, 119.0, 113.7 (t, $^1J_{\text{C-F}}$ = 291.3 Hz), 61.3, 36.1 (dd, 2J = 11.5, 8.9 Hz), 31.5, 29.8 ppm (dd, 2J = 13.2, 9.8 Hz); ^{19}F NMR (376 MHz, CDCl₃): δ = -132.6 (dd, 2J = 153.9 Hz, $J_{\text{F-H}}$ = 14.8 Hz, 1F), -136.3 ppm (dd, 2J = 153.8 Hz, $J_{\text{F-H}}$ = 14.0 Hz, 1F); $\bar{\nu}$ /(film) = 2982, 2360, 2343, 1656, 1627, 1425, 1354, 1252, 1169, 1001 cm⁻¹; MS (CI): m/z (%): 296 (12) [M+C₂H₅]⁺, 268 (52) [M+H]⁺, 248

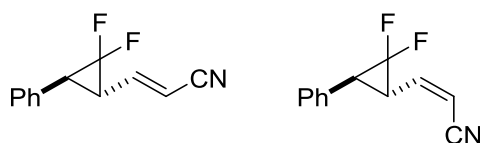
(100) $[M-F]^+$, 217 (8) $[M-(F-OMe)]$, 187 (8); HRMS (APCI): calcd for $C_{14}H_{16}F_2NO_2$, 268.1144 $[M+H]^+$ found 268.1145; t_R (GC) = 13.37 minutes.

Preparation of ethyl (*E*)-3-((1*R,3*S**)-2,2-difluoro-3-phenylcyclopropyl)-2-methylacrylate (**212**)**



Ester **212** was prepared from alcohol **144** (340 mg, 1.47 mmol), TEMPO (26 mg, 0.47 mmol), BAIB (512 mg, 1.62 mmol), (carboethoxyethylidene)triphenylphosphorane (692 mg, 1.9 mmol) and anhydrous DCM (10 mL) according to general procedure H with an oxidation time of 4 hours and an olefination time of 17 hours. Column chromatography on silica gel (1:19 Et₂O in hexane) afford ester **212** as a yellow oil (290 mg, 74%); R_f = 0.47 (1:4 Et₂O in hexane); ¹H NMR (400 MHz, CDCl₃): δ = 7.39-7.30 (m, ArH, 3H), 7.29-7.25 (m, ArH, 2H), 6.59 (ddd, J = 9.7 Hz, ⁴ J_{H-F} = 3.0 Hz, ⁴ J = 1.5 Hz, CH=CCH₃, 1H), 4.25 (q, J = 7.2 Hz, OCH₂CH₃, 2H), 2.86 (dd, J_{H-F} = 14.9 Hz, J = 7.2 Hz, ArCHCF₂CH, 1H), 2.70 (ddd, J_{H-F} = 13.3 Hz, J = 9.7, 7.3 Hz, CHCH=CH₃, 1H), 2.00 (d, ⁴ J = 1.2 Hz, CH=C(CH₃), 3H), 1.34 ppm (t, J = 7.2 Hz, OCH₂CH₃, 3H); ¹³C NMR (100 MHz, CDCl₃): δ = 167.2, 133.4 (d, ⁴ J_{C-F} = 4.9 Hz) 132.6, 130.8, 128.7, 127.9, 127.6, 113.8 (t, ¹ J_{C-F} = 292.5 Hz), 60.8, 36.2 (dd, ² J_{C-F} = 11.8, 9.6 Hz), 31.2 (t, ² J_{C-F} = 11.2 Hz), 14.3, 13.1 ppm; ¹⁹F NMR (376 MHz, CDCl₃): δ = -130.73 (dd, ² J = 154.4 Hz, J_{F-H} = 14.6 Hz, 1F), -135.5 (dd, ² J = 154.8 Hz, J_{F-H} = 13.5 Hz, 1F); $\bar{\nu}$ /(film) = 2984, 2359, 2342, 1705, 1441, 1259 cm⁻¹; MS (CI): m/z (%): 275 (8) $[(M-F)+C_2H_5]^+$, 247 (100), $[M-F]^+$, 219 (11), $[(M+H)-F-Et]$, 201 (20), 173 (39); HRMS (APCI): calcd for $C_{15}H_{17}F_2O_2$, 267.1191 $[M+H]^+$ found 267.1192; t_R (GC) = 12.46 minutes.

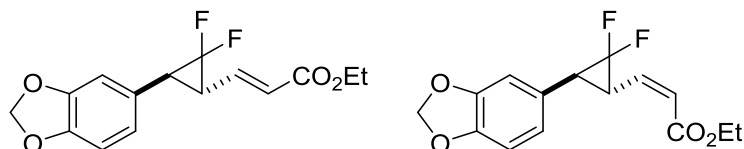
Preparation of ethyl (*E*)-3-((1*R**,3*S**)-2,2-difluoro-3-phenylcyclopropyl)acrylonitrile (**213a**) and (*Z*)-3-((1*R**,3*S**)-2,2-difluoro-3-phenylcyclopropyl)acrylonitrile (**213b**) mixture



(Triphenylphosphoranylidene)acetonitrile (536 mg, 1.8 mmol) was added to a colourless solution of aldehyde **145** (250 mg, 1.37 mmol) in anhydrous DCM (6 mL) at room temperature under nitrogen. The resulting yellow reaction mixture changed to a red solution after being stirred for 2.5 hours. The reaction mixture was concentrated under reduced pressure and the resulting ^1H NMR of crude product confirmed complete conversion of **145**. Column chromatography on silica gel (1:4 Et₂O in hexane) afforded a 3:2 diastereoisomeric mixture of cyano-**213a** and **213b** (237 mg, 84%). Mixed data for **213a** and **213b**: R_f = 0.29 (1:4 Et₂O in hexane); HRMS (APCI): calcd for C₁₂H₁₀F₂N, 206.0776 [M+H]⁺ found 206.0774; $\bar{\nu}$ /(film) = 3291, 2912, 1495, 1476, 1437, 1236, 1167, 1103, 1036, 1011, 930 cm⁻¹; Extracted data for **213a**: ^1H NMR (400 MHz, CDCl₃): δ = 7.42-7.24 (m, ArH, 5H), 6.53 (ddt, J = 16.3, 9.6 Hz, $^4J_{\text{H-F}}$ = 1.3 Hz, CH=CHCN, 1H), 5.60 (d, J = 16.4 Hz, CH=CHCN, 1H), 3.00-2.93 (m, ArCH, 1H), 2.65 ppm (ddd, $J_{\text{H-F}}$ = 12.3 Hz, J = 9.6, 7.2 Hz, CHCH=CH, 1H); ^{13}C NMR (100 MHz, CDCl₃): δ = 146.9 (d, $^4J_{\text{C-F}}$ = 4.9 Hz), 131.5, 128.9, 128.1, 127.9, 116.8, 112.8 (t, $^1J_{\text{C-F}}$ = 293.6 Hz), 101.8, 36.4 (dd, $^2J_{\text{C-F}}$ = 11.9, 9.6 Hz), 34.2 ppm (t, $^2J_{\text{C-F}}$ = 11.6 Hz); ^{19}F NMR (376 MHz, CDCl₃): δ = -129.9 (dd, 2J = 158.1 Hz, $J_{\text{F-H}}$ = 15.3 Hz, 1F), -135.5 ppm (dd, 2J = 158.1 Hz, $J_{\text{F-H}}$ = 12.10 Hz, 1F); MS (CI): m/z (%): 246 (11) [M+C₃H₅]⁺, 234 (23) [M+C₂H₅]⁺, 206 (94) [M+H]⁺, 186 (100) [M-F]⁺; t_R (GC) = 11.45 minutes. Extracted data for **213b**: ^1H NMR (400 MHz, CDCl₃): δ = 7.42-7.24 (m, ArH, 5H), 6.32 (ddt, J = 11.0, 9.8 Hz, $^4J_{\text{H-F}}$ = 1.1 Hz, CHCH=CHCN, 1H), 5.55 (d, J = 11.1 Hz, CH=CHCN, 1H), 3.09 (ddd, $J_{\text{H-F}}$ = 12.3 Hz, J = 9.8, 6.9 Hz, CHCH=, 1H), 3.00-2.93 ppm (m, ArCH, 1H); ^{13}C NMR (100 MHz, CDCl₃): δ = 146.2 (d, $^4J_{\text{C-F}}$ = 5.4 Hz), 131.2, 128.9, 128.1, 127.9, 115.8, 112.8 (t, $^1J_{\text{C-F}}$ = 293.1 Hz), 101.4, 36.6 (d, $^2J_{\text{C-F}}$ = 11.8, 9.22), 33.1 ppm (d, $^2J_{\text{C-F}}$ = 13.3, 10.4); ^{19}F NMR (376 MHz, CDCl₃): δ = -130.0 (dd, 2J = 156.9, $J_{\text{H-F}}$ = 15.0 Hz, 1F), -

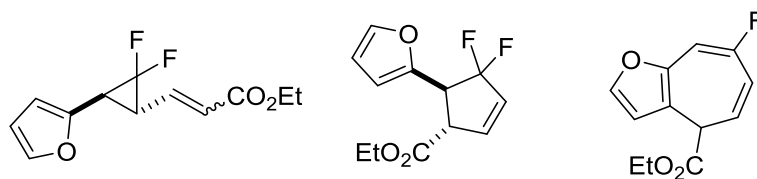
135.8 ppm (dd, $^2J = 156.9$, $J_{H-F} = 12.2$ Hz, 1F); MS (CI): m/z (%): 246 (6) $[M+C_3H_5]^+$, 234 (15) $[M+C_2H_5]^+$, 206 (22) $[M+H]^+$, 186 (100) $[M-F]^+$; t_R (GC) = 11.86 minutes.

Preparation of ethyl (*E*)-3-((1*R**,3*S**)-3-(benzo[d][1,3]dioxol-5-yl)-2,2-difluorocyclopropyl)acrylate (**214a**) and of ethyl (*Z*)-3-((1*R**,3*S**)-3-(benzo[d][1,3]dioxol-5-yl)-2,2-difluorocyclopropyl)acrylate (**214b**)



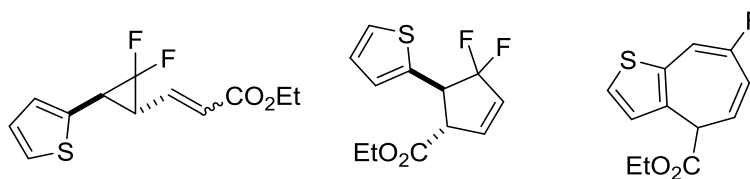
Ester **214** was prepared from alcohol **199d** (36.5 mg, 0.16 mmol), TEMPO (3.7 mg, 0.02 mmol), BAIB (57 mg, 0.18 mmol), (ethoxycarbonylmethylene)triphenylphosphorane (85 mg, 0.21 mmol) and anhydrous DCM (2 mL) according to General Procedure H with an oxidation time of 4 hours and an olefination time of 4 hours. Column chromatography on silica gel (1:9 diethyl ether in hexane) afforded **214a** (23.5 mg, 50%) and a mixture of **214a** and **214b** (10 mg, 21%) as pale yellow oils. Data for **214a**: $R_f = 0.25$ (1:4 Et₂O in hexane); 1H NMR (400 MHz, CDCl₃): $\delta = 6.81$ - 6.72 (m, ArH, 3H), 6.77 (dd, $J = 15.3$, 8.9 Hz, CH=CHCO₂Et, 1H), 6.08 (d, $J = 15.5$ Hz, CH=CHCO₂Et, 1H), 5.98 (s, OCH₂O, 2H), 4.23 (q, $J = 7.1$ Hz, OCH₂CH₃, 2H), 2.84 ($J_{H-F} = 14.7$ Hz, $J = 7.1$ Hz, ArCH, 1H), 2.54 (ddd, $J_{H-F} = 13.0$ Hz, $J = 8.9$, 7.1 Hz, CHCH=CH, 1H), 1.33 (t, $J = 7.1$ Hz, OCH₂CH₃, 3H); ^{13}C NMR (100 MHz, CDCl₃): $\delta = 165.2$, 147.5, 146.7, 139.8 (d, $J_{C-F} = 4.7$ Hz), 125.2, 123.1, 121.2, 112.7 (t, $^1J_{C-F} = 292.4$ Hz), 107.9, 107.7, 100.8, 60.1, 35.2 (dd, $^2J_{C-F} = 12.1$, 9.3 Hz), 33.4 (t, $^2J_{C-F} = 11.7$ Hz), 13.7 ppm; ^{19}F NMR (376 MHz, CDCl₃): $\delta = -130.6$ (dd, $^2J = 156.5$ Hz, $J_{F-H} = 14.7$ Hz, 1F), -135.5 (dd, $^2J = 156.2$ Hz, $J_{F-H} = 13.0$ Hz, 1F); $\bar{\nu}$ /(film) = 2924, 2359, 2342, 1715, 1505, 1493, 1445, 1256, 1188 1165, 1096, 1038, 1018, 789 cm⁻¹; MS (CI): m/z (%): 325 (4) $[M+C_2H_5]^+$, 305 (9) $[(M-F)+C_2H_5]^+$, 277 (100) $[M-F]^+$, 259 (11) $[M-F_2]^+$, 231 (44), 203 (24), 175 (5); HRMS (APCI): calcd for C₁₅H₁₈F₂O₄N, 314.1198 $[M+NH_4]^+$ found 314.1199; t_R (GC) = 14.30 minutes. Extracted Data for **214b**: $R_f = 0.40$ (1:4 Et₂O in hexane); ^{19}F NMR (376 MHz, CDCl₃): $\delta = -132.5$ (dd, $^2J = 154.4$ Hz, $J_{F-H} = 14.8$ Hz, 1F), -136.1 (dd, $^2J = 153.6$ Hz, $J_{F-H} = 13.5$ Hz, 1F).

Attempted preparation of ethyl (*E*)-3-((1*R,3*S**)-2,2-difluoro-3-(furan-2-yl)cyclopropyl)acrylate (**215a/215b**)**



The synthesis of ester **215** was attempted from alcohol **199a** (1.33 g, 7.6 mmol), BAIB (2.67 mg, 8.36 mmol), TEMPO (60 mg, 1.52 mmol), (ethoxycarbonylmethylene)triphenylphosphorane (5.3 g, 9.8 mmol) and DCM (30 mL) according to general procedure H with an oxidation time of 3 h and olefination time of 16 h. The ^{19}F NMR of the resulting crude reaction mixture confirmed complete consumption of **199a**. Column chromatography on silica gel (1:19 Et₂O in hexane) afforded a set of fractions containing rearrangement product **220a** with trace amounts of difluorocyclopentene **222a** (1.06 g, 80%) as a pale yellow oil. Further purification attempts failed as isolated compounds showed signs of decomposition (solution turned black). No evidence of ester **215** was observed during the reaction and initial purification, consistent with rearrangement occurring at room temperature. ^1H and ^{19}F NMR spectra are consistent with heptadiene **220a** and show similarities with the corresponding thiophene based product (**221a**) which was fully characterised (*vide infra*). Extracted data for **220a**: $R_f = 0.38$ (1:4 Et₂O in hexane); ^1H NMR (400 MHz, CDCl₃): $\delta = 7.54$ (d, $J = 2.0$ Hz, ArH, 1H), 6.57 (dddd, $J_{\text{H-F}} = 15.2$ Hz, $^4J = 2.0$ Hz, $^5J = 0.7, 0.5$ Hz, C-CH=CF, 1H), 6.28 (dd, $J = 2.0$ Hz, $^4J = 0.6$ Hz, ArH, 1H), 6.17 (dddd, $J_{\text{H-F}} = 11.5$ Hz, $J = 10.7$ Hz, $^4J = 2.0$ Hz, 0.5 Hz, (F)CCH=CH, 1H), 5.89 (ddd, $J = 10.7, 7.2$ Hz, $^4J_{\text{H-F}} = 4.1$ Hz, $^5J = 0.5$ Hz), 4.23 (ABq, $J = 7.4$ Hz, $^2J = 1.4$ Hz, OCH_aH_bCH₃, 2H), 4.18 (br. d, $J = 7.5$ Hz, C(H)CO₂Et, 1H), 1.29 ppm (t, $J = 7.2$ Hz, CH₂CH₃, 3H); ^{19}F NMR (376 MHz, CDCl₃): $\delta = -105.67$ ppm (ddd, $J_{\text{F-H}} = 15.2, 11.5$ Hz, $^4J_{\text{F-H}} = 4.2$ Hz).

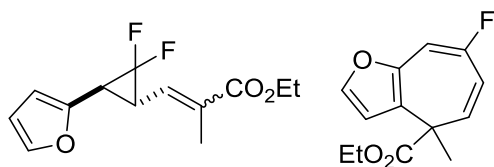
Attempted preparation of ethyl (*E*)-3-((1*R,3*S**)-2,2-difluoro-3-(thiophen-2-yl)cyclopropyl)acrylate (**216a/216b**)**



The synthesis of ester **216** was attempted from alcohol **199c** (684 mg, 3.6 mmol), BAIB (1.26 g, 3.96 mmol), TEMPO (28 mg, 0.72 mmol), (ethoxycarbonylmethylene)triphenylphosphorane (1.64 g, 4.68 mmol) and DCM (15 mL) according to general procedure **H** with an oxidation time of 3 h and an olefination time of 16 h. The ^1H NMR spectrum of the crude reaction mixture confirmed complete consumption of **199c**. Column chromatography on silica gel (1:19 Et₂O in hexane) afforded a set of fractions containing **216b** (12 mg), a mixture of rearrangement products and alkenoates **216a** (420 mg) and a mixture of rearrangement products **221a** and **223a** (212 mg). A solution of crude product containing **216a** in CDCl₃ (1 mL) and **216b** in CDCl₃ (1 mL) were heated at 40 °C and 50 °C, respectively for 17 h. ^1H and ^{19}F NMR showed complete consumption of VCP-precursors. Product samples containing a clean mixture of **221a** and **223a** were combined and concentrated under reduced pressure to afford a brown oil (488 mg). HPLC purification on a Kromasil C18 cartridge (2:5 to 1:1 gradient of MeCN containing 0.1% ammonia solution in 10 mM ammonium bicarbonate for 10 minutes then 1:1 to 9.9:10 of the same eluent for 30 minutes) afford clean heptadiene **221a** (112 mg, 14%) as an orange oil and a brown oil containing a mixture of **221a** and difluorocyclopentene **223a** (24 mg, 1:1 by ^1H NMR, the latter characterised by the distinctive ^{19}F NMR signals). Data for **221a**: R_f = 0.42 (1:4 Et₂O in hexane); ^1H NMR (400 MHz, CDCl₃): δ = 7.38 (d, J = 5.2 Hz, ArH, 1H), 6.80 (dd, $J_{\text{H-F}}$ = 15.6 Hz, 4J = 1.7 Hz, C-CH=CF, 1H), 6.77 (d, J = 5.24 Hz, ArH, 1H), 6.21 (dddd, J = 10.9 Hz, $J_{\text{H-F}}$ = 7.3 Hz, 4J = 1.7, 0.8 Hz, CHCH=CH-CF, 1H), 6.01 (ddd, J = 10.9, 7.0 Hz, $^4J_{\text{H-F}}$ = 4.6 Hz, CH-CH=CH, 1H), 4.29 (ABq, J = 7.2 Hz, 2J = 1.4 Hz, OCH_aH_bCH₃, 2H), 3.98 (d, J = 7.0 Hz, C(H)CO₂Et, 1H), 1.32 ppm (t, J = 7.2 Hz, CH₂CH₃, 3H); ^{13}C NMR (100 MHz, CDCl₃): δ = 170.6, 158.8 (d, $^1J_{\text{C-F}}$ = 246 Hz), 132.3 (d, $J_{\text{C-F}}$ = 14.9 Hz), 129.7, 126.8

(d, $^5J_{C-F} = 3.1$ Hz), 125.8 (d, $J_{C-F} = 13.0$ Hz), 125.5, 120.5 (d, $^2J_{C-F} = 35.2$ Hz), 106.1 (d, $^2J_{C-F} = 31.4$ Hz), 60.9, 44.7, 13.7 ppm; ^{19}F NMR (376 MHz, CDCl_3): $\delta = -103.4$ ppm (ddd, $J_{F-H} = 15.6, 7.3$ Hz, $^4J_{F-H} = 4.6$ Hz); $\bar{\nu}/(\text{film}) = 2980, 2937, 1733, 1632, 1444, 1402, 1370, 1333, 1308, 1186, 1137$ cm^{-1} ; MS (CI): m/z (%): 239 (41) $[\text{M}+\text{H}]^+$, 219 (35) $[\text{M}-\text{F}]^+$, 193 (25) $[\text{M}-\text{OEt}]^+$, 165 (100) $[\text{M}-\text{CO}_2\text{Et}]^+$, 147 (9); HRMS (APCI): calcd for $\text{C}_{12}\text{H}_{12}\text{FSO}_2$, 239.0542 $[\text{M}+\text{H}]^+$ found 239.0548; t_R (GC) = 12.91 minutes. Extracted data for **223a**: ^1H NMR (400 MHz, CDCl_3): $\delta = 7.31$ (dd, $J = 5.1$ Hz, $^4J = 1.3$ Hz, ArH, 1H), 7.09-7.07 (br m, containing d $J = 3.7$ Hz, ArH, 1H), 7.04 (dd, $J = 5.1, 3.7$ Hz, ArH, 1H), 6.46 (dt, $J = 6.0, 1.9$ Hz, $^4J = 1.9$ Hz, $\text{CF}_2\text{-CH}=\text{CH}$, 1H), 6.10 (dd, $J = 6.0$ Hz, $^4J = 2.7$ Hz, $\text{CF}_2\text{-CH}=\text{CH}$, 1H), 4.34-4.24 (m, under peak for **221a**, ArCH, 1H), 4.21 (q, $J = 7.2$ Hz, OCH_2CH_3 , 2H), 3.94-3.88 (m, CHCO_2Et , 1H), 1.28 ppm (t, $J = 7.2$ Hz, CH_2CH_3 , 3H); ^{19}F NMR (376 MHz, CDCl_3): $\delta = -92.4$ (ddd, $^2J = 250.5$ Hz, $J_{F-H} = 14.8$ Hz, $^4J_{F-H} = 7.6$ Hz, CF_aF_b , 1F), -93.7 ppm (ddd, $^2J = 250.5$ Hz, $J_{F-H} = 14.6$ Hz, $^4J_{F-H} = 5.4$ Hz, CF_aF_b , 1F); MS (CI): m/z (%): 267 (7) $[\text{M}-\text{F}+\text{C}_2\text{H}_5]^+$, 239 (100) $[\text{M}-\text{F}]^+$, 221 (8) $[\text{M}-\text{F}_2+\text{H}]^+$, 193 (25), 165 (12); t_R (GC) = 12.11 minutes.

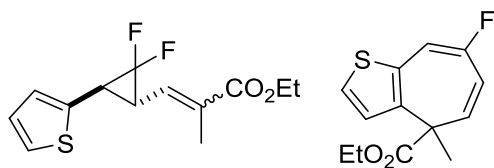
Attempted preparation of ethyl (*E*)-3-((1*R**,3*S**)-2,2-difluoro-3-(furan-2-yl)cyclopropyl)acrylate (**217a/217b**)



The synthesis of ester **217** was attempted from alcohol **199a** (52 mg, 0.3 mmol), BAIB (106 mg, 0.33 mmol), TEMPO (5 mg, 0.03 mmol), (carbethoxyethylidene)triphenylphosphorane (142 mg, 0.39 mmol) and DCM (2 mL) according to general procedure **H** with an oxidation time of 3 h and an olefination time of 14 h. The ^1H NMR spectrum of the crude reaction mixture confirmed complete consumption of **199a**, forming cycloheptadiene **220b** exclusively. The crude reaction mixture was transferred onto a pad of silica (10 g) in a sinter funnel which had been conditioned with hexane. The pad was eluted with 0:1 to 1:9 Et_2O in hexane to afford cycloheptadiene **220b** as a pale yellow oil (34 mg, 48%). $R_f = 0.41$ (1:4 Et_2O in hexane); ^1H NMR (400 MHz, CDCl_3): $\delta = 7.53$ (d, $J = 2.0$ Hz, ArH, 1H),

6.57 (dddd, $J_{\text{H-F}} = 14.9$ Hz, $^4J = 2.0$, 0.7 Hz, $^5J = 0.6$ Hz, C-CH=CF, 1H), 6.28 (dd, $J = 2.0$ Hz, $^4J = 0.7$ Hz, ArH, 1H), 6.14 (ddd, $J = 11.7$ Hz, $J_{\text{H-F}} = 10.3$ Hz, $^4J = 2.0$ Hz, C(F)-CH=CH, 1H), 5.76 (dd, $J = 11.7$ Hz, $^4J_{\text{H-F}} = 4.2$ Hz, C(F)-CH=CH, 1H), 4.18 (q, $J = 7.2$ Hz, OCH₂CH₃, 2H), 1.64 (s, CH₃, 3H), 1.25 ppm (t, $J = 7.2$ Hz, CH₂CH₃, 3H); ¹³C NMR (150 MHz, CDCl₃): $\delta = 173.9$, 157.8 (d, $^1J_{\text{C-F}} = 241.0$ Hz), 146.2 (d, $^4J_{\text{C-F}} = 15.9$ Hz), 144.4 (d, $^5J_{\text{C-F}} = 4.1$ Hz), 133.2 (d, $J_{\text{C-F}} = 13.1$ Hz), 120.5 (d, $^2J_{\text{C-F}} = 37.7$ Hz), 120.3 (d, $J_{\text{C-F}} = 3.9$ Hz), 109.9, 102.5 (d, $J_{\text{C-F}} = 33.7$ Hz), 61.4, 44.9, 24.0, 14.1 ppm; ¹⁹F NMR (376 MHz, CDCl₃): $\delta = -107.05$ (ddd, $J_{\text{F-H}} = 14.9$, 10.3 Hz, $^4J_{\text{F-H}} = 4.2$ Hz); $\bar{\nu}$ /(film) = 2980, 2934, 1794, 1731, 1641, 1459, 1405, 1376, 1251, 1216, 1149, 1108, 1017 cm⁻¹; MS (CI): m/z (%): 237 (33) [M+H]⁺, 217 (30) [M-F]⁺, 191 (15) [M-OEt]⁺, 189 (13) [M-(F+Et)+H]⁺, 163 (100) [M-CO₂Et]⁺, 145 (8) [M-(CO₂Et+F)+H]⁺; HRMS (APCI): calcd for C₁₃H₁₇F₁N₁O₃, 254.1187 [M+NH₄]⁺ found 254.1189; t_{R} (GC) = 12.05 minutes.

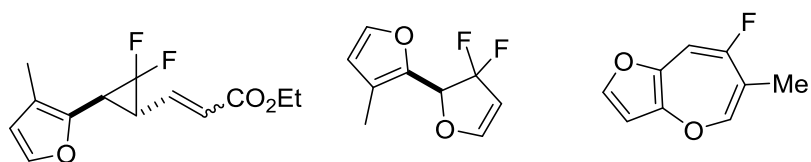
Attempted preparation of ethyl (*E*)-3-((1*R,3*S**)-2,2-difluoro-3-(thiophen-2-yl)cyclopropyl)acrylate (**218a/218b**)**



The synthesis of ester **218** was attempted from alcohol **199c** (93 mg, 0.48 mmol), BAIB (171 mg, 0.53 mmol), TEMPO (7.5 mg, 0.05 mmol), (carbethoxyethylidene)triphenylphosphorane (226 mg, 0.62 mmol) and DCM (3.2 mL) according to general procedure **H** with an oxidation time of 3 h and an olefination time of 14 h. The ¹H NMR spectrum of the crude reaction mixture confirmed complete consumption of **199c**, forming cycloheptadiene **221b** exclusively. The crude reaction mixture was transferred onto a pad of silica (10 g) in a sinter funnel which had been conditioned with hexane. The pad was eluted with 0:1 to 1:9 Et₂O in hexane to afford cycloheptadiene **221b** as a pale yellow oil (66 mg, 55%). $R_f = 0.39$ (1:4 Et₂O in hexane); ¹H NMR (400 MHz, CDCl₃): $\delta = 7.39$ (d, $J = 5.4$ Hz, ArH, 1H), 6.88 (d, $J = 5.4$ Hz, ArH, 1H), 6.76 (dd, $J_{\text{H-F}} = 15.4$ Hz, $^4J = 2.0$ Hz, C-CH=CF, 1H), 6.24 (ddd, $J = 11.1$ Hz, $J_{\text{H-F}} = 8.2$ Hz, $^4J = 2.0$ Hz, CF-CH=CH, 1H), 5.80 (dd, $J = 11.1$ Hz, $^4J_{\text{H-F}} = 4.6$ Hz, CF-CH=CH, 1H), 4.14 (q, $J = 7.2$ Hz, OCH₂CH₃, 2H), 1.79 (s,

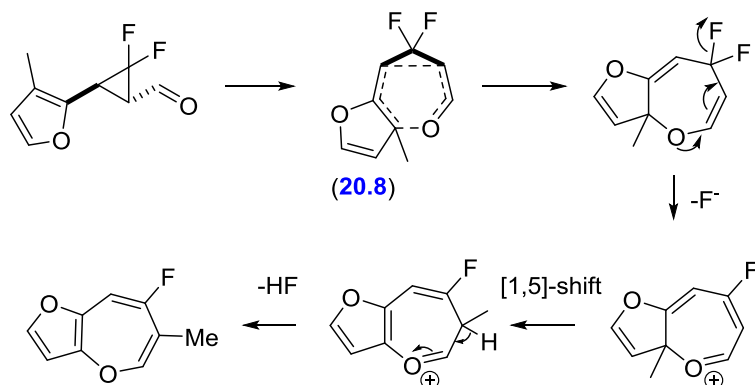
C-CH₃, 3H), 1.20 ppm (t, *J* = 7.2 Hz, CH₂CH₃, 3H); ¹³C NMR (100 MHz, CDCl₃): δ = 173.8, 158.2 (d, ¹*J*_{C-F} = 244.5 Hz), 135.4 (d, ⁴*J*_{C-F} = 2.0 Hz), 132.9 (d, *J*_{C-F} = 13.1 Hz), 132.0 (d, *J*_{C-F} = 13.5 Hz), 126.4 (d, ⁵*J*_{C-F} = 3.3 Hz), 125.3, 120.0 (d, ²*J*_{C-F} = 36.0 Hz), 105.9 (d, ²*J*_{C-F} = 31.3 Hz), 60.8, 47.6, 23.3, 13.6 ppm; ¹⁹F NMR (376 MHz, CDCl₃): δ = -106.10 (ddd, *J*_{F-H} = 15.4, 8.2 Hz, ⁴*J*_{F-H} = 4.6 Hz); $\bar{\nu}$ /(film) = 2980, 2937, 1733, 1632, 1444, 1402, 1370, 1333, 1308, 1186, 1137 cm⁻¹; MS (CI): *m/z* (%): 253 (31) [M+H]⁺, 233 (53) [M-F]⁺, 207 (19) [M-OEt]⁺, 179 (100) [M-CO₂Et]⁺, 161 (8) [M-(CO₂Et+F)+H]⁺; HRMS (APCI): calcd for C₁₃H₁₄F₁S₁O₂, 253.0693 [M+H]⁺ found 253.0696; *t*_R (GC) = 13.17 minutes.

Attempted preparation of ethyl (*E*)-3-((1*R,3*S**)-2,2-difluoro-3-(2'-furyl-3-methyl)cyclopropyl)acrylate (**219a/219b**)**



The synthesis of ester **219a** was attempted from alcohol **199h** (71 mg, 0.38 mmol), BAIB (144 mg, 0.45 mmol), TEMPO (11 mg, 0.08 mmol), (carbethoxyethylidene)triphenylphosphorane (183 mg, 0.53 mmol) and DCM (3 mL) according to general procedure H with an oxidation time of 6 h and an olefination time of 16 h. Crude ¹H and ¹⁹F NMR after oxidation suggested rearrangement had occurred before addition of phosphorane. The reaction mixture was concentrated under reduced pressure and crude ¹H and ¹⁹F NMR showed no new formation of rearrangement products. Attempted chromatographic purification on silica gel (0:1 to 1:4 Et₂O in hexane) failed to isolated desired rearrangement products either due to product volatility or decomposition on silica. ¹⁹F NMR of crude products showed strong similarities to 3,3-difluoro-4,5-dihydrofurans reported by Hammond and Arimitsu (¹⁹F NMR: δ = -84.6 (ddd, *J* = 248.0, 23.1, 19.8 Hz, 1F) -87.2 ppm (ddd, *J* = 248.0, 13.2, 13.2 Hz, 1F))^{S203} and benzoheptadiene compounds reported previously by ourselves (¹⁹F NMR: δ = -100.7 ppm (dt, *J*_{F-H} = 18.2, 5.2 Hz, ⁴*J*_{F-H} = 5.2 Hz, 1F).^{S164} Due to these similarities the crude products were tentatively assigned as dihydrofuran **226** and ether **225** (1:2.5 ratio respectively by ¹⁹F NMR); the doublet

of doublet observed for the latter suggest the methyl group underwent [1,5]-shift during the re-aromatisation of the furan (**Scheme S1**).

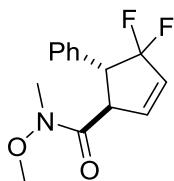


Scheme S123: Proposed mechanism rearrangement of 18h to 34 through rearrangements (ΔG^\ddagger value (blue) quoted in kcal mol⁻¹)

Data for **226**: ¹⁹F NMR (376 MHz, CDCl₃): δ = -81.9 (dd, ²*J* = 248.0 Hz, *J*_{F-H} = 20.0 Hz, 1F), -89.3 ppm (dt, ²*J* = 248.0 Hz, *J*_{F-H} = 13.8 Hz, 1F). Data for **225**: ¹⁹F NMR (376 MHz, CDCl₃): δ = -99.4 ppm (dd, *J*_{F-H} = 34.0 Hz, ⁴*J*_{F-H} = 18.5 Hz).

General Procedure I: Thermal Rearrangement of Vinyl Difluorocyclopanes

Preparation of (1*R**,5*R**)-4,4-difluoro-*N*-methoxy-*N*-methyl-5-phenylcyclopent-2-ene-1-carboxamide (**228**)



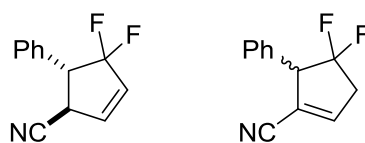
A solution of **221a** (7.0 mg, 0.026 mmol) in toluene (0.3 mL) was heated to 95 °C in a sealed microwave vial for 17 hours in a DrySyn block. After cooling and venting the vial, ¹⁹F NMR confirmed complete consumption of **221a**. The reaction mixture was transferred to a round bottom flask using DCM (5 mL) and concentrated under reduced pressure to afford difluorocyclopentene **228** (6.8 mg, 97%) as a yellow oil. *R*_f = 0.36 (1:1 Et₂O in hexane); ¹H NMR (400 MHz, CDCl₃): δ = 7.40-7.31 (m, ArH, 5H), 6.40 (dt, *J* = 6.0, 1.6 Hz, *J*_{H-F} = 1.6 Hz, =CHCHCO, 1H), 6.10 (dd, *J* = 6.0 Hz, ⁴*J* = 2.5 Hz, CF₂CH=CH, 1H), 4.34 (dddd, ⁴*J*_{H-F} = 8.9, 5.2 Hz, *J* = 6.7, 1.6 Hz, COCH, 1H), 4.11 (ddd, *J*_{H-F} = 16.1, 15.4 Hz, *J* = 6.7 Hz, PhCH, 1H), 3.49 (s, OCH₃, 3H), 3.20 ppm (s, OCH₃, 3H);

^{13}C NMR (100 MHz, CDCl_3): δ = 170.5, 139.1 (t, $J_{\text{C-F}}$ = 10.0 Hz), 134.1, 129.6 (t, $^1J_{\text{C-F}}$ = 254.7 Hz), 128.9, 128.3 (dd, $^2J_{\text{C-F}}$ = 30.1, 25.2 Hz), 128.0, 127.3, 60.9, 53.2 (t, $^2J_{\text{C-F}}$ = 24.5 Hz), 51.4 (d, $J_{\text{C-F}}$ = 5.3 Hz), 31.9 ppm; ^{19}F NMR (376 MHz, CDCl_3): δ = -90.2 (ddd, 2J = 251.0 Hz, $J_{\text{F-H}}$ = 16.1, $^4J_{\text{H-F}}$ = 8.9 Hz, 1F), -92.0 ppm (ddd, 2J = 251.1 Hz, $J_{\text{F-H}}$ = 15.4, $^4J_{\text{H-F}}$ = 5.2 Hz, 1F); $\bar{\nu}$ /(film) = 2963, 2940, 2361, 2342, 1661, 1456, 1418, 1387, 1364, 1350, 1169, 1051, 1034, 1026, 1093 cm^{-1} ; MS (CI): m/z (%): 296 (19) [(M+H)-F] $^+$, 276 (26) [(M+H)-F] $^+$, 248 (100) [M-F] $^+$, 218 (10) [(M+H)-OMe-F] $^+$, 187 (16), 161 (6); HRMS (APCI): calcd for $\text{C}_{14}\text{H}_{15}\text{F}_2\text{NO}_2\text{Na}$, 290.0963 [M+Na] $^+$ found 290.0964; t_{R} (GC) = 12.97 minutes.

Thermolysis of (Z)-3-((1R*,3S*)-2,2-difluoro-3-phenylcyclopropyl)-N-methoxy-N-methylacrylamide (229)

A solution of **212a** (126 mg, 0.47 mmol) in Ph_2O (0.5 mL) was heated at 165 °C for 17 h according to General Procedure I. The crude reaction mixture was loaded onto a silica pad (10 g) conditioned with hexane. Ph_2O was eluted with hexane then crude products were eluted with Et_2O , collected and concentrated under reduced pressure to afford a brown oil (53 mg). ^1H and ^{19}F NMR confirmed full consumption of alkenoate **212a**. Column chromatography on silica gel (1:9 to 2:5 EtOAc in hexane) was used to separate two major unknown products as yellow oils; unknown **S1** (13 mg) and unknown **S2** (7 mg). Lack of distinctive Weinreb amide signals in the ^1H NMR suggests decomposition had occurred. Data for **S1**: R_f = 0.21 (1:1 Et_2O in hexane); ^{19}F NMR (376 MHz, CDCl_3): δ = -100.41 (d, $J_{\text{F-H}}$ = 15.9 Hz). Data for **S2**: R_f = 0.39 (1:1 Et_2O in hexane); ^{19}F NMR (376 MHz, CDCl_3): δ = -87.39 (s).

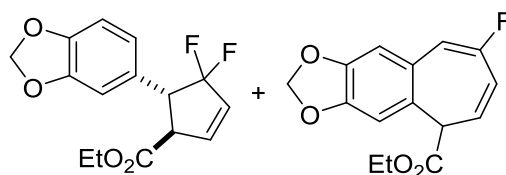
Preparation of (1R*,5R*)-4,4-difluoro-5-phenylcyclopent-2-ene-1-carbonitrile (230) and 4,4-difluoro-5-phenylcyclopent-1-ene-1-carbonitrile (236)



A solution of mixture **231a/231b** (100 mg, 0.48 mmol) in Ph_2O (1.0 mL) was heated to 90 °C in a sealed microwave vial for 17 hours in a DrySyn block. After cooling and venting, the resulting ^{19}F NMR spectrum confirmed full conversion of **213a**. The

microwave vial was resealed and heated to 160 °C for 17 hours in a DrySyn block. After cooling and venting, the resulting ^{19}F NMR spectrum confirmed full consumption of **213b**. The crude reaction mixture was transferred onto a pad of silica (15 g) in a sinter funnel which has been conditioned with hexane. Ph_2O was eluted using hexane and then crude product fractions were eluted using Et_2O , collected and concentrated under reduced pressure to afford a red oil (106 mg). Column chromatography on silica gel (0:1 to 1:9 Et_2O in hexane) afforded a mixture difluorocyclopentenenes **230** and **236** (6:1 ratio by ^1H NMR) as a yellow oil (44.7 mg, 48%). Data for mixture of **230** and **236**: $R_f = 0.21$ (1:9 Et_2O in hexane); $\bar{\nu}/(\text{film}) = 3091, 3069, 3036, 2915, 2249, 2229, 1502, 1457, 1349, 1178 \text{ cm}^{-1}$; HRMS (APCI): calcd for $\text{C}_{12}\text{H}_8\text{F}_2\text{N}$, 204.0625 [M-H] found 204.0634; Data for **230**: ^1H NMR (400 MHz, CDCl_3): $\delta = 7.47\text{-}7.40$ (m, ArH, 3H), 7.35-7.32 (m, ArH, 2H), 6.45 (dt, $J = 6.0, 1.9$ Hz, $^4J_{\text{H-F}} = 1.3$ Hz, $\text{C}(\text{F}_2)\text{CH}=\text{CH}$, 1H) 6.26 (dd, $J = 6.0$ Hz, $J_{\text{H-F}} = 2.6$ Hz, $\text{C}(\text{F}_2)\text{-CH}=\text{CH}$, 1H), 3.99 (dddd, $J = 7.6, 2.0$ Hz, $^4J_{\text{H-F}} = 9.6, 5.0$ Hz, $\text{C}(\text{H})\text{CN}$, 1H), 3.90 ppm (ddd, $J = 7.6$ Hz, $J_{\text{H-F}} = 14.6, 13.7$ Hz, ArCH, 1H); ^{13}C NMR (100 MHz, CDCl_3): $\delta = 134.8$ (t, $J_{\text{C-F}} = 10.0$ Hz), 131.0, 130.4 (dd, $^2J_{\text{C-F}} = 30.1, 24.1$ Hz), 128.5, 128.4 (represents 2 carbon atoms), 127.4 (t, $^1J_{\text{C-F}} = 246.7$ Hz), 117.3 (d, $^4J_{\text{C-F}} = 5.2$ Hz), 5.4 (t, $^2J_{\text{C-F}} = 25.4$ Hz), 38.3 ppm (d, $J_{\text{C-F}} = 6.4$ Hz); ^{19}F NMR (376 MHz, CDCl_3): $\delta = -90.98$ (ddd, $^2J = 255.6$ Hz, $J_{\text{F-H}} = 14.9$ Hz, $^4J_{\text{F-H}} = 9.6$ Hz, CF_aF_b , 1F), -93.00 ppm (ddd, $^2J = 255.6$ Hz, $J_{\text{F-H}} = 13.7$ Hz, $^4J_{\text{F-H}} = 14.6$ Hz, CF_aF_b , 1F); MS (CI): m/z (%): 246 (10) $[\text{M}+\text{C}_3\text{H}_5]^+$, 234 (20) $[\text{M}+\text{C}_2\text{H}_5]^+$, 206 (77) $[\text{M}+\text{H}]^+$, 186 (100) $[\text{M-F}]^+$; t_R (GC) = 11.31 minutes. Data for **236**: ^1H NMR (400 MHz, CDCl_3): $\delta = 7.47\text{-}7.40$ (m, ArH, 3H), 7.24-7.22 (m, ArH, 2H), 6.87 (dt, $J = 5.0$ Hz, $^4J_{\text{H-F}} = 2.6$ Hz, $^4J = 2.2$ Hz, $\text{CF}_2\text{-CH}_2\text{-CH=}$, 1H), 4.36 (dddt, $J_{\text{H-F}} = 18.0, 7.9$ Hz, $^4J = 2.2, 1.4$ Hz, ArCH, 1H), 3.17-3.09 (m, $\text{CF}_2\text{-CH}_2\text{-CH=}$, 2H); ^{13}C NMR (100 MHz, CDCl_3): $\delta = 143.9$ (t, $J_{\text{C-F}} = 4.1$ Hz), 129.9, 128.3, 128.2 (represents 2 carbon atoms), 127.1 (t, $^1J_{\text{C-F}} = 255.1$ Hz), 115.9 (dd, $J_{\text{C-F}} = 6.7, 2.8$ Hz), 114.1, 58.7 (dd, $^2J_{\text{C-F}} = 26.7, 25.4$ Hz), 41.9 ppm (dd, $J_{\text{C-F}} = 28.9, 28.3$ Hz); ^{19}F NMR (376 MHz, CDCl_3): $\delta = (-90.62)\text{-}(-91.40)$ (m, CF_aF_b , underneath ^{19}F signal for major product **230**), $(-98.05)\text{-}(-98.76)$ ppm (m, containing d, $^2J = 233.1$ Hz, CF_aF_b); MS (CI): m/z (%): 246 (7) $[\text{M}+\text{C}_3\text{H}_5]^+$, 234 (17) $[\text{M}+\text{C}_2\text{H}_5]^+$, 206 (100) $[\text{M}+\text{H}]^+$, 186 (35) $[\text{M-F}]^+$; t_R (GC) = 11.50 minutes.

Preparation of ethyl (1R,5R)-5-(benzo[d][1,3]dioxol-5-yl)-4,4-difluorocyclopent-2-ene-1-carboxylate (232) and ethyl 8-fluoro-5H-cyclohepta[4,5]benzo[1,2-d][1,3]dioxole-5-carboxylate (237)



A solution of **214a** (445 mg, 0.07 mmol) in a toluene (7.5 mL) was heated to 70 °C for 17 h according the General Procedure I. ^1H and ^{19}F NMR showed full consumption of **214a** to a mixture of difluorocyclopentene **232** and benzoheptadiene **237** (42:58 respectively, relative ratio by ^{19}F NMR). HPLC purification on a Kromasil C18 cartridge (3:10 to 9.9:10 gradient of MeCN containing 0.1% ammonia solution in 10 mM ammonium bicarbonate) afford clean fluoroheptadiene **237** (45 mg, 11%) as a white solid and difluorocyclopentene **232** (82 mg, 18%). Note: poor yield could be due to partial solubility of crude reaction mixture in loading solvent for HPLC purification (1:1 DMSO/MeOH). Data for **232**: R_f = 0.35 (1:4 Et₂O in hexane); ^1H NMR (400 MHz, CDCl₃): δ = 6.81 (s, ArH, 3H), 6.48 (ddd, J = 6.0 Hz, $J_{\text{H-F}}$ = 1.7 Hz, 4J = 1.7 Hz, CF₂-CH=CH, 1H), 6.07 (dd, J = 6.0, 2.5 Hz, CH=CH, 1H), 5.98 (s, O₂CH₂, 2H), 4.19 (q, J = 7.0 Hz, OCH₂CH₃, 2H), 3.95-3.82 (m, ArCH and HCCO₂Et, 2H), 1.26 ppm (t, J = 7.0 Hz, CH₂CH₃, 3H); ^{13}C NMR (100 MHz, CDCl₃): δ = 170.2 (d, $^4J_{\text{C-F}}$ = 2.7 Hz), 147.3, 146.8, 138.4 (t, $J_{\text{C-F}}$ = 10.4 Hz), 129.0 (t, $^1J_{\text{C-F}}$ = 245.7 Hz), 128.4 (dd, $^2J_{\text{C-F}}$ = 30.8, 24.5 Hz), 127.2, 122.3, 108.8, 107.7, 100.6, 61.0, 54.2 (d, $J_{\text{C-F}}$ = 5.8 Hz), 53.1 (t, $^2J_{\text{C-F}}$ = 24.0 Hz), 13.6 ppm; ^{19}F NMR (376 MHz, CDCl₃): δ = -90.21 (ddd, 2J = 252.5 Hz, $J_{\text{F-H}}$ = 16.4, $^4J_{\text{F-H}}$ = 8.6 Hz, CF_aF_b, 1F), -93.07 ppm (ddd, 2J = 252.5 Hz, $J_{\text{F-H}}$ = 14.1, $^4J_{\text{F-H}}$ = 5.1 Hz, CF_aF_b, 1F); $\bar{\nu}$ /(film) = 2982, 2904, 1614, 1731, 1506, 1493, 1446, 1245, 1167, 1018 cm⁻¹; MS (CI): m/z (%): 277 (100) [M-F]⁺, 231 (16), 203 (15), 175 (4) [M-C₇O₂H₅]⁺; HRMS (APCI): calcd for C₁₅H₁₄FO₄, 277.0876 [M-F] found 277.0905; t_R (GC) = 14.09 minutes. Data for **237**: m.p. = 118-120 °C (chloroform/pentane); R_f = 0.40 (1:4 Et₂O in hexane); ^1H NMR (400 MHz, CDCl₃): δ = 6.82 (s, ArH, 1H), 6.80 (d, $J_{\text{H-F}}$ = 18.1 Hz, C-CH=CF, 1H), 6.59 (s, ArH, 1H), 6.22-6.14 (m, representing CF-CH=CH and C(H)-CH=CH, 2H), 6.01 (d, 2J = 1.4 Hz, OCH₂H₂O, 1H),

5.98 (d, $^2J = 1.4$ Hz, $\text{OCH}_a\text{H}_b\text{O}$, 1H), 4.30 (ABq, $J = 7.2$ Hz, $^2J = 1.9$ Hz, $\text{OCH}_a\text{H}_b\text{CH}_3$, 2H), 3.69 (d, $J = 5.2$ Hz, HCCO_2Et , 1H), 1.31 ppm (t, $J = 7.2$ Hz, CH_2CH_3 , 3H); ^{13}C NMR (100 MHz, CDCl_3): $\delta = 171.0$, 158.6 (d, $^2J_{\text{C-F}} = 245.5$ Hz), 148.6, 146.1, 127.7 (d, $J_{\text{C-F}} = 12.5$ Hz), 126.0 (d, $J_{\text{C-F}} = 11.4$ Hz), 125.8, 119.3 (d, $^2J_{\text{C-F}} = 35.1$ Hz), 113.0 (d, $^2J_{\text{C-F}} = 27.9$ Hz), 107.0 (d, $^5J_{\text{C-F}} = 3.8$ Hz), 105.1, 101.1, 60.9, 48.9, 13.7 ppm; ^{19}F NMR (376 MHz, CDCl_3): $\delta = -102.97$ ppm (ddd, $J_{\text{F-H}} = 18.1$, 4.8 Hz, $^4J_{\text{C-F}} = 4.8$ Hz); $\bar{\nu}/(\text{film}) = 2982$, 2904, 1733, 1645, 1506, 1485, 1374, 1333, 1305, 1238, 1193 cm^{-1} ; MS (CI): m/z (%): 305 (11) $[\text{M}+\text{C}_2\text{H}_5]^+$, 277 (65) $[\text{M}+\text{H}]^+$, 257 (41) $[\text{M}+\text{H}]^+$, 231 (100) $[\text{M}-\text{OEt}]^+$, 203 (40) $[\text{M}-\text{CO}_2\text{Et}]^+$, 57 (80); HRMS (ASAP+): calcd for $\text{C}_{15}\text{H}_{14}\text{FO}_4$, 277.0876 $[\text{M}+\text{H}]^+$ found 277.0884; t_R (GC) = 14.97 minutes.

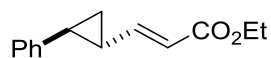
Preparation of ((1S*,2S*)-2-phenylcyclopropyl)methanol (**239**)



Diiodomethane (1 ml, 12.5 mmol) was added dropwise to a solution of diethylzinc (6.25 mL of a 1 M solution in hexane, 6.25 mmol) in DCM (2 mL) at 0 °C over a period of 5 minutes and stirred for 20 minutes under nitrogen. A solution of cinnamyl alcohol (335 mg, 1.25 mmol) in DCM (1.5 mL) was added dropwise and the reaction mixture and stirred for 2.5 hours at 0 °C. The reaction mixture was quenched with saturated aqueous NH_4Cl (10 ml) and EtOAc (10 ml). The organic layer was separated and the aqueous layer extracted further with EtOAc (3 x 10 ml). The original organic layer and extracts were combined, dried (MgSO_4) and concentrated under reduced pressure to remove volatile organic solvent. Column chromatography on silica gel (2:3 EtOAc in hexane) afforded alcohol **239** as a yellow oil (93 mg, 52%). $R_f = 0.23$ (1:1 Et_2O in hexane); ^1H NMR (400 MHz, CDCl_3): $\delta = 7.29$ -7.26 (m, ArH , 2H), 7.17 (tt, $J = 7.3$ Hz, $^4J = 1.2$ Hz, ArH , 1H), 7.10-7.08 (m, ArH , 2H), 3.64 (dd, $^2J = 11.3$ Hz, $J = 6.8$ Hz, $\text{CH}_a\text{H}_b\text{OH}$, 1H), 3.62 (dd, $^2J = 11.3$ Hz, $J = 6.8$ Hz, $\text{CH}_a\text{H}_b\text{OH}$, 1H), 1.84 (td, $J = 9.8$, 4.9 Hz, PhCH , 1H), 1.78 (br. s, OH , 1H), 1.50-1.44 (m, $\text{CH}_2\text{CH}(\text{CH}_2)\text{CH}$, 1H), 1.00-0.92 ppm (m, CH_2 , 2H); ^{13}C NMR (100 MHz, CDCl_3): $\delta = 142.5$, 128.4, 125.9, 125.7, 66.5, 25.3, 21.3, 13.8 ppm; $\bar{\nu}/(\text{film}) = 3333$, 3026, 3003, 2361, 2342, 1605, 1497, 1018, 743, 696 cm^{-1} ; MS (CI): m/z (%): 159 (14) $[(\text{M}+\text{H})-$

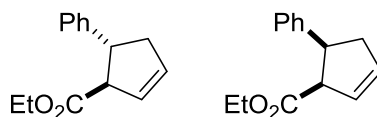
OH]⁺, 131 (100) [M-OH]⁺; 117 (29), 91 (28); *t*_R (GC) = 11.10 minutes. Data was in agreement with those reported by Charette and co-workers.²⁴³

Preparation of ethyl (*E*)-3-((1*R**,2*S**)-2-phenylcyclopropyl)acrylate (**227a**)



Ester **227a** was prepared from alcohol **239** (100 mg, 0.67 mmol), TEMPO (10 mg, 0.067 mmol), BAIB (237 mg, 0.74 mmol), (carbethoxyethylidene)triphenylphosphorane (303 mg, 0.87 mmol) and anhydrous DCM (1 mL) according to general procedure D with an oxidation time of 3.5 hours and an olefination time of 20 hours. Column chromatography on silica gel (1:9 Et₂O in hexane) afforded ester **227a** as a colourless oil (100 mg, 67%). *R*_f = 0.42 (1:4 Et₂O in hexane); ¹H NMR (400 MHz, CDCl₃): δ = 7.33-7.28 (m, ArH, 2H), 7.21 (tt, *J* = 7.3 Hz, ⁴*J* = 1.3 Hz, ArH, 1H), 7.12-7.09 (m, ArH, 2H), 6.62 (dd, *J* = 15.5, 9.9 Hz, CHCH=CH, 1H), 5.92 (d, *J* = 15.5 Hz, CH=CH, 1H), 4.21 (q, *J* = 7.2 Hz, OCH₂CH₃, 2H), 2.20 (ddd, *J* = 9.5, 6.2, 4.3 Hz, PhCH, 1H), 1.84 (dddd, *J* = 9.9, 8.4, 5.4, 4.1 Hz, CH₂CHCH=CH, 1H), 1.47 (ddd, ²*J* = 8.5, *J* = 6.6, 5.2 Hz, CHCH₀H₀CH, 1H), 1.36-1.30 ppm (m, (incl. 1.31 ppm, t, *J* = 7.2 Hz, OCH₂CH₃, 3H), 4H); ¹³C NMR (100 MHz, CDCl₃): δ = 166.2, 151.0, 140.3, 128.0, 125.7, 125.4, 118.4, 59.6, 26.4, 26.2, 17.2, 13.8 ppm; $\bar{\nu}$ /(film) = 2980, 2359, 2342, 1709, 1643, 1256, 1175, 1036 cm⁻¹; MS (CI): *m/z* (%): 245 (6) [M+C₂H₅]⁺, 217 (56) [M+H]⁺, 171 (50) [M-OEt]⁺, 143 (100) [M-CO₂Et]⁺, HRMS (APCI): calcd for C₁₄H₁₇O₂, 217.1223 [M+H]⁺ found 217.1224; *t*_R (GC) = 13.57 minutes.

Preparation of ethyl (1*R**,5*R**)-5-phenylcyclopent-2-ene-1-carboxylate (**231a**) and ethyl (1*R**,5*S**)-5-phenylcyclopent-2-ene-1-carboxylate (**231b**)



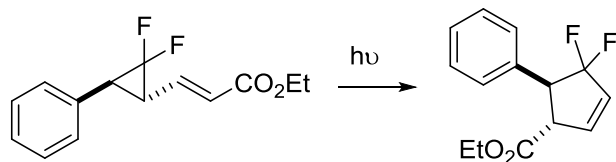
A solution of **227a** (100 mg, 0.46 mmol) in a Ph₂O (0.5 mL) was heated to 220 °C for 17 h according the General Procedure I. The crude reaction mixture was transferred onto a pad of silica (10 g) in a sinter funnel which has been conditioned with hexane. Ph₂O was eluted using hexane and then crude product fractions were eluted using Et₂O, collected and concentrated under reduced pressure to afford an

orange oil (80 mg). Column chromatography on silica gel (0:1 to 1:9 Et₂O in hexane) afforded a *trans*-**231a** (40 mg, 40%) and *cis*-**231b** (22 mg, 22%, compound started to decompose slowly after isolation to an unknown side product) as pale yellow oils. Data for *trans*-**231a**: $R_f = 0.65$ (1:4 Et₂O in hexane); ¹H NMR (400 MHz, CDCl₃): $\delta = 7.35\text{--}7.27$ (m, ArH, 3H), 7.25–7.21 (m, ArH, 2H), 5.96 (ddt, $J = 5.7, 2.5$ Hz, $^4J = 2.3$ Hz, CH₂CH=CH, 1H), 5.79 (ddt, $J = 5.7, 2.4$ Hz, $^4J = 2.2$ Hz, CH₂CH=CH, 1H), 4.17 (q, $J = 7.2$ Hz, OCH₂CH₃, 2H), 3.83 (dt, $J = 9.2, 6.6$ Hz, ArCH, 1H), 3.67 (dddd, $J = 9.2, 2.5$ Hz, $^4J = 2.5, 2.2$ Hz, HCCO₂Et, 1H), 3.00 (dddd, $^2J = 16.9$ Hz, $J = 9.2, 2.4$ Hz, $^4J = 2.6, 2.3$ Hz, -CH_aH_b-, 1H), 2.56 (dddd, $^2J = 16.9$ Hz, $J = 6.6, 2.4$ Hz, $^4J = 2.6, 2.3$ Hz, -CH_aH_b-, 1H), 1.27 ppm (t, $J = 7.2$ Hz, 3H); ¹³C NMR (100 MHz, CDCl₃): $\delta = 173.6, 145.0, 132.2, 128.1, 127.7, 126.6, 125.9, 60.2, 59.0, 45.8, 41.1, 13.7$ ppm; $\bar{\nu}$ /(film) = 3060, 3029, 2980, 2932, 2906, 2854, 1731, 1495, 1457, 1245, 1176 cm⁻¹; MS (CI): m/z (%): 245 (2) [M+C₂H₅]⁺, 217 (8) [M+H]⁺, 171 (19) [M-OEt]⁺, 143 (100) [M-CO₂Et]⁺, HRMS (APCI): calcd for C₁₄H₁₇O₂, 217.1228 [M+H]⁺ found 217.1229; t_R (GC) = 12.44 minutes. Data *cis*-**231b**: $R_f = 0.52$ (1:4 Et₂O in hexane); ¹H NMR (400 MHz, CDCl₃): $\delta = 7.27\text{--}7.28$ (m, ArH, 4H), 7.22–7.17 (m, ArH, 1H), 6.15 (ddt, $J = 5.7, 2.2$ Hz, $^4J = 2.1$ Hz, CH₂CH=CH, 1H), 5.85 (ddt, $J = 5.7, 2.3$ Hz, $^4J = 1.9$ Hz, CH₂CH=CH, 1H), 3.93 (dddt, $J = 9.1, 2.1$ Hz, $^4J = 2.0, 1.9$ Hz, HCCO₂Et, 1H), 3.85 (dt, $J = 9.1, 7.2$ Hz, ArCH, 1H), 3.78–3.61 (m, OCH_aH_bCH₃, 2H); 2.83 (dddd, $J = 7.2, 2.3$ Hz, $^4J = 2.2, 1.9$ Hz, CH-CH₂-CH=CH-, 2H), 0.85 ppm (t, $J = 7.0$ Hz, CH₂CH₃, 3H); ¹³C NMR (100 MHz, CDCl₃): $\delta = 172.2, 141.5, 133.8, 128.0, 127.5, 127.4, 126.0, 59.6, 55.9, 46.3, 38.4, 13.2$ ppm; $\bar{\nu}$ /(film) = 3060, 3029, 2980, 2932, 2904, 1729, 1495, 1457, 1370, 1178 cm⁻¹; MS (CI): m/z (%): 245 (5) [M+C₂H₅]⁺, 217 (14) [M+H]⁺, 171 (20) [M-OEt]⁺, 143 (100) [M-CO₂Et]⁺; HRMS (TOF): calcd for C₁₄H₁₇O₂, 216.1150 [M] found 216.1155; t_R (GC) = 12.28 minutes.

7.6. Compounds from Chapter 4

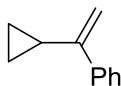
6.6.1. Experimental Procedure

UV Irradiation of ethyl 3-((1'*R**,3'*S**)-2',2'-difluoro-3'-phenylcyclopropyl) prop-2E-enoate (**147a**)



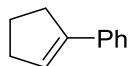
A solution of cyclopropyl **147a** in degassed MeCN (3.4 mL) was loaded into an FEP batch reactor (preconditioned with degassed MeCN (6 mL)) coiled around a quartz immersion well containing a low pressure UV lamp (wavelength 254 nm, 16 W). The reaction mixture was loaded further into the reactor by the addition of degassed MeCN (1.5 mL) and irradiated for 19 h at room temperature (maximum temperature reached was 25.1 °C). The FEP tubing was flushed with 20 mL MeCN and the reaction mixture collected, concentrated under reduced pressure and analysed by ^1H and ^{19}F NMR. No rearrangement was observed and the crude reaction mixture re-loaded into the reactor using the procedure described above and irradiated for a further 90 h at room temperature (maximum temperature reached was 23.7 °C). The FEP tubing was flushed with MeCN (20 mL) and the reaction mixture collected, concentrated under reduced pressure. ^{19}F NMR analysis confirmed a mixture of four diastereoisomers of cyclopropyl **147/152** present; only trace amounts of rearrangement was observed over the 109 hours of irradiation.

Preparation of (1-cyclopropylvinyl)benzene (**251**)



Butyl lithium (3.5 mL of a 1.9 M in THF, 6.6 mmol) was added dropwise over 5 minutes to a cooled solution of methyltriphenylphosphonium iodide (3.57 g, 10 mmol) in anhydrous THF (20 mL) and stirred under nitrogen for 2 hours. The resulting saturated yellow solution was cooled to -10 °C and cyclopropyl phenyl ketone (1.4 mL, 10.2 mmol) was added neat into the reaction mixture and stirred for 3 hours, quenched with aq. NH₄Cl (sat., 10 mL) and allowed to warm to room temperature. The reaction mixture was concentrated under reduced pressure to remove the organic solvent, then Et₂O (20 mL) added and the resulting layers separated and collected. The aqueous layer was extracted further with Et₂O (2 x 20 mL) and the organic extracts combined with the original organic layer, dried (MgSO₄) and concentrated under reduced pressure (40 °C, 300 mbar). ¹H NMR analysis of crude product showed 61% conversion to desired product. Purification on silica gel (hexane) afforded desired product **251** as a colourless oil (1.15 g), acetone (2 x 10 mL) was added to azeotrope any remaining hexane to afford **251** (720 mg, 50%), as a colourless oil. *R_f* = 0.6 (hexane); ¹H NMR (400 MHz, CDCl₃): δ = 7.63-7.61 (m, ArH, 2H), 7.39-7.34 (m, ArH, 2H), 7.32-7.28 (m, ArH, 1H), 5.30 (d, ²J = 0.9 Hz, C=CH_aH_b, 1H), 4.96 (dd, ⁴J = 1.2 Hz, ²J = 0.9 Hz, C=CH_aH_b, 1H), 1.68 (dddt, *J* = 8.3, 7.9, 5.4 (t), ⁴J = 1.2 Hz, CH, 1H), 0.87 (ddd, *J* = 8.3, 6.3, 4.1 Hz, C(H)CH₂CH₂, 2H), 0.64-0.60 ppm (CH₂, 2H); ¹³C NMR (400 MHz, CDCl₃): δ = 148.9, 141.2, 127.7, 127.0, 125.7, 108.6, 76.8, 15.2, 6.2 ppm; $\bar{\nu}$ /(film) = 3083, 3057, 3003, 1625, 1575, 1496, 1446, 1262, 1022, 890, 776, 703 cm⁻¹; *m/z* (%): 173 (5) [M+C₂H₅]⁺, 145 (100) [M+H]⁺, 130 (25) [(M-CH₂)+H]⁺, 129 (24) [M-CH₂-H]⁺, 117 (50) [(M-C₂H₄)+H]⁺, 91 (28) [M-C₃H₅-CH₂]⁺, 67 (94) [M-Ph]; *t_R* (GC) = 9.787 minutes. Data was in agreement with those reported by Gonzalez-de-Castro and Xiao.²⁴⁴

Preparation of cyclopent-1-en-1-ylbenzene (**252**)



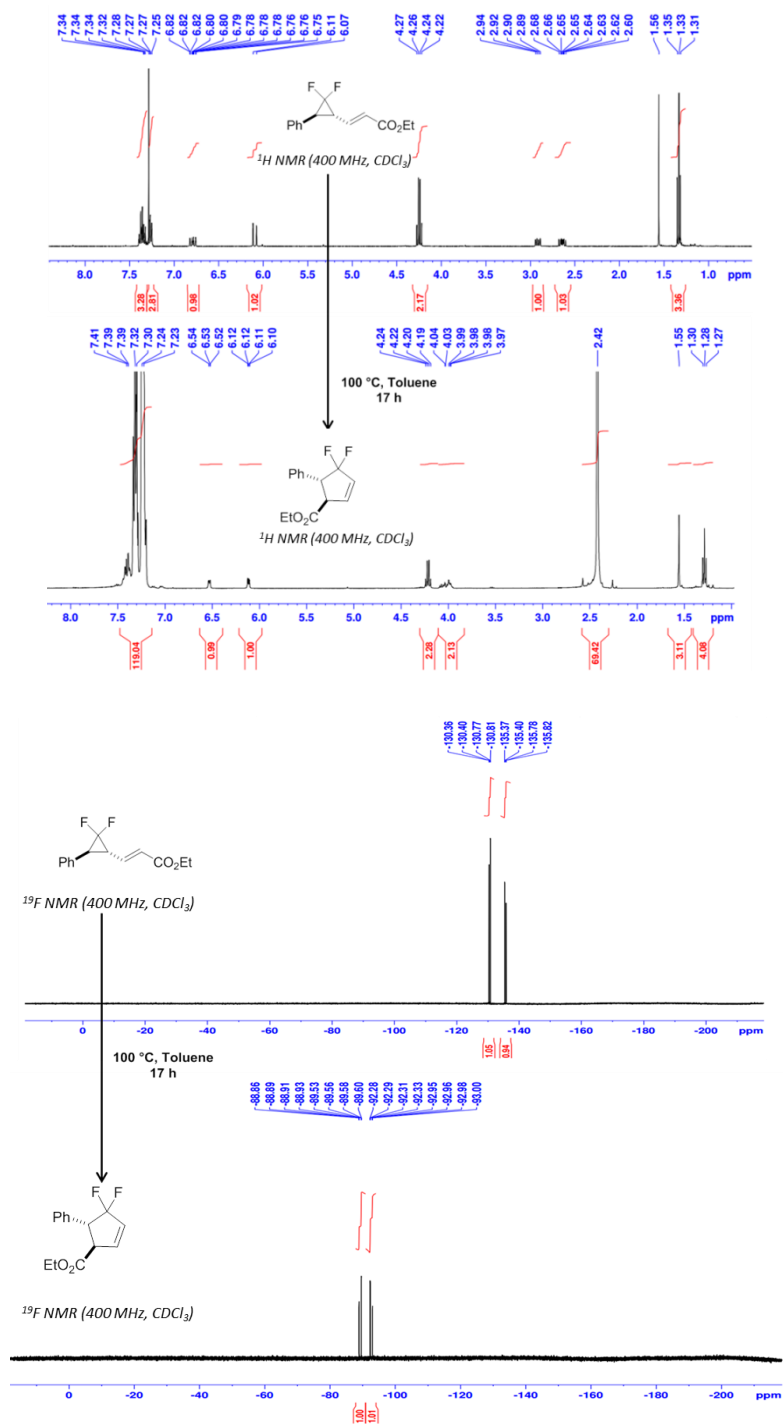
A solution of $\text{Ni}(\text{cod})_2$ (9.6 mg, 0.035 mmol) and 1,3-Bis(2,6-diisopropylphenyl)imidazol-2-ylidene (IPr, 27.2 mg, 0.07 mmol) in anhydrous $[\text{D}_6]$ -benzene (0.5 mL) was shaken and added to a vial containing alkene **251** and the start time for the reaction recorded in the glovebox. The reaction mixture was mixed using a syringe and transferred to a NMR tube which was sealed, removed from the glovebox and followed by ^1H NMR at room temperature. Starting alkene was characterised by proton signal at 5.25 ppm (1H) and product by proton signal at 6.01 ppm (1H). Signals representative of free cyclooctadiene were also evident (5.56 ppm). Full consumption of alkene **251** was observed after 3.5 hours at room temperature.

All Ni-mediated reaction conditions screened with difluorocyclopropyl **147a** followed the same procedure above and followed by ^{19}F NMR.

Appendix

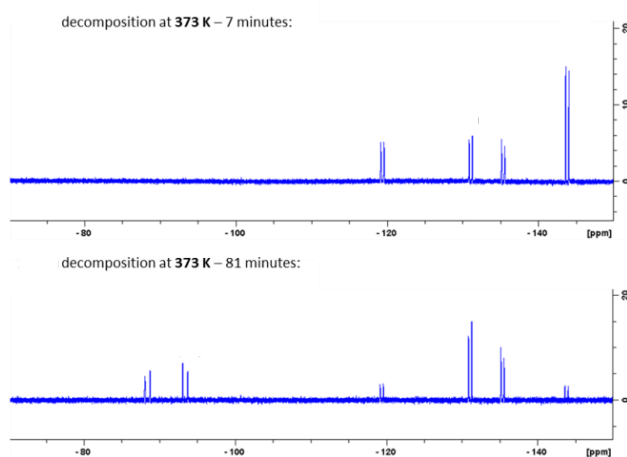
Supporting Information for Chapter 2

Crude NMR spectra for rearrangement of **147a**



Experimental procedure for VT ^{19}F NMR Kinetics

^{19}F NMR spectra were acquired on a Brüker AV400 instrument equipped with a QNP-z probe and a temperature control unit. Data was collected at 376 MHz using 8 scans per data point. Settings for spectra acquisition were as follows: NS = 8 scans; D1 = 1.5 s; SW = 199.77 ppm and O1P = -100 ppm. The samples were held at reaction temperature for the duration of the experiment: 373 K for reaction profiles for **147a** and **147b**, and **152a** and **152b**, and 363, 373, 383 and 393 K for Arrhenius plots with **147a**. d_8 -Toluene and d_{10} -xylene were purchased from Cambridge Isotope Laboratories, Inc. and Sigma Aldrich, respectively and used as received. A solution of VCPR precursor (typically 0.07-0.36 M) was made up in a clean, dry NMR tube and the tube was capped. The tube was inserted into the magnet and the instrument's internal temperature was set to the desired reaction temperature and allowed to equilibrate (approx. 2-7 minutes heating time). The sample was then analysed at appropriate intervals using a Brüker Topspin automated script, *multi_zgvd2b*. Samples were automatically shimmed using *topshim* between acquisitions. Relative percentages were determined by averaging the manual integration for each compound on the resulting spectra using proprietary software. **Example spectra:**



Kinetic Data

147a Reaction Profile

¹⁹F NMR integration data for the VCPR of **147a** in d₈-toluene (0.15 M) heated at 373 K (AV400, QNP-z probe); 8 scans, D₁ = 1.5 s, TE = 373 K.

| Time (sec) | Average Integration | | | Relative Percentage (%) | | |
|------------|---------------------|------|-------|-------------------------|-------|-------|
| | 147a | 152a | 153 | 147a | 152a | 153 |
| 0 | 10.53 | 1.03 | 0.58 | 86.72 | 8.51 | 4.77 |
| 420 | 9.40 | 1.46 | 1.25 | 77.64 | 12.03 | 10.33 |
| 720 | 9.51 | 1.69 | 1.90 | 72.57 | 12.92 | 14.51 |
| 1020 | 10.18 | 1.84 | 2.72 | 69.08 | 12.47 | 18.46 |
| 1320 | 10.16 | 1.87 | 3.29 | 66.33 | 12.22 | 21.45 |
| 1620 | 9.96 | 1.66 | 3.70 | 65.01 | 10.82 | 24.17 |
| 1920 | 9.26 | 1.74 | 4.33 | 60.39 | 11.36 | 28.25 |
| 2220 | 8.88 | 1.68 | 4.78 | 57.91 | 10.92 | 31.17 |
| 2520 | 9.28 | 1.79 | 5.75 | 55.16 | 10.64 | 34.20 |
| 2820 | 8.72 | 1.66 | 6.15 | 52.74 | 10.05 | 37.22 |
| 3120 | 9.22 | 1.77 | 7.17 | 50.78 | 9.73 | 39.49 |
| 3420 | 8.66 | 1.54 | 7.42 | 49.15 | 8.76 | 42.09 |
| 3720 | 8.53 | 1.66 | 7.93 | 47.07 | 9.16 | 43.76 |
| 4020 | 8.23 | 1.51 | 8.36 | 45.47 | 8.34 | 46.20 |
| 4320 | 8.42 | 1.68 | 9.36 | 43.27 | 8.63 | 48.10 |
| 4620 | 8.11 | 1.58 | 9.74 | 41.74 | 8.11 | 50.14 |
| 4920 | 7.71 | 1.42 | 9.91 | 40.48 | 7.45 | 52.07 |
| 5220 | 7.49 | 1.38 | 10.34 | 39.00 | 7.17 | 53.83 |
| 5520 | 7.62 | 1.35 | 11.41 | 37.41 | 6.61 | 55.98 |
| 5820 | 7.94 | 1.45 | 12.70 | 35.94 | 6.57 | 57.50 |
| 6120 | 7.82 | 1.59 | 13.31 | 34.40 | 7.01 | 58.59 |
| 6420 | 7.52 | 1.36 | 14.09 | 32.75 | 5.92 | 61.33 |
| 6720 | 7.18 | 1.22 | 13.79 | 32.35 | 5.51 | 62.14 |
| 7020 | 6.43 | 1.04 | 13.23 | 31.04 | 5.04 | 63.91 |
| 7320 | 6.53 | 1.11 | 14.10 | 30.04 | 5.11 | 64.85 |
| 7620 | 6.30 | 1.35 | 14.32 | 28.68 | 6.15 | 65.17 |
| 7920 | 7.29 | 1.30 | 17.78 | 27.64 | 4.91 | 67.45 |
| 8220 | 7.09 | 0.90 | 18.54 | 26.71 | 3.40 | 69.88 |
| 8520 | 5.87 | 1.00 | 16.01 | 25.66 | 4.37 | 69.97 |
| 8820 | 5.83 | 0.91 | 16.80 | 24.78 | 3.86 | 71.35 |
| 9120 | 5.70 | 0.96 | 17.33 | 23.76 | 4.01 | 72.23 |
| 9420 | 5.70 | 0.94 | 18.39 | 22.78 | 3.74 | 73.48 |
| 9720 | 5.41 | 0.85 | 18.38 | 21.95 | 3.45 | 74.60 |
| 10020 | 5.20 | 0.77 | 18.57 | 21.18 | 3.13 | 75.69 |
| 10320 | 5.59 | 0.94 | 21.37 | 20.05 | 3.37 | 76.58 |
| 10620 | 4.88 | 0.75 | 19.06 | 19.77 | 3.03 | 77.19 |
| 36000 | 0.15 | 0.03 | 24.83 | 0.59 | 0.12 | 99.28 |

147a Reaction Profile

¹⁹F NMR integration data for the VCPR of **147a** in d₈-toluene (0.15 M) heated at 373 K (AV400, QNP-z probe); 8 scans, D₁ = 1.5 s, TE = 373 K.

| Time (sec) | Average Integration | | | Relative Percentage (%) | | |
|------------|---------------------|------|-------|-------------------------|-------|-------|
| | 147a | 152a | 153 | 147a | 152a | 153 |
| 420 | 0.88 | 1.06 | 0.00 | 45.38 | 54.62 | 0.00 |
| 540 | 0.65 | 0.71 | 0.00 | 47.87 | 52.13 | 0.00 |
| 900 | 1.44 | 0.70 | 0.08 | 64.95 | 31.41 | 3.64 |
| 1260 | 1.91 | 0.71 | 0.22 | 67.11 | 25.00 | 7.89 |
| 1620 | 2.52 | 0.70 | 0.35 | 70.63 | 19.70 | 9.66 |
| 1980 | 2.85 | 0.68 | 0.52 | 70.44 | 16.79 | 12.77 |
| 2340 | 3.18 | 0.67 | 0.73 | 69.37 | 14.62 | 16.01 |
| 2700 | 3.44 | 0.69 | 0.90 | 68.35 | 13.73 | 17.93 |
| 3060 | 3.30 | 0.69 | 1.07 | 65.27 | 13.65 | 21.07 |
| 3420 | 3.68 | 0.72 | 1.37 | 63.80 | 12.44 | 23.76 |
| 3780 | 3.48 | 0.68 | 1.48 | 61.78 | 12.02 | 26.20 |
| 4140 | 3.41 | 0.67 | 1.68 | 59.15 | 11.69 | 29.16 |
| 4500 | 3.59 | 0.68 | 1.99 | 57.35 | 10.91 | 31.74 |
| 4860 | 3.67 | 0.66 | 2.21 | 56.14 | 10.07 | 33.79 |
| 5220 | 3.47 | 0.71 | 2.30 | 53.56 | 10.94 | 35.50 |
| 5580 | 3.28 | 0.67 | 2.45 | 51.23 | 10.54 | 38.23 |
| 5940 | 3.96 | 0.71 | 3.16 | 50.57 | 9.08 | 40.35 |
| 6300 | 3.64 | 0.69 | 3.14 | 48.77 | 9.21 | 42.02 |
| 6660 | 3.56 | 0.63 | 3.36 | 47.21 | 8.33 | 44.46 |
| 7020 | 3.74 | 0.64 | 3.73 | 46.08 | 7.86 | 46.06 |
| 7380 | 3.33 | 0.67 | 3.59 | 43.88 | 8.83 | 47.29 |
| 7740 | 3.20 | 0.71 | 3.69 | 42.12 | 9.37 | 48.51 |
| 8100 | 3.56 | 0.67 | 4.34 | 41.53 | 7.83 | 50.64 |
| 8460 | 3.57 | 0.67 | 4.71 | 39.87 | 7.44 | 52.68 |
| 8820 | 3.79 | 0.70 | 5.26 | 38.91 | 7.13 | 53.96 |
| 9180 | 3.56 | 0.64 | 5.25 | 37.62 | 6.82 | 55.56 |
| 9540 | 3.47 | 0.64 | 5.51 | 36.10 | 6.61 | 57.29 |
| 9900 | 3.52 | 0.61 | 5.88 | 35.20 | 6.06 | 58.73 |
| 10260 | 3.78 | 0.66 | 6.54 | 34.40 | 5.97 | 59.63 |
| 10620 | 3.85 | 0.64 | 7.15 | 33.06 | 5.52 | 61.42 |
| 10980 | 3.64 | 0.62 | 7.12 | 31.99 | 5.49 | 62.52 |
| 11340 | 3.89 | 0.64 | 7.96 | 31.13 | 5.09 | 63.78 |
| 11700 | 3.31 | 0.64 | 7.33 | 29.36 | 5.66 | 64.97 |
| 12060 | 3.40 | 0.67 | 7.64 | 29.05 | 5.72 | 65.23 |
| 12420 | 3.84 | 0.68 | 9.13 | 28.15 | 4.95 | 66.90 |
| 12780 | 3.96 | 0.69 | 10.11 | 26.83 | 4.64 | 68.53 |
| 36000 | 2.86 | 0.73 | 67.44 | 4.03 | 1.03 | 94.95 |

147b Reaction Profile

¹⁹F NMR integration data for the VCPR of **147b** in *d*₈-toluene (0.36 M) heated at 373 K (AV400, QNP-z probe); 8 scans, *D*₁ = 1.5 s, *TE* = 373 K.

| Time (sec) | Average Integration | | Relative Percentage (%) | |
|------------|---------------------|------|-------------------------|-------|
| | 147b | 152b | 147b | 152b |
| 420 | 0.92 | 0.09 | 91.15 | 8.85 |
| 720 | 1.00 | 0.15 | 86.80 | 13.20 |
| 1020 | 0.93 | 0.18 | 83.81 | 16.19 |
| 1320 | 0.91 | 0.18 | 83.27 | 16.73 |
| 1620 | 0.90 | 0.20 | 81.97 | 18.03 |
| 1920 | 0.92 | 0.21 | 81.51 | 18.49 |
| 2220 | 0.92 | 0.22 | 80.41 | 19.59 |
| 2520 | 0.91 | 0.22 | 80.84 | 19.16 |
| 2820 | 0.93 | 0.25 | 78.80 | 21.20 |
| 3120 | 0.90 | 0.23 | 79.34 | 20.66 |
| 3420 | 0.92 | 0.25 | 78.94 | 21.06 |
| 3720 | 0.90 | 0.27 | 77.07 | 22.93 |
| 4020 | 0.91 | 0.25 | 78.22 | 21.78 |
| 4320 | 0.91 | 0.24 | 79.42 | 20.58 |
| 4620 | 0.92 | 0.26 | 77.68 | 22.32 |
| 4920 | 0.93 | 0.26 | 77.91 | 22.09 |
| 5220 | 0.91 | 0.25 | 78.65 | 21.35 |
| 5520 | 0.92 | 0.25 | 78.55 | 21.45 |

152b Reaction Profile

¹⁹F NMR integration data for the VCPR of **152b** in *d*₈-toluene (0.07 M) heated at 373 K (AV400, QNP-z probe); 8 scans, *D*₁ = 1.5 s, *TE* = 373 K.

| Time (sec) | Average Integration | | Relative Percentage (%) | |
|------------|---------------------|------|-------------------------|-------|
| | 147b | 152b | 147b | 152b |
| 300 | 0.65 | 1.27 | 33.81 | 66.19 |
| 480 | 0.45 | 0.70 | 38.18 | 59.10 |
| 840 | 0.88 | 0.71 | 53.58 | 43.54 |
| 1200 | 1.13 | 0.70 | 60.50 | 37.39 |
| 1560 | 1.46 | 0.69 | 66.67 | 31.23 |
| 1920 | 1.79 | 0.69 | 71.05 | 27.41 |
| 2280 | 2.01 | 0.68 | 72.92 | 24.78 |
| 2640 | 2.20 | 0.69 | 74.50 | 23.26 |
| 3000 | 2.33 | 0.69 | 76.09 | 22.43 |
| 3360 | 2.39 | 0.68 | 75.69 | 21.53 |
| 3720 | 2.55 | 0.69 | 76.87 | 20.92 |
| 4080 | 2.58 | 0.69 | 76.73 | 20.35 |
| 4440 | 2.58 | 0.68 | 77.20 | 20.35 |
| 4800 | 2.63 | 0.69 | 78.32 | 20.41 |
| 5160 | 2.60 | 0.67 | 77.58 | 20.07 |
| 5520 | 2.59 | 0.67 | 77.61 | 20.03 |
| 5880 | 2.58 | 0.71 | 76.14 | 20.88 |
| 6240 | 2.58 | 0.69 | 76.37 | 20.56 |
| 6600 | 2.65 | 0.70 | 76.90 | 20.27 |
| 6960 | 2.70 | 0.68 | 78.18 | 19.58 |
| 7320 | 2.81 | 0.72 | 76.95 | 19.69 |

NMR Simulation

The NMR concentration/time data obtained for **147a**, **152a** and **153** (including measured endpoints) was imported into Berkeley Madonna software^{S171} from text files and simulated running the method below:

METHOD RK4

STARTIME = 0

STOPTIME = 36000

DT = 0.05

A0=0 {Start concentration of trans cyclopropane}

Init A=A0

B0=0 {Start concentration of cyclopentene}

Init B=B0

C0=100 {Start concentration of cis cyclopropane}

Init C=C0

k1=0.0001 {k1 is the VCPR}

k2=0.0001 {k2 is the isomerisation to cis}

k_2=0.0001 {k_2 is the isomerisation back to trans}

*d/dt (A)=-k1*A-k2*A+k_2*C*

*d/dt (B)=k1*A*

*d/dt (C)=k2*A-k_2*C*

LIMIT A>=0

LIMIT B>=0

LIMIT C>=0

Arrhenius Data

120 °C Data:

¹⁹F NMR integration data for the VCPR of **147a** in *d*₁₀-xylene (0.35 M) heated at **393 K** (AV400, QNP-z probe); 8 scans, *D*₁ = 1.5 s, *TE* = **393 K**.

| Time (s) | Average Integrals | | | Relative Percentage | | |
|----------|-------------------|------|-------|---------------------|-------|-------|
| | 147a | 152a | 153 | 147a | 152a | 153 |
| 180 | 0.98 | 0.17 | 0.00 | 85.06 | 14.91 | 0.03 |
| 300 | 0.92 | 0.21 | 0.43 | 59.35 | 13.34 | 27.31 |
| 420 | 0.91 | 0.20 | 0.82 | 47.16 | 10.49 | 42.35 |
| 600 | 0.90 | 0.20 | 1.24 | 38.63 | 8.49 | 52.88 |
| 780 | 0.90 | 0.17 | 1.70 | 32.40 | 6.25 | 61.35 |
| 960 | 0.90 | 0.16 | 2.33 | 26.65 | 4.76 | 68.59 |
| 1140 | 0.92 | 0.17 | 2.99 | 22.57 | 4.13 | 73.30 |
| 1320 | 0.91 | 0.14 | 3.84 | 18.66 | 2.76 | 78.58 |
| 1500 | 0.90 | 0.15 | 4.71 | 15.60 | 2.65 | 81.75 |
| 1680 | 0.87 | 0.13 | 5.71 | 12.97 | 1.87 | 85.16 |
| 1860 | 0.89 | 0.09 | 7.07 | 11.07 | 1.12 | 87.81 |
| 2040 | 0.90 | 0.11 | 9.03 | 9.01 | 1.07 | 89.92 |
| 2220 | 0.92 | 0.08 | 11.50 | 7.35 | 0.64 | 92.01 |
| 2400 | 0.91 | 0.09 | 13.81 | 6.17 | 0.62 | 93.21 |
| 2580 | 0.93 | 0.14 | 14.33 | 6.05 | 0.90 | 93.05 |
| 2760 | 0.95 | 0.11 | 22.09 | 4.11 | 0.46 | 95.43 |
| 2940 | 0.85 | 0.02 | 25.90 | 3.16 | 0.08 | 96.76 |
| 3120 | 1.01 | 0.03 | 35.55 | 2.75 | 0.09 | 97.16 |
| 3300 | 0.92 | 0.00 | 25.67 | 3.47 | 0.00 | 96.53 |
| 3480 | 0.95 | 0.00 | 42.87 | 2.16 | 0.00 | 97.84 |
| 3660 | 0.99 | 0.00 | 39.47 | 2.44 | 0.00 | 97.56 |

110 °C Data:

¹⁹F NMR integration data for the VCPR of **147a** in d₁₀-xylene (0.35 M) heated at **383 K** (AV400, QNP-z probe); 8 scans, D₁ = 1.5 s, TE = **383 K**.

| Time (s) | Average Integrals | | | Relative Percentage | | |
|----------|-------------------|------|------|---------------------|-------|-------|
| | 147a | 152a | 153 | 147a | 152a | 153 |
| 300 | 0.90 | 0.08 | 0.05 | 87.10 | 8.06 | 4.84 |
| 360 | 0.90 | 0.13 | 0.10 | 79.42 | 11.78 | 8.80 |
| 540 | 0.90 | 0.18 | 0.21 | 69.62 | 14.00 | 16.37 |
| 720 | 0.91 | 0.16 | 0.27 | 67.84 | 12.05 | 20.11 |
| 900 | 0.90 | 0.17 | 0.35 | 63.21 | 11.94 | 24.85 |
| 1080 | 0.90 | 0.17 | 0.48 | 58.50 | 10.71 | 30.79 |
| 1260 | 0.91 | 0.17 | 0.58 | 54.82 | 10.05 | 35.13 |
| 1440 | 0.91 | 0.17 | 0.72 | 50.51 | 9.30 | 40.19 |
| 1620 | 0.91 | 0.16 | 0.83 | 47.98 | 8.40 | 43.62 |
| 1800 | 0.90 | 0.15 | 0.95 | 45.14 | 7.29 | 47.57 |
| 1980 | 0.91 | 0.16 | 1.09 | 41.91 | 7.54 | 50.56 |
| 2160 | 0.91 | 0.17 | 1.24 | 39.31 | 7.18 | 53.51 |
| 2340 | 0.90 | 0.16 | 1.40 | 36.66 | 6.32 | 57.02 |
| 2520 | 0.91 | 0.15 | 1.56 | 34.71 | 5.57 | 59.72 |
| 2700 | 0.89 | 0.15 | 1.71 | 32.44 | 5.58 | 61.98 |
| 2880 | 0.89 | 0.14 | 1.90 | 30.40 | 4.84 | 64.76 |
| 3060 | 0.90 | 0.16 | 2.03 | 29.04 | 5.12 | 65.84 |
| 3240 | 0.89 | 0.13 | 2.24 | 27.26 | 4.10 | 68.65 |
| 3420 | 0.89 | 0.15 | 2.46 | 25.49 | 4.34 | 70.17 |
| 3600 | 0.89 | 0.15 | 2.61 | 24.28 | 4.22 | 71.51 |
| 3780 | 0.89 | 0.14 | 2.94 | 22.45 | 3.64 | 73.91 |
| 3960 | 0.90 | 0.14 | 3.17 | 21.42 | 3.43 | 75.16 |
| 4140 | 0.87 | 0.14 | 3.47 | 19.42 | 3.04 | 77.55 |
| 4320 | 0.91 | 0.14 | 3.84 | 18.54 | 2.95 | 78.52 |
| 4500 | 0.89 | 0.14 | 4.08 | 17.45 | 2.65 | 79.90 |
| 4680 | 0.88 | 0.12 | 4.37 | 16.44 | 2.16 | 81.40 |
| 4860 | 0.89 | 0.10 | 4.79 | 15.43 | 1.81 | 82.76 |
| 5040 | 0.91 | 0.10 | 5.35 | 14.30 | 1.63 | 84.07 |
| 5220 | 0.88 | 0.13 | 5.77 | 12.98 | 1.86 | 85.16 |
| 5400 | 0.90 | 0.10 | 6.06 | 12.71 | 1.36 | 85.93 |
| 5580 | 0.92 | 0.11 | 6.71 | 11.88 | 1.41 | 86.71 |

100 °C Data:

¹⁹F NMR integration data for the VCPR of **147a** in d₁₀-xylene (0.35 M) heated at **373 K** (AV400, QNP-z probe); 8 scans, D₁ = 1.5 s, TE = **373 K**.

| Time (s) | Average Integrals | | | Relative Percentage | | |
|----------|-------------------|------|------|---------------------|-------|-------|
| | 147a | 152a | 153 | 147a | 152a | 153 |
| 420 | 0.91 | 0.05 | 0.03 | 92.22 | 5.04 | 2.74 |
| 540 | 0.90 | 0.07 | 0.03 | 89.75 | 6.90 | 3.34 |
| 840 | 0.90 | 0.11 | 0.07 | 83.36 | 9.97 | 6.66 |
| 1140 | 0.91 | 0.12 | 0.09 | 81.08 | 10.69 | 8.23 |
| 1440 | 0.91 | 0.14 | 0.13 | 77.24 | 11.74 | 11.02 |
| 1740 | 0.90 | 0.14 | 0.16 | 74.70 | 11.72 | 13.58 |
| 2040 | 0.90 | 0.14 | 0.20 | 72.32 | 11.33 | 16.35 |
| 2340 | 0.90 | 0.15 | 0.24 | 69.61 | 11.60 | 18.79 |
| 2640 | 0.91 | 0.15 | 0.29 | 67.35 | 11.45 | 21.20 |
| 2940 | 0.90 | 0.16 | 0.31 | 65.74 | 11.42 | 22.84 |
| 3240 | 0.90 | 0.15 | 0.37 | 63.35 | 10.60 | 26.05 |
| 3540 | 0.91 | 0.15 | 0.40 | 62.16 | 10.32 | 27.51 |
| 3840 | 0.91 | 0.16 | 0.46 | 59.69 | 10.32 | 29.98 |
| 4140 | 0.90 | 0.15 | 0.51 | 57.68 | 9.53 | 32.80 |
| 4440 | 0.91 | 0.15 | 0.56 | 56.24 | 9.28 | 34.48 |
| 4740 | 0.91 | 0.18 | 0.61 | 53.76 | 10.33 | 35.91 |
| 5040 | 0.90 | 0.14 | 0.65 | 53.07 | 8.48 | 38.45 |
| 5340 | 0.90 | 0.15 | 0.72 | 50.94 | 8.70 | 40.37 |
| 5640 | 0.90 | 0.14 | 0.75 | 50.29 | 7.96 | 41.75 |
| 5940 | 0.91 | 0.15 | 0.81 | 48.61 | 7.91 | 43.48 |
| 6240 | 0.90 | 0.14 | 0.86 | 47.32 | 7.52 | 45.16 |
| 6540 | 0.90 | 0.15 | 0.91 | 45.76 | 7.50 | 46.74 |
| 6840 | 0.90 | 0.15 | 0.99 | 44.39 | 7.24 | 48.37 |
| 7140 | 0.91 | 0.15 | 1.04 | 43.31 | 7.03 | 49.66 |
| 7440 | 0.90 | 0.14 | 1.09 | 42.29 | 6.79 | 50.92 |
| 7740 | 0.90 | 0.14 | 1.14 | 41.26 | 6.54 | 52.20 |
| 8040 | 0.90 | 0.17 | 1.23 | 39.16 | 7.41 | 53.43 |
| 8340 | 0.92 | 0.17 | 1.29 | 38.64 | 7.21 | 54.15 |
| 8640 | 0.90 | 0.14 | 1.34 | 37.90 | 5.87 | 56.23 |
| 8940 | 0.90 | 0.14 | 1.44 | 36.35 | 5.68 | 57.97 |
| 9240 | 0.91 | 0.17 | 1.46 | 35.83 | 6.74 | 57.43 |

90 °C Data:

¹⁹F NMR integration data for the VCPR of **147a** in *d*₁₀-xylene (0.36 M) heated at **363 K** (AV400, QNP-z probe); 8 scans, *D*₁ = 1.5 s, *TE* = **363 K**.

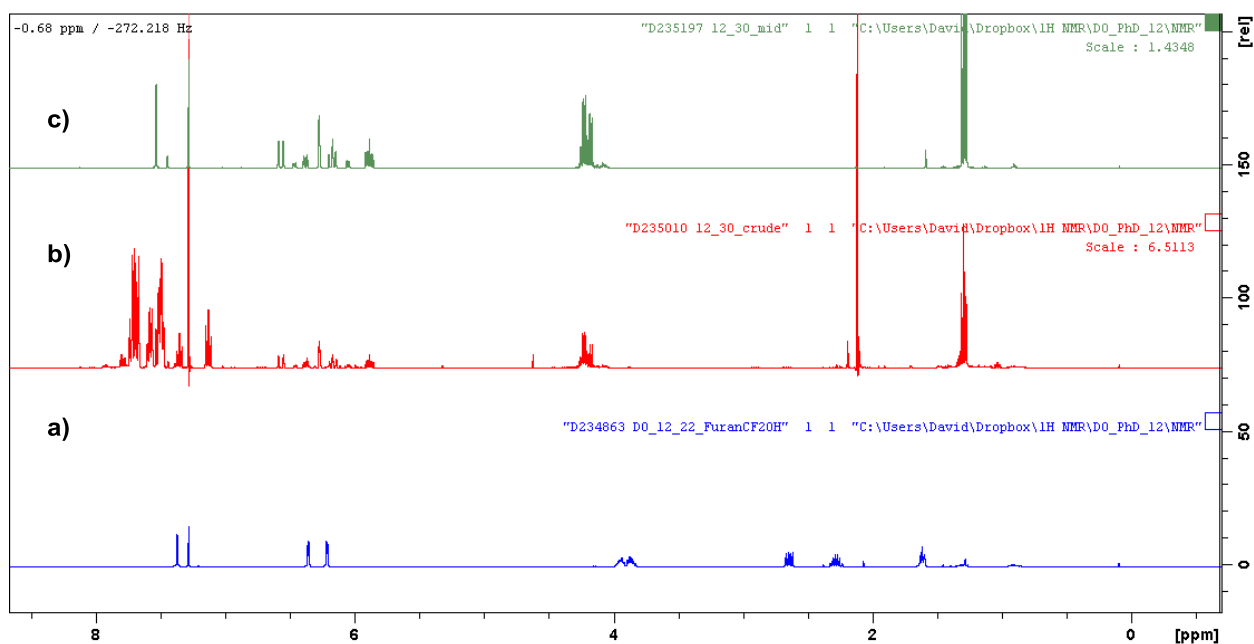
| Time (s) | Average Integrals | | | Relative Percentage | | |
|----------|-------------------|-------------|------------|---------------------|-------------|------------|
| | 147a | 152a | 153 | 147a | 152a | 153 |
| 480 | 0.91 | 0.03 | 0.02 | 94.36 | 3.60 | 2.04 |
| 540 | 0.91 | 0.04 | 0.02 | 93.32 | 4.40 | 2.28 |
| 840 | 0.91 | 0.04 | 0.01 | 94.05 | 4.51 | 1.44 |
| 1140 | 0.90 | 0.05 | 0.02 | 92.79 | 5.61 | 1.61 |
| 1440 | 0.91 | 0.08 | 0.05 | 87.63 | 7.95 | 4.42 |
| 1740 | 0.90 | 0.09 | 0.06 | 85.98 | 8.51 | 5.51 |
| 2040 | 0.90 | 0.10 | 0.07 | 84.73 | 8.94 | 6.33 |
| 2340 | 0.91 | 0.11 | 0.09 | 81.94 | 9.82 | 8.24 |
| 2640 | 0.90 | 0.11 | 0.11 | 80.37 | 10.10 | 9.52 |
| 2940 | 0.91 | 0.12 | 0.13 | 78.14 | 10.40 | 11.46 |
| 3240 | 0.91 | 0.13 | 0.14 | 77.27 | 11.01 | 11.73 |
| 3540 | 0.90 | 0.13 | 0.15 | 76.85 | 10.74 | 12.41 |
| 3840 | 0.91 | 0.12 | 0.18 | 74.88 | 10.25 | 14.88 |
| 4140 | 0.91 | 0.13 | 0.20 | 73.33 | 10.29 | 16.38 |
| 4440 | 0.91 | 0.13 | 0.21 | 72.86 | 10.05 | 17.08 |
| 4740 | 0.91 | 0.13 | 0.23 | 71.26 | 10.40 | 18.34 |
| 5040 | 0.91 | 0.13 | 0.25 | 70.30 | 10.35 | 19.35 |
| 5340 | 0.91 | 0.17 | 0.30 | 65.97 | 12.38 | 21.64 |
| 5640 | 0.91 | 0.14 | 0.29 | 67.73 | 10.79 | 21.48 |
| 5940 | 0.91 | 0.13 | 0.30 | 67.83 | 9.84 | 22.33 |
| 6240 | 0.91 | 0.13 | 0.32 | 67.08 | 9.41 | 23.52 |
| 6540 | 0.90 | 0.13 | 0.34 | 65.91 | 9.53 | 24.56 |
| 6840 | 0.91 | 0.14 | 0.35 | 64.89 | 10.17 | 24.94 |
| 7140 | 0.91 | 0.12 | 0.36 | 65.31 | 8.63 | 26.06 |
| 7440 | 0.91 | 0.13 | 0.40 | 62.86 | 9.29 | 27.85 |
| 7740 | 0.90 | 0.13 | 0.43 | 61.66 | 9.08 | 29.26 |
| 8040 | 0.91 | 0.13 | 0.44 | 61.47 | 8.62 | 29.91 |
| 8340 | 0.91 | 0.13 | 0.46 | 60.60 | 8.53 | 30.87 |
| 8640 | 0.91 | 0.13 | 0.48 | 59.88 | 8.86 | 31.27 |
| 8940 | 0.91 | 0.13 | 0.50 | 59.12 | 8.40 | 32.48 |
| 9240 | 0.90 | 0.13 | 0.51 | 58.57 | 8.35 | 33.08 |
| 9540 | 0.92 | 0.17 | 0.57 | 55.13 | 10.37 | 34.50 |
| 9840 | 0.91 | 0.14 | 0.57 | 56.21 | 8.54 | 35.25 |
| 10140 | 0.91 | 0.13 | 0.59 | 55.62 | 8.01 | 36.37 |
| 10440 | 0.90 | 0.14 | 0.60 | 55.08 | 8.34 | 36.58 |
| 10740 | 0.89 | 0.10 | 0.62 | 55.40 | 6.47 | 38.13 |
| 11040 | 0.91 | 0.12 | 0.66 | 53.68 | 7.23 | 39.09 |
| 11340 | 0.90 | 0.11 | 0.66 | 54.08 | 6.45 | 39.46 |
| 11640 | 0.90 | 0.12 | 0.70 | 52.61 | 6.76 | 40.63 |
| 11940 | 0.91 | 0.13 | 0.71 | 51.90 | 7.45 | 40.65 |
| 12240 | 0.91 | 0.14 | 0.76 | 50.50 | 7.78 | 41.72 |
| 12540 | 0.90 | 0.12 | 0.75 | 50.99 | 6.66 | 42.36 |
| 12840 | 0.90 | 0.13 | 0.78 | 49.73 | 6.96 | 43.31 |
| 13140 | 0.91 | 0.13 | 0.81 | 49.27 | 6.94 | 43.79 |
| 13440 | 0.90 | 0.11 | 0.83 | 48.96 | 6.09 | 44.95 |
| 13740 | 0.90 | 0.12 | 0.87 | 47.54 | 6.31 | 46.15 |
| 14040 | 0.91 | 0.17 | 0.92 | 45.50 | 8.60 | 45.90 |
| 14340 | 0.92 | 0.12 | 0.94 | 46.43 | 6.23 | 47.34 |
| 14640 | 0.91 | 0.13 | 0.94 | 46.10 | 6.45 | 47.45 |

Supporting Information for Chapter 3

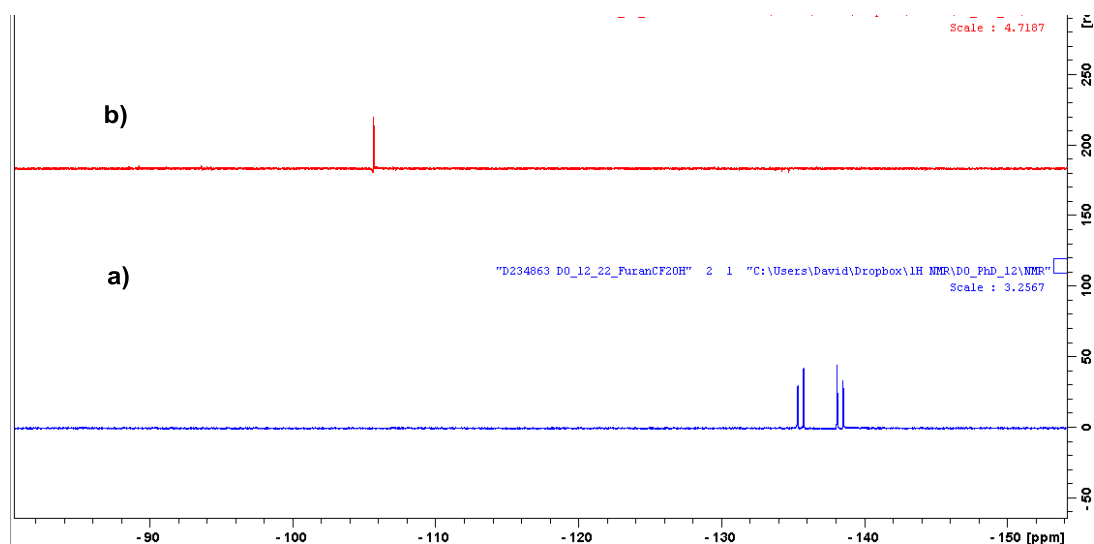
Crude Spectra for Low Temperature Rearrangement Precursors

Spectra below highlight the results of oxidation/Wittig chemistry on highly reactive heteroaromatic substituents.

- Furyl Alcohol **199a** with (ethoxycarbonylmethylene)triphenylphosphorane

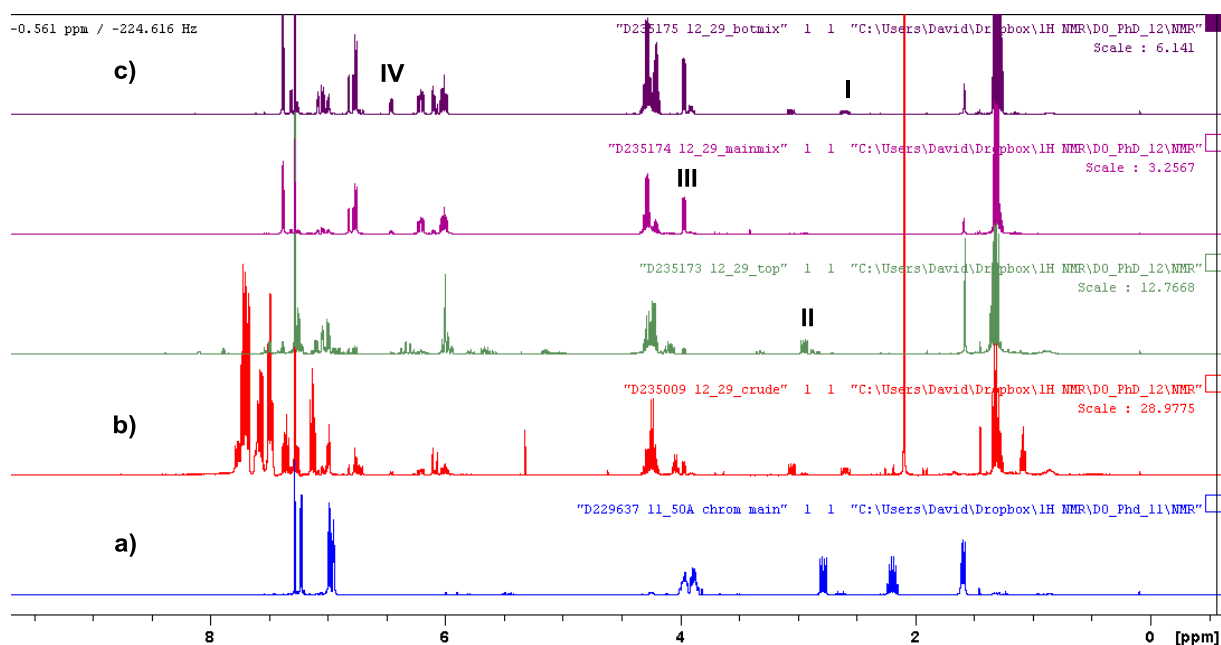
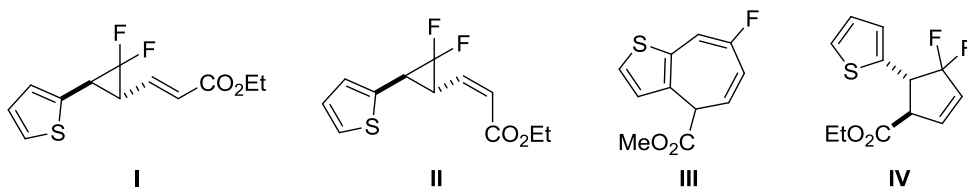


a) Isolated ¹H NMR for alcohol **199a** b) Crude ¹H NMR after oxidation/Wittig reaction showing no evidence of peaks relating to cyclopropane proton atoms. c) ¹H NMR of main fraction isolated from first purification on silica.

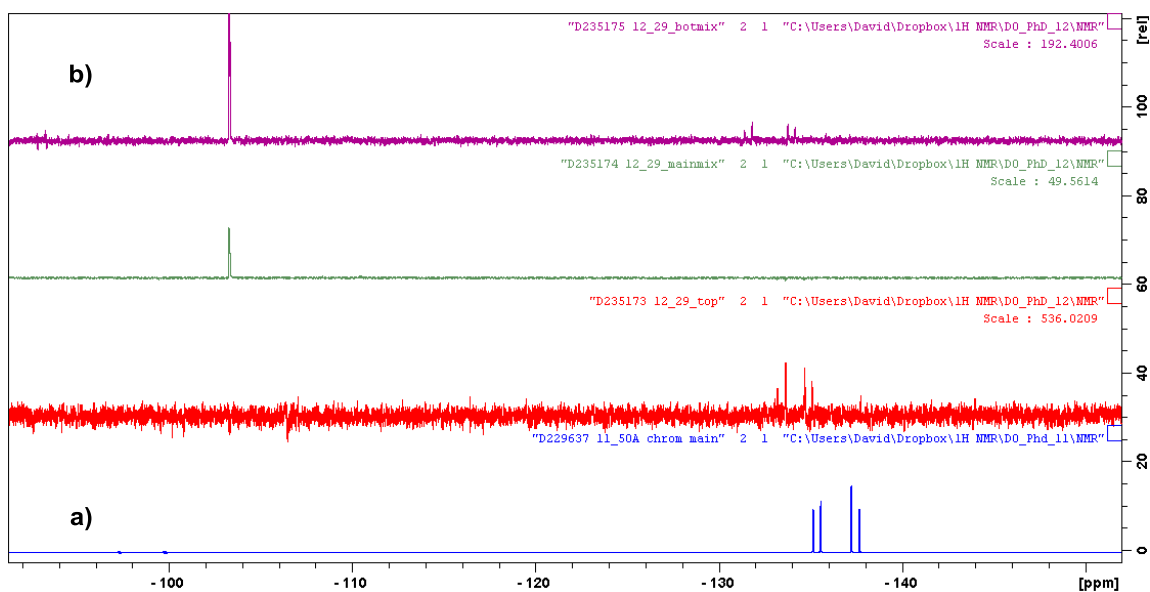


a) Isolated ¹⁹F NMR for furyl alcohol **199a** b) ¹⁹F NMR of main fraction isolated from first purification after oxidation/Wittig.

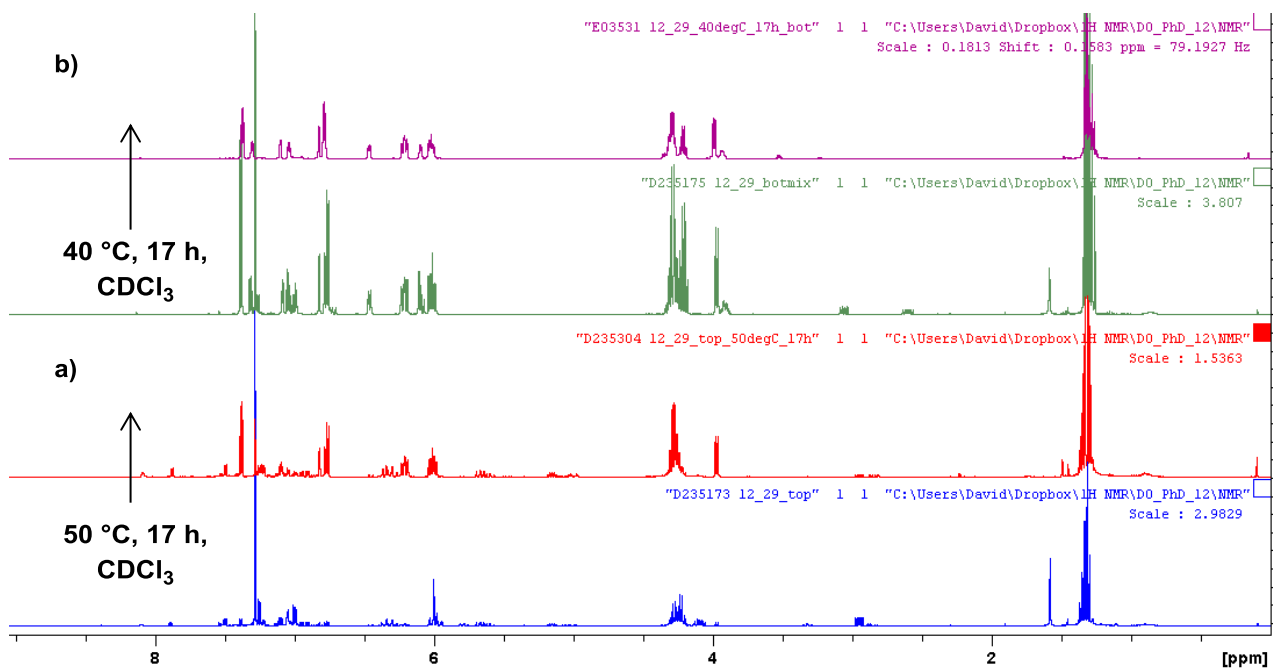
- Thiophenyl alcohol **199c** with (ethoxycarbonylmethylene)triphenylphosphorane



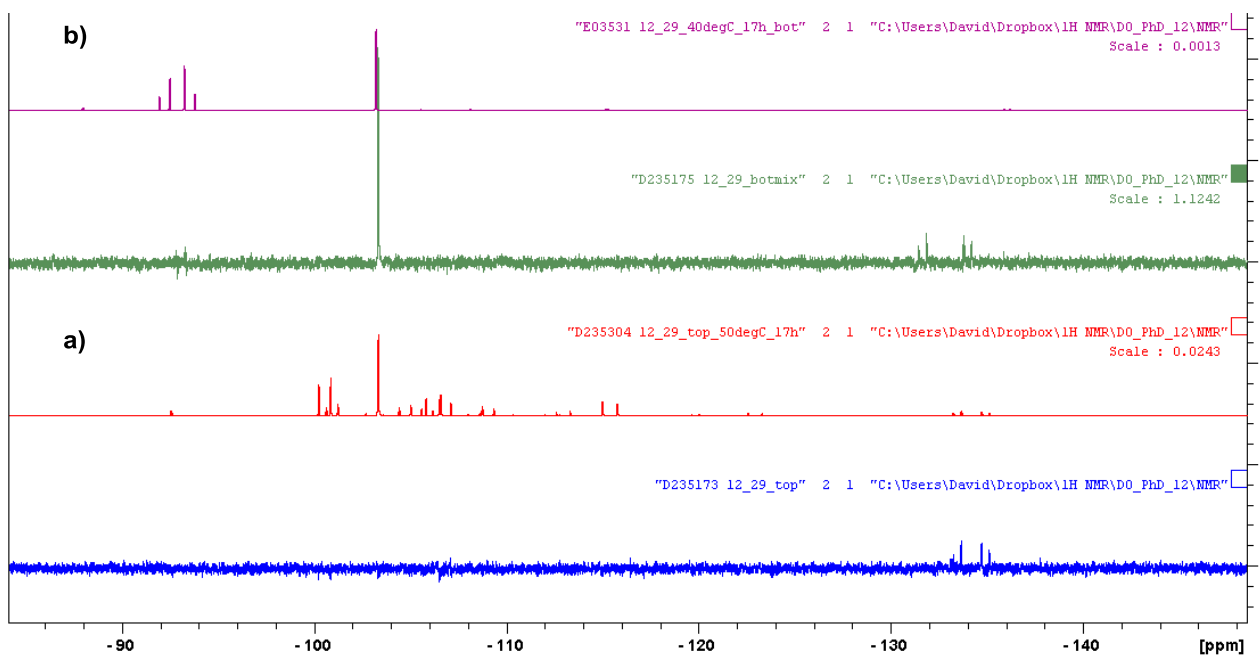
a) ¹H NMR of isolated thiophenyl alcohol **199c**. b) Crude ¹H NMR after oxidation/Wittig reaction. c) Three different fractions isolated after first purification on silica. (Assignment of crude spectra based on previous knowledge on *E/Z* cyclopropane isomers and ¹⁹F NMR data for products which was confirmed on isolation of products).



a) Crude ^{19}F NMR for isolated thiophenyl alcohol **199c**. b) ^{19}F NMR for isolated fractions highlighted for purification above.

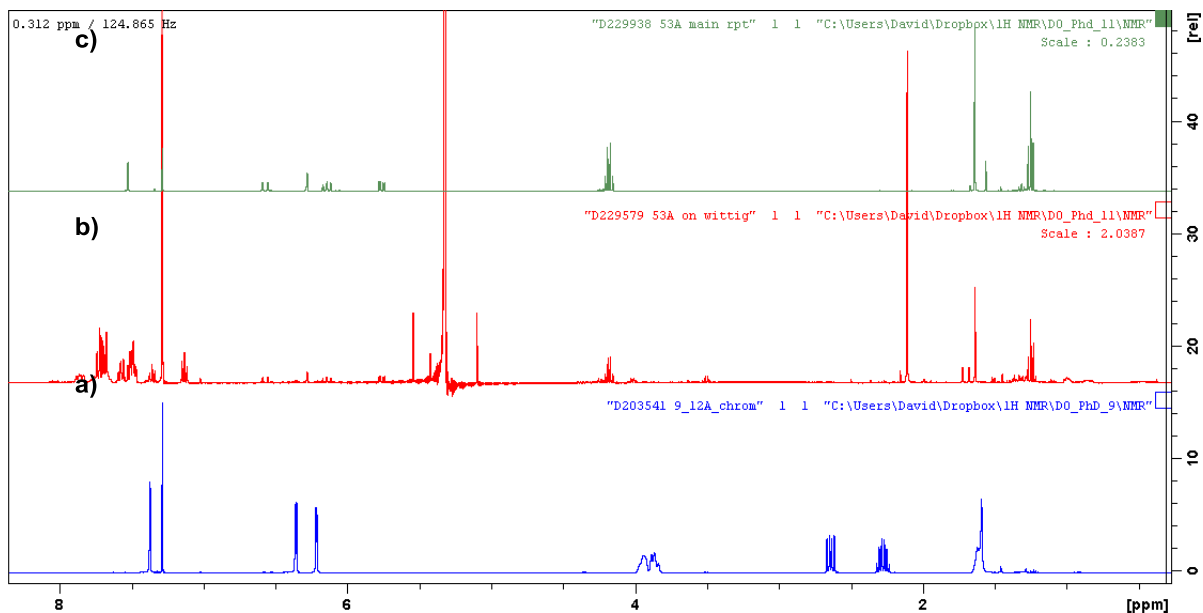


a) Thermolysis of < 10 mg sample containing *Z*-thiophenyl **216b** at 50 °C for 17 hours resulting in full conversion to heptadiene **216a** alongside other side products. b) Thermolysis of 420 mg sample containing *E*-thiophenyl **216a** at 40 °C for 17 hours resulting in full conversion to a mixture of VCPR and [3,3] product.

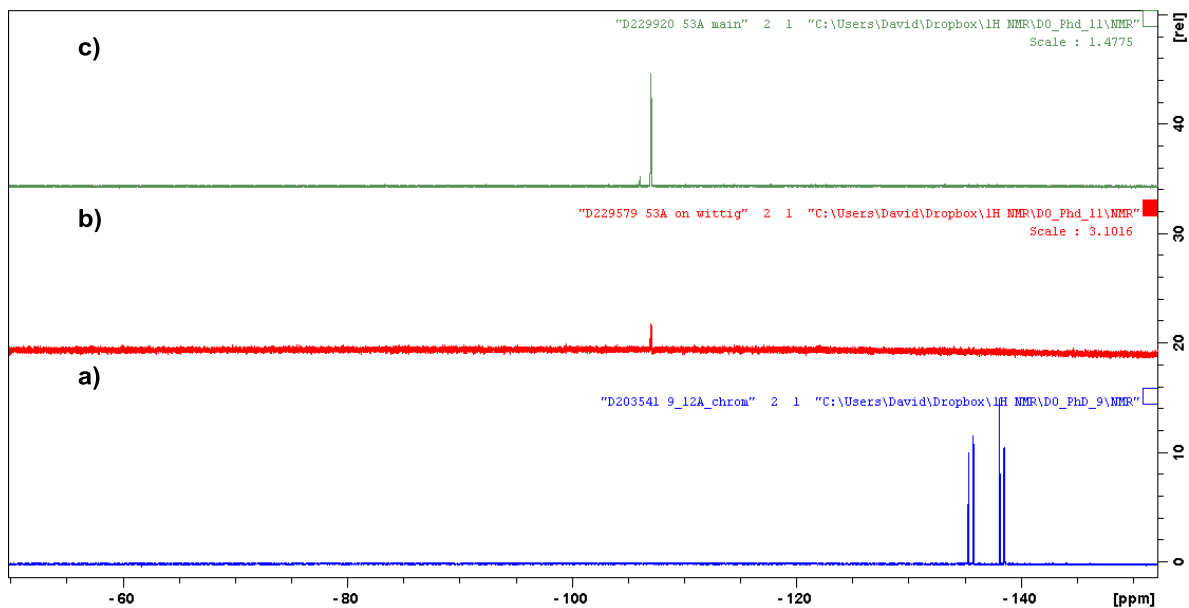


Corresponding crude ^{19}F NMR for **216**.

- Furyl alcohol **199a** with (carbethoxyethylidene)triphenylphosphorane

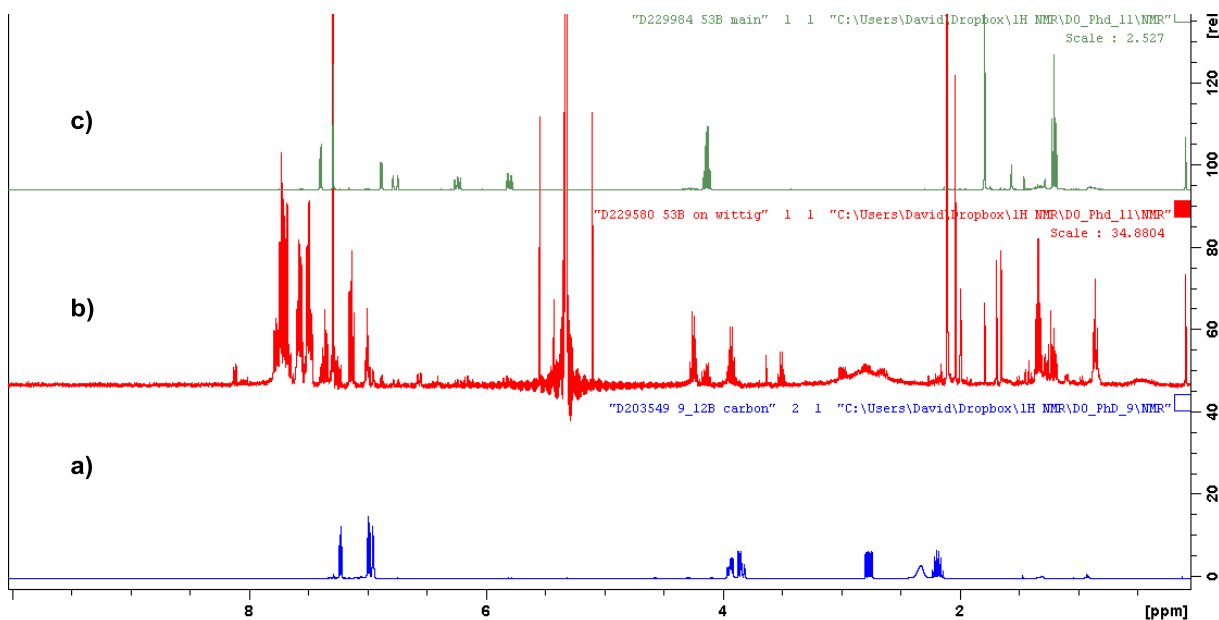


a) ^1H NMR of isolated furyl alcohol **199a**. b) Crude ^1H NMR after oxidation/Wittig with (carbethoxyethylidene)triphenylphosphorane c) ^1H NMR after 1st purification on silica.

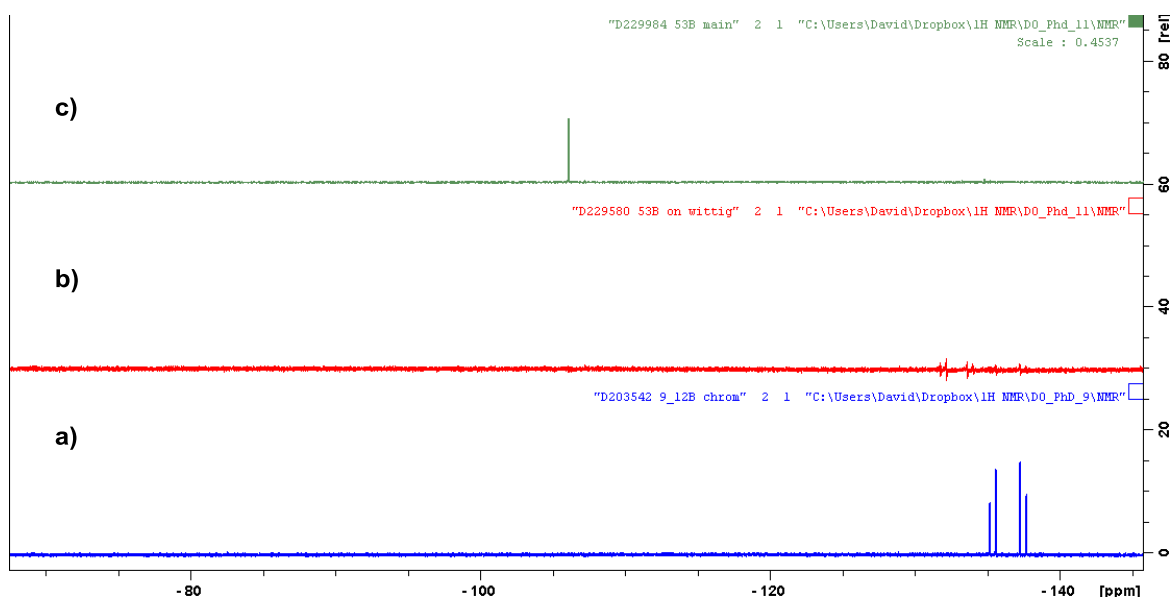


a) ^{19}F NMR for isolated furyl alcohol **199a** b) Crude ^{19}F NMR after oxidation/Wittig with (carbethoxyethylidene)triphenylphosphorane c) ^{19}F NMR after 1st purification on silica.

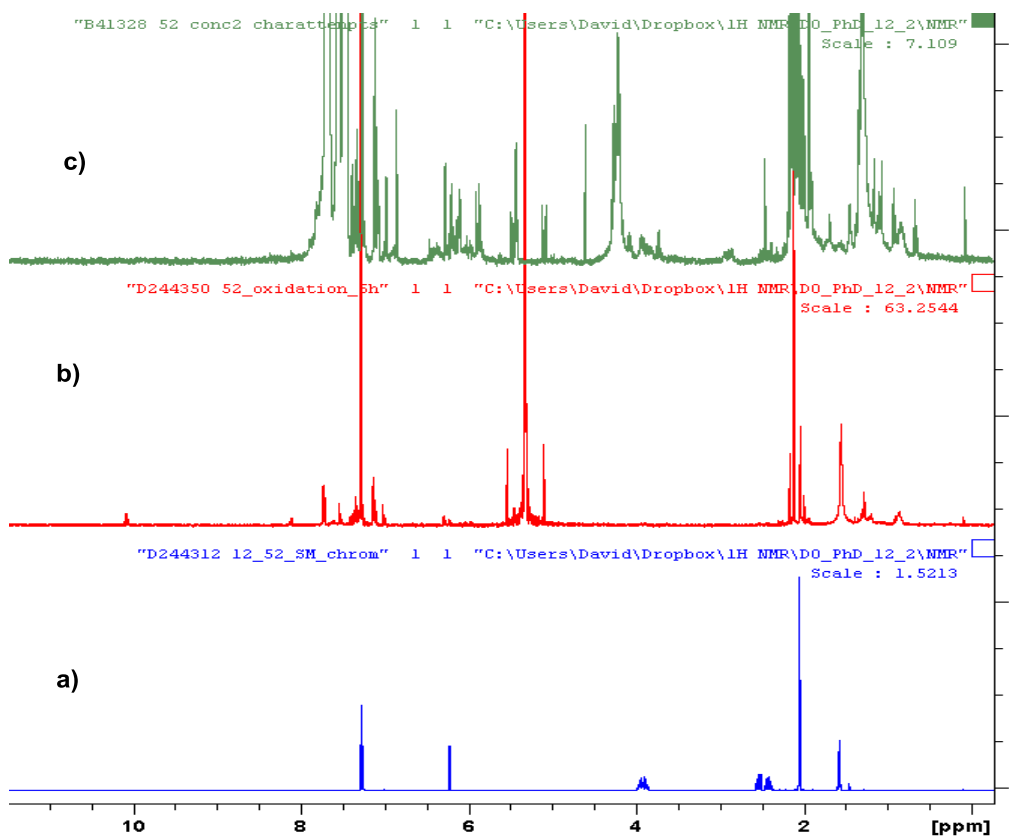
- Thiophenyl alcohol **199c** with (carbethoxyethylidene)triphenylphosphorane



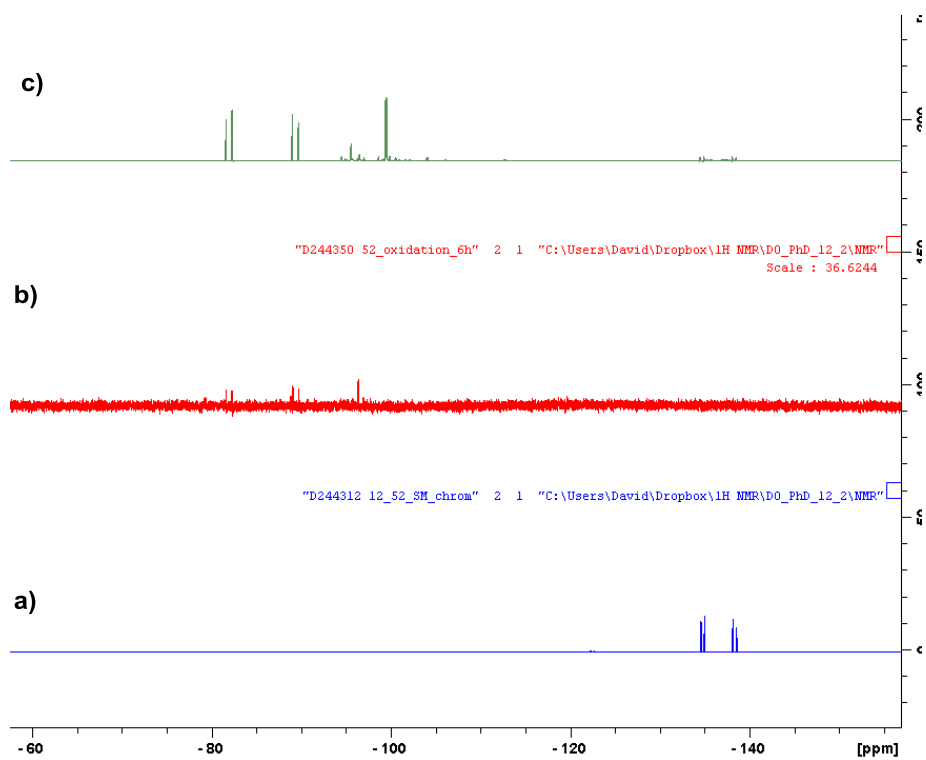
a) ^1H NMR for isolated thiophenyl alcohol **199c** b) Crude ^1H NMR after oxidation/Wittig with (carbethoxyethylidene)triphenylphosphorane c) ^1H NMR after 1st purification on silica.



a) ¹⁹F NMR for isolated thiophenyl alcohol **199c** b) Crude ¹⁹F NMR after oxidation/Wittig with (carboethoxyethylidene)triphenylphosphorane c) ¹⁹F NMR after 1st purification on silica.



a) ¹H NMR for isolated 3-methyl-furyl alcohol **199h** b) Crude ¹H NMR after oxidation with (ethoxycarbonylmethylene)triphenylphosphorane c) ¹H NMR after olefination and concentration of reaction mixture.



^{19}F NMR for isolated 3-methyl-furyl alcohol **199h** b) Crude ^{19}F NMR after oxidation with (ethoxycarbonylmethylene)triphenylphosphorane c) ^{19}F NMR after olefination and concentration of reaction mixture.

Rearrangement of Isolated VCP – Crude Spectra

- (*E*)-Weinreb Amide **211a**

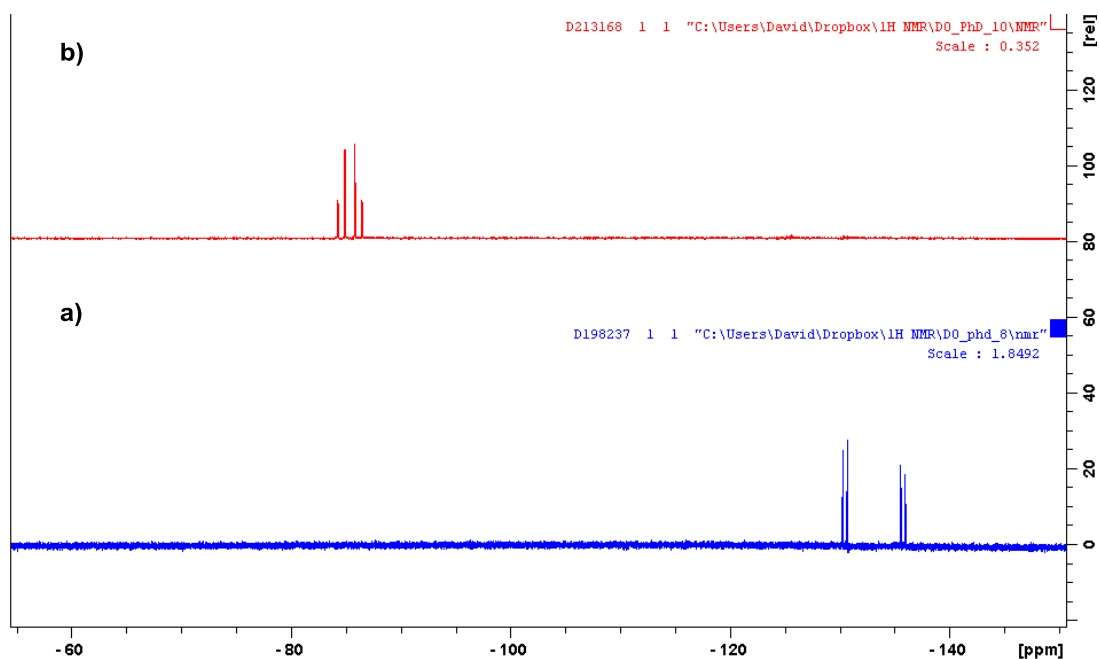
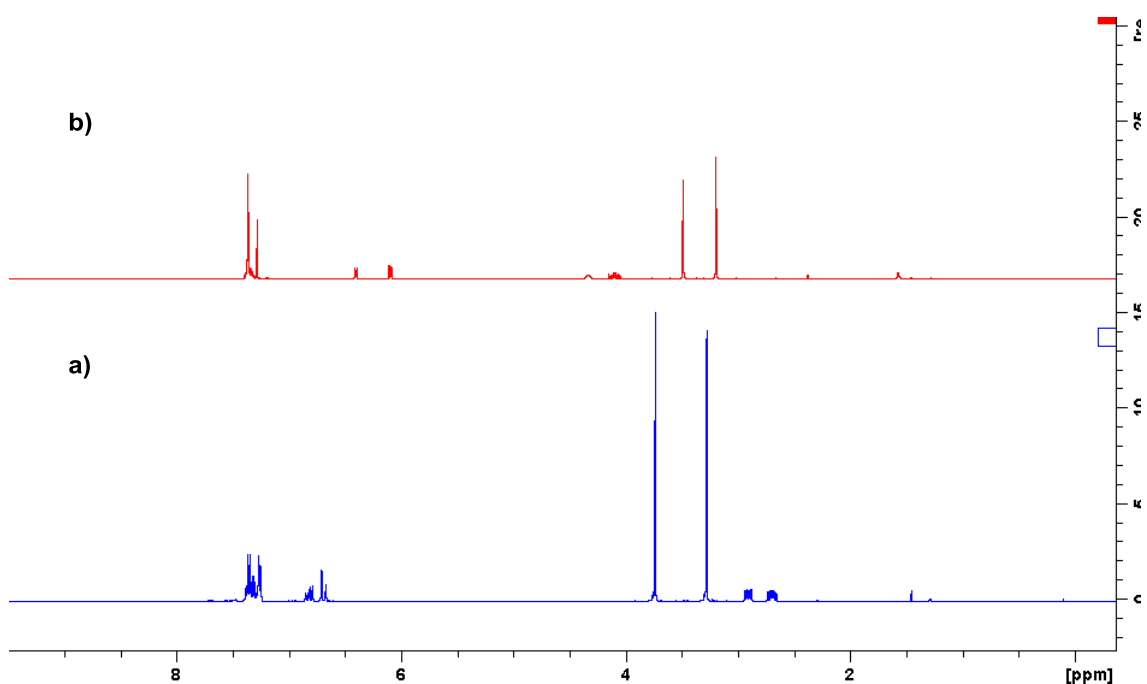
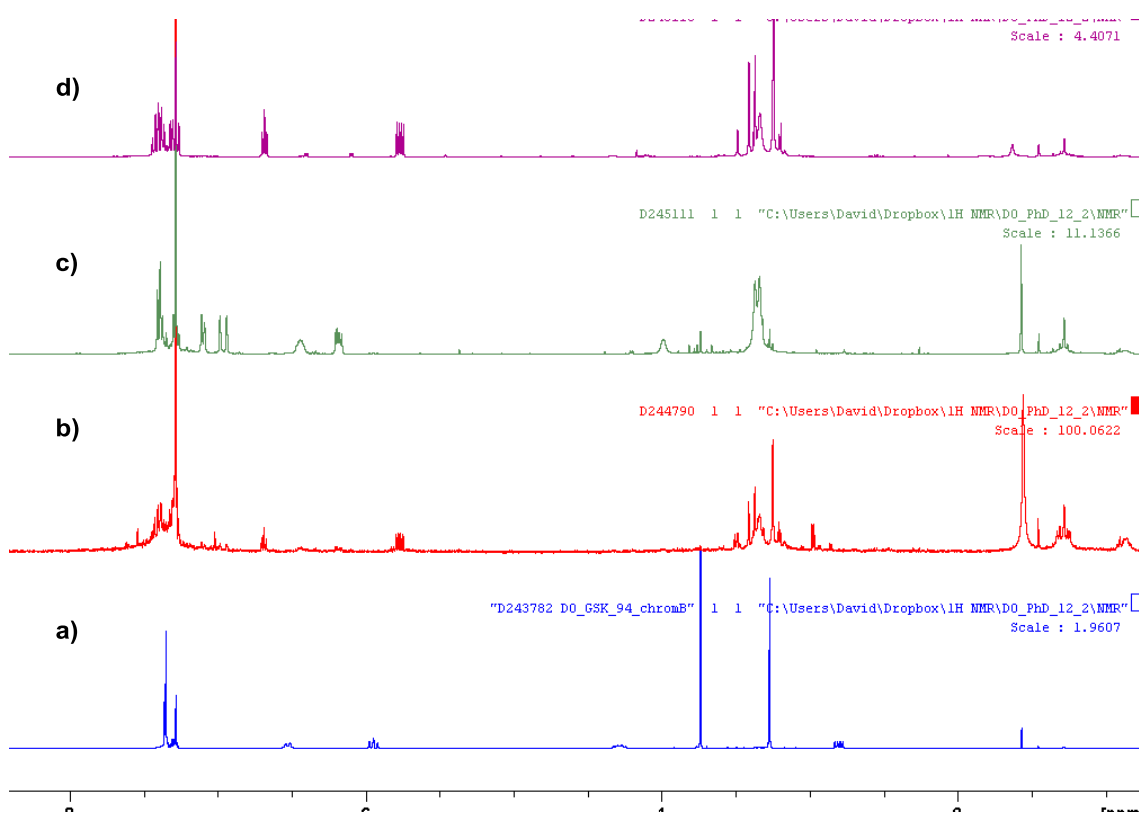


Figure S74: a) ^{19}F NMR of isolated *E*-Weinreb amide VCP **211a**. b) Crude ^{19}F NMR for rearrangement of **228** at 95 °C for 17 hours.

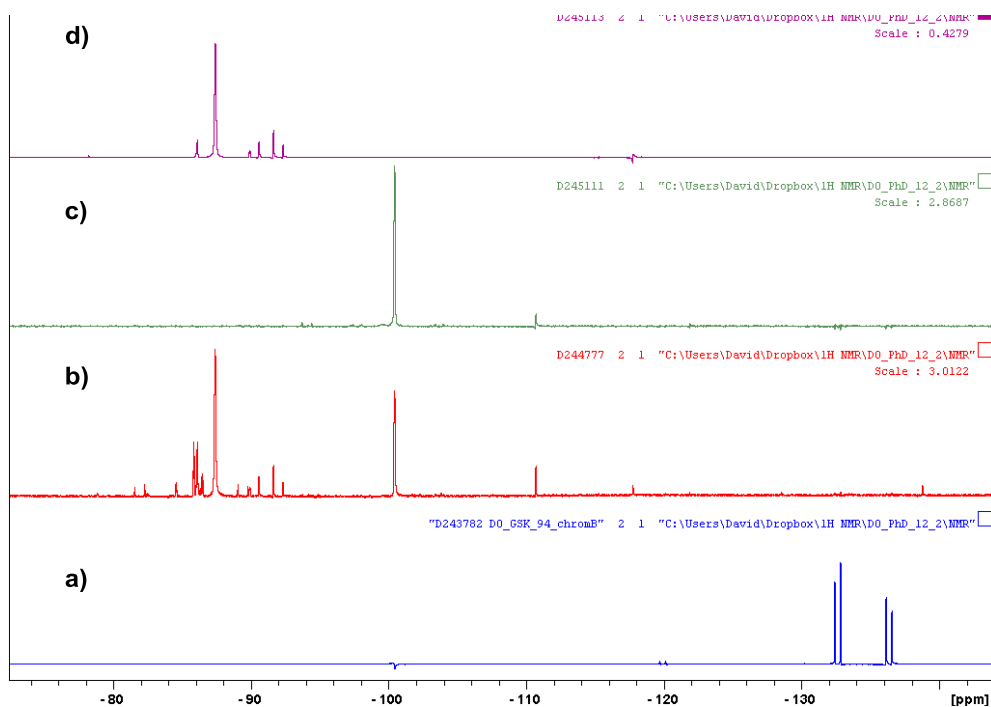


a) ^1H NMR of isolated *E*-Weinreb amide VCP **211a**. b) Crude ^1H NMR for rearrangement of **228** at 95 °C for 17 hours.

- (Z)-Weinreb Amide (**211b**)



a) ^1H NMR of isolated ZWeinreb amide VCP **211b**. b) Crude ^1H NMR of **211b** after rearrangement at 165 °C for 17 hours (silica pad used to remove Ph_2O solvent c) and d) ^1H NMR of isolated products after chromatography.



a) ^{19}F NMR of isolated Z-Weinreb amide VCP **211b**. b) Crude ^{19}F NMR of **211b** after rearrangement at 165 °C for 17 hours (silica pad used to remove Ph_2O solvent). c) and d) ^{19}F NMR of isolated products after chromatography.

- **α -Methyl Ester 212a**

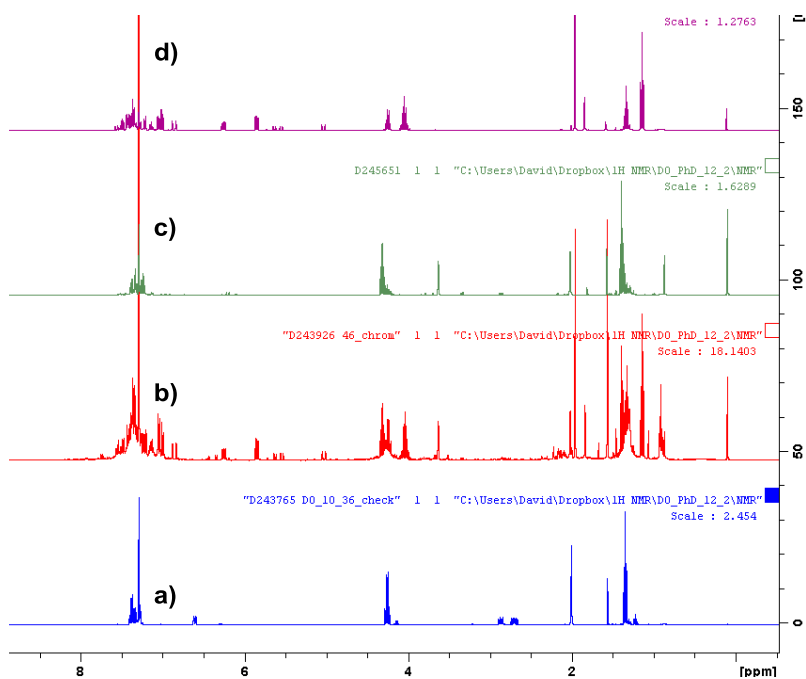
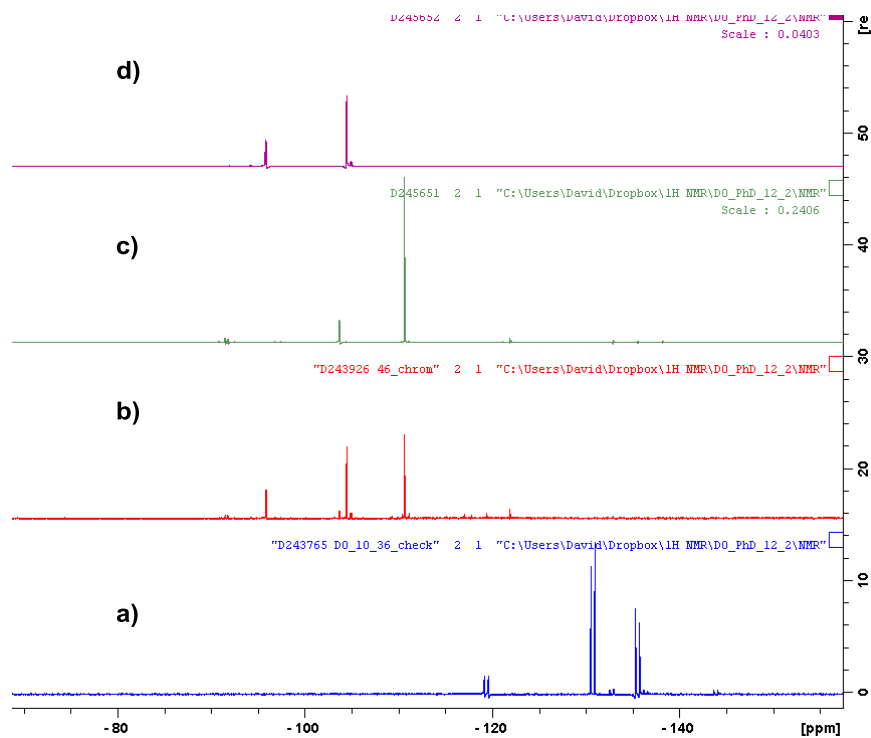
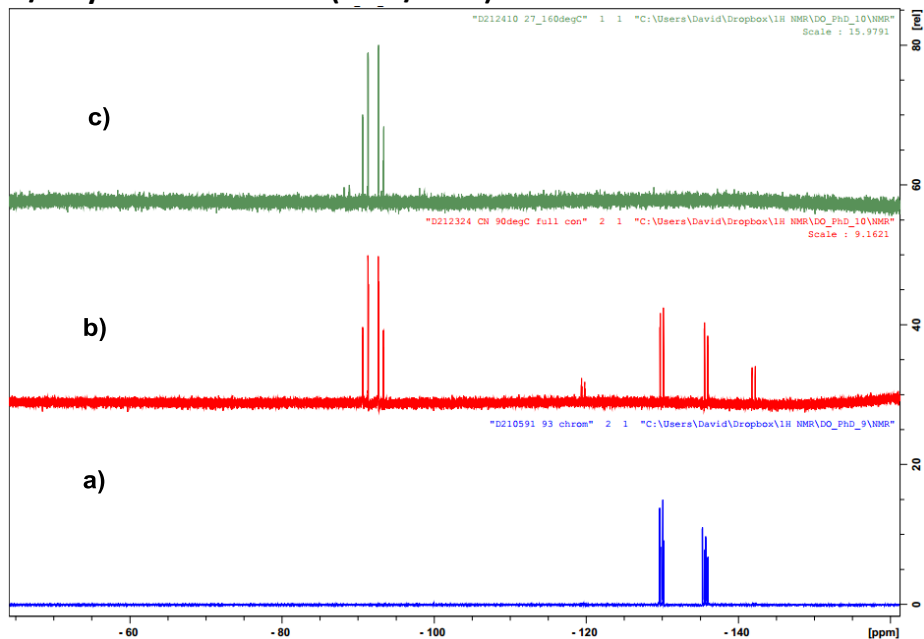


Figure S75: a) ^1H NMR of isolated alkenoate **212a** b) Crude ^1H NMR of **212a** after rearrangement at 155 °C for 17 hours (silica pad used to remove Ph_2O solvent). c) and d) ^1H NMR of isolated products after chromatography.

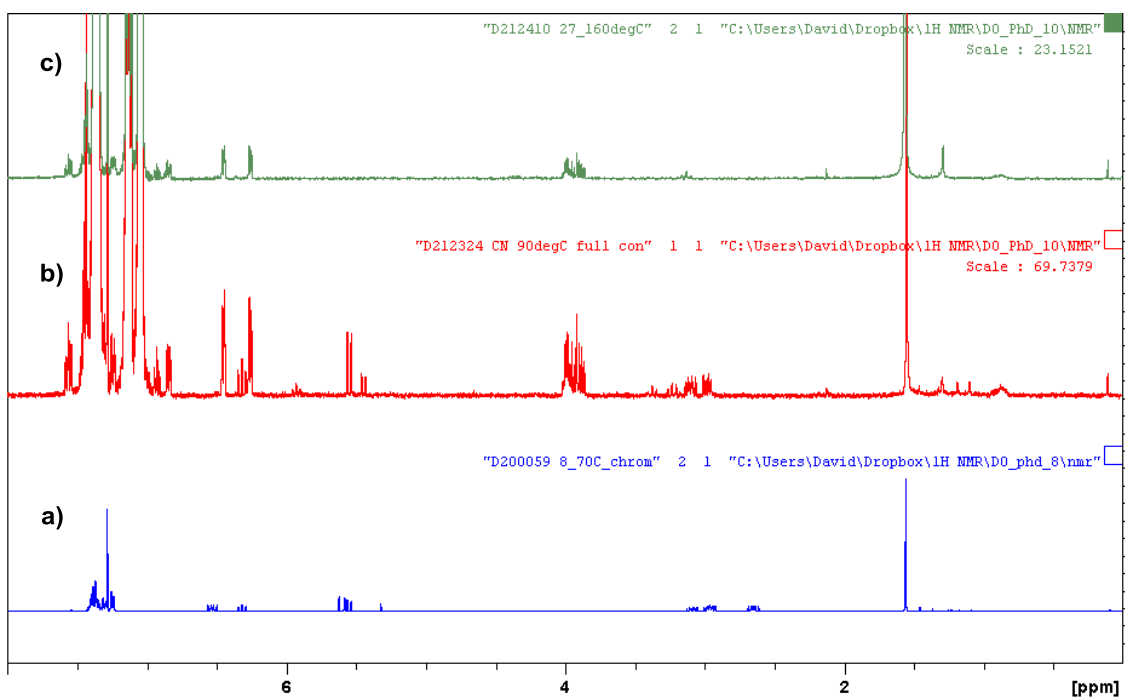


a) ^{19}F NMR of isolated alkenoate **212a**. b) Crude ^{19}F NMR of **212a** after rearrangement at 155 °C for 17 hours (silica pad used to remove Ph_2O solvent). c) and d) ^{19}F NMR of unknown products after chromatography.

- ***E/Z*-Cyano VCP mixture (213a/213b)**

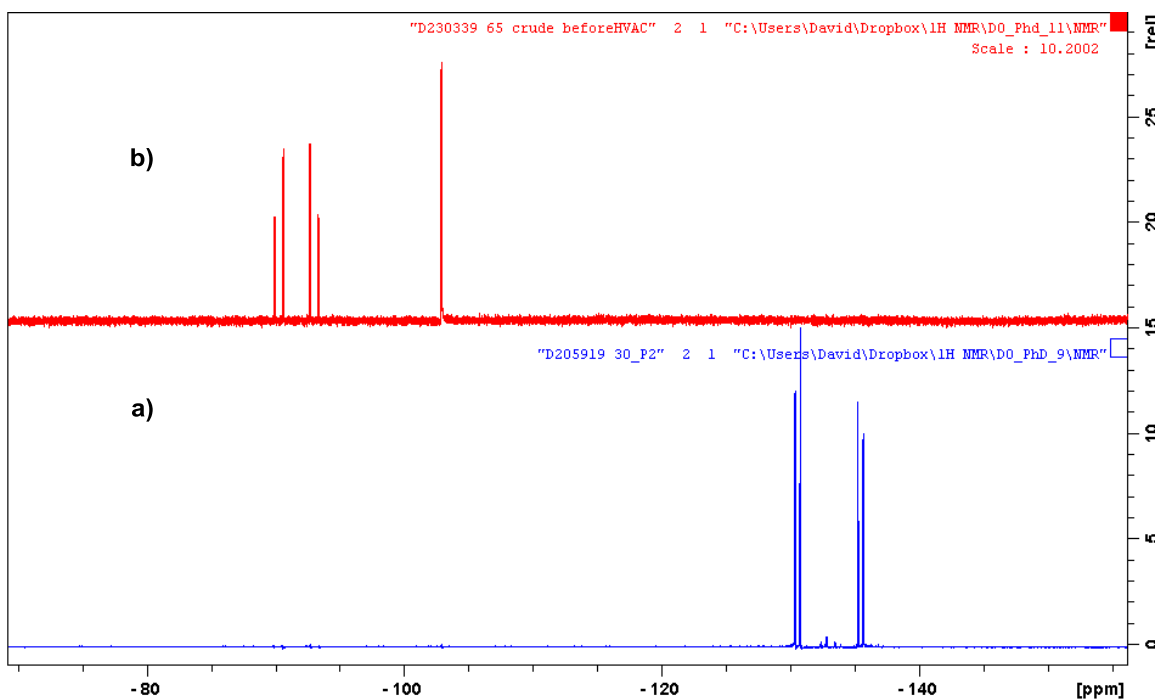


a) ^{19}F NMR spectra of **213a/213b** mixture. b) ^{19}F NMR spectra for the rearrangement of **213a/213b** at 90 °C for 17 h resulting in full conversion of **213a** to difluorocyclopentene **230** and only cyclopropane stereoisomerization of **213b** to **235** c) ^{19}F NMR spectra after the rearrangement of crude mixture in b) at 160 °C for 17 h.

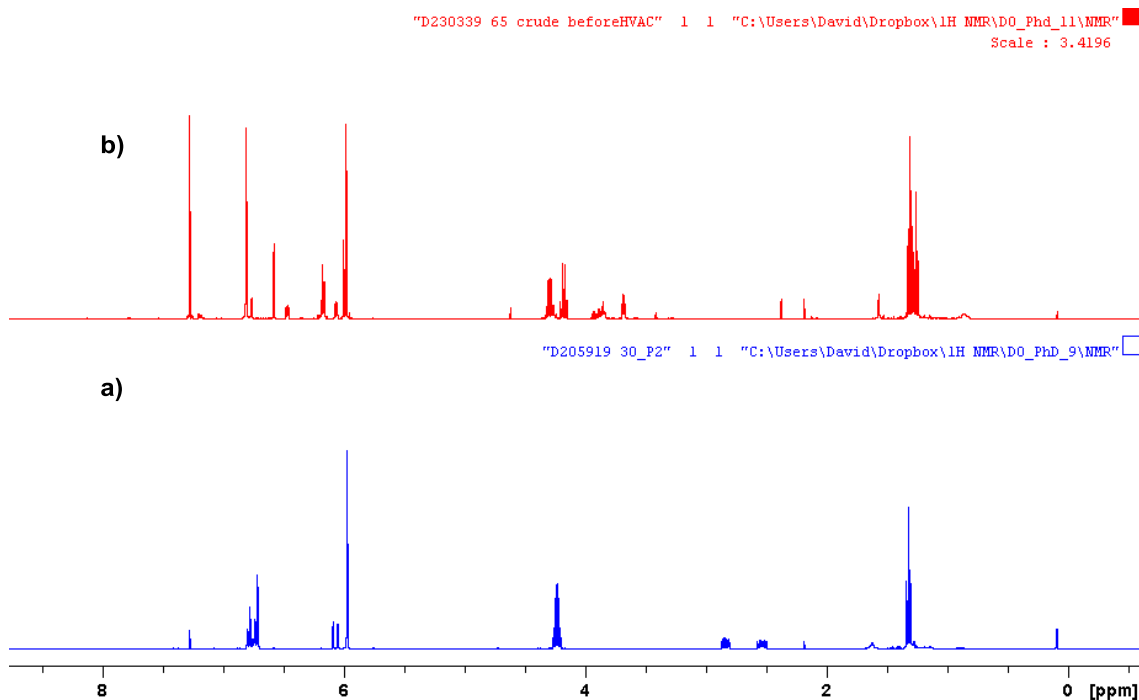


Corresponding ^1H spectra for mixture **213a/213b**.

- **Piperonyl 214a**

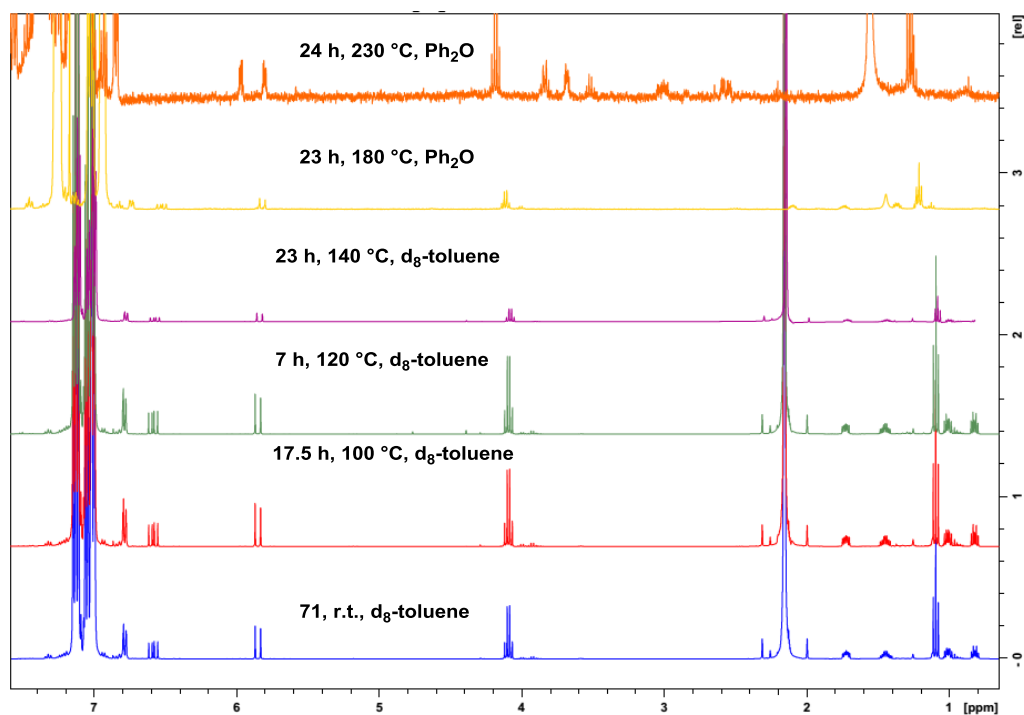


a) ^{19}F NMR of isolated piperonyl VCP **214a**. b) ^{19}F NMR of crude reaction mixture after rearrangement at 70 °C for 17 h.

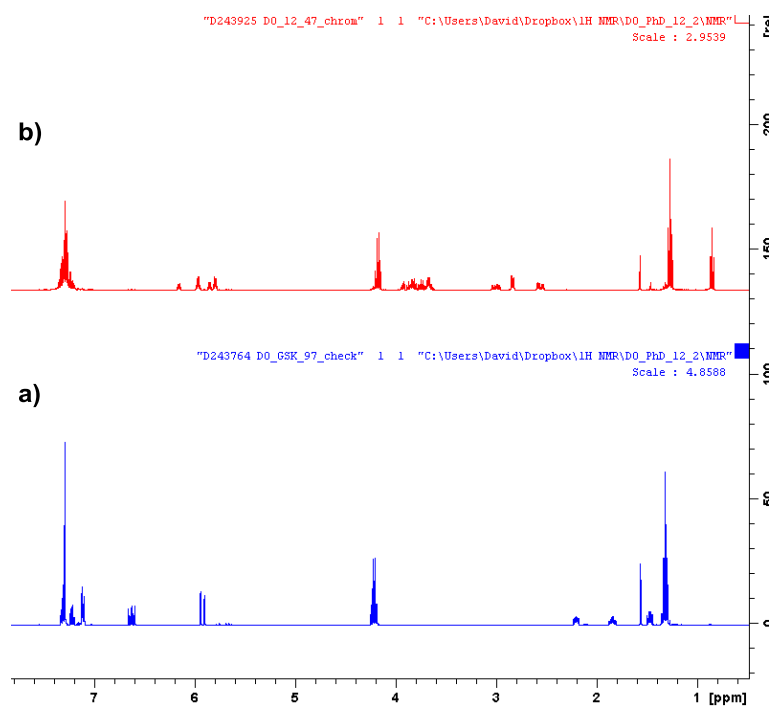


Corresponding ^1H NMR spectra for **214a**.

- **Non-fluorinated 227a**



Rearrangement temperature screening show temperatures > 180 °C are required for the rearrangement of non-fluorinated VCP **227a**.



a) ^1H NMR for isolated alkenoate **227a** b) Crude ^1H NMR for the rearrangement of isolated non-fluorinated **227a** at 210 °C for 17 h (after removal of Ph_2O solvent).

Arrhenius Plot

Chapter 2

Decay plots of **147a** relative percentage vs time were generated on Excel and exponential curves fitted using the trendline function. Rates at four different temperatures were calculated from first order exponential decay equation **1**

$$A = A_0 e^{-kt} \quad (1)$$

Arrhenius Data

| | | | | |
|---|----------|----------|----------|----------|
| Temperature (K) | 363 | 373 | 383 | 393 |
| 1/T (K ⁻¹) | 0.002755 | 0.002681 | 0.002611 | 0.002545 |
| k x 10 ⁻⁴ (s ⁻¹) | 0.5 | 1.0 | 3.6 | 10.1 |
| Ln k | -9.92063 | -9.18117 | -7.92943 | -6.89783 |

From Arrhenius equation **2**, a plot of Ln k vs 1/T was generated on Excel and a line fitted using the trendline function. The equation of the line (**3**) was calculated using the *LINEST* statistical function and the gradient used to calculate E_a . The errors in the values were estimated by plotting two lines which would result from the maximum errors ($\pm 5\%$) in the outermost points and averaging the gradient to determine E_a .

$$\ln k = \frac{-E_a}{R} \frac{1}{T} + \ln A \quad (2)$$

$$y = -14693.925 x + 30.424 \quad (3)$$

$$E_a = +29.2 \pm 0.6 \text{ kcal mol}^{-1}$$

$$A = 1.6 \times 10^{13} \text{ s}^{-1}$$

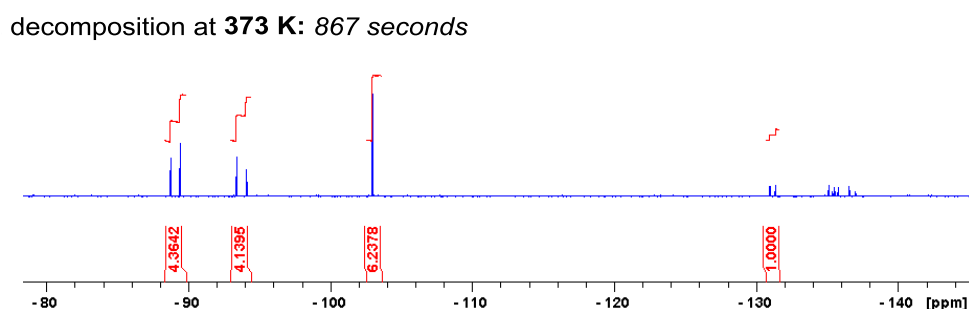
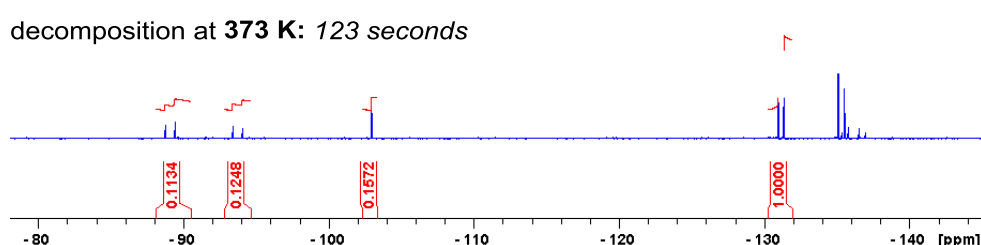
Piperonyl 214a Rearrangement: Kinetic Modelling

VT ¹⁹F NMR Procedure for Piperonyl 214a

¹⁹F NMR spectra were acquired on a Brüker AV400 instrument equipped with a QNP-z probe and a temperature control unit. Data was collected at 376 MHz using 8 scans per data point. Settings for spectra acquisition were as follows: NS = 8 scans; D1 = 1.5 s; SW = 199.77 ppm and O1P = -100 ppm. The samples were held at reaction temperature for the duration of the experiment: 343, 353, 363 and 373 K for Arrhenius plots with **214a**. [D8]-Toluene was purchased from and Sigma Aldrich and used as received. A solution of VCPR precursor (typically 0.13-0.15 M) was

made up in a clean, dry NMR tube and the tube was capped. The tube was inserted into the magnet and the instrument's internal temperature was set to the desired reaction temperature and allowed to equilibrate (approx. 2 minutes heating time). The sample was then analysed at appropriate intervals using a Bruker Topspin automated script, *multi_zgvd2b*. Samples were automatically shimmed using *topshim* between acquisitions. In order to obtain sufficient data points for kinetic analysis; the above procedure was altered slightly for rearrangements at temperatures of 363 and 373 K. Reactions at both temperatures used *noshim* to cancel any shimming between spectra acquisition, allowing time points to be taken every 40 or 25 seconds (respectively) instead of 60 seconds with shimming between samples. A sacrificial sample was used to shim the reaction mixture at 373 K. This was ejected and replaced with a fresh sample which was locked and followed at 25 second intervals (*multi_zgvd2b*) after solvent locking. This procedure allowed the first time point to be taken after 50 seconds instead of 180 seconds. Relative percentages were determined by averaging the manual integration for each compound on the resulting spectra using proprietary software.^{S245}

Example Spectra:



Raw Kinetic Data for Piperonyl 214a

¹⁹F NMR integration data for the VCPR of **214a** in d8-toluene (0.13 M) heated at 343 K (AV400, QNP-z probe); 8 scans, D1= 1.5 s, TE = 343 K.

| Time (s) | Average Integrations | | | Relative Percentage | | |
|-------------|----------------------|------|------|---------------------|------|------|
| | SM | VCPR | 3,3 | SM | VCPR | 3,3 |
| 0 | 1.00 | 0.03 | 0.01 | 96.4 | 3.1 | 0.5 |
| 360 | 1.00 | 0.05 | 0.02 | 93.7 | 4.6 | 1.7 |
| 480 | 1.00 | 0.07 | 0.04 | 90.0 | 6.3 | 3.7 |
| 720 | 1.00 | 0.07 | 0.06 | 88.5 | 6.2 | 5.3 |
| 960 | 1.00 | 0.11 | 0.09 | 83.5 | 9.1 | 7.5 |
| 1200 | 1.00 | 0.11 | 0.09 | 83.0 | 9.3 | 7.7 |
| 1440 | 1.00 | 0.14 | 0.15 | 77.2 | 10.9 | 11.9 |
| 1680 | 1.00 | 0.16 | 0.17 | 74.9 | 12.2 | 12.8 |
| 1920 | 1.00 | 0.19 | 0.20 | 71.8 | 14.0 | 14.2 |
| 2160 | 1.00 | 0.22 | 0.22 | 69.5 | 15.0 | 15.6 |
| 2400 | 1.00 | 0.25 | 0.27 | 66.0 | 16.4 | 17.5 |
| 2640 | 1.00 | 0.28 | 0.30 | 63.2 | 17.7 | 19.1 |
| 2880 | 1.00 | 0.28 | 0.31 | 63.0 | 17.5 | 19.5 |
| 3120 | 1.00 | 0.32 | 0.36 | 59.6 | 19.0 | 21.4 |
| 3360 | 1.00 | 0.34 | 0.36 | 58.7 | 20.1 | 21.2 |
| 3600 | 1.00 | 0.40 | 0.44 | 54.4 | 21.6 | 24.0 |
| 3840 | 1.00 | 0.38 | 0.45 | 54.4 | 20.9 | 24.7 |
| 4080 | 1.00 | 0.46 | 0.52 | 50.7 | 23.1 | 26.2 |
| 4320 | 1.00 | 0.45 | 0.51 | 50.9 | 22.9 | 26.2 |
| 4560 | 1.00 | 0.50 | 0.55 | 48.8 | 24.2 | 27.0 |
| 4800 | 1.00 | 0.57 | 0.68 | 44.5 | 25.2 | 30.3 |
| 5040 | 1.00 | 0.60 | 0.70 | 43.5 | 26.1 | 30.4 |
| 5280 | 1.00 | 0.62 | 0.72 | 42.8 | 26.4 | 30.7 |
| 5520 | 1.00 | 0.62 | 0.77 | 41.9 | 26.1 | 32.1 |
| 5760 | 1.00 | 0.69 | 0.79 | 40.2 | 27.9 | 31.9 |
| 6000 | 1.00 | 0.76 | 0.83 | 38.5 | 29.5 | 32.0 |
| 6240 | 1.00 | 0.78 | 0.95 | 36.6 | 28.5 | 34.8 |
| 6480 | 1.00 | 0.82 | 0.99 | 35.7 | 29.1 | 35.2 |
| 6720 | 1.00 | 0.88 | 1.02 | 34.5 | 30.5 | 35.0 |
| 6960 | 1.00 | 0.90 | 1.08 | 33.6 | 30.3 | 36.1 |
| 7200 | 1.00 | 0.99 | 1.15 | 31.8 | 31.7 | 36.5 |
| 7440 | 1.00 | 1.02 | 1.23 | 30.8 | 31.3 | 37.9 |
| 7680 | 1.00 | 1.09 | 1.32 | 29.3 | 32.0 | 38.8 |
| 7920 | 1.00 | 1.15 | 1.38 | 28.4 | 32.6 | 39.0 |
| 8160 | 1.00 | 1.22 | 1.51 | 26.8 | 32.6 | 40.6 |
| 8400 | 1.00 | 1.26 | 1.45 | 27.0 | 34.0 | 39.1 |

| Time (s) | Average Integrations | | | Relative Percentage | | |
|-------------|----------------------|------|------|---------------------|------|------|
| | SM | VCPR | 3,3 | SM | VCPR | 3,3 |
| 8640 | 1.00 | 1.27 | 1.56 | 26.1 | 33.2 | 40.6 |
| 8880 | 1.00 | 1.44 | 1.77 | 23.8 | 34.2 | 42.0 |
| 9120 | 1.00 | 1.54 | 1.84 | 22.8 | 35.2 | 42.0 |
| 9360 | 1.00 | 1.50 | 1.83 | 23.1 | 34.6 | 42.3 |
| 9600 | 1.00 | 1.66 | 1.96 | 21.6 | 35.9 | 42.5 |
| 9840 | 1.00 | 1.77 | 2.12 | 20.4 | 36.2 | 43.3 |
| 10080 | 1.00 | 1.81 | 2.20 | 19.9 | 36.1 | 43.9 |
| 10320 | 1.00 | 1.83 | 2.10 | 20.3 | 37.1 | 42.6 |
| 10560 | 1.00 | 1.89 | 2.37 | 19.0 | 36.0 | 45.0 |
| 10800 | 1.00 | 1.93 | 2.43 | 18.6 | 36.0 | 45.4 |
| 11280 | 1.00 | 2.09 | 2.60 | 17.6 | 36.7 | 45.7 |
| 63960 | 0.00 | 0.97 | 1.26 | 0.0 | 43.6 | 56.4 |

¹⁹F NMR integration data for the VCPR of **214a** in d8-toluene (0.13 M) heated at 353 K (AV400, QNP-z probe); 8 scans, D1= 1.0 s, TE = 353 K.

| Time (s) | Average Integrations | | | Relative Percentage | | |
|-------------|----------------------|-------|-------|---------------------|------|------|
| | SM | VCPR | 3,3 | SM | VCPR | 3,3 |
| 0 | 1.00 | 0.04 | 0.02 | 94.0 | 3.9 | 2.2 |
| 240 | 1.00 | 0.06 | 0.05 | 90.1 | 5.8 | 4.1 |
| 420 | 1.00 | 0.12 | 0.06 | 84.4 | 10.2 | 5.4 |
| 600 | 1.00 | 0.18 | 0.18 | 73.8 | 13.1 | 13.2 |
| 780 | 1.00 | 0.23 | 0.24 | 67.6 | 15.8 | 16.5 |
| 960 | 1.00 | 0.27 | 0.31 | 63.2 | 17.1 | 19.7 |
| 1140 | 1.00 | 0.33 | 0.38 | 58.3 | 19.5 | 22.1 |
| 1320 | 1.00 | 0.43 | 0.49 | 52.1 | 22.3 | 25.6 |
| 1500 | 1.00 | 0.47 | 0.57 | 49.1 | 22.9 | 28.1 |
| 1680 | 1.00 | 0.55 | 0.65 | 45.6 | 25.0 | 29.4 |
| 1860 | 1.00 | 0.59 | 0.75 | 42.7 | 25.3 | 32.0 |
| 2040 | 1.00 | 0.73 | 0.89 | 38.2 | 27.9 | 33.8 |
| 2220 | 1.00 | 0.81 | 1.03 | 35.2 | 28.4 | 36.4 |
| 2400 | 1.00 | 0.94 | 1.15 | 32.3 | 30.5 | 37.2 |
| 2580 | 1.00 | 1.00 | 1.32 | 30.1 | 30.2 | 39.7 |
| 2760 | 1.00 | 1.20 | 1.55 | 26.7 | 32.1 | 41.3 |
| 2940 | 1.00 | 1.21 | 1.55 | 26.6 | 32.2 | 41.2 |
| 3120 | 1.00 | 1.40 | 1.78 | 23.9 | 33.5 | 42.6 |
| 3300 | 1.00 | 1.48 | 1.91 | 22.8 | 33.7 | 43.6 |
| 3480 | 1.00 | 1.71 | 2.24 | 20.2 | 34.6 | 45.2 |
| 3660 | 1.00 | 2.01 | 2.64 | 17.7 | 35.6 | 46.7 |
| 3840 | 1.00 | 2.03 | 2.59 | 17.8 | 36.1 | 46.1 |
| 4020 | 1.00 | 2.27 | 2.91 | 16.2 | 36.7 | 47.1 |
| 4200 | 1.00 | 2.85 | 3.80 | 13.1 | 37.3 | 49.6 |
| 4380 | 1.00 | 2.75 | 3.64 | 13.5 | 37.2 | 49.3 |
| 4560 | 1.00 | 3.23 | 4.31 | 11.7 | 37.8 | 50.5 |
| 4740 | 1.00 | 3.32 | 4.34 | 11.5 | 38.3 | 50.2 |
| 4920 | 1.00 | 4.35 | 5.59 | 9.1 | 39.8 | 51.1 |
| 5100 | 1.00 | 4.13 | 5.38 | 9.5 | 39.3 | 51.2 |
| 5280 | 1.00 | 4.26 | 5.65 | 9.2 | 39.1 | 51.8 |
| 5460 | 1.00 | 5.00 | 6.58 | 7.9 | 39.8 | 52.3 |
| 5640 | 1.00 | 4.81 | 6.06 | 8.4 | 40.5 | 51.1 |
| 5820 | 1.00 | 6.21 | 8.21 | 6.5 | 40.3 | 53.2 |
| 6000 | 1.00 | 6.75 | 8.85 | 6.0 | 40.7 | 53.3 |
| 6180 | 1.00 | 8.11 | 10.43 | 5.1 | 41.5 | 53.4 |
| 6360 | 1.00 | 5.79 | 7.55 | 7.0 | 40.4 | 52.7 |
| 6540 | 1.00 | 9.03 | 12.02 | 4.5 | 41.0 | 54.5 |
| 6720 | 1.00 | 9.71 | 12.64 | 4.3 | 41.6 | 54.1 |
| 6900 | 1.00 | 10.78 | 14.33 | 3.8 | 41.3 | 54.9 |
| 7080 | 1.00 | 9.40 | 12.23 | 4.4 | 41.5 | 54.0 |
| 7260 | 1.00 | 10.10 | 12.74 | 4.2 | 42.4 | 53.4 |
| 7440 | 1.00 | 12.65 | 16.46 | 3.3 | 42.0 | 54.7 |
| 7620 | 1.00 | 12.47 | 16.40 | 3.3 | 41.7 | 54.9 |
| 15120 | 0.00 | 1.01 | 1.61 | 0.0 | 38.4 | 61.6 |

¹⁹F NMR integration data for the VCPR of **214a** in d8-toluene (0.13 M) heated at 363 K (AV400, QNP-z probe); 8 scans, D1= 1.0 s, TE = 363 K.

| Time | Average Integrations | | | Relative Percentage | | | Time | Average Integrations | | | Relative Percentage | | |
|------|----------------------|------|------|---------------------|------|------|------|----------------------|-------|-------|---------------------|------|------|
| | (s) | SM | VCPR | 3,3 | SM | VCPR | | 3,3 | (s) | SM | VCPR | 3,3 | SM |
| 0 | 1.00 | 0.03 | 0.02 | 95.0 | 2.8 | 2.1 | 1295 | 1.00 | 1.69 | 2.41 | 19.6 | 33.1 | 47.3 |
| 120 | 1.00 | 0.11 | 0.10 | 82.8 | 8.8 | 8.4 | 1325 | 1.00 | 1.87 | 2.51 | 18.6 | 34.8 | 46.6 |
| 160 | 1.00 | 0.12 | 0.13 | 80.0 | 9.9 | 10.0 | 1355 | 1.00 | 1.86 | 2.60 | 18.3 | 34.1 | 47.6 |
| 190 | 1.00 | 0.15 | 0.15 | 77.2 | 11.4 | 11.4 | 1385 | 1.00 | 1.95 | 2.65 | 17.9 | 34.8 | 47.3 |
| 210 | 1.00 | 0.17 | 0.19 | 73.2 | 12.8 | 14.0 | 1415 | 1.00 | 2.48 | 3.36 | 14.6 | 36.2 | 49.1 |
| 245 | 1.00 | 0.18 | 0.22 | 71.4 | 13.1 | 15.5 | 1445 | 1.00 | 2.31 | 3.18 | 15.4 | 35.6 | 49.0 |
| 275 | 1.00 | 0.22 | 0.27 | 67.2 | 14.6 | 18.2 | 1475 | 1.00 | 2.65 | 3.57 | 13.9 | 36.6 | 49.5 |
| 305 | 1.00 | 0.23 | 0.30 | 65.7 | 14.9 | 19.4 | 1505 | 1.00 | 2.31 | 3.08 | 15.6 | 36.1 | 48.2 |
| 335 | 1.00 | 0.26 | 0.31 | 63.4 | 16.7 | 19.9 | 1535 | 1.00 | 2.70 | 3.55 | 13.8 | 37.2 | 49.0 |
| 365 | 1.00 | 0.30 | 0.34 | 61.0 | 18.1 | 20.9 | 1565 | 1.00 | 2.65 | 3.68 | 13.6 | 36.2 | 50.2 |
| 395 | 1.00 | 0.32 | 0.37 | 59.2 | 18.8 | 22.0 | 1595 | 1.00 | 3.04 | 4.27 | 12.0 | 36.5 | 51.4 |
| 425 | 1.00 | 0.36 | 0.43 | 55.9 | 20.1 | 24.1 | 1625 | 1.00 | 3.07 | 4.41 | 11.8 | 36.2 | 52.0 |
| 455 | 1.00 | 0.36 | 0.47 | 54.4 | 19.8 | 25.7 | 1655 | 1.00 | 2.96 | 4.16 | 12.3 | 36.5 | 51.2 |
| 485 | 1.00 | 0.43 | 0.51 | 51.8 | 22.1 | 26.2 | 1685 | 1.00 | 3.04 | 4.26 | 12.1 | 36.6 | 51.3 |
| 515 | 1.00 | 0.43 | 0.55 | 50.6 | 21.7 | 27.7 | 1715 | 1.00 | 3.22 | 4.44 | 11.6 | 37.2 | 51.3 |
| 545 | 1.00 | 0.44 | 0.55 | 50.3 | 21.9 | 27.8 | 1745 | 1.00 | 4.05 | 5.63 | 9.4 | 37.9 | 52.7 |
| 575 | 1.00 | 0.48 | 0.63 | 47.3 | 22.8 | 29.8 | 1775 | 1.00 | 3.50 | 4.64 | 10.9 | 38.3 | 50.8 |
| 605 | 1.00 | 0.52 | 0.66 | 45.7 | 24.0 | 30.3 | 1805 | 1.00 | 3.63 | 4.95 | 10.4 | 37.9 | 51.7 |
| 635 | 1.00 | 0.54 | 0.71 | 44.5 | 23.9 | 31.6 | 1835 | 1.00 | 4.26 | 5.99 | 8.9 | 37.9 | 53.2 |
| 665 | 1.00 | 0.59 | 0.80 | 42.0 | 24.6 | 33.4 | 1865 | 1.00 | 4.10 | 5.49 | 9.4 | 38.7 | 51.8 |
| 695 | 1.00 | 0.64 | 0.83 | 40.5 | 25.9 | 33.6 | 1895 | 1.00 | 4.71 | 6.66 | 8.1 | 38.1 | 53.9 |
| 725 | 1.00 | 0.69 | 0.85 | 39.3 | 27.1 | 33.6 | 1925 | 1.00 | 5.27 | 7.43 | 7.3 | 38.4 | 54.3 |
| 755 | 1.00 | 0.70 | 0.92 | 38.2 | 26.8 | 35.0 | 1955 | 1.00 | 4.75 | 6.31 | 8.3 | 39.4 | 52.3 |
| 785 | 1.00 | 0.73 | 0.98 | 36.9 | 26.8 | 36.3 | 1985 | 1.00 | 5.47 | 7.64 | 7.1 | 38.8 | 54.1 |
| 815 | 1.00 | 0.77 | 1.06 | 35.3 | 27.1 | 37.5 | 2015 | 1.00 | 4.68 | 6.58 | 8.2 | 38.2 | 53.7 |
| 845 | 1.00 | 0.86 | 1.13 | 33.5 | 28.8 | 37.7 | 2045 | 1.00 | 4.82 | 6.57 | 8.1 | 38.9 | 53.0 |
| 875 | 1.00 | 0.86 | 1.15 | 33.2 | 28.6 | 38.2 | 2075 | 1.00 | 6.13 | 8.45 | 6.4 | 39.4 | 54.2 |
| 905 | 1.00 | 0.93 | 1.23 | 31.7 | 29.4 | 39.0 | 2105 | 1.00 | 5.63 | 7.83 | 6.9 | 38.9 | 54.2 |
| 935 | 1.00 | 0.96 | 1.28 | 30.8 | 29.8 | 39.4 | 2135 | 1.00 | 5.74 | 8.28 | 6.7 | 38.2 | 55.1 |
| 965 | 1.00 | 1.02 | 1.35 | 29.7 | 30.3 | 40.0 | 2165 | 1.00 | 6.95 | 9.38 | 5.8 | 40.1 | 54.1 |
| 995 | 1.00 | 1.09 | 1.47 | 28.0 | 30.7 | 41.3 | 2315 | 1.00 | 12.12 | 16.74 | 3.3 | 40.6 | 56.1 |
| 1025 | 1.00 | 1.16 | 1.64 | 26.3 | 30.5 | 43.2 | 2465 | 1.00 | 11.96 | 16.63 | 3.4 | 40.4 | 56.2 |
| 1055 | 1.00 | 1.18 | 1.65 | 26.1 | 30.8 | 43.1 | 2525 | 1.00 | 10.33 | 14.72 | 3.8 | 39.6 | 56.5 |
| 1085 | 1.00 | 1.30 | 1.72 | 24.9 | 32.4 | 42.7 | 2585 | 1.00 | 10.78 | 15.52 | 3.7 | 39.5 | 56.9 |
| 1115 | 1.00 | 1.27 | 1.75 | 24.9 | 31.6 | 43.5 | 2645 | 1.00 | 14.73 | 21.04 | 2.7 | 40.0 | 57.2 |
| 1145 | 1.00 | 1.41 | 1.91 | 23.2 | 32.6 | 44.2 | | | | | | | |
| 1175 | 1.00 | 1.38 | 1.88 | 23.5 | 32.4 | 44.1 | | | | | | | |
| 1205 | 1.00 | 1.56 | 2.07 | 21.6 | 33.7 | 44.7 | | | | | | | |
| 1235 | 1.00 | 1.78 | 2.43 | 19.2 | 34.2 | 46.7 | | | | | | | |
| 1265 | 1.00 | 1.72 | 2.35 | 19.7 | 34.0 | 46.3 | | | | | | | |
| | | | | | | | 6360 | 1.00 | 55.62 | 98.61 | 0.6 | 35.8 | 63.5 |

¹⁹F NMR integration data for the VCPR of **214a** in d8-toluene (0.15 M) heated at 373 K (AV400, QNP-z probe); 8 scans, D1= 1.0 s, TE = 373 K.

| Time (s) | Average Integrations | | | Relative Percentage | | | Time (s) | Average Integrations | | | Relative Percentage | | |
|-------------|----------------------|------|-------|---------------------|------|------|-------------|----------------------|--------|--------|---------------------|------|------|
| | SM | VCPR | 3,3 | SM | VCPR | 3,3 | | SM | VCPR | 3,3 | SM | VCPR | 3,3 |
| 51 | 1.00 | 0.07 | 0.04 | 90.6 | 6.1 | 3.4 | 1011 | 1.00 | 7.67 | 10.89 | 5.1 | 39.2 | 55.7 |
| 75 | 1.00 | 0.08 | 0.04 | 90.0 | 6.8 | 3.3 | 1035 | 1.00 | 6.99 | 10.21 | 5.5 | 38.4 | 56.1 |
| 99 | 1.00 | 0.10 | 0.11 | 82.6 | 7.9 | 9.5 | 1059 | 1.00 | 6.96 | 9.74 | 5.6 | 39.3 | 55.0 |
| 123 | 1.00 | 0.12 | 0.16 | 78.4 | 9.3 | 12.3 | 1083 | 1.00 | 8.89 | 12.55 | 4.5 | 39.6 | 55.9 |
| 147 | 1.00 | 0.18 | 0.22 | 71.1 | 13.1 | 15.8 | 1107 | 1.00 | 10.62 | 14.97 | 3.8 | 39.9 | 56.3 |
| 171 | 1.00 | 0.24 | 0.29 | 65.2 | 15.9 | 18.9 | 1131 | 1.00 | 9.79 | 14.16 | 4.0 | 39.2 | 56.8 |
| 195 | 1.00 | 0.28 | 0.35 | 61.6 | 17.0 | 21.4 | 1155 | 1.00 | 14.57 | 21.05 | 2.7 | 39.8 | 57.5 |
| 219 | 1.00 | 0.32 | 0.42 | 57.2 | 18.6 | 24.2 | 1179 | 1.00 | 12.66 | 17.92 | 3.2 | 40.1 | 56.7 |
| 243 | 1.00 | 0.35 | 0.52 | 53.4 | 18.9 | 27.6 | 1203 | 1.00 | 16.53 | 23.12 | 2.5 | 40.7 | 56.9 |
| 267 | 1.00 | 0.43 | 0.58 | 49.7 | 21.3 | 29.0 | 1227 | 1.00 | 16.37 | 22.65 | 2.5 | 40.9 | 56.6 |
| 291 | 1.00 | 0.51 | 0.68 | 45.7 | 23.2 | 31.1 | 1251 | 1.00 | 16.80 | 23.88 | 2.4 | 40.3 | 57.3 |
| 315 | 1.00 | 0.56 | 0.77 | 42.8 | 24.2 | 33.0 | 1275 | 1.00 | 23.06 | 33.48 | 1.7 | 40.1 | 58.2 |
| 339 | 1.00 | 0.61 | 0.85 | 40.5 | 24.9 | 34.6 | 1299 | 1.00 | 20.64 | 28.65 | 2.0 | 41.0 | 57.0 |
| 363 | 1.00 | 0.66 | 0.95 | 38.3 | 25.2 | 36.5 | 1323 | 1.00 | 41.69 | 61.14 | 1.0 | 40.2 | 58.9 |
| 387 | 1.00 | 0.76 | 1.08 | 35.2 | 26.7 | 38.1 | 1347 | 1.00 | 22.65 | 32.25 | 1.8 | 40.5 | 57.7 |
| 411 | 1.00 | 0.85 | 1.23 | 32.5 | 27.6 | 39.9 | 1371 | 1.00 | 29.39 | 42.34 | 1.4 | 40.4 | 58.2 |
| 435 | 1.00 | 0.93 | 1.36 | 30.4 | 28.4 | 41.2 | 1395 | 1.00 | 28.58 | 40.41 | 1.4 | 40.8 | 57.7 |
| 459 | 1.00 | 0.99 | 1.41 | 29.4 | 29.1 | 41.4 | 1419 | 1.00 | 39.00 | 56.55 | 1.0 | 40.4 | 58.6 |
| 483 | 1.00 | 1.10 | 1.57 | 27.2 | 30.0 | 42.8 | 1443 | 1.00 | 38.19 | 54.13 | 1.1 | 40.9 | 58.0 |
| 507 | 1.00 | 1.22 | 1.83 | 24.7 | 30.2 | 45.1 | 1467 | 1.00 | 34.78 | 50.50 | 1.2 | 40.3 | 58.5 |
| 531 | 1.00 | 1.34 | 1.88 | 23.7 | 31.7 | 44.6 | 1635 | 1.00 | 382.68 | 547.06 | 0.1 | 41.1 | 58.8 |
| 555 | 1.00 | 1.52 | 2.20 | 21.2 | 32.2 | 46.6 | | | | | | | |
| 579 | 1.00 | 1.59 | 2.34 | 20.3 | 32.3 | 47.5 | | | | | | | |
| 603 | 1.00 | 1.76 | 2.58 | 18.7 | 33.0 | 48.3 | | | | | | | |
| 627 | 1.00 | 1.97 | 2.92 | 17.0 | 33.4 | 49.6 | | | | | | | |
| 651 | 1.00 | 2.21 | 3.16 | 15.7 | 34.7 | 49.7 | | | | | | | |
| 675 | 1.00 | 2.13 | 3.13 | 16.0 | 34.0 | 50.0 | | | | | | | |
| 699 | 1.00 | 2.43 | 3.56 | 14.3 | 34.8 | 50.9 | | | | | | | |
| 723 | 1.00 | 2.70 | 3.87 | 13.2 | 35.6 | 51.2 | | | | | | | |
| 747 | 1.00 | 2.88 | 4.15 | 12.4 | 35.8 | 51.7 | | | | | | | |
| 771 | 1.00 | 2.98 | 4.32 | 12.0 | 35.9 | 52.1 | | | | | | | |
| 795 | 1.00 | 3.59 | 5.19 | 10.2 | 36.7 | 53.1 | | | | | | | |
| 819 | 1.00 | 3.78 | 5.38 | 9.8 | 37.2 | 53.0 | | | | | | | |
| 843 | 1.00 | 3.36 | 4.88 | 10.8 | 36.3 | 52.8 | | | | | | | |
| 867 | 1.00 | 4.25 | 6.24 | 8.7 | 37.0 | 54.3 | | | | | | | |
| 891 | 1.00 | 5.13 | 7.42 | 7.4 | 37.9 | 54.7 | | | | | | | |
| 915 | 1.00 | 6.12 | 8.78 | 6.3 | 38.5 | 55.2 | | | | | | | |
| 939 | 1.00 | 5.47 | 7.85 | 7.0 | 38.2 | 54.8 | | | | | | | |
| 963 | 1.00 | 6.99 | 10.23 | 5.5 | 38.4 | 56.2 | | | | | | | |
| 987 | 1.00 | 6.75 | 9.82 | 5.7 | 38.4 | 55.9 | | | | | | | |

Rearrangement Reaction Profiles for 214a (343-373 K)

The reaction profile (relative percentage conversion vs time) was plotted using the NMR data above on Excel.

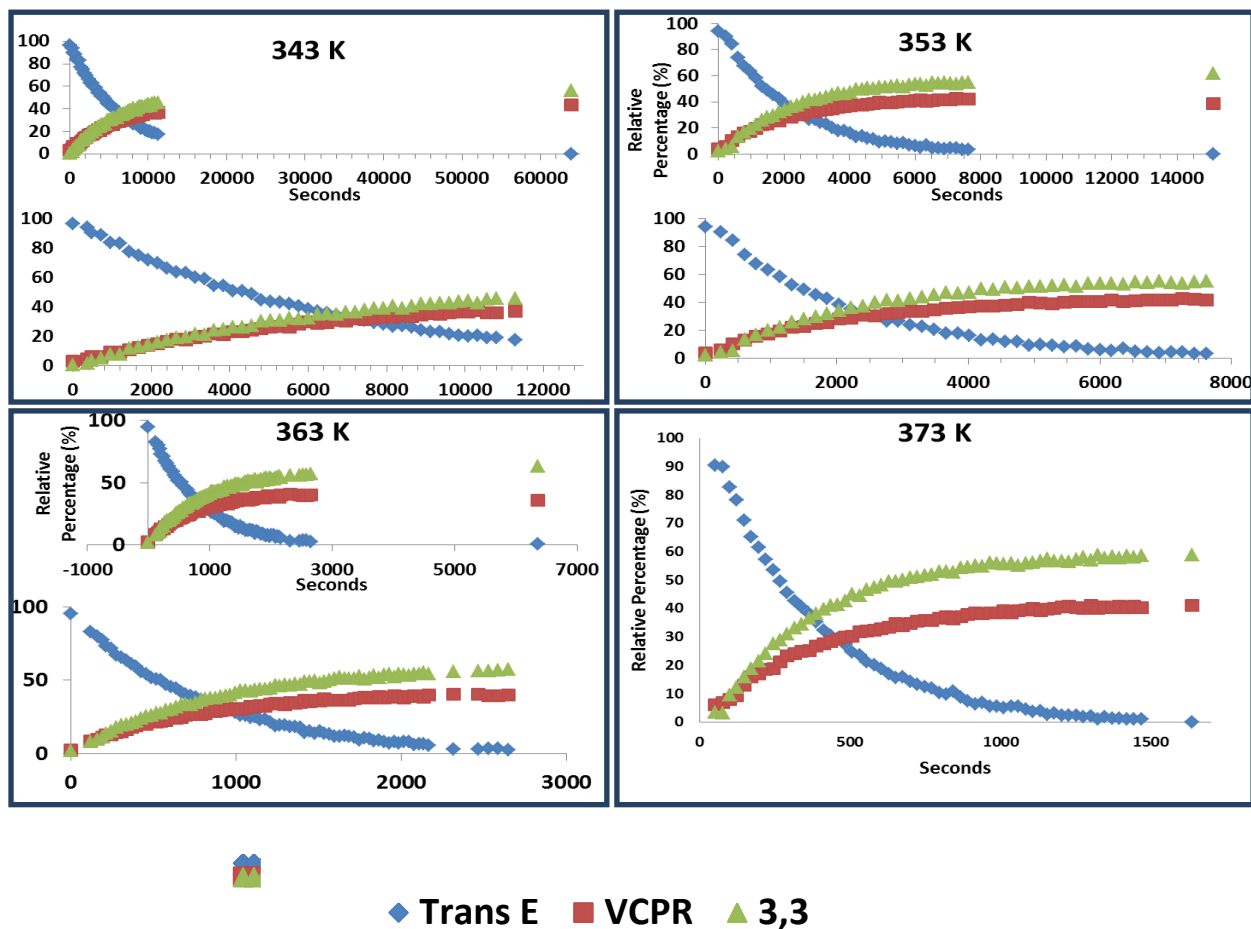


Figure S76: Reaction profiles for the rearrangement of 214a at 343-373 K.

Simulation Procedure: The NMR concentration/time data obtained for **214a** (including a measured endpoint) was imported into Berkeley Madonna software^{S171} from text files and simulated using the two methods discussed below:

Model A

STARTTIME = 0
STOPTIME=43200
DT = 0.05

A0=100 {start concentration of trans cyclopropane}
Init A=A0
B0=0 {start concentration of cis cyclopropane}
Init B=B0
C0=0 {start concentration of cyclopentene}
Init C=C0
D0=0 {start concentration of benzoheptadiene}
Init D=D0

k1=0.0001 {k1 is isomerisation to cis}
k_1=0.0001 {k_1 is isomerisation to trans}
k2=0.0001 {k2 is the VCPR}
k3=0.0001 {k3 is the 3,3}

d/dt (A)=-k1*A-k2*A+k_1*B
d/dt (B)=-k_1*B-k3*B+k1*A
d/dt (C)=k2*A
d/dt (D)=k3*B

LIMIT A>=0
LIMIT B>=0
LIMIT C>=0
LIMIT D>=0

Model B

STARTTIME = 0
STOPTIME=43200
DT = 0.05

A0=100 {start concentration of trans cyclopropane}
Init A=A0
C0=0 {start concentration of cyclopentene}
Init C=C0
D0=0 {start concentration of benzoheptadiene}
Init D=D0

k2=0.0001 {k2 is the VCPR}
k4=0.0001 {k4 is the 3,3}

d/dt (A)=-k2*A-k4*A
d/dt (C)=k2*A
d/dt (D)=k4*A

LIMIT A>=0
LIMIT C>=0
LIMIT D>=0

Arrhenius Plot for Piperonyl 214a

Rate data from **Model B** was changed into the desired Arrhenius parameters.

Arrhenius Data

| Temperature (K) | 1/T | $k_2 (10^{-4} \text{ s}^{-1})$ | Ln k_2 | $k_4 (10^{-4} \text{ s}^{-1})$ | Ln k_4 |
|-----------------|-------------|--------------------------------|----------|--------------------------------|----------|
| 344.1 | 0.002906132 | 0.7338 | -9.51986 | 0.8725 | -9.34673 |
| 354.2 | 0.002823264 | 2.0242 | -8.50517 | 2.632 | -8.2426 |
| 364.2 | 0.002745744 | 5.4558 | -7.51366 | 7.484 | -7.19757 |
| 374.2 | 0.002672368 | 11.0977 | -6.8036 | 15.7878 | -6.4511 |

From Arrhenius equation **1**, a plot of Ln k_2 or Ln k_4 vs 1/T was generated on Excel and a line fitted using the trendline function. The equation of the line was calculated using the *LINEST* statistical function and the gradient used to calculate E_a . The errors in the values were estimated by plotting two lines which would result from the maximum errors ($\pm 5\%$) in the outermost points and averaging the gradient to determine the E_a .

$$\ln k = \frac{-E_a}{R} \frac{1}{T} + \ln A \quad (1)$$

Computational Dipole Investigations

The difference in dipole between the VCPR and aromatic-vinylcyclopropane rearrangement transition states for the rearrangement of piperonyl-VCP precursors (*trans*-**181f** and *cis*-**240**, respectively) was used to assess the potential effect solvent would have on electronic structure calculations.

Solvation Effect on VCPR and [3,3]-Rearrangement Dipole Moments

| Solvent | Solvent Properties | | Difference in Dipole Moment (Debyes) ^[c] | |
|------------------|--------------------|---------------|---|---------------|
| | Dielectric | Dipole Moment | 168a -> TS9a | 181f -> TS14f |
| Gas Phase (n.a.) | n.a. | n.a. | 0.11 | 0.74 |
| Toluene | 2.37 | 0.36 | 0.30 | 0.74 |
| Diphenyl Ether | 3.73 | 1.30 | 0.63 | 0.73 |
| 1-Pentanol | 15.13 | 1.70 | 0.50 | 1.06 |
| Acetonitrile | 35.70 | 3.92 | 0.53 | 1.06 |

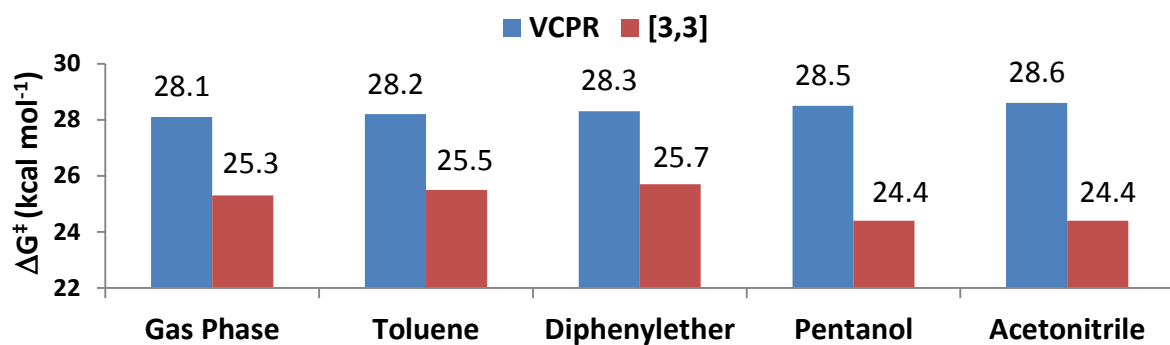
[a] Data reported in Gaussian'09 user's reference.⁵²⁴⁶ [b] Data reported by National Institute of Standards and Technology (NIST).⁵²⁴⁷ [c] Gaussian'09, (U)M05-2X/6-31+G*, 298 K, solvation parameterised using Self-Consistent Reaction Field (SCRF)⁵²⁴⁸ using the Conductor-like Polarizable Continuum Model (CPCM).⁵²⁴⁹

Due to the slightly higher dipole moment for the [3,3]-pathway, more polar solvents (1-pentanol, acetonitrile) gave lower ΔG^\ddagger values compared with gas phase or less polar solvents (toluene, diphenyl ether); approximately 1.0 kcal mol⁻¹ lower energy barrier.

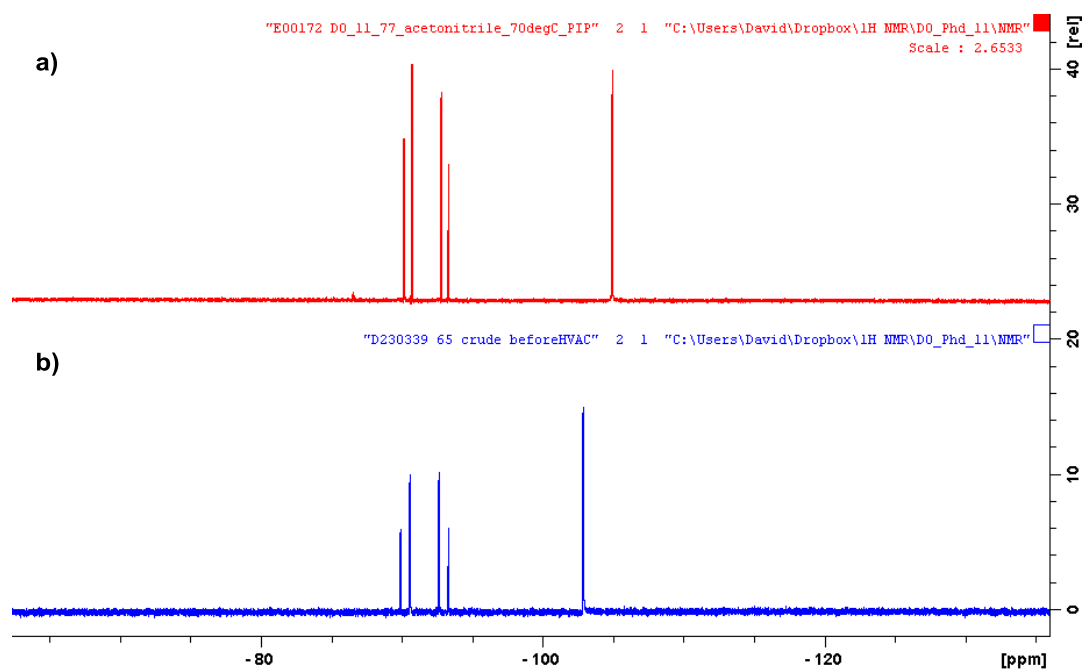
Solvent Effect on Rearrangement Free Energies of Activation (ΔG^\ddagger)

| Solvation | ΔG^\ddagger ((U)M05-2X/6-31+G*, 298 K, Gaussian'09) | | |
|---------------|---|-------|---|
| | VCPR | [3,3] | $\Delta\Delta G^\ddagger$ ($\Delta G^\ddagger_{\text{VCPR}} - \Delta G^\ddagger_{[3,3]}$) |
| Gas Phase | 28.1 | 25.3 | 2.8 |
| Toluene | 28.2 | 25.5 | 2.7 |
| Diphenylether | 28.3 | 25.7 | 2.6 |
| 1-Pentanol | 28.5 | 24.4 | 4.1 |
| Acetonitrile | 28.6 | 24.4 | 4.2 |

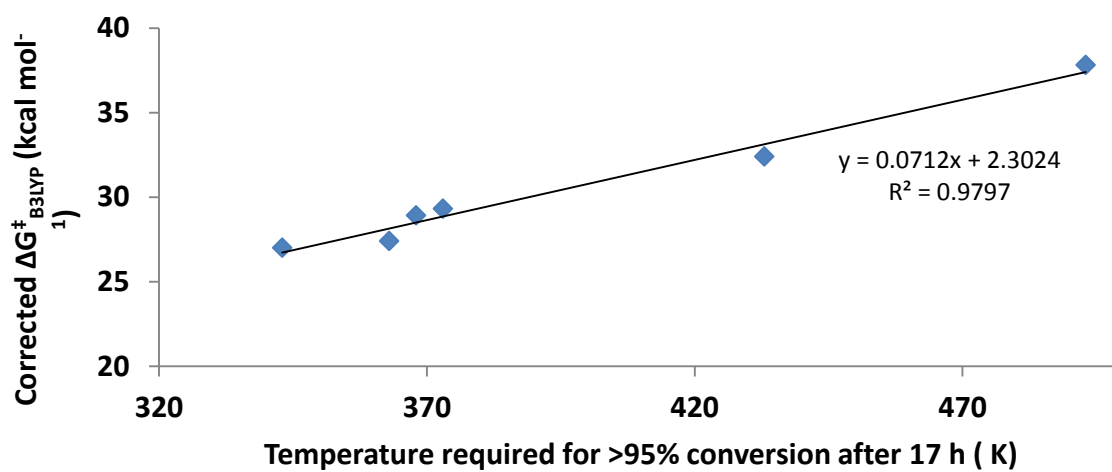
All units are in kcal mol⁻¹.



Solvent effect on calculated ΔG^\ddagger values for the VCPR of 181f and [3,3]-rearrangement of 240.



Crude ¹⁹F NMR for thermal rearrangement of 214a in a) [D3]acetonitrile and b) [D8]toluene.



References

- (1) (a) Babudri, F.; Farinola, G. M.; Naso, F.; Ragni, R., *Chem. Commun.*, **2007**, 1003; (b) Berger, R.; Resnati, G.; Metrangolo, P.; Weber, E.; Hulliger, J., *Chem. Soc. Rev.*, **2011**, *40*, 3496.
- (2) Roesky, H., W. *Efficient Preparations of Fluorine Compounds*; 1st ed.; John Wiley & Sons, Inc: Hoboken, New Jersey, **2013**.
- (3) O'Hagan, D.; S. Rzepa, H., *Chem. Commun.*, **1997**, 645.
- (4) (a) Purser, S.; Moore, P. R.; Swallow, S.; Gouverneur, V., *Chem. Soc. Rev.*, **2008**, *37*, 320; (b) Meanwell, N. A., *J. Med. Chem.*, **2011**, *54*, 2529; (c) Hagmann, W. K., *J. Med. Chem.*, **2008**, *51*, 4359.
- (5) (a) Van Heek, M.; France, C. F.; Compton, D. S.; Mcleod, R. L.; Yumibe, N. P.; Alton, K. B.; Sybertz, E. J.; Davis, H. R., *J. Pharm. Exp. Ther.*, **1997**, *283*, 157; (b) Rosenblum, S. B.; Huynh, T.; Afonso, A.; Davis, H. R.; Yumibe, N.; Clader, J. W.; Burnett, D. A., *J. Med. Chem.*, **1998**, *41*, 973.
- (6) Crane, S. N.; Black, W. C.; Palmer, J. T.; Davis, D. E.; Setti, E.; Robichaud, J.; Paquet, J.; Oballa, R. M.; Bayly, C. I.; McKay, D. J.; Somoza, J. R.; Chauret, N.; Seto, C.; Scheiget, J.; Wesolowski, G.; Massé, F.; Desmarais, S.; Ouellet, M., *J. Med. Chem.*, **2006**, *49*, 1066.
- (7) Rowley, M.; Hallett, D. J.; Goodacre, S.; Moyes, C.; Crawforth, J.; Sparey, T. J.; Patel, S.; Marwood, R.; Patel, S.; Thomas, S.; Hitzel, L.; O'Connor, D.; Szeto, N.; Castro, J. L.; Hutson, P. H.; MacLeod, A. M., *J. Med. Chem.*, **2001**, *44*, 1603.
- (8) Fujimura, K.-i.; Sasabuchi, Y., *ChemMedChem*, **2010**, *5*, 1254.
- (9) (a) Gakh, Y. G.; Gakh, A. A.; Gronenborn, A. M., *Magn. Reson. Chem.*, **2000**, *38*, 551; (b) Dalvit, C., *Prog. Nucl. Mag. Res. Sp.*, **2007**, *51*, 243; (c) Chen, H.; Viel, S.; Ziarelli, F.; Peng, L., *Chem. Soc. Rev.*, **2013**, *42*, 7971.
- (10) Jordan, J. B.; Poppe, L.; Xia, X.; Cheng, A. C.; Sun, Y.; Michelsen, K.; Eastwood, H.; Schnier, P. D.; Nixey, T.; Zhong, W., *J. Med. Chem.*, **2011**, *55*, 678.
- (11) Dolbier Jr, W. R., *J. Fluorine Chem.*, **2005**, *126*, 157.

- (12) (a) O'Hagan, D.; Schaffrath, C.; Cobb, S. L.; Hamilton, J. T. G.; Murphy, C. D., *Nature*, **2002**, *416*, 279; (b) Eustáquio, A. S.; O'Hagan, D.; Moore, B. S., *J. Nat. Prod.*, **2010**, *73*, 378.
- (13) (a) Furuya, T.; Kuttruff, C. A.; Ritter, T., *Curr. Opin. Drug Discov. Devel.*, **2008**, *11*, 903; (b) Kirk, K. L., *Org. Process Res. Dev.*, **2008**, *12*, 305; (c) Ni, C.; Hu, M.; Hu, J., *Chem. Rev.*, **2015**, *115*, 765.
- (14) Lal, G. S.; Pez, G. P.; Pesaresi, R. J.; Prozonic, F. M.; Cheng, H., *J. Org. Chem.*, **1999**, *64*, 7048.
- (15) Umemoto, T.; Singh, R. P.; Xu, Y.; Saito, N., *J. Am. Chem. Soc.*, **2010**, *132*, 18199.
- (16) Nielsen, M. K.; Ugaz, C. R.; Li, W.; Doyle, A. G., *J. Am. Chem. Soc.*, **2015**, *137*, 9571.
- (17) (a) Sandford, G., *J. Fluorine Chem.*, **2007**, *128*, 90; (b) McPake, C. B.; Sandford, G., *Org. Process Res. Dev.*, **2012**, *16*, 844.
- (18) Campbell, M. G.; Ritter, T., *Chem. Rev.*, **2015**, *115*, 612.
- (19) Percy, J. M., *Top. Curr. Chem.*, **1997**, *193*, 131.
- (20) (a) Bégué, J.-P.; Bonnet-Delpon, D.; Crousse, B., *Synlett*, **2004**, *1*, 18; (b) Shuklov, I. A.; Dubrovina, N. V.; Börner, A., *Synthesis*, **2007**, *19*, 2925.
- (21) DeBoos, G. A.; Fullbrook, J. J.; Percy, J. M., *Org. Lett.*, **2001**, *3*, 2859.
- (22) Cox, L. R.; DeBoos, G. A.; Fullbrook, J. J.; Percy, J. M.; Spencer, N., *Tetrahedron: Asymmetry*, **2005**, *16*, 347.
- (23) Crowley, P. J.; Fawcett, J.; Griffith, G. A.; Moralee, A. C.; Percy, J. M.; Salafia, V., *Org. Biomol. Chem.*, **2005**, *3*, 3297.
- (24) Anderl, T.; Audouard, C.; Miah, A.; Percy, J. M.; Rinaudo, G.; Singh, K., *Org. Biomol. Chem.*, **2009**, *7*, 5200.
- (25) (a) Patel, S. T.; Percy, J. M.; Wilkes, R. D., *Tetrahedron*, **1995**, *51*, 9201; (b) Howarth, J. A.; Martin Owton, W.; Percy, J. M.; Rock, M. H., *Tetrahedron*, **1995**, *51*, 10289.
- (26) Wilson, P. G.; Percy, J. M.; Redmond, J. M.; McCarter, A. W., *J. Org. Chem.*, **2012**, *77*, 6384.

- (27) DeBoos, G. A.; Fullbrook, J. J.; Owton, W. M.; Percy, J. M.; Thomas, A. C., *Synlett*, **2000**, 0963.
- (28) Crowley, P. J.; Moralee, A. C.; Percy, J. M.; Spencer, N. S., *Synlett*, **2000**, *12*, 1737.
- (29) Crowley, P. J.; Howarth, J. A.; Owton, W. M.; Percy, J. M.; Stansfield, K., *Tetrahedron Lett.*, **1996**, *37*, 5975.
- (30) (a) Kyne, S. H.; Percy, J. M.; Pullin, R. D. C.; Redmond, J. M.; Wilson, P. G., *Org. Biomol. Chem.*, **2011**, *9*, 8328; (b) Frieman, J.; Percy, J. M.; Tolfrey, A., *Unpublished results*.
- (31) Ichikawa, J., *J. Fluorine Chem.*, **2000**, *105*, 257.
- (32) Katz, J. D.; Lapointe, B. T.; Dinsmore, C. J., *J. Org. Chem.*, **2009**, *74*, 8866.
- (33) Percy, J. M., Wilson, P. G., *Manuscript in preparation*.
- (34) Bonney, K. J.; Schoenebeck, F., *Chem. Soc. Rev.*, **2014**, *43*, 6609.
- (35) DiMartino, G.; Percy, J. M., *Chem. Commun.*, **2000**, 2339.
- (36) DiMartino, G.; Hursthouse, M. B.; Light, M. E.; Percy, J. M.; Spencer, N. S.; Tolley, M., *Org. Biomol. Chem.*, **2003**, *1*, 4423.
- (37) (a) Wang, S. Y.; Borden, W. T., *J. Am. Chem. Soc.*, **1989**, *111*, 7282; (b) Bennett, W. A., *J. Org. Chem.*, **1969**, *34*, 1772.
- (38) (a) Fischer, E. O.; Maasböl, A., *Angew. Chem. Int. Ed.*, **1964**, *3*, 580; (b) Schrock, R. R., *Acc. Chem. Res.*, **1979**, *12*, 98.
- (39) (a) Glorius, F., *Top. Organomet. Chem.*, **2006**, *21*, 1; (b) Marion, N.; Díez-González, S.; Nolan, S. P., *Angew. Chem. Int. Ed.*, **2007**, *46*, 2988; (c) Nolan, S. P. *N-Heterocyclic Carbenes in Synthesis*; 1st ed.; Wiley-VCH: Weinheim, **2006**.
- (40) (a) Bourissou, D.; Guerret, O.; Gabbai, F. P.; Bertrand, G., *Chem. Rev.*, **1999**, *100*, 39; (b) Bertrand, G. *Carbene Chemistry: From Fleeting Intermediates to Powerful Reagents*; 1st ed.; CRC Press: Danver, Massachusetts, **2002**; (c) Strassner, T., *Top. Organomet. Chem.*, **2004**, *13*, 1.
- (41) Birchall, J. M.; Cross, G. E.; Haszeldine, R. N., *Proc. Chem. Soc.*, **1960**, 81.
- (42) Harrison, J. F.; Liedtke, R. C.; Liebman, J. F., *J. Am. Chem. Soc.*, **1979**, *101*, 7162.
- (43) Brahms, D. L. S.; Dailey, W. P., *Chem. Rev.*, **1996**, *96*, 1585.

- (44) (a) Dolbier, W. R.; Battiste, M. A., *Chem. Rev.*, **2003**, *103*, 1071; (b) Fedoryński, M., *Chem. Rev.*, **2003**, *103*, 1099; (c) Thankachan, A. P.; Sindhu, K. S.; Krishnan, K. K.; Anilkumar, G., *Org. Biomol. Chem.*, **2015**, *13*, 8780.
- (45) Birchall, J. M.; Fields, R.; Haszeldine, R. N.; McLean, R. J., *J. Fluorine Chem.*, **1980**, *15*, 487.
- (46) Birchall, J. M.; Haszeldine, R. N.; Roberts, D. W., *Chem. Commun. (London)*, **1967**, 287.
- (47) Sargeant, P. B., *J. Org. Chem.*, **1970**, *35*, 678.
- (48) Robinson, G. C., *Tetrahedron Lett.*, **1965**, *6*, 1749.
- (49) Hine, J.; Porter, J. J., *J. Am. Chem. Soc.*, **1957**, *79*, 5493.
- (50) Weyersta.P; Schwartz.U; Nerdel, F., *Liebigs Ann. Chem.*, **1973**, 2100.
- (51) Wang, F.; Zhang, W.; Zhu, J.; Li, H.; Huang, K.-W.; Hu, J., *Chem. Commun.*, **2011**, *47*, 2411.
- (52) Yudin, A. K.; Prakash, G. K. S.; Deffieux, D.; Bradley, M.; Bau, R.; Olah, G. A., *J. Am. Chem. Soc.*, **1997**, *119*, 1572.
- (53) Wang, F.; Luo, T.; Hu, J.; Wang, Y.; Krishnan, H. S.; Jog, P. V.; Ganesh, S. K.; Prakash, G. K. S.; Olah, G. A., *Angew. Chem. Int. Ed.*, **2011**, *50*, 7153.
- (54) Prakash, G. K. S.; Yudin, A. K., *Chem. Rev.*, **1997**, *97*, 757.
- (55) Prakash, G. K. S.; Jog, P. V.; Batamack, P. T. D.; Olah, G. A., *Science*, **2012**, *338*, 1324.
- (56) (a) Mitsch, R. A., *J. Am. Chem. Soc.*, **1965**, *87*, 758; (b) Moss, R. A.; Wang, L.; Krogh-Jespersen, K., *J. Am. Chem. Soc.*, **2009**, *131*, 2128.
- (57) Dolbier, W. R.; Wojtowicz, H.; Burkholder, C. R., *J. Org. Chem.*, **1990**, *55*, 5420.
- (58) (a) Bessard, Y.; Müller, U.; Schlosser, M., *Tetrahedron*, **1990**, *46*, 5213; (b) Burton, D. J.; Naae, D. G., *J. Am. Chem. Soc.*, **1973**, *95*, 8467.
- (59) Aikawa, K.; Toya, W.; Nakamura, Y.; Mikami, K., *Org. Lett.*, **2015**, *17*, 4996.
- (60) Flynn, R. M.; Manning, R. G.; Kessler, R. M.; Burton, D. J.; Hansen, S. W., *J. Fluorine Chem.*, **1981**, *18*, 525.
- (61) Eujen, R.; Hoge, B., *J. Organomet. Chem.*, **1995**, *503*, C51.

- (62) (a) Seyferth, D.; P. Hopper, S., *J. Organomet. Chem.*, **1971**, *26*, C62; (b) Seyferth, D.; Hopper, S. P., *J. Org. Chem.*, **1972**, *37*, 4070.
- (63) Seyferth, D.; Dertouzos, H.; Suzuki, R.; Mui, J. Y. P., *J. Org. Chem.*, **1967**, *32*, 2980.
- (64) (a) Taguchi, T.; Kurishita, M.; Shibuya, A.; Aso, K., *Tetrahedron*, **1997**, *53*, 9497; (b) Itoh, T.; Mitsukura, K.; Furutani, M., *Chem. Lett.*, **1998**, *27*, 903; (c) Csuk, R.; Eversmann, L., *Tetrahedron*, **1998**, *54*, 6445; (d) Shibuya, A.; Sato, A.; Taguchi, T., *Bioorg. Med. Chem. Lett.*, **1998**, *8*, 1979; (e) Koizumi, N.; Takegawa, S.; Mieda, M.; Shibata, K., *Chem. Pharm. Bull.*, **1996**, *44*, 2162; (f) Shibuya, A.; Okada, M.; Nakamura, Y.; Kibashi, M.; Horikawa, H.; Taguchi, T., *Tetrahedron*, **1999**, *55*, 10325.
- (65) Oshiro, K.; Morimoto, Y.; Amii, H., *Synthesis*, **2010**, *12*, 2080.
- (66) Gill, D. M.; McLay, N.; Waring, M. J.; Wilkinson, C. T.; Sweeney, J. B., *Synlett*, **2014**, *25*, 1756.
- (67) Fujioka, Y.; Amii, H., *Org. Lett.*, **2008**, *10*, 769.
- (68) Tian, F.; Kruger, V.; Bautista, O.; Duan, J.-X.; Li, A.-R.; Dolbier Jr, W. R.; Chen, Q.-Y., *Org. Lett.*, **2000**, *2*, 563.
- (69) Dolbier Jr, W. R.; Tian, F.; Duan, J.-X.; Li, A.-R.; Ait-Mohand, S.; Bautista, O.; Buathong, S.; Marshall Baker, J.; Crawford, J.; Anselme, P.; Cai, X. H.; Modzelewska, A.; Koroniak, H.; Battiste, M. A.; Chen, Q.-Y., *J. Fluorine Chem.*, **2004**, *125*, 459.
- (70) Aono, T.; Sasagawa, H.; Fuchibe, K.; Ichikawa, J., *Org. Lett.*, **2015**, *17*, 5736.
- (71) Eusterwiemann, S.; Martinez, H.; Dolbier, W. R., *J. Org. Chem.*, **2012**, *77*, 5461.
- (72) Hudlicky, T.; Reed, J. W., *Angew. Chem. Int. Ed.*, **2010**, *49*, 4864.
- (73) Neureiter, N., *J. Org. Chem.*, **1959**, *24*, 2044.
- (74) Vogel, E., *Angew. Chem.*, **1960**, *72*, 4.
- (75) (a) Trost, B. M.; Bogdanowicz, M. J., *J. Am. Chem. Soc.*, **1973**, *95*, 5311; (b) Corey, E. J.; Walinsky, S. W., *J. Am. Chem. Soc.*, **1972**, *94*, 8932.
- (76) Danheiser, R. L.; Martinez-Davila, C.; Morin, J. M., *J. Org. Chem.*, **1980**, *45*, 1340.
- (77) Evans, D. A.; Golob, A. M., *J. Am. Chem. Soc.*, **1975**, *97*, 4765.

- (78) Paquette, L. A.; Meehan, G. V.; Henzel, R. P.; Eizember, R. F., *J. Org. Chem.*, **1973**, *38*, 3250.
- (79) Hudlicky, T.; Heard, N. E.; Fleming, A., *J. Org. Chem.*, **1990**, *55*, 2570.
- (80) Hudlicky, T.; Koszyk, F. F.; Kutchan, T. M.; Sheth, J. P., *J. Org. Chem.*, **1980**, *45*, 5020.
- (81) Morizawa, Y.; Oshima, K.; Nozaki, H., *Tetrahedron Lett.*, **1982**, *23*, 2871.
- (82) (a) Murakami, M.; Nishida, S., *Chem. Lett.*, **1979**, *8*, 927; (b) Zuo, G.; Louie, J., *Angew. Chem. Int. Ed.*, **2004**, *43*, 2277.
- (83) Wellington, C. A., *J. Phys. Chem.*, **1962**, *66*, 1671.
- (84) Lewis, D. K.; Charney, D. J.; Kalra, B. L.; Plate, A.-M.; Woodard, M. H.; Cianciosi, S. J.; Baldwin, J. E., *J. Phys. Chem. A*, **1997**, *101*, 4097.
- (85) Schlag, E. W.; Rabinovitch, B. S., *J. Am. Chem. Soc.*, **1960**, *82*, 5996.
- (86) (a) Benson, S. W.; Bose, A. N.; Nangia, P., *J. Am. Chem. Soc.*, **1963**, *85*, 1388; (b) Egger, K. W.; Golden, D. M.; Benson, S. W., *J. Am. Chem. Soc.*, **1964**, *86*, 5420.
- (87) Woodward, R. B.; Hoffmann, R., *Angew. Chem. Int. Ed.*, **1969**, *8*, 781.
- (88) (a) Willcott, M. R.; Cargle, V. H., *J. Am. Chem. Soc.*, **1967**, *89*, 723; (b) Willcott, M. R.; Cargle, V. H., *J. Am. Chem. Soc.*, **1969**, *91*, 4310.
- (89) Ellis, R. J.; Frey, H. M., *J. Chem. Soc.*, **1964**, 5578.
- (90) Baldwin, J. E., *Chem. Rev.*, **2003**, *103*, 1197.
- (91) Baldwin, J. E.; Bonacorsi, S., *J. Org. Chem.*, **1994**, *59*, 7401.
- (92) Asuncion, L. A.; Baldwin, J. E., *J. Am. Chem. Soc.*, **1995**, *117*, 10672.
- (93) Baldwin, J. E.; Bonacorsi, S. J., *J. Am. Chem. Soc.*, **1996**, *118*, 8258.
- (94) Baldwin, J. E.; Villarica, K. A.; Freedberg, D. I.; Anet, F. A. L., *J. Am. Chem. Soc.*, **1994**, *116*, 10845.
- (95) Baldwin, J. E., *J. Comput. Chem.*, **1998**, *19*, 222.
- (96) Quirante, J. J.; Enriquez, F.; Hernando, J. M., *J. Mol. Struct. - Theochem*, **1990**, *204*, 193.
- (97) Houk, K. N.; Li, Y.; Evanseck, J. D., *Angew. Chem. Int. Ed.*, **1992**, *31*, 682.
- (98) Davidson, E. R.; Gajewski, J. J., *J. Am. Chem. Soc.*, **1997**, *119*, 10543.

- (99) Houk, K. N.; Nendel, M.; Wiest, O.; Storer, J. W., *J. Am. Chem. Soc.*, **1997**, *119*, 10545.
- (100) Nendel, M.; Sperling, D.; Wiest, O.; Houk, K. N., *J. Org. Chem.*, **2000**, *65*, 3259.
- (101) (a) Doubleday, C.; Nendel, M.; Houk, K. N.; Thweatt, D.; Page, M., *J. Am. Chem. Soc.*, **1999**, *121*, 4720; (b) Doubleday, C., *J. Phys. Chem. A*, **2001**, *105*, 6333; (c) Doubleday, C.; Li, G.; Hase, W. L., *Phys. Chem. Chem. Phys.*, **2002**, *4*, 304.
- (102) Sicking, W.; Sustmann, R.; Mulzer, J.; Huisgen, R., *Helv. Chim. Acta*, **2011**, *94*, 1389.
- (103) Wang, S. C.; Tantillo, D. J., *J. Organomet. Chem.*, **2006**, *691*, 4386.
- (104) (a) Trost, B. M.; Morris, P. J., *Angew. Chem. Int. Ed.*, **2011**, *50*, 6167; (b) Mei, L.-y.; Wei, Y.; Xu, Q.; Shi, M., *Organometallics*, **2012**, *31*, 7591.
- (105) Tombe, R.; Kurahashi, T.; Matsubara, S., *Org. Lett.*, **2013**, *15*, 1791.
- (106) Wang, S. C.; Troast, D. M.; Conda-Sheridan, M.; Zuo, G.; LaGarde, D.; Louie, J.; Tantillo, D. J., *J. Org. Chem.*, **2009**, *74*, 7822.
- (107) (a) Dolbier, W. R., *Acc. Chem. Res.*, **1981**, *14*, 195; (b) Roth, W. R.; Kirmse, W.; Hoffmann, W.; Lennartz, H.-W., *Chem. Ber.*, **1982**, *115*, 2508.
- (108) Mitsch, R. A.; Neuvar, E. W., *J. Phys. Chem.*, **1966**, *70*, 546.
- (109) Smart, B. E.; Krusic, P. J.; Roe, D. C.; Yang, Z.-Y., *J. Fluorine Chem.*, **2002**, *117*, 199.
- (110) Zeiger, D. N.; Liebman, J. F., *J. Mol. Struct.*, **2000**, *556*, 83.
- (111) Dolbier, W. R.; Al-Sader, B. H.; Sellers, S. F.; Koroniak, H., *J. Am. Chem. Soc.*, **1981**, *103*, 2138.
- (112) Erbes, P.; Boland, W., *Helv. Chim. Acta*, **1992**, *75*, 766.
- (113) (a) Brown, J. M.; Golding, B. T.; Stofko, J. J., *J. Chem. Soc., Chem. Commun.*, **1973**, 319b; (b) Schneider, M., *Angew. Chem. Int. Ed.*, **1975**, *14*, 707.
- (114) Maskill, H., *The Physical Basis of Organic Chemistry*, OUP, Oxford, **1985**, Chapter 6, 242.
- (115) Tu-Hsin, Y.; Paquette, L. A., *Tetrahedron Lett.*, **1982**, *23*, 3227.
- (116) Hudlicky, T.; Natchus, M., *J. Org. Chem.*, **1992**, *57*, 4740.
- (117) Murray, C. K.; Yang, D. C.; Wulff, W. D., *J. Am. Chem. Soc.*, **1990**, *112*, 5660.

- (118) (a) Theodoridis, G. In *Advances in Fluorine Science*; 1st ed.; Alain, T., Ed.; Elsevier Science: **2006**; Vol. 2, p 121; (b) Swallow, S. In *Fluorine in Pharmaceutical and Medicinal Chemistry From Bioaspects to Clinical Applications*; Gouverneur, V., Müller, K., Eds.; Imperial Collage Press: Covent Garden, London, **2012**, p 141; (c) Bremer, M.; Kirsch, P.; Klasen-Memmer, M.; Tarumi, K., *Angew. Chem. Int. Ed.*, **2013**, 52, 8880; (d) Wang, J.; Sánchez-Roselló, M.; Aceña, J. L.; del Pozo, C.; Sorochinsky, A. E.; Fustero, S.; Soloshonok, V. A.; Liu, H., *Chem. Rev.*, **2013**, 114, 2432.
- (119) Mase, T.; Houpis, I. N.; Akao, A.; Dorziotis, I.; Emerson, K.; Hoang, T.; Iida, T.; Itoh, T.; Kamei, K.; Kato, S.; Kato, Y.; Kawasaki, M.; Lang, F.; Lee, J.; Lynch, J.; Maligres, P.; Molina, A.; Nemoto, T.; Okada, S.; Reamer, R.; Song, J. Z.; Tschäen, D.; Wada, T.; Zewge, D.; Volante, R. P.; Reider, P. J.; Tomimoto, K., *J. Org. Chem.*, **2001**, 66, 6775.
- (120) (a) Morikawa, T.; Kodama, Y.; Uchida, J.; Takano, M.; Washio, Y.; Taguchi, T., *Tetrahedron*, **1992**, 48, 8915; (b) Barth, F.; O-Yang, C., *Tetrahedron Lett.*, **1991**, 32, 5873; (c) Buttle, L. A.; Motherwell, W. B., *Tetrahedron Lett.*, **1994**, 35, 3995.
- (121) Yang, Y.-Y.; Meng, W.-D.; Qing, F.-L., *Org. Lett.*, **2004**, 6, 4257.
- (122) Munemori, D.; Narita, K.; Nokami, T.; Itoh, T., *Org. Lett.*, **2014**, 16, 2638.
- (123) (a) Miyaura, N.; Suzuki, A., *Chem. Rev.*, **1995**, 95, 2457; (b) Suzuki, A., *Angew. Chem. Int. Ed.*, **2011**, 50, 6722.
- (124) Jover, J.; Fey, N.; Purdie, M.; Lloyd-Jones, G. C.; Harvey, J. N., *J. Mol. Catal. A: Chem*, **2010**, 324, 39.
- (125) Matos, K.; Soderquist, J. A., *J. Org. Chem.*, **1998**, 63, 461.
- (126) Carrow, B. P.; Hartwig, J. F., *J. Am. Chem. Soc.*, **2011**, 133, 2116.
- (127) (a) Amatore, C.; Jutand, A.; Le Duc, G., *Chem. Eur. J.*, **2011**, 17, 2492; (b) Amatore, C.; Jutand, A.; Le Duc, G., *Chem. Eur. J.*, **2012**, 18, 6616; (c) Amatore, C.; Le Duc, G.; Jutand, A., *Chem. Eur. J.*, **2013**, 19, 10082.
- (128) Charette, A. B.; Giroux, A., *J. Org. Chem.*, **1996**, 61, 8718.
- (129) Jana, R.; Pathak, T. P.; Sigman, M. S., *Chem. Rev.*, **2011**, 111, 1417.

- (130) (a) de Lang, R. J.; Brandsma, L., *Synth. Commun.*, **1998**, *28*, 225; (b) Sarabia, F.; Martín-Gálvez, F.; Chammaa, S.; Martín-Ortiz, L.; Sánchez-Ruiz, A., *J. Org. Chem.*, **2010**, *75*, 5526.
- (131) Fang, G.-H.; Yan, Z.-J.; Deng, M.-Z., *Org. Lett.*, **2004**, *6*, 357.
- (132) Wang, X.-Z.; Deng, M.-Z., *J. Chem. Soc., Perkin Trans. 1*, **1996**, *0*, 2663.
- (133) Krasovskiy, A.; Knochel, P., *Synthesis*, **2006**, *2006*, 0890.
- (134) Bach, R. D.; Dmitrenko, O., *J. Am. Chem. Soc.*, **2004**, *126*, 4444.
- (135) (a) Lu, C. C.; Peters, J. C., *J. Am. Chem. Soc.*, **2004**, *126*, 15818; (b) Sperrle, M.; Gramlich, V.; Consiglio, G., *Organometallics*, **1996**, *15*, 5196.
- (136) Lennox, A. J. J.; Lloyd-Jones, G. C., *J. Am. Chem. Soc.*, **2012**, *134*, 7431.
- (137) Tsuji, J. *Palladium Reagents and Catalysts: Innovations in Organic Synthesis*; John Wiley & Sons Ltd: Chichester, 1997.
- (138) (a) Grigg, R.; Stevenson, P.; Worakun, T., *J. Chem. Soc., Chem. Commun.*, **1985**, 971; (b) Grigg, R.; Stevenson, P.; Worakun, T., *Tetrahedron*, **1988**, *44*, 2049.
- (139) Muñiz, K., *Angew. Chem. Int. Ed.*, **2009**, *48*, 9412.
- (140) Casado, A. L.; Espinet, P., *Organometallics*, **1998**, *17*, 954.
- (141) (a) Ohashi, M.; Kambara, T.; Hatanaka, T.; Saijo, H.; Doi, R.; Ogoshi, S., *J. Am. Chem. Soc.*, **2011**, *133*, 3256; (b) Ohashi, M.; Shibata, M.; Saijo, H.; Kambara, T.; Ogoshi, S., *Organometallics*, **2013**, *32*, 3631; (c) Ohashi, M.; Saijo, H.; Shibata, M.; Ogoshi, S., *Eur. J. Org. Chem.*, **2013**, *2013*, 443.
- (142) Zhou, S.-M.; Deng, M.-Z., *Tetrahedron Lett.*, **2000**, *41*, 3951.
- (143) Soper, A. K.; Benmore, C. J., *Phys. Rev. Lett.*, **2008**, *101*, 065502.
- (144) Zhou, S.-M.; Deng, M.-Z.; Xia, L.-J.; Tang, M.-H., *Angew. Chem. Int. Ed.*, **1998**, *37*, 2845.
- (145) (a) Namboodiri, V. V.; Varma, R. S., *Green Chem.*, **2001**, *3*, 146; (b) Sharma, A. K.; Gowdahalli, K.; Krzeminski, J.; Amin, S., *J. Org. Chem.*, **2007**, *72*, 8987.
- (146) Ma, N. L.; Siu, F. M.; Tsang, C. W., *Chem. Phys. Lett.*, **2000**, *322*, 65.
- (147) (a) Tucker, C. E.; Davidson, J.; Knochel, P., *J. Org. Chem.*, **1992**, *57*, 3482; (b) Pereira, S.; Srebnik, M., *Organometallics*, **1995**, *14*, 3127.
- (148) Zhao, Y.; Snieckus, V., *Org. Lett.*, **2014**, *16*, 390.

- (149) (a) Ishiyama, T.; Murata, M.; Miyaura, N., *J. Org. Chem.*, **1995**, *60*, 7508; (b) Takagi, J.; Takahashi, K.; Ishiyama, T.; Miyaura, N., *J. Am. Chem. Soc.*, **2002**, *124*, 8001.
- (150) Schwartz, J.; Labinger, J. A., *Angew. Chem. Int. Ed.*, **1976**, *15*, 333.
- (151) Wipf, P.; Jahn, H., *Tetrahedron*, **1996**, *52*, 12853.
- (152) Wang, Y. D.; Kimball, G.; Prashad, A. S.; Wang, Y., *Tetrahedron Lett.*, **2005**, *46*, 8777.
- (153) Qing-Yun, C., *J. Fluorine Chem.*, **1995**, *72*, 241.
- (154) Milne, K.; Percy, J. M., Final Year Masters Thesis, **2015**.
- (155) Foris, A., *Magn. Reson. Chem.*, **2004**, *42*, 534.
- (156) Hagooley, Y.; Cohen, O.; Rozen, S., *Tetrahedron Lett.*, **2009**, *50*, 392.
- (157) Houk, K. N.; Rondan, N. G.; Mareda, J., *Tetrahedron*, **1985**, *41*, 1555.
- (158) C. A. Sader, K. N. Houk, *ARKIVOC*, **2014**, *3*, 170–183.
- (159) Barnett, C. J.; Huff, B.; Kobierski, M. E.; Letourneau, M.; Wilson, T. M., *J. Org. Chem.*, **2004**, *69*, 7653.
- (160) (a) Hall, M. I.; Pridmore, S. J.; Williams, J. M. J., *Adv. Synth. Catal.*, **2008**, *350*, 1975; (b) Lee, E. Y.; Kim, Y.; Lee, J. S.; Park, J., *Eur. J. Org. Chem.*, **2009**, *2009*, 2943.
- (161) Ireland, R. E.; Norbeck, D. W., *J. Org. Chem.*, **1985**, *50*, 2198.
- (162) Vatèle, J.-M., *Tetrahedron Lett.*, **2006**, *47*, 715.
- (163) Dolbier, W. R.; Sellers, S. F., *J. Am. Chem. Soc.*, **1982**, *104*, 2494.
- (164) Orr, D.; Percy, J. M.; Tuttle, T.; Kennedy, A. R.; Harrison, Z. A., *Chem. Eur. J.*, **2014**, *20*, 14305.
- (165) (a) Fawcett, J.; Griffith, G. A.; Percy, J. M.; Uneyama, E., *Org. Lett.*, **2004**, *6*, 1277; (b) Fawcett, J.; Moralee, A. C.; Percy, J. M.; Salafia, V.; Vincent, M. A.; Hillier, I. H., *Chem. Commun.*, **2004**, *0*, 1062.
- (166) Adam, W.; van Barneveld, C.; Golsch, D., *Tetrahedron*, **1996**, *52*, 2377.
- (167) <http://openflask.blogspot.co.uk/2014/01/tfdo-synthesis-procedure.html>, Accessed February 2014.
- (168) (a) Houk, K. N.; Liu, J.; DeMello, N. C.; Condroski, K. R., *J. Am. Chem. Soc.*, **1997**, *119*, 10147; (b) Jenson, C.; Liu, J.; Houk, K. N.; Jorgensen, W. L., *J. Am. Chem.*

- Soc.*, **1997**, *119*, 12982; (c) Schneebeli, S. T.; Hall, M. L.; Breslow, R.; Friesner, R., *J. Am. Chem. Soc.*, **2009**, *131*, 3965.
- (169) (a) Padwa, A.; Dent, W., *J. Org. Chem.*, **1987**, *52*, 235; (b) Beebe, X.; Darczak, D.; Henry, R. F.; Vortherms, T.; Janis, R.; Namovic, M.; Donnelly-Roberts, D.; Kage, K. L.; Surowy, C.; Milicic, I.; Niforatos, W.; Swensen, A.; Marsh, K. C.; Wetter, J. M.; Franklin, P.; Baker, S.; Zhong, C.; Simler, G.; Gomez, E.; Boyce-Rustay, J. M.; Zhu, C. Z.; Stewart, A. O.; Jarvis, M. F.; Scott, V. E., *Bioorg. Med. Chem.*, **2012**, *20*, 4128.
- (170) (a) Nunez, M. T.; Martin, V. S., *J. Org. Chem.*, **1990**, *55*, 1928; (b) Carlsen, P. H. J.; Katsuki, T.; Martin, V. S.; Sharpless, K. B., *J. Org. Chem.*, **1981**, *46*, 3936.
- (171) Zahnley, T.; Macey, R.; Oster, G. In *Berkley Madonna*; 8.3.18 eq.; University of California at Berkeley: Berkeley, California, **2010**.
- (172) (a) Becke, A. D., *J. Chem. Phys.*, **1993**, *98*, 5648; (b) Lee, C.; Yang, W.; Parr, R. G., *Phys. Rev. B*, **1988**, *37*, 785; (c) Vosko, S. H.; Wilk, L.; Nusair, M., *Can. J. Phys.*, **1980**, *58*, 1200; (d) Stephens, P. J.; Devlin, F. J.; Chabalowski, C. F.; Frisch, M. J., *J. Phys. Chem.*, **1994**, *98*, 11623.
- (173) Zhao, Y.; Schultz, N. E.; Truhlar, D. G., *J. Chem. Phys.*, **2005**, *123*, 161103.
- (174) Zhao, Y.; Truhlar, D., *Theor. Chem. Acc.*, **2008**, *120*, 215.
- (175) (a) Antony, J.; Grimme, S., *Phys. Chem. Chem. Phys.*, **2006**, *8*, 5287; (b) Grimme, S., *J. Comput. Chem.*, **2006**, *27*, 1787.
- (176) Spartan '08, Wavefunction, Irvine, CA, **2008**.
- (177) Spartan '10, Wavefunction, Irvine, CA, **2010**.
- (178) Frisch, M. J., Gaussian'09, Revision A.1 ed., Gaussian Inc: Wallingford CT, **2009**.
- (179) Loncharich, R. J.; Schwartz, T. R.; Houk, K. N., *J. Am. Chem. Soc.*, **1987**, *109*, 14.
- (180) Bakalova, S. M.; Santos, A. G., *J. Org. Chem.*, **2004**, *69*, 8475.
- (181) (a) Hudlicky, T.; Fan, R.; Reed, J. W.; Gadamasetti, K. G. In *Organic Reactions*; John Wiley & Sons, Inc.: 2004; Vol. 41, p 1; (b) Krüger, S.; Gaich, T., *Beilstein J. Org. Chem.*, **2014**, *10*, 163.
- (182) Hess, B. A.; Baldwin, J. E., *J. Org. Chem.*, **2002**, *67*, 6025.
- (183) (a) Bachrach, S. M. *Computational Organic Chemistry*; 2nd ed.; John Wiley & Sons, Inc.: Hoboken, New Jersey, 2014; (b) Crammer, C. J. *Essentials of*

Computational Chemistry: Theories and Models; 2nd ed.; John Wiley & Sons, Ltd.: Chichester, West Sussex, 2004.

(184) (a) Liang, Y.; Mackey, J. L.; Lopez, S. A.; Liu, F.; Houk, K. N., *J. Am. Chem. Soc.*, **2012**, *134*, 17904; (b) Jiménez-Osés, G.; Brockway, A. J.; Shaw, J. T.; Houk, K. N., *J. Am. Chem. Soc.*, **2013**, *135*, 6633; (c) Houk, K. N.; Cheong, P. H.-Y., *Nature*, **2008**, *455*, 309; (d) Nguyen, Q. N. N.; Tantillo, D. J., *Chem. Asian J.*, **2014**, *9*, 674; (e) Tsang, A. S. K.; Sanhueza, I. A.; Schoenebeck, F., *Chem. Eur. J.*, **2014**, *20*, 16432.

(185) Hansch, C.; Leo, A.; Taft, R. W., *Chem. Rev.*, **1991**, *91*, 165.

(186) Creary, X., *Acc. Chem. Res.*, **2006**, *39*, 761.

(187) (a) Agirbas, H.; Jackson, R. A., *J. Chem. Soc., Perkin Trans. 2*, **1983**, 739; (b) Jiang, X.; Ji, G., *J. Org. Chem.*, **1992**, *57*, 6051; (c) Dust, J. M.; Arnold, D. R., *J. Am. Chem. Soc.*, **1983**, *105*, 1221.

(188) (a) Zipse, H. In *Radicals in Synthesis I*; Gansäuer, A., Ed.; Springer Berlin Heidelberg: 2006; Vol. 263, p 163; (b) Henry, D. J.; Parkinson, C. J.; Mayer, P. M.; Radom, L., *J. Phys. Chem. A*, **2001**, *105*, 6750.

(189) Creary, X.; Wolf, A.; Miller, K., *Org. Lett.*, **1999**, *1*, 1615.

(190) (a) Schneider, T. F.; Werz, D. B., *Org. Lett.*, **2011**, *13*, 1848; (b) Schneider, T. F.; Kaschel, J.; Werz, D. B., *Angew. Chem. Int. Ed.*, **2014**, *53*, 5504.

(191) Bruno, I.; Cole, J.; Lommerse, J. M.; Rowland, R. S.; Taylor, R.; Verdonk, M., *J. Comput. Aided Mol. Des.*, **1997**, *11*, 525.

(192) (a) Olsen, R. K.; Feng, X.; Campbell, M.; Shao, R.-I.; Math, S. K., *J. Org. Chem.*, **1995**, *60*, 6025; (b) Hartley, R. C.; Li, J.; Main, C. A.; McKiernan, G. J., *Tetrahedron*, **2007**, *63*, 4825.

(193) Meek, S. J.; O'Brien, R. V.; Llaveria, J.; Schrock, R. R.; Hoveyda, A. H., *Nature*, **2011**, *471*, 461.

(194) Knölker, H.-J.; Winterfeldt, E., *Liebigs Ann. Chem.*, **1986**, *1986*, 465.

(195) Lohre, C.; Fröhlich, R.; Glorius, F., *Synthesis*, **2008**, *2008*, 2221.

(196) Brnardic, E. J.; Converso, A.; Fraley, M. E.; Garbaccio, R. M.; Huang, S. Y, PCT Int. Appl. (2009), WO 2009140163 A1 Nov 19, 2009.

(197) Chen, Q.; Wu, S., *J. Org. Chem.*, **1989**, *54*, 3023.

- (198) (a) Fuchibe, K.; Koseki, Y.; Aono, T.; Sasagawa, H.; Ichikawa, J., *J. Fluorine Chem.*, **2012**, *133*, 52; (b) Thomason, C. S.; Dolbier, W. R., *J. Org. Chem.*, **2013**, *78*, 8904; (c) Thomason, C. S.; Wang, L.; Dolbier, W. R., *J. Fluorine Chem.*, **2014**, *168*, 34; (d) Li, L.; Wang, F.; Ni, C.; Hu, J., *Angew. Chem. Int. Ed.*, **2013**, *52*, 12390; (e) Deng, X.-Y.; Lin, J.-H.; Zheng, J.; Xiao, J.-C., *Chem. Commun.*, **2015**, *51*, 8805.
- (199) Zhou, J.; Campbell-Conroy, E. L.; Silina, A.; Uy, J.; Pierre, F.; Hurley, D. J.; Hilgraf, N.; Frieman, B. A.; DeNinno, M. P., *J. Org. Chem.*, **2015**, *80*, 70.
- (200) Xu, W.; Chen, Q.-Y., *Org. Biomol. Chem.*, **2003**, *1*, 1151.
- (201) Aris, V.; Brown, J. M.; Conneely, J. A.; Golding, B. T.; Williamson, D. H., *J. Chem. Soc., Perkin Trans. 2*, **1975**, 4.
- (202) Larsen, S. D., *J. Am. Chem. Soc.*, **1988**, *110*, 5932.
- (203) Arimitsu, S.; Hammond, G. B., *J. Org. Chem.*, **2007**, *72*, 8559.
- (204) Denmark, S. E.; Edwards, J. P., *J. Org. Chem.*, **1991**, *56*, 6974.
- (205) Yanai, T.; Tew, D. P.; Handy, N. C., *Chem. Phys. Lett.*, **2004**, *393*, 51.
- (206) Özkan, İ.; Zora, M., *J. Org. Chem.*, **2003**, *68*, 9635.
- (207) Maas, G., *Chem. Ber.*, **1979**, *112*, 3241.
- (208) Maas, G.; Hummel, C., *Chem. Ber.*, **1980**, *113*, 3679.
- (209) Ohlinger, W. S.; Klunzinger, P. E.; Deppmeier, B. J.; Hehre, W. J., *J. Phys. Chem. A*, **2009**, *113*, 2165.
- (210) Curtiss, L. A.; Raghavachari, K.; Pople, J. A., *J. Chem. Phys.*, **1993**, *98*, 1293.
- (211) (a) Domalski, E., S., *J. Phys. Chem. Ref. Data*, **1972**, *1*, 221; (b) Hubbard, W. N.; Scott, D. W.; Frow, F. R.; Waddington, G., *J. Am. Chem. Soc.*, **1955**, *77*, 5855.
- (212) Cohen, N., *J. Phys. Chem. Ref. Data*, **1996**, *25*, 1411.
- (213) Simon, L.; Goodman, J. M., *Org. Biomol. Chem.*, **2011**, *9*, 689.
- (214) Mulzer, J.; Huisgen, R.; Arion, V.; Sustmann, R., *Helv. Chim. Acta*, **2011**, *94*, 1359.
- (215) Viridi, A.; Gupta, V. P.; Sharma, A., *J. Mol. Struct. - Theochem*, **2004**, *678*, 239.
- (216) Ni, Y.; Montgomery, J., *J. Am. Chem. Soc.*, **2006**, *128*, 2609.
- (217) Ryu, I.; Ikura, K.; Tamura, Y.; Maenaka, J.; Ogawa, A.; Sonoda, N., *Synlett*, **1994**, *1994*, 941.

- (218) Böhm, V. P. W.; Gstöttmayr, C. W. K.; Weskamp, T.; Herrmann, W. A., *Angew. Chem. Int. Ed.*, **2001**, *40*, 3387.
- (219) Louie, J.; Gibby, J. E.; Farnworth, M. V.; Tekavec, T. N., *J. Am. Chem. Soc.*, **2002**, *124*, 15188.
- (220) Wu, J.; Faller, J. W.; Hazari, N.; Schmeier, T. J., *Organometallics*, **2012**, *31*, 806.
- (221) Iglesias, M. J.; Blandez, J. F.; Fructos, M. R.; Prieto, A.; Álvarez, E.; Belderrain, T. R.; Nicasio, M. C., *Organometallics*, **2012**, *31*, 6312.
- (222) Dible, B. R.; Sigman, M. S., *Inorg. Chem.*, **2006**, *45*, 8430.
- (223) Iglesias, M. J.; Prieto, A.; Nicasio, M. C., *Adv. Synth. Catal.*, **2010**, *352*, 1949.
- (224) Iglesias, M. J.; Prieto, A.; Nicasio, M. C., *Org. Lett.*, **2012**, *14*, 4318.
- (225) (a) Pietruszka, J.; Witt, A., *J. Chem. Soc., Perkin Trans. 1*, **2000**, *0*, 4293; (b) Brondani, P. B.; Dudek, H.; Reis, J. S.; Fraaije, M. W.; Andrade, L. H., *Tetrahedron: Asymmetry*, **2012**, *23*, 703.
- (226) Sreedhar, B.; Radhika, P.; Neelima, B.; Hebalkar, N., *J. Mol. Catal. A: Chem*, **2007**, *272*, 159.
- (227) (a) Azizi, N.; Baghi, R.; Ghafari, H.; Bolourtchian, M.; Hashemi, M., *Synlett*, **2010**, 379; (b) Ying, A.; Li, Z.; Yang, J.; Liu, S.; Xu, S.; Yan, H.; Wu, C., *J. Org. Chem.*, **2014**, *79*, 6510.
- (228) Takemoto, K., Sakamoto, H., *Jpn. Kokai Koho* (**2010**), JP2010126514 A 20100610.
- (229) Shao, T.; Fang, X.; Yang, X., *Synlett*, **2015**, *26*, 1835.
- (230) Lagiakos, H. R.; Walker, A.; Aguilar, M.-I.; Perlmutter, P., *Tetrahedron Lett.*, **2011**, *52*, 5131.
- (231) Queval, P.; Jahier, C.; Rouen, M.; Artur, I.; Legeay, J.-C.; Falivene, L.; Toupet, L.; Crévisy, C.; Cavallo, L.; Baslé, O.; Mauduit, M., *Angew. Chem. Int. Ed.*, **2013**, *52*, 14103.
- (232) Sheldrick, G., *Acta Crystallogr. Sect. A*, **2008**, *64*, 112.
- (233) Coulson, D. R.; Satek, L. C.; Grim, S. O. In *Inorganic Syntheses*; John Wiley & Sons, Inc.: 2007, p 121.
- (234) Duhamel, L.; Plaquevent, J.-C., *J. Organomet. Chem.*, **1993**, *448*, 1.

- (235) Waser, J.; Gaspar, B.; Nambu, H.; Carreira, E. M., *J. Am. Chem. Soc.*, **2006**, *128*, 11693.
- (236) Kobayashi, Y.; Taguchi, T.; Morikawa, T., *J. Fluorine Chem.*, **1982**, *21*, 60.
- (237) Kim, I. S.; Dong, G. R.; Jung, Y. H., *J. Org. Chem.*, **2007**, *72*, 5424.
- (238) Kobayashi, Y.; Taguchi, T.; Morikawa, T.; Takase, T.; Takanashi, H., *J. Org. Chem.*, **1982**, *47*, 3232.
- (239) Lebel, H.; Davi, M., *Adv. Synth. Catal.*, **2008**, *350*, 2352.
- (240) Iwasaki, M.; Kobayashi, Y.; Li, J. P.; Matsuzaka, H.; Ishii, Y.; Hidai, M., *J. Org. Chem.*, **1991**, *56*, 1922.
- (241) Acharya, A.; Eickhoff, J. A.; Jeffrey, C. S., *Synthesis*, **2013**, *45*, 1825.
- (242) Bulman Page, P. C.; Appleby, L. F.; Chan, Y.; Day, D. P.; Buckley, B. R.; Slawin, A. M. Z.; Allin, S. M.; McKenzie, M. J., *J. Org. Chem.*, **2013**, *78*, 8074.
- (243) Charette, A. B.; Juteau, H.; Lebel, H.; Molinaro, C., *J. Am. Chem. Soc.*, **1998**, *120*, 11943.
- (244) Gonzalez-de-Castro, A.; Xiao, J., *J. Am. Chem. Soc.*, **2015**, *137*, 8206.
- (245) Topspin, 3.2 ed., Bruker: Billerica, MA, **2012**.
- (246) http://www.gaussian.com/g_tech/g_ur/k_scrf.htm, Accessed on 9th Nov. 2015.
- (247) Nelson, R. D., Lide, D. R., Maryott, A. A., & United States. National Bureau of Standards. (1967). *Selected values of electric dipole moments for molecules in the gas phase*. Washington, D.C.: U.S. Dept. of Commerce, National Bureau of Standards. (<http://www.nist.gov/data/nsrds/NSRDS-NBS-10.pdf>, Accessed 9th Nov. 2015).
- (248) Tomasi, J.; Mennucci, B.; Cammi, R., *Chem. Rev.*, **2005**, *105*, 2999.
- (249) Cossi, M.; Rega, N.; Scalmani, G.; Barone, V., *J. Comput. Chem.*, **2003**, *24*, 669.